
**Novel Coronary
Atherothrombosis Genes
Identified By Blood Cell
Transcriptomics**

PhD

2012

Unni Krishnan

*This thesis is dedicated to Hari and Radhika Krishnan,
my personal experiments in human genetics.*

ABSTRACT

Rationale: Coronary artery disease (CAD) is a complex phenotype with multiple genetic and environmental risk factors. The circulating monocyte plays a key role in CAD and contributes to atherogenesis, plaque progression and atherothrombosis, especially through its interactions with platelets. This study tested the hypothesis that gene expression profiling of monocytes in a resting state, and following platelet-mediated stimulation would identify novel molecules that may determine the inherited risk of CAD.

Methods: Four groups of subjects were recruited: patients with a premature MI (PMI) <65 years (n=19) and age/gender matched healthy controls (n=19), healthy young men with a strong family history of PMI (n=22) and matched controls with no significant family history of CAD (n=17). Monocyte RNA was extracted before and after platelet-mediated stimulation (for 4 hours) from all subjects for whole genome microarray analysis. Differentially expressed genes were validated by QPCR and those genes with similar trends in expression in the PMI patients and the healthy young men with a family history of PMI were selected for further analysis. These were tested *in silico* in CARDIoGRAM, a large scale genome wide association study (GWAS) to identify genetic variants that showed either strong associations with CAD or with gene expression in monocytes (expression quantitative trait locus - eQTL).

Results: This work revealed similar trends in differential expression of specific monocyte genes between PMI patients and healthy men with a strong genetic risk of PMI compared with their respective healthy controls. These include genes implicated in lipid metabolism (ACAD10), sterol transport (CYP27A1, ARV1) and inflammation (CCL3, EGR1). Of these, ACAD10 and CYP27A1 were the genes which were most statistically significant. In the follow-up analysis of these genes, a genetic variant (rs2238151) in ACAD10 showed a significant association with risk of CAD (risk allele frequency (RAF): 0.63, OR: 1.08, corrected p: 5.85×10^{-6}) and MI (RAF: 0.57, OR: 1.09, corrected p: 6.24×10^{-6}) in the CARDIoGRAM GWAS meta-analysis and a variant in CYP27A1 (rs933994) was noted to be an eQTL for CYP27A1 expression in monocytes ($p=2.9 \times 10^{-70}$).

Conclusions: Gene expression profiling in resting and stimulated monocytes from subjects with premature CAD and those with an increased genetic risk of CAD have revealed novel gene variants which associate with susceptibility to CAD.

ACKNOWLEDGEMENTS

First and foremost I am indebted to my supervisors, Professors Nilesh Samani and Alison Goodall. This work would not have happened without either of them and it is my hope that they would feel I have done some justice to the opportunity given to me.

Prof Samani continues to be a constant source of inspiration to me at a personal and professional level and I owe him the most for supporting my career aspirations in academic cardiology. He has always encouraged and supported me in my project as well as at crucial stages in my career and I can confidently say that I would not have achieved any of my professional milestones without his guidance and good will.

Alison has been as much a friend as a patient and supportive supervisor throughout this project. She has always accommodated me at short notice at various critical stages in my research, steering my thought process and work in the right direction. Her expertise in platelet biology and the vast academic experience at her disposal have been invaluable in helping me overcome the various hurdles I encountered during this project.

I should also mention those who started as colleagues and ended as close friends during my time in the department. Joy (Wright), I can only describe as my 'partner in crime' for the kinship I feel from all the hours we spent immersed in labwork and agonizing over our experiments. Tina (James) was crucial to the day-to-day running of the project while unassuming Jackie (Appleby) helped me on countless occasions with her amazing insights into laboratory work. Jas (Moore) taught me everything about PCR and did it with an indelible smile, while Veryan (Codd) was always happy to troubleshoot. In 'The Office' I thank everyone who made my time enjoyable, especially Jay (Gracey) for her raucous laughter, Kim (Mason) for being my tireless source of administrative information and an endless supplier of tea and Terry (Smith) for being the only other cricket fan around. Everyone in the department pitched in when I was looking for healthy recruits, providing a constant stream of friends and relatives who willingly donated their time and blood.

I am grateful to the Bloodomics project for funding my research fellowship and for the expertise of the various collaborators within the consortium, especially Prof Willem Ouwehand, Dr Nick Watkins and Dr Rosienne Farrugia (University of Cambridge) and Dr Cordelia Langford and Dr Peter Ellis (Wellcome Trust Sanger Institute, Hinxton). In the latter part of my project, Dr Chris Nelson (Medical Statistician, University of Leicester) was immensely supportive in conducting the genome wide integrative analyses.

I would like to thank my clinical supervisors in Liverpool, especially Dr Nick Palmer and Dr Raphael Perry for facilitating my multiple trips to Leicester to ensure that I progress with my thesis while in full time clinical training. I should also mention Dr Philip Weston who gave me a very timely 'pep talk' to keep me focused on completing my thesis.

My parents have supported me without question in all that I have attempted. My father taught me to persevere with what I believe in, especially when the going gets tough, while I learnt to appreciate the joy in attention to detail from my mother, who I also thank for showing me how to balance analytical rigour with intuition. Everyone in the family and my circle of friends have put up with my mood swings admirably and I thank them all for their patience and understanding.

To my children, Hari and Radhika, I owe an apology for all the kites that were not flown and all the puddles that went unassaulted. For all those times when I had to choose my thesis over the two of you, I hope I can make up to you some day.

Above all, I owe everything to my constant companion and best friend, my greatest no-holds-barred critic and unashamed supporter, who has seen the worst in me more than anyone else, who understands me and believes in me even when I don't, who loves me warts and all – my wife Dhanya, who incidentally also beat me to it by successfully defending *her* PhD last year!

TABLE OF CONTENTS

Identification of Novel Genes Involved In Coronary Atherothrombosis by Blood Cell Transcriptome Profiling	Error! Bookmark not defined.
Abstract.....	3
Acknowledgements	4
Table of contents.....	5
List of Tables and Figures	11
Abbreviations	16
Chapter 1	20
Introduction.....	20
1.1 Coronary artery disease (CAD) – the problem.....	21
1.2 Atherosclerosis – a complex phenotype	21
1.3 Risk factors for CAD	22
1.4 Heritability of CAD	24
1.5 Elucidation of genetic contributions to CAD	25
1.6 Cellular and molecular pathways in CAD.....	32
1.6.3.1 Monocytes.....	33
1.6.3.1.1 The role of monocyte gene expression in atherosclerosis.....	35
1.6.3.2 Platelets	37
1.6.3.3 Monocyte-platelet interactions in atherothrombosis	40
1.6.3.4 Platelet-mediated stimulation of circulating monocytes.....	42
1.7 Original principal hypotheses.....	44
1.8 Aims of this study	44
Chapter 2	46
Materials and Methods.....	46
2.1 Recruitment.....	47
2.2 Clinical data collection and blood sampling	51
2.2.1.1 Post MI and healthy controls	51
2.2.1.2 Offspring of MI and controls.....	54
2.2.1.3 Details of family history of offspring groups	56
2.2.1.3.1 Parental history of premature MI and other atherosclerotic disease....	56
2.2.1.3.2 Grandparental history of MI and other atherosclerotic disease	56
2.3 isolation of blood cells and supernatant.....	58
2.3.2.1 AutoMACS vs. Dynabeads: results of comparison experiments	60
2.3.3.1 Selection of stimulus relevant to atherosclerosis	63
2.3.3.2 Platelet-mediated stimulation protocol using CRP-XL.....	64
2.3.4.1 Analysis of monocytes and monocyte-platelet aggregates by flowcytometry:	65
2.4 RNA extraction and microarray analysis.....	67
2.4.1.1 Preparation of stock for on-column DNA clean up (Qiagen Cat# 79254).....	70
2.5 Post hybridisation data analysis	78
2.5.2.1 Quantile normalisation of microarray data	80
2.5.2.2 Detection thresholds.....	81
2.5.2.3 Statistical correction for multiple testing.....	81
2.5.2.4 Graphical depiction of differential gene expression – volcano plots	82
2.5.2.5 Filtering of datasets to identify differentially expressed genes	83
2.6 Bioinformatic analysis of microarray data	83
2.7 Quantitative Reverse Transcriptase-PCR (RT-PCR) of differentially expressed genes.....	89
Chapters 3-9	93
Results	93
Overview of the results Chapters.....	94

Chapter 3: Results	96
Response of the monocyte transcriptome to a platelet mediated stimulation	96
3.1 Introduction	97
3.2 Differentially expressed genes: summary	99
3.3 Gene Ontology analysis of differentially expressed monocyte genes after CRP-XL stimulation.....	107
3.3.2.1 Network 1: Inflammatory Response, Cellular Movement, Cell-To-Cell Signaling and Interaction.....	111
3.3.2.2 Network 2: Cell-To-Cell Signaling and Interaction, Tissue Development, Cardiovascular System Development and Function	113
3.3.2.3 Network 3: Inflammatory Response, Gastrointestinal Disease, Hematological Disease.....	115
3.4 Candidate genes and pathways	118
3.4.1.1 Genes up-regulated after stimulation with platelets common to all groups	119
3.4.1.1.1 Oxidized LDL receptor 1 (OLR1, LOX1, CLEC8A); Chr 12p13.2-p12.3	119
3.4.1.1.3 Chemokines	123
Monocyte chemoattractant protein 1 (MCP1/CCL2); Chr 17q11.2-q12.....	123
Monocyte chemoattractant protein 3 (MCP3/CCL7); 17q11.2-q12	123
3.4.1.1.4 Interleukin 8 (IL8, CXCL8); Chr 4q13-q21.....	125
3.4.1.1.5 Secreted phosphoprotein 1 (SPP1, osteopontin); Chr 4q22.1.....	126
3.4.1.1.6 Oncostatin-M (OSM); Chr: 22q12	127
3.4.1.1.7 DNA damage inducible transcript 4 (DDIT4, REDD1); Chr 10pter-q26.12.....	128
3.4.1.2 Genes down regulated after stimulation with platelets common to all groups.....	129
3.4.1.2.1 Interleukin 15 (IL15); Chr 4q31	129
3.4.1.2.2 G-protein coupled bile acid receptor 1 (GPBAR1/TGR5); Chr2q35...	130
3.4.1.2.3 Thrombospondin receptor (CD36/GP4); Chr 7q11.2.....	131
3.4.1.2.4 CD33; Chr 19q13.3.....	132
3.4.1.2.5 Fractalkine receptor (CX3CR1); Chr3p21.3	133
3.4.1.2.6 Endothelial differentiation gene 2 (EDG2, LPAR1); Chr9q31.3	134
3.4.1.2.7 Apolipoprotein L 3 (APOL3); Chr22q13:1	135
3.4.1.2.8 Beta-2 adrenergic receptor (ADRB2); Chr5q31-q32	136
3.4.2.1 LXR/RXR Activation	137
3.4.2.2 TREM1 signalling	138
3.5 Discussion.....	138
Chapter 4: Results	143
Post MI vs. Controls – differences in monocyte gene expression at baseline and after platelet mediated stimulation.....	143
4.1 Introduction	144
4.2 Baseline gene expression: initial analysis.....	145
4.3 Baseline gene expression: Links with CAD.....	149
4.4 Baseline gene expression: Genes and Pathways.....	150
4.4.1.1 Inflammatory markers.....	150
4.4.1.1.1 Tumour necrosis factor (TNF/TNF α); Chr 6p21.3	150
4.4.1.1.2 Orosomucoid 1 (ORM1); Chr 9q34.1-34.3.....	152
4.4.1.1.3 Peptidoglycan recognition protein-1 (PGLYRP1); Chr19q13.2-q13.3	153
4.4.1.1.4 Testis derived transcript (TES); Chr7q31.2.....	154
4.4.2 Pathways	155
4.4.2.1 Wnt signalling pathway.....	155
4.4.2.1.1 CXXC5 (CF5/RINF); Chr 5q31.2.....	156
4.4.2.1.2 Olfactomedin 1 (OLFM1); Chr 9q34.3.....	157

4.4.2.1.3 Hypothetical roles of differentially expressed genes in Wnt signalling	158
4.5. Analysis of Differentially expressed monocytes genes after platelet mediated stimulation (CRP-XL).....	160
4.6 Gene expression in activated monocytes: Initial Analysis	160
4.7 Gene Expression in activated monocytes: Links with CAD	167
4.8 Gene Expression in activated monocytes: Genes and pathways.....	168
4.8.1.1 Regulators of coagulation (Figure 4.19).....	168
4.8.1.1.1 Tissue factor pathway inhibitor (TFPI); Chr 2q32.....	169
4.8.1.1.2 Thrombomodulin (THBD); Chr 20p11.2	171
4.8.1.1.3 Syndecan 2 (SDC2); Chr 8q22-q23	172
4.8.1.1.4 Protein C Receptor (PROCR/EPCR/CD201 antigen); Chr 20q11.2 ..	173
4.8.1.1.5 Cathepsin L (CTSL); Chr 9q21.33	174
4.8.1.1.6 Heparanase (HPSE); Chr 4q21.3	175
4.8.1.1.7 Legumain (LGMN1/PRSC1); Chr 14q32.1	176
4.8.1.1.8 Regulators of coagulation: summary	176
4.8.1.2 Cholesterol metabolism	178
4.8.1.2.1 Cytochrome P450; subfamily XXVIIA, polypeptide 1 (CYP27A1), Chr 2q33-qter.....	178
4.8.1.2.2 Acetyl-CoA acetyltransferase 2 (ACAT2); Chr 6q25.3	180
4.8.1.2.3 Nicotinic acid receptors	181
4.8.1.2.4 Leptin (LEP); Chr 7q31.3.....	182
4.8.1.3 Chemokines (Figure 4.34)	183
4.8.1.4 Enzymes	185
4.8.1.4.1 Arginase 1 (ARG1); Chr 6q23.....	185
4.8.1.4.2 5' nucleotidase (NT5E/CD73); Chr 6q14-q21.....	186
4.8.1.5 Transcription factors	187
4.8.1.5.1 Transcription Factor 4 (TCF4); Chr 18q21.1	188
4.8.1.5.2 (Sex determining region Y)-box 4 (SOX4); Chr 6p22.3.....	189
4.8.1.6 Other genes	190
4.8.1.6.1 DNAJ/HSP40 Homolog; subfamily B; member 1 (DNAJB1, HDJ1); Chr 19p13.2).....	190
4.8.1.6.2 CD86 (B7.2; LAB72); Chr 3q21	191
4.8.1.7 Genes with differential expression at baseline and after CRP-XL stimulation.....	192
4.8.1.7.1 Orosomucoid 1 (ORM1, alpha-1 acid glycoprotein); Chr9q34.1-34.3)	192
4.8.1.7.2 Peptidoglycan recognition protein-1 (PGLYRP1); 19q13.2-q13.3	193
4.8.2.1 Wnt signalling.....	194
4.8.2.1.1 Wingless-type MMTV integration site family, member 5A (Wnt5A); Chr 3p21-p14.....	194
4.8.2.1.2 Interactions of differentially expressed genes with beta catenin.....	195
4.9 Discussion.....	198
Chapter 5: results.....	203
Offspring of MI vs. Controls – differences in monocyte gene expression at baseline and after platelet mediated stimulation.....	203
5.1 Introduction	204
5.2 Baseline gene Expression: Initial analysis	204
5.3 Baseline Gene Expression: links with cad	208
5.4 Baseline GENE expression: Candidate genes and pathways	209
5.4.1.1 Acyloxyacyl hydrolase (AOAH); Chr 7p14-p12	209
5.4.1.2 Transcription factors.....	211
5.4.1.2.1 Early growth response protein 1 (EGR1); Chr 5q31.1	211

5.4.1.2.2 Aryl hydrocarbon receptor nuclear translocator (ARNT/HIF1 β); Chr 1q21.....	213
5.4.1.2.3 Finkel-Biskis-Jenkins murine osteosarcoma viral oncogene homolog B (FOSB); Chr 19q13.32.....	214
5.4.1.2.4 V-myc myelocytomatosis viral oncogene homolog (MYC/c-MYC); 8q24.21.....	215
5.4.1.2.5 Zinc finger protein 274 (ZNF274); Chr 19qter.....	216
5.4.1.2.6 Role of hypoxia in differential expression of transcription factors.....	217
5.4.1.3 Other genes.....	218
5.4.1.3.1 Cytochrome P450, family 27, subfamily A, polypeptide 1 (CYP27A1); Chr2q33-qter.....	218
5.4.1.3.2 Chemokine (C-C motif) ligand 3 (CCL3/macrophage inflammatory protein-1 α); Chr 17q11-q21.....	219
5.4.1.3.3 Actin, alpha 2, smooth muscle, aorta (ACTA2), Chr 10q23.3.....	222
5.4.2.1 VEGF signaling.....	223
5.5 Analysis of Differentially expressed monocytes genes after platelet mediated stimulation (CRP-XL).....	224
5.6 Differential Gene Expression in activated monocytes: Initial Analysis.....	224
5.7 Differential Gene Expression in activated monocytes: links with cad.....	229
5.8 Candidate genes and pathways.....	230
5.8.1.1 Heat shock proteins.....	230
5.8.1.1.1 Heat shock protein 90kDa alpha (cytosolic), class B member 1 (HSP90AB1/HSP90 β); Chr 6 p12.....	231
5.8.1.1.2 Stress induced phosphoprotein 1 (STIP1/P60/HOP/STI1); Chr 11q13.....	233
5.8.1.1.3 DnaJ (Hsp40) homolog, subfamily B, member 6 (DNAJB6; Ch4 7q36.3).....	235
5.8.1.1.4 FK506 binding protein 4 (FKBP4/FKBP52/PPIase/HSP56; Chr 12p13.33).....	236
5.8.1.1.5 DnaJ (Hsp40) homolog, subfamily A, member 4 (DNAJA4), Chr 15q25.1.....	237
5.8.1.1.6 Heat shock protein B1 (HSPB1, HSP27); Chr 7q11.23.....	238
5.8.1.2 Other candidate genes.....	240
5.8.1.2.1 Diacyl glycerol kinase delta (DGKD); Chr 2q37.1.....	240
5.8.1.2.2 Inhibitor of DNA binding 3 (ID3/HEIR-1); Chr 1p36.13-p36.12.....	241
5.8.1.2.3 Transporter 2, ATP-binding cassette, sub-family B (TAP2); Chr 6p21.3.....	242
5.8.1.2.4 Latexin (LXN), Chr 3q25.32.....	243
5.8.2.1 Nrf2 mediated oxidative stress response.....	245
5.8.2.2 Wnt/beta catenin signalling.....	246
5.9 Discussion.....	247
Chapter 6: Results.....	251
Genes shared between Post MI and Offspring of MI.....	251
6.1 Introduction.....	252
6.2 analysis of shared genes.....	255
6.2.1.1 FOSB (AP-1); Chr 19q13.32.....	258
6.2.1.2 EGR1; Chr 5q31.1.....	260
6.2.1.3 Immediate early response 2 (IER2);Chr 19p13.2.....	262
6.2.2 Lipid metabolism and transport.....	264
6.2.2.1 Cytochrome P450, family 27, subfamily A, polypeptide 1 (CYP27A1); Chr2q33-qter.....	264
6.2.2.2 Leptin (LEP); Chr 7q31.3.....	266
6.2.2.3 Acyl coenzyme A dehydrogenase family, member 10 (ACAD10); Chr 12q24.12.....	267

6.2.2.4 ARV1 homolog (ARV1); Chr 1q42.2	268
6.2.3 Chemokines	270
6.2.3.1 Chemokine (C-C motif) ligand 3-like 3 (CCL3L3); Chr 17q21.1	270
6.2.3.2 Chemokine (C-C ligand) 7 (CCL7/MCP3); Chr 17q11.2-q12.....	271
6.2.3.3 Chemokine binding protein 2 (CCBP2/D6/CCR9/CCR10); Chr 3p21.3	272
6.2.4 Heat shock proteins.....	273
6.2.4.1 DnaJ (Hsp40) homolog, subfamily B, member 1 (DNAJB1/HSP40); Chr 19p13.2.....	273
6.2.4.2 FK506 binding protein 4 (FKBP4/HSP56/PPlase); Chr 12p13.33	274
6.2.5 Cell senescence.....	275
6.2.5.1 B cell translocation gene 2 (BTG2; Chr 1q32).....	275
6.2.5.2 Huntington interacting protein 1 (HIP1); Chr 7q11.23	276
6.2.6 Response to hypoxia.....	277
6.2.6.1 Family with sequence similarity 13, member A (FAM13A1); Chr 4q22.1	277
6.2.7 Tumour suppressor	278
6.2.7.1 Latexin (LXN); Chr 3q25.32.....	278
6.2.8 Receptors and signaling	279
6.2.8.1 Killer cell immunoglobulin-like receptor, two domains, long cytoplasmic tail, 4 (KIR2DL4/G9P/CD158D); 19q13.4	279
6.2.8.2 Solute carrier family 5 (sodium/myo-inositol cotransporter), member 3 (SLC5A3/SMIT/SMIT2); Chr 21q22.12.....	280
6.2.9 Summary of shared trends in monocyte gene expression in high risk groups.....	281
6.3 validation of key microarray results by Q-PCR	283
6.4 Correlating genetic variants with monocyte gene expression	287
6.4.1.1 CARDIoGRAM Study	288
6.4.1.2 Selection of genes.....	289
6.4.1.3 Findings.....	291
6.4.1.3.1 Association with CAD:	291
6.4.1.3.2 Association with MI:.....	295
6.4.2.1 Background.....	298
6.4.2.2 Cardiogenics – a GWE/GWAS study of human monocytes.....	298
6.4.2.3 eQTLs in differentially expressed genes.....	299
6.5 Discussion.....	303
Chapter 7	307
Discussion	307
7.1 The challenge of CAD in the 21 st century	308
7.2 Rationale, design and outcomes of the study	309
7.2.1 Rationale for the use of transcriptome analysis	309
7.2.2 Design of the current study.....	310
7.2.2.1 Subject selection and definition of study groups	312
7.2.2.2 Sample processing.....	314
7.2.3 Study objectives	314
7.2.3.1 Transcriptome of resting and stimulated monocytes in overt atherosclerotic coronary artery disease (Post MI vs Controls).....	315
7.2.3.3 Shared genes – Post MI and Offspring of MI	318
7.2.3.4 Genetic variations associate with gene expression.....	318
7.2.3.5 The effect of collagen activated platelets on monocyte gene expression	319
7.4 Main conclusions.....	320
7.5 Limitations of the study.....	323
7.6 Future directions.....	327
CYP27A1 – a key regulator of cholesterol efflux.....	327

CCL3 – a biomarker for early stage atherosclerosis	329
PGLYRP1 and ORM1 – plasma biomarkers for genetic risk of CAD	330
7.7 Conclusion	331
References.....	333
Appendix.....	373
Optimisation of methods and protocols	373
Platelet-Mediated Stimulation experiment (CRP-XL)	374
Platelet Flow Cytometry	374
Fibrinogen binding and P-selectin expression	376
Whole blood MPA flow cytometric assay – Optilyse®C method	377
Whole blood Annexin binding assay (see Tube Plan below).....	378
R scripts for statistical analysis.....	379
# Analysis 1: PMIt4 vs CONt4	380
# Analysis 2: PMIt0 vs CONt0	381
# Analysis 3: PMIt4 vs PMIt0.....	382
# Analysis 4: CONt4 vs CONt0.....	383
# Analysis 1: CB vs CC	385
# Analysis 2: MB vs MC	386
# Analysis 3: MB vs CB #.....	387
# Analysis 4: MC vs CC #.....	388
Selection of a control gene	389

LIST OF TABLES AND FIGURES

Figure 1.1: Role of transcriptome analysis in CAD.....	29
Figure 1.2: The role of the monocyte in atherogenesis.	35
Figure 1.3: The role of the monocyte in atherosclerosis.	36
Figure 1.4: Platelet structure and function.	39
Figure 1.5: Mechanisms of Monocyte-Platelet interaction.....	41
Figure 2.1: Schematic diagram of study groups and experiments.....	50
Table 2.1: Demographic and biometric data for Post MI patients and healthy controls. ...	52
Table 2.2: Baseline blood tests for Post MI patients and healthy controls.....	52
Table 2.3: Pharmacotherapy in patients Post MI.	53
Table 2.4: Demographic and biometric data for Offspring of MI and healthy controls.	54
Table 2.5: Baseline blood tests for Offspring of MI and healthy controls.....	55
Figure 2.2: Relative efficacy of CRP-XL and CRP-18 (flowcytometry).	64
Table 2.6: Flowcytometry protocol for detection of monocyte platelet aggregates.	66
Figure 2.3: NanoDrop® method of RNA assessment.	71
Figure 2.4: Assessment of cross-lineage cell contamination.....	71
Figure 2.5: RNA integrity.	73
Figure 2.6: 18S PCR to assess contamination of RNA samples with genomic DNA.....	74
Figure 2.7: Design characteristics of the Sentrix BeadChip (modified from Illumina Gene Expression Datasheet).....	77
Figure 2.8: Scheme of analysis of microarray signal intensity data.	78
Table 2.7: Scheme for statistical analysis of gene expression profiles.....	80
Figure 2.9: Sample volcano plot of differential gene expression.	82
Figure 2.10: Interaction map (ChiLiBot) of candidate genes linked to term 'atherosclerosis'.	86
Table 2.8: List of TaqMan primers.....	91
Figure 3.1: Scheme of platelet-mediated stimulation for all study groups.	97
Figure 3.2: Flowcytometry of activated monocytes following platelet-mediated stimulation.	98
Figure 3.3: Heat map of microarray signal intensities.	99
Figure 3.4a: Sigmoid plots of signal intensity in resting and stimulated monocyte samples.	100
Figure 3.4b: Sigmoid plots of signal intensity in resting and stimulated monocyte samples.	101
Figure 3.5: Volcano plots of differential gene expression in monocytes after platelet-mediated stimulation in all study groups.	102
Figure 3.6: Venn diagram of up-regulated genes following platelet-mediated stimulation.	103
Figure 3.7: Venn diagram of down regulated genes following platelet-mediated stimulation.....	104
Table 3.1: Common differentially expressed genes following CRP-XL stimulation.....	106
Table 3.2: Up-regulated genes classified according to molecular function.....	107
Table 3.3: Up-regulated genes classified according to biological process.	108
Table 3.4: Up-regulated genes classified according to protein class.....	108
Table 3.5: Up-regulated genes classified according to pathway.	108
Table 3.6: Down regulated genes classified according to molecular function.....	109
Table 3.7: Down regulated genes classified according to biological process.	109
Table 3.8: Down regulated genes classified according to protein class.	109
Table 3.9: Down regulated genes classified according to pathway.	109
Table 3.12: Biological networks involving differentially expressed genes after CRP-XL.	110
Figure 3.8: Inflammatory Response, Cellular Movement, Cell-To-Cell Signalling and Interaction.	112

Figure 3.9: Cell-To-Cell Signalling and Interaction, Tissue Development, Cardiovascular System Development and Function.....	114
Figure 3.10: Inflammatory Response, Gastrointestinal Disease, Haematological Disease.....	116
Figure 3.11: Interaction map (ChiLiBot) of candidate gene linked to atherosclerosis	117
Figure 3.12: Interaction map (ChiLiBot) of candidate gene linked to oxidative stress.....	118
Figure 3.13: Microarray signal intensities of OLR1 in all four study groups.....	120
Figure 3.14: Microarray signal intensities of TGM2 in all four study groups.	122
Figure 3.15: Microarray signal intensities of CCL2 in all four study groups.....	124
Figure 3.16: Microarray signal intensities of CCL7 in all four study groups.....	124
Figure 3.17: Microarray signal intensities of IL8 in all four study groups.	125
Figure 3.18: Microarray signal intensities of SPP1 in all four study groups.....	126
Figure 3.19: Microarray signal intensities of OSM in all four study groups.....	127
Figure 3.20: Microarray signal intensities of DDIT4 in all four study groups.....	128
Figure 3.21: Microarray signal intensities of IL15 in all four study groups.....	129
Figure 3.22: Microarray signal intensities of GPBAR1 in all four study groups.....	130
Figure 3.23: Microarray signal intensities of CD36 in all four study groups.....	131
Figure 3.24: Microarray signal intensities of CD33 in all four study groups.....	132
Figure 3.25: Microarray signal intensities of CX3CR1 in all four study groups.....	133
Figure 3.26: Microarray signal intensities of EDG2 in all four study groups.....	134
Figure 3.27: Microarray signal intensities of APOL3 in all four study groups.....	135
Figure 3.28: Microarray signal intensities of ARDB2 in all four study groups.....	136
Figure 3.29: Summary of differentially expressed genes following CRP-XL.....	140
Figure 4.2: Sigmoid plots of fluorescent signal intensity in resting monocytes.....	145
Figure 4.3: Volcano plot of Post MI vs. controls at baseline.....	146
Figure 4.4: Gene transcript filtering strategy to identify differentially expressed genes. .	147
Table 4.1: Post MI vs. Controls – differentially expressed genes at baseline.....	148
Figure 4.5: Lists of interactions on PubMed for each candidate gene (ChiLiBot).	149
Figure 4.6: Microarray signal intensities of TNF in Post MI patients and controls.	151
Figure 4.7: Interaction of TNF with other candidate genes and search terms (ChiLiBot).	151
Figure 4.8: Microarray signal intensities of ORM1 in Post MI patients and controls.	152
Figure 4.9: Microarray signal intensities of PGLYRP1 in Post MI patients and controls.	153
Figure 4.10: Microarray signal intensities of TES in Post MI patients and controls.....	154
Figure 4.11: Microarray signal intensities of CXXC5 in Post MI patients and controls....	156
Figure 4.12: Microarray signal intensities of OLFM1 in Post MI patients and controls....	157
Figure 4.13: Differentially expressed genes with roles in Wnt signalling.	159
Figure 4.14: Scheme of analysis – Post MI vs. Controls after platelet mediated stimulation.	160
Figure 4.15: Sigmoid plots of fluorescent signal intensity in stimulated monocytes.....	161
Figure 4.16: Volcano plot of Post MI vs. controls after CRP-XL stimulation.....	161
Figure 4.17: Gene transcript filtering strategy to identify differentially expressed genes.	162
Table 4.2: Post MI vs. Controls – differentially expressed genes after platelet-mediated stimulation.....	166
Figure 4.18: Lists of interactions on PubMed for each candidate gene (ChiLiBot).	167
Figure 4.19: Lists of interactions on PubMed for regulators of coagulation (ChiLiBot). ..	168
Figure 4.20: Microarray signal intensities of TFPI in Post MI patients and controls.....	169
Figure 4.21: quantitative PCR of TFPI in Post MI patients and controls.....	170
Figure 4.22: Microarray signal intensities of THBD in Post MI patients and controls.....	171
Figure 4.23: Microarray signal intensities of SDC2 in Post MI patients and controls.	172
Figure 4.24: Microarray signal intensities of PROCR in Post MI patients and controls... ..	173
Figure 4.25: Microarray signal intensities of CTSL in Post MI patients and controls.	174
Figure 4.26: Microarray signal intensities of HPSE in Post MI patients and controls.....	175
Figure 4.27: Microarray signal intensities of LGMN in Post MI patients and controls.	176

Figure 4.28: Differential expression of regulators of coagulation and endothelial function.	177
Figure 4.29: Microarray signal intensities of CYP27A1 in Post MI patients and controls.	179
Figure 4.30: quantitative PCR of CYP27A1 in Post MI patients and controls.	179
Figure 4.31: Microarray signal intensities of ACAT2 in Post MI patients and controls.	180
Figure 4.32: Microarray signal intensities of GPR19A&B in Post MI patients and controls.	181
Figure 4.33: Microarray signal intensities of Leptin in Post MI patients and controls.	182
Figure 4.34: Microarray signal intensities of chemokines in Post MI patients and controls.	184
Figure 4.37: Microarray signal intensities of ARG1 in Post MI patients and controls.	185
Figure 4.36: Microarray signal intensities of NT5E in Post MI patients and controls.	186
Figure 4.37: Lists of interactions on PubMed for transcription factors (ChiLiBot).	187
Figure 4.38: Microarray signal intensities of TCF4 in Post MI patients and controls.	188
Figure 4.39: Microarray signal intensities of SOX4 in Post MI patients and controls.	189
Figure 4.40: Microarray signal intensities of DNAJB1 in Post MI patients and controls.	190
Figure 4.41: Microarray signal intensities of CD86 in Post MI patients and controls.	191
Figure 4.42: Microarray signal intensities of ORM1 in Post MI patients and controls.	192
Figure 4.43: Microarray signal intensities of PGLYRP1 in Post MI patients and controls.	193
Figure 4.44: Microarray signal intensities of Wnt5A in Post MI patients and controls.	195
Figure 4.45: Proposed roles of differentially expressed genes in Wnt signalling.	196
Figure 4.46: Microarray signal intensities of FOXO3A in Post MI patients and controls.	197
Figure 4.47: Microarray signal intensities of PPARG in Post MI patients and controls.	198
Figure 5.1: Scheme of analysis – Offspring of MI vs. Controls at baseline.	204
Figure 5.2: Sigmoid plots of fluorescent signal intensity in resting monocytes.	205
Figure 5.3: Volcano plot of Offspring of MI vs. controls at baseline.	205
Figure 5.4: Gene transcript filtering strategy to identify differentially expressed genes.	206
Table 5.1: Offspring of MI vs. Controls – differentially expressed genes at baseline.	207
Figure 5.5: Interaction map (ChiLiBot) of candidate gene linked to atherosclerosis.	208
Figure 5.6: Microarray signal intensities of AOA in Offspring of MI and controls.	210
Figure 5.7: Quantitative PCR of AOA in Offspring of MI and controls.	210
Figure 5.8: Microarray signal intensities of EGR1 in Offspring of MI and controls.	212
Figure 5.9: Quantitative PCR of EGR1 in Offspring of MI and controls.	212
Figure 5.10: Microarray signal intensities of ARNT in Offspring of MI and controls.	213
Figure 5.11: Microarray signal intensities of FOSB in Offspring of MI and controls.	214
Figure 5.12: Microarray signal intensities of MYC in Offspring of MI and controls.	215
Figure 5.13: Microarray signal intensities of ZNF274 in Offspring of MI and controls.	216
Figure 5.14: Monocyte mediated mechanisms of atherogenesis in Offspring of MI.	217
Figure 5.15: Microarray signal intensities of CYP27A1 in Offspring of MI and controls.	218
Figure 5.16: quantitative PCR of CYP27A1 in Offspring of MI and controls.	219
Figure 5.17: Microarray signal intensities of CCL3 in Offspring of MI and controls.	220
Figure 5.18: quantitative PCR of CCL3 in Offspring of MI and controls.	220
Figure 5.19: Signal intensities of CCL3L1 and CCL3L3 in Offspring of MI and controls.	221
Figure 5.20: Microarray signal intensities of MYC in Offspring of MI and controls.	222
Figure 5.21: Offspring of MI vs. Controls after platelet-mediated stimulation.	224
Figure 5.22: Sigmoid plots of fluorescent signal intensity in stimulated monocytes.	225
Figure 5.23: Volcano plot of Offspring of MI vs. controls after platelet-mediated stimulation.	225
Figure 5.24: Gene transcript filtering strategy to identify differentially expressed genes.	226
Table 5.2: Offspring of MI vs. Controls – differentially expressed genes in circulating monocytes after platelet-mediated stimulation.	228
Figure 5.25: Interaction map (ChiLiBot) of candidate gene linked to atherosclerosis.	229
Table 5.3: List of differentially expressed heat shock proteins.	230

Figure 5.26: Interaction map (ChiLiBot) of key words and genes linked to HSP90AB1. .	231
Figure 5.27: Microarray signal intensities of HSP90AB1 in Offspring of MI and controls.	232
Figure 5.28: quantitative PCR of HSP90AB1 in Offspring of MI and controls.....	233
Figure 5.29: Microarray signal intensities of STIP1 in Offspring of MI and controls.....	234
Figure 5.30: quantitative PCR of STIP1 in Offspring of MI and controls.....	234
Figure 5.31: Microarray signal intensities of DNAJB6 in Offspring of MI and controls. ...	235
Figure 5.32: Microarray signal intensities of FKBP4 in Offspring of MI and controls.	236
Figure 5.33: Microarray signal intensities of DNAJA4 in Offspring of MI and controls. ...	237
Figure 5.34: HSPB1 in the atherosclerotic plaque.	239
Figure 5.35: Microarray signal intensities of HSPB1 in Offspring of MI and controls.	239
Figure 5.36: Microarray signal intensities of DGKD in Offspring of MI and controls.	240
Figure 5.37: quantitative PCR of DGKD in Offspring of MI and controls.	241
5.38: Microarray signal intensities of ID3 in Offspring of MI and controls.	242
Figure 5.39: Microarray signal intensities of TAP2 in Offspring of MI and controls.....	243
Figure 5.40: Microarray signal intensities of LXN in Offspring of MI and controls.....	244
Figure 5.41: Heat shock proteins and their interactions.	247
Figure 6.1: Trends in differential gene expression across experiments.....	252
Table 6.1: Genes with shared trends in unstimulated monocytes (baseline).....	253
Table 6.2: Genes with shared trends after platelet-mediated monocyte stimulation (CRP-XL).	254
Figure 6.2: Classification of shared genes according to biological function.....	255
Figure 6.3: Interaction map (ChiLiBot) of shared candidate gene to predefined search terms.....	256
Table 6.3: Genes shared by Post MI and Offspring of MI groups linked to CAD.	257
Figure 6.4: Differential expression of FOSB in Offspring of MI and patients Post MI.....	259
Figure 6.5: Differential expression of EGR1 in Offspring of MI and patients Post MI.....	261
Figure 6.6: Differential expression of IER2 in patients Post MI and Offspring of MI.	263
Figure 6.7: Differential expression of CYP27A1 in Offspring of MI and Post MI.	265
Figure 6.8: Differential expression of LEP in patients Post MI and Offspring of MI.....	266
Figure 6.9: Differential expression of ACAD10 in Offspring of MI and Post MI.....	267
Figure 6.10: Differential expression of ARV1 in Offspring of MI and Post MI.	269
Figure 6.11: Differential expression of CCL3L3 in Offspring of MI and Post MI.....	270
Figure 6.12: Differential expression of CCL7 in Post MI and Offspring of MI.....	271
Figure 6.13: Differential expression of CCBP2 in Offspring of MI and Post MI.....	272
Figure 6.14: Differential expression of DNAJB1 in Post MI and Offspring of MI.	273
Figure 6.15: Differential expression of FKBP4 in Offspring of MI and Post MI.	274
Figure 6.16: Differential expression of BTG2 in Offspring of MI and Post MI.	275
Figure 6.17: Differential expression of HIP1 in Post MI and Offspring of MI.....	276
Figure 6.18: Differential expression of FAM13A1 in Post MI and Offspring of MI.	277
Figure 6.19: Differential expression of LXN in Post MI and Offspring of MI.....	278
Figure 6.20: Differential expression of KIR2DL4 in Offspring of MI and Post MI.	279
Figure 6.21: Differential expression of SLC5A3 in Offspring of MI and Post MI.	280
Figure 6.22: Summary of shared genes in Post MI and Offspring of MI.	282
Figure 6.23: Perturbations in sterol metabolism in Post MI and Offspring of MI.	282
Figure 6.24: Microarray and Q-PCR results of EGR1 in Offspring of MI and controls. ...	283
Figure 6.25: Microarray and Q-PCR results of EGR1 in patients Post MI and controls. .	284
Figure 6.26: Microarray and Q-PCR for CYP271 in Offspring of MI and controls.....	285
Figure 6.27: Microarray and Q-PCR for CYP27A1 in Offspring of MI and controls.....	285
Figure 6.28: Microarray and Q-PCR results of CYP27A1 in Post MI and controls.	286
Figure 6.29: Correlating GWE with GWAS - scheme of analysis	287
Table 6.4: List of shared genes selected for CARDIoGRAM analysis	289
Table 6.5: List of genes in Post MI vs. Controls selected for CARDIoGRAM analysis ...	290

Table 6.6: List of genes in Offspring of MI vs. Controls selected for CARDIoGRAM analysis.....	290
Table 6.7: SNPs in differentially expressed genes with significant association with CAD	291
Figure 6.30: Genetic variant in ACAD10 (rs2238151) associated with CAD and MI.....	292
Figure 6.31: Genetic variant in DRD3 (rs7649438) associated with CAD.	293
Figure 6.32: Genetic variant in PGLYRP1 (rs11672503) associated with CAD.....	294
Figure 6.33: Differential expression of DRD3 and PGLYRP1 in Post MI.....	294
Table 6.8: SNPs in differentially expressed genes with significant association with MI ..	295
Figure 6.34: Genetic variant in ARV1 (rs4506448) associated with CAD.	296
Figure 6.34: Genetic variant in CCL3L3 (rs991479) associated with CAD.	297
Figure 6.35: Candidate genes with eQTLs in Cardiogenics	299
Table 6.9: Candidate genes with eQTLs in Cardiogenics	300
Figure 6.36: eQTL in gene CYP27A1	301
Figure 6.37: CYP27A1 gene expression according to genotype.....	302
Figure 7.1: Role of monocyte transcriptome analysis in CAD	322

ABBREVIATIONS

ACAD10	Acyl Coenzyme A Dehydrogenase Family, Member 10
ACAT2	Acetyl-Coa Acetyltransferase 2
ACTA2	Actin, Alpha 2, Smooth Muscle, Aorta
ADRB2	Adrenergic, Beta-2-, Receptor
AMI	Acute Myocardial Infarction
APOL3	Apolipoprotein L, 3
ARG1	Arginase 1
ARNT	Aryl Hydrocarbon Receptor Nuclear Translocator
ARV1	Arv1 Homolog
BTG2	B Cell Translocation Gene 2
CAD	Coronary Artery Disease
CCBP2	Chemokine Binding Protein 2
CCL2	Chemokine (C-C Motif) Ligand 2 (Mcp1)
CCL3	Chemokine (C-C Motif) Ligand 3
CCL7	Chemokine (C-C Motif) Ligand 7 (Mcp3)
CD36	Cd86 Molecule (Thrombospondin Receptor)
CD86	Cd86 Molecule (B-Lymphocyte Activation Antigen B7-2)
CRP-XL	Cross Linked Collagen Related Peptide
CSV	Comma Separated Value
CTSL	Cathepsin L
CXCR1	Fractalkine Receptor
CXXC5	Cxxc Finger Protein 5
CYP27A1	Cytochrome P 27 A1
DDIT4	Dna-Damage-Inducible Transcript 4
DNA	Deoxy-Ribo Nucleic Acid
DNAJA4	Dnaj (Hsp40) Homolog, Subfamily A, Member 4
DNAJB1	Dnaj/Hsp40 Homolog; Subfamily B; Member 1
DNAJB6	Dnaj (Hsp40) Homolog, Subfamily B, Member 6
ECG	Electrocardiogram
EDTA	Ethylene Diamine Tetra Acetic Acid
EGR1	Early Growth Response 1
EIF3S5	Eukaryotic Translation Initiation Factor 3 Subunit 5
EQTL	Expression Quantitative Trait Locus
FAM	6-Carboxy Fluorescein
FAM13A1	Family With Sequence Similarity 13, Member A
FC	Flowcytometry
FITC	Fluorescein Isothiocyanate
FKBP4	Fk506 Binding Protein 4
FOSB	Finkel-Biskis-Jenkins Murine Osteosarcoma Viral Oncogene Homolog B
GAPDH	Glyceraldehyde-3-Phosphate Dehydrogenase
GPBAR1	G Protein Coupled Bile Acid Receptor 1
GPIB-V-IX	Glycoprotein Ib-V-Ix
GPVI	Glycoprotein Vi
GWAS	Genome Wide Association Study
GWE	Genome Wide Expression
HDL	High Density Lipoprotein
HIP1	Huntington Interacting Protein 1
HMBS	Hydroxymethylbilane Synthase
HMGCOA	3-Hydroxy 3-Methylglutaryl Coenzyme A
HPRT1	Hypoxanthine Phosphoribosyltransferase 1
HPSE	Heparanase

HSP90AB1	Heat Shock Protein 90kda Alpha (Cytosolic), Class B Member 1
HSPB1	Heat Shock Protein B1
ICAM1	Intercellular Adhesion Molecule-1
ID3	Inhibitor Of Dna Binding 3
IFN	Interferon
IHOP	Information Hyperlinked Over Proteins
IL15	Interleukin 15
IL8	Interleukin 8
IPA	Ingenuity Pathway Analysis
IVT	In Vitro Transcription
JAM	Junctional Adhesion Molecule
KIR2DL4	Killer Cell Immunoglobulin-Like Receptor, Two Domains, Long Cytoplasmic Tail, 4
LDL	Low Density Lipoprotein
LEP	Leptin
LGMN	Legumain
LP(A)	Lipoprotein A
LPS	Lipopolysaccharide
LXN	Latexin
MACS	Magnet Assisted Cell Sorting
MCP1	Monocyte Chemoattractant Protein 1
MCP1	Monocyte Chemoattractant Protein-1 (Ccl2)
MCP3	Monocyte Chemoattractant Protein-3 (Ccl7)
MCSF	Monocyte Colony Stimulating Factor
MINAP	Myocardial Infarction National Audit Project
MINAP	Myocardial Infarction National Audit Project
MIP1 α	Macrophage Inflammatory Protein-1 α
MPA	Monocyte Platelet Aggregates
NCBI	National Centre For Biotechnology Information
NSF	National Service Framework
NSTEMI	Non St Segment Elevation Myocardial Infarction
NT5E	5' Nucleotidase
OLFM1	Olfactomedin1
OLR1	Oxidised Ldl Receptor 1 (Lox1)
ORM1	Orosomuroid 1
OSM	Oncostatin M
PBS	Phosphate Buffered Saline
PCR	Polymerase Chain Reaction
PECAM1	Platelet Endothelial Cell Adhesion Molecule-1
PGLYRP1	Peptidoglycan Recognition Protein 1
PLA2G4B	Phospholipase A2, Group Ivb
PPARG	Peroxisome Proliferator-Activated Receptor Gamma
PPIA	Peptidylprolyl Isomerase A (Cyclophilina)
PROCR	Protein C Receptor
PSGL-1	P Selectin Glycoprotein Ligand-1
PYGB	Phosphorylase, Glycogen; Brain
Q-PCR	Quantitative Polymerase Chain Reaction
RANTES	Regulated On Activation Normal T-Cell Expressed And Secreted
RNA	Ribonucleic Acid
RPE-CY5	R-Phycoerythrin-Cyanine 5
RPL13A	Ribosomal Protein L13a
RPLP	60s Acidic Ribosomal Protein P0
RTPCR	Reverse Transcriptase Polymerase Chain Reaction
SDC2	Syndecan 2

SDHA	Succinate Dehydrogenase A
SDHB	Succinate Dehydrogenase B
SLC5A3	Solute Carrier Family 5 (Sodium/Myo-Inositol Cotransporter), Member 3
SNP	Single Nucleotide Polymorphism
SOX4	Sex Determining Region Y Box 4
SPP1	Secreted Phosphoprotein 1 (Osteopontin 1)
SSA	Site Specific Assessment
STEMI	St Segment Elevation Myocardial Infarction
STIP1	Stress Induced Phosphoprotein 1
TAP2	Transporter 2, Atp-Binding Cassette, Sub-Family B
TBP	Tata Box Protein
TCF4	Transcription Factor 4
TF	Tissue Factor
TFPI	Tissue Factor Pathway Inhibitor
TGF β	Transforming Growth Factor β
TGM2	Transglutaminase 2
THBD	Thrombomodulin
TLR	Toll-Like Receptor
TLR4	Toll Like Receptor 4
TNF	Tumour Necrosis Factor (Alpha)
UA	Unstable Angina
VCAM1	Vascular Cell Adhesion Molecule-1
LDL	Very Low Density Lipoprotein
Wnt5A	Wingless-Type Mmtv Integration Site Family, Member 5a
ZNF274	Zinc Finger Protein 274

CHAPTER 1

Introduction

1.1 CORONARY ARTERY DISEASE (CAD) - THE PROBLEM

Atherosclerotic coronary artery disease is one of the leading causes of mortality worldwide. The World Health Organisation (WHO) describes it as a true pandemic with 'no geographic, gender or socio-economic boundaries'. By the year 2030, CAD is likely to cause over 8 million deaths per year and remain the leading cause of global mortality accounting for 1 in 6 deaths worldwide (Mathers and Loncar, 2006). In the UK approximately one in five men and one in six women die from CAD (Allender, 2007). The long term morbidity and socio-economic burden of CAD is considerable. CAD cost the health care system in the UK around £3.2 billion annually according to the latest estimates in 2006 (Allender et al., 2008). This represents a cost per capita of over £50. In addition, production losses due to mortality and morbidity associated with CAD cost the UK over £3.9 billion, with around 55% of this cost due to death and 45% due to illness in those of working age. Awareness of such economic impacts of CAD led to the formulation of the National Service Framework (NSF) for Coronary Heart Disease in 2000 to set national standards for the prevention, diagnosis and treatment of CAD in England.

1.2 ATHEROSCLEROSIS - A COMPLEX PHENOTYPE

The challenge of coronary atherosclerosis lies in the insidious progression of atheromatous plaques over many years which then undergo acute and often unpredictable deterioration due to plaque rupture or erosion resulting in intraluminal atherothrombosis. The anatomical organisation of coronary circulation and the spatial localisation of plaque rupture accounts for the often fatal clinical presentation of acute myocardial infarction (AMI). The last 40 years has seen a

significant paradigm shift in the clinician's approach to AMI, from management of complications to early intervention at presentation and prevention of CAD progression by timely modification of risk factors. Observational studies demonstrate encouraging declines in death rates due to AMI over time from the impact of primary and secondary prevention strategies (Ford et al., 2007, Bata et al., 2006, Goldberg et al., 2006). However as patients have diverse baseline risks for AMI, the very sick patients of high risk may become the major determinants of outcome in clinical trials, thereby diluting the effects of therapeutic strategies when applied to routine clinical practice (Ioannidis and Lau, 1997, Kent et al., 2008). This highlights the importance of defining person specific risk profiles through a better molecular level characterisation of coronary atherosclerosis.

Atherosclerosis is now recognized as a complex inflammatory disease affecting the arterial circulation (Ross, 1999). Genetic (Lloyd-Jones et al., 2004) and environmental (Yusuf et al., 2004) influences modulate interactions between the vascular endothelium and circulating cells at the molecular level. The initiation of atherosclerotic lesion formation starts as early as the prenatal period as shown by histological studies on foetal aortas (Napoli et al., 1997). The cumulative effects of risk factors modify the qualitative and quantitative progression of these initial 'fatty streaks'.

1.3 RISK FACTORS FOR CAD

As early as the middle of the 20th century various epidemiological studies were in progress which identified the role of common risk factors in coronary disease (Kannel et al., 1961, Chapman and Massey, 1964, Kannel et al., 1965, Gordon and Kannel, 1971), including hypercholesterolaemia (Kannel et al., 1971, Sharrett

et al., 2001), hypertension (Kannel et al., 1980, Kannel, 2000), diabetes mellitus (Kannel and McGee, 1979), cigarette smoking (Kannel et al., 1968) and obesity (Gordon and Kannel, 1976).

These 'traditional' risk factors are prevalent alone or in combination in up to 90% of the patients with clinically evident CAD (Khot et al., 2003). In addition, these and other environmental risk factors including dietary habits, physical activity and psychological well being have been shown to influence the risk of MI in large scale studies (Yusuf et al., 2004) and account for over 90% of the population attributable risk for MI.

A family history of CAD has been identified as an independent risk factor in population based studies (Hopkins et al., 1988, Schildkraut et al., 1989). Such genetic predisposition applies not only to CAD but also the risk factors for CAD such as hypertension (Williams et al., 1988), hyperlipidaemia (Breslow, 2000) and diabetes mellitus (Harvald, 1967).

There is evidence that first degree relatives with established CAD share morphological features such as location of atherosclerotic lesion in the coronary circulation (Fischer et al., 2005). A study in asymptomatic young adults with a family history of MI has shown a significant correlation between structural changes in the coronary circulation and a positive family history of premature CAD (Philips et al., 2007). In addition, the traditionally recognised risk factors for CAD such as hypertension, dyslipidaemia and dysglycaemia are more prevalent in offspring of parents with premature CAD (Bao et al., 1995).

1.4 HERITABILITY OF CAD

A large scale screening of more than 130,000 families across three states in the USA found that a family history of premature CAD (<55years for men and <65 years for women) was seen in only 14% of the general population compared to 48% of patients with CAD and 72% of those with premature CAD (Williams et al., 2001). The relative risk attributable to a family history of premature MI ranges from 1.5 for affected parent to 8.0 for affected monozygotic twin (Mayer et al., 2007). In the Swedish Twin Registry, a definite trend emerged in the magnitude of the relative hazard of death from CAD which underpins the complex genetic-environmental interactions in coronary atherosclerosis. Among both the men and the women, whether monozygotic or dizygotic twins, the influence of sibling (twin) CAD decreased as the age at which one's twin died of coronary heart disease increased (Marenberg et al., 1994). In the Framingham Study, a family history of CAD in parents was noted to be a stronger contributing factor to premature CAD (<60 years) compared to late onset CAD (>60 years) (Schildkraut et al., 1989). In the North Karelia study, the risk of sibling CAD decreased from >10 fold to <2 fold with an increase in the age of incidence of CAD in the proband from <46 years to >55 years (Rissanen, 1979b). The same authors also reported that the relative risk for CAD was more in male siblings (70%) than for male parents (30%). In addition, the risk was greater in male siblings or parents compared to female first degree relatives (Rissanen, 1979a). This risk may be attributable to a similar familial risk of hypertension and hyperlipidaemia which were more frequent (2-3 fold) in families of men with premature myocardial infarction (Rissanen and Nikkila, 1979). This highlights the importance of selecting patients with premature CAD to study heritable trends in CAD. It also suggests that the mechanisms by which the

increased genetic risk of CAD is transmitted include abnormalities of lipid metabolism and vascular function. Therefore studying apparently healthy offspring of patients with premature CAD is important to understand the genetic signatures that underlie CAD. By selecting healthy young subjects without established CAD or known risk factors, segregated according to a family history of CAD, the primary genetic factors which determine risk of disease are more likely to be identified. Considering that these subjects are not on pharmacotherapy and do not have cardiovascular comorbidities (which may potentially affect measurement of the phenotype of interest and possibly gene expression), the overall association between gene and phenotype is purer and more immune to confounding.

1.5 ELUCIDATION OF GENETIC CONTRIBUTIONS TO CAD

Various approaches including hypothesis driven candidate gene analyses, linkage studies in families and genome-wide association studies have been used to identify the genetic determinants of CAD. Studies have focused on direct phenotypes (myocardial infarction, death from CAD etc) as well as intermediate phenotypes such as traditional risk factors (hypertension, dyslipidaemia), haemostatic abnormalities (prothrombotic tendencies) and the genetic determinants of response to therapy in CAD.

Candidate gene studies assess the frequency of finite numbers of gene variants in CAD which require prior knowledge of the role of these genes (Wang et al., 2010a, Berg, 1990). Although the number of subjects required in such analyses is relatively small, in most instances such studies tend to refute (Schelleman et al., 2007) rather than confirm previously noted associations, arising mainly from false

positive conclusions (Lluis-Ganella et al., 2009, Sagoo et al., 2008, Wang et al., 2011c).

Linkage analyses are performed in families to identify 'quantitative trait loci – QTL' - regions of interest in chromosomes which are shared by family members with phenotypic evidence of disease (Chiodini and Lewis, 2003, Klos et al., 2001). There are two main forms of linkage analysis: first, classical segregation analysis in large pedigrees where the disease is suspected to be due to a Mendelian gene mutation. This does not apply to most families with CAD although a few instances of Mendelian forms of MI have been described (Wang et al., 2003). The second approach is to analyse large number of affected sibling pairs (ASP) to search for areas of the genome that are inherited more frequently by the affected siblings than would be expected by chance (Hauser et al., 2004). This approach was applied in the British Heart Foundation Family Heart Study (BHF-FHS) which assembled over 2000 families (Samani et al., 2005) and in the PROCARDIS Study (Farrall et al., 2006). Although both studies found some loci showing excess sharing none of these exceeded the genome-wide significance threshold LOD score of 3.0. Although unbiased, in retrospect, on the basis of findings emerging from genome-wide association studies it would appear that such linkage analyses were probably underpowered.

Genome wide association studies (GWAS) use an unbiased approach to the identification of genetic risk factors. Typically, large case-control studies of unrelated individuals are undertaken where the entire genome is analysed for variations in frequency of single nucleotide polymorphisms (SNPs) which associate with the disease. The results then need to be validated in a 'replication

set' of subjects to confirm the association. However, the challenge in SNP based analyses lies in identifying a functional role for the observed associations as noted in an expert commentary at the turn of the 21st century (Winkelmann and Hager, 2000).

GWAS have identified areas of the genome with significant associations with CAD. The 9p21.3 chromosome locus has shown the most consistent, replicable and highly significant association with CAD (McPherson et al., 2007, Helgadottir et al., 2007, Samani et al., 2007, Johansen et al., 2010). The rs1333049 SNP has emerged in meta-analysis to confer a 29% increased risk of MI (Preuss et al., 2010). However, the 9p21 locus is a gene desert and functional significance of this locus is yet to be elucidated (Harismendy et al., 2011). The locus is devoid of protein coding genes, but overlaps with the cyclin dependent kinase inhibitors 2A and 2B (CDKN 2A/2B) and the antisense non coding RNA in the INK4 locus (ANRIL) (Holdt and Teupser, 2012). These genes have been shown to be expressed in the atherosclerotic plaque (Holdt et al., 2011) and implicated in modulation of vascular smooth muscle cell growth (Congrains et al., 2012b) and tissue remodelling (Congrains et al., 2012a). Other studies also link the 9p21 locus to inflammatory phenotypes (Harismendy et al., 2011) or even platelet responses (Musunuru et al., 2010).

Other loci have been reported in a series of studies over the past 4-5 years. Recently CARDIoGRAM, a meta-analysis of 14 GWAS of CAD with more than 22,000 cases and 64,000 controls and validated in an additional 60,000 individuals, has identified an additional 13 novel loci in addition to the 20 or more previously known SNPs with a significant association with CAD (Schunkert et al.,

2011). The study unifies samples from the Atherosclerotic Disease Vascular function and genetic Epidemiology study, CADomics, Cohorts for Heart and Aging Research in Genomic Epidemiology, deCODE, the German Myocardial Infarction Family Studies I, II, and III, Ludwigshafen Risk and Cardiovascular Health Study/AtheroRemo, MedStar, Myocardial Infarction Genetics Consortium, Ottawa Heart Genomics Study, PennCath, and the Wellcome Trust Case Control Consortium (Preuss et al., 2010). This study also confirmed the association of 10 previously published genetic variants with CAD. However, of the 23 gene variants analysed in this study, only 4 had previously known mechanistic roles contributing to CAD. This suggests that the molecular mechanisms of candidate genetic markers identified by GWAS remain largely unknown.

1.5.1 Gene expression analysis and genetic risk of CAD

Genome wide expression (GWE) profiling (transcriptomics) is a systematic analysis of the transcriptome, i.e., the entire RNA content in a cell or tissue. The central paradigm surrounding the transcriptome is that it acts as a 'messenger' within the cell, conveying the information contained within the genetic sequence in the nucleus (the genotype) to other cellular organelles which determine normal and abnormal cell behaviour (the phenotype) through protein synthesis. Some of these proteins in turn have regulatory roles on the genome itself in negative or positive feedback loops.

However unlike the genome, the transcriptome is responsive to both genetic and environmental influences (Figure 1.1). Changes in physiology such as ageing (de Magalhaes et al., 2009) and exercise (Buttner et al., 2007b), pathological changes such as oxidative stress (Crujeiras et al., 2008) and external factors such as cigarette smoke (Buttner et al., 2007a) have been shown to modulate gene expression in animal and human cells including circulating mononuclear leukocytes.

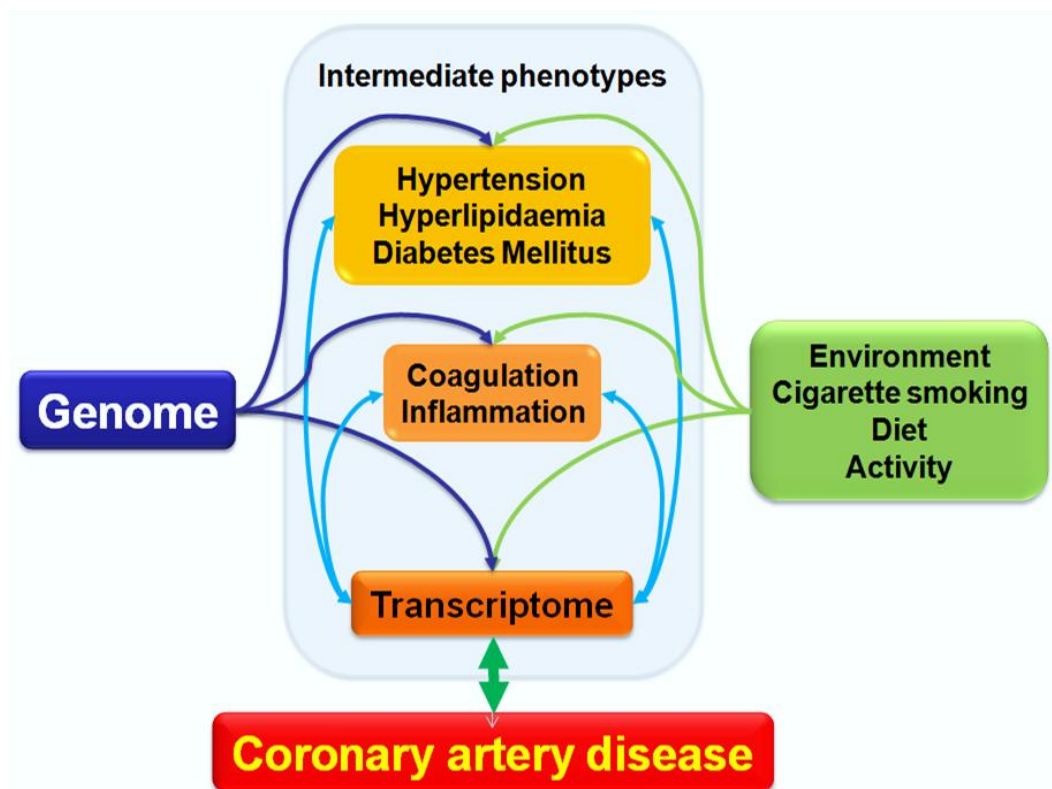


Figure 1.1: Role of transcriptome analysis in CAD

The transcriptome can be considered an intermediate phenotype at a molecular level under the influence of genetic variations. In addition, it is also responsive to the environment as well as other clinical intermediate phenotypes leading to CAD.

In the context of CAD, the transcriptome is influenced by well known clinical intermediate phenotypes such as hypertension, hypercholesterolaemia, vascular inflammation and diabetes (Figure 1.1). Interactions between these risk factors and other environmental factors such as smoking and diet, which influence the progression of CAD, are mediated through the transcriptome. Therefore the

transcriptome can be seen as a useful 'intermediate' phenotype which documents the genetic and environmental perturbations which would complement GWAS analysis in understanding mechanisms of complex diseases (Nica and Dermitzakis, 2008).

Another approach is to combine GWAS and GWE analysis to understand their interaction in a disease process (Gilad et al., 2008). GWE data is considered as a quantitative trait in such analysis and attempts are made to identify variations in the genome which determine variations in gene expression. The genetic loci of such genomic variations which result in differential gene expression are termed expression Quantitative Trait Loci or eQTLs. Such eQTLs may be adjacent in position to the genes they influence (*cis* eQTL) or distant in position, in some instances even on different chromosomes (*trans* eQTL).

The development of microarray technology (Schena et al., 1995) has been a major advance in providing such genome and transcriptome -wide overviews into complex phenotypes such as CAD. This platform uses cDNA 'probe sets' on the arrays which are reverse transcribed unique strands of complimentary DNA (oligonucleotides, usually 25-100 nucleotides long) to all known genes in the human genome. This provides a highly specific binding of RNA in the sample to the cDNA probes thereby separating expressed genes from others, which helps to identify those genes which are relevant to the phenotype under investigation. Advances in microarray chip design allow the hybridization of multiple samples to the same chip, thereby reducing technical variability of such high throughput analysis.

A case-control study design using microarrays can be used in GWE analysis to identify genetic risk factors underlying polygenic diseases such as CAD (Taurino et al., 2010) for the following reasons:

1. The approach does not make prior assumptions regarding candidate genes. This is especially of relevance in the era of systems biology which attempts to delineate the complexity of biological networks at a sub cellular scale.
2. GWE analysis offers an opportunity to study the effect of environmental stimuli on gene expression. This helps to identify candidate genes which differ in expression profiles only in the presence of appropriate environmental stimuli.
3. GWE analysis provides unbiased mechanistic insights into the disease process including aetiology, progression (Van Assche et al., 2011), clinical subtypes and response to external agents such as pharmacotherapy (Sivapalaratnam et al., 2011a).
4. Obtaining cell specific transcriptome 'signatures' (Burton et al., 2009) mapping the perturbations in intracellular organelles and function help to unravel complex phenotypes such as CAD which involves multiple cell types (Patino et al., 2005).
5. Genes which are differentially expressed can be studied further in either direction, i.e., upstream to identify genetic variations that associate with the differential expression (Smith et al., 2006) and downstream to analyse the effect of differential expression at protein/organelle/cellular levels or using a systems biology approach (Nookaew et al., 2010).

Although significant progress has been made in the various steps in transcriptome analyses including a shift of focus from tissue to cell specific profiling, distortion free amplification of RNA samples (McClain et al., 2005) and standardisation of

post array analyses - both statistical (Qin and Kerr, 2004, Kooperberg et al., 2002) and bioinformatic (Sadlier et al., 2005), the challenge lies in translating the results of such studies into biologically meaningful information with potential clinical applications. Subsequent analysis of candidate genes require the ability to make intelligent choices in 'filtering' data, in looking at magnitude (fold change) and strength (statistical significance) of differential expression, in identifying the biological role of candidate genes which pass the filtering steps by the creation of molecular networks and functional maps (Chen and Sharp, 2004) and importantly, validating the observed differences by specific assays such as PCR.

GWE therefore is not a standalone tool in understanding the genetic basis of CAD. Used in a complementary manner to GWAS and importantly, as an informed starting point for further functional studies to understand the biological roles of the differentially expressed genes which associate with CAD, it provides a useful overview of alterations at a molecular level which underpin this complex disease.

1.6 CELLULAR AND MOLECULAR PATHWAYS IN CAD

1.6.1 Atherogenesis and atherothrombosis at the molecular level

The initiation and progression of atherosclerosis is driven by the complex interactions between the vascular (arterial) endothelium, smooth muscle cells, circulating blood cells (platelets, monocytes and T lymphocytes) and blood flow characteristics (alterations in laminar flow and shear stress) in the presence of 'atherogenic' lipoproteins: oxidised LDL, beta-VLDL and Lp(a), which are formed as a result of an aggravated vascular inflammatory state. Various inflammatory mediators including adhesion molecules and cytokines released from vascular endothelium as well as interferons, interleukins (1,12,18) and tumour necrosis

factor from T lymphocytes (Jawien, 2008) promote the progression of coronary atherosclerosis, which is now recognised as a systemic inflammatory disease affecting the large and medium sized elastic and muscular arteries (Ross, 1999). It is an excessively protective fibroproliferative response to vascular stress and injury resulting from exposure to environmental and genetic risk factors (Ross, 1995).

1.6.2 The role of oxidative stress in atherosclerosis

Cellular oxidative stress is an early event in atherogenesis (Bonomini et al., 2008) and continues to play a role in lesion progression and plaque rupture. Oxidative stress results in endothelial dysfunction and increases platelet aggregation, monocyte adhesion and vascular inflammation (Taddei et al., 2000). Oxidative stress mediated by reactive oxygen species has also been shown to activate platelets (Ovechkin et al., 2007) and monocytes (Sanguigni et al., 2005). 3-hydroxy 3-methylglutaryl coenzyme A inhibitors (HMG CoA inhibitors/ 'statins') have been shown to attenuate oxidative stress (Rosenson, 2001).

1.6.3 Circulating monocytes and platelets in atherosclerosis

1.6.3.1 Monocytes

Monocytes are relatively undifferentiated blood cells in circulation capable of maturation along functionally and morphologically diverse pathways into a range of cell types depending on the local environment and interactions with other cells and humoral mediators. They are precursors to inflammatory and phagocytic macrophages and dendritic cells with an important role in immunity, response to infection and inflammation (Tacke and Randolph, 2006). The role of the monocyte in atherogenesis and plaque progression has gained prominence with the recognition of atherosclerosis as an active systemic inflammatory disease rather

than an anomaly of lipid storage. The earliest identifiable lesion in atherosclerosis, the fatty streak is a purely inflammatory lesion consisting of monocyte derived macrophages and T lymphocytes suggesting the central role of the monocyte in the initiation and progression of atherosclerotic plaque (Napoli et al., 1997). Animal studies have confirmed that monocyte accumulation in atheroma correlate directly with disease severity (Swirski et al., 2006) and that these develop into lipid laden foam cells. Circulating monocytes marginate and adhere to endothelial cells secondary to the derangement in structural and functional integrity of the endothelium, although monocytes can also induce the surface expression of selectins and other adhesion molecules on intact endothelium (Tsouknos et al., 2003). In addition the vascular endothelium responds to shear stress; alteration of blood flow from laminar to turbulent causes a change in endothelial expression of adhesion molecules and triggers the synthesis of chemokines thereby promoting leukocyte recruitment (Figure 1.2).

Vascular cell adhesion molecule-1 (VCAM-1, CD102) is one of the earliest inducible endothelium derived adhesion molecules that mediates monocyte recruitment and a marker of early atherosclerosis (Rao et al., 2007). Intercellular adhesion molecule-1 (ICAM-1) aids leukocyte adhesion and is expressed by endothelial cells in advanced lesions. Platelet endothelial cell adhesion molecule-1 (PECAM-1, CD31) and junctional adhesion molecules A-C (JAM-A,B,C) are abundant at endothelial cell junctions with a role in paracellular migration of monocytes into the subendothelial layer. Circulating modified LDL stimulates endothelial cells to produce monocyte chemoattractant protein -1 (MCP-1) (Navab et al., 2004) and P-selectin (Vora et al., 1997) which recruit circulating monocytes to areas of subendothelial LDL accumulation. It also promotes the differentiation of

monocytes into tissue macrophages by inducing the release of monocyte colony stimulating factor (M-CSF) which influences the differentiation, survival, proliferation, migration and metabolism of monocyte-derived macrophages in atherosclerotic lesions (Rajavashisth et al., 1990).

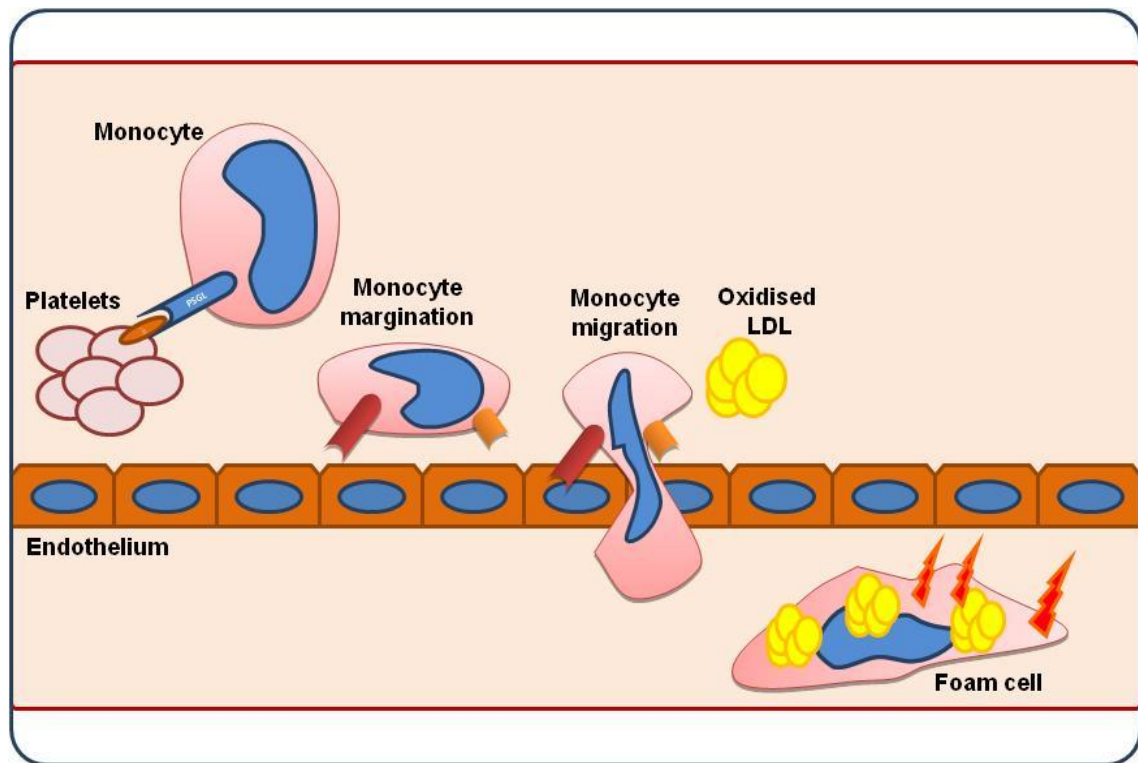


Figure 1.2: The role of the monocyte in atherogenesis.

Circulating monocytes are activated by platelets by P-selectin: PSGL-1 binding. Activated monocytes express integrins and other adhesive molecules which allow their margination and transendothelial migration. Oxidised LDL is taken up by monocyte derived macrophages which enhances pro-inflammatory signalling.

1.6.3.1.1 The role of monocyte gene expression in atherosclerosis

As described above, monocytes play a central role in atherosclerosis (Figure 1.3). They are responsive to perturbations in vascular structure and function, undergo transformation to macrophages which are central to atherosclerotic plaque development and they are integral to atherothrombosis where they closely associate with platelets following plaque rupture in the setting of acute coronary syndromes. Monocyte gene expression has been shown to be an integrator of

genetic and environmental influences in chronic inflammatory conditions (Zeller et al., 2010). In addition, they are easily isolated from peripheral blood and can be considered as reporters of endothelial function and inflammation in the context of atherosclerosis (Patino et al., 2005).

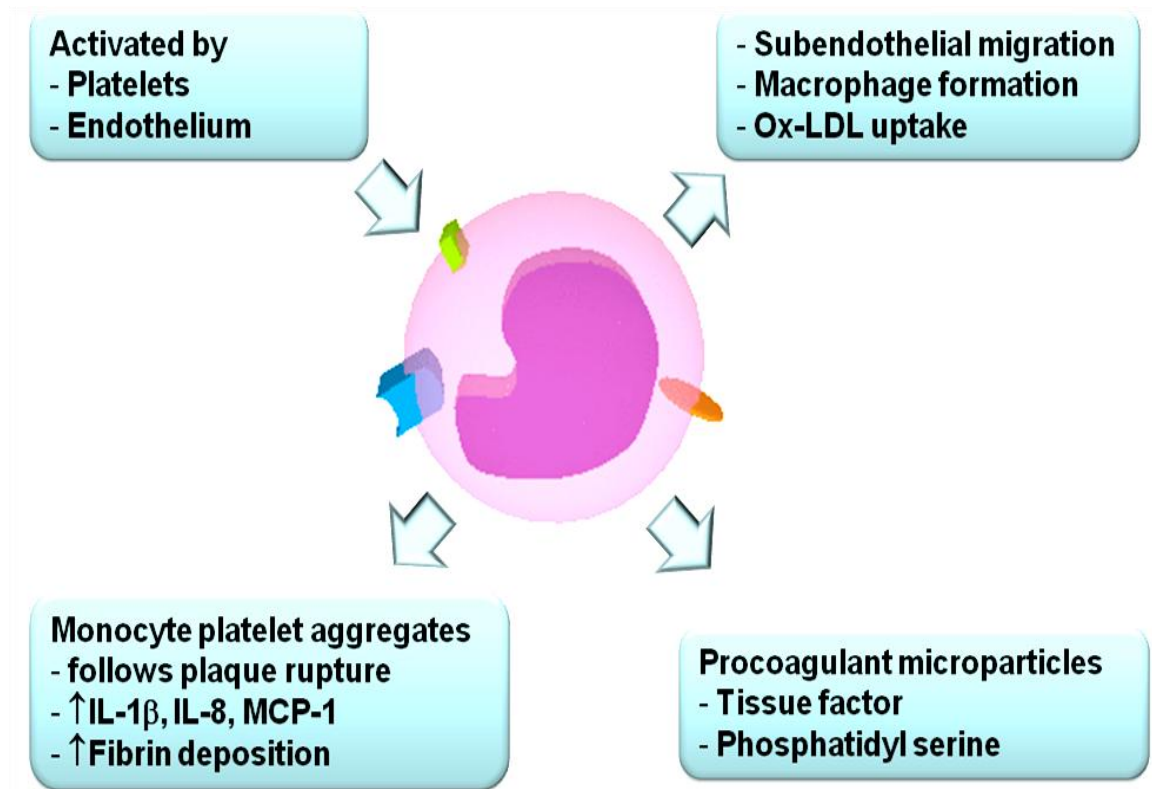


Figure 1.3: The role of the monocyte in atherosclerosis.

The circulating monocyte is activated by alterations in other cell types, undergoes morphological and functional alterations in response to such stimuli and is an integral part of atherosclerosis throughout its course from plaque formation to rupture.

A large scale analysis of unrelated individuals in the Gutenberg Heart Study (Zeller et al., 2010) has employed a combined approach of GWAS and GWE of circulating monocytes in an attempt to identify links between variations in the genome and phenotype of disease. Monocytes were obtained from 1,490 unrelated individuals (35 to 74 years, 760 men) and GWE profiles were analysed. In this study, differential gene expression in monocytes associated with variations

in gene sequence (eQTLs) as well as with classical risk factors such as hypercholesterolaemia, hypertension and smoking.

This suggests two potential mechanisms by which gene expression in the circulating monocyte associates with CAD risk:

1. Through variations in genomic content which strongly associate with differential gene expression – the eQTLs. This accounts for the genetically accumulated risk which manifests as differential gene expression.
2. Through the response of the monocyte transcriptome to environmental influences. This may reflect changes in clinically quantifiable intermediate phenotypes such as hypertension and hypercholesterolaemia.

1.6.3.2 Platelets

Platelets are small discoid anucleate cellular elements in circulation derived from megakaryocytes in bone marrow and lung (Ogawa, 1993). They are central to primary haemostasis and repair, but also play an important role in the initiation and progression of stable coronary atherosclerosis (Linden and Jackson, 2010) and in acute atherothrombosis following plaque rupture (Davi and Patrono, 2007).

Platelets interact with other cell types, predominantly circulating monocytes and vascular endothelial cells to promote vascular inflammation and atherosclerosis (Antoniades et al., 2010). Platelets also play a role in atherogenesis and promote progression of atherosclerotic lesions (Massberg et al., 2002). Such pro-inflammatory interactions are mediated by the contents of platelet granules, which are of two types: alpha and dense granules (Figure 1.4). These granules contain

various proinflammatory and prothrombotic molecules which upon activation of the platelet, are released into membrane-bound platelet microparticles (PMPs).

Activation of platelets is mediated primarily through the glycoprotein VI (GPVI) receptor which binds collagen (Jung et al., 2009) and the various G-protein coupled receptors for thrombin (PAR1 and PAR4 in human platelets), ADP (P2Y1 and P2Y12) and thromboxane (TP). In addition, the glycoprotein Ib-IX-V (GPIb-IX-V) receptor which binds to von Willebrand Factor (vWF) (Chen and Lopez, 2005) slows down the circulating platelet and facilitates its attachment to the subendothelium. Slowing down of vWF activated platelets in circulation under high shear stress facilitates collagen mediated GPVI receptor activation (Inoue et al., 2008) and activation via thrombin, ADP and thromboxane.

Platelet activation results in morphological changes and activation of integrin adhesion receptors; most notably the GPIIb-IIIa (or $\alpha 2b\beta 3$) receptor for fibrinogen that allows platelets to aggregate, and expression of P-selectin which promotes platelet-leukocyte adhesion. Other integrins, such as the GPIaIIa ($\alpha 5\beta 1$) collagen receptor help to stabilize the binding of platelets to the sub-endothelial matrix. Activated platelets bound to collagen in the vessel wall attract and bind circulating progenitor cells and promote their differentiation to macrophages, foam cells and dendritic cells (Gawaz et al., 2008).

The interaction of activated platelets with circulating monocytes is mediated via the binding of platelet surface P-selectin with its ligand P-selectin glycoprotein ligand-1 (PSGL-1) on the monocyte. This is facilitated by the chemokine RANTES (regulated on activation normal T cell expressed and secreted; CCL5) (von Hundelshausen et al., 2005, McGregor et al., 2006) as shown in Figure 1.4. P-selectin binding stimulates the synthesis of chemotactic factors and interleukins by the activated monocytes (Weyrich et al., 1996).

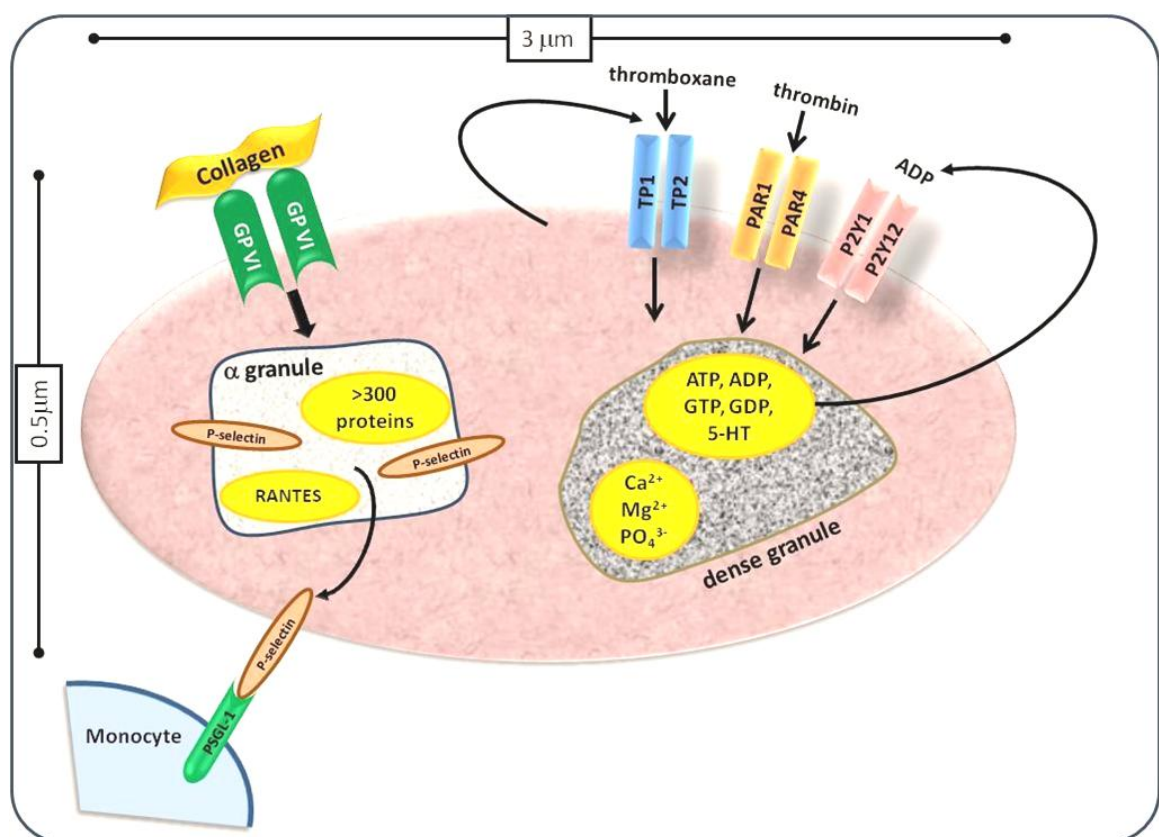


Figure 1.4: Platelet structure and function.

The major cellular organelles of platelets and their contents are shown. A large number of pro-inflammatory molecules are stored and secreted by platelets in their alpha and dense granules. Collagen activates platelets by binding to the dimeric glycoprotein VI (GPVI) receptor. The main cellular interaction is with monocytes through P-selectin: PSGL-1 binding.

1.6.3.3 Monocyte-platelet interactions in atherothrombosis

Flowcytometry studies have shown that collagen activated platelets express P-selectin and bind to P-selectin glycoprotein ligand-1 (PSGL-1) on monocytes (McGregor et al., 2006) to form monocyte-platelet aggregates (MPA) following which the activated monocytes increase surface expression of tissue factor, factor Xa and fibrinogen (Barnard et al., 2005) (Figure 1.5).

Activation of monocytes via the PSGL-1 ligand results in increased expression of adhesion molecules and facilitates the transendothelial migration of monocytes (da Costa Martins et al., 2006). This is mediated by the enhanced expression of $\beta 1$ and $\beta 2$ integrins (da Costa Martins et al., 2006). The intracellular signalling triggered by PSGL-1 activation augments the rolling (through activation of ERM proteins (Snapp et al., 2002)) and migration (through activation of mTOR (Fox et al., 2007)) of circulating monocytes (van Gils et al., 2009). Not surprisingly, inhibition of P-selectin/PSGL-1 interaction reduces vascular inflammation (van Gils et al., 2009). Shear resistant monocyte arrest on the endothelium is facilitated by platelet derived RANTES (von Hundelshausen et al., 2001). Thus platelet mediated monocyte activation is a key step in localisation of monocytes to sites of vascular injury and subsequent atherosclerosis (Linden and Jackson, 2010).

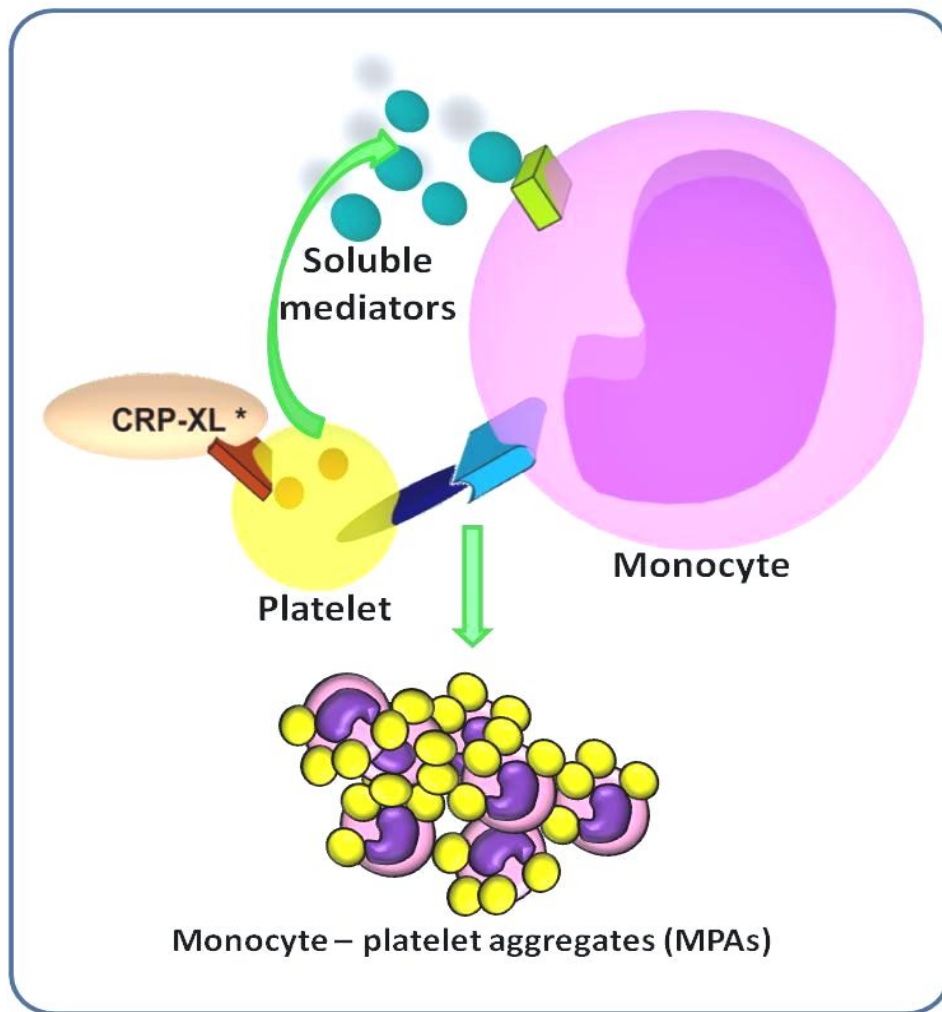


Figure 1.5: Mechanisms of Monocyte-Platelet interaction.

Circulating monocytes are activated by platelets directly via P-selectin: PSGL-1 binding and indirectly via soluble mediators released from activated platelets. This results in the formation of monocyte-platelet aggregates (MPAs) in circulation. The presence of MPAs in circulation is a reliable marker for platelet activation and cross talk between platelets and monocytes.

It has been shown that activation of circulating platelets with increased surface expression of P-selectin, phosphatidyl serine and formation of monocyte-platelet aggregates (MPA) is significantly higher in patients with hyperlipidaemia (Sener et al., 2005). Following rupture of atherosclerotic plaques, platelet activation increases the levels of circulating MPAs (van Gils et al., 2009). Elevated levels of circulating MPAs have been seen in stable and unstable coronary artery disease (Furman et al., 2001), ischaemic stroke, hypertension and diabetes. In patients with chest pain, presence of >30% circulating MPA levels has been shown to

discriminate acute myocardial infarction from other causes (Lippi et al., 2007) with a high degree of confidence.

Flowcytometric analysis of circulating MPAs has been shown to be a more sensitive marker of platelet activation than platelet surface expression of P-selectin (Michelson et al., 2001).

1.6.3.4 Platelet-mediated stimulation of circulating monocytes

As previously described, the circulating monocyte has an impressive potential for differentiation along varying morphological and functional lines depending on the environmental stimulus. It also has recognised roles in various pathophysiological processes including infection, immunity, inflammation, apoptosis and atherosclerosis. Therefore, the challenge in studying the monocyte lies in selecting the appropriate stimulus of relevance to the condition of interest.

Various stimuli have been used to activate circulating monocytes to study changes in gene expression relevant to atherosclerosis. These include stimulation followed by cell culture to differentiate into macrophages and activation *in vitro* to study the effects in undifferentiated monocytes. Lipopolysaccharide (bacterial endotoxin) has been used as an *in vitro* stimulus for monocytes to study differences in gene expression (Lawrence et al., 2007). Signalling pathways activated in the monocyte in response to LPS include the toll-like receptor (TLR) and type 1 interferon (IFN) pathways (Ovstebo et al., 2008). In addition, it has been shown that other factors including non-LPS fraction of bacteria (Ovstebo et al., 2008) and presence of LPS-binding protein (Kato et al., 2004) affect monocyte response to LPS.

The well recognised role of platelets in the activation of circulating monocytes during various stages of atherosclerosis provides an alternative stimulus for

monocytes which is likely to focus monocyte activation in a direction of relevance to CAD. It has been shown that collagen activates platelets in a glycoprotein VI (GPVI) dependent manner which results in platelet aggregation (Jung and Moroi, 2008). Cross linked collagen related peptide (CRP-XL) containing a repeat Gly-Pro-Hyp sequence recognised by the GPVI receptor induces platelet signalling similar to that induced by collagen (Kehrel et al., 1998). This is a platelet specific stimulus which does not affect the monocyte other than via activated platelets so that the observed gene expression profiles are a direct consequence of platelet-monocyte interactions.

Differential gene expression in the monocyte may reflect or even precede the pathophysiological changes that underlie CAD progression (Zeller et al., 2010). These changes may be unmasked or amplified by the use of an appropriate stimulus, such as CRP-XL and differential expression in cases and controls may be used to identify patterns of gene expression with a strong association with CAD. These observations may result in the identification of mechanisms of disease progression which are mediated through the circulating monocyte.

1.7 ORIGINAL PRINCIPAL HYPOTHESES

Variations in gene expression of the circulating peripheral blood monocyte determine individual susceptibility to atherosclerotic coronary artery disease.

1.8 AIMS OF THIS STUDY

To investigate this hypothesis the following questions were addressed:

What are the key changes in gene expression in monocytes induced by platelet driven stimulation?

Are there differences in transcriptome profiles of resting and stimulated monocytes from individuals with overt atherosclerotic coronary artery disease compared to controls?

Are there differences in transcriptome profiles of resting and stimulated monocytes between groups of individuals with contrasting heritable risk of atherosclerotic coronary artery disease?

Is there genetic regulation of monocyte gene expression in any of the genes that show differential expression in 2 and 3 above and are genetic variants in these genes associated with risk of CAD/MI?

CHAPTER 2

Materials and Methods

2.1 RECRUITMENT

Site specific ethics approval (SSA) was obtained from the Derby Main Research Ethics Committee (REC ref no: 06/Q2401/134) and the institutional Research and Development Department (Ref: RM61056). The study was funded by the EU FP6 Programme (Ref: LSHM-CT-2004-503485, Bloodomics).

The study recruited four groups of subjects (Figure 2.1). Northern European Caucasians from the same geographic area were recruited to limit biological and genetic heterogeneity. Cases and controls were matched for age, gender and current smoking status. Patients with diabetes mellitus, bleeding disorders including platelet dysfunction, inflammatory disorders such as malignancy, autoimmune disorders and active infections were excluded.

2.1.1 Subjects with premature MI (Group 1)

Group 1 consisted of individuals under the age of 65 years admitted to hospital with a first ST segment elevation MI (STEMI). Eligible patients were identified from the Myocardial Infarction National Audit Project (MINAP), introduced in 1998 as part of the National Service Framework (NSF) for coronary artery disease. All acute care hospitals treating patients with acute myocardial infarction have a responsibility to maintain MINAP databases containing demographic and clinical data of admissions with a diagnosis of myocardial infarction. Suitable subjects presenting with acute myocardial infarction to the Regional Cardiothoracic Centre, Glenfield Hospital, Leicester were selected from the institutional MINAP database.

Recruitment was limited to STEMI patients for two reasons: STEMI has universally recognised diagnostic criteria which allow bedside diagnosis at the time of

admission based on clinical presentation and ECG. The acute plaque rupture within the coronary artery resulting in luminal occlusion is a characteristic feature of STEMI. This provides an ideal phenotype to study coronary atherosclerosis and atherothrombosis.

Other types of acute coronary syndromes – non ST segment elevation MI (NSTEMI) and unstable angina (UA) are not always diagnosed at the time of presentation and tend to be variably associated with plaque rupture or erosion with subtotal and transient coronary luminal occlusion.

The intention was to recruit these subjects at the time of initial admission and repeat samples at ≥ 3 months post STEMI when in a stable clinical condition. The aim of recruiting patients in the acute phase of STEMI was to obtain monocyte RNA samples before the initiation of long term secondary prevention therapy including statins and antiplatelet drugs which may modify the monocyte and platelet transcriptome. However, in the acute stage, the monocyte transcriptome may represent changes due to the acute stress response and prothrombotic state and not necessarily a reflection of the underlying atherosclerotic disease.

Six acute STEMI patients were recruited within hours of presentation after thrombolytic therapy or primary angioplasty, but before the initiation of statins or drugs which act on the renin-angiotensin-aldosterone pathway. However it became apparent that there was significant platelet contamination of the monocyte isolates from these individuals, possibly due to the formation of monocyte – platelet aggregates in the setting of an acute plaque rupture event. Therefore further recruitment was limited to patients ≥ 3 months post STEMI in a clinically stable condition without symptomatic angina or congestive cardiac failure.

2.1.2 Subjects with a family history of premature MI (Group 2)

Two strategies were used to recruit healthy Caucasian men with a family history of premature myocardial infarction:

1. Existing databases from previous studies in cardiovascular genetics within the Department were used to identify suitable participants. Healthy individuals (age range 18-40 years) with a positive family history of premature CAD (age of myocardial infarction: parent <55yrs +/- grandparent <65 yrs) were recruited for this study.
2. Patients admitted to Glenfield hospital with a premature myocardial infarction were approached for recruitment of suitable male offspring.

All recruits were between 18 and 40 years of age. A significant family history of premature myocardial infarction was defined as one of the parents having had a myocardial infarction under the age of 55 years. A proportion of recruits also had a grandparent with a myocardial infarction under the age of 65 years.

2.1.3 Healthy volunteers (control groups 3 and 4)

Two groups of controls were recruited for the study. Group 3 consisted of healthy volunteers matched for age, gender and smoking status to subjects in Group 1. Group 4 consisted of healthy volunteers with no family history of premature CAD in two preceding generations matched for age and gender to subjects in Group 2.

Healthy volunteers were recruited by advertisement within the hospital premises. All controls were free of illnesses and were not on any regular medication. They were matched with cases for age, gender and smoking status.

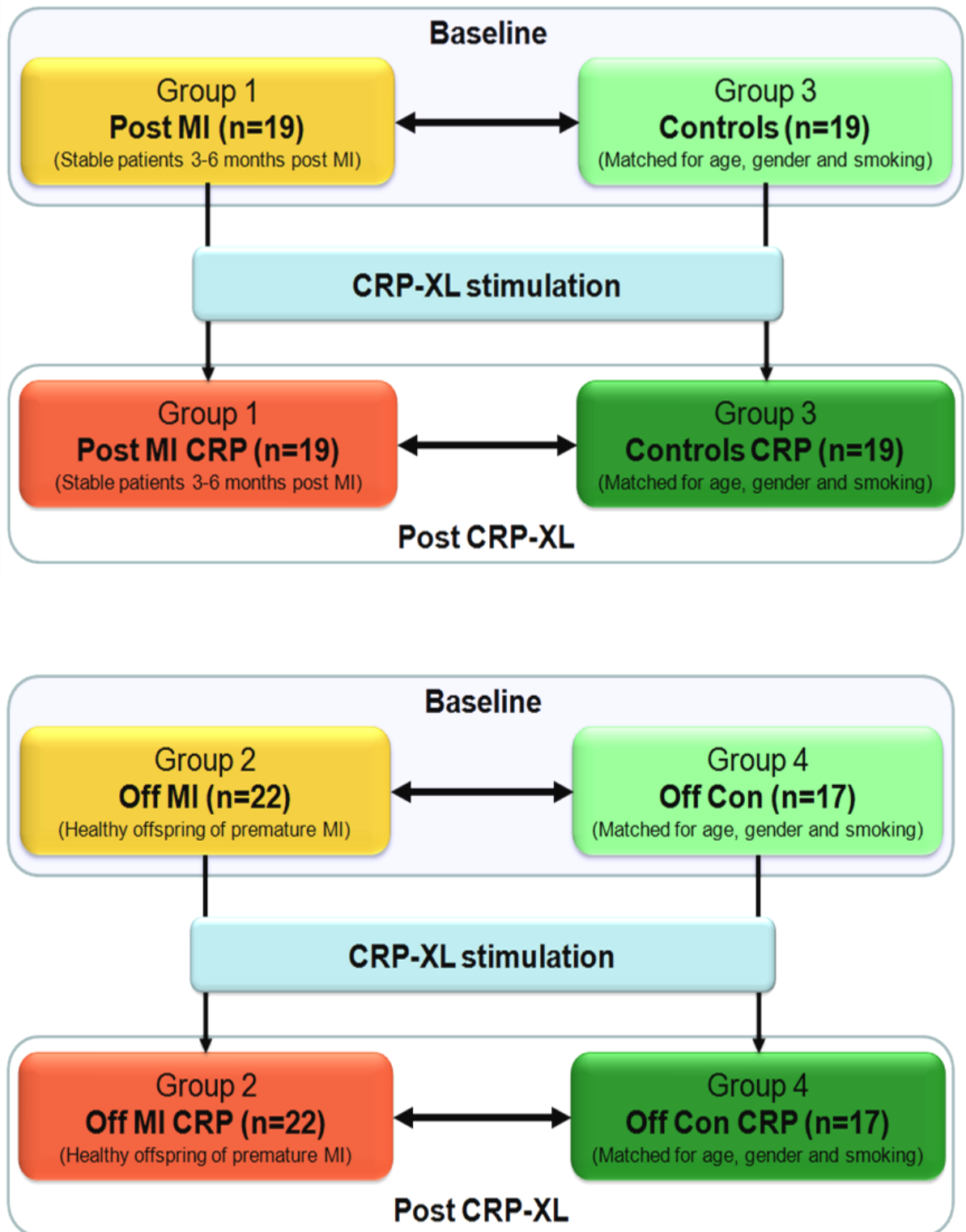


Figure 2.1: Schematic diagram of study groups and experiments.

The two study groups (1 & 2) and control groups (3 & 4) are shown. Groups were compared at baseline and after CRP-XL stimulation as shown. In addition, within group analyses of changes in the monocyte transcriptome were carried out in all four groups.

2.2 CLINICAL DATA COLLECTION AND BLOOD SAMPLING

All subjects underwent a face to face interview with the research fellow (U.K.) during which relevant clinical information including medical and family history, biometric measurements, resting 12 lead ECG and a fasting venous blood sample were obtained. Subjects were fasting for a minimum of 10 hours and had refrained from consuming caffeine for a minimum of 12 hours prior to blood sampling. Blood samples were collected into BD Vacutainer® glass tubes. To minimise platelet activation, the procedure was performed in a quiet room with the subject supine for at least 10 minutes and the initial 2ml blood was not used for monocyte isolation.

The samples were collected in the following order:

- (i) 2ml blood in EDTA tubes for full blood count.
- (ii) 15 ml blood in citrate tubes for baseline plasma isolation, monocyte stimulation and flowcytometry.
- (iii) 20 ml in EDTA tubes for resting monocyte isolation.
- (iv) 10 ml blood in serum tubes for storage and estimation of fasting lipid profile.
- (v) 2ml blood in fluoride tubes for fasting glucose estimation.

2.2.1 Demographic and biometric data

2.2.1.1 Post MI and healthy controls

Twenty patients were recruited three to six months after acute STEMI (Post MI group, Group 1) followed by twenty healthy controls (Group 3) matched for age, gender and current smoking status. One from each group was later excluded (see below). The demographic and biometric data are summarised in Table 2.1 and baseline fasting blood test results in Table 2.2

Measurement	Post MI (n=19)	Control (n=19)	p value
Age (years)	53 ±7	51 ±7	0.44
Female	2/19	2/19	1.0
Current smokers	4/19	4/19	1.0
BMI	29.79 ±4.04	26.47 ±2.81	0.003
W:H ratio	0.93 ±0.06	0.9 ±0.06	0.19
SBP (mm Hg)	127 ±18	138 ±19	0.07
DBP (mm Hg)	80 ±11	88 ±14	0.13
Pulse (bpm)	55±8	63±9	0.04

Table 2.1: Demographic and biometric data for Post MI patients and healthy controls.

Measurement	Post MI (n=19)	Control (n=19)	p value
WBC (x10 ³ /uL)	6.5 ±1.6	5.3 ±1.2	0.02
Monocyte (x10 ³ /uL)	0.47 ±0.2	0.28 ±0.2	0.002
Platelet (x10 ³ /uL)	242 ±62	218 ±51	0.12
TC:HDL	4.1 ±0.8	4.9 ±1.3	0.02
LDL (mmol/L)	2.4 ±0.5	3.6 ±1.0	<0.0001
TG (mmol/L)	1.5 ±0.7	1.5 ±0.8	0.69
FPG (mmol/L)	5.3 ±0.6	4.8 ±0.3	0.02

Table 2.2: Baseline blood tests for Post MI patients and healthy controls.

Post MI (STEMI) patients and controls were well matched in terms of age, gender and current smoking status. However the Post MI group had significantly higher body mass index although the waist to hip ratios of both groups were comparable.

The Post MI group had significantly lower systolic blood pressure, pulse rate, TC:HDL ratio and LDL levels as a consequence of secondary prevention therapy (Table 2.3). Although both groups had monocyte counts and glucose levels within the normal range, these were both significantly higher in the Post MI patients.

All patients recruited 3 to 6 months after STEMI were on established long term pharmacotherapy as given in Table 2.3.

Medication	Number (%) of patients
Aspirin	19 (100)
Clopidogrel	13 (68)
HMGCoA reductase inhibitors ('statin')	19 (100)
βblockers	17 (89)
ACEi	16 (84)
ARB	3 (16)
Aldosterone antagonists	1 (5)
Diuretics	2 (11)

Table 2.3: Pharmacotherapy in patients Post MI.

In addition, 7 patients (35%) were on proton pump inhibitors, one patient was on dihydropyridine calcium channel blocker while another was on PPAR alpha antagonist ('fibrate') therapy. None of the patients were on antianginals. One of the controls for STEMI was on two antihypertensive medications and therefore was excluded from further analysis.

Resting 12 lead ECGs were obtained on all subjects. In the Post MI group, 12 out of 20 patients had inferior or infero-posterior q waves, 4 patients had anterior q waves and the rest had no obvious pathological q waves on ECG although they had a definite diagnosis of STEMI on admission. One patient was in atrial

fibrillation. In the control group for premature MI patients, 14 out of 20 subjects had normal ECGs, two had borderline first degree heart block, two had right bundle branch block, one had left bundle branch block and one had significant left ventricular hypertrophy. The person with left bundle branch block had previously undergone extensive investigation including cardiac MRI scanning which ruled out structural heart disease and therefore he was included in the study. The person with left ventricular hypertrophy was also on antihypertensive medications and therefore was excluded from further analysis.

2.2.1.2 Offspring of MI and controls

Case (Group 2) and control (Group 4) offspring subjects were recruited in parallel over a four month period. Recruitment was stopped when 23 and 20 individuals were recruited to groups 2 and 4 respectively (target: 20 in each group). However four subjects were later excluded from the study (see below). The demographic and biometric data are summarised in Table 2.4 and baseline fasting blood test results in Table 2.5.

Measurement	Offspring of MI (n=22)	Control offspring (n=17)	p value
Age (years)	29 ±7	31 ±5	0.22
Current smokers	7/22	5/17	0.74
BMI	26.25±4.4	26.47 ±3.3	0.75
W:H ratio	0.87 ±0.06	0.86±0.05	0.94
SBP (mm Hg)	134 ±13	123 ±9	0.02
DBP (mm Hg)	80 ±10	75 ±6	0.03
Pulse (bpm)	68±8	61±7	0.01

Table 2.4: Demographic and biometric data for Offspring of MI and healthy controls.

Measurement	Offspring of MI (n=22)	Control offspring (n=17)	p value
WBC (x10 ³ /uL)	5.8±1.7	5.3 ±1.2	0.02
Monocyte	0.39 ±0.2	0.37 ±0.1	0.86
Platelet (x10 ³ /uL)	223 ±51	212 ±57	0.35
TC:HDL	5.1 ±1.4	4.4 ±0.8	0.17
LDL (mmol/L)	3.4 ±1.1	3.1 ±0.7	0.4
TG (mmol/L)	1.4 ±0.7	1.01 ±0.4	0.09
FPG (mmol/L)	4.8 ±0.4	4.8 ±0.3	0.8

Table 2.5: Baseline blood tests for Offspring of MI and healthy controls.

The two groups with (Offspring of MI, Group 2) and without a family history of premature MI (Control offspring, Group 4) were matched for age and smoking status. Although the mean age of the Offspring of MI was less than controls by two years, they had significantly higher systolic and diastolic blood pressures and pulse rate. Such observations have been made previously in subjects with a positive family history of vascular disease (Musil et al., 2012).

Although none of the subjects had active infections or inflammatory disorders, there was a significantly higher total WBC count in the Offspring of MI. However, the cell counts were well within normal limits. There were no significant differences in monocyte and platelet counts, cholesterol profiles or blood glucose levels.

All men in the offspring groups had normal ECGs except one person with right bundle branch block, one with asymptomatic intermittent Wenkebach phenomenon and one with left ventricular hypertrophy. The latter had high blood pressure readings but none of the subjects were on any regular medications and all declared to have refrained from medication that could affect platelet function for ≥10 days prior to study.

2.2.1.3 Details of family history of offspring groups

2.2.1.3.1 Parental history of premature MI and other atherosclerotic disease

15 out of 22 subjects in the Offspring of MI group (Group 2) had a paternal history of MI under the age of 55 (mean [\pm SD] = 45 [\pm 6 years]), while 5 out of 22 had a maternal history of MI under the age of 55 (mean [\pm SD] = 48 [\pm 3 years]). In one case both parents had suffered an MI (mother at 43 years, father at 64 years) while in two other instances one parent had MI before the age of 55 years and the other parent had angina or CVA before 60 years. One recruit had a parental history of MI above 55 years (father had MI at 60 years).

None of the subjects in the Control offspring group had parents with known coronary disease or other vascular disease at the time of recruitment. However two subjects in this group were subsequently excluded from the study. In one instance, a parent of one of the subjects had an unconfirmed myocardial infarction in their 60s while another subject had a parental history of sudden death (cause unknown).

2.2.1.3.2 Grandparental history of MI and other atherosclerotic disease

10 of 22 Offspring of MI had a grandparent with MI before 65 years while another two had MI before 75 years (mean [\pm SD] = 55 [\pm 12 years]). None of the Control offspring (Group 4) had grandparents with known atherosclerotic disease before 65 years. Three had a grandparent with MI (mean age = 74 years) while two had a grandparent with CVA (mean age = 73 years).

2.2.2 Exclusions – all groups

- One of the MI patients (Group 1) was excluded due to poor RNA sample quality.
- One of the Controls for MI (Group 3) on pharmacotherapy for hypertension was excluded.
- Two offspring (one in Group 2 and one in Group 4) had previously undiagnosed diabetes mellitus (detected on fasting glucose test arranged as part of the study) and were excluded.
- Two Control offspring (Group 4) with parents with either suspected coronary disease or sudden death (presumed cardiovascular cause) after recruitment were excluded.

2.3 ISOLATION OF BLOOD CELLS AND SUPERNATANT

2.3.1 Serum and plasma isolation

Plasma was separated by centrifugation at 1800g for 30 minutes at 4°C. Serum was allowed to separate by incubation at room temperature for 60 minutes followed by centrifugation at 1800g for 30 minutes at room temperature. Following incubation of blood samples with CRP-XL (see below), further plasma samples were collected by centrifugation at 1800g for 30 minutes at 4°C.

2.3.2 Monocyte isolation at baseline

The study plan was to isolate monocytes from whole blood using CD14+ve magnetic beads. Prior to the study different methods were tested to determine the optimal method for use in the collection of samples from the cohort.

Monocyte gene expression has been shown to be affected by mechanical stress and time of processing. Therefore, available methods for cell isolation including Lymphoprep™ (Axis-Shield) density gradient separation and magnetic cell separation platforms (RoboSep, AutoMACS and Dynabeads) were compared.

Lymphoprep™ (Ficoll-Isopaque) is a commercially available sterile, endotoxin free medium for separation of mononuclear cells. Although this is a reliable method for separating monocytes from granulocytes, it does not allow separation from other mononuclear cells including T and B lymphocytes, natural killer cells etc. In addition, the repeated centrifugation and washing steps may result in monocyte gene activation which is inducible by mechanical stress.

Three magnetic cell separation platforms were tested for the project. All platforms used paramagnetic micro beads with cell specific antibody coating (CD14 for

monocyte isolation) to allow separation with >95% purity and >75% yield. Positive selection protocols on all three platforms were compared as they consistently yielded better purity compared to negative ('no touch') isolation.

(i) RoboSep® (StemCell technologies) is an automated robotic platform which can separate up to 4 samples simultaneously. The beads are 150nm in diameter and compatible with flowcytometry to assess cell purity. The protocol required multiple pipetting/washing steps followed by CD14 separation in a magnetic field. The method takes 75 minutes to isolate monocytes from whole blood.

(ii) AutoMACS® (Miltenyi) is a semi-automated cell separation platform that uses flowcytometry compatible beads 50nm in diameter. An initial incubation/wash step with paramagnetic beads followed by injection of the sample through a magnetic steel mesh column traps monocytes attached to the paramagnetic beads. This protocol allowed monocyte isolation from whole blood in 45 minutes. The AutoMACS Pro allows positive or negative cell isolation from three samples in series.

(iii) Dynabeads® (Dyna, Invitrogen) are coated paramagnetic beads of 5-6 µm diameter that allow cell separation using a manual protocol that does not involve multiple pipetting steps, centrifugation or injection through columns. The beads were added to the undiluted venous blood samples which were then incubated in a cold room on a rotary mixer followed by separation in a magnetic field. This protocol allowed monocyte isolation from whole blood within 30 minutes of venesection.

AutoMACS and RoboSep platforms are compatible with flowcytometric analysis to assess purity by virtue of their small bead size. Dynabead separation does not

allow assessment of purity by flowcytometry as the bead size interferes with cell counting.

After testing all three platforms, it was evident that the RoboSep platform did not provide a significant advantage except in instances where multiple unsupervised isolation protocols were warranted. Therefore further comparison experiments were conducted using the AutoMACS and Dynal platforms.

2.3.2.1 AutoMACS vs. Dynabeads: results of comparison experiments

10 ml venous blood was collected from the antecubital vein from six donors (five male, one female) and divided into two; 5ml whole blood each for manual separation using the Dynal protocol and automated separation by the Miltenyi AutoMACS Pro protocol. Both protocols required the addition of 50 microlitres of anti-CD14 antibody coated paramagnetic beads per ml of whole blood. The Dynal protocol allowed parallel processing of all six samples in 60 minutes. By comparison, the AutoMACS platform isolated monocytes from 3 samples in series in 120 minutes. At the end of the monocyte isolation protocol, the samples were stored at -80°C in TRizol and subsequently used for RNA extraction.

Both platforms yielded similar quantities of total monocyte RNA (Dynal: 0.54 – 2.06 micrograms; Miltenyi: 0.8 – 2.2 micrograms) from 5 ml venous blood. However, the Dynal platform had two significant advantages, that it allowed sample processing in parallel and that the protocol was shorter. In addition, the manual Dynal method was less likely to induce mechanical stress related monocyte activation.

The Dynal protocol was further optimized to reduce the volume of anti-CD14 antibody coated paramagnetic beads added per ml blood. Comparison

experiments showed that from 8ml venous blood with a total monocyte count of 3.2×10^6 , addition of 25 and 50 microlitres of Dynabeads yielded 2.5 and 2.8 micrograms of total RNA from monocytes. As the minimum requirement of RNA for microarray experiments was 500 nanograms, the protocol was revised to 25 microlitres Dynabeads per ml blood.

Purity of samples was verified by PCR of lineage specific cell surface antigens (Watkins et al., 2009). This confirmed that the samples were free of contamination by platelets and other mononuclear cells (see below; section on confirmation of RNA purity).

After testing the three platforms for cell isolation, the Dynabeads method was chosen as it was the quickest and the least likely to cause mechanical stress during processing. The assessment of purity was made by PCR of specific cell type markers which provided greater sensitivity and accuracy than flowcytometry in detecting contaminating cells.

The original Dynal protocol included a dilution step prior to the addition of antibody coated beads. However this method was modified to avoid delay and mechanical stress which could activate the monocytes, and to improve yield. Pilot experiments indicated that within the normal range of monocyte counts ($0.2-0.8 \times 10^6$ cells/ml), from 10ml venous blood, more than 10^6 monocytes were consistently isolated, thereby yielding a minimum of 1 μ g RNA. For the above reasons, the final protocol was modified as described below.

- At baseline, venous blood was collected into two 8ml EDTA tubes. 100 μ l was used for cell counts and the rest was used for immediate monocyte isolation. A

separate 500 µl aliquot collected in citrate anticoagulant was kept aside for flowcytometry.

- CD14 coated Dynabeads which were freshly washed in sterile endotoxin free phosphate buffered saline (PBS) was added to the sample at a concentration of 25 µl beads/ml blood. The samples were then mixed by gentle inversion and incubated at 4°C on a rotary mixer for 20 minutes, following which they were kept on a rack in a magnetic field which allows the paramagnetic beads with the CD14 +ve monocytes attached to move to the sides of the sample tubes within 30-60 seconds. The blood, now depleted of monocytes was pipetted out and the beads were washed twice in sterile PBS by gentle mixing on the magnetic rack till the supernatant turned clear. TRIzol reagent was then added to the beads and the samples vigorously pipetted to lyse the attached monocytes. This was then used for RNA extraction.
- The three 5ml aliquots collected into citrate tubes (see below) were processed in a similar manner after 4 hours incubation at 37°C with collagen related peptide (see below). The CD14 depleted blood was used for plasma extraction.

2.3.3 Platelet mediated stimulation of monocytes

2.3.3.1 Selection of stimulus relevant to atherosclerosis

Stimulation by collagen related peptide activates monocytes through a platelet dependent pathway which is functionally relevant to both early cellular processes in atherogenesis and clinical events arising from atherothrombosis.

As previously described, collagen related peptide (CRP) activates the platelet GPVI receptor, a key mediator of collagen induced platelet procoagulant activity. Following activation, platelets release P-selectin which then binds to the P-selectin glycoprotein ligand-1 (PSGL-1) on the monocyte to activate it.

Two forms of collagen related peptide (CRP) were compared for consistency and effectiveness of platelet activation – CRP-18 and CRP-XL, provided Dr Richard Farndale, Dept of Biochemistry, University of Cambridge (Pugh et al., 2010). Optimisation experiments were carried out in three doses of each reagent: 10, 1.0 and 0.1 micrograms per ml sample.

The extent of platelet activation (measured by fibrinogen binding and expressed in percentage) ranged from 74 to 94% with increasing doses of CRP-18, whilst the response with CRP-XL was less variable, ranging from 89% to 95% (Figure 2.2).

Based on these experiments, it was decided that 1.0µg of CRP-XL per ml of whole blood would provide optimum stimulation. Titration curves of P-selectin expression (as a marker of platelet activation in response to CRP-XL) were obtained in pilot experiments to confirm adequate stimulation at this concentration.

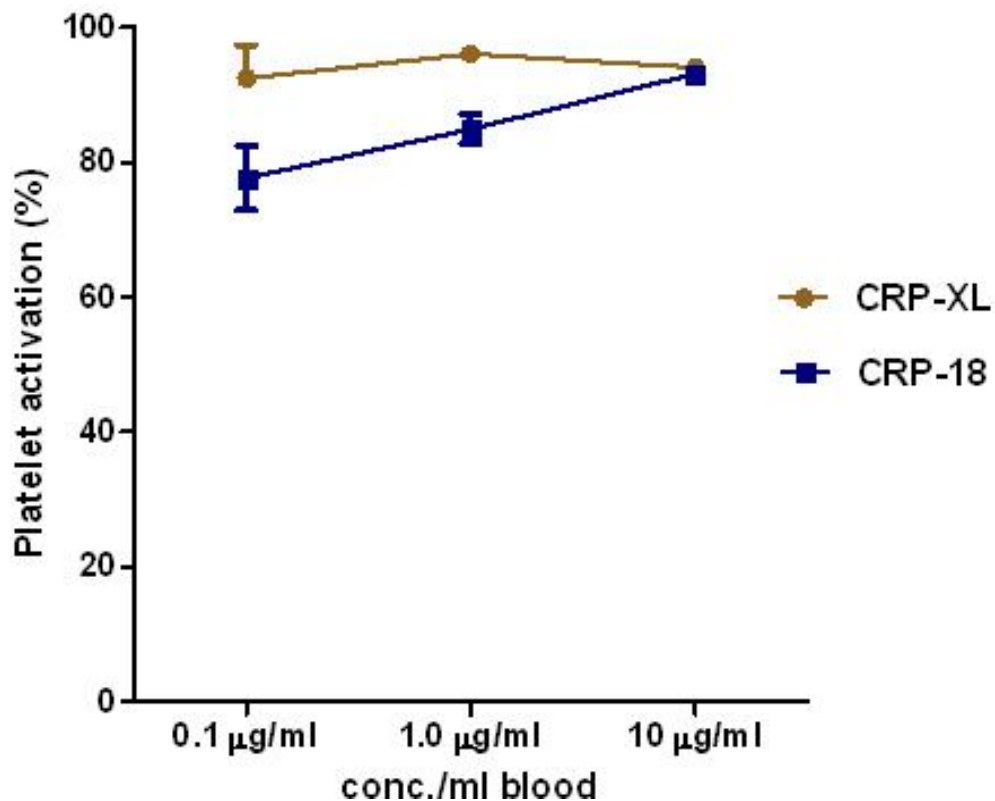


Figure 2.2: Relative efficacy of CRP-XL and CRP-18 (flowcytometry). Efficacy of both agents was tested at three concentrations. CRP-XL was used for subsequent experiments due to higher and more consistent platelet response.

2.3.3.2 Platelet-mediated stimulation protocol using CRP-XL

15 ml aliquots of venous blood collected into citrate tubes were used in the stimulation experiment. Cross linked collagen related peptide was added to the blood sample at a concentration of 1 μg per ml blood. Following the addition of CRP-XL, the blood samples were incubated at 37°C for four hours. During this period, the samples were mixed gently on a tilting plate mixer to attain uniform stimulation. This experiment was carried out in glass tubes to prevent monocyte adhesion.

2.3.4 Flowcytometry

This was performed at two time points:

- At baseline, we demonstrated that there was no significant platelet activation. For this we used a flowcytometric assay to measure monocyte-platelet aggregates (MPA). CD42b was used as the platelet surface marker while CD14 was selected as the monocyte marker for this assay.
- After 4 hours incubation with CRP-XL, we obtained samples for MPA assay to confirm monocyte activation.

2.3.4.1 Analysis of monocytes and monocyte-platelet aggregates by flowcytometry:

Reagents: Phosphate buffered saline (pH 7.4), Hepes buffered saline, Optilyse[®]C (Beckman Coulter#A11895), antibodies: MOPC31C IgG1k (Sigma M9035) - 5 μ L, P-Selectin blocking Mab 9E1 (R&D BBA30) - 2 μ L, CD14-RPE-Cy5 Mouse α Human (Serotec MCA1568C) - 5 μ L, RPE-Cy5 IgG2a isotype -ve control for CD14.RPEcy5 (Serotec MCA 929C) - 2 μ L, CD42b-RPE Mouse α Human (DAKO R7014) - 2 μ L, RPE IgG2a -ve isotype for CD42b (DAKO X0950) - 2 μ L.

50 μ L HBS was added to four LP4 tubes and antibodies were added as shown in Table 2.6. 50 μ L citrated blood was added to each tube and incubated for 30 minutes at room temperature, following which 250 μ L Optilyse[®]C solution was added and the tubes were mixed and allowed to stand at room temperature for 15 minutes, following which 250 μ L PBS was added. Following a further incubation at room temperature for 5 minutes, these were analysed on the flowcytometer (MCL-XL; Beckman Coulter Ltd, Milton Keynes, UK).

Tube	HBS	MOP C31 IgG1 k	Mab 9E1	RPE Cy5 IgG ₁ 2a Isotype control	CD14 RPE Cy5	RPE IgG2a Isotype control	CD42b RPE	Blood
ISOTYPE CONTROL #1 FOR RPE.CY5	50µL	5µL	2µL	2µL			-	50µL
ISOTYPE CONTROL #2 FOR RPE	50µL	5µL	2µL	-	5µl	2µl		50µL
3	50µL	5µL	2µL	-	5µl		2µL	50µL
4	50µL	5µL	2µL	-	5µl		2µL	50µL

Table 2.6: Flowcytometry protocol for detection of monocyte platelet aggregates.

2.3.5 Isolation of platelets

Analysis of the platelet transcriptome was one of the initial aims of this project. However, it was evident from pilot experiments that there was no reliable method for isolating platelet RNA from relatively small volumes of blood (<50ml) without significant leukocyte (especially monocyte) contamination. This is mainly attributable to the relative abundance of RNA in nucleated cells compared to platelets. Leukocytes contain approximately 10,000 fold the RNA content in platelets and therefore a single contaminating leukocyte per 100 platelets would contribute to 50% of the RNA from the sample (Fink et al., 2003). The volume of blood obtained was limited by the Ethics Committee to 50ml. This was not sufficient for the preparation of adequate amounts of platelet rich plasma to provide 0.5 microgram of total platelet RNA consistently. Therefore all microarray and PCR analyses in the subsequent sections were performed on monocyte RNA samples only.

2.4 RNA EXTRACTION AND MICROARRAY ANALYSIS

Stringent standards have to be maintained when extracting RNA, especially for downstream applications such as in-vitro transcription (IVT) and microarray hybridisation.

The factors that determine the quality and quantity of extracted RNA are:

- (i) Sample size – one million nucleated cells yield 1-10µg of RNA. This variation in yield depends on the state of transcriptional activity of the cell (for instance, cells in culture usually contain more RNA than freshly extracted cells whilst frozen cells yield relatively lower quantities of RNA).
- (ii) Time delay from sample collection to extraction – immediate freezing in storage solutions such as 'RNA *later*'[®] help to limit RNA degradation; however this cannot always ensure adequate RNA yields. Therefore, the best strategy is to aim for immediate RNA extraction following sample collection and cell lysis. Even when samples are frozen immediately, the quality and purity of RNA cannot be guaranteed.
- (iii) Lysis buffer – various commercially available buffers are used for cell lysis prior to RNA extraction. An effective chaotropic agent is essential to ensure adequate cell lysis and release of nucleic acids. TRIzol reagent (Invitrogen Cat# 15596-026), a solution containing guanidinium thiocyanate and phenol, achieves effective and reliable cell lysis and denaturation of proteins and DNA at room temperature while maintaining RNA integrity. However, the isopropanol precipitation step may result in variable yield and purity when the sample size is limited (<500,000 cells). Therefore, this step was substituted by a silica gel column method (RNeasy columns; Qiagen Cat# 74106). This

ensured adequate sample recovery from all samples. However, column based methods do not allow extraction of short RNA strands such as siRNA and miRNA. This was not considered necessary for the project which was centred on the analysis of mRNA.

(iv) RNA purity – Phase lock gel tubes (Eppendorf Cat# 955154045) help to separate the aqueous layer containing RNA from the phenol phase containing proteins and DNA. Salts and solvents used in the extraction steps are common contaminants in RNA samples which may interfere with the efficiency of downstream RNA amplification such as in vitro transcription and PCR. A column based centrifugation protocol reduces such contamination, as evidenced by consistently high 260/280 and 260/230 ratios (>2.00) on spectrophotometry. Poor 260/280 and 260/230 ratios are indicative of significant contamination of the RNA samples by proteins and solvents (such as phenol) respectively. In addition, it is important to ensure that the sample is free of DNA contamination. On-column DNase treatment was used to eliminate DNA contamination. An 'RT negative' sample was then used for 18s QPCR for 40 cycles to demonstrate absence of DNA in the samples (described below).

(v) Reducing RNase contamination – RNases are ubiquitous enzymes which degrade RNA samples; long transcripts and low abundance transcripts are especially vulnerable. It is important to ensure that the work surface is cleaned regularly and before each extraction. RNase free water should be used for all experiments. Using an ultraviolet lamp hood to pre-treat pipettes and racks helps to minimise RNase contamination. Commercially available RNase

elimination solutions maybe considered in addition to the above measures, although this is not essential.

2.4.1 Modified TRIzol-RNeasy method with on-column DNase treatment

Empty 2ml phase lock tubes were spun at high speed (13,000 RPM) for 20 seconds. To this, homogenised samples in 1ml TRIzol were added and incubated at room temperature for 5 minutes, following which 200 µl chloroform was added per 1ml of TRIzol and the tubes shaken vigorously, without vortexing, for 20 seconds. This was followed by incubation at room temperature for 2-3 minutes during which the clear aqueous layer containing the RNA formed a supernatant. The tubes were then spun at 14,000 rpm for 10 minutes at room temperature which resulted in separation of the clear aqueous layer containing RNA above the gel interphase and the pink, slightly turbid phenol layer containing DNA and proteins below. This step was repeated by adding 200µl chloroform if cell counts were low. The aqueous phase was then pipetted to an RNase free tube and mixed well with an equal volume of 70% ethanol (usually 600µl). The sample was then pipetted onto an RNeasy column (maximum 650µl) and spun at 10,000 rpm for 30 seconds which adsorbs the RNA onto the column (the flow through was discarded). The step was repeated with the rest of the sample, following which 350µL RWI buffer (part of the RNeasy kit) was added to column and spun at 10,000 rpm for 30 seconds (flow through discarded). DNase (prepared as given below) was added to the column and incubated for 20 minutes at room temperature. The wash step was then repeated with 350 µl RWI buffer as before. From the RNeasy kit, 500µl of RPE buffer was added to the column and left at room temperature for 5 minutes, following which the sample was centrifuged at 10,000 rpm for 1 minute. This second wash step with RPE buffer was then

repeated with a longer centrifugation step (2 minutes). After discarding the flow through, an additional 'dry spin' was done at maximum speed for 2 minutes to eliminate any remaining buffer. After transferring the column to a labelled 1.5ml Eppendorf tube, 25µl RNase free water was added to the centre of the column and centrifuged at 10,000 rpm for 90 seconds to elute the RNA off the column.

2.4.1.1 Preparation of stock for on-column DNA clean up (Qiagen Cat# 79254)

Solid DNase I (1500 Kunitz units) was dissolved in 550ml RNase free water, mixed by gentle inversion and divided into 10µl aliquots of stock solution at -20°C. When required, these were thawed and made up to 80µl with RDD buffer stored at 4°C.

2.4.2 Quantification of mRNA

The NanoDrop spectrophotometer (Thermo Scientific) was used to quantify the extracted mRNA. It measures absorbance spectra of nucleic acids and provides a ratio of the absorbance of ultraviolet rays at 260 nm (DNA and RNA) to that at 280 nm (proteins) and 230 nm (salts such as thiocyanates, phenolates). In addition the platform allows absolute quantification of samples (Figure 2.3).

All DNase treated RNA samples were analysed using the NanoDrop. Only samples in excess of 0.5 µg RNA with a 260/280 ratio >1.8 and a 260/230 ratio >2.0 were selected for further analysis. All samples were extracted and stored in 20µl aliquots at -80°C until the end of the recruitment phase (3-6 months).

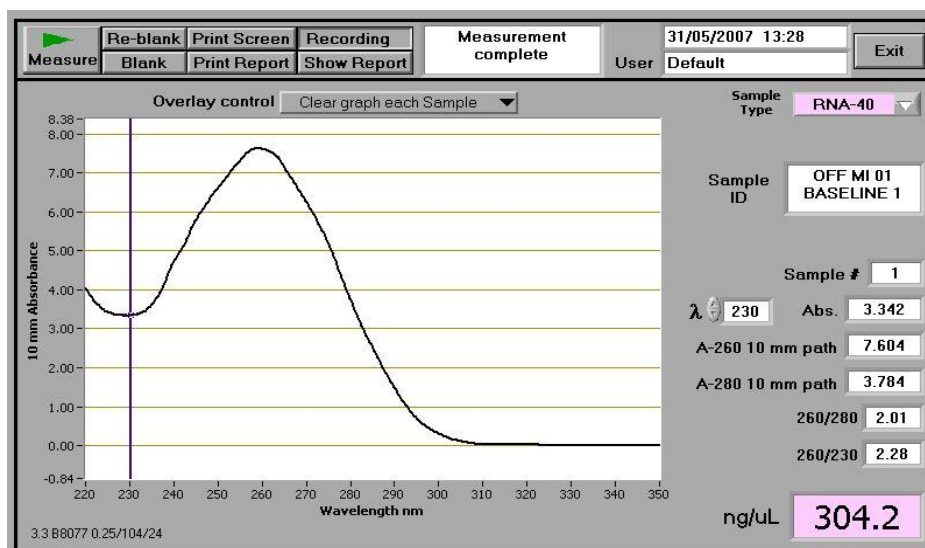


Figure 2.3: NanoDrop® method of RNA assessment.

The graph shows UV absorbance of different wavelengths by the RNA sample. 260/280 and 260/230 ratios >2.0 as shown (lower right corner of the image) confirm that the sample is of the required quality. RNA quantity is also sufficient at 304.2ng/μL (i.e., 6μg/20μL aliquot).

2.4.3 Confirmation of purity of RNA samples

Contamination by other cell types would invalidate the experiments. Monocyte RNA purity was assessed prior to transcriptome profiling by Q-PCR of lineage specific markers for RBCs (Glycophorin-A), platelets (GPIX), T lymphocytes (CD3), B lymphocytes (CD19), natural killer cells (CD56) and neutrophils (CD66b). No significant contamination was noted after 40 cycles of PCR (Figure 2.4).

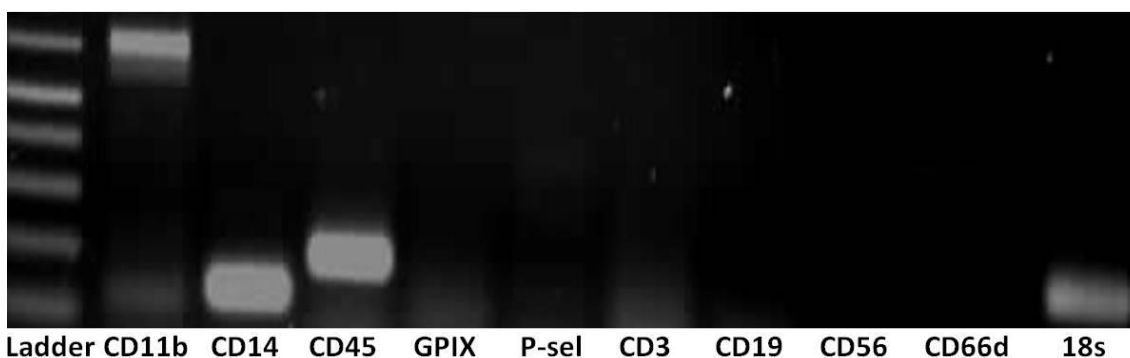


Figure 2.4: Assessment of cross-lineage cell contamination

The lanes 2 and 3 (CD11b and CD14) from the left show positive bands for lineage specific monocyte markers. Lane 4 (CD45) is a pan leukocyte marker. Lanes 5-10 confirm the absence of contamination by platelets (lanes 5-6, GP IX and P-selectin), T lymphocytes (lane 7, CD3), B lymphocytes (lane 8, CD19), natural killer cells (lane 9, CD56) and neutrophils (lane 10, CD66b).

2.4.4 Assessment of integrity of RNA samples

RNA samples are extremely susceptible to degradation. Over time, the lesser abundant and longer transcripts are the ones most likely to degrade. Therefore it is important to assess the integrity of these samples prior to microarray experiments. Traditionally, agarose gel electrophoresis has been used to assess the integrity of the RNA. Typically, on agarose gel, the sample shows two bands (28s and 18s) with the mRNA 'smear' straddling the 28s band. If any genomic DNA is present, this forms a band at the sample well. Degraded samples do not have the two bands; instead a homogenous smear concentrated at the low molecular weight region is observed.

However, agarose gel electrophoresis requires large quantities of RNA (at least 0.5 μg). Therefore, a microfluidics platform (2100 Bioanalyzer, Agilent) was used for analysis of RNA integrity. The Bioanalyzer chip has a microfluidics platform (gel impregnated interconnecting lattice of channels which analyses up to 12 $1\mu\text{l}$ samples containing $\geq 5\text{ng}$ total RNA simultaneously). This uses electrophoretic separation of RNA samples on the platform and subsequent quantification of laser induced fluorescence. Following this, an electropherogram and gel-like images are generated by the Bioanalyzer software.

The integrity of RNA samples was assessed prior to amplification and expressed as the RNA integrity number (RIN). The RIN is generated by a software algorithm which assesses degradation of the RNA sample by measuring the relative amplitudes of the 18S and 28S bands on the electropherogram (Figure 2.5) and comparing it to the degree of 'noise' in the baseline.

For eukaryotic RNA, RIN values are assigned from 1 to 10 in decreasing order of degradation, with 1 being the most degraded. The majority of the samples tested in optimisation experiments (n=24) had a RIN > 8.0 which is comparable to the expected quality for RNA samples following TRIzol extraction on the RIN database: http://www.chem.agilent.com/rin/_rinsearch.aspx. Study samples were analysed at the Wellcome Trust Sanger Institute (WTSI) and all passed their standard quality control assessment prior to microarray hybridisation.

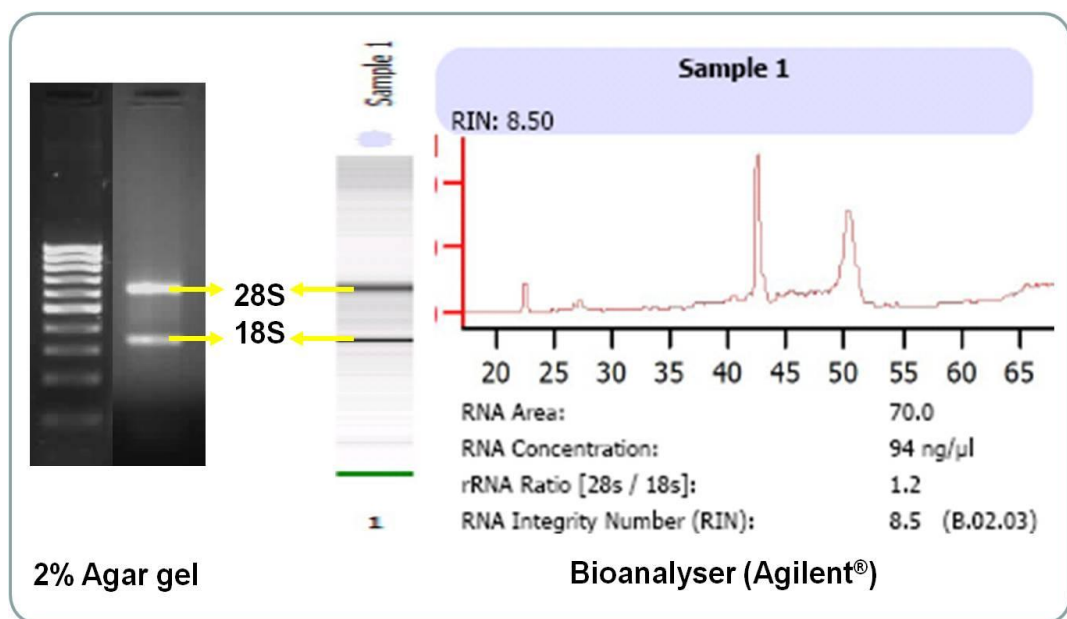


Figure 2.5: RNA integrity.

Assessment of RNA integrity by 2% agar gel is shown on the left. The two distinct bands (18S and 28S) are labelled. There is no evidence of degradation of the sample. A ladder is also shown for reference. On the right are shown the results of RNA sample analysis using an Agilent Bioanalyser. An image similar to the agar gel assay can be derived using the Bioanalyser software which again shows the distinct bands (18S and 28S). In addition, the software also allows derivation of a RIN value which confirms that the sample is of the quality expected from a TRIzol extraction protocol.

2.4.5 Confirmation of DNA elimination - 18S PCR

Ribosomal RNA (rRNA) components are encoded by genes that are organized as tandem rDNA repeating units (RNR1-5), in the p12 region of chromosomes 13, 14, 15, 21 and 22. Each rDNA unit encodes a 45S rRNA which is a precursor for 18S, 5.8S and 28S rRNA. Usually 30 to 40 repeats are found on each chromosome

although the numbers vary between individuals. In addition, 18S is a single exon gene with a highly conserved sequence in eukaryotic organisms. These features make it a very sensitive marker for the presence of genomic DNA.

18s primers (F&R) and probe, TaqMan® master mix and the RNA sample were made up to 10µl in nuclease free water and 40 cycles of Q-PCR was performed. The samples were then run on a 2% agarose gel for 30 minutes, stained with ethidium bromide and imaged using ultraviolet light. Samples with and without the gDNA elimination step are shown for comparison. As shown in this optimization experiment (Figure 2.6), all samples were free of gDNA after extraction.

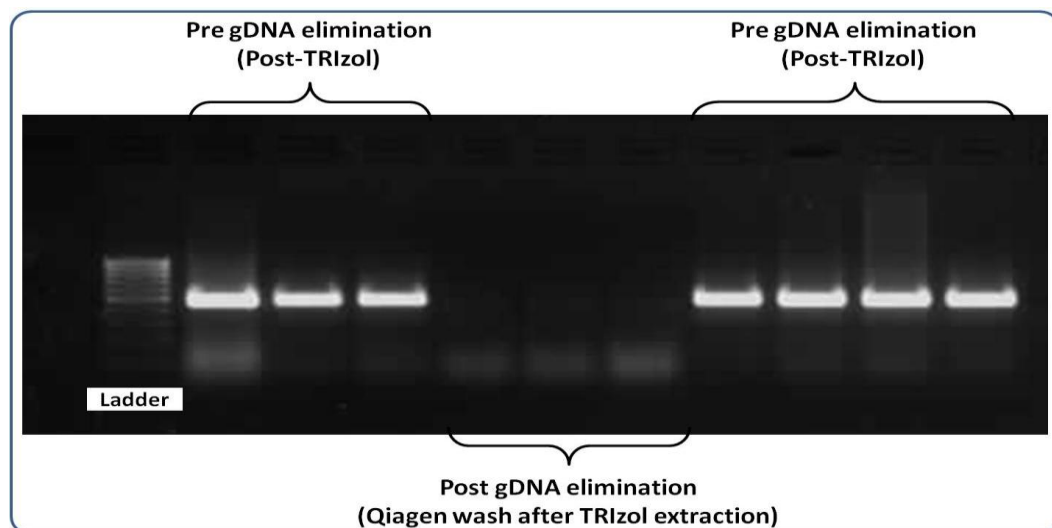


Figure 2.6: 18S PCR to assess contamination of RNA samples with genomic DNA.

The left lane shows the ladder followed by 10 lanes of samples. Of these, lanes 4-6 have samples treated with the on column DNase whilst samples in lanes 1-3 and 7-10 contain RNA samples which are not treated with the DNase. Significant contamination by genomic DNA is evident from the distinct 18S bands in the untreated samples.

2.4.6 Amplification of RNA samples by in vitro transcription (IVT)

Various methods have been employed for the amplification of messenger RNA prior to microarray hybridisation. We chose the in vitro transcription method to convert the RNA samples to cRNA using the Illumina TotalPrep® RNA

amplification kit (Ambion Cat# AMIL1791) which was recommended for use with the microarray platform. In vitro transcription is a linear amplification method which uses reverse transcription followed by a T7 RNA polymerase reaction for amplification. The TotalPrep® protocol allows amplification of small amounts of RNA (50-500ng) to yield biotinylated cRNA (100-1000 copies of each transcript after one round of amplification).

All total RNA samples for amplification were brought to a standard concentration of 100ng in 11µl of RNase free water. The first strand of cDNA was synthesised by adding 9µl of first strand master mix to the sample and incubating at 42°C for 2 hours, followed by the addition of 80µl of second strand master mix and incubation at 16°C in a thermal cycler for two hours. The next step was to collect the cDNA for in vitro transcription. For this 250µl of cDNA binding buffer was added to the sample and spun on a cDNA binding column for 1 minute at 10,000 rpm, followed by a second spin with a wash buffer. The cDNA was then eluted off the columns in two stages by addition of 10 and then 9µl nuclease free water at 55°C and centrifugation at 10,000 rpm for two minutes each. The double stranded cDNA was collected into a nuclease free Eppendorf (approximately 17.5µl) and after addition of 7.5µl IVT master mix incubated overnight (16 hours) at 37°C.

The IVT reaction was stopped the next morning by addition of 75µl nuclease free water and the cRNA was extracted using the cRNA filter cartridges. In this step, the cRNA (in 100µl aliquots) was mixed with 350µl cRNA binding buffer followed by 250µl absolute ethanol. The samples were then immediately spun at 10,000 rpm for 1 minute on the cRNA filter columns which adsorbs the cRNA. The columns were then washed using 650µl wash buffer which was centrifuged out

after 1-2 minutes incubation on the columns at room temperature. Additional dry spins ensured that all columns were devoid of any remaining traces of buffer (which may increase salt contamination). The cRNA was then eluted off the columns by addition of 100µl nuclease free water at 55°C and centrifugation at 10,000 rpm for 90 seconds. The cRNA was then quantified on the NanoDrop® spectrophotometer and 20µl aliquots were prepared containing 3µg cRNA which were hybridised on Illumina Human-6 v2 expression microarrays.

2.4.7 Hybridisation of amplified RNA to cDNA microarrays

The Illumina Human-6 expression BeadChip® (Figure 2.7) allows the analysis of six samples simultaneously. The array contains >48,000 probes derived from human genes in the National Center for Biotechnology Information (NCBI) Reference Sequence (RefSeq) and UniGene databases. Specifically, of the 48,804 transcript probe sets, 27,455 are coding transcripts and 446 are non-coding transcripts with well established annotation. An additional 8,066 transcripts with provisional annotation (7,870 coding and 196 non-coding) and a further 12,837 mRNA sequences that align to expressed sequence tags (UniGene Build 199) are also represented on this array.

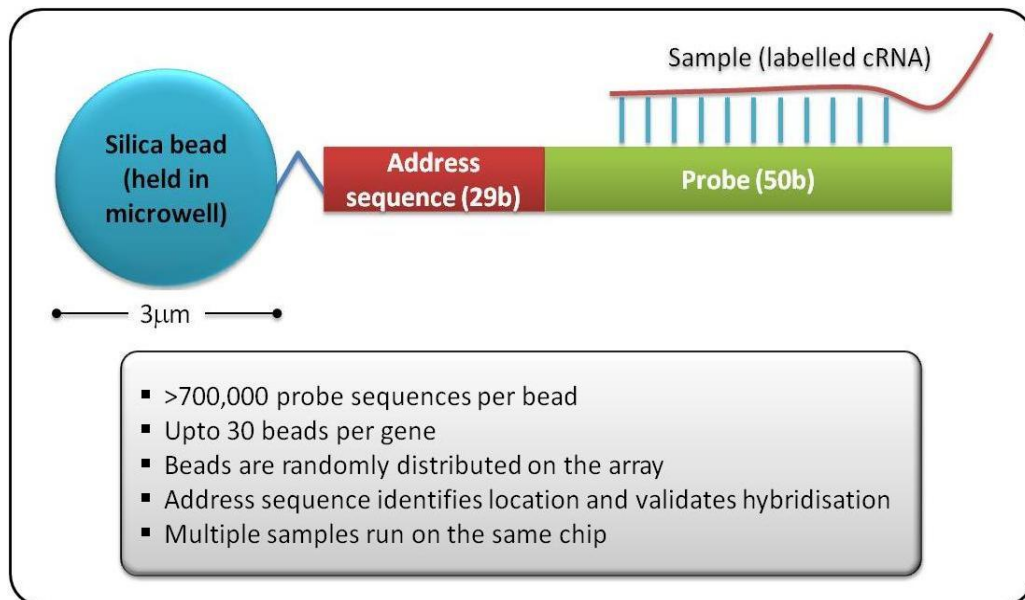


Figure 2.7: Design characteristics of the Sentrix BeadChip (modified from Illumina Gene Expression Datasheet)

The Illumina Sentrix BeadChip requires 1.5-3 μ g of cRNA for whole genome transcription profiling. The amplified IVT product was hybridised to the bead chip array and scanned using a Beadarray fluorescence reader. All microarray experiments were carried out at the Microarray suite in the Wellcome Trust Sanger Institute, Hinxton by Dr Peter Ellis. The Beadarray Reader takes 9 hours to scan each array and the results are obtained as fluorescent signal intensities.

2.5 POST HYBRIDISATION DATA ANALYSIS

The various steps in the analysis of raw microarray signal intensity data are summarized in Figure 2.8 below.

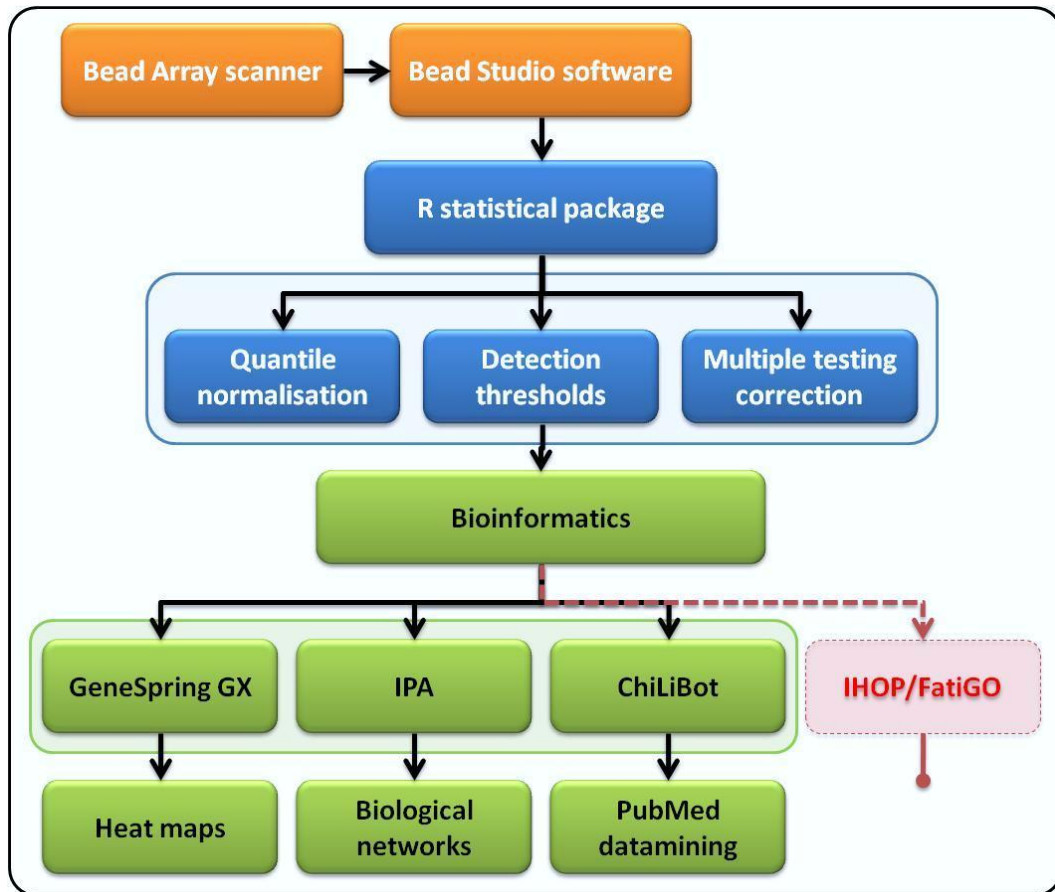


Figure 2.8: Scheme of analysis of microarray signal intensity data.

The three stages of Post Microarray data analysis are shown in this Figure. IHOP/FatiGo analysis at the bottom was not pursued further as they were superseded by the other bioinformatic analyses. (IPA – Ingenuity Pathway Analysis).

2.5.1 Bead Studio analysis

The single colour fluorescent signal intensities of each probe set on the array were quantified by the Beadarray Reader and then analysed using Bead Studio, a dedicated software that outputs the information on the arrays to a 'comma

separated values (.CSV)' file (access to facilities in the Platelet Group Laboratory, National Blood Centre, Cambridge kindly provided by Dr Nick Watkins).

The following information was obtained on each array:

- (i) the number of beads in each probe set (≥ 20 for 99.99% of probe sets)
- (ii) minimum, mean and maximum signal intensities of each probe set
- (iii) the standard deviation of signal intensities in the probe set
- (iv) the detection threshold signal intensity ($>99^{\text{th}}$ percentile of background fluorescence)

This signal intensity file is the reference file for all further statistical and bioinformatic analyses. The Beadarray scanner and Beadstudio conduct various pre-processing steps which include: (i) correction for local background fluorescence on the array and verification of positive controls, (ii) removal of outlier beads for each probe set, (iii) quantile normalization of fluorescent signal intensity data across multiple microarrays in the sample set and (iv) use of a clustering algorithm to exclude outlier data. All subsequent analyses described below were performed on the average signal intensities for all probe sets on the array.

2.5.2 Statistical analysis

The large datasets generated by microarray experiments, especially those at a whole genome scale, require powerful statistical tools. R is a commonly used statistical program and language which enables a variety of data analyses and graphical output.

The software was downloaded from <http://www.r-project.org/>. After installing R, the following packages for microarray analyses were downloaded from <http://www.bioconductor.org/> and installed: Akima, multtest, Affy, OCPlus,

Biobase, Affyio and preprocessCore. 'R scripts' (specific command prompts for statistical analyses – appendix page 379) were run for each of the comparisons shown in Table 2.7. The initial step was the preparation of a .TXT file containing the BeadStudio output file and a sample list ordered according to sample number and group.

	Post MI CRP	Control Baseline	Off MI CRP	Off Con Baseline
Post MI Baseline	Within group	Between groups		
Control CRP	Between groups	Within group		
Off MI Baseline			Within group	Between groups
Off Con CRP			Between groups	Within group

Table 2.7: Scheme for statistical analysis of gene expression profiles.

2.5.2.1 Quantile normalisation of microarray data

This protocol was initially developed for Affymetrix probe set arrays and uses the whole dataset. No assumptions are made in this normalization step about the distribution of signal intensities. Instead, this normalization method reorders the distribution of probe intensities by ranking the intensities in ascending or descending order in all arrays included in the analysis. The average signal intensity of each probe set was log transformed and then quantile normalized using the 'Affy' package in R.

2.5.2.2 Detection thresholds

To the normalised data set, 'detection thresholds' were applied to define 'present calls'. Present calls were determined based on the mean signal intensity of probe sets compared to the mean background signal intensity of the microarray. The 99th percentile of background signal intensity was chosen as the threshold for a probe set to return a 'present call'. By defining present calls with such stringency, a semi quantitative analysis of signal intensities was achieved, i.e., for each probe set, it was possible to determine the proportion of samples which returned present calls thereby allowing segregation of genes which returned present calls in all samples and those which were present only in a subset of samples. In addition, this helped to eliminate false positives arising from variations of small magnitude (below the resolution power of the Beadarray reader).

2.5.2.3 Statistical correction for multiple testing

The normalised dataset was analysed using the independent sample t-test for 'between groups' comparisons and the paired sample t-test for 'within group' comparisons. Additional statistical analyses were performed to account for false positives. The 'fdr2d' command was used to derive p values 'corrected' for multiple statistical testing as previously described (Ploner et al., 2006). Briefly, this is a statistical correction for false positive results, i.e., the false discovery rate (fdr) in more than one dimension (2D). This provides a 'local' or gene specific correction to the p value obtained for each gene depending on the magnitude of the differential expression compared to background signal intensity. This correction is less conservative than the Bonferroni correction for multiple testing.

2.5.2.4 Graphical depiction of differential gene expression – volcano plots

In large datasets such as microarray signal intensities, volcano plots (Figure 2.9) are useful means of summarising the magnitude and vector of changes in gene expression between two data sets. Such plots arrange genes according to fold change (x axis) and statistical significance (y axis). In this study volcano plots were generated for log₂ fold change (x axis) vs. -log₁₀ p-values (y axis).

The former gives an indication of the ‘biological’ differences between sample groups and the latter denotes the ‘strength’ of the observed differences. These plots have a typical ‘v’ shape with the least differentially regulated genes populating the middle of the dataset and the most differentially expressed genes with robust statistical significance found towards the top corners of the plot.

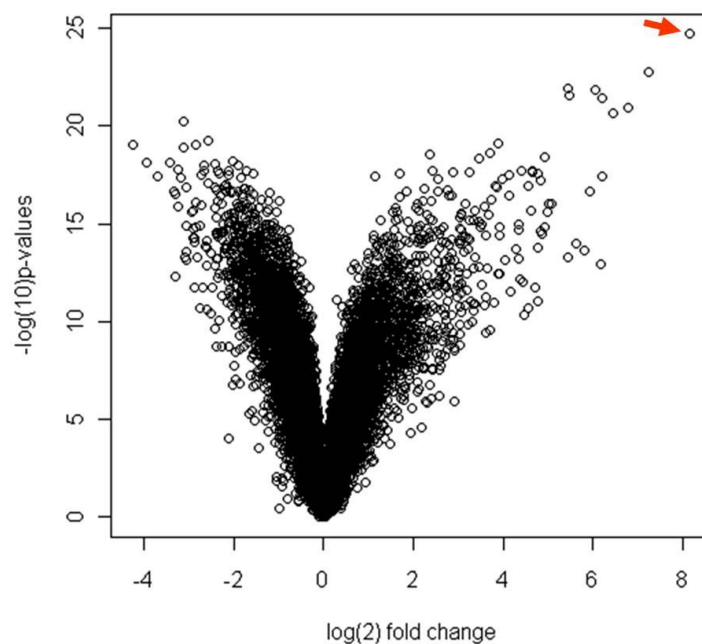


Figure 2.9: Sample volcano plot of differential gene expression.

Fold change is expressed in log₂ transformed values on the X axis and statistical significance is plotted on the Y axis as log₁₀ of p values. This plot shows the genes which are most differentially expressed after platelet mediated stimulation in Group 1 (Post MI). The arrow denotes the most up-regulated gene with the lowest p value (OLR1 - up-regulated >256 fold with a p value <10⁻²⁵).

2.5.2.5 Filtering of datasets to identify differentially expressed genes

After statistical analyses, the data was filtered as follows: (i) genes which did not return present calls (as determined by the detection thresholds set in the statistical analysis) in any of the samples were excluded, (ii) two statistical thresholds were used to filter the data, the crude p value (<0.05) and the fdr_{2d} corrected p value (<0.5), (iii) thresholds were set for the degree of change in transcript signal intensities (fold change) to identify the number of genes in the data set that were differentially expressed at a given p value threshold.

2.6 BIOINFORMATIC ANALYSIS OF MICROARRAY DATA

The genes with significant differences in transcript levels in each comparison were studied further using various bioinformatic resources (see Figure 2.8 above). In brief, the strategy was as follows:

1. GeneSpring GX was used to generate heat maps of differentially expressed genes in each comparison experiment (within group and between groups).
2. ChiLiBot was used for a systematic review of PubMed indexed literature on the candidate genes and their relationships with coronary disease.
3. Ingenuity Pathway Analysis (IPA) was used to generate molecular networks which integrate the functional roles of the differentially expressed genes.
4. IHOP and FatiGo were two other resources which were considered, but later superseded by IPA analysis.

2.6.1 GeneSpring GX

This is a gene expression data visualisation and analysis software which enables statistical and biological analysis of candidate genes.

It creates 'heat maps' of gene expression – these are visual representations of quantitative gene expression. The fluorescent signal intensities were colour coded by the software to indicate relative increases and reductions in gene expression. The expression profiles were clustered into groups based on conditions (resting vs. stimulated) or sample subject groups (cases vs. controls). In addition, this allowed the exploration of the role of biological factors in gene expression – such as age, cholesterol levels and other biometric variables.

Gene ontology analyses attribute descriptions to genes and gene products. This allowed a broad classification of genes based on their molecular function, the cellular component(s) they are located in and the biological process or pathway they contribute to. Such analyses helped to identify common pathways of association in apparently unrelated genes.

Once such clusters of genes were identified, the software allowed the analysis of patterns of expression of gene clusters to identify and describe molecular processes which involve multiple genes which could be selectively activated or inhibited in certain sample groups or conditions. GeneSpring also allowed the identification of 'shared genes' across groups, i.e., the generation of Venn diagrams to identify and explore genes which are differentially expressed in more than one comparison.

2.6.2 ChiLiBot analysis (<http://www.chilibot.net/>)

ChiLiBot (Chip based Literature searching robot) is a text mining software robot specially suited for 'PubMed' literature. This uses natural language processing (NLP) which allows the software to decipher the structure of sentences (in English) and the interaction between words. It is especially suited for microarray analyses in identifying previously described 'relationships' between candidate genes. It greatly simplifies literature mining by using 'syntax based rules' to define grammatical relationships between candidate genes.

For instance, it differentiates between 'interactive' relationships and 'parallel' relationships – the former where the candidate genes have an effect on each other (up-regulate/ activate/ modify etc) and the latter where they are merely in proximity to each other (mentioned in consecutive sentences, but not related by function).

Unlike PubMed which lists abstracts containing the key words, ChiLiBot provides the keywords in graphical form with a network of relationships with other candidate genes (or search terms). Another novel feature of ChiLiBot is the 'hypothesis generation' function. This is enabled by the ability to chart indirect relationships between genes. This is important in identifying causal relationships in complex biological processes where many genes interact at different stages in the process affecting the final outcome.

Using ChiLiBot, interactive networks were obtained for the candidate genes in all comparisons (between groups and within group) which identified and classified relationships between genes and also the relation of genes to specific search terms: 'atherosclerosis', 'coronary artery disease' and 'myocardial infarction'. The

synonym function on ChiLiBot allows the user to enter one search term for which the software generates all previously described synonyms in literature.

Figure 2.10 demonstrates the syntax based classification which allows ChiLiBot to generate interactive maps of search terms. The terms in pink boxes (spokes) are analysed for interactions with each other and with those terms in blue boxes (hubs) while the latter are not searched against each other.

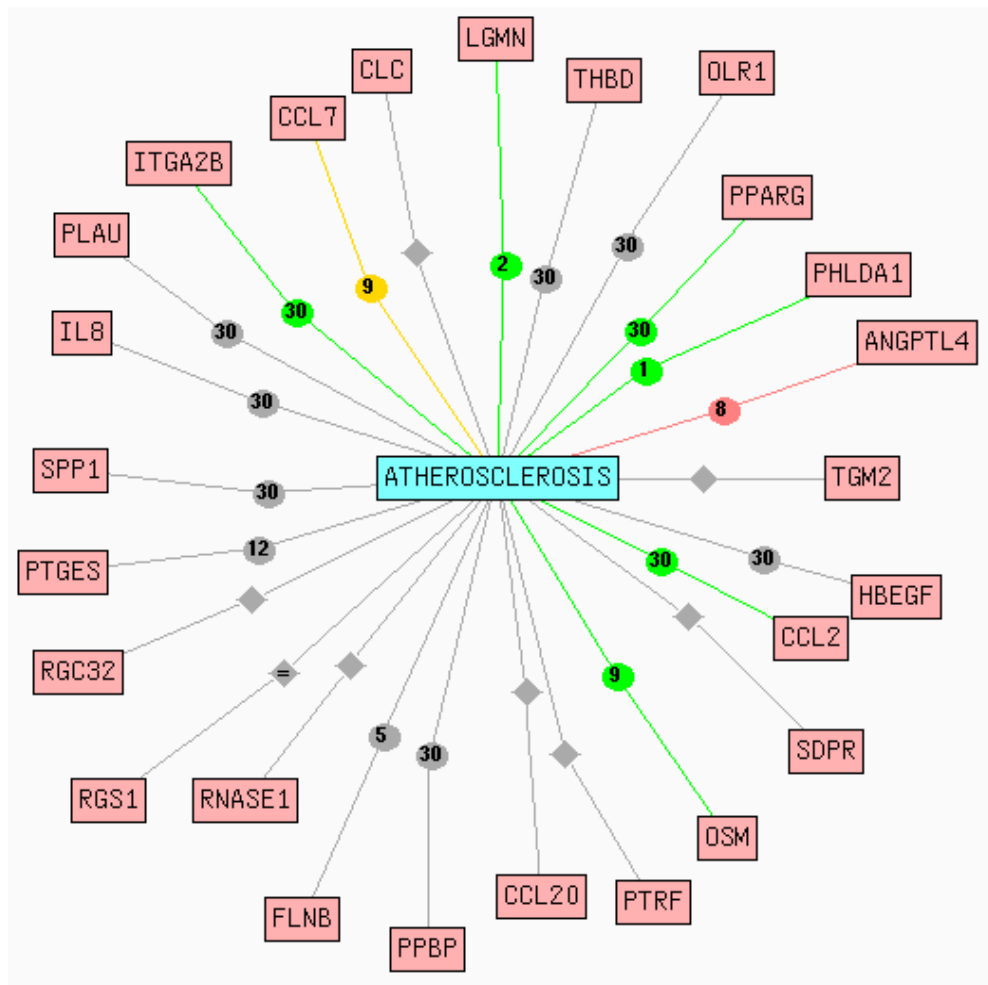


Figure 2.10: Interaction map (ChiLiBot) of candidate genes linked to term ‘atherosclerosis’.

The genes which have a parallel relationship with atherosclerosis in literature are connected by grey lines. These are terms which appear in literature in adjacent sentences without any direct link with the ‘hub’. By contrast, the green lines

connect terms which 'up-regulate' the 'hub', the yellow lines connect those which have a 'neutral' but definite interaction with the 'hub' and the red lines connect terms which 'down regulate' the 'hub' term. The numbers in the nodes indicate the number of abstracts in PubMed which provide evidence for these interactions.

2.6.3 IHOP (<http://www.ihop-net.org>)

Information Hyperlinked Over Proteins (IHOP) is an online search engine which allows the user to identify abstracts in PubMed citing the candidate gene(s). This also allows the visualisation of genes or proteins in the human genome which are mentioned in the same abstract as the gene of interest, thereby aiding the identification of novel associations between genes. However, this is purely a text based search engine with a high likelihood of false associations which were 'found' but were not validated by following up the apparent associations. Overall, the use of IHOP was limited to targeted search of literature on candidate genes for rapid literature review.

2.6.4 FatiGo in Babelomics

Babelomics is an online resource which allows functional analysis and interpretation of genome scale data thereby reducing the likelihood of false positive (i.e., statistically robust, yet functionally irrelevant) observations.

FatiGo, one of the web tools on Babelomics assigns the most characteristic Gene Ontology (GO) term to each gene list, then uses the Fisher's exact test (corrected for multiple testing) to compare two lists of genes and identify the GO terms which are significantly different (adjusted p value) in the two lists. Although this was used for initial data analysis, it was superseded by Ingenuity Pathway analysis (IPA)

2.6.5 Ingenuity pathway analysis (Ingenuity Systems, CA)

Ingenuity pathway analysis (IPA) is an online analytical tool for gene expression data in a biological context. It assigns molecular functions, interactions, biological networks and canonical signalling pathways to the gene expression dataset. It also allows identification of phenotype states which have known associations with the candidate genes of interest as well as transcription factors with regulatory roles on these genes. IPA uses the Ingenuity® Knowledge Base, a repository of biological interactions and functional annotations derived from published literature after manual review of full text articles. IPA generates schematics and interaction maps of the genes of interest which incorporates the structural details, functional roles and sub cellular location of the proteins coded by these genes.

IPA analysis was carried out on the common genes expressed in all groups following stimulation and the differentially expressed genes in each case/control experiment. Only the data for the common genes expressed in monocytes in all groups after CRP-XL mediated stimulation is included in the thesis (Chapter 3).

2.7 QUANTITATIVE REVERSE TRANSCRIPTASE-PCR (RT-PCR) OF DIFFERENTIALLY EXPRESSED GENES

Following analysis of microarray data, candidate genes were selected on the basis of statistical and biological significance for validation by Q-PCR. All stored RNA samples were DNase treated (in addition to the on column DNase treatment during initial RNA extraction) prior to RT-PCR using the AMP-D1 (Sigma) kit. RNA samples were incubated at room temperature for 15 minutes with DNase 1 and reaction buffer, following which a stop solution was added to inactivate DNase 1 which was then denaturised by 10 minute incubation at 70°C. Following this, all samples were converted to cDNA by RT-PCR.

2.7.1 Synthesis of cDNA from mRNA for quantitative RT-PCR

The DNase treated samples were incubated at 65°C for five minutes with dNTPs and a combination of oligoDT and random hexamer primers. After cooling on ice (one minute), the samples were centrifuged and then mixed with first strand buffer, 0.1M DTT, RNaseOUT and SuperScript III. Following this they were incubated at 25°C for five minutes and ramped up in 5°C increments (30 seconds each) to 45°C. Following 60 minutes incubation at this temperature, the reaction was inactivated by heating to 70°C for 15 minutes.

2.7.2 Selection of a control gene (see appendix page: 389 for details)

The first step was the identification of a suitable control gene. Although genes such as 18S and GAPDH are commonly used control genes in Q-PCR, there were important issues to consider in these analyses.

1. The cycle lengths of the control gene and the gene of interest should be comparable. As one cycle of Q-PCR equates to a two fold increase in sample, high abundance genes such as 18S which frequently amplify at 10-12 cycles may mask small fold changes in gene expression of low abundance transcripts. Therefore 18S was used as a control gene for some of the initial experiments but this was then replaced by TBP (see below).
2. The use of a stimulus (CRP-XL) affects the expression of many genes, including commonly used control genes. To assess this further, microarray gene expression analysis software (GeneSpring GX, see below) was used to analyse fluorescent signal intensities of commonly used control genes including β 2 microglobulin, β actin, cyclophilin A, GAPDH, HMBS, HPRT1, PLA2 G4B, RPLP, SDH and TBP. The control gene which had least variation following stimulation experiments was selected following this analysis.

The gene that satisfied the two criteria mentioned above was TATA box protein (TBP). This is a low to moderate abundance transcript in nucleated cells which does not show significant variation in expression following CRP-XL stimulation. This was used in the majority of the Q-PCR experiments as the control gene.

2.7.3 Amplification of cDNA by quantitative PCR (Q-PCR)

Absolute quantification was used for validation given the small fold changes in microarray signal intensity of differentially expressed genes. Inventoried TaqMan® (Applied Biosystems) primers and probes (FAM) were used (Table 2.8). A second colour probe (Yakima yellow) was used for the control gene (TBP; Eurogentec Cat# RT-CKYD-TBP) in a duplex PCR reaction which allowed the generation of a standard curve and absolute quantification of gene expression.

In each reaction 2µl of cDNA was incubated with 18µl master mix (comprising of 10µl TaqMan GE master mix, 1µl TaqMan probe, 1.2µl TBP protein primer, 0.4µl TBP probe, 5.4µl RNase free water). To minimise technical and pipetting error, case and control samples were included on the same 96 well plate. All reactions were conducted in triplicate and outliers were excluded where applicable from analysis.

Gene	Catalogue no:
AOAH	HS00155735_M1
CCL3	HS00234142_M1
CYP27A1	HS00168003_M1
DGKD	HS00177552_M1
EGR1	HS00152928_M1
HPSE	HS0018D737_M1
HSP90AB1	HS00607336_8H
ITGB1	HS00236976_M1
MEIS1	HS00180020_M1
ONCOSTATIN M	HS00171165_M1
OROSOMUCOID 1	HS01590791_M1
PROCR	HS00941182_M1
STIP1	HS00428979_M1
TBP (control gene)	HS00920494_M1
TFPI	HS00196731_M1
THBD	HS00264920_S1

Table 2.8: List of TaqMan primers.

Q-PCR was performed on a 7900HT Fast Real Time PCR system (ABI) as follows: Stage 1: 50°C for 2 minutes, Stage 2: 95°C for 10 minutes, Stage 3: 40 cycles of 95°C for 15 seconds and 60°C for 1 minute. 50 cycles were used in Stage 3 for low abundance genes. Transcript abundance was determined from the fluorescent signal intensities on microarray.

CHAPTERS 3-9

Results

OVERVIEW OF THE RESULTS CHAPTERS

The first Chapter in this section (**Chapter 3**) describes changes in monocyte gene expression following a platelet-mediated stimulus (CRP-XL) that were common to all four groups. This explores the cellular and molecular responses of the monocyte to a pathophysiologically relevant stimulus and substantiates the hypothesis that *platelet driven stimulation of circulating monocytes plays an important role in the initiation, progression and manifestation of atherosclerotic coronary artery disease*. Differentially expressed genes across all four study groups are analysed for molecular interactions of relevance to atherosclerosis. This Chapter is unique in its perspective in that the aim is to gain a mechanistic insight into the monocyte response following exposure to activated platelets.

The following Chapter (**Chapter 4**) focuses on the differences in gene expression in subjects with premature CAD when compared to healthy control subjects. This starts with a descriptive analysis of the differentially expressed genes in resting monocytes followed by the changes in gene expression after stimulation with CRP-XL activated platelets. Following this, a similar analysis is performed on the offspring groups to identify patterns in gene expression in resting and stimulated monocytes (**Chapter 5**).

Chapter 6 examines whether the same genes are differentially expressed in the MI and Offspring of MI groups. Gene transcripts with similar trends in expression profiles in the two groups are considered an enriched dataset for further analysis for their causal involvement in MI. This is followed by an analysis of these genes to identify associations of variants in the genes with risk of MI and CAD and eQTLs in these genes that associate with monocyte gene expression.

CHAPTER 3: RESULTS

Response of the monocyte transcriptome to a platelet mediated stimulation

3.1 INTRODUCTION

Platelet mediated stimulation of circulating monocytes is the central experiment in this project. This was performed to identify changes in gene expression following stimulation and to amplify differences in gene expression in cases vs. controls. This Chapter provides an account of the changes to monocyte gene expression in all four study groups following platelet-mediated stimulation (CRP-XL).

Peripheral venous whole blood samples from all four study groups were incubated for four hours with CRP-XL (Figure 3.1). This achieved platelet-mediated stimulation of circulating monocytes as evidenced by a high percentage of monocyte platelet aggregates (MPAs) detected by flowcytometry (Figure 3.2), resulting in significant differential gene expression compared to unstimulated (baseline) samples. The genes at the extremes of differential expression were the same in all groups. Further analyses of differentially expressed genes were performed to identify common trends in gene expression following platelet-mediated stimulation (CRP-XL).

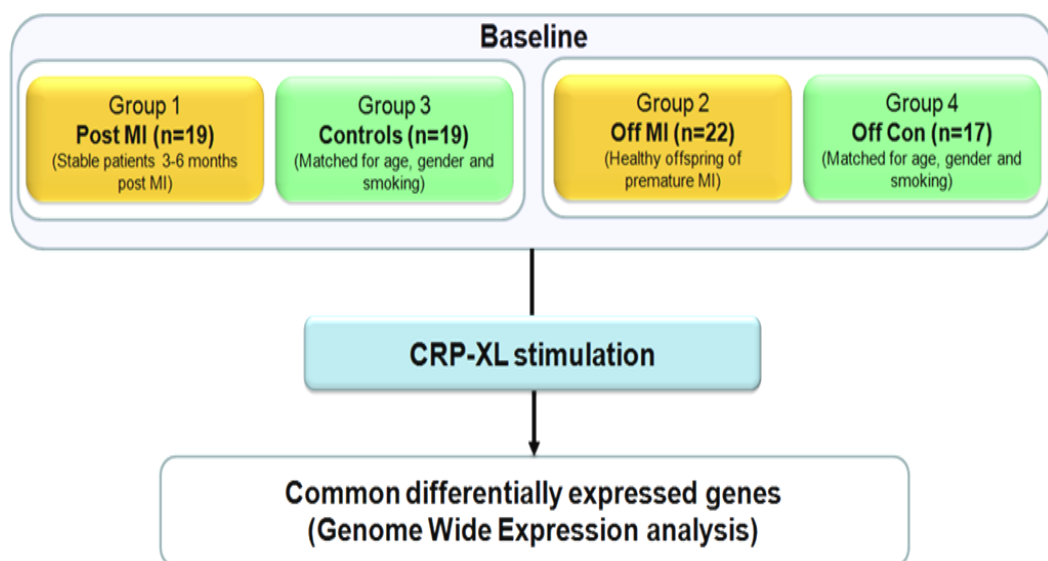


Figure 3.1: Scheme of platelet-mediated stimulation for all study groups.

Identical protocols for stimulation with CRP-XL were used in all groups. Flowcytometry was used at baseline to confirm that the monocytes were in a resting state and after stimulation to ensure adequacy of the platelet mediated stimulus. Figure 3.2 below shows that all groups had <20% MPAs at baseline, but this rose significantly in all groups following platelet-mediated stimulation.

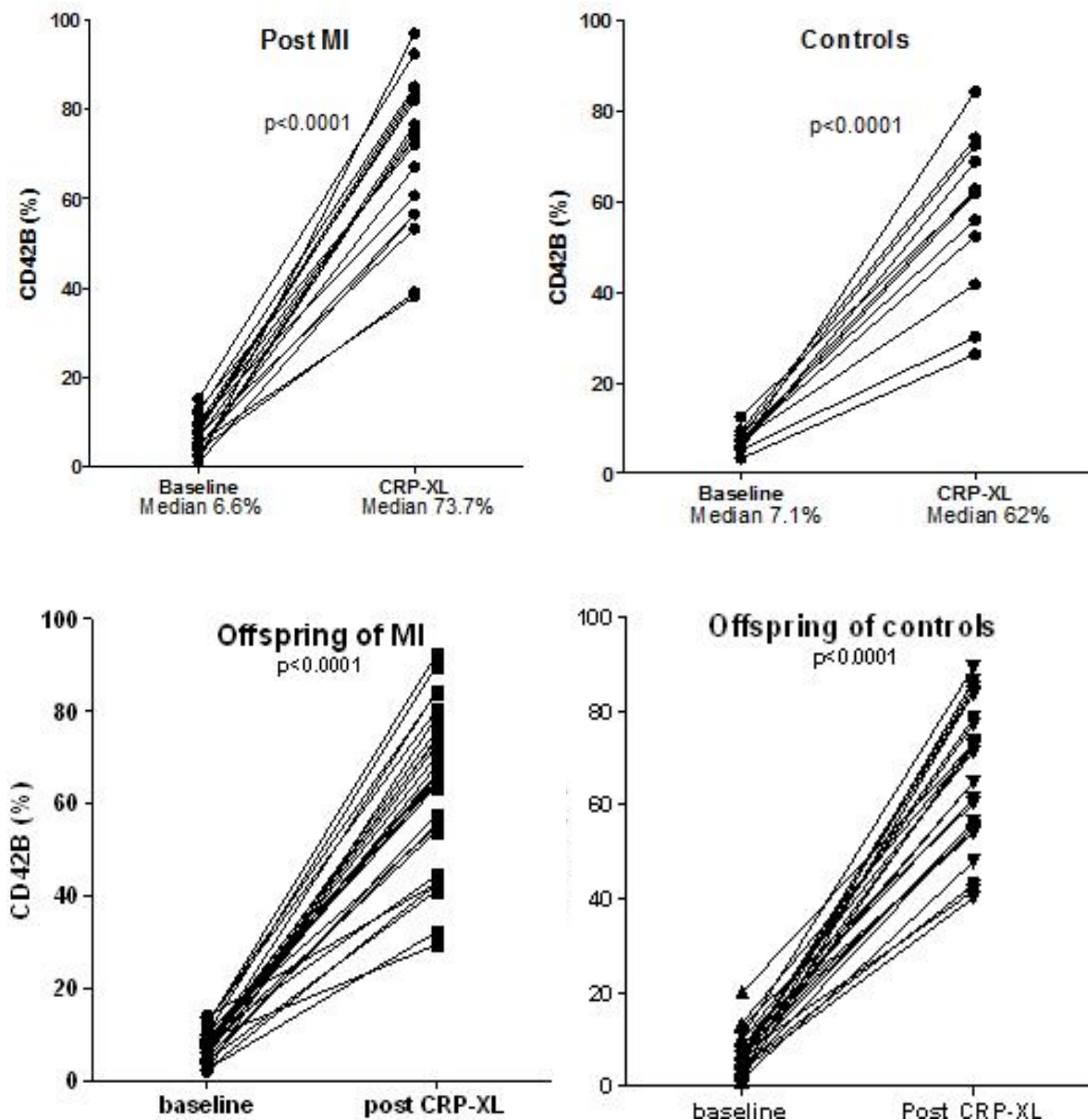


Figure 3.2: Flowcytometry of activated monocytes following platelet-mediated stimulation. At baseline, there is minimal platelet mediated monocyte stimulation as evidenced by low levels of monocyte-platelet aggregates (MPA) in all four groups. Following CRP-XL stimulation, a significant increase in MPA formation is seen in all groups indicating high levels of monocyte activation (shown on the y-axis as the % of CD42b+ve monocytes).

3.2 DIFFERENTIALLY EXPRESSED GENES: SUMMARY

The microarray signal intensities were quantile normalised and clustered according to treatment type (baseline vs. stimulated) for each study group. Heat maps were generated for all groups with transcript probes coloured according to signal intensity. Up-regulated transcripts were coded in yellow and down regulated transcripts in blue. As an example, the monocyte transcriptome before and after platelet-mediated stimulation in a control group (Group 4) is shown (Figure 3.3).

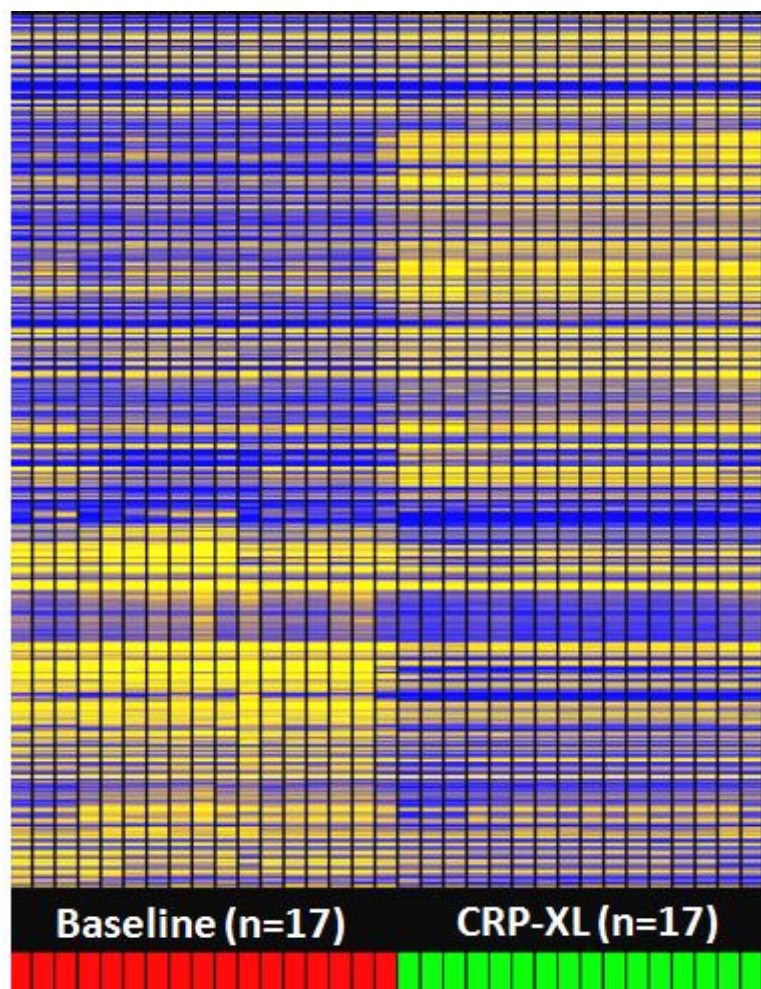


Figure 3.3: Heat map of microarray signal intensities.

Signal intensities of monocyte gene expression from 17 offspring controls in Group 4 before and after platelet-mediated stimulation are shown. The up-regulated genes following CRP-XL are represented as yellow blocks and the down regulated genes as blue blocks. The red bars at the bottom mark the baseline samples while the green bars denote samples following platelet-mediated stimulation (17 in each group). Cluster analysis revealed perfect alignment of gene expression profiles into baseline and CRP-XL groups. Similar heat maps were obtained in all other groups.

Sigmoid plots (Figure 3.4 a & b) are useful in depicting the profiles of gene expression across the entire dataset. Baseline signal intensities for each probe set are averaged across all subjects in a group. These are depicted graphically with the probe sets on the x axis in the order of increasing fluorescent signal intensities on a \log_{10} scale on the y axis. The corresponding signal intensities for the same probe sets after platelet-mediated stimulation demonstrate differential gene expression. For example, in Figure 3.4a below, the first row shows average signal intensities for each probe set at baseline and the second row shows the corresponding signal intensities after stimulation. This reveals that platelet-mediated stimulation results in significant differential expression of genes across the entire range of signal intensity in both groups.

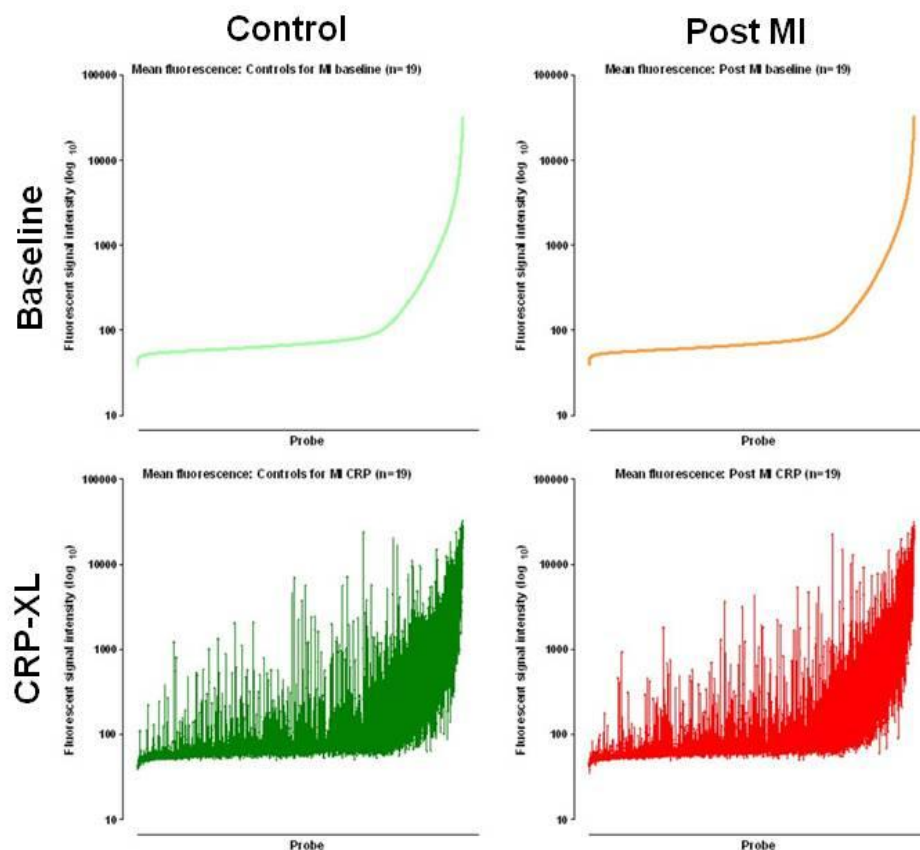


Figure 3.4a: Sigmoid plots of signal intensity in resting and stimulated monocyte samples.

This shows baseline fluorescent signal intensities of all probe sets and corresponding changes in signal following platelet-mediated stimulation (CRP-XL) in Post MI (Group 1) and control group (Group 3).

Figure 3.4b shows a similar trend in gene expression profiles in Offspring of MI and Control offspring.

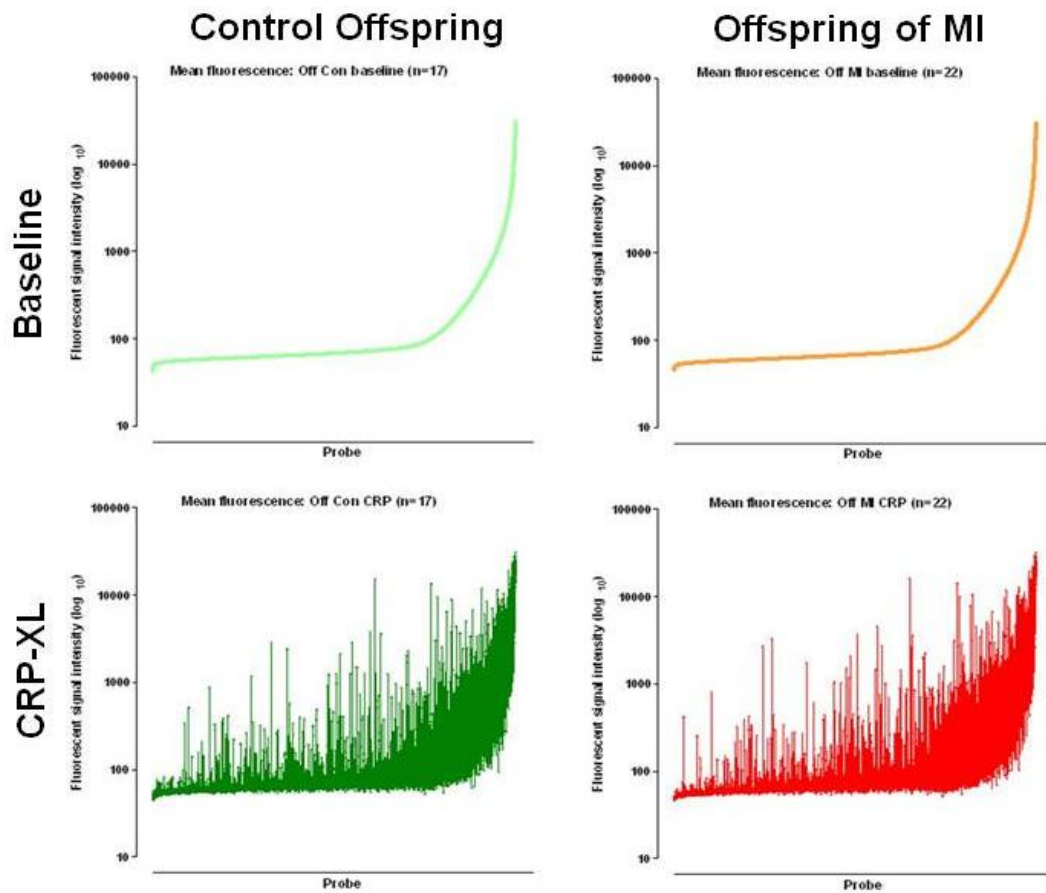


Figure 3.4b: Sigmoid plots of signal intensity in resting and stimulated monocyte samples.

This shows baseline fluorescent signal intensities of all probe sets and corresponding changes in signal following platelet-mediated stimulation in Offspring of MI (Group 2) and Control offspring (Group 4).

All gene transcripts with a p value <0.05 , a false discovery rate (FDR2D) of $<1\%$ (a stringent threshold was applied to select the most significant changes in gene expression after stimulation), and present calls in one or more subjects per group qualified for further analysis. A subset of genes which showed >10 fold up-regulation or <0.2 fold down regulation (CRP-XL/baseline) were arbitrarily deemed as showing significant differential expression and analysed further. The volcano plots (Figure 3.5) illustrate the subset of genes in each group which fulfilled the above filtering criteria.

Considering the top left volcano plot in Figure 3.5 (Post MI baseline vs CRP) as an example, on the x axis, the down regulated genes constitute the left limb of the volcano plot while the up-regulated genes populate the right limb. Therefore the most differentially expressed genes lie at the extreme ends of the x axis. The y axis denotes the statistical significance of the observed differential expression. Differentially expressed genes with increasing statistical significance are higher on the y axis. Therefore the top left and top right regions of the volcano plot (shaded blue and yellow respectively) contain the most differentially expressed and statistically significant genes which were selected for further analysis.

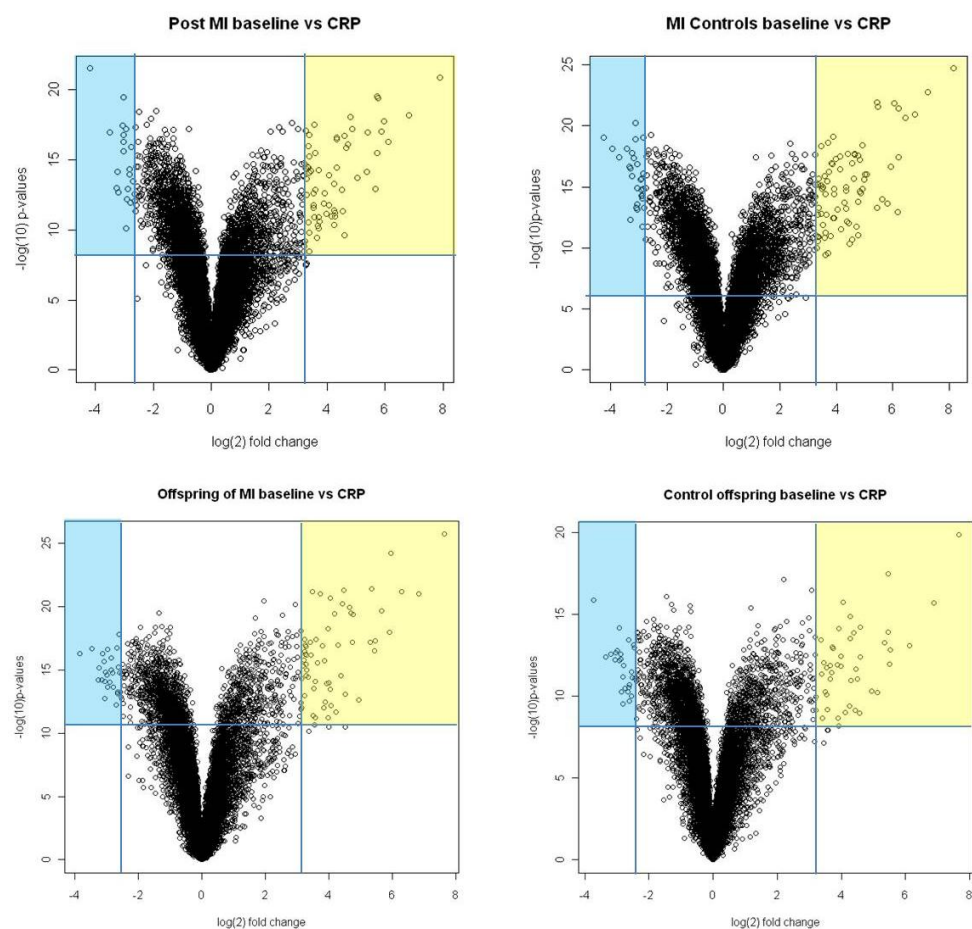


Figure 3.5: Volcano plots of differential gene expression in monocytes after platelet-mediated stimulation in all study groups.

Distribution of differentially expressed CD14⁺ monocyte gene transcripts following stimulation of whole blood for 4 hours at 37°C with CRP-XL. Log₂ of fold change (CRP-XL/baseline) is plotted on the x-axis and log₁₀ of p-values (t test, uncorrected) is plotted on the y-axis. The yellow and blue shaded regions contain up and down regulated transcripts respectively which fulfil the filtering criteria for subsequent candidate gene analyses.

3.2.1 Identification of shared up-regulated gene transcripts after platelet mediated stimulation

The Venn diagram (Figure 3.6) below shows each of the four groups in different rectangles: Post MI (Group 1, blue), Controls for MI (Group 3, orange), Offspring of MI (Group 2, purple) and Control offspring (Group 4, green).

The red circle in the centre denotes the 36 transcripts that were up-regulated >10 fold when compared to baseline in all four groups. The green circle highlights the 2 transcripts that were up-regulated to this degree in the Post MI and Offspring of MI groups while the 1 transcript that was up-regulated in the two control groups are shown in the blue circle. The latter two groups of transcripts were studied separately (see Chapter 6).

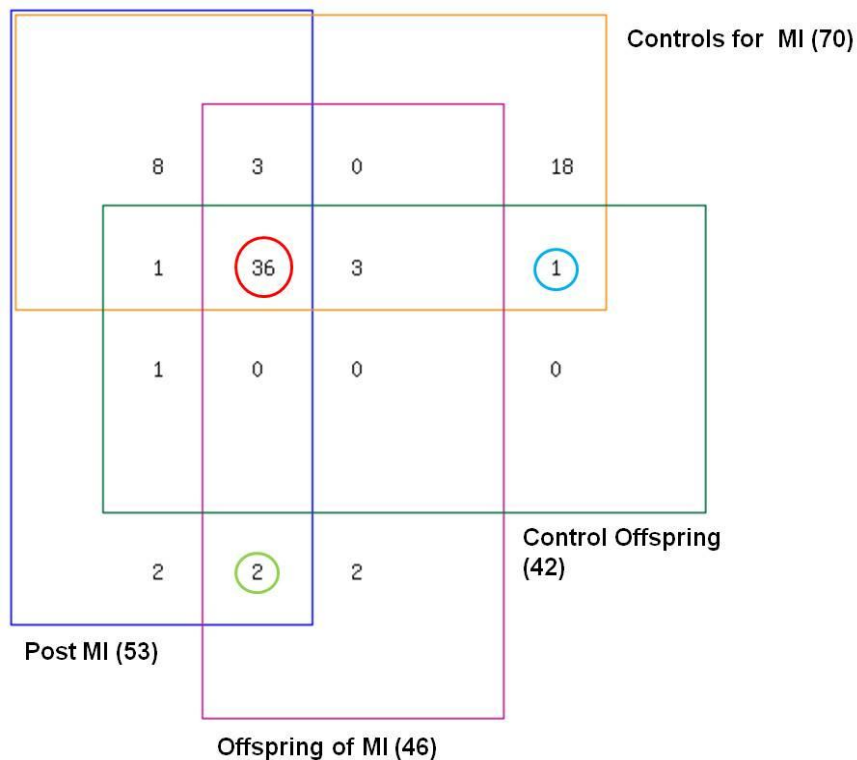


Figure 3.6: Venn diagram of up-regulated genes following platelet-mediated stimulation.

Distribution of up-regulated CD14⁺ monocyte gene transcripts following stimulation of whole blood for 4 hours at 37°C with CRP-XL. The red circle contains transcripts shared by all groups, the green circle contains those shared by study groups (Post MI and Offspring of MI) while the blue circle contains those shared by the controls (Controls for MI and offspring controls).

3.2.2 Identification of shared down regulated gene transcripts after platelet mediated stimulation

Shared down regulated genes across all four groups were identified as shown within the red circle in the Venn diagram (Figure 3.7). 25 transcripts were down regulated to <0.2 of baseline expression levels (i.e., >5 fold down regulation) in all four groups when compared to baseline.

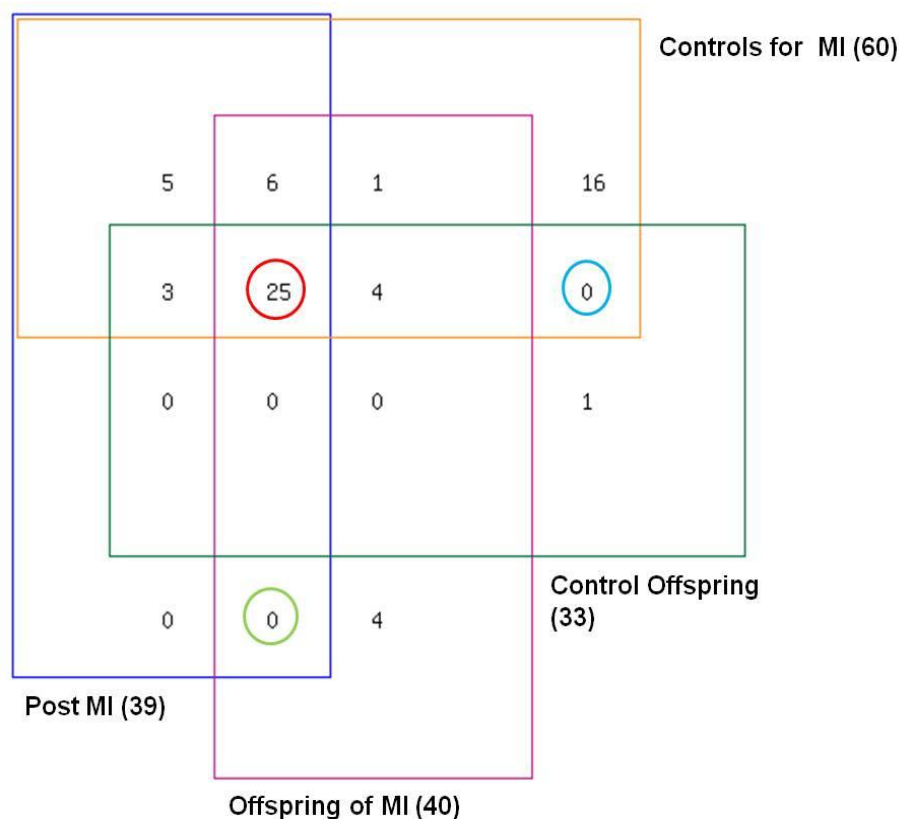


Figure 3.7: Venn diagram of down regulated genes following platelet-mediated stimulation. The Figure shows the distribution of down regulated gene transcripts following stimulation of whole blood for 4 hours at 37°C. The red circle contains transcripts shared by all groups, the green circle contains those shared by study groups (Post MI and Offspring of MI) while the blue circle contains those shared by the controls (Controls for MI and offspring controls).

Differentially expressed genes common to all four groups – 36 up-regulated (yellow) and 25 down regulated (blue) – are listed in Table 3.1 below according to fold change.

Probe_ID	Gene ID	Fold change after platelet-mediated stimulation			
		Post MI	MI Controls	Offspring (MI)	Control offspring
ILMN_17381	OLR1	237.65	284.87	199.07	202.05
ILMN_7641	TGM2	113.32	152.04	113.37	117.65
ILMN_13176	DDIT4	69.72	56.29	59.98	45.52
ILMN_2226	C15orf48	62.43	73.14	61.89	45.93
ILMN_13668	RIS1	58.94	110.81	77.99	69.44
ILMN_13832	PHLDA1	53.64	87.22	39.40	40.92
ILMN_12432	DHRS3	52.67	65.72	40.98	43.62
ILMN_23315	TKTL1	52.64	43.90	43.86	23.68
ILMN_9394	SPP1	50.37	72.79	22.83	21.62
ILMN_1789	CCL20	42.67	73.06	43.17	30.98
ILMN_13137	OSM	41.24	49.62	50.31	44.14
ILMN_13922	GP1BB	32.72	60.59	22.99	22.79
ILMN_20242	LGMN	28.90	44.62	26.99	23.90
ILMN_11463	STX1A	28.18	43.50	26.11	22.06
ILMN_19154	FPRL2	26.23	30.62	25.09	24.05
ILMN_22301	PTRF	25.29	20.23	16.50	12.65
ILMN_25446	SLC7A5	24.38	25.13	22.24	19.44
ILMN_2247	IL8	24.07	27.22	30.59	34.98
ILMN_3436	RGS1	22.89	20.33	11.80	13.01
ILMN_14549	RGC32	20.26	25.19	19.61	19.53
ILMN_13131	C12orf59	20.03	23.34	12.41	16.71
ILMN_2778	PTGES	19.94	28.77	14.90	14.76
ILMN_20440	ANGPTL4	19.36	28.84	16.87	11.83
ILMN_22847	RNASE1	19.15	27.51	16.11	19.81
ILMN_13741	IL7R	19.09	24.67	17.99	15.19
ILMN_25185	CCL2	18.94	32.49	15.70	18.96
ILMN_21428	G0S2	17.63	13.16	15.19	11.85
ILMN_18708	CLEC5A	16.66	27.42	21.55	20.93
ILMN_10556	SLC16A10	15.90	28.60	26.86	14.85
ILMN_22074	PPBP	15.09	34.04	14.34	15.87
ILMN_24123	CCL7	14.84	31.79	11.72	17.47
ILMN_10912	THBD	13.05	21.36	14.54	11.72
ILMN_11513	SDPR	12.51	30.12	10.37	11.32

Probe_ID	Gene ID	Fold change after platelet-mediated stimulation			
		Post MI	MI Controls	Offspring (MI)	Control offspring
ILMN_21371	FLNB	12.12	17.43	13.35	13.36
ILMN_13020	HBEGF	11.68	12.27	13.83	10.37
ILMN_17241	MARCKSL1	10.39	13.15	12.06	13.23
ILMN_19500	LRRRC33	0.20	0.12	0.13	0.17
ILMN_29052	ALS2CR13	0.20	0.15	0.18	0.16
ILMN_23335	EVA1	0.19	0.14	0.14	0.16
ILMN_2211	GIMAP7	0.18	0.14	0.12	0.14
ILMN_820	SLC27A3	0.18	0.16	0.18	0.19
ILMN_18797	LOC340061	0.18	0.17	0.19	0.19
ILMN_27567	EDG2	0.17	0.12	0.16	0.16
ILMN_9671	DPYSL2	0.17	0.11	0.15	0.13
ILMN_8572	APOL3	0.16	0.13	0.12	0.14
ILMN_24441	CD33	0.16	0.15	0.15	0.18
ILMN_657	C4orf18	0.16	0.14	0.16	0.16
ILMN_8593	CX3CR1	0.14	0.13	0.17	0.19
ILMN_7981	GPBAR1	0.14	0.14	0.12	0.15
ILMN_5569	RTN1	0.14	0.09	0.10	0.12
ILMN_8583	CHST13	0.14	0.13	0.12	0.16
ILMN_6869	GIMAP8	0.13	0.12	0.13	0.14
ILMN_2022	ADRB2	0.13	0.17	0.16	0.20
ILMN_16803	IL15	0.12	0.11	0.13	0.14
ILMN_10869	TSCOT	0.12	0.10	0.14	0.14
ILMN_14069	FUCA1	0.12	0.11	0.09	0.11
ILMN_6233	C6orf192	0.12	0.10	0.11	0.13
ILMN_13694	C20orf27	0.11	0.10	0.11	0.12
ILMN_19730	E2F2	0.11	0.08	0.12	0.13
ILMN_1013	RASSF4	0.09	0.06	0.10	0.10
ILMN_1908	CACNA2D3	0.06	0.05	0.07	0.08

Table 3.1: Common differentially expressed genes following CRP-XL stimulation.

The up-regulated transcript IDs are in yellow (n=36) and the down regulated in blue (n=25). Fold change across all four groups are tabulated. All transcripts fulfilled the filtering thresholds (present calls in >1, fold change >10 or < 0.2, uncorrected p value <0.05, false discovery rate [FDR2D] <0.01).

3.3 GENE ONTOLOGY ANALYSIS OF DIFFERENTIALLY EXPRESSED MONOCYTE GENES AFTER CRP-XL STIMULATION

These genes showed similar profiles of expression following platelet-mediated stimulation in all groups and therefore constitute the ‘response to platelets’ in human monocytes. Among the most highly up-regulated genes in all four groups (>10 fold with a false discovery rate <1%) Oxidised LDL Receptor 1 (OLR1) was most differentially expressed at 200 fold from baseline signal intensity while calcium channel, voltage-dependent, alpha 2/delta subunit 3 (CACNA2D3) was down regulated to 0.05 fold.

3.3.1 Gene Ontology analysis of genes after stimulation

The list of 36 up-regulated transcripts was analysed further using the PANTHER classification system. Interrogation of the PANTHER database limiting to the human genome identified 23 genes from this list. Gene ontological analyses were performed to classify these 23 candidate genes according to molecular function (Table 3.2), biological process (Table 3.3), protein class (Table 3.4) and functional pathway (Table 3.5) as follows.

Molecular function	Genes (n)	Gene ID
Binding	11	ANGPTL4, CCL2, CCL20, CCL7, CLEC5A, HBEGF, IL8, MARCKSL1, OLR1, OSM, PPBP
Catalytic activity	4	DHRS3, LGMN, NMES1, PTGES
Receptor activity	3	CLEC5A, FPR3, OLR1

Table 3.2: Up-regulated genes classified according to molecular function.

Biological process	Genes (n)	Gene ID
Cell communication	12	ANGPTL4, CCL2, CCL20, CCL7, CLEC5A, FPR3, HBEGF, IL8, MARCKSL1, OLR1, OSM, PPBP
Cellular process	12	ANGPTL4, CCL2, CCL20, CCL7, CLEC5A, FPR3, HBEGF, IL8, MARCKSL1, OLR1, OSM, PPBP
Immune system process	11	ANGPTL4, CCL2, CCL20, CCL7, CLEC5A, FPR3, IL8, OLR1, OSM, PPBP, PTGES
Response to stimulus	9	ANGPTL4, CCL2, CCL20, CCL7, CLEC5A, IL8, OLR1, PPBP, PTGES

Table 3.3: Up-regulated genes classified according to biological process.

Protein class	Genes (n)	Gene ID
Signalling molecule	11	ANGPTL4, CCL2, CCL20, CCL7, CLEC5A, HBEGF, IL8, MARCKSL1, OLR1, OSM, PPBP
Defence/immunity protein	3	ANGPTL4, CLEC5A, OLR1
Receptor	3	CLEC5A, FPR3, OLR1

Table 3.4: Up-regulated genes classified according to protein class.

Pathway	Genes (n)	Gene ID
Inflammation mediated by chemokines and cytokine signalling pathway	5	CCL2, CCL20, CCL7, CLEC5A, FPR3, IL8

Table 3.5: Up-regulated genes classified according to pathway.

25 transcripts were down regulated <0.2 fold when compared to baseline. The list of down regulated genes was analysed further using the PANTHER classification system. Interrogation of the PANTHER database limiting to the human genome identified 25 genes from the list of 25 transcripts with significant down regulation.

Gene ontological analyses were performed to classify these 25 candidate genes according to molecular function (Table 3.6), biological process (Table 3.7), protein class (Table 3.8) and functional pathway (Table 3.9) as follows.

Molecular function	Genes (n)	Gene ID
Binding	6	BUD31, CD33, E2F2, IL15, RASSF4, RIN2
Receptor activity	6	CD33, CX3CR1, DRB2, GPBAR1, LPAR1, LRRC33
Transporter activity	5	APOL3, C6orf192, CACNA2D3, MPZL2, SLC27A3
Catalytic activity	4	CHST13, DPYSL2, FUCA1, SLC27A3
Transcription regulator	2	BUD31, E2F2

Table 3.6: Down regulated genes classified according to molecular function.

Biological process	Genes (n)	Gene ID
Cellular process	11	ADRB2, CACNA2D3, CD33, CX3CR1, E2F2, GPBAR1, IL15, LPAR1, LRRC33, MPZL2, RASSF4
Cell communication	10	ADRB2, CACNA2D3, CD33, CX3CR1, E2F2, GPBAR1, IL15, LPAR1, LRRC33, RASSF4
Transport	9	ADRB2, APOL3, C6orf192, CACNA2D3, MPZL2, RIN2, RTN1, SLC27A3, SCL46A2
Immune system process	5	CD33, CX3CR1, GIMAP7, GIMAP8, IL15, LRRC33
Cell adhesion	3	CD33, LRRC33, MPZL2
Apoptosis	3	IL15, RASSF4

Table 3.7: Down regulated genes classified according to biological process.

Protein class	Genes (n)	Gene ID
Receptor	6	ADRB2, CD33, CX3CR1, GPBAR1, LPAR1, LRRC33
Transporter	5	APOL3, C6orf192, CACNA2D3, MPZL2, SLC27A3
Transcription factor	2	BUD31, E2F2
Cell adhesion molecule	2	CD33, MPZL2

Table 3.8: Down regulated genes classified according to protein class.

Pathway	Genes (n)	Gene ID
Inflammation mediated by chemokine and cytokine signalling pathway	2	CX3CR1, IL15
Beta2 adrenergic receptor signalling pathway	1	ADRB2
Interleukin signalling pathway	1	IL15

Table 3.9: Down regulated genes classified according to pathway.

3.3.2 Common genes after platelet-mediated stimulation: Identification of biological networks

The 48 differentially expressed genes (23 up-regulated and 25 down regulated) were analysed as a single group to identify molecular interactions. Identification of such biological networks was performed using the online resource, Ingenuity Pathway Analysis (IPA).

This is a dynamic analysis which compares the observed frequency of interactions between the molecules of interest compared to the expected frequency of interactions and assigns a score depending on the strength of the former. This does not represent established signalling or metabolic pathways, but uses reported interactions from scientific literature stored in a dedicated online database, Ingenuity Knowledge Base (IKB) to draw network maps. A 'p score' is assigned to each network which expresses the probability of clustering the genes into a network by random association ($p \text{ score} = (-) \log_{10} p\text{-value}$). A $p \text{ score} > 3$ denotes a $p \text{ value} < 0.001$ or a 99.9% probability that the network is not generated by chance alone. Three biological networks were identified as listed in Table 3.12.

Biological network	P score	Genes (n)
Inflammatory Response, Cellular Movement, Cell-To-Cell Signalling and Interaction	19	13
Cell-To-Cell Signalling and Interaction, Tissue Development, Cardiovascular System Development and Function	14	10
Inflammatory Response, Gastrointestinal Disease, Haematological Disease	5	5

Table 3.12: Biological networks involving differentially expressed genes after CRP-XL.

IPA allowed spatial and functional depiction of genes of interest. Interaction maps were generated for each biological network depicting the sub-cellular location of candidate genes and their molecular interactions. A brief description of these networks is provided in the following section.

3.3.2.1 Network 1: Inflammatory Response, Cellular Movement, Cell-To-Cell Signaling and Interaction

The 13 differentially expressed genes in this network (Figure 3.8) included 10 genes which were up-regulated and 3 genes which were down regulated after platelet-mediated stimulation.

The up-regulated genes included cytokines (monocyte chemoattractant protein 1 [MCP1/CCL2], monocyte chemoattractant protein 3 [MCP3/CCL7], monocyte-derived neutrophil chemotactic factor [IL8], Oncostatin M and Osteopontin [SPP1]), enzymes (RNASE1, prostaglandin E synthase [PTGES]), transporter (apolipoprotein L3 [APOL3]) and other molecules (apoptosis-associated nuclear protein [PHLDA1], G0/G1switch 2[G0S2]). The down regulated genes included cytokines (IL15) and G-protein coupled receptors (Fractalkine receptor [CX3CR1], lysophosphatidic acid receptor 1 [LPAR1/EDG2]).

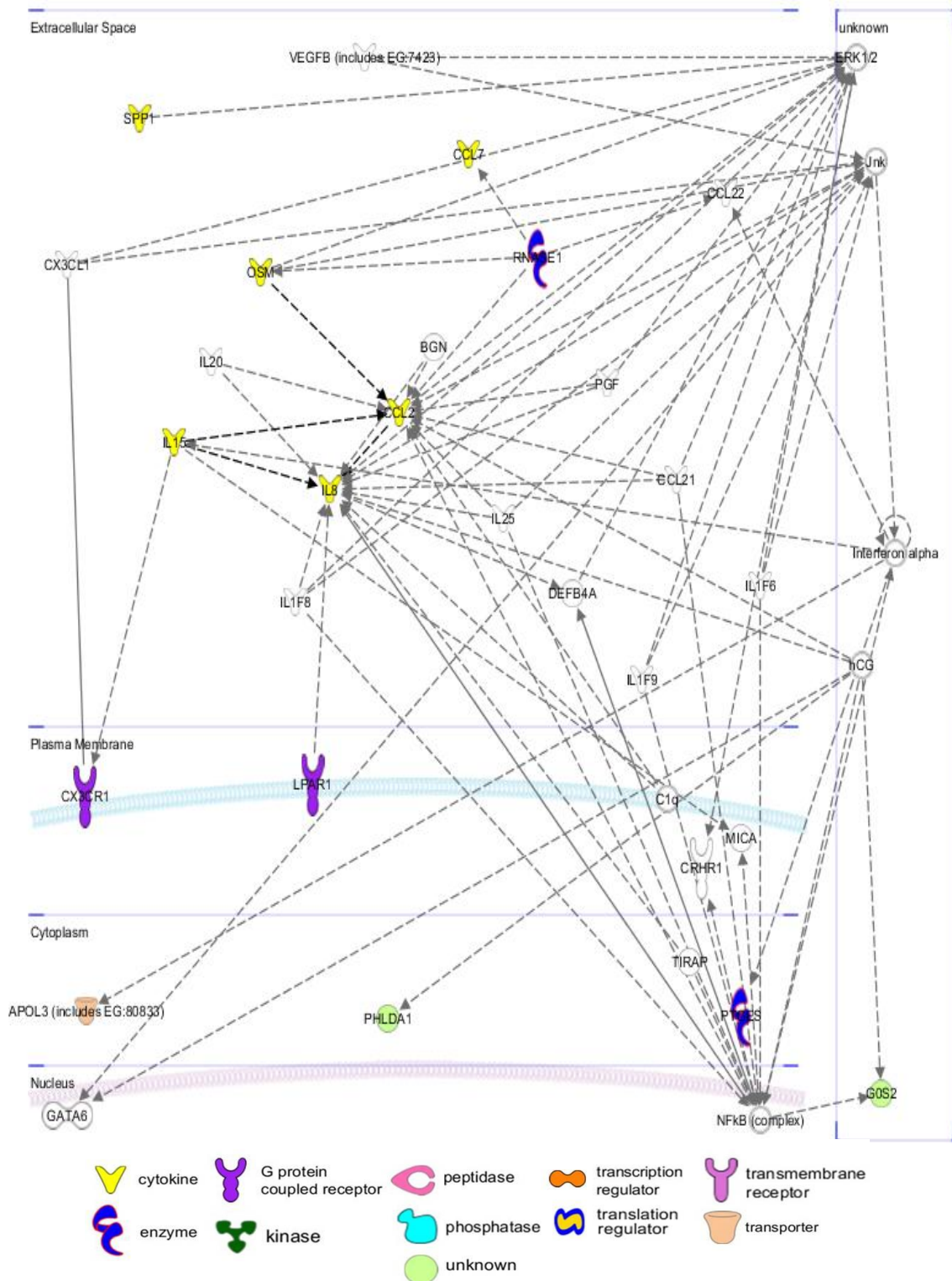


Figure 3.8: Inflammatory Response, Cellular Movement, Cell-To-Cell Signalling and Interaction.

The molecules highlighted in colour are those which were differentially expressed in all groups following platelet mediated stimulation of monocytes for 4 hours at 37°C. A key is provided at the bottom of the Figure.

3.3.2.2 Network 2: Cell-To-Cell Signaling and Interaction, Tissue Development, Cardiovascular System Development and Function

The 10 differentially expressed genes in this network (Figure 3.9) included 9 genes which were up-regulated and 1 gene which was down regulated after platelet-mediated stimulation.

The up-regulated genes included cytokines (beta-thromboglobulin [BTG1/PPBP/CXCL7], heparin-binding epidermal growth factor [HBEGF]), transmembrane receptors (oxidized low-density lipoprotein receptor 1 [OLR1], IL7 receptor [IL7R]) and other molecules (PPARG angiopoietin related protein [ANGPTL4], glycoprotein Ib (platelet), beta polypeptide [GP1BB], DNA-damage-inducible transcript 4 [DDIT4], filamin B [FLNB] and macrophage myristoylated alanine-rich C kinase substrate [MARCKSL1]). The down regulated gene was the G-protein coupled receptor, beta-2 adrenergic receptor [ADRB2].

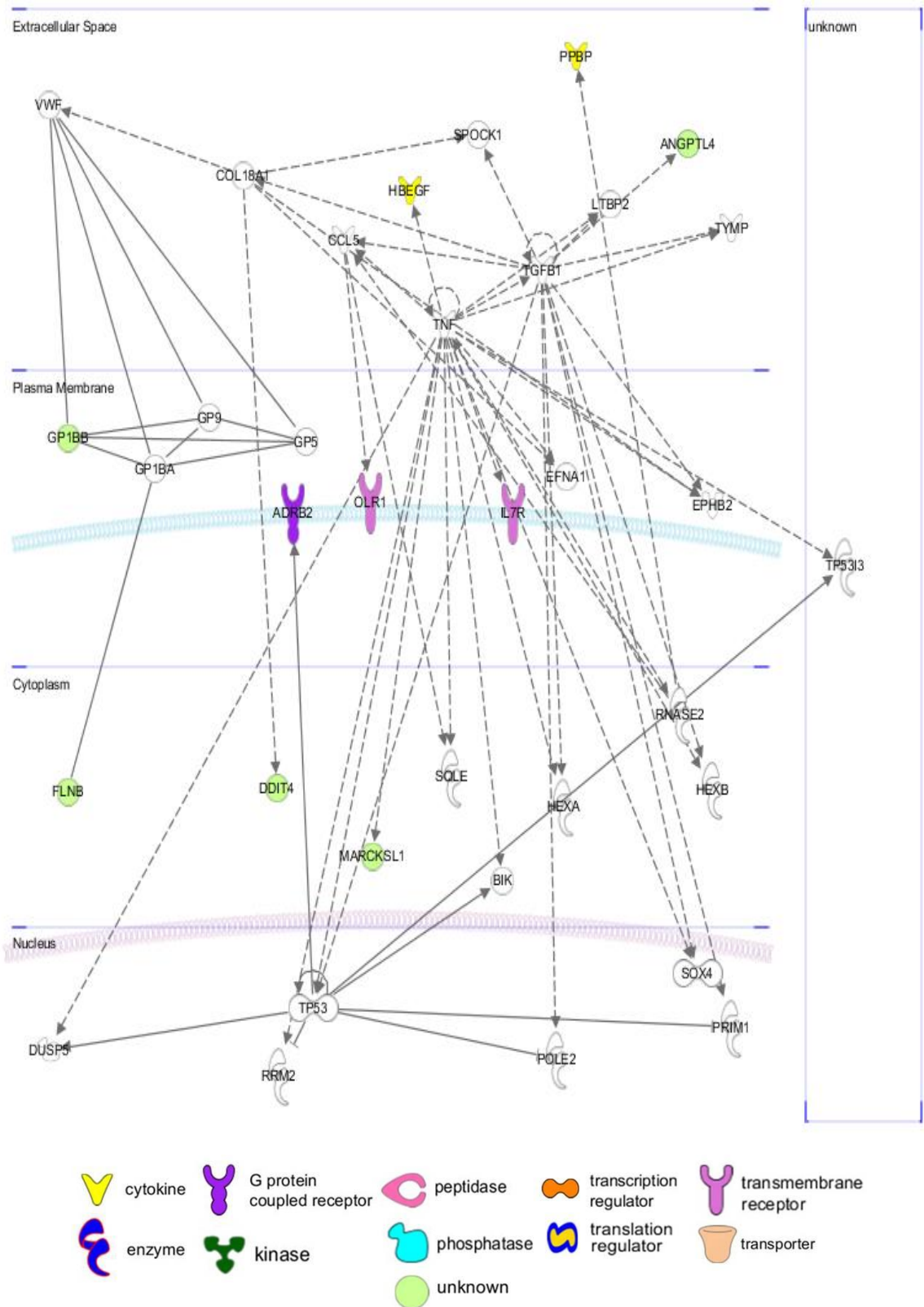


Figure 3.9: Cell-To-Cell Signalling and Interaction, Tissue Development, Cardiovascular System Development and Function.

The molecules highlighted in colour are those which were differentially expressed in all groups following platelet mediated stimulation of monocytes for 4 hours at 37°C. A key is provided at the bottom of the Figure.

3.3.2.3 Network 3: Inflammatory Response, Gastrointestinal Disease, Hematological Disease

The 5 differentially expressed genes in this network (Figure 3.10) included 4 genes which were up-regulated and 1 gene which were down regulated after platelet-mediated stimulation.

The up-regulated genes included the cytokine macrophage inflammatory protein 3 alpha [CCL20], the transmembrane receptor, thrombomodulin [THBD], the cytoplasmic enzyme transglutaminase 2 [TGM2) and serum deprivation-response protein [SDPR]. The down regulated gene was the myeloid cell surface antigen CD33.

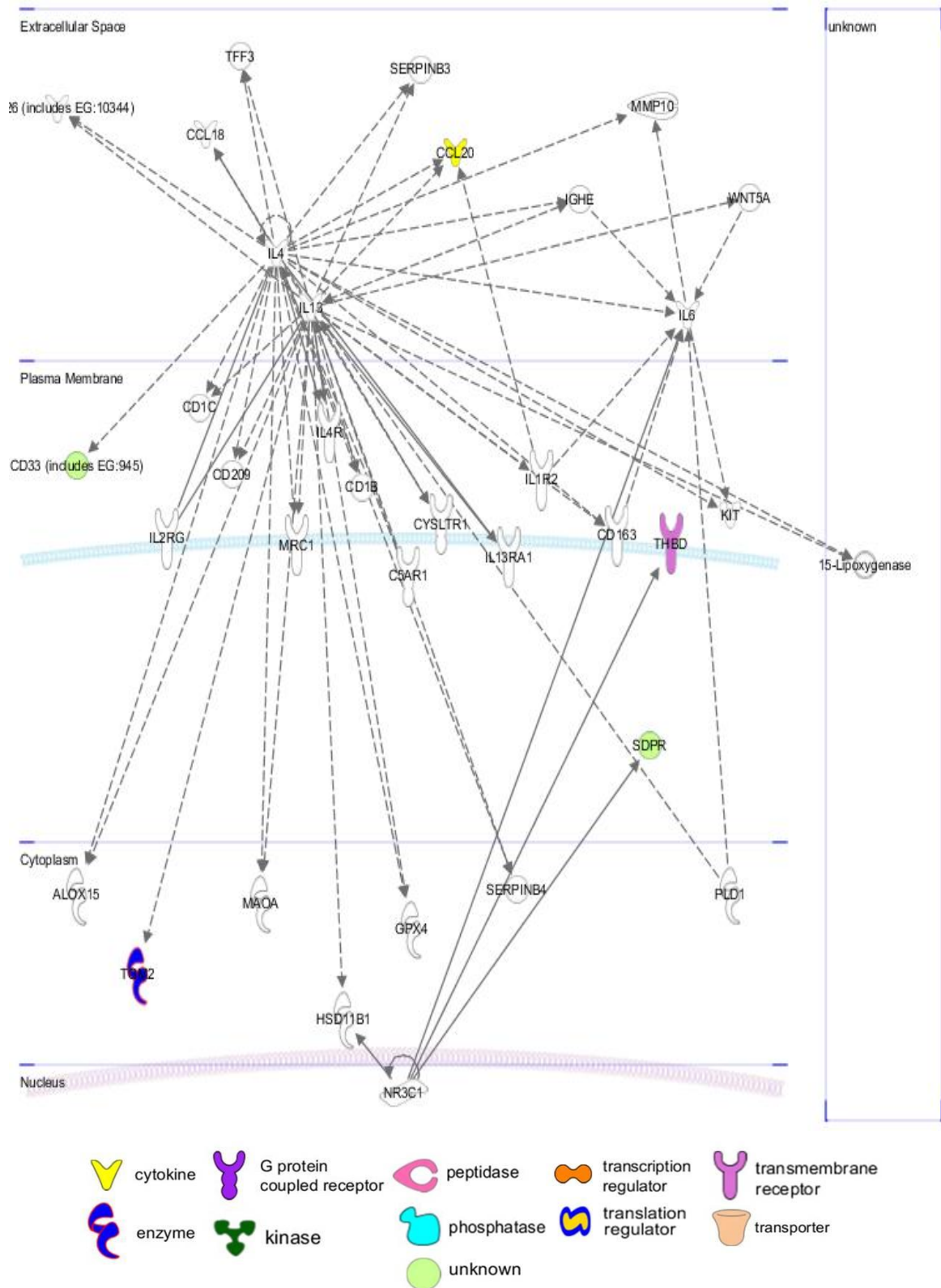


Figure 3.10: Inflammatory Response, Gastrointestinal Disease, Haematological Disease.

The molecules highlighted in colour are those which were differentially expressed in all groups following platelet mediated stimulation of monocytes for 4 hours at 37°C. A key is provided at the bottom of the Figure.

3.4.1.1 Genes up-regulated after stimulation with platelets common to all groups

3.4.1.1.1 Oxidized LDL receptor 1 (OLR1, LOX1, CLEC8A); Chr 12p13.2-p12.3

Oxidised LDL receptor 1 belongs to the c-type lectin super family and is regulated through the cyclic AMP signalling pathway. Oxidised LDL up-regulates OLR1 and promotes endothelial cell proliferation, apoptosis, and vascular remodelling (Lu et al., 2011a). OLR1 expression in vascular smooth muscle cells and tissue macrophages is inducible by various stimuli including $TNF\alpha$, $TGF\beta$ and fluid shear stress (Hayashida et al., 2005). This receptor takes up oxidized LDL (Sakurai and Sawamura, 2003), mediates endothelial phagocytosis of apoptotic cells and promotes platelet adhesion (Kakutani et al., 2000, Morawietz, 2010). OLR1 also functions as a receptor for the heat shock protein HSP60 (Xie et al., 2010).

The expression profiles of OLR1 before and after CRP-XL (platelet-mediated) stimulation in all four study groups are shown in Figure 3.13. In all groups, OLR1 is essentially 'switched off' in resting monocytes (baseline) as evidenced by the consistently low signal intensities in all groups. After stimulation, there is a significant up-regulation of OLR1 expression. The fluorescent signal intensities in the 20-40,000 range suggests that OLR1 is a highly expressed gene in monocytes following platelet-mediated stimulation.

The fold change following stimulation was higher in controls of MI than in the Post MI group. This is likely to be a result of statin therapy in the Post MI group which has been shown to reduce OLR1 expression (Puccetti et al., 2005). OLR1 was expressed at similar levels in Offspring of MI and their controls.

The significant up-regulation of OLR1 in circulating monocytes following a platelet mediated stimulus using cross linked collagen related peptide suggests possible

mechanisms of OLR1 up-regulation *in vivo*. Collagen mediated activation of platelets and subsequent platelet-mediated OLR1 up-regulation in monocytes may lead to oxidised LDL uptake and atherogenesis.

This may also occur after a plaque rupture event as suggested by studies in patients presenting to hospital with acute coronary syndromes. These patients have significantly higher levels of soluble OLR1 compared to patients with stable angina and those with normal coronary arteries (Kume et al., 2010) .

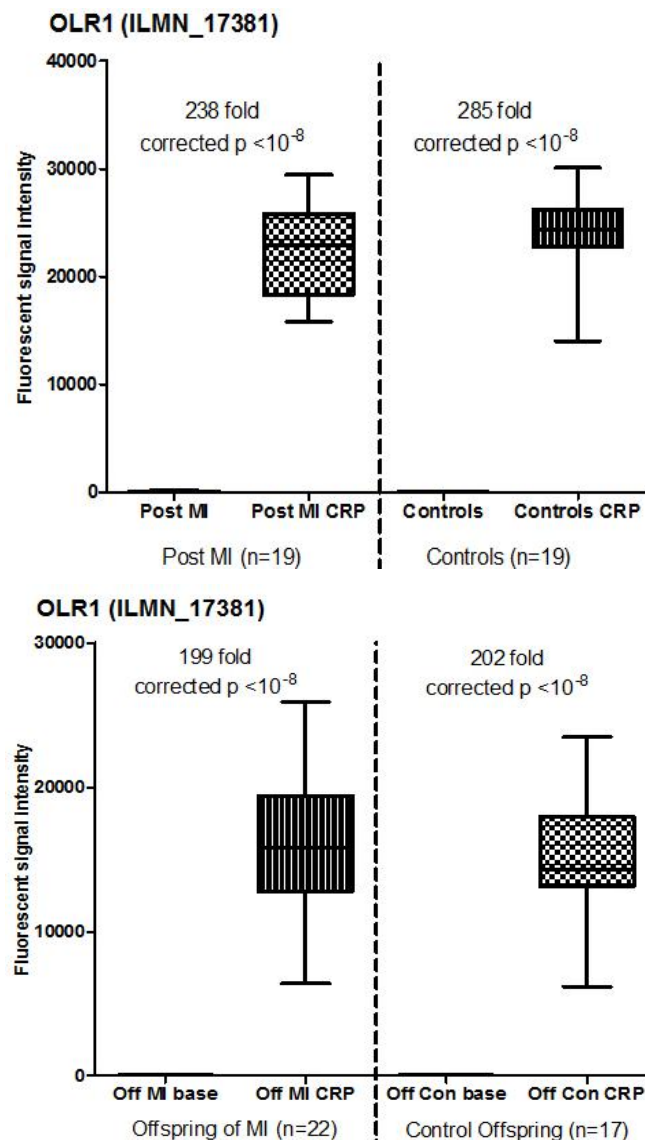


Figure 3.13: Microarray signal intensities of OLR1 in all four study groups.

Fluorescent signal intensities in all four groups before and after platelet-mediated stimulation are shown. Error bars denote the range of expression. Fold changes and false discovery corrected p values are provided.

3.4.1.1.2 Transglutaminase 2 (TGM2/TGase2/TGC); Chr20q12

Transglutaminase 2 is a ubiquitous calcium dependent cross-linking enzyme that catalyses irreversible post translational modification of proteins (Shin et al., 2008). Modification by TGM2 results in precipitation and aggregation of intracellular proteins with breakdown of intracellular architecture (Shin et al., 2008). However, activation of TGM2 does not always result in apoptosis and in some contexts, in fact aids cell survival (Lentile et al., 2007). Other studies have shown that TGM2 activates the pro-inflammatory transcription factor nuclear factor kappa B (NF κ B) by polymerizing its inhibitor I- κ B (Cho et al., 2008).

In the context of atherosclerosis, its presence in the shoulder regions of plaques confers stability to the lesions by promoting fibrosis and calcification (Haroon et al., 2001). At a molecular level, this is achieved by the formation of epsilon(gamma-glutamyl)lysine isopeptide bonds which cross-link extra cellular matrix proteins such as fibronectin and collagen (Van Herck et al., 2010). TGM2 is essential for the differentiation of smooth muscle cells from a contractile to a chondro-osseous phenotype (Johnson et al., 2008). The release of transforming growth factor beta (TGF β) by macrophages during phagocytosis is TGM2 dependent (Szondy et al., 2003). In addition, it also promotes the activity of TGF β in the extra cellular matrix by activating its latent form (Kojima et al., 1993).

In the current study, TGM2 levels were below the microarray detection threshold in all groups at baseline. Following stimulation TGM2 was up-regulated more than 110 fold in all groups. Fluorescent signal intensities rose in all groups to the 10-30,000 range suggesting that TGM2 is highly expressed in monocytes following CRP-XL stimulation. It was most up-regulated in controls of MI; however the levels

were not significantly different from the levels in the Post MI group. The levels in Offspring of MI and their matched controls were similar after CRP-XL stimulation.

The significant up-regulation of TGM2 (Figure 3.14) following CRP-XL stimulation may indicate a response to oxidative stress similar to the up-regulation of OLR1.

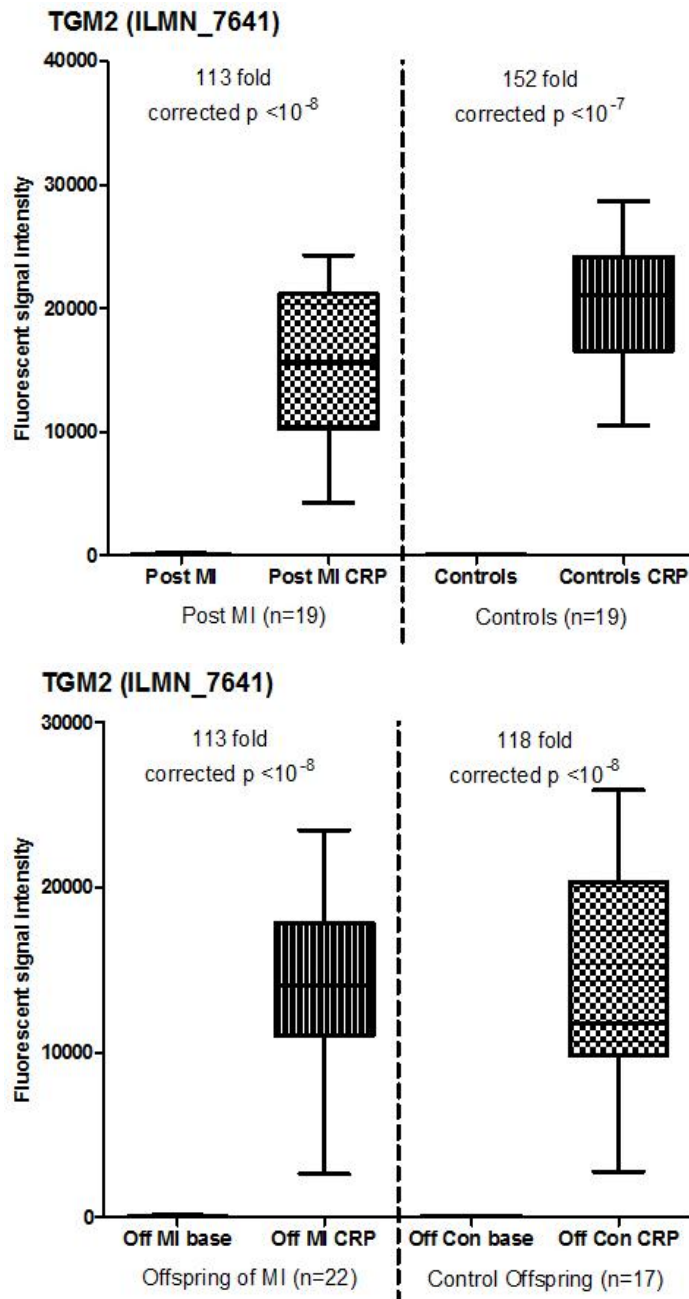


Figure 3.14: Microarray signal intensities of TGM2 in all four study groups.

Fluorescent signal intensities in all four groups before and after platelet-mediated stimulation are shown. Error bars denote the range of expression. Fold changes and false discovery corrected p values are provided.

3.4.1.1.3 Chemokines

Monocyte chemoattractant protein 1 (MCP1/CCL2); Chr 17q11.2-q12

MCP1/CCL2 belongs to the CXC family of cytokines and displays chemotactic activity preferentially for monocytes and basophils. Endothelial cells release MCP1 in response to interleukin 1 β (Takahashi et al., 1995b) and there is evidence that cross talk between endothelial cells and peripheral blood monocytes augments MCP1 release from both cell types (Takahashi et al., 1995a). MCP1 augments CD40L induced tissue factor expression on U937 cell lines (Nomura et al., 2009). It has also been noted that MCP1 levels in circulation were raised in hyperlipidaemic patients compared to controls and that treatment with pitavastatin reduced these levels (Nomura et al., 2009).

Monocyte chemoattractant protein 3 (MCP3/CCL7); 17q11.2-q12

MCP3 is expressed in vascular smooth muscles following pro-inflammatory stimuli and in rat carotid artery following balloon angioplasty (Wang et al., 2000). Circulating levels of CCL7 correlate with clinically relevant coronary artery disease (Ardigo et al., 2007).

At baseline, low signal intensities were noted for both CCL2 and CCL7. Following stimulation (Figures 3.15, 3.16), transcript levels were raised significantly in all groups to more than 10 fold from baseline levels. Both cytokines were expressed to moderately high levels in stimulated monocytes (2-20,000).

CCL2 and CCL7 levels in Post MI patients were lower than that in controls which may be explained by statin therapy (Vieira et al., 2005, Wang et al., 2011d).

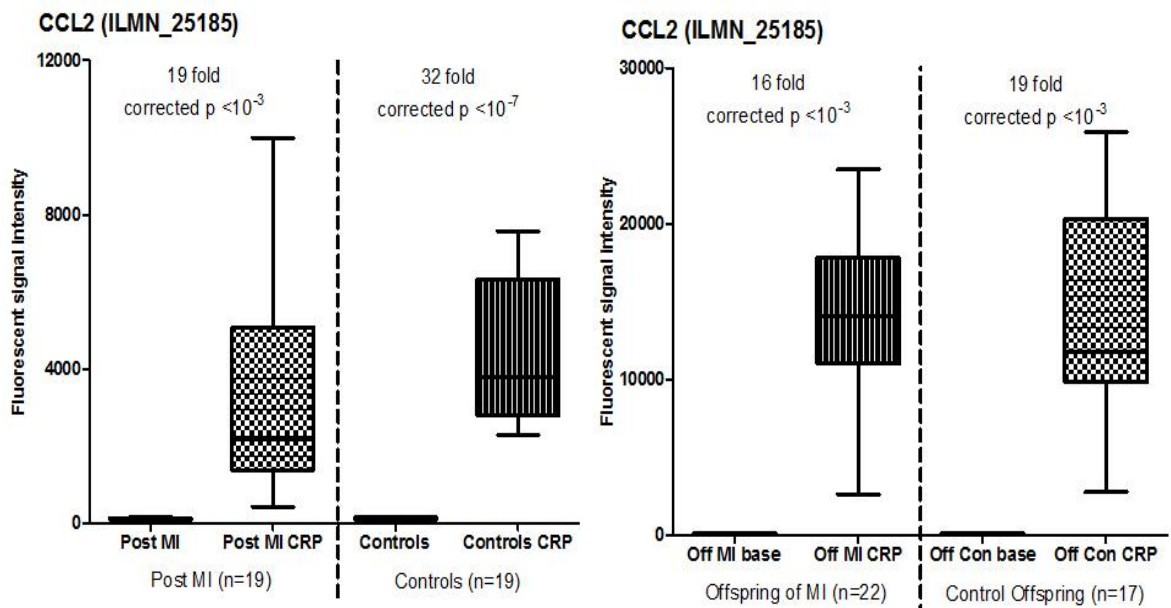


Figure 3.15: Microarray signal intensities of CCL2 in all four study groups.

Fluorescent signal intensities in all four groups before and after platelet-mediated stimulation are shown. Error bars denote the range of expression. Fold changes and false discovery corrected p values are provided.

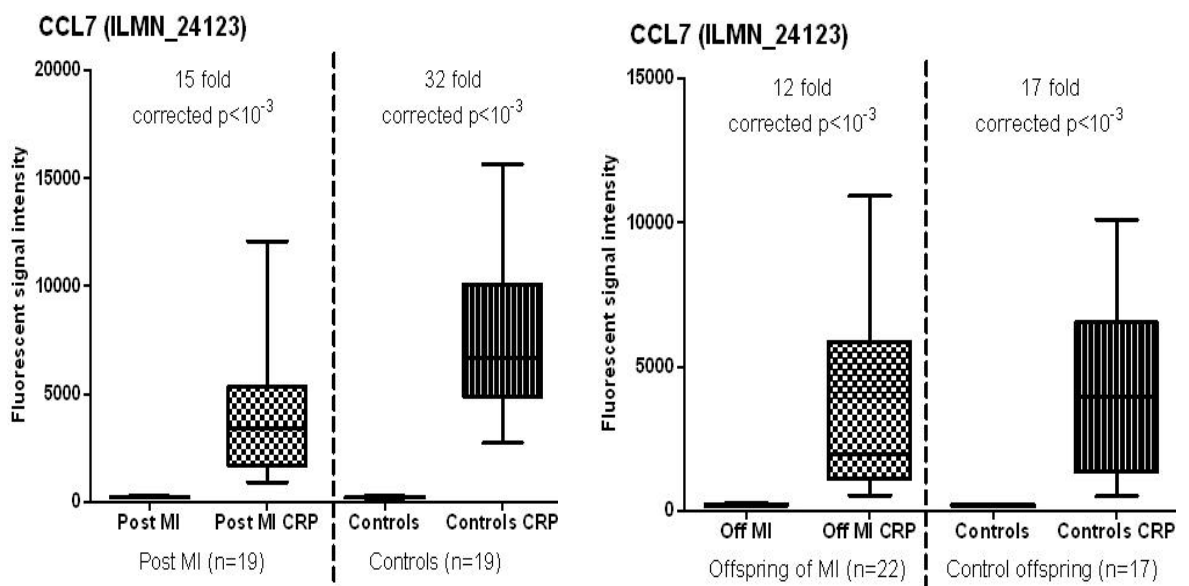


Figure 3.16: Microarray signal intensities of CCL7 in all four study groups.

Fluorescent signal intensities in all four groups before and after platelet-mediated stimulation are shown. Error bars denote the range of expression. Fold changes and false discovery corrected p values are provided.

3.4.1.1.4 Interleukin 8 (IL8, CXCL8); Chr 4q13-q21

IL8 is a member of the CXC cytokine family and is a potent chemotactic and angiogenic factor. Factor VIIa induces IL8 expression in smooth muscle cells in the presence of tissue factor (Demetz et al.). Following myocardial infarction, elevated IL8 levels have shown a positive correlation with the extent of myocardial damage, especially in the first few days after the event (Orn et al., 2009).

In the present study (Figure 3.17), IL8 was expressed at low levels in resting monocytes in all groups. Following stimulation, levels were raised more than 20 fold in all groups. The gene is expressed to high levels following stimulation as evidenced by the signal intensity range (10-20,000).

It is noteworthy that IL8 levels were not higher in Post MI patients compared to controls after stimulation. This may be due to their stable clinical state and statin therapy, which is known to reduce levels of IL8 (Dje N'Guessan et al., 2009).

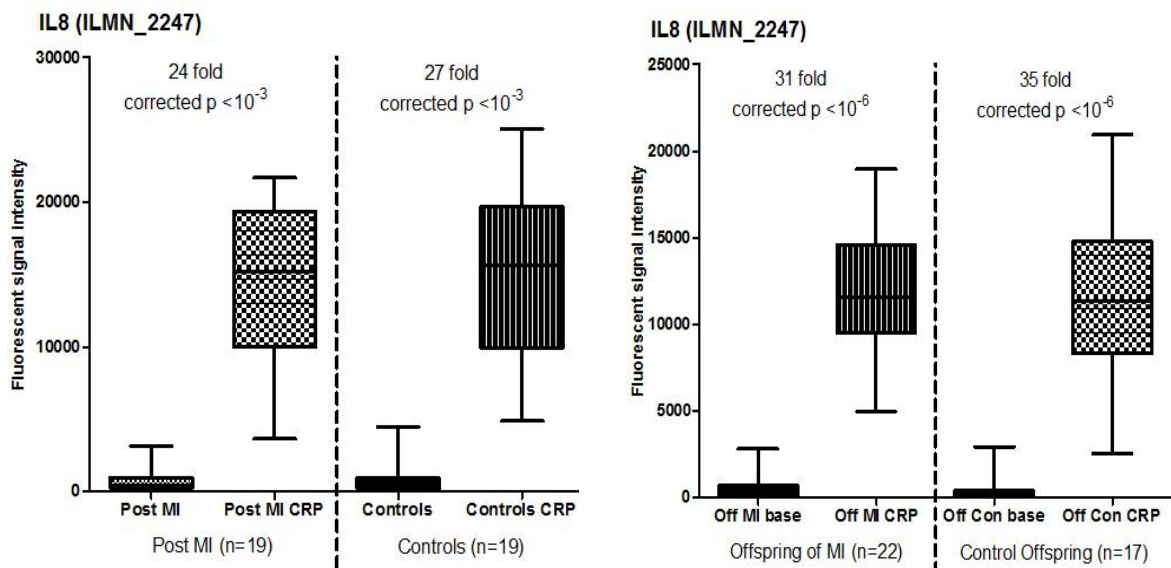


Figure 3.17: Microarray signal intensities of IL8 in all four study groups.

Fluorescent signal intensities in all four groups before and after platelet-mediated stimulation are shown. Error bars denote the range of expression. Fold changes and false discovery corrected p values are provided.

3.4.1.1.5 Secreted phosphoprotein 1 (SPP1, osteopontin); Chr 4q22.1

Osteopontin (Opn) is a glyco-phosphoprotein which promotes cell adhesion and chemotaxis (El-Tanani, 2008). It has been co-localised by immunohistochemistry to arteries of diabetic patients and promotes platelet-derived growth factor (PDGF)-mediated DNA synthesis in vascular smooth muscle cells (Takemoto et al., 2000). In mouse models of hypertension, SPP1 promotes oxidative stress (Irita et al., 2011). Gene silencing of SPP1 in macrophages resulted in impaired migration, an increased rate of apoptosis and decreased expression of macrophage scavenger receptor A type 1 (Nystrom et al., 2007).

SPP1 expression levels were below the detection threshold in all groups at baseline. Following stimulation, SPP1 gene expression increased to moderate levels (2-10,000) in all groups. Higher fold changes (>50 fold) were seen in the Post MI group and their age matched controls (Figure 3.18), although levels were not significantly different between the two groups.

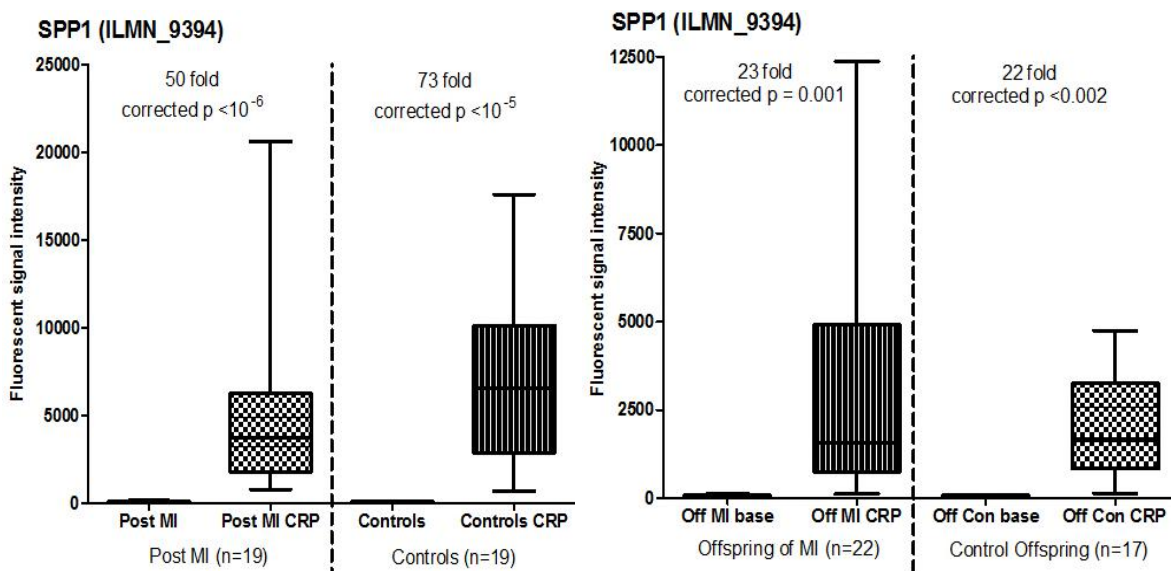


Figure 3.18: Microarray signal intensities of SPP1 in all four study groups.

Fluorescent signal intensities in all four groups before and after platelet-mediated stimulation are shown. Error bars denote the range of expression. Fold changes and false discovery corrected p values are provided.

3.4.1.1.6 Oncostatin-M (OSM); Chr: 22q12

This is a member of the cytokine family secreted by circulating monocytes and tissue macrophages. Of interest to atherothrombosis is the up-regulation of OSM in macrophages by thrombin. This is mediated by the translocation of transcription factors, c-fos and c-jun as a result of thrombin binding to the cell surface, suggesting a link between thrombosis and inflammation (Kastl et al., 2009, Vasse et al., 1999). OSM has an angiogenic effect on capillary endothelial cells with implications for atherosclerosis (Vasse et al., 1999). OSM is expressed by smooth muscle cells in human carotid atherosclerotic lesions (Albasanz-Puig et al., 2011).

OSM was expressed at low levels in unstimulated monocytes in all groups. Signal intensities were raised to a moderate degree (5-10,000) following CRP-XL stimulation in all groups (Figure 3.19) with higher fluorescent intensities in the Post MI group and their controls compared to the offspring groups.

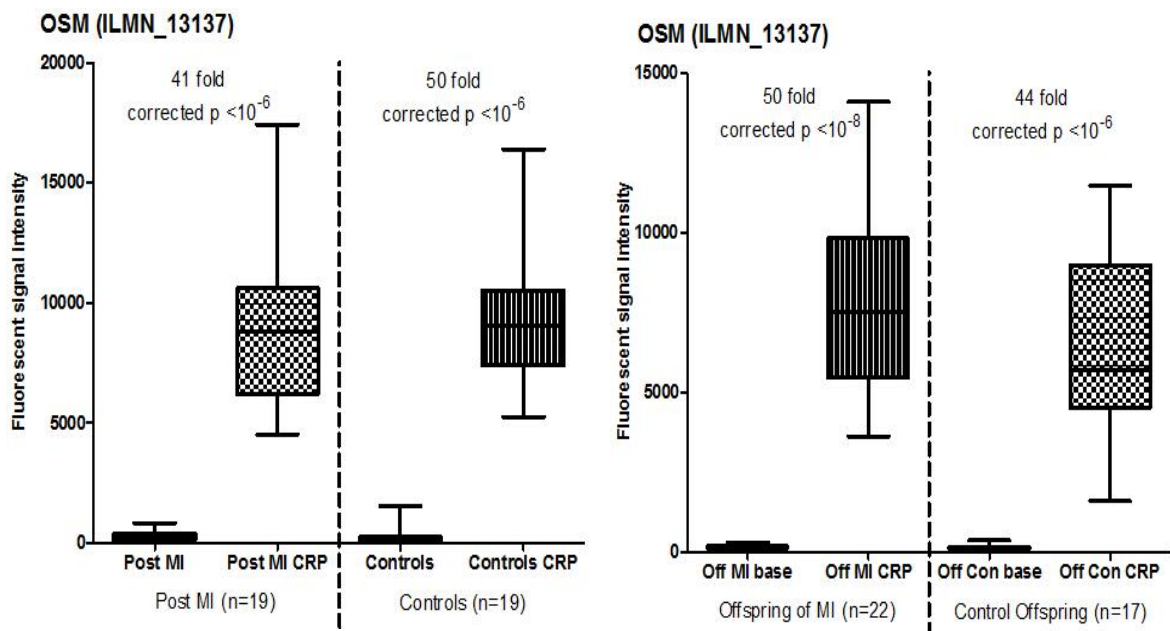


Figure 3.19: Microarray signal intensities of OSM in all four study groups.

Fluorescent signal intensities in all four groups before and after platelet-mediated stimulation are shown. Error bars denote the range of expression. Fold changes and false discovery corrected p values are provided.

3.4.1.1.7 DNA damage inducible transcript 4 (DDIT4, REDD1); Chr 10pter-q26.12

Although not previously linked to atherosclerosis, DDIT4 is recognised as a stress response gene which is up-regulated by both hypoxia and energy stress (Ellisen, 2005). This is a regulatory molecule which controls the expression of the mammalian target of rapamycin (mTOR) by suppressing it following hypoxic stress (Vadysirisack and Ellisen, 2012). mTOR signalling is critical to the recovery of cells following hypoxic injury and this requires degradation of DDIT4 (Katiyar et al., 2009). DDIT4 has been shown to enhance oxidative stress mediated cell death (Yoshida et al., 2010).

DDIT4 expression was raised to moderate levels of fluorescent signal intensity (5-20,000) following stimulation in all four groups (Figure 3.20). Levels were higher in Post MI and their controls compared to the offspring groups. The response to CRP-XL suggests the possibility of significant oxidative stress with the stimulus.

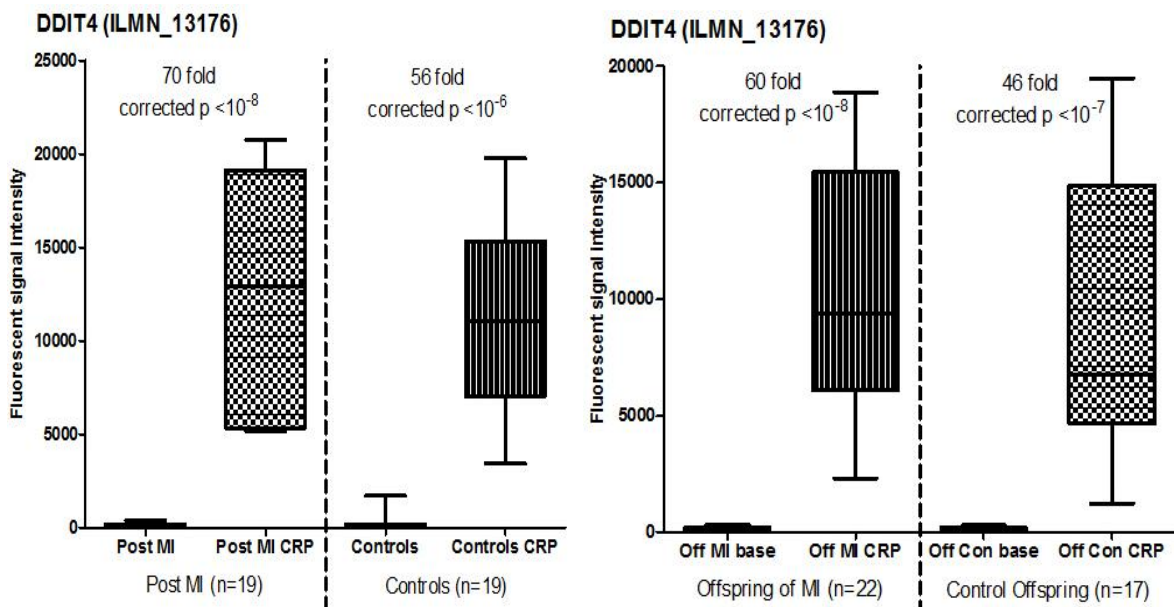


Figure 3.20: Microarray signal intensities of DDIT4 in all four study groups.

Fluorescent signal intensities in all four groups before and after platelet-mediated stimulation are shown. Error bars denote the range of expression. Fold changes and false discovery corrected p values are provided.

3.4.1.2 Genes down regulated after stimulation with platelets common to all groups

3.4.1.2.1 Interleukin 15 (IL15); Chr 4q31

Interleukin 15 (IL-15) has been detected in atherosclerotic plaques where it appears to have a regulatory role. In vitro studies have shown that IL-15 inhibits smooth muscle cell expression of fractalkine (FKN, CX3CL1) and its receptor CX3CR1. Mouse models have shown that both IL-15 and FKN-CX3CR1 are activated following arterial injury. The former opposes intimal thickening while the latter aggravates it. IL-15 is thought to maintain atherosclerotic plaque stability in a platelet derived growth factor dependent manner by stimulating smooth muscle cells (van der Meer et al., 2011).

IL15 was expressed at moderate levels in resting monocytes but expression was significantly suppressed in all groups following CRP-XL stimulation (Figure 3.21).

No significant differences were noted between cases and controls.

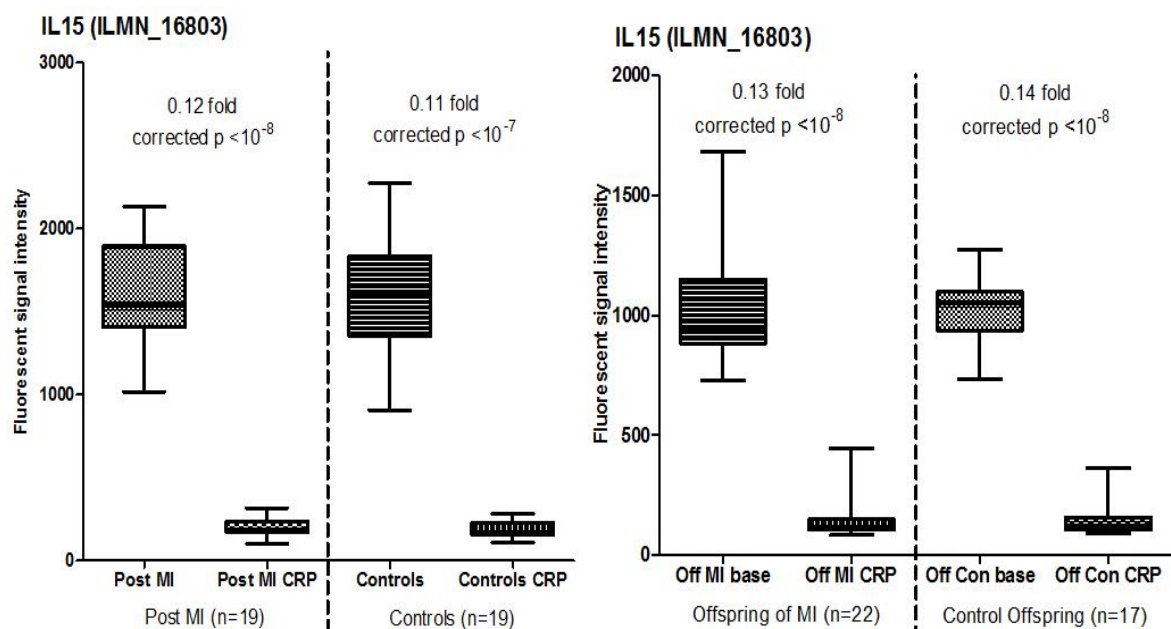


Figure 3.21: Microarray signal intensities of IL15 in all four study groups.

Fluorescent signal intensities in all four groups before and after platelet-mediated stimulation are shown. Error bars denote the range of expression. Fold changes and false discovery corrected p values are provided.

3.4.1.2.2 G-protein coupled bile acid receptor 1 (GPBAR1/TGR5); Chr2q35

GPBAR1 is a G protein coupled bile acid receptor with immunomodulatory properties. It is a negative regulator of NF kappa B and has an anti-inflammatory effect (Wang et al., 2011e). It suppresses cytokine production in human macrophages in response to LPS (Kawamata et al., 2003). Up-regulation of GPBAR1 regulates energy expenditure in brown adipose tissue and skeletal muscle (Trauner et al., 2010), Down regulation of GPBAR1 resulted in a decrease in the bile acid pool, increased fat accumulation and weight gain in a mouse knockout model, indicating its role in energy homeostasis (Maruyama et al., 2006).

In this study, GPBAR1 was expressed at moderate levels in resting monocytes. It was down regulated in all groups following CRP-XL stimulation (Figure 3.22).

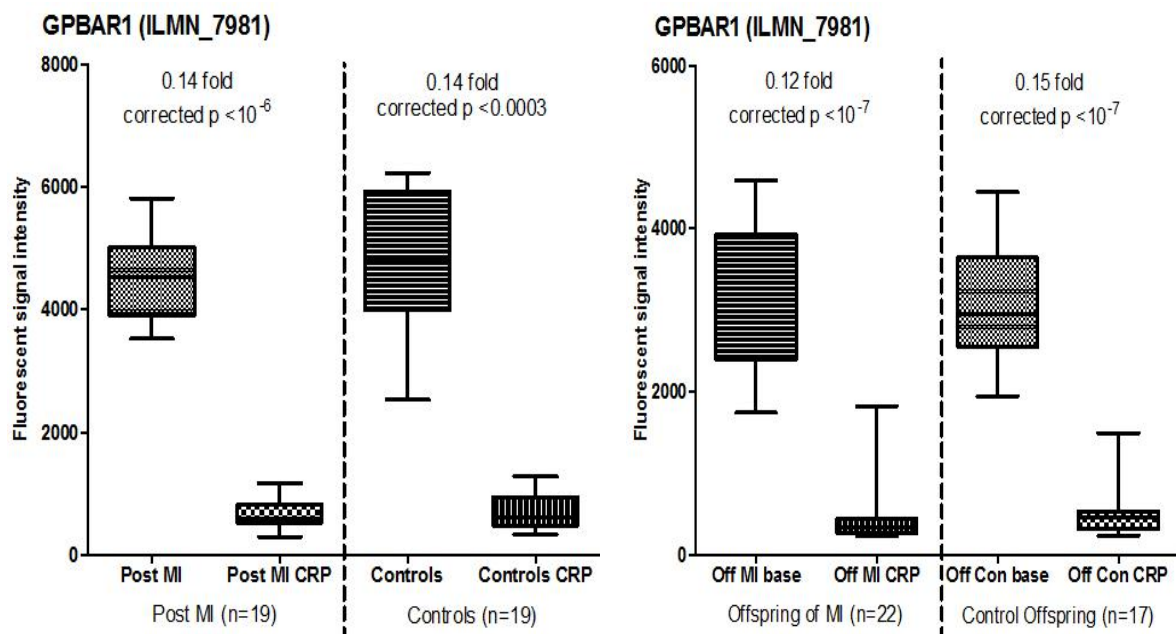


Figure 3.22: Microarray signal intensities of GPBAR1 in all four study groups.

Fluorescent signal intensities in all four groups before and after platelet-mediated stimulation are shown. Error bars denote the range of expression. Fold changes and false discovery corrected p values are provided.

3.4.1.2.3 Thrombospondin receptor (CD36/GP4); Chr 7q11.2

CD36 is a cell surface oxidized LDL receptor expressed on platelets, monocytes, macrophages and endothelial cells (Yamashita et al., 2007). CD36 deficiency results in hyperlipidaemia and metabolic syndrome (Yamashita et al., 2007). However, this also promotes atherogenesis by enhancing macrophage spreading and subintimal macrophage trapping (Park et al., 2009). Flowcytometry of human monocytes suggested that tissue factor surface expression (and resultant prothrombotic reactivity to lipopolysaccharide) was inversely proportional to CD36 expression (Sovershaev et al., 2007) suggesting that platelet-mediated activation may promote a prothrombotic monocyte phenotype by suppressing CD36.

Moderate levels of CD36 expression was noted in resting monocytes with numerically higher levels in the Post MI group and their controls compared to the two offspring groups (Figure 3.23). There was significant down regulation of CD36 in all groups following stimulation. Post MI patients had numerically levels higher following stimulation, although the difference was not statistically significant.

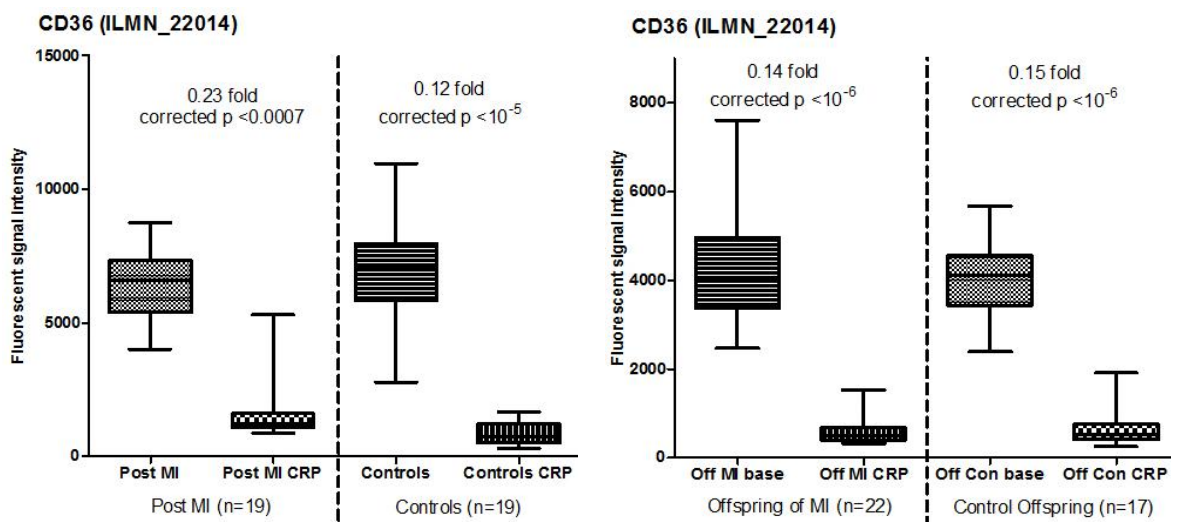


Figure 3.23: Microarray signal intensities of CD36 in all four study groups.

Fluorescent signal intensities in all four groups before and after platelet-mediated stimulation are shown. Error bars denote the range of expression. Fold changes and false discovery corrected p values are provided.

3.4.1.2.4 CD33; Chr 19q13.3

CD33 is a myeloid cell surface antigen with a role in vascular inflammation. Differences in CD33 surface expression (CD33 low vs. high) determine the degree of scavenger receptor expression and LDL uptake by monocytes (Draude et al., 1999). Shear stress induced platelet microparticles promotes CD33 expression in THP-1 monocytic cell lines (Nomura et al., 2001). Considering that collagen stimulation releases soluble mediators from platelets, the down regulation of CD33 following stimulation suggests an alternative mechanism. Addition of anti-CD33 antibodies to CD14⁺ monocytes in culture prevented their maturation to dendritic cells and promoted apoptosis (Ferlazzo et al., 2000) suggesting that CD33 down regulation may be a pro-apoptotic change induced by CRP-XL (Figure 3.24).

Figure 3.24 shows moderate levels of CD33 expression in resting monocytes, 4-8,000 in Post MI and controls with lower levels (2-6,000) in the offspring groups. Similar degrees of down regulation were noted following stimulation.

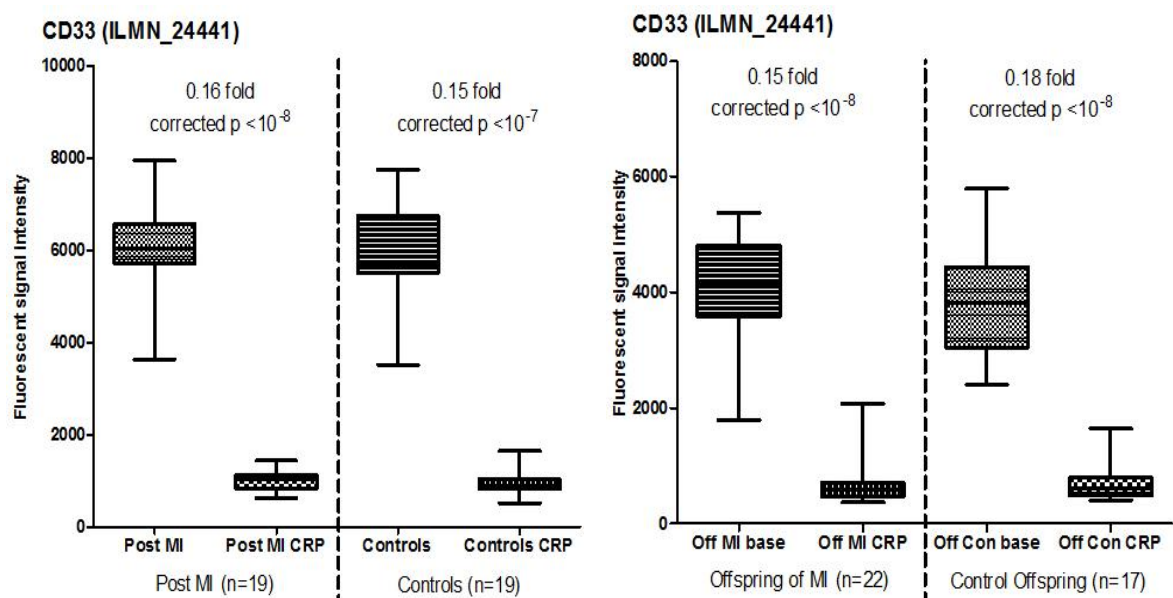


Figure 3.24: Microarray signal intensities of CD33 in all four study groups.

Fluorescent signal in all four groups before and after platelet-mediated stimulation are shown. Error bars denote the range of expression. Fold changes and false discovery corrected p values are provided.

3.4.1.2.5 Fractalkine receptor (CX3CR1); Chr3p21.3

Fractalkine (CX3CL1) is a trans-membrane chemokine expressed by endothelial cells involved in the adhesion (membrane bound form) and chemotaxis (soluble plasma form) of leukocytes; CX3CR1 is its receptor expressed in monocytes and lymphocytes (Imaizumi et al., 2004). CX3CR1 expression on peripheral blood mononuclear cells is up-regulated by IL2 and down regulated by IL15 (Barlic et al., 2003). Fractalkine signalling also has anti inflammatory properties under certain circumstances - it reduces cytokine signalling and production of TNF alpha, MCP1, MIP1 alpha and RANTES in macrophages following CCL4 stimulation (Aoyama et al., 2010). It also has a role in wound repair through chemotactic signalling of monocyte derived macrophages (Ishida et al., 2008).

Low to moderate levels of CXCR1 expression (500-1500) was noted in all groups at baseline (Figure 3.25). CXCR1 expression was significantly suppressed following CRP-XL stimulation in all groups in this study.

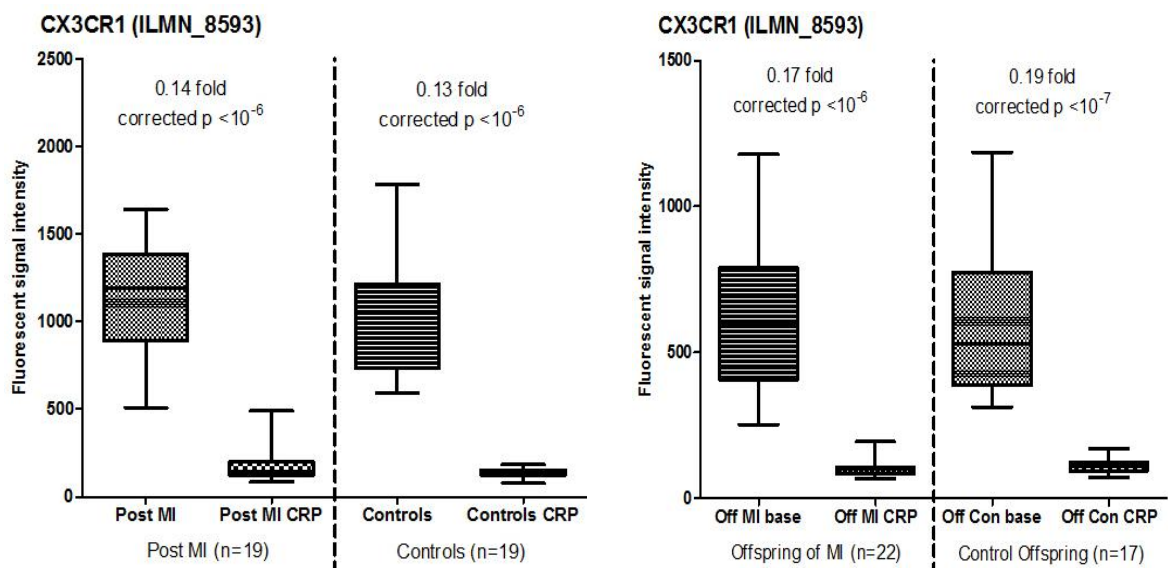


Figure 3.25: Microarray signal intensities of CX3CR1 in all four study groups.

Fluorescent signal intensities in all four groups before and after platelet-mediated stimulation are shown. Error bars denote the range of expression. Fold changes and false discovery corrected p values are provided.

3.4.1.2.6 Endothelial differentiation gene 2 (EDG2, LPAR1); Chr9q31.3

EDG2 (Type 1 LPA) is an integral endothelial cell membrane protein of the G protein coupled receptor family. Its ligand, lysophosphatidic acid promotes IL-8 and MCP-1 driven monocyte adhesion to vascular endothelium (Lin et al., 2007).

Low to moderate level expression was seen in all groups at baseline. CRP-XL suppressed EDG2 expression in all groups, but a statistically significant higher expression was seen in the Post MI group compared to controls (Figure 3.26).

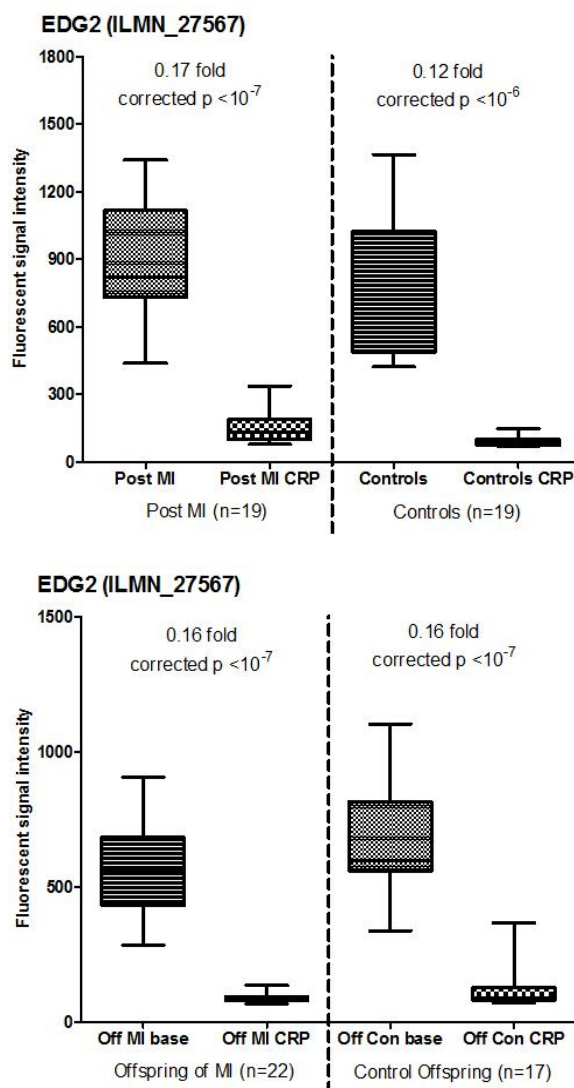


Figure 3.26: Microarray signal intensities of EDG2 in all four study groups.

Fluorescent signal intensities in all four groups before and after platelet-mediated stimulation are shown. Error bars denote the range of expression. Fold changes and false discovery corrected p values are provided.

3.4.1.2.7 Apolipoprotein L 3 (APOL3); Chr22q13:1

APOL3 is a cytoplasmic protein that regulates the intracellular transport of lipids including cholesterol. It is expressed in normal and atherosclerotic vascular walls in response to TNF (Horrevoets et al., 1999).

APOL3 was expressed at moderate levels in resting monocytes (Figure 3.27). Following stimulation, significant down regulation was noted in all groups. Although the levels were higher in the Post MI group, this was not significantly different from the controls.

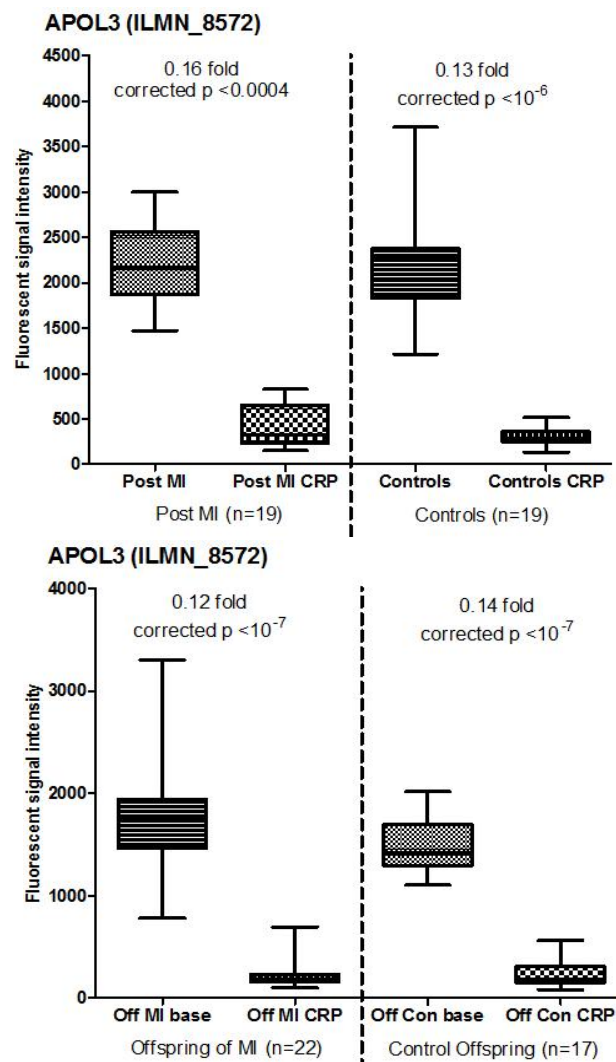


Figure 3.27: Microarray signal intensities of APOL3 in all four study groups.

Fluorescent signal intensities in all four groups before and after platelet-mediated stimulation are shown. Error bars denote the range of expression. Fold changes and false discovery corrected p values are provided.

3.4.1.2.8 Beta-2 adrenergic receptor (ADRB2); Chr5q31-q32

ADRB2 was down regulated in all groups following CRP-XL (Figure 3.28) which may be due to oxidative stress as noted in a rat heart membrane model exposed to high concentrations of hydrogen peroxide (Persad et al., 1998). Although levels were higher in the Post MI group compared to healthy controls, this did not achieve statistical significance.

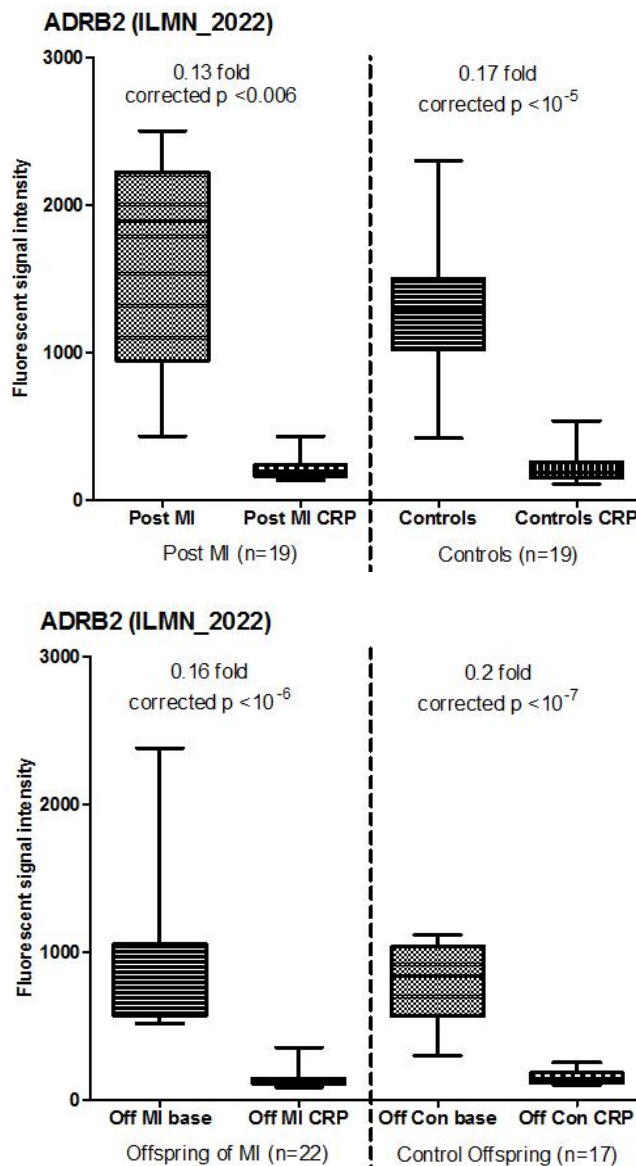


Figure 3.28: Microarray signal intensities of ARDB2 in all four study groups.

Fluorescent signal intensities in all four groups before and after platelet-mediated stimulation are shown. Error bars denote the range of expression. Fold changes and false discovery corrected p values are provided.

3.4.2 Pathways

IPA analysis revealed that several molecular and signalling pathways were over-represented within the differentially expressed genes following CRP-XL stimulation.

3.4.2.1 LXR/RXR Activation

The liver x receptors α (LXR α /NR1H3) and β (LXR β /NR1H2) are nuclear receptors which influence macrophage function and form heterodimers with 9-cis retinoic acid receptor α (RXR α /NR2B1) to act as regulators of intracellular sterol content (Edwards et al., 2002). Oxidized cholesterol compounds (oxysterols) are natural ligands of these receptors (Beltowski, 2008). As oxysterols are formed in proportion to cellular cholesterol content, this enables LXRs to function as 'cholesterol sensors'. LXR activation limits cholesterol overload by various mechanisms including reduced intestinal cholesterol absorption and increased HDL mediated reverse cholesterol transport (Beltowski, 2008).

Two members of this signalling pathway, CCL2 and CCL7, were up-regulated in this study across all groups following CRP-XL stimulation. It has been shown that ligands for RXR promote CCL2 expression in monocytes which promotes monocyte activation and migration (Zhu et al., 1999). In addition, there is also evidence that phagocytosis of apoptotic cells by macrophages (*efferocytosis*) is regulated through a liver x receptor – retinoic acid receptor alpha (LXR-RAR α) mediated mechanism which requires TGM2, which was up-regulated in all groups after stimulation. ATP binding cassette transporter A1 (ABCA1) mediated reverse cholesterol transport is also regulated by RAR through TGM2 (Boisvert et al., 2006).

3.4.2.2 TREM1 signalling

Triggering receptor expressed on monocytes-1 (TREM1) signalling potentiates the inflammatory response of monocytes and macrophages in chronic inflammatory conditions (Schenk et al., 2007). This signalling cascade increases expression of TNF, IL6, IL8 and CCL2 (Tessarz et al., 2007). Hypoxic stress is a major stimulus for expression of TREM-1 in monocyte derived dendritic cells (Bosco et al., 2011). Interfering with TREM1 signalling has been shown to reduce CCL2 expression in peritoneal macrophages and reduce inflammation (Wang et al., 2012a). Increased CCL2 expression following CRP-XL suggests a proinflammatory change in monocytes.

3.5 DISCUSSION

3.5.1 Platelet mediated activation of monocytes results in an oxidative stress response

CRP-XL binds to the GPVI receptor on the platelet surface (Polanowska-Grabowska et al., 2003). This activates platelets which then stimulate monocytes directly (P-selectin:PSGL) and indirectly (platelet microparticles). This Chapter describes the changes in the monocyte transcriptome following platelet mediated activation. Many of the differentially expressed genes following this stimulation have well established roles in cellular response to oxidative stress.

OLR1 levels increase following oxidative stress and results in increased generation of reactive oxygen species alongside decreased NO production (Sakurai and Sawamura, 2003). Consequently, it increases activity of matrix metalloproteinases 2&9, osteopontin, fibronectin and NADPH oxidase (Hu et al.,

2008). There is also evidence that OLR1 up-regulation following oxidized LDL exposure results in DNA damage as suggested by the significant up-regulation of DNA damage inducible transcripts (Thum and Borlak, 2008). C reactive protein induces TNF α mediated release of a soluble form of OLR1 from macrophages (Zhao et al.). Animal studies have shown that OLR1 correlates to tissue factor expression, apoptotic events and morphologic vulnerability in atheromatous plaques (Kuge et al., 2008).

In response to oxidative stress, transglutaminase 2 is up-regulated in cardiomyocytes and mediates apoptosis (Song et al.). There is also evidence that TGM2 up-regulates and polymerises macrophage osteopontin (SPP1) resulting in enhanced adhesion to calcified elastic lamellae (Kaartinen et al., 2007).

CCL2 (MCP1) is up-regulated following oxidative stress (Masai et al.) and promotes initiation (Libby, 2002) and progression (Aiello et al., 1999) of atherosclerosis by inducing diapedesis and subendothelial migration of monocytes. CCL7 (MCP3) is another chemokine that is expressed in response to oxidative stress (Michalec et al., 2002).

IL8 is produced in response to oxidative stress (Neri et al., 2007) and facilitates pro-atherogenic events such as LDL binding to endothelium and increased expression of leukocyte adhesion molecules (Hung et al., 2008, Hajjar et al., 1989). DDIT4 enhances oxidative stress dependent cell death (Yoshida et al., 2010). It has been shown to activate the pro-inflammatory transcription factor nuclear factor kappa B (NF κ B) and promote apoptosis and inflammation (Yoshida et al., 2010).

Figure 3.29 provides an overview of the differentially expressed genes following CRP-XL stimulation and their roles in oxidative stress injury.

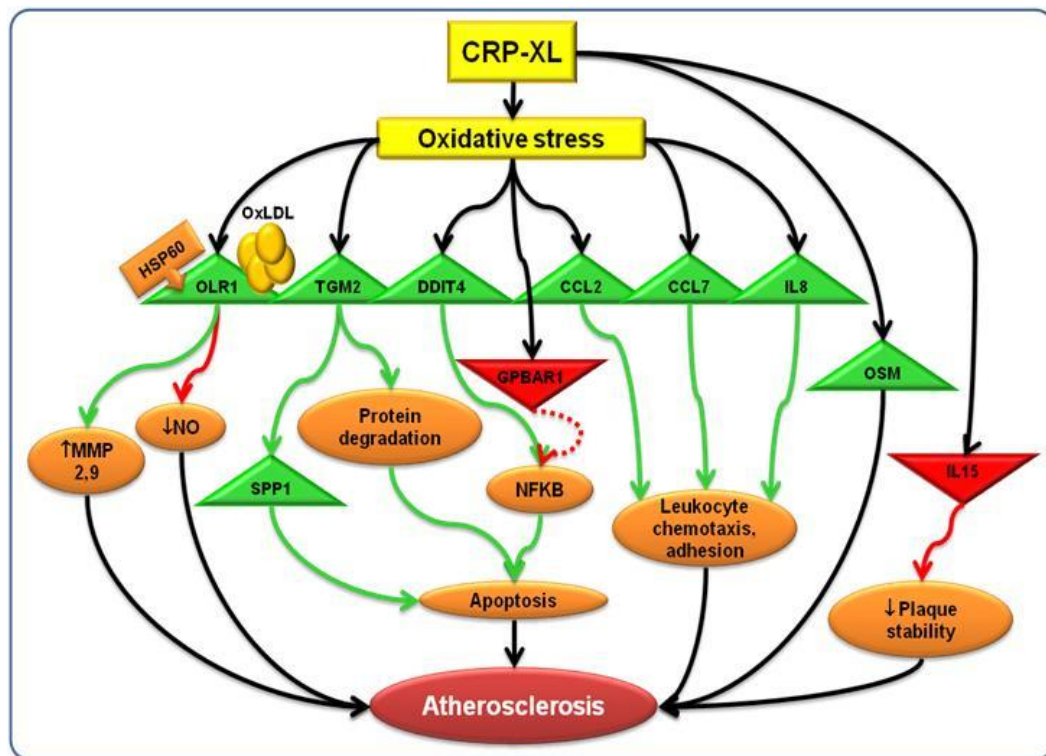


Figure 3.29: Summary of differentially expressed genes following CRP-XL.

CRP-XL stimulation results in a significant oxidative stress as evidenced by the differentially expressed genes. The up-regulated genes are shown in green and down regulated genes in red. Green arrows denote stimulation, red arrows denote suppression and dotted arrows denote release from suppression.

In this Chapter, we have demonstrated that platelet mediated stimulation induces expression of monocyte genes with relevance to vascular inflammation and atherosclerosis, predominantly by triggering an oxidative stress response. Cellular oxidative stress is an early event in atherogenesis (Bonomini et al., 2008) and is also the unifying mechanism for many of the classical risk factors for CAD (Madamanchi et al., 2005), suggesting that this model of collagen (CRP-XL) induced, platelet mediated stimulation of monocytes is a useful tool in delineating the functional biology of the monocyte/macrophage lineage in atherosclerosis. A 25-35% increase in monocyte expression of P-selectin glycoprotein ligand-1

(PSGL-1) was noted in all four study groups (data not shown) which is further confirmation of the platelet mediated monocyte stimulation achieved in this study. This Chapter also serves to demonstrate that the response to CRP-XL in all four study groups is similar when considering the expression profiles of the most differentially expressed genes.

This sets the stage for the type of analyses and the format for presentation of results in subsequent Chapters. Whereas this Chapter focused on common themes in gene expression in stimulated monocytes to justify the rationale for the stimulation experiment, subsequent Chapters focus on the differences between groups in gene expression – at baseline in unstimulated monocytes as well as following platelet-mediated (CRP-XL) stimulation.

CHAPTER 4: RESULTS

Post MI vs. Controls – differences

in monocyte gene expression at

baseline and after platelet

mediated stimulation

4.1 INTRODUCTION

The aim of the experiments described in this Chapter was to identify gene expression abnormalities in monocytes isolated from subjects with confirmed premature MI. All subjects in the premature MI group ('Post MI', Group 1) had a confirmed STEMI in the preceding 3-6 months and had no pre-existing history of CAD or MI. Healthy controls matched for age, gender and smoking status were recruited who had no history of MI, CAD or risk factors for atherosclerosis such as hypertension and hypercholesterolaemia. To avoid potential confounders which may influence monocyte gene expression, none of the subjects in either group had diabetes mellitus or other chronic inflammatory diseases and were free of infections at the time of recruitment.

A two stage analysis is described in this Chapter. In the first stage, differences in gene expression in resting monocytes are described (Figure 4.1) followed by the changes in the monocyte transcriptome after platelet-mediated stimulation.

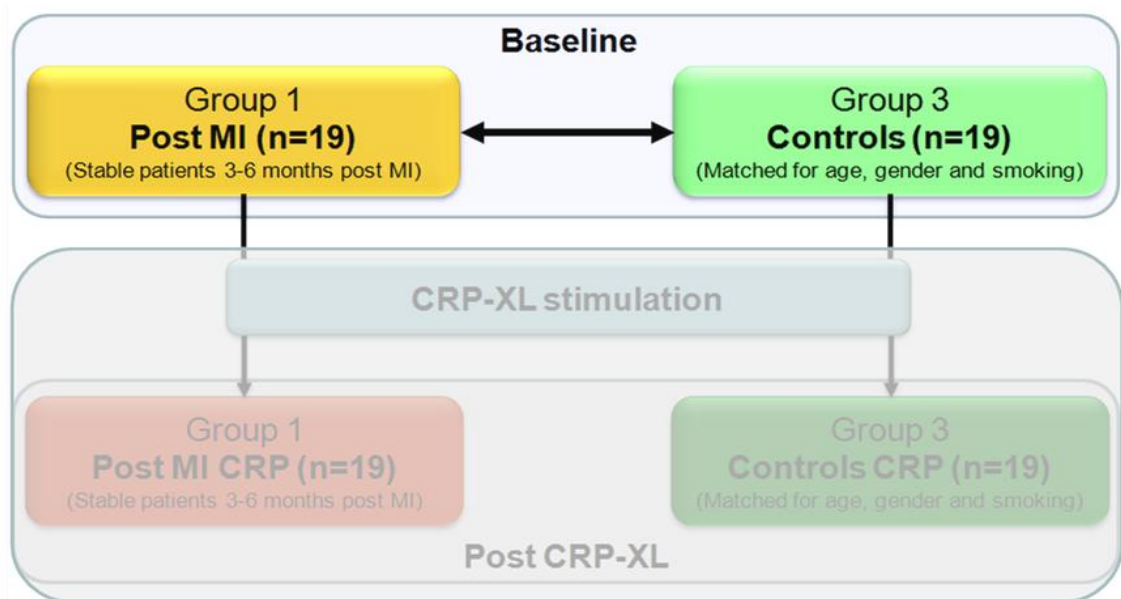


Figure 4.1: Scheme of analysis – Post MI vs. Controls at baseline.

4.2 BASELINE GENE EXPRESSION: INITIAL ANALYSIS

Peripheral venous blood samples collected in EDTA were used to isolate CD14⁺ monocytes and RNA was extracted in TRIzol within 50 minutes of venesection. Absence of platelet mediated monocyte activation was confirmed by monocyte platelet aggregate (MPA) assay on flowcytometry.

Microarray signal intensities were quantile normalized following which they were compared (Post MI vs. Controls at baseline) and statistically analysed for significant differential expression. Global expression of transcripts in Post MI patients with reference to healthy controls are shown in sigmoid plots (Figure 4.2).

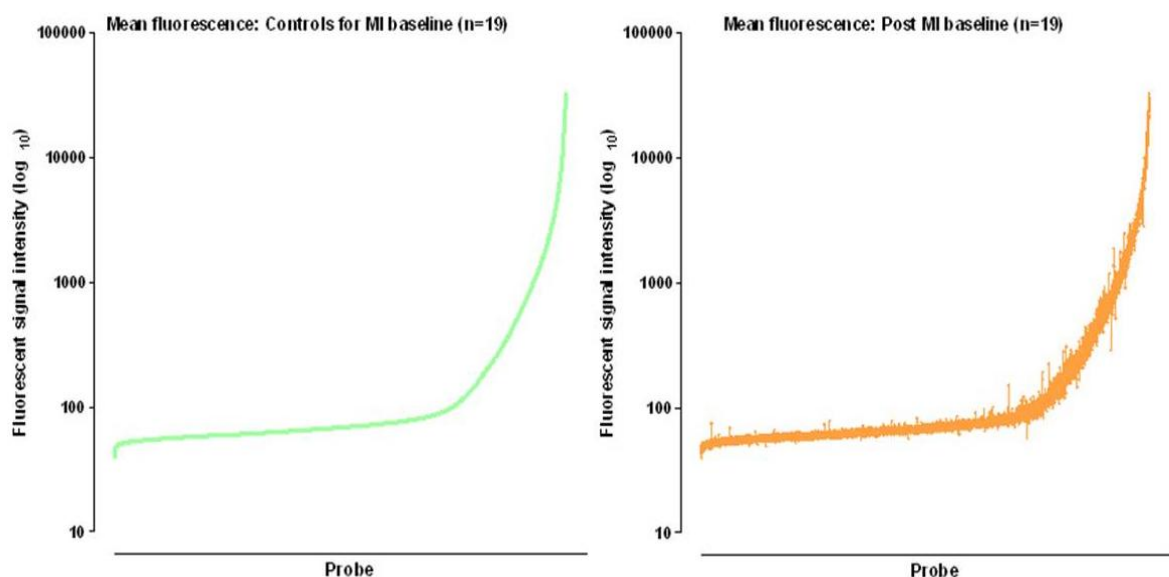


Figure 4.2: Sigmoid plots of fluorescent signal intensity in resting monocytes.

The graph shows baseline mean fluorescent signal intensities of all probe sets in healthy controls (left) and corresponding changes in signal intensities in the same probe sets in the Post MI group, i.e., the ‘delta change’ in signal intensities (right). The probe sets are plotted on the x axis in the order of the probe ID numbers according to increasing fluorescent signal intensities on a log₁₀ scale plotted on the y axis.

Both graphs have the probe IDs plotted on the x-axis in ascending order of their signal intensity in the *control* group (Group 3). By doing so, differences signal intensity for each probe ID in the *cases* (Group 1) is made apparent (right panel).

Two observations are noteworthy from this graph: (i) there are differences in gene expression across the spectrum of transcript abundance – from very low to very highly expressed genes; (ii) differences between cases and controls are not as marked as the differences before and after stimulation within the same group (see Figures 3.4a&b).

Degree (fold change) and significance (p value) of transcript probesets are graphically represented in Figure 4.3. The shaded areas contain the genes which were selected for further analysis after initial filtering steps as described below. Unlike the volcano plots in Chapter 3, this Figure shows that the majority of transcripts are not differentially expressed between cases and controls.

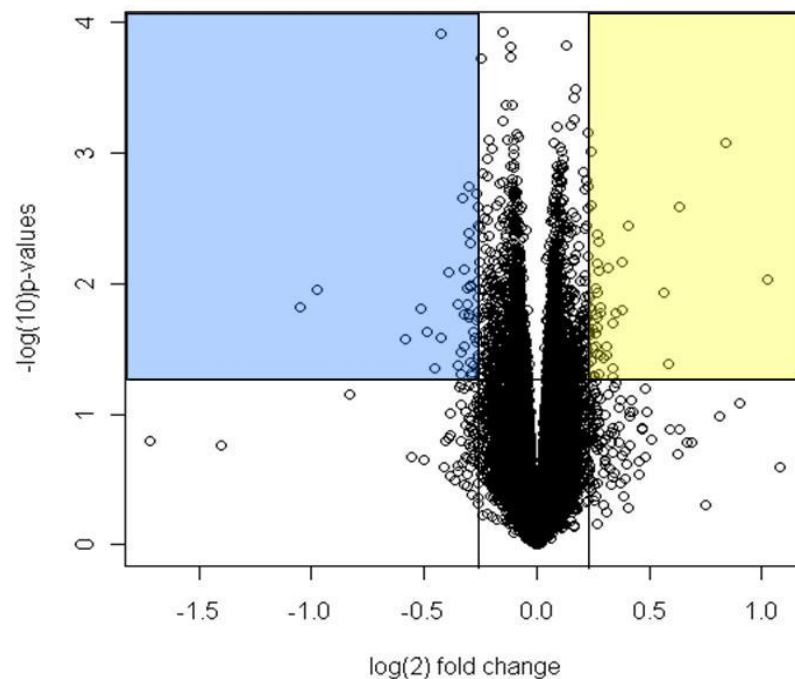


Figure 4.3: Volcano plot of Post MI vs. controls at baseline.

Log₂ of fold change (Post MI/controls) is plotted on the x-axis and log₁₀ of p-values (t test, uncorrected) is plotted on the y-axis. The yellow and blue shaded regions contain up and down regulated transcripts respectively which fulfil the filtering criteria for subsequent candidate gene analyses.

Differentially expressed genes were analysed according to the fold change in gene expression. In the initial screening step, genes which did not return 'present' calls in any of the samples were excluded. The first level statistical filter excluded those genes which had an uncorrected p value >0.05 and a false discovery rate $>50\%$. 676 transcript probes were selected using this strategy. All transcripts which fulfilled these filtering criteria had a low false discovery rate ($fdr_{2D} < 0.05$).

To further identify the most significant differences in gene expression, additional filtering steps were performed (Figure 4.4) to select 27 transcripts which were up-regulated >1.25 fold or down regulated <0.8 fold. 11 of these genes were up-regulated while 16 were down regulated in patients with premature MI compared to controls. All transcripts conformed to an uncorrected p value of <0.05 and a false discovery rate of $<5\%$ (Table 4.1).

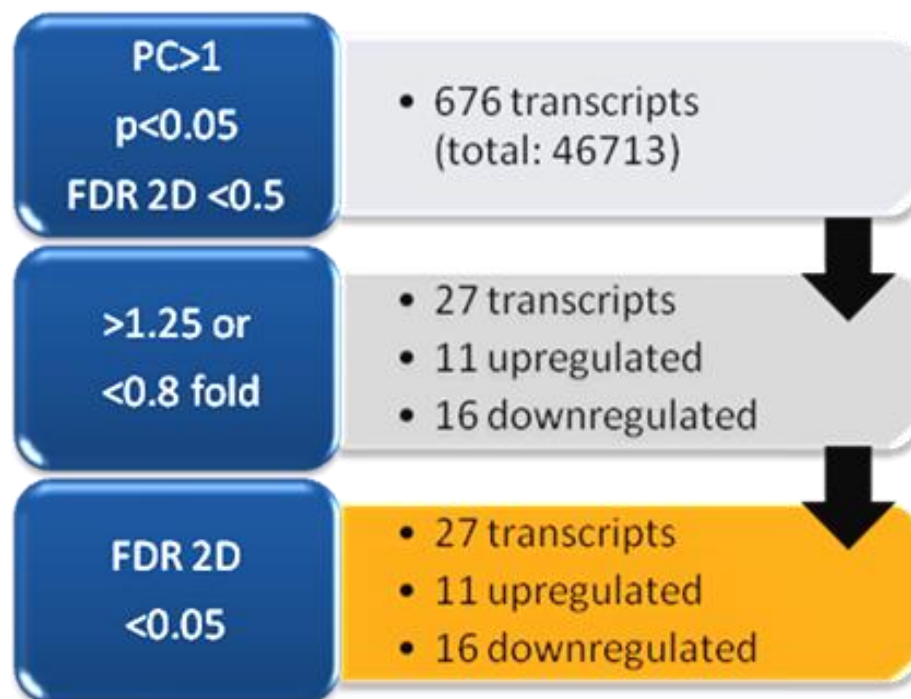


Figure 4.4: Gene transcript filtering strategy to identify differentially expressed genes. The orange panel highlights the filtering threshold used for subsequent candidate gene analyses (PC=present call).

Probe ID	Gene ID	Fold change	p values	fdr2D
ILMN_2829	OAS1	2.03	0.03	0.01
ILMN_17138	ORM1	1.78	0.03	0.01
ILMN_6493	TRK1	1.55	0.03	0.01
ILMN_12464	PGLYRP1	1.50	0.05	0.01
ILMN_24087	TNF	1.48	0.04	0.01
ILMN_8088	PEX11G	1.33	0.02	0.01
ILMN_18708	CLEC5A	1.30	0.03	0.01
ILMN_8019	ANKRD35	1.30	0.01	0.01
ILMN_12423	IER2	1.26	0.01	0.01
ILMN_14509	SLC16A6	1.26	0.04	0.01
ILMN_26614	H1FX	0.80	0.03	0.01
ILMN_21544	PYGB	0.79	0.03	0.01
ILMN_26329	OPN3	0.79	0.04	0.01
ILMN_14919	TES	0.79	0.05	0.01
ILMN_6637	SS18	0.78	0.05	0.01
ILMN_6733	SNX5	0.78	0.03	0.01
ILMN_137372	DRD3	0.76	0.01	0.01
ILMN_1435	OLFM1	0.74	0.03	0.01
ILMN_10449	CXXC5	0.74	0.02	0.01
ILMN_22808	TIMM10	0.73	0.03	0.01
ILMN_27341	OLFM1	0.67	0.02	0.01
ILMN_2789	HBA1	0.51	0.04	0.01
ILMN_28875	HBB	0.48	0.03	0.01

Table 4.1: Post MI vs. Controls – differentially expressed genes at baseline.

The up-regulated gene IDs are in yellow and the down regulated in blue. Fold changes (Post MI/Controls) are tabulated. All transcripts fulfilled the filtering thresholds (present calls in >1, fold change >1.25 or < 0.8, uncorrected p value <0.05, false discovery rate [fdr2D] <0.05). Unmapped transcripts are not shown.

4.3 BASELINE GENE EXPRESSION: LINKS WITH CAD

To identify known relationships of the differentially expressed genes with each other and with atherosclerosis, further text mining analysis was performed using ChiLiBot. The candidate genes were analysed for interactions within published literature with each other and with the following key words: atherogenesis, atherosclerosis, atherothrombosis, coronary artery disease, myocardial infarction, monocyte, macrophage and collagen.

Nine genes had established links with the aforementioned key words in published literature after further filtering to exclude co-occurrence in abstracts without interactive relationships (Figure 4.5). This analysis enabled the selection of genes with the strongest pathophysiological links to atherosclerosis from the candidate genes which showed maximal differential expression in resting monocytes. However, only four genes were studied further after reviewing the ChiLiBot results as the rest did not have robust links with the keywords.

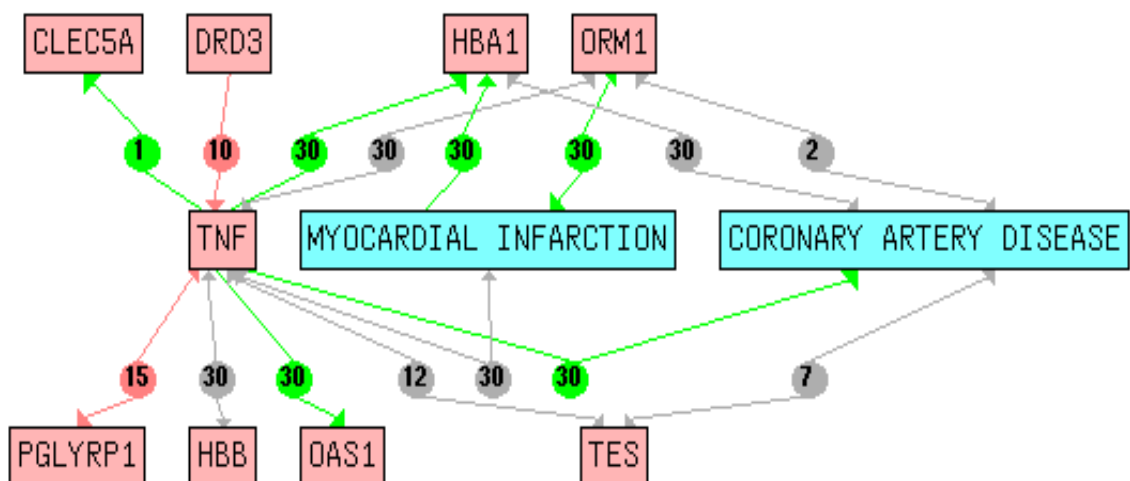


Figure 4.5: Lists of interactions on PubMed for each candidate gene (ChiLiBot).

The arrows in green denote a positive association between terms (up-regulation, activation, enhancement etc), red arrows denote a negative association (inhibition, down regulation, suppression etc) while the grey arrows denote associations with no such directionality. The numbers within the circles denote the number of interactive sentences.

4.4 BASELINE GENE EXPRESSION: GENES AND PATHWAYS

4.4.1 Genes

This section describes the characteristics of the differentially expressed genes and their putative roles in atherosclerosis. The graphs for each gene show the fluorescent signal intensities at baseline alongside those after platelet-mediated stimulation (CRP-XL). Although these genes are differentially expressed in resting monocytes, their expression profiles in Post MI and Control groups are similar after stimulation in some instances.

4.4.1.1 Inflammatory markers

4.4.1.1.1 Tumour necrosis factor (TNF/TNF α); Chr 6p21.3

TNF is a proinflammatory cytokine secreted by macrophages and involved in a multitude of pathways including cell proliferation, apoptosis and autoimmunity. Increased levels of TNF can occur as a result of Post MI ventricular remodelling (Stumpf et al., 2008). Secondary prevention therapy (including dual anti-platelet agents, HMGCoA reductase inhibitors [statins] and inhibitors of the renin-angiotensin-aldosterone axis [ACE inhibitors, angiotensin receptor blockers and aldosterone antagonists]) has regulatory effects on TNF activity. Statins counter the effects of TNF on cardiomyocytes (Saito et al., 2007b), but do not influence circulating TNF levels (Smetanina et al., 2006). Combined aspirin and clopidogrel therapy (Chen et al., 2006) as well as angiotensin converting enzyme (ACE) inhibitors (We et al., 2002) reduce circulating TNF levels Post MI. This also explains the subdued increase in TNF gene expression in Post MI patients compared to controls following platelet-mediated stimulation described in later sections in this Chapter.

TNF gene expression levels were 1.48 fold (fdr adjusted $p=0.01$) higher in patients with a history of premature MI at baseline (Figure 4.6). The Figure shows that TNF is expressed to moderate levels (1-3,000) in the resting monocytes and that following stimulation, levels rise in both groups.

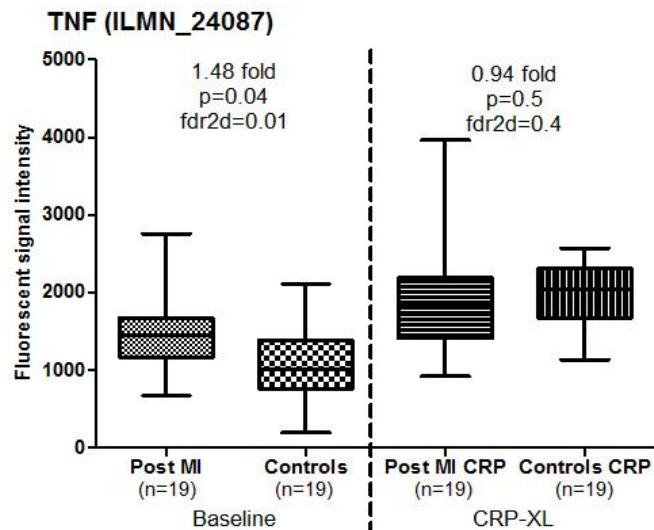


Figure 4.6: Microarray signal intensities of TNF in Post MI patients and controls. Fluorescent signal intensities in Post MI patients and controls before and after platelet-mediated stimulation are shown. Error bars denote the range of expression. Fold changes, p values and false discovery rates are provided.

ChiLiBot analysis (Figure 4.7) revealed that TNF had the most number of links with atherosclerosis in published literature amongst the differentially expressed genes.

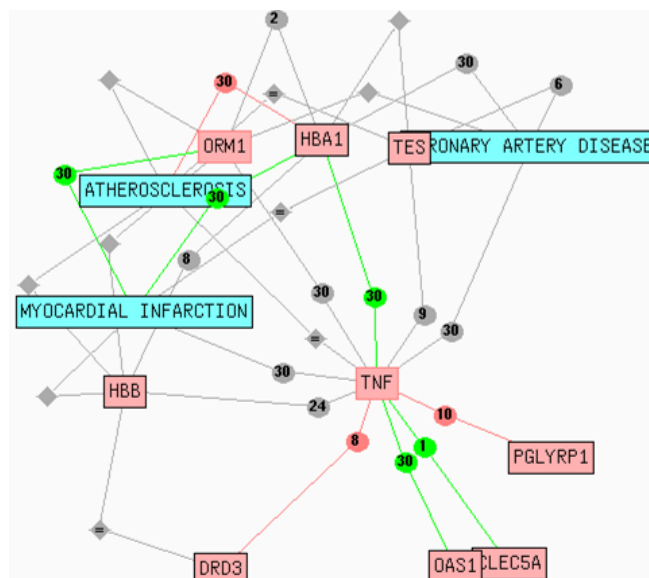


Figure 4.7: Interaction of TNF with other candidate genes and search terms (ChiLiBot).

4.4.1.1.2 Orosomucoid 1 (ORM1); Chr 9q34.1-34.3

ORM1 is recognized as a biomarker of atherosclerotic coronary disease (Correale et al., 2008) and other inflammatory conditions such as metabolic syndrome (Kvasnicka et al., 2003) and type II diabetes mellitus (Schmidt et al., 1999). Although small size studies (n=150) indicate that elevated blood levels of ORM1 (alpha 1 acid glycoprotein) associate with adverse outcome for patients after myocardial infarction (Chapelle et al., 1981), this has not been validated on a larger scale. Epidemiological studies have not revealed any relationship between raised ORM1 levels and future risk of MI (Kuller et al., 1996).

ORM1 expression levels were 1.78 fold (fdr adjusted p=0.01) higher in patients with a history of premature MI (Figure 4.8). ORM1 is expressed at low levels in resting monocytes (<500) but following platelet-mediated stimulation, levels rise significantly in Post MI patients compared to controls.

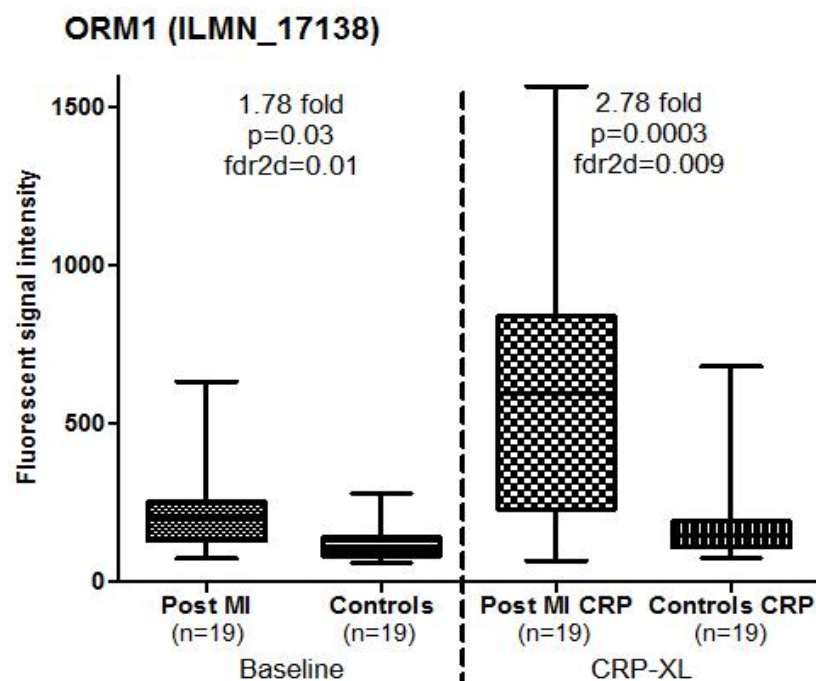


Figure 4.8: Microarray signal intensities of ORM1 in Post MI patients and controls.

Fluorescent signal intensities in Post MI patients and controls before and after platelet-mediated stimulation are shown. Error bars denote the range of expression. Fold changes, p values and false discovery rates are provided.

4.4.1.1.3 Peptidoglycan recognition protein-1 (PGLYRP1); Chr19q13.2-q13.3

PGLYRP1 is a highly conserved member of the innate immune response and plays a role in defence against bacterial infections and also in autoimmune diseases such as inflammatory arthritis and psoriasis (Dziarski and Gupta, 2010). This has been found to have an independent association with atherosclerotic burden in coronary and other vascular beds (Rohatgi et al., 2009).

PGLYRP1 gene expression levels were 1.5 fold (fdr adjusted $p=0.01$) higher in patients with a history of MI premature (Figure 4.9) at baseline. This was only expressed at low levels in resting monocytes but the levels were raised significantly in the Post MI group after stimulation.

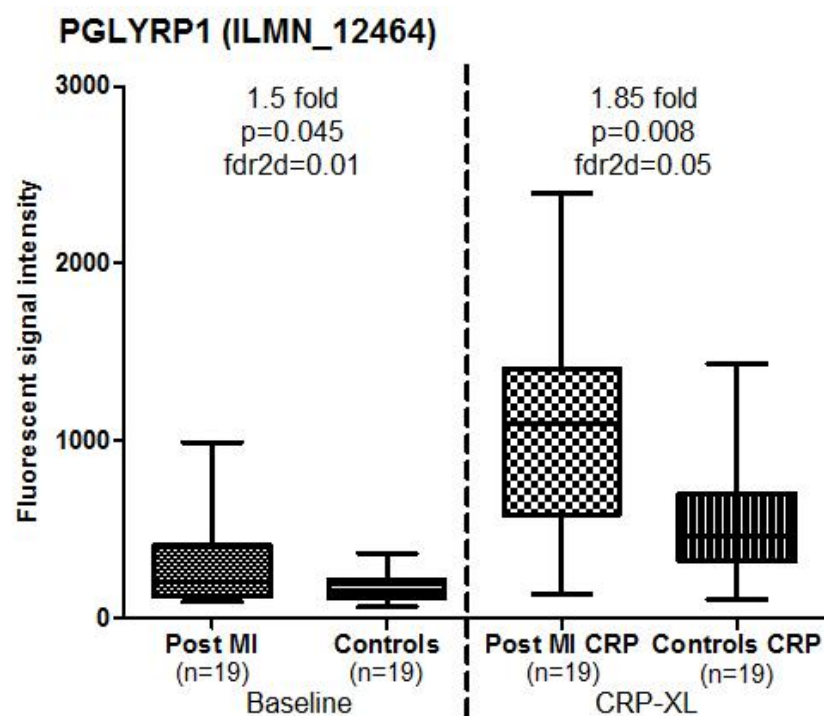


Figure 4.9: Microarray signal intensities of PGLYRP1 in Post MI patients and controls. Fluorescent signal intensities in Post MI patients and controls before and after platelet-mediated stimulation are shown. Error bars denote the range of expression. Fold changes, p values and false discovery rates are provided.

4.4.1.1.4 Testis derived transcript (TES); Chr7q31.2

This gene is similar to the mouse gene testin and contains zinc-finger motifs called LIM domains which mediate interactions between transcription factors, cytoskeletal proteins and signalling molecules. Low levels of TES have been noted at RNA and protein level in coronary arteries of patients with CAD compared to controls (sections obtained from explanted hearts and rejected donor hearts from a transplant programme) and in addition, TES expression has been shown to have a regulatory role in endothelial cells by preventing adhesion of monocytes activated by oxidized LDL (Archacki et al., 2012).

In this study, TES levels were significantly lower in the Post MI group (Figure 4.10) at baseline (0.79 fold, *fdr* adjusted *p* value = 0.01). Signal intensities increased in both groups after platelet mediated stimulation to similar levels (*p*=ns).

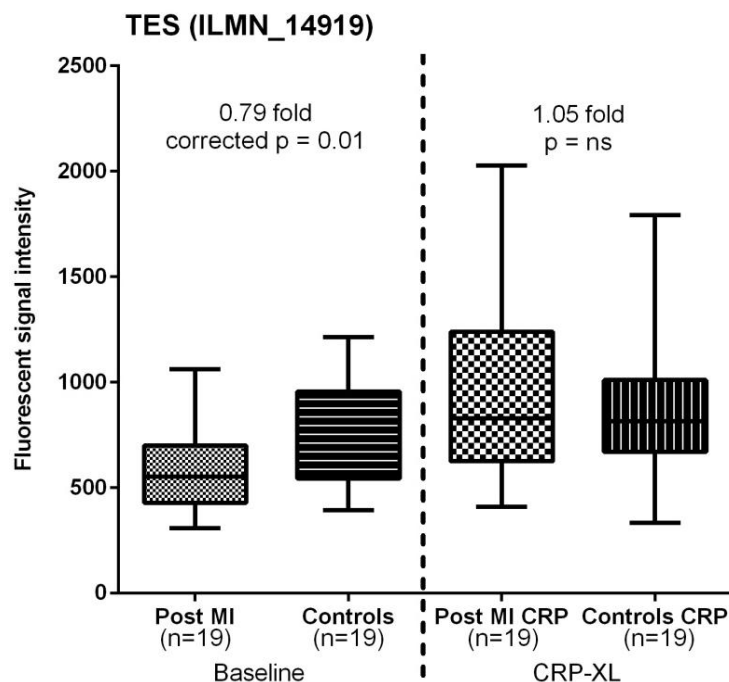


Figure 4.10: Microarray signal intensities of TES in Post MI patients and controls.

Fluorescent signal intensities in Post MI and controls before and after platelet-mediated stimulation are shown. Error bars denote the range. Fold changes, *p* values and false discovery rates are provided.

As shown in this section, the differentially expressed genes at baseline do not always maintain such differences after stimulation. The trends before and after platelet-mediated monocyte stimulation are shown together for these genes to provide an overview of their expression profile under both conditions.

4.4.2 Pathways

In addition to the ChiLiBot analysis described earlier, genes were analysed to identify common molecular pathways which may explain the observed patterns of gene expression. One such pathway which includes three of the differentially expressed genes in this experiment is the Wnt signalling pathway.

4.4.2.1 Wnt signalling pathway

This pathway is a key determinant of cell fate, proliferation and division and has a role in mediating inflammation (Gustafson and Smith, 2006) as well as response to injury (Dell'accio et al., 2008) and repair (Oerlemans et al., 2010) depending on varying stimuli and conditions (Kato, 2008). Activation of this pathway results in monocyte adhesion to endothelial cells (Lee et al., 2006). Wnt proteins have been co-localised to human and murine atherosclerotic plaques (Christman et al., 2008). In addition, Wnt5a has been linked to toll like receptor 4 (TLR4) which is an innate receptor implicated in atherosclerosis. In response to lipopolysaccharide (LPS), a known ligand of TLR4, increased expression of Wnt5a is seen in murine macrophages (Christman et al., 2008). Wnt signalling is also implicated in arterial calcification (Shao et al., 2007) and apoptosis (Zhang et al., 2009b).

Three genes differentially expressed in Post MI patients, TNF, CXCL5 and olfactomedin, have established roles in regulating the Wnt signalling pathway. The

gene expression profile of TNF has been previously described in this Chapter. The other two genes are described below.

4.4.2.1.1 CXXC5 (CF5/RINF); Chr 5q31.2

CXXC5 (retinoid inducible nuclear factor, RINF) is a transcriptional regulator in myeloid cell differentiation (Pendino et al., 2009).

CXXC5 gene expression was 0.74 fold ($p=0.02$, $fdr_{2d}=0.01$) in patients with premature MI (Figure 4.11). This was expressed to moderate levels in resting monocytes and the levels rose in response to platelet-mediated stimulation. Lower levels were seen in Post MI patients compared to controls under both conditions, although the difference was not statistically significant after stimulation.

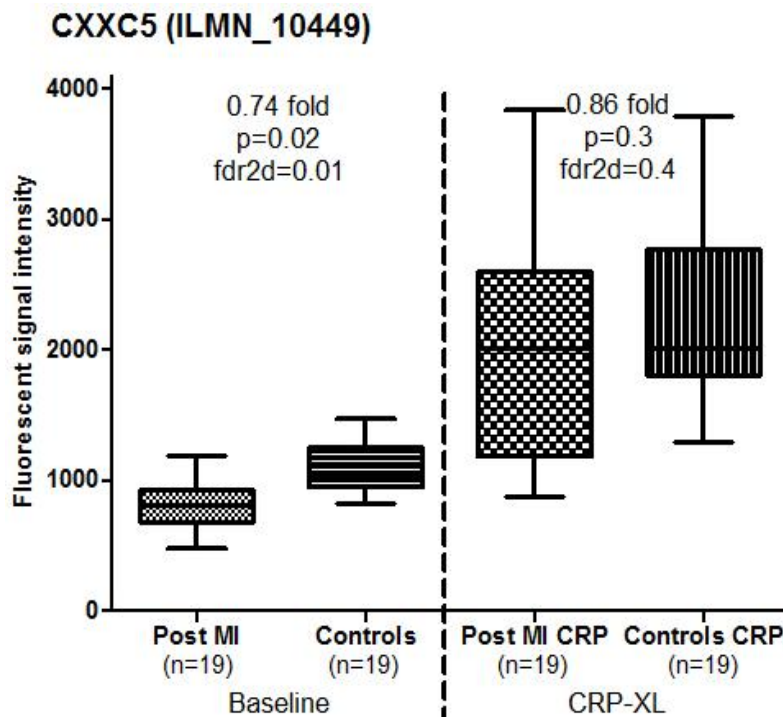


Figure 4.11: Microarray signal intensities of CXXC5 in Post MI patients and controls.

Fluorescent signal intensities in Post MI patients and controls before and after platelet-mediated stimulation are shown. Error bars denote the range of expression. Fold changes, p values and false discovery rates are provided.

4.4.2.1.2 Olfactomedin 1 (OLFM1); Chr 9q34.3

OLFM1 is involved in differentiation of neuronal tissue. This was represented by two probes on the microarray platform (ILMN_1435, ILMN_27345). The signal intensities (Figure 4.12) indicate that it is a low abundance gene in the monocyte (range 100-400). Both probes showed significantly lower gene expression in patients with premature MI (0.74 fold and 0.67 fold respectively, $fdr_{2d}=0.01$ for both). Gene expression was down regulated after platelet-mediated stimulation in both groups.

Low abundance genes with small amplitude changes can give rise to errors in interpretation of microarray signal intensities. However in this instance, the consistent magnitude and direction of change in signal intensities for both probes representing the same gene makes a false positive result unlikely.

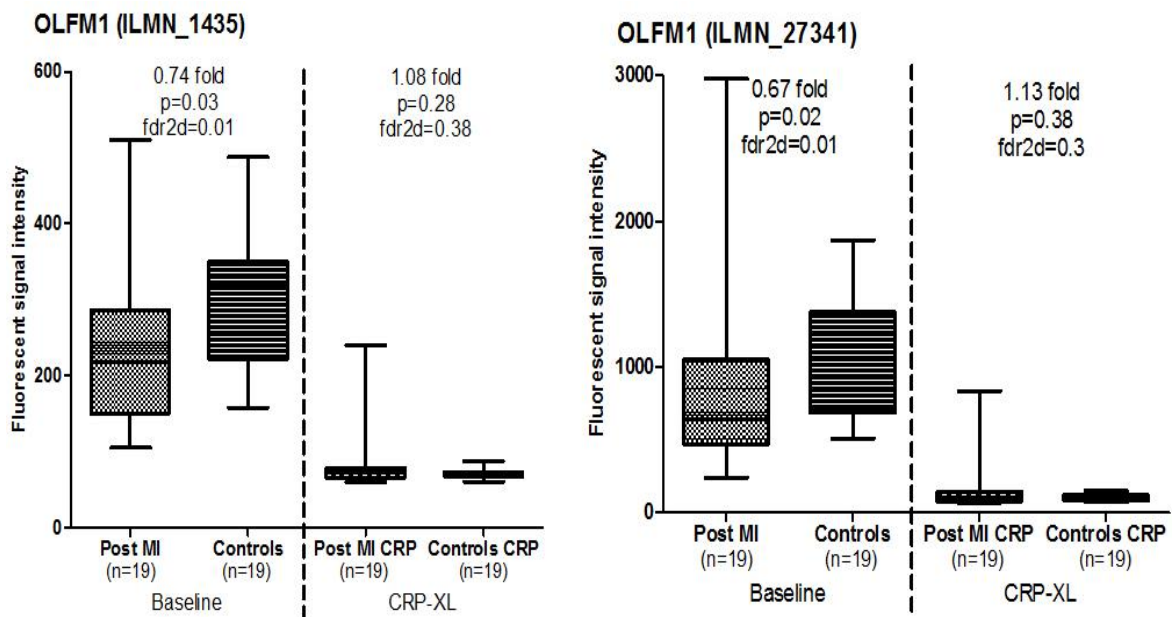


Figure 4.12: Microarray signal intensities of OLFM1 in Post MI patients and controls.

Fluorescent signal intensities in Post MI patients and controls before and after platelet-mediated stimulation are shown. Error bars denote the range of expression. Fold changes, p values and false discovery rates are provided.

4.4.2.1.3 Hypothetical roles of differentially expressed genes in Wnt signalling

TNF promotes arterial calcification in animal models by inducing Wnt signalling in the vessel wall (Al-Aly, 2008). Msx2, a muscle segment homeobox gene family member has been shown to up-regulate expression of wnt3a and wnt7a (Shao et al., 2005) in a TNF dependent manner. This has been shown to be mediated through the transcription factor nuclear factor kappa B (NFkB) and promotes vascular smooth muscle calcification (Lee et al., 2010). There is emerging evidence that oxidative stress injury activates TNF and plays a role in Msx2-Wnt dependent aortic calcification (Lai et al., 2012).

In certain tissues, CXXC5 has an inhibitory effect on Wnt signalling. CXXC5 suppresses Wnt signalling in neural stem cells (Andersson et al., 2009). The down regulation of CXXC5 seen in this analysis may indicate a release of the Wnt pathway from regulation by CXXC5. CXXC5 is also known as Wilms' tumour 1 (WT1) induced inhibitor of Dishevelled (WID). Dishevelled is a protein that promotes Wnt signalling (Gao and Chen, 2010). By inhibiting Dishevelled, CXXC5 inhibits Wnt/beta catenin signalling (Kim et al., 2010). In a rat model of myocardial infarction, increased levels of Dishevelled and beta catenin, its downstream target in the Wnt signalling pathway have been noted in areas of neovascularisation in injured myocardium (Blankesteyn et al., 2000) suggesting a role for Wnt signalling in cell proliferation and migration.

OLFM1 protein is involved in differentiation of neuronal tissue and modulates Wnt signalling (Nakaya et al., 2008). Wnt signalling is important in actin stress fibre mediated cell motility and adhesion (Uren et al., 2004, Bohr et al., 2011). OLFM1 is over expressed during phases of tissue repair and promotes Wnt mediated actin cytoskeletal reorganization (Bohr et al., 2011). The down regulation of OLFM1 in Post MI patients may indicate a reduced potential for cell repair. Figure 4.13 summarises the proposed roles of these genes in Wnt signalling.

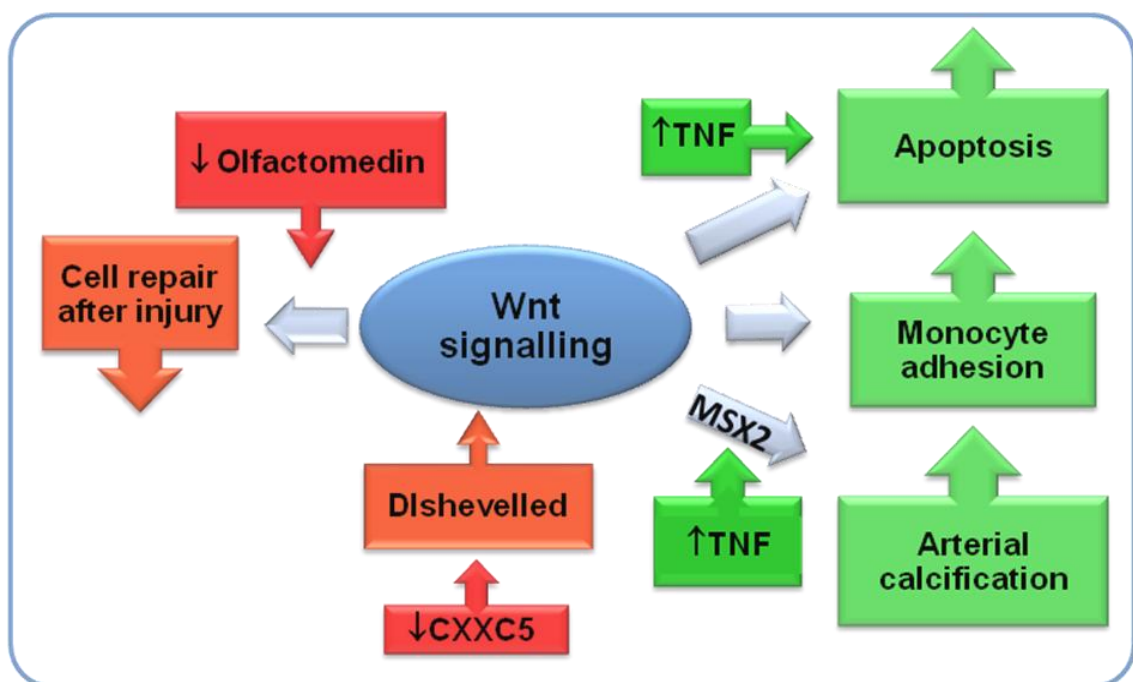


Figure 4.13: Differentially expressed genes with roles in Wnt signalling.

CXXC5 and OLFM1, the two down regulated genes in the red boxes are important in regulation of tissue repair processes mediated by Wnt signalling. TNF, the up-regulated gene in the green box drives the Wnt pathway in a pro-apoptotic and proatherosclerotic direction.

4.5. ANALYSIS OF DIFFERENTIALLY EXPRESSED MONOCYTES GENES AFTER PLATELET MEDIATED STIMULATION (CRP-XL)

The differences in monocyte gene expression between Post MI and control groups following platelet mediated stimulation by incubation of whole blood samples with CRP-XL are explored in this section (Figure 4.14).

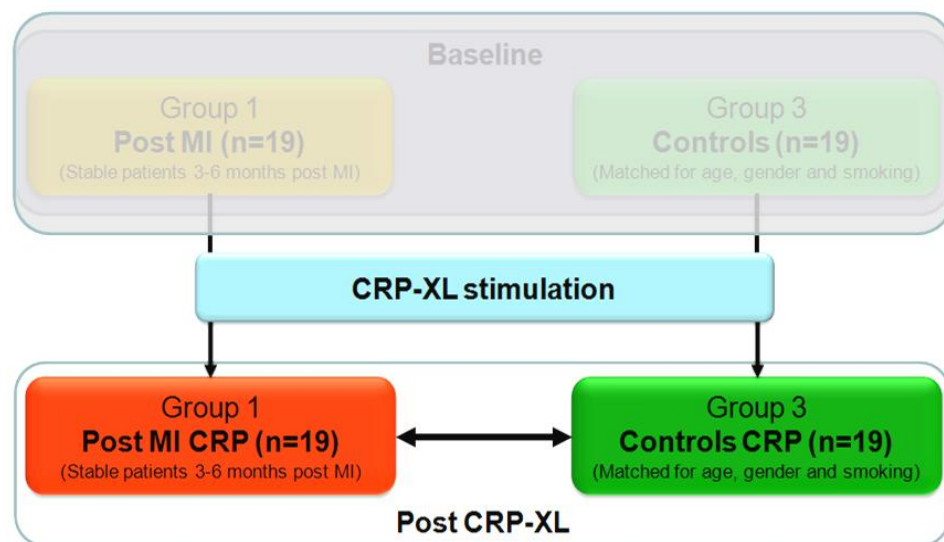


Figure 4.14: Scheme of analysis – Post MI vs. Controls after platelet mediated stimulation.

4.6 GENE EXPRESSION IN ACTIVATED MONOCYTES: INITIAL ANALYSIS

Peripheral venous blood samples collected in citrate tubes were stimulated with activated platelets (confirmed by MPA formation on flowcytometry) following which CD14⁺ monocytes were isolated and RNA was extracted in TRIzol. The microarray signal intensities were quantile normalized and then compared (Post MI (Group 1) vs. Controls (Group 3)) and statistically analysed for significant differential expression. Differential expression of transcripts in the Post MI group in comparison to healthy controls was confirmed in sigmoid plots (Figure 4.15).

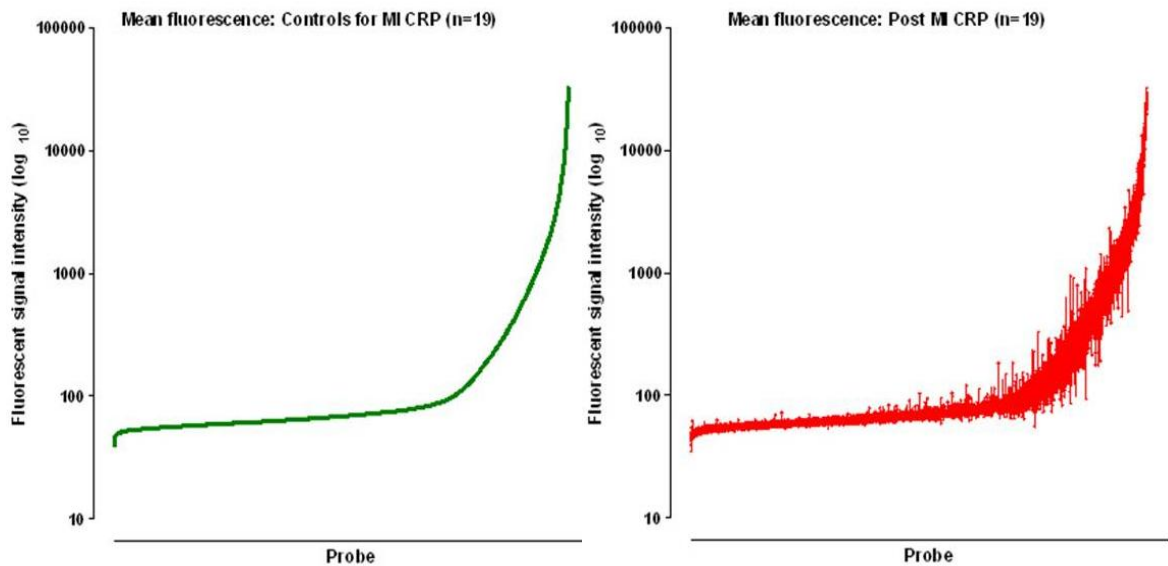


Figure 4.15: Sigmoid plots of fluorescent signal intensity in stimulated monocytes.

The graph shows mean fluorescent signal intensities of all probe sets following stimulation in healthy Controls (left) and corresponding changes in signal intensities in the Post MI group (right). The ‘noise’ in the graph on the right denotes the change in gene expression for each probe on the array in the Post MI group when compared to controls.

Degree (fold change) and significance (p value) of each transcript probe set are graphically represented in Figure 4.16.

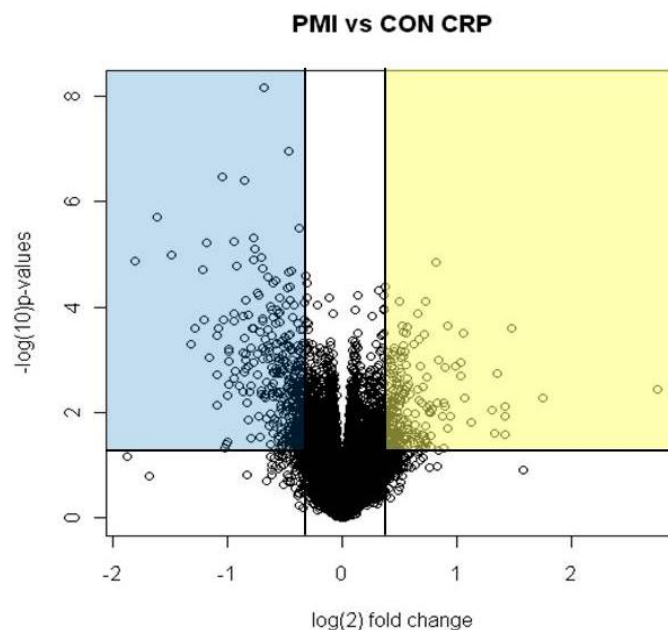


Figure 4.16: Volcano plot of Post MI vs. controls after CRP-XL stimulation.

\log_2 of fold change (Post MI/controls) is plotted on the x-axis and \log_{10} of p-values (t test, uncorrected) is plotted on the y-axis. The yellow and blue shaded regions contain up and down regulated transcripts respectively which fulfil the filtering criteria for subsequent candidate gene analyses.

Differentially expressed genes were analysed according to the fold change in gene expression. In the initial screening step, genes which did not return 'present' calls in any of the samples were excluded. The first level statistical filter excluded those genes which had an uncorrected p value >0.05 and a false discovery rate $>50\%$ ($fdr_{2D}>0.5$). More genes (742 transcripts) were differentially expressed in stimulated monocytes than in resting monocytes in the Post MI group compared to controls.

To further identify the most significant differences in gene expression, additional filtering steps were performed (Figure 4.17) to select transcripts which were up-regulated >1.25 fold or down regulated <0.8 fold. In addition, the false discovery rate was set to $<5\%$. This identified 169 transcripts, of which 24 were up-regulated and 145 were down regulated in patients with premature MI compared to controls (Table 4.2).

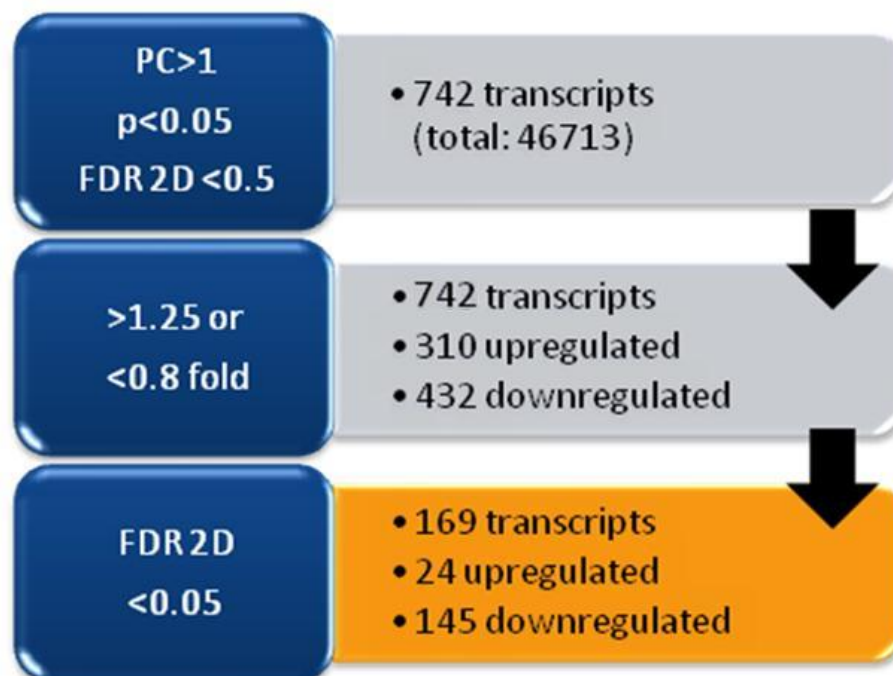


Figure 4.17: Gene transcript filtering strategy to identify differentially expressed genes. The orange panel highlights the filtering threshold used for candidate gene analyses (PC=present call).

Probe ID	Symbol	Fold change	p values	FDR2D
ILMN_8881	RAB8A	6.70	0.00	0.00
ILMN_10827	LEP	3.36	0.01	0.01
ILMN_17138	ORM1	2.78	0.00	0.01
ILMN_8723	HIG2	2.68	0.01	0.02
ILMN_10067	FAM13A1	2.55	0.00	0.02
ILMN_46649	LOC641710	2.48	0.01	0.02
ILMN_19494	ARG1	2.10	0.01	0.04
ILMN_6296	ACN9	2.04	0.00	0.03
ILMN_26372	GPR109A	2.04	0.00	0.03
ILMN_22584	GPR109B	1.99	0.00	0.03
ILMN_19740	DNAJB1	1.85	0.01	0.05
ILMN_19500	LRRC33	1.76	0.00	0.00
ILMN_2033	CYP27A1	1.66	0.00	0.03
ILMN_27567	EDG2	1.58	0.00	0.03
ILMN_21141	HIP1	1.55	0.00	0.05
ILMN_8232	CASP5	1.47	0.00	0.04
ILMN_11630	CLEC10A	1.46	0.00	0.05
ILMN_10994	KMO	1.45	0.00	0.05
ILMN_20480	IRF8	1.45	0.00	0.05
ILMN_23335	EVA1	1.44	0.00	0.05
ILMN_13014	CCDC47	1.29	0.00	0.00
ILMN_34995	LOC653257	1.29	0.00	0.02
ILMN_13138	ACAT2	1.29	0.00	0.04
ILMN_13755	CLDN7	1.28	0.00	0.04
ILMN_3312	PARP15	0.80	0.00	0.04
ILMN_18062	NGFB	0.80	0.00	0.04
ILMN_15870	ST7	0.79	0.00	0.03
ILMN_19125	RUNX1	0.79	0.00	0.03
ILMN_15279	CLCN3	0.79	0.00	0.04
ILMN_20831	FHL2	0.79	0.00	0.05
ILMN_19522	CDK2AP1	0.78	0.00	0.04
ILMN_1204	KCTD9	0.78	0.00	0.05
ILMN_139066	SLC25A15	0.78	0.00	0.03
ILMN_3945	PLCB1	0.78	0.00	0.04
ILMN_19796	MPP1	0.78	0.00	0.05
ILMN_16947	C9orf5	0.78	0.00	0.04
ILMN_14672	GMFB	0.77	0.00	0.04
ILMN_28419	HCRTR1	0.77	0.00	0.03
ILMN_20942	HSA277841	0.77	0.00	0.03
ILMN_1833	PPAPDC1B	0.77	0.00	0.04
ILMN_29976	TFDP2	0.76	0.00	0.03
ILMN_12727	ADAM19	0.76	0.00	0.05
ILMN_45804	LOC389850	0.76	0.00	0.04

Probe ID	Symbol	Fold change	p values	FDR2D
ILMN_45056	LOC440895	0.76	0.00	0.05
ILMN_18176	CALCRL	0.75	0.00	0.05
ILMN_10040	ITSN1	0.75	0.00	0.05
ILMN_10494	ANXA2P1	0.75	0.00	0.05
ILMN_23756	CD86	0.75	0.00	0.02
ILMN_7118	N4BP2	0.74	0.00	0.02
ILMN_17847	PLEKHA5	0.74	0.00	0.04
ILMN_6698	OR51B5	0.73	0.00	0.01
ILMN_39737	LOC284964	0.73	0.00	0.03
ILMN_139014	ZAK	0.73	0.00	0.03
ILMN_6130	ZMYND11	0.73	0.00	0.01
ILMN_12419	PFTK1	0.73	0.00	0.01
ILMN_25073	MICAL-L1	0.73	0.00	0.02
ILMN_23265	RBBP7	0.73	0.00	0.03
ILMN_4738	ITGB1	0.72	0.00	0.00
ILMN_27344	CABP5	0.72	0.00	0.03
ILMN_20899	PTK2	0.72	0.00	0.01
ILMN_28222	AMY1C	0.72	0.00	0.04
ILMN_21502	ACVR1	0.72	0.00	0.02
ILMN_23979	SNTB1	0.72	0.00	0.03
ILMN_15850	C20orf22	0.72	0.00	0.01
ILMN_12895	VRK2	0.72	0.00	0.03
ILMN_26838	CDCP1	0.72	0.00	0.04
ILMN_137635	ZAK	0.72	0.00	0.04
ILMN_21371	FLNB	0.72	0.00	0.04
ILMN_5465	CDCA4	0.71	0.00	0.02
ILMN_24480	SDC4	0.71	0.00	0.01
ILMN_43377	ZNF469	0.71	0.00	0.01
ILMN_12126	TCF4	0.71	0.00	0.03
ILMN_15188	DOCK10	0.71	0.00	0.02
ILMN_3785	ATP1B3	0.70	0.00	0.03
ILMN_21073	C5orf4	0.70	0.00	0.04
ILMN_2058	FLJ20054	0.70	0.00	0.02
ILMN_415	CALD1	0.70	0.00	0.03
ILMN_25419	FAM102B	0.70	0.00	0.04
ILMN_43240	LOC653486	0.70	0.00	0.02
ILMN_19382	MEIS1	0.69	0.00	0.02
ILMN_20806	CLDN5	0.69	0.00	0.02
ILMN_14904	NFIB	0.69	0.00	0.04
ILMN_19752	ITGAE	0.69	0.00	0.01
ILMN_17456	SOX4	0.69	0.00	0.01
ILMN_23051	GALNT6	0.69	0.00	0.02
ILMN_18092	SCGB1C1	0.69	0.00	0.02

Probe ID	Symbol	Fold change	p values	FDR2D
ILMN_26025	PGBD5	0.68	0.00	0.04
ILMN_21711	PROCR	0.68	0.00	0.01
ILMN_26360	EPAS1	0.68	0.00	0.04
ILMN_9320	AKAP12	0.68	0.00	0.03
ILMN_137372	DRD3	0.68	0.00	0.02
ILMN_30352	HAK	0.68	0.00	0.02
ILMN_4227	PDE5A	0.68	0.00	0.04
ILMN_138607	ATP1B3	0.68	0.00	0.01
ILMN_20242	LGMN	0.68	0.00	0.04
ILMN_20369	MFAP4	0.67	0.00	0.01
ILMN_137673	CRLF2	0.67	0.00	0.02
ILMN_11463	STX1A	0.67	0.00	0.02
ILMN_24244	HBQ1	0.67	0.00	0.04
ILMN_29267	ALOX12	0.67	0.00	0.04
ILMN_8814	CTSL	0.66	0.00	0.00
ILMN_20088	ANPEP	0.66	0.00	0.01
ILMN_18609	CRLF2	0.66	0.00	0.04
ILMN_28610	NT5E	0.66	0.00	0.01
ILMN_5990	GRAP2	0.65	0.00	0.01
ILMN_3923	CXorf20	0.65	0.00	0.01
ILMN_12877	CRADD	0.65	0.00	0.02
ILMN_7756	SRGAP1	0.64	0.00	0.02
ILMN_138322	PHLDA1	0.64	0.00	0.02
ILMN_21395	CCL22	0.64	0.00	0.02
ILMN_9952	ABHD6	0.64	0.00	0.00
ILMN_28273	FGFRL1	0.64	0.00	0.02
ILMN_27871	DOCK7	0.64	0.00	0.01
ILMN_7859	FLJ20701	0.63	0.00	0.02
ILMN_10912	THBD	0.63	0.00	0.01
ILMN_37532	LOC402538	0.62	0.00	0.00
ILMN_30353	SCCPDH	0.62	0.00	0.00
ILMN_23523	FREQ	0.62	0.00	0.01
ILMN_25344	SPTBN5	0.62	0.00	0.02
ILMN_16305	FLJ45337	0.62	0.00	0.02
ILMN_3531	TMSB4Y	0.62	0.00	0.01
ILMN_6240	PSD3	0.61	0.00	0.00
ILMN_11680	GUCY1A3	0.61	0.00	0.01
ILMN_8714	PGRMC1	0.60	0.00	0.00
ILMN_11682	TSC22D1	0.60	0.00	0.02
ILMN_16763	DNAH17	0.60	0.00	0.05
ILMN_27069	HPSE	0.60	0.00	0.00
ILMN_6113	PSD3	0.59	0.00	0.00
ILMN_28140	TINAGL1	0.59	0.00	0.00

Probe ID	Symbol	Fold change	p values	FDR2D
ILMN_23858	GPR56	0.59	0.00	0.01
ILMN_28958	NRIP3	0.59	0.00	0.00
ILMN_15510	FSTL1	0.58	0.00	0.03
ILMN_15414	CDCP1	0.58	0.00	0.01
ILMN_30091	TSPAN9	0.58	0.00	0.02
ILMN_1789	CCL20	0.57	0.00	0.03
ILMN_13668	RIS1	0.57	0.00	0.01
ILMN_6950	SGNE1	0.56	0.00	0.00
ILMN_22648	ACRBP	0.56	0.00	0.02
ILMN_13440	MGC13057	0.56	0.00	0.04
ILMN_4207	MMD	0.56	0.00	0.02
ILMN_14624	Wnt5A	0.56	0.00	0.04
ILMN_1429	TFPI	0.55	0.00	0.00
ILMN_12108	SDC2	0.55	0.00	0.01
ILMN_16991	NEK6	0.55	0.00	0.02
ILMN_137523	SMOX	0.53	0.00	0.00
ILMN_31298	LOC58489	0.53	0.00	0.04
ILMN_28857	MYO10	0.52	0.00	0.01
ILMN_8663	CML2	0.52	0.00	0.01
ILMN_13834	TMEPAI	0.52	0.00	0.00
ILMN_2477	TPST1	0.50	0.00	0.02
ILMN_9078	C21orf7	0.50	0.00	0.01
ILMN_3962	CLEC1B	0.49	0.00	0.01
ILMN_17834	TFPI	0.48	0.00	0.00
ILMN_18096	COL22A1	0.47	0.00	0.01
ILMN_24123	CCL7	0.47	0.00	0.01
ILMN_11451	WDR69	0.44	0.00	0.00
ILMN_2172	SIGLEC12	0.43	0.00	0.01
ILMN_22074	PPBP	0.43	0.00	0.00
ILMN_21398	CXCL5	0.41	0.00	0.04
ILMN_10606	KIAA1199	0.36	0.00	0.00
ILMN_2147	CMKOR1	0.33	0.00	0.00

Table 4.2: Post MI vs. Controls – differentially expressed genes after platelet-mediated stimulation.

The up-regulated gene IDs are in yellow and the down regulated in blue. Fold changes (Post MI/Controls) are tabulated. All transcripts fulfilled the filtering thresholds (present calls in >1, fold change >1.25 or < 0.8, uncorrected p value <0.05, false discovery rate [fdr2D] <0.05). Unmapped transcripts are not shown.

4.7 GENE EXPRESSION IN ACTIVATED MONOCYTES: LINKS WITH CAD

To identify known relationships of the candidate molecules with each other and with atherosclerosis, further text mining analysis was performed using ChiLiBot. The candidate genes were analysed for previously reported interactions in published literature with each other and with the following key words: atherogenesis, atherosclerosis, atherothrombosis, coronary artery disease, myocardial infarction, monocyte, macrophage and collagen.

Of the differentially expressed genes, 11 molecules had established links with the aforementioned key words in published literature after further filtering to exclude co-occurrence in abstracts without interactive relationships (Figure 4.18). This analysis enabled the selection of genes with the strongest pathophysiological links to atherosclerosis from the candidate genes which showed maximal differential expression following platelet mediated monocyte stimulation.

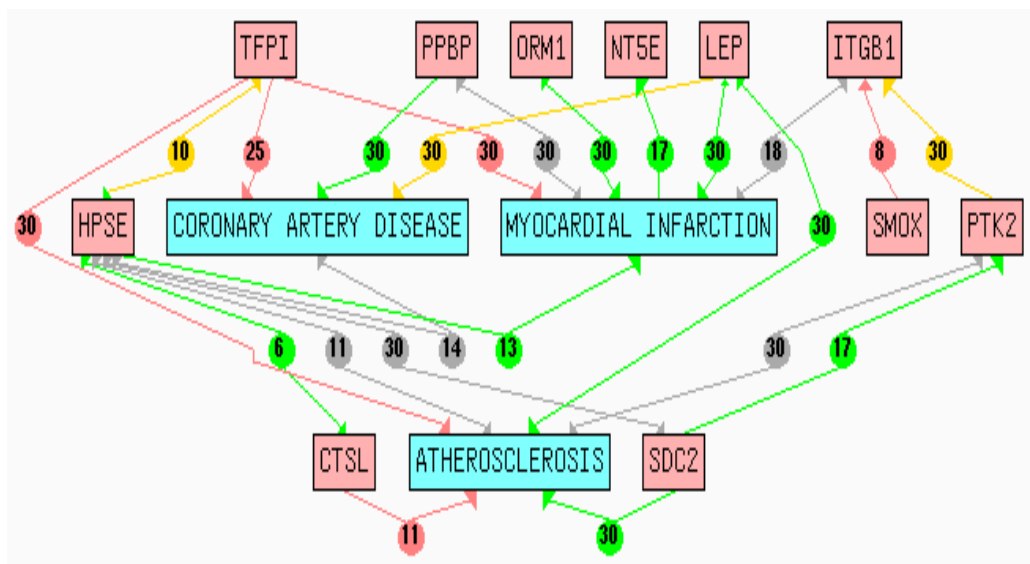


Figure 4.18: Lists of interactions on PubMed for each candidate gene (ChiLiBot).

The candidate genes include regulators of metabolism (leptin, coagulation (TFPI, HPSE) and enzymes (NT5E).

4.8 GENE EXPRESSION IN ACTIVATED MONOCYTES: GENES AND PATHWAYS

4.8.1 Genes

4.8.1.1 Regulators of coagulation (Figure 4.19)

Differentially expressed genes after platelet-mediated stimulation included tissue factor pathway inhibitor (TFPI), thrombomodulin, protein C receptor, syndecan 2, heparanase and cathepsin L. Legumain, a regulator of cathepsin L was also differentially expressed. Further analysis of published literature was performed to assess which of these are likely to be an effect of pharmacotherapy.

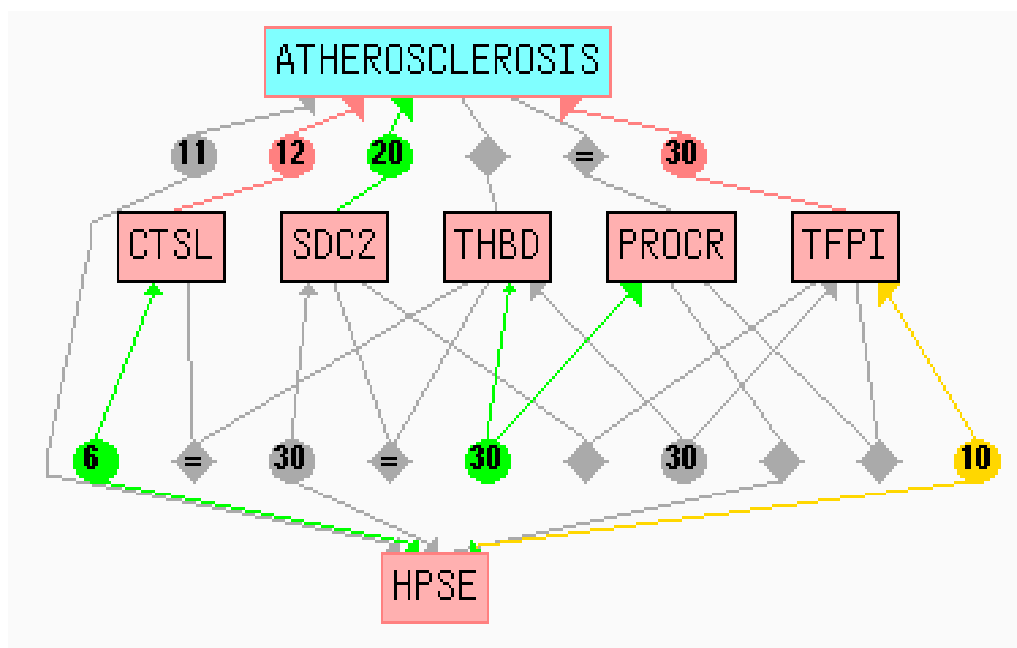


Figure 4.19: Lists of interactions on PubMed for regulators of coagulation (ChiLiBot).

The arrows in green denote a positive association between terms (up-regulation, activation, enhancement etc), red arrows denote a negative association (inhibition, down regulation, suppression etc) while the grey arrows denote associations with no such directionality. The numbers within the circles denote the number of interactive sentences.

Quantitative PCR for validation of microarray fluorescent signal intensities was performed on one of the genes (TFPI) which had the most significant differential expression in the Post MI group compared to matched healthy controls.

4.8.1.1.1 Tissue factor pathway inhibitor (TFPI); Chr 2q32

TFPI was represented by two probes on the microarray (ILMN_1429, ILMN_17834). Both showed (Figure 4.20) significantly lower gene expression in patients with premature MI (0.48 fold and 0.55 fold respectively, $fdr_{2d}=0.01$). Signal intensities of the two probes indicate that TFPI is expressed at low levels in resting monocytes and that there is a significant increase in expression following platelet-mediated stimulation. This was confirmed by Q-PCR (Figure 4.21).

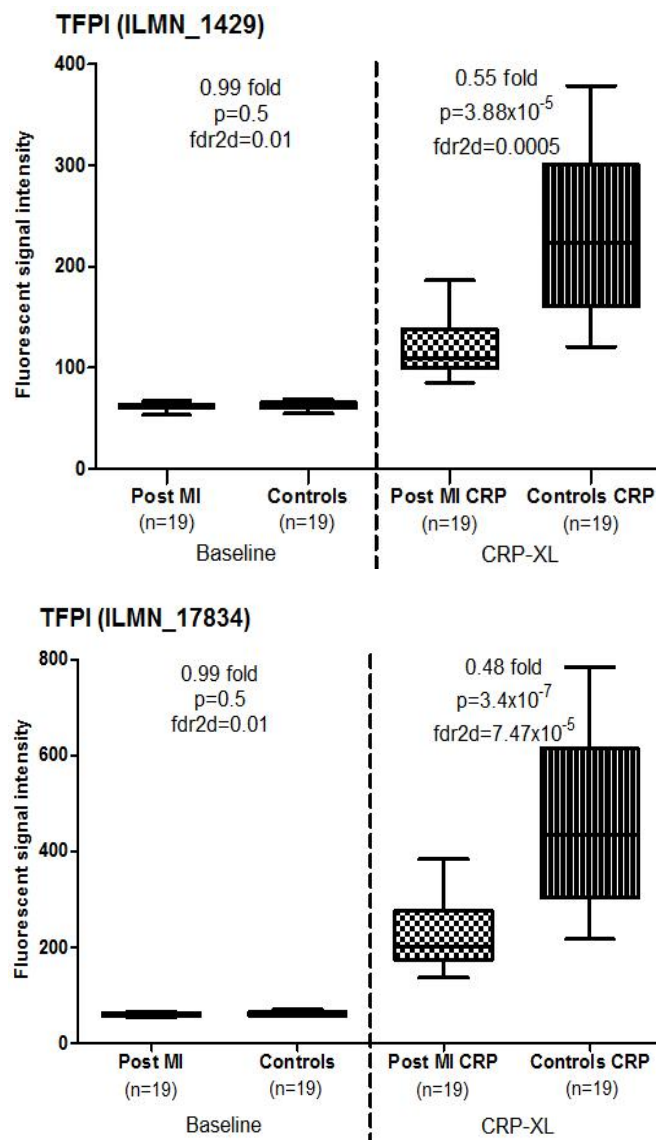


Figure 4.20: Microarray signal intensities of TFPI in Post MI patients and controls.

Fluorescent signal intensities in Post MI patients and controls before and after platelet-mediated stimulation are shown. Error bars denote the range of expression. Fold changes, p values and false discovery rates are provided.

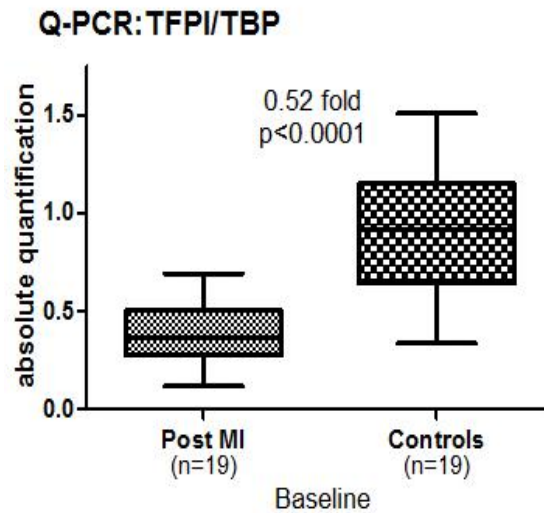


Figure 4.21: quantitative PCR of TFPI in Post MI patients and controls.

Q-PCR of TFPI with tata box protein as control gene is shown. Error bars denote the range of expression. Fold change and p value are provided.

Following monocyte activation, TFPI levels increased in both groups, however the rise was less impressive in patients with MI. This is not readily explained by pharmacotherapy. There is no evidence in published literature that either aspirin or clopidogrel affect TFPI levels. There is evidence that dyslipidaemia reduces levels of TFPI (Zawadzki et al., 2007) whilst statins have been shown to increase TFPI levels (Tetik et al., 2010). TFPI expression was up-regulated within plaque macrophages with increasing atherosclerotic burden (Crawley et al., 2000) and was associated with attenuated tissue factor activity (Caplice et al., 1998).

The relative deficiency of TFPI in patients with MI compared to controls indicates the possible pathophysiology underlying acute luminal occlusion of coronary arteries after plaque rupture in the Post MI patients. All of these patients had clinical and electrocardiographic evidence of acute coronary luminal occlusion at the time of their MI (STEMI). The reduction in TFPI release from monocytes at the site of plaque rupture may result in accelerated atherothrombosis due unopposed action of TF resulting in rapid coronary luminal thrombosis.

4.8.1.1.2 Thrombomodulin (THBD); Chr 20p11.2

THBD is an endothelial thrombin binding receptor which activates Protein C. It modulates cellular proliferation, adhesion and inflammation (Li et al., 2009b) and has anticoagulant properties on par with TFPI and activated protein C (Saito et al., 2007a). Thrombomodulin plays a role in arterial remodelling and neointimal proliferation (Li et al., 2006). Thrombomodulin is critical to thrombin mediated activation of protein C (Van de Wouwer et al., 2004).

Fluorescent signal intensities suggest that THBD is expressed at moderate levels in activated monocytes. Although platelet-mediated stimulation resulted in increased expression of THBD in both groups, levels were 0.63 fold (fdr adjusted $p=0.014$) lower in the Post MI group (Figure 4.22).

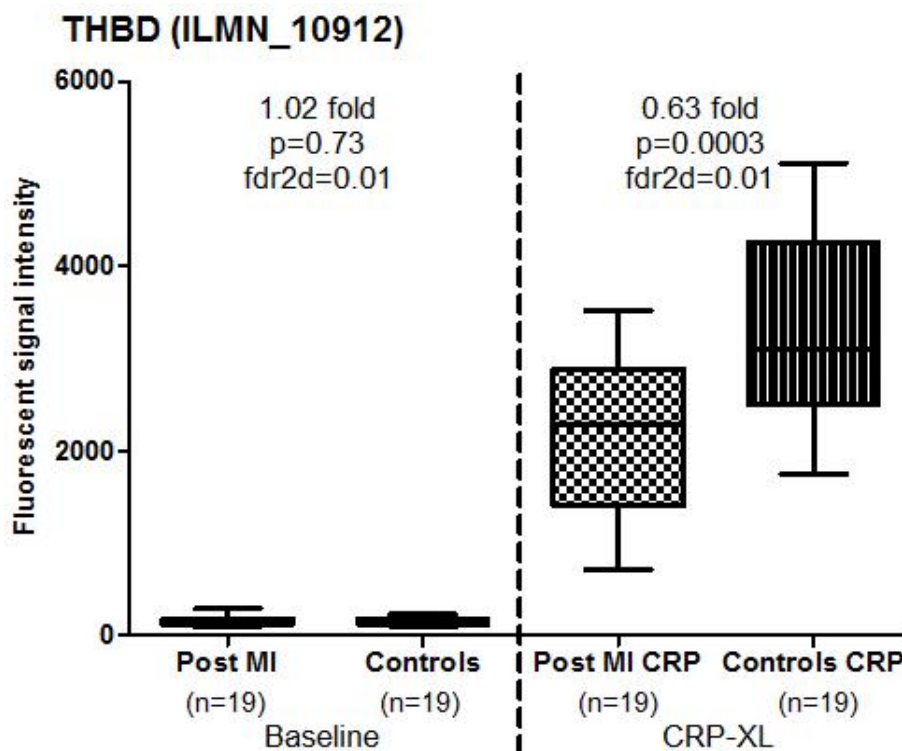


Figure 4.22: Microarray signal intensities of THBD in Post MI patients and controls.

Fluorescent signal intensities in Post MI patients and controls before and after platelet-mediated stimulation are shown. Error bars denote the range of expression. Fold changes, p values and false discovery rates are provided.

4.8.1.1.3 Syndecan 2 (SDC2); Chr 8q22-q23

SDC2 is a transmembrane heparan sulphate proteoglycan (HSPG) and a key constituent of the subendothelial extracellular matrix which affect basement membrane permeability and cellular adhesion. Vascular HSPGs decrease during atherosclerosis (Pillarsetti, 2000). Endothelial cells exposed to oxidised LDL increase the expression of heparanase which reduces cell surface expression of HSPG allowing subendothelial migration and binding of oxidised LDL to fibronectin (Pillarsetti et al., 1997). Increased SDC2 activity in endothelial cells is associated with reduced monocyte binding and a decreased tendency to atherosclerosis (Duan et al., 2005).

SDC2 levels were significantly raised in both groups after stimulation (Figure 4.23), However this was expressed 0.55 fold (fdr2d p = 0.008) lower in patients with premature MI after platelet-mediated monocyte stimulation.

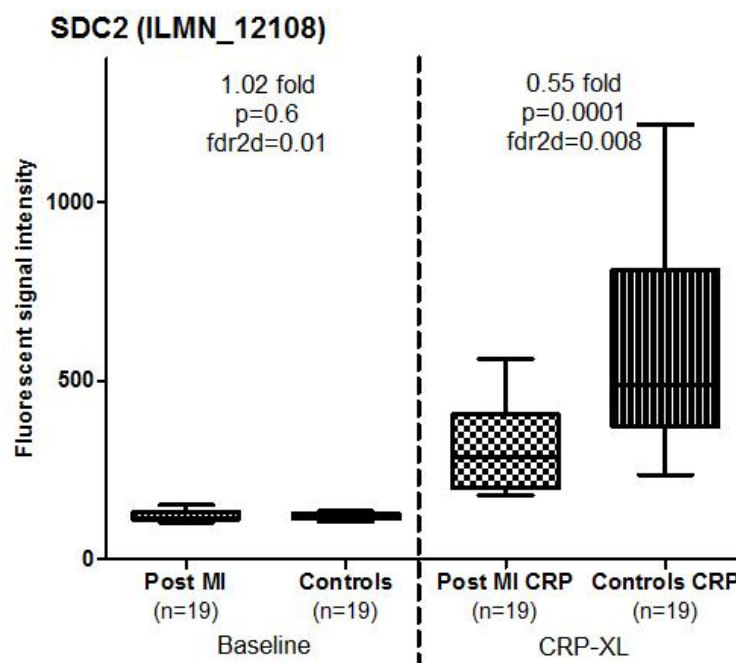


Figure 4.23: Microarray signal intensities of SDC2 in Post MI patients and controls.

Fluorescent signal intensities in Post MI patients and controls before and after platelet-mediated stimulation are shown. Error bars denote the range of expression. Fold changes, p values and false discovery rates are provided.

4.8.1.1.4 Protein C Receptor (PROCR/EPCR/CD201 antigen); Chr 20q11.2

Two polymorphisms in the PROCR gene are protective against MI (Medina et al., 2008) and associated with either high levels of activated protein C or PROCR. The inflammatory marker, C reactive protein has been shown to down regulate the expression of PROCR and THBD in endothelial cells (Nan et al., 2005). In circulating monocytes, PROCR expression in response to activated protein C reduced monocyte chemoattractant protein-1 (MCP-1) induced chemotaxis and suppressed TNF-alpha expression (Xue et al., 2007).

PROCR was expressed 0.68 fold lower (fdr2d p=0.01) in patients Post MI after platelet-mediated stimulation (Figure 4.24). No significant difference was noted in resting monocytes.

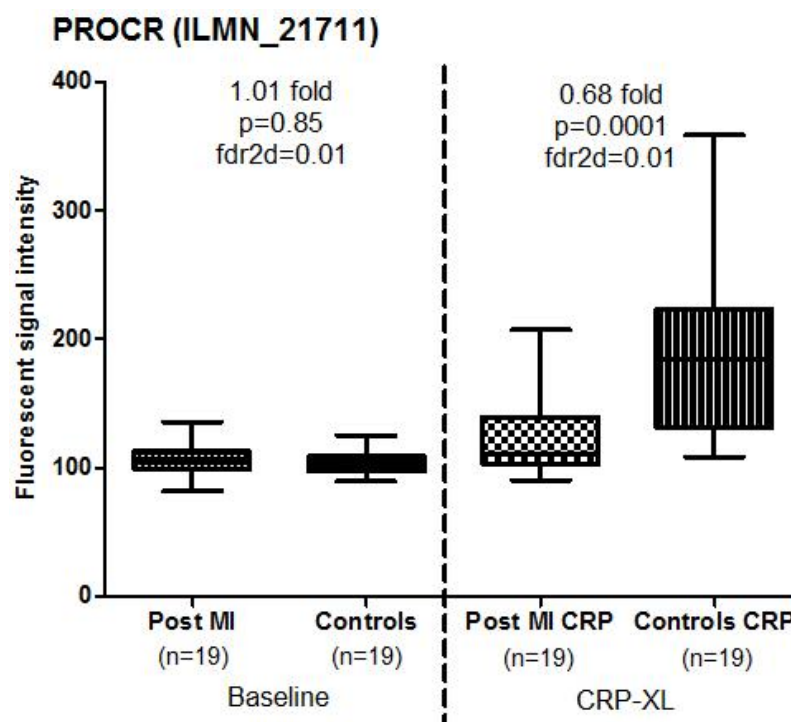


Figure 4.24: Microarray signal intensities of PROCR in Post MI patients and controls.

Fluorescent signal intensities in Post MI patients and controls before and after platelet-mediated stimulation are shown. Error bars denote the range of expression. Fold changes, p values and false discovery rates are provided.

4.8.1.1.5 Cathepsin L (CTSL); Chr 9q21.33

CTSL is a lysosomal cysteine proteinase with a role in atherosclerosis. High levels of cathepsin L have been associated with macrophage death, necrotic core formation and atherosclerotic plaque destabilisation (Li et al., 2009a). Serum cathepsin levels positively correlate with coronary stenoses on angiography (Liu et al., 2006).

CTSL is expressed at moderate levels in resting monocytes (1-2,000) in both groups (Figure 4.25). Following platelet-mediated stimulation, levels rose to >3 fold in healthy controls, but to a lesser extent in Post MI patients. This subdued response to CRP-XL stimulation may be an effect of statin therapy which has been shown to reduce cathepsin L expression (Abisi et al., 2008). A relative 0.66 fold decrease in CTSL levels were seen in the Post MI group compared to healthy controls who were not on statin therapy.

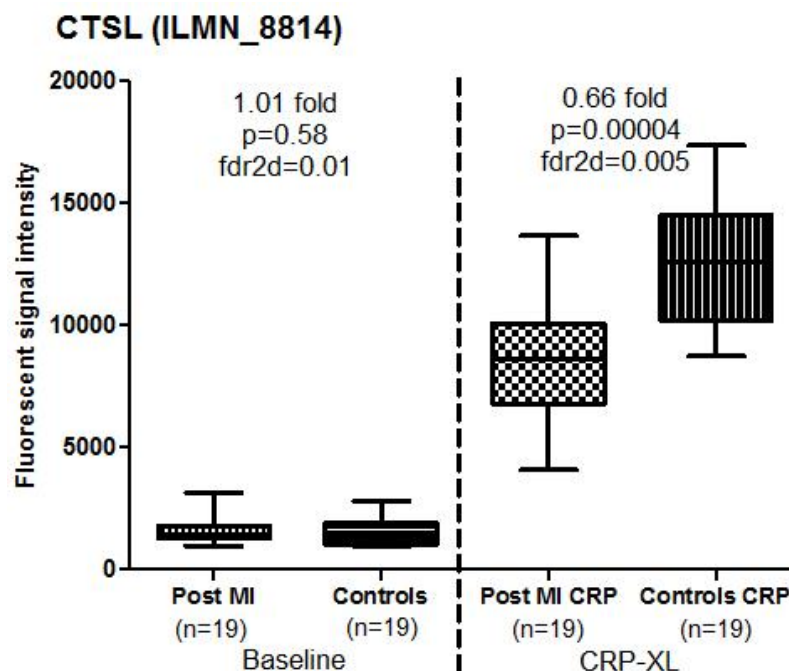


Figure 4.25: Microarray signal intensities of CTSL in Post MI patients and controls.

Fluorescent signal intensities in Post MI patients and controls before and after platelet-mediated stimulation are shown. Error bars denote the range of expression. Fold changes, p values and false discovery rates are provided.

4.8.1.1.6 Heparanase (HPSE); Chr 4q21.3

HPSE is an enzyme that cleaves heparan sulphate proteoglycans (including SDC2) on the cell surface and promotes angiogenesis, tumour invasion and tumour growth (Murry et al., 2005). It promotes coagulation by directly stimulating tissue factor synthesis and by dissociating TFPI from the endothelial surface (Nadir et al., 2008). A rat carotid balloon injury model experiment demonstrated that heparanase promotes neointimal hyperplasia by releasing fibroblast growth factor bound to heparan sulphate (Myler et al., 2006). Proteolytic processing by cathepsin L activates heparanase from its precursor molecule proheparanase (Abboud-Jarrous et al., 2008, Vlodayvsky et al., 2008).

HPSE is expressed at moderate levels in resting monocytes (Figure 4.26). Following stimulation, levels increased to >2 fold in healthy controls while levels were relatively lower in Post MI patients (0.59 fold; fdr2d p = 0.003). This is likely to be due to the low levels of cathepsin, and indirectly an effect of statin therapy.

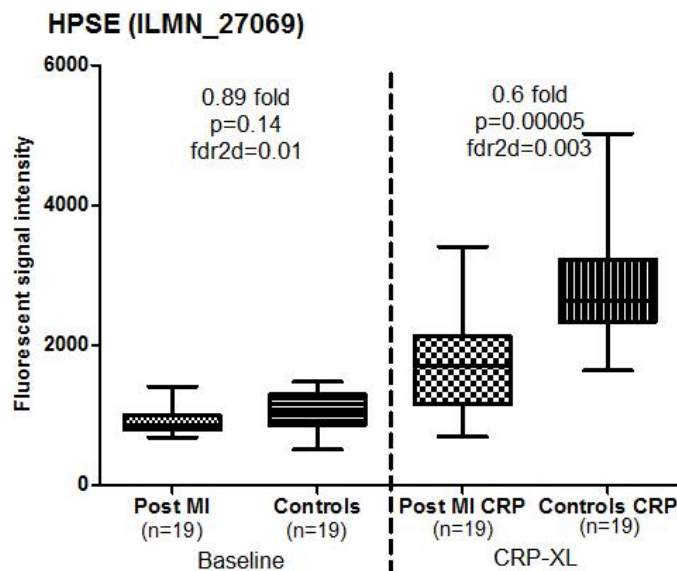


Figure 4.26: Microarray signal intensities of HPSE in Post MI patients and controls.

Fluorescent signal intensities in Post MI patients and controls before and after platelet-mediated stimulation are shown. Error bars denote the range of expression. Fold changes, p values and false discovery rates are provided.

4.8.1.1.7 Legumain (LGMN1/PRSC1); Chr 14q32.1

LGMN is a cysteine protease that activates cathepsin L and promotes chemotaxis of monocytes (Clerin et al., 2008) and plaque rupture (Mattock et al., 2010). Levels of legumain are reduced in response to statin therapy (Wang et al., 2010b).

Legumain gene expression increased significantly after platelet-mediated stimulation (Figure 4.27). The relatively lower levels of legumain expression in the Post MI group (0.68 fold, $fdr_{2d} p=0.04$) following stimulation may be an effect of statin therapy.

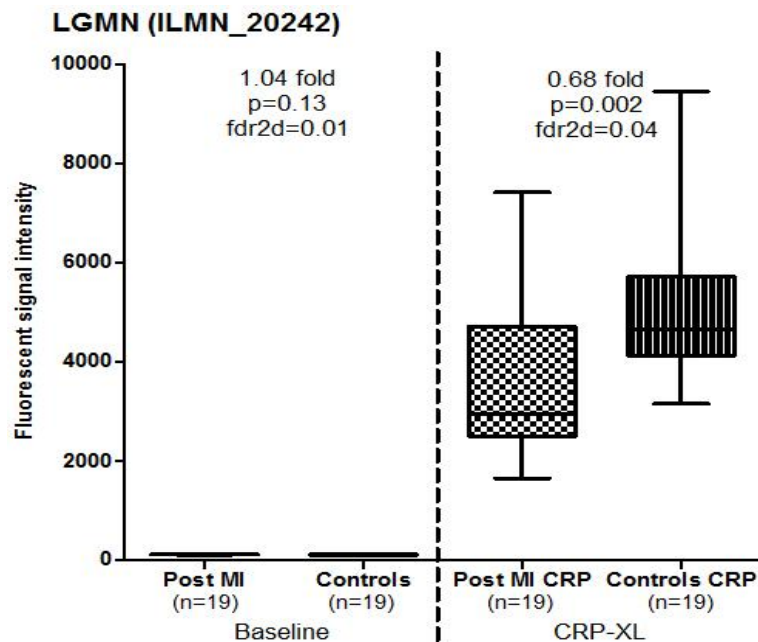


Figure 4.27: Microarray signal intensities of LGMN in Post MI patients and controls.

Fluorescent signal intensities in Post MI patients and controls before and after platelet-mediated stimulation are shown. Error bars denote the range of expression. Fold changes, p values and false discovery rates are provided.

4.8.1.1.8 Regulators of coagulation: summary

The candidate genes described above have important roles in regulating the functional integrity of the vascular endothelium. It has been previously proposed that circulating monocytes act as reporters of endothelial function (Patino et al., 2005). The response of these genes to platelet-mediated stimulation of monocytes

in patients with established coronary atherosclerotic disease may reflect pathophysiological changes in the vascular endothelium.

Figure 4.28 summarises the proposed mechanisms for the observed differences in gene expression of these molecules and their interactions derived from published literature. The probable effects of pharmacotherapy are separated from those which are likely to be related to the disease. In the upper panel, the relatively reduced expression of legumain, cathepsin L and heparanase may be an effect of statin therapy in Post MI patients. Heparanase appears to play an important regulatory role in the surface expression of SDC2 and TFPI as shown in the lower panel. By cleaving SDC2 from the endothelial surface, this promotes uptake of oxidized LDL while reduced levels of TFPI has a procoagulant effect. The reduced levels of SDC2 and PROCr also promote monocyte chemotaxis while low levels of THBD may decrease the activation of protein C.

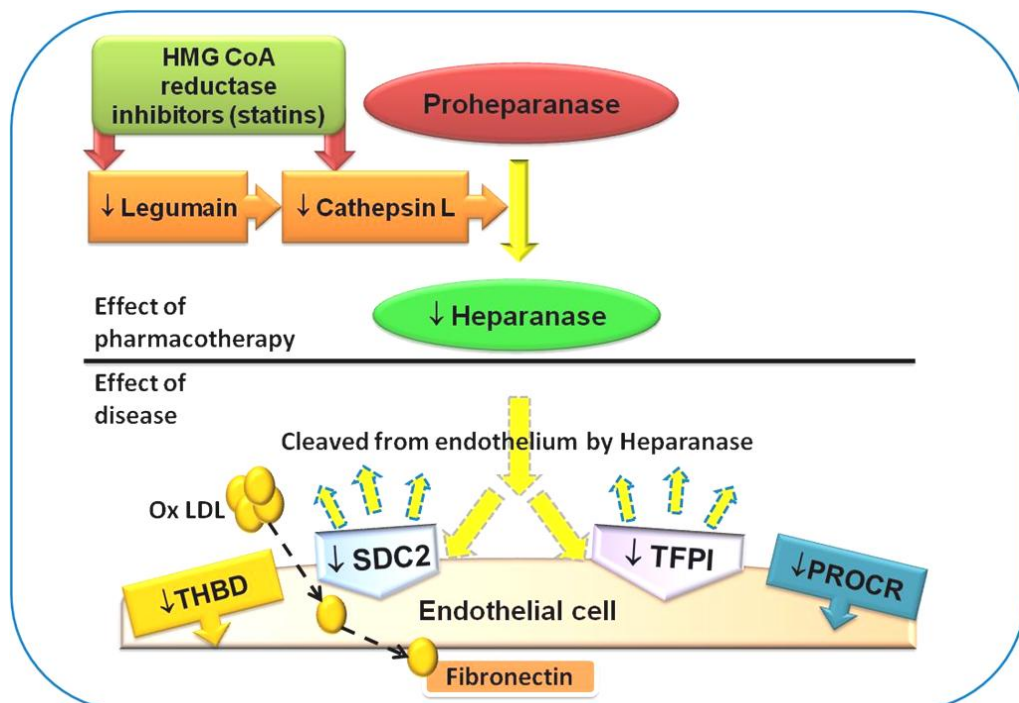


Figure 4.28: Differential expression of regulators of coagulation and endothelial function. The differentially expressed genes which regulate coagulation and vascular inflammation are summarised with the possible mechanisms underlying the microarray results.

4.8.1.2 Cholesterol metabolism

4.8.1.2.1 Cytochrome P450; subfamily XXVIIA, polypeptide 1 (CYP27A1), Chr 2q33- qter

CYP27A1 (sterol 27 hydroxylase) is a multifunctional hepatic hydroxylase in the bile acid (Pikuleva et al., 1998) and vitamin D (Sawada et al., 2000) synthetic pathways. This is also secreted by macrophages in culture (Babiker et al., 1997) and has a role in cholesterol efflux from monocyte derived macrophages and endothelial cells. Previous studies (Bjorkhem et al., 1994) indicate that CYP27A1 has the ability to repeatedly hydroxylate the same methyl group in cholesterol thereby allowing the efflux of 27-hydroxycholesterol and 3-beta-hydroxy-5-cholestenoic acid in varying amounts depending on the extracellular acceptor. In addition, the relative proportions of cholesterol and 27-hydroxycholesterol secreted by macrophages is governed by the availability of HDL, with preferential efflux of the latter when HDL availability is limited (Babiker et al., 1997). This observation suggests that CYP27A1 provides an alternative route to reverse cholesterol transport from tissue macrophages, especially in dyslipidaemic individuals with low HDL. The higher level expression of CYP27A1 may also be an effect of increased TNF activity in these individuals. TNF activates the JNK pathway (Zhang et al., 2006) which modulates the expression of CYP27A1 (Norlin et al.). PPAR gamma, which was up-regulated in both groups following CRP-XL stimulation has also been shown to increase CYP27A1 mRNA levels in human monocyte derived macrophages (Quinn et al., 2005).

Figure 4.29 shows that at baseline, Post MI patients had relatively lower levels of CYP27A1. Platelet-mediated stimulation suppressed levels in both groups, however, patients Post MI had a 1.66 fold (FDR adjusted $p = 0.03$) higher

expression level compared to controls. The observed difference in microarray fluorescent signal intensities were validated by Q-PCR (Figure 4.30)

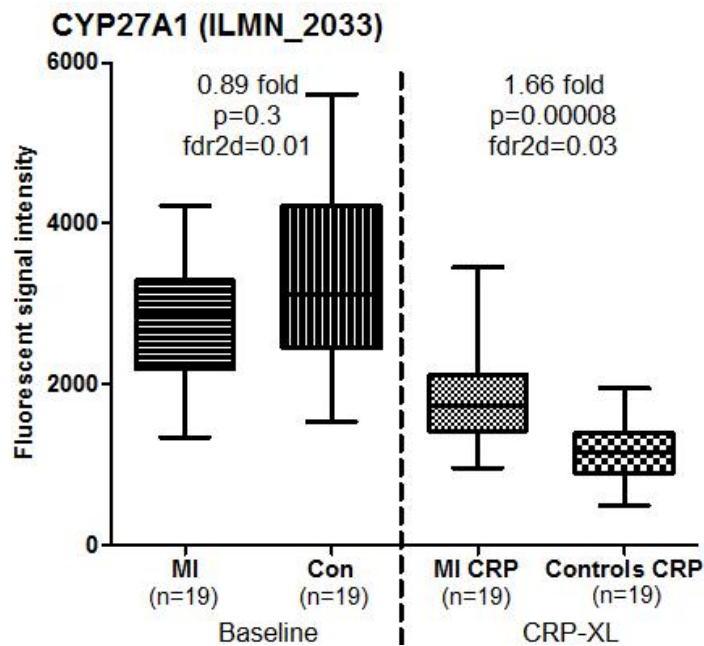


Figure 4.29: Microarray signal intensities of CYP27A1 in Post MI patients and controls. Fluorescent signal intensities in Post MI patients and controls before and after platelet-mediated stimulation are shown. Error bars denote the range of expression. Fold changes, p values and false discovery rates are provided.

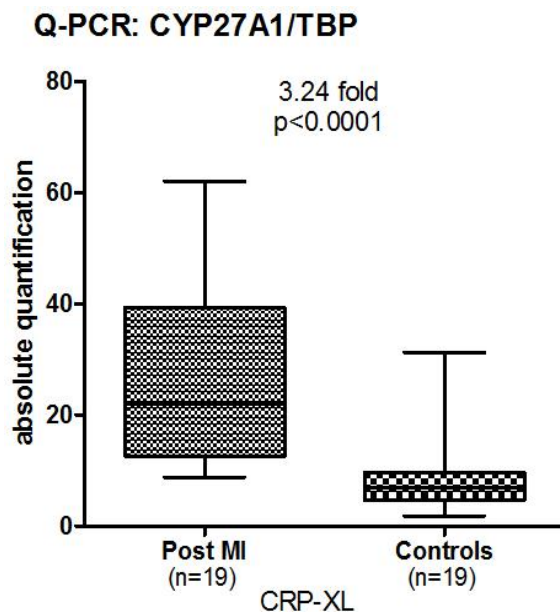


Figure 4.30: quantitative PCR of CYP27A1 in Post MI patients and controls. Q-PCR of TFPI with tata box protein as control gene is shown. Error bars denote the range of expression. Fold change and p value are provided.

4.8.1.2.2 Acetyl-CoA acetyltransferase 2 (ACAT2); Chr 6q25.3

ACAT2 is regulated by intracellular cholesterol in a dose dependant manner (Pramfalk et al., 2007). This enzyme plays a role in intra-cellular lipid storage and absorption of cholesterol from the intestine (Chang et al., 2001). Levels of hepatocyte ACAT2 activity correlate negatively with plasma HDL levels suggesting that ACAT2 regulates the availability of intracellular cholesterol for secretion into HDL (Parini et al., 2009). ACAT2 also selectively promotes the secretion of cholesteryl esters in the atherogenic apo-B containing lipoproteins (Temel et al., 2007). Inhibition of ACAT2 has been shown to attenuate hypercholesterolaemia and atherosclerosis in animal models (Ohshiro et al., 2011).

In this study, the low baseline levels of ACAT2 in the Post MI group (Figure 4.31) are likely to be due to statin therapy (Pramfalk et al., 2007) while the relative increase following stimulation may indicate the underlying atherogenic phenotype.

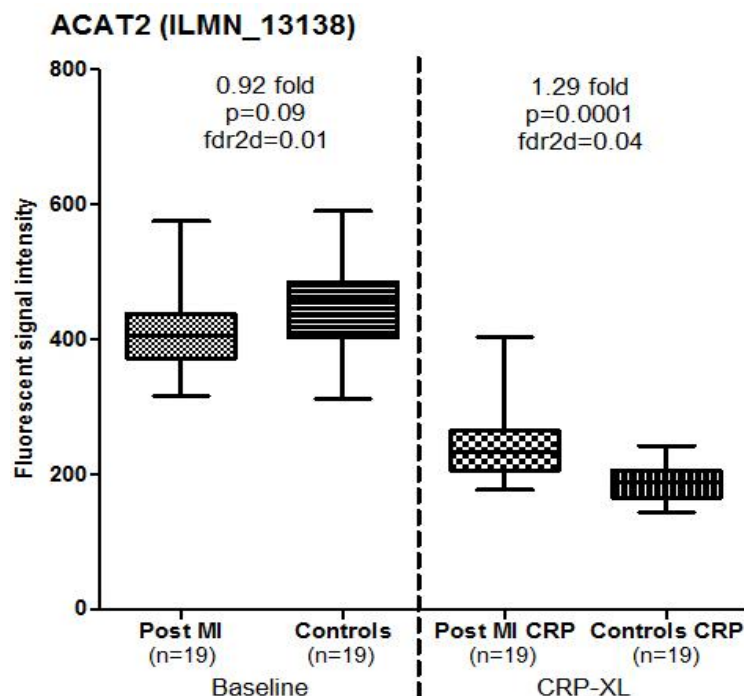


Figure 4.31: Microarray signal intensities of ACAT2 in Post MI patients and controls.

Fluorescent signal intensities in Post MI patients and controls before and after platelet mediated stimulation are shown. Error bars denote the range of expression. Fold changes, p values and false discovery rates are provided.

4.8.1.2.3 Nicotinic acid receptors

GPR109A (hydroxycarboxylic acid receptor 2/HCAR2/HM74a; Chr 12q24.31) and **GPR109B** (HCAR3/HM74/PUMAG; Chr 12q24.31) are nicotinic acid receptors (Kamanna and Kashyap, 2007). The therapeutic actions of nicotinic acid (niacin) are mediated predominantly through the GPR109A receptor which is expressed in adipocytes and macrophages (Richman et al., 2007).

Figure 4.32 shows that levels of both receptors were low in both groups at baseline. However, following platelet-mediated stimulation a significant increase in expression levels was noted in the Post MI group. None of the Post MI patients were on niacin and therefore, the selective up-regulation of GPR109 receptors in this group following stimulation may suggest a compensatory mechanism following an atherogenic stimulus in Post MI patients compared to controls (Figure 4.32).

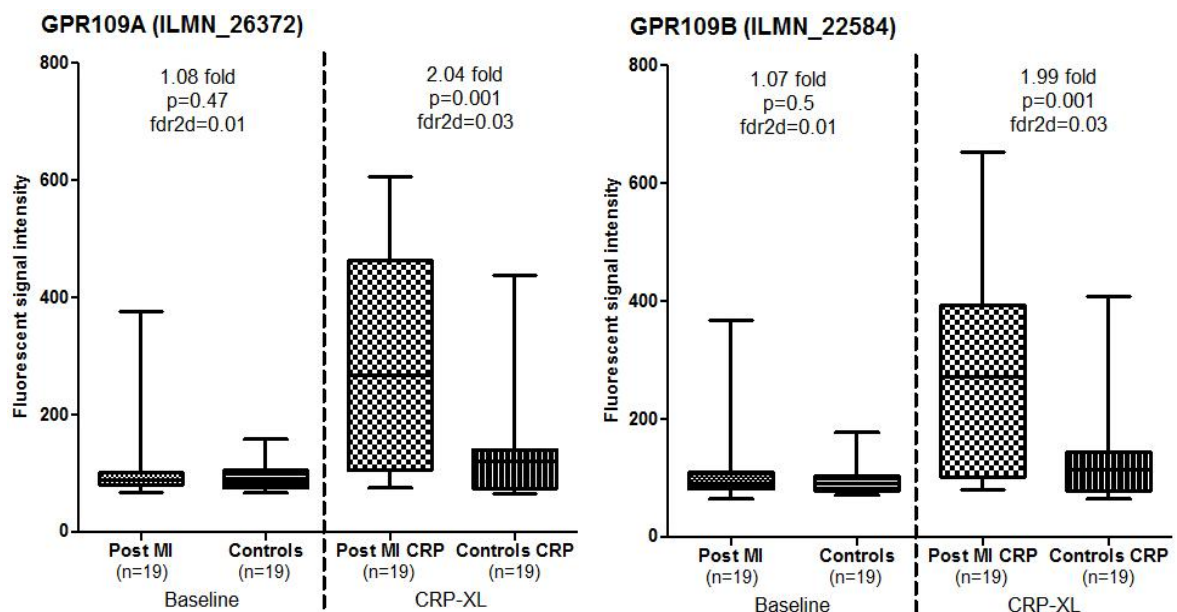


Figure 4.32: Microarray signal intensities of GPR19A&B in Post MI patients and controls. Fluorescent signal intensities in Post MI patients and controls before and after platelet-mediated stimulation are shown. Error bars denote the range of expression. Fold changes, p values and false discovery rates are provided.

4.8.1.2.4 Leptin (LEP); Chr 7q31.3

Leptin is mainly secreted by white adipocytes and regulates body weight. In the context of obesity, it promotes atherogenesis by proliferative, prothrombotic and proinflammatory mechanisms (Katagiri et al., 2007). Specifically, it up-regulates the expression of cholesterol acyl transferase-1 (ACAT-1) in cultured monocyte-derived macrophages which promotes atherosclerosis (Bai et al., 2004). Leptin also up-regulates CYP27A1 in hepatocytes (VanPatten et al., 2001). This is a relevant observation as CYP27A1 is a cholesterol efflux mediator in macrophages (Babiker et al., 1997) which is up-regulated in atheroma and has been noted to be over expressed in the Post MI group in this study (see above).

Leptin was expressed at very low levels in resting monocytes in both groups (Figure 4.33). Following stimulation, there was a 3.36 fold (FDR adjusted $p = 0.008$) increase in the Post MI group compared to controls.

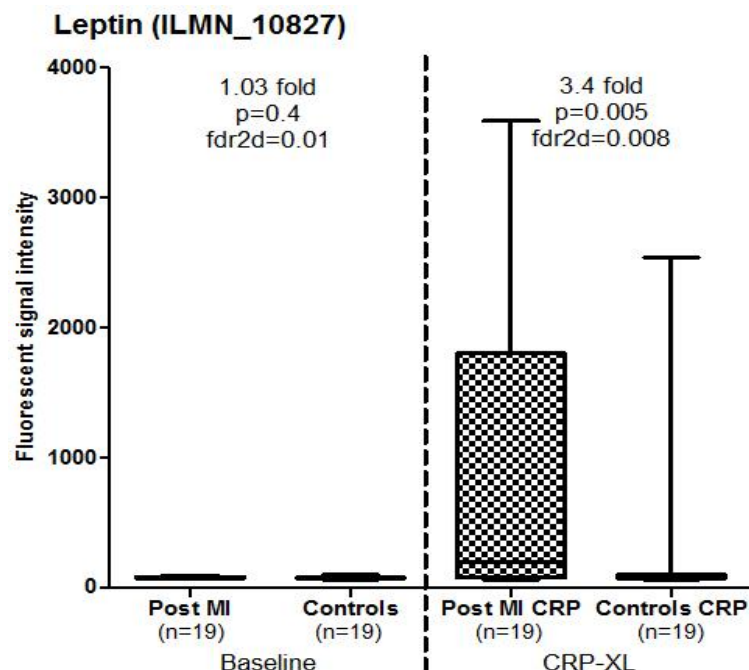


Figure 4.33: Microarray signal intensities of Leptin in Post MI patients and controls.

Fluorescent signal intensities in Post MI patients and controls before and after platelet-mediated stimulation are shown. Error bars denote the range of expression. Fold changes, p values and false discovery rates are provided.

4.8.1.3 Chemokines (Figure 4.34)

CXCL5 (epithelial-derived neutrophil activating protein 78; Chr 4q12-q13), **CCL7** (monocyte chemoattractant protein 3; Chr 17q11.2-q12), **CCL20** (macrophage inflammatory protein 3 alpha; Chr 2q33-q37) and **CCL22** (macrophage derived chemokine; Chr 16q13) have been implicated in various stages of atherosclerotic coronary artery disease. CXCL5 is released from peripheral blood mononuclear cells on stimulation with oxidized LDL (Holm et al., 2003). Genotyping of the 156 G>C polymorphism (rs352046) of CXCL5 have revealed an association with C/C genotype and 3 year mortality after MI (Zineh et al., 2008). CCL7 is released by smooth muscle cells in response to inflammatory stimuli and a similar expression has been observed in rats after balloon angioplasty of carotid arteries, which indicates a potential role in vascular injury (Wang et al., 2000). CCL20 plays a role in myocardial remodelling after ischaemia and infarction (Moro et al., 2007). There is evidence that adipocyte secretory products induce HUVECs to express MIP3 α (CCL20) (Sommer et al., 2009). Coronary artery ligation experiments in rats have shown release of CCL20 in the post infarct phase alongside TNF α and IL6 (Moro et al., 2007).

Figure 4.34 shows that levels of all four chemokines were below the detection threshold of the array. Following stimulation, levels were raised in both groups indicating that platelet-mediated stimulation promotes an atherogenic phenotype in monocytes. The reduction in these inflammatory cytokines in Post MI patients may be an effect of pharmacotherapy. The observation that CXCL5 is down regulated in endothelial cells following addition of atorvastatin lends credibility to this assumption (Zineh et al., 2008). A similar decreased expression has been noted in circulating monocytes after atorvastatin therapy (Wang et al., 2011d).

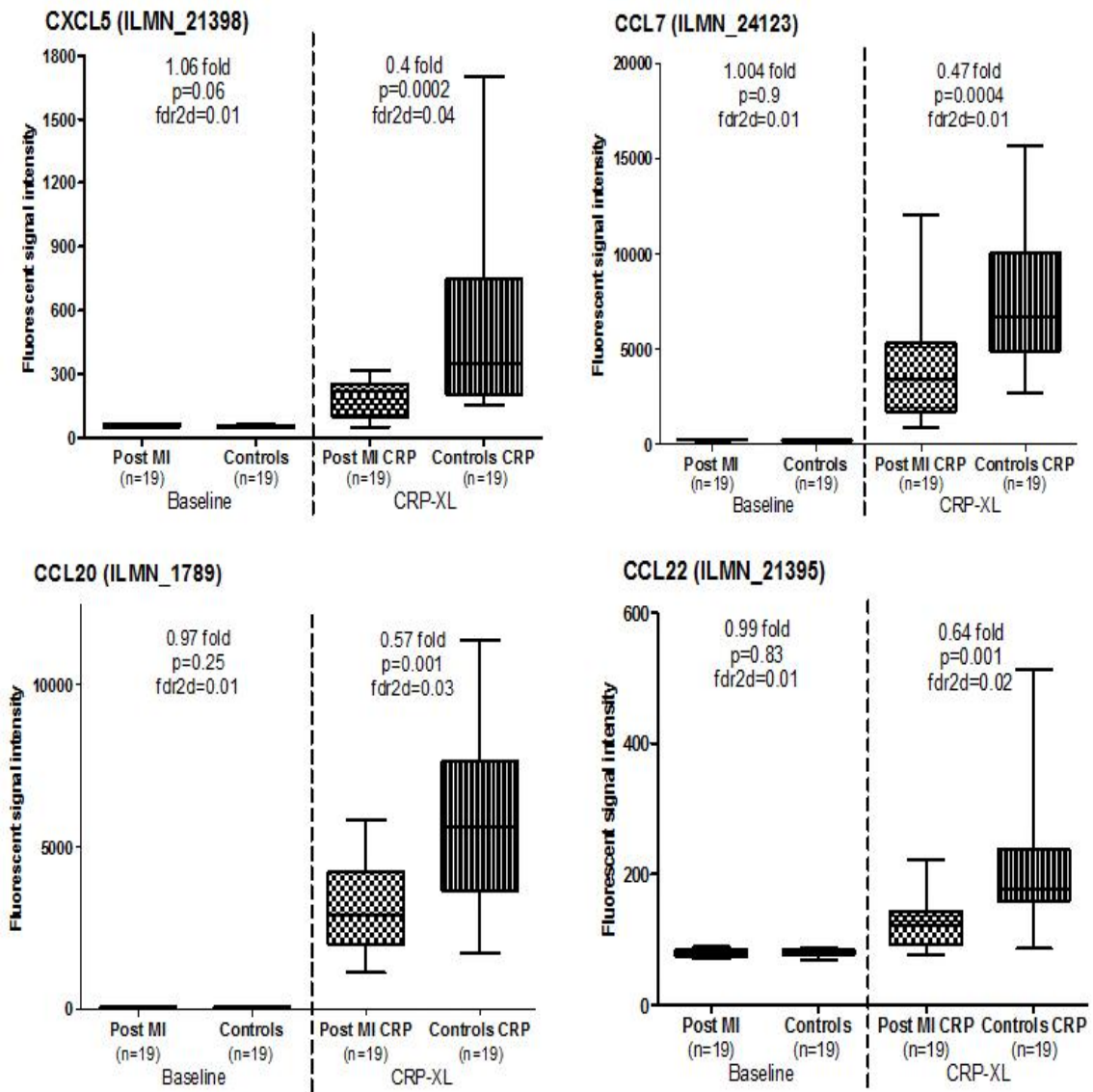


Figure 4.34: Microarray signal intensities of chemokines in Post MI patients and controls. Fluorescent signal intensities in Post MI patients and controls before and after platelet-mediated stimulation are shown. Error bars denote the range of expression. Fold changes, p values and false discovery rates are provided.

4.8.1.4 Enzymes

4.8.1.4.1 Arginase 1 (ARG1); Chr 6q23

Polymorphisms in the ARG1 gene have previously been implicated in myocardial infarction. The rs2781666 GT polymorphism has been associated with myocardial infarction and carotid artery intima media thickness (Dumont et al., 2007). However, the exact role of this molecule is unclear as animal studies indicate that macrophage ARG1 may protect against atherosclerosis (Teupser et al., 2006). The findings in the current study may reflect a compensatory up-regulation of ARG1 in individuals with established atherosclerosis.

At baseline, there was a non significant relative increase in ARG1 levels in the Post MI group (Figure 4.35). A 2.09 fold (FDR adjusted $p = 0.035$) increase was noted in the Post MI group after platelet mediated stimulation (Figure 4.35).

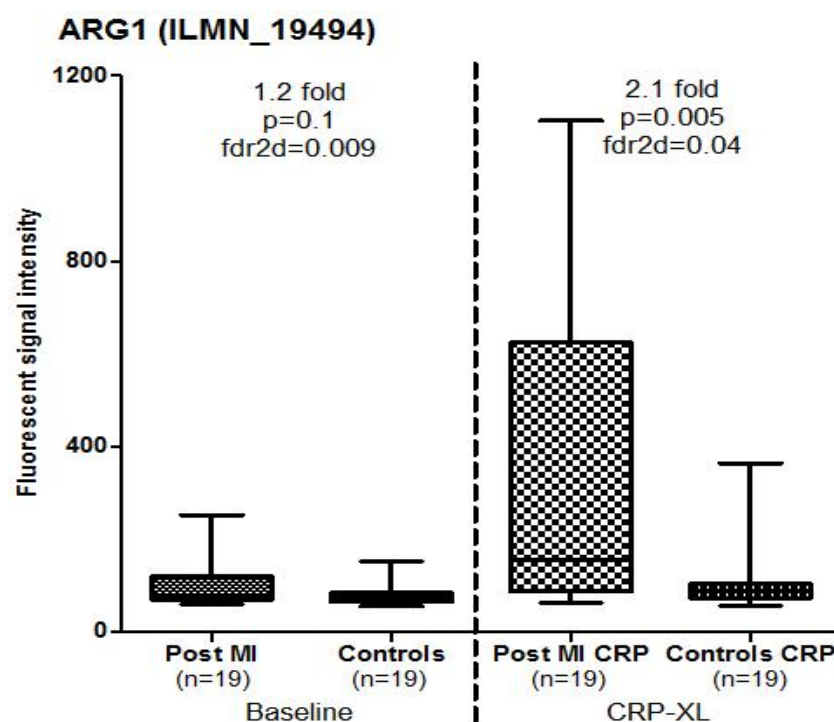


Figure 4.37: Microarray signal intensities of ARG1 in Post MI patients and controls.

Fluorescent signal intensities in Post MI patients and controls before and after platelet-mediated stimulation are shown. Error bars denote the range of expression. Fold changes, p values and false discovery rates are provided.

4.8.1.4.2 5' nucleotidase (NT5E/CD73); Chr 6q14-q21

This plasma membrane enzyme converts extracellular nucleotides to membrane permeable nucleosides. Low levels of NT5E are associated with increased arterial calcification and increased cardiovascular risk (St Hilaire et al., 2011). Low NT5E activity levels were seen in lymphocytes of patients with atherosclerosis and their children (Ryzhova et al., 2001).

NT5E expression levels were not significantly different between groups at baseline (Figure 4.36). Platelet-mediated stimulation resulted in an increase in expression levels in both groups. However levels were significantly lower in patients with MI.

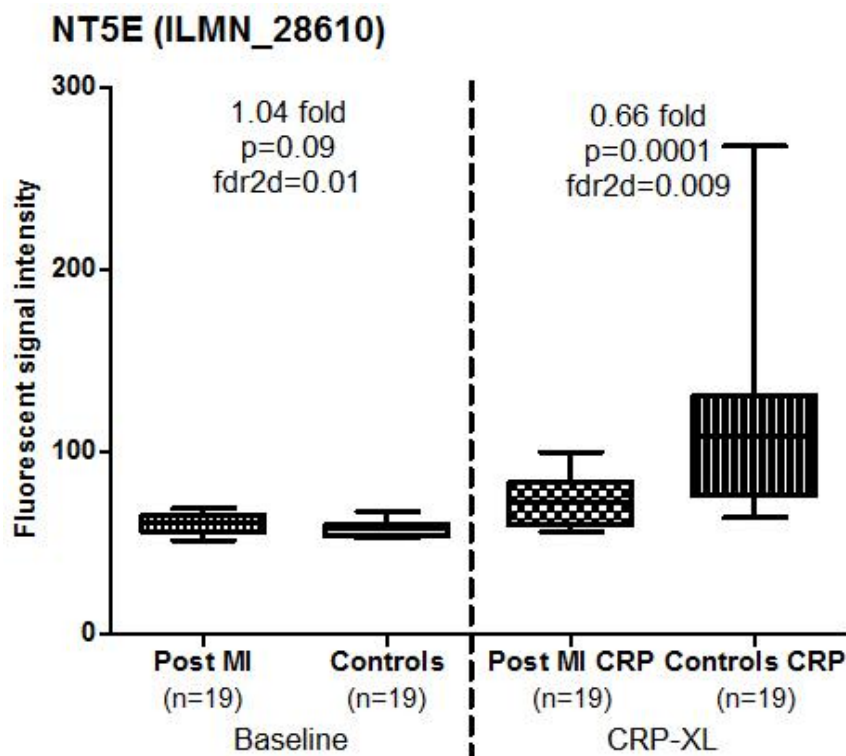


Figure 4.36: Microarray signal intensities of NT5E in Post MI patients and controls. Fluorescent signal intensities in Post MI patients and controls before and after platelet-mediated stimulation are shown. Error bars denote the range of expression. Fold changes, p values and false discovery rates are provided.

4.8.1.5 Transcription factors

Of the 15 transcription factors that were differentially expressed in patients compared to controls, 10 interacted with or indirectly influenced Wnt/beta catenin signalling (Figure 4.37). In addition, Wnt5A was differentially expressed after platelet-mediated stimulation in patients Post MI.

Down regulation or subdued up-regulation of these transcription factors was noted in the Post MI group after stimulation. Following interactive mapping using ChiLiBot, TCF4 emerged as the gene which had the strongest relationship with Wnt signalling.

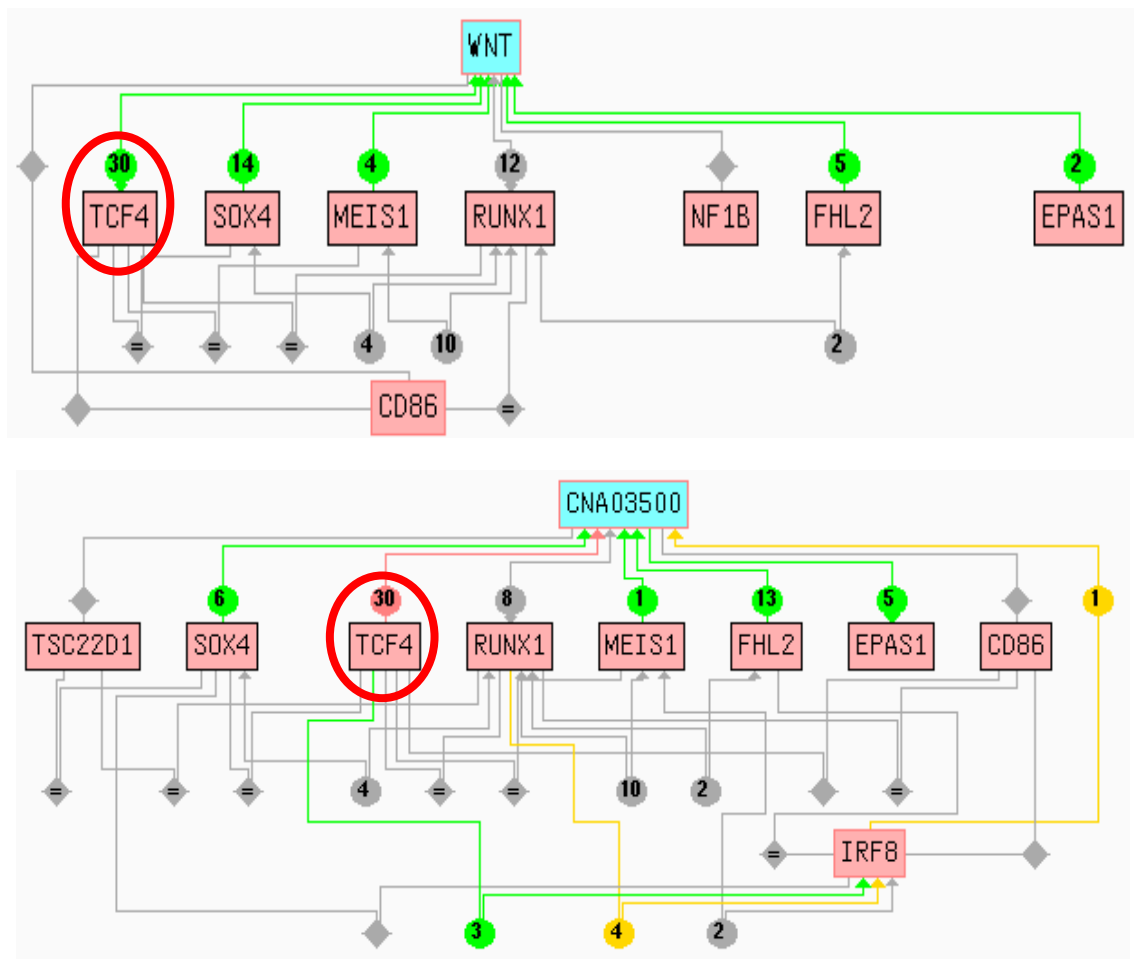


Figure 4.37: Lists of interactions on PubMed for transcription factors (ChiLiBot).

The top panel shows the candidate genes in pink boxes which interact with Wnt and the bottom panel shows interactions with beta catenin (CNA03500). TCF4 with the most number of interactions with other candidate genes is highlighted in the red circle.

4.8.1.5.1 Transcription Factor 4 (TCF4); Chr 18q21.1

TCF4 is a modulator of the Wnt signalling pathway. It stabilises beta catenin and promotes cell growth and proliferation (Wu et al., 2010). This is relevant to the response of smooth muscle cells to oxidised LDL (Bedel et al., 2008) and smooth muscle proliferation (Quasnichka et al., 2006). In a rat carotid artery balloon injury model, up-regulation and interaction of beta catenin and TCF4 promoted proliferation and prevented smooth muscle apoptosis (Wang et al., 2002).

Low levels were seen in both groups before and after stimulation (Figure 4.38). In the Post MI group, mean signal intensity decreased from (240 ± 44) to (172 ± 37) while in controls, there was a numerical increase from (245 ± 55) to (248 ± 74) after stimulation. The down regulation of TCF4 after stimulation in the Post MI group (Figure 4.38) may suggest a pro-apoptotic response in this group in contrast to healthy controls. Although aspirin has been shown to suppress TCF4, there was no difference in expression at baseline between the groups, suggesting that the primary stimulus is likely to be oxidative stress following monocyte stimulation.

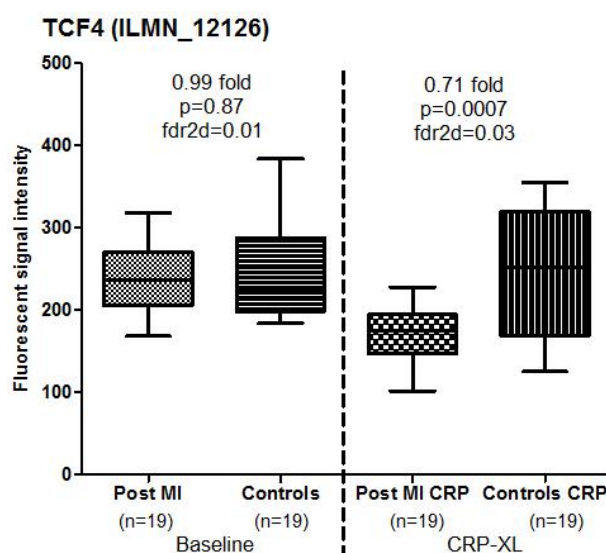


Figure 4.38: Microarray signal intensities of TCF4 in Post MI patients and controls.

Fluorescent signal intensities in Post MI patients and controls before and after platelet-mediated stimulation are shown. Error bars denote the range of expression. Fold changes, p values and false discovery rates are provided.

4.8.1.5.2 (Sex determining region Y)-box 4 (SOX4); Chr 6p22.3

SOX4 is a transcription factor that regulates cell fate and development. This has been shown to enhance beta catenin/TCF4 mediated signalling by stabilising available intracellular beta catenin (Lee et al., 2011a, Sinner et al., 2007).

Figure 4.39 suggests that SOX4 is a low abundance transcript in monocytes (signal intensity <1000). There was no significant difference in expression at baseline between groups. Following platelet-mediated stimulation, SOX4 levels were reduced in both groups, but more so in the Post MI group.

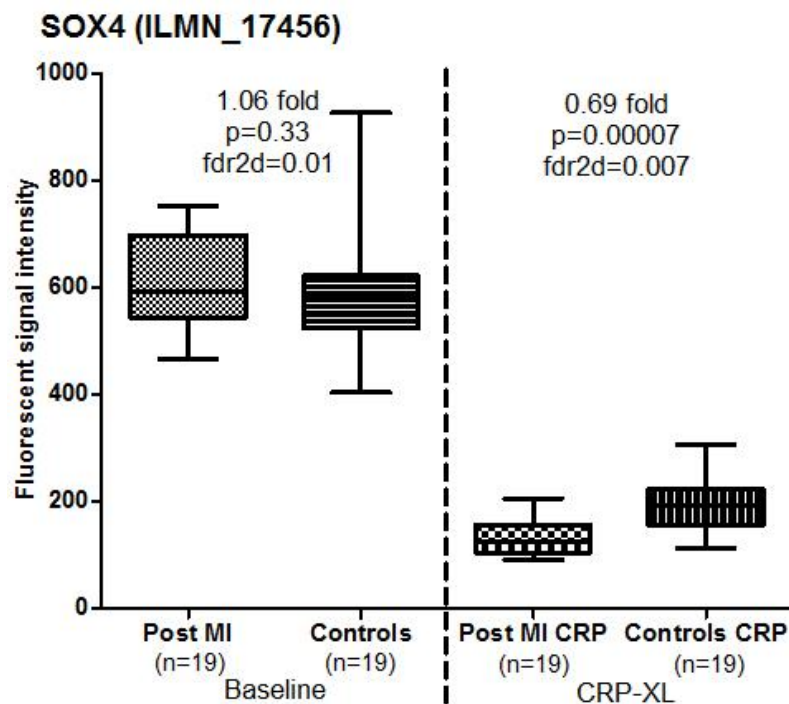


Figure 4.39: Microarray signal intensities of SOX4 in Post MI patients and controls.

Fluorescent signal intensities in Post MI patients and controls before and after platelet-mediated stimulation are shown. Error bars denote the range of expression. Fold changes, p values and false discovery rates are provided.

4.8.1.6 Other genes

4.8.1.6.1 DNAJ/HSP40 Homolog; subfamily B; member 1 (DNAJB1, HDJ1); Chr 19p13.2)

This chaperone molecule is a member of the heat shock protein family and has a role in protein folding. This is mediated via functional interaction with another heat shock protein, HSP70 (Freeman and Morimoto, 1996). Heat shock protein expression is triggered by cellular stress secondary to exposure to non native proteins (Voellmy and Boellmann, 2007). A closely related molecule, DNAJA1 (HDJ2) is up-regulated in carotid artery plaques and correlates with the degree of stenosis in ulcerated plaques (Nguyen et al., 2001).

Signal intensities were very low in resting monocytes (Figure 4.40). Following stimulation with activated platelets, DNAJB1 was elevated 1.85 fold in Post MI patients (FDR corrected $p=0.04$). In the Post MI group, there is a significant increase in expression levels in contrast to controls.

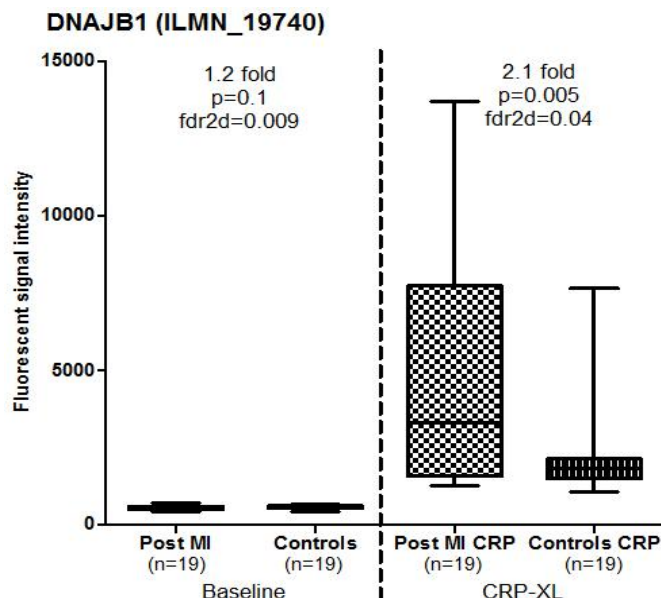


Figure 4.40: Microarray signal intensities of DNAJB1 in Post MI patients and controls.

Fluorescent signal intensities in Post MI patients and controls before and after platelet-mediated stimulation are shown. Error bars denote the range of expression. Fold changes, p values and false discovery rates are provided.

4.8.1.6.2 CD86 (B7.2; LAB72); Chr 3q21

CD86 encodes a type I membrane protein that is a member of the immunoglobulin super family. This protein is expressed by antigen-presenting cells and a ligand for CD28 antigen and cytotoxic T-lymphocyte-associated protein 4 (CTLA-4) on the T-cell surface (Ellis et al., 1996). CD86 binding with CD28 antigen is a co-stimulatory signal for T-cell activation whilst binding of CD86 with CTLA-4 negatively regulates T-cell activation and diminishes the immune response (Lane, 1997).

Figure 4.41 suggests that CD86 is expressed at moderate levels in monocytes (3-6,000). Expression levels were comparable in resting monocytes but a relative reduction in levels was noted in the patients following platelet-mediated stimulation – expression levels did not rise in the Post MI patients unlike healthy controls. This differential expression is likely to be due to statin therapy in the Post MI patients as it has been shown that LPS stimulated human monocytes show reduced CD86 expression if treated with simvastatin or atorvastatin (Yilmaz et al., 2006).

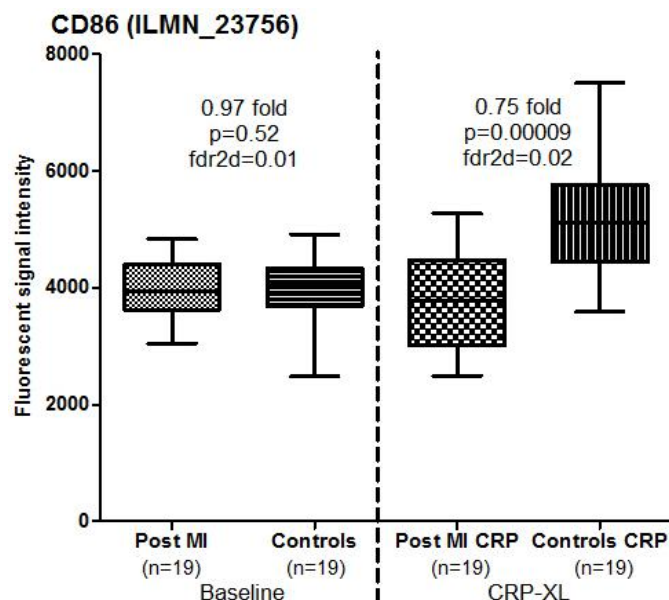


Figure 4.41: Microarray signal intensities of CD86 in Post MI patients and controls.

Fluorescent signal intensities in Post MI patients and controls before and after platelet-mediated stimulation are shown. Error bars denote the range of expression. Fold changes, p values and false discovery rates are provided.

4.8.1.7 Genes with differential expression at baseline and after CRP-XL stimulation

Of the differentially expressed genes at baseline described in the first part of this Chapter, ORM1 and PGLYRP1 were also differentially expressed after CRP-XL stimulation (Figures 4.42, 4.43). Both genes showed an increase in the fold change observed at baseline.

4.8.1.7.1 Orosomucoid 1 (ORM1, alpha-1 acid glycoprotein); Chr9q34.1-34.3

ORM1 is expressed at low levels in monocytes (Figure 4.42). ORM1 was expressed 1.78 fold higher in Post MI patients at baseline and this rose to a relative fold change of 2.78 after stimulation. From Figure 4.42, it is apparent that the levels of ORM1 did not change significantly in healthy controls after stimulation while a definite increase in expression was seen in the Post MI group.

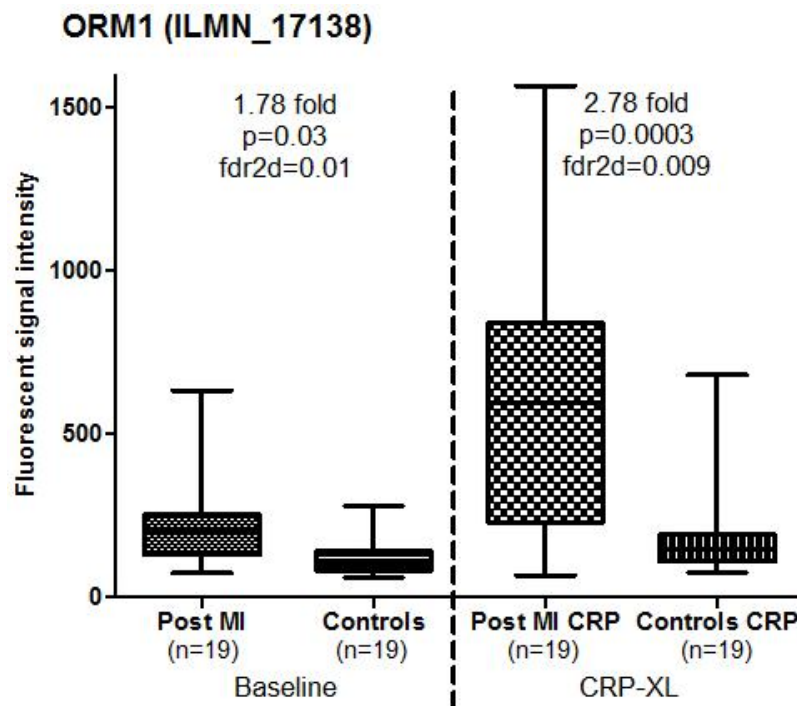


Figure 4.42: Microarray signal intensities of ORM1 in Post MI patients and controls.

Fluorescent signal intensities in Post MI patients and controls before and after platelet-mediated stimulation are shown. Error bars denote the range of expression. Fold changes, p values and false discovery rates are provided.

4.8.1.7.2 Peptidoglycan recognition protein-1 (PGLYRP1); 19q13.2-q13.3

PGLYRP1 expression in the Post MI group was significantly higher than in controls at baseline and after stimulation (Figure 4.43). Signal intensities reveal that it is expressed at low to moderate levels in monocytes. An increase in expression levels was seen in both groups after platelet-mediated stimulation. Levels were 1.85 fold higher in the Post MI group.

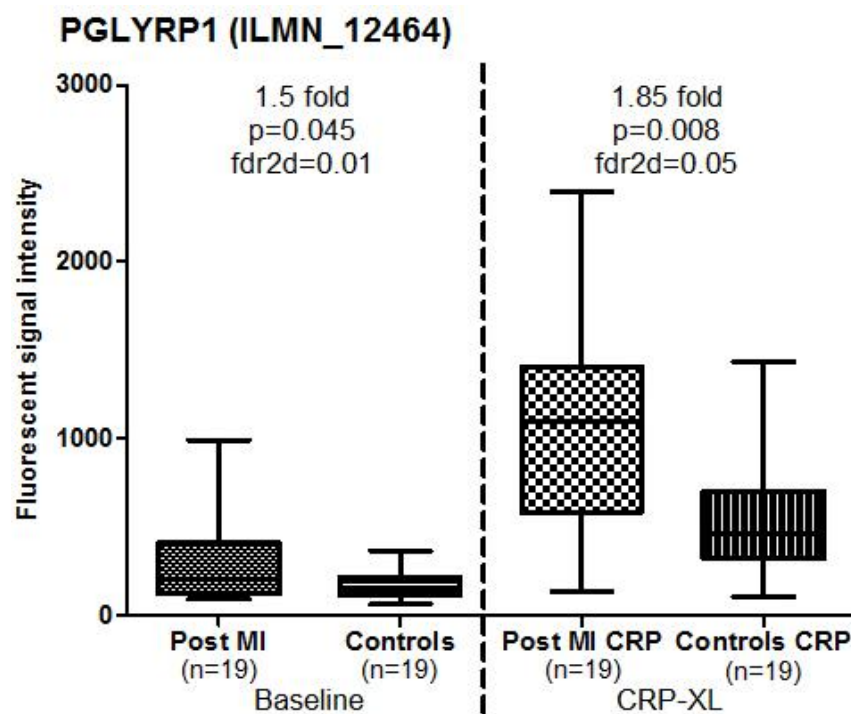


Figure 4.43: Microarray signal intensities of PGLYRP1 in Post MI patients and controls.

Fluorescent signal intensities in Post MI patients and controls before and after platelet-mediated stimulation are shown. Error bars denote the range of expression. Fold changes, p values and false discovery rates are provided.

Other differentially expressed genes at baseline (TNF, TES, CXXC5 and OLFM1) did not maintain a significant difference in expression levels in Post MI patients compared to controls after platelet-mediated stimulation.

4.8.2 Pathways

4.8.2.1 Wnt signalling

As described earlier in section 4.4.2.1, this pathway has a role in mediating inflammation (Gustafson and Smith, 2006) as well as response to injury (Dell'accio et al., 2008) and repair (Oerlemans et al., 2010). Wnt proteins have been co-localised to human and murine atherosclerotic plaques (Christman et al., 2008). Wnt signalling is also implicated in arterial calcification (Shao et al., 2007) and apoptosis (Zhang et al., 2009b).

4.8.2.1.1 Wingless-type MMTV integration site family, member 5A (Wnt5A); Chr 3p21-p14

Wnt5A is a non canonical member of the Wnt family (Ishitani et al., 2003). It is present in human atherosclerotic lesions where it co-localises with Toll like receptor 4 (TLR4) which is an innate receptor implicated in atherosclerosis (Christman et al., 2008). In response to lipopolysaccharide (LPS), a known ligand of TLR4, increased expression of Wnt5a is seen in murine macrophages (Christman et al., 2008). Wnt5A mediates the inflammatory response of macrophages to bacterial antigens (Blumenthal et al., 2006) and has a role in cellular proliferation and repair (Cheng et al., 2008). It can either inhibit or stimulate activity of the beta catenin-TCF4 complex depending on the cellular and receptor context (Mikels and Nusse, 2006). In cell lines Wnt5a regulates the translocation of beta-catenin from cytoplasm to nucleus and suppresses beta catenin/TCF-dependent transcriptional activity (Yuan et al., 2011).

Wnt5A was not expressed in resting monocytes but levels rose following CRP-XL stimulation (Figure 4.44). The Post MI group had a 0.56 fold (fdr2d p=0.04)

expression of Wnt5A compared to controls after stimulation (Figure 4.44). This is unlikely to be due to pharmacotherapy. Statins have been reported to increase Wnt5A levels in bone marrow derived cells (Zhang et al., 2009a) and renal mesangial cells where apoptotic changes reduced Wnt5A levels which were restored by simvastatin (Lin et al., 2008).

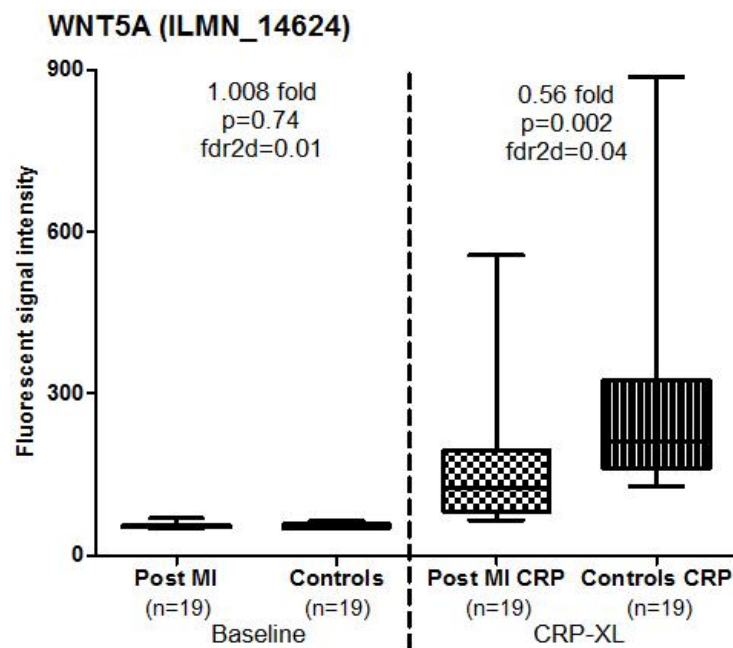


Figure 4.44: Microarray signal intensities of Wnt5A in Post MI patients and controls. Fluorescent signal intensities in Post MI patients and controls before and after platelet-mediated stimulation are shown. Error bars denote the range of expression. Fold changes, p values and false discovery rates are provided.

4.8.2.1.2 Interactions of differentially expressed genes with beta catenin

The differential expression of genes following stimulation in the Post MI group suggests a diversion of beta catenin, a key component of the Wnt pathway away from TCF4 as depicted in Figure 4.45. Following stimulation, there is a reduction in SOX4 expression levels. SOX4 facilitates the interaction of beta catenin with TCF4. This in addition to the reduction in TCF4 may result in reduced beta catenin/TCF4 coupling. There may also be increased availability of beta catenin considering the reduction in Wnt5A which is a regulator of beta catenin activity.

This suggests a change from proliferative signalling to oxidative stress mediated pathways following stimulation. The significant up-regulation (>200 fold) of oxidised LDL receptor 1 (OLR1) in all groups (Chapter 3) suggests that platelet-mediated stimulation induces an oxidative stress response in monocytes. OLR1 correlates with oxidative stress in CAD (Kamezaki et al., 2009) and is up-regulated in endothelial cells following oxidative stress (Sakurai and Sawamura, 2003).

Beta catenin has been shown to act as a molecular switch depending on cellular stress and can be activated by transcription factors other than TCF4 (Thevenod and Chakraborty, 2010). In response to oxidative stress, beta catenin combines with fork head box O (FOXO) proteins or with TCF4 and achieve very different cellular responses. Beta catenin-FOXO coupling promotes cell senescence and apoptosis while beta catenin-TCF4 interaction promotes proliferation and development (Jin et al., 2008). The relative abundance of FOXO proteins with the observed reduction in TCF4 may therefore result in a diversion of beta catenin signalling from a proliferative to apoptotic pathway.

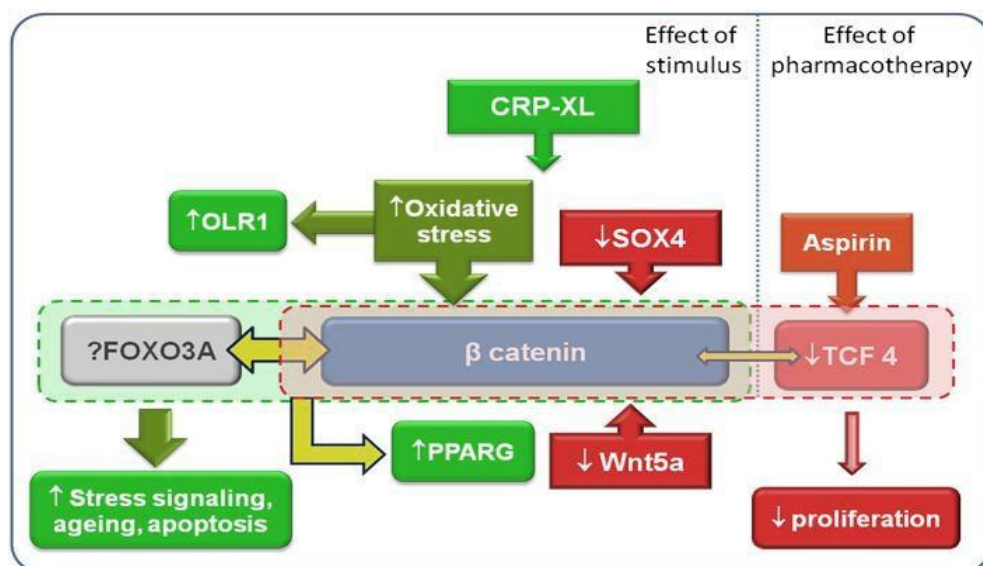


Figure 4.45: Proposed roles of differentially expressed genes in Wnt signalling.

The differentially expressed genes which regulate Wnt/beta catenin signalling are summarised with the possible mechanisms underlying the microarray results.

To explore this further, specific interrogation of microarray signal intensities was performed which revealed a significant up-regulation of Fork head box O3A (FOXO3A) in both groups with a non significant numerically higher level in the Post MI group (Figure 4.46). This protein has been shown to defend against oxidative stress (Ambrogini et al., 2010).

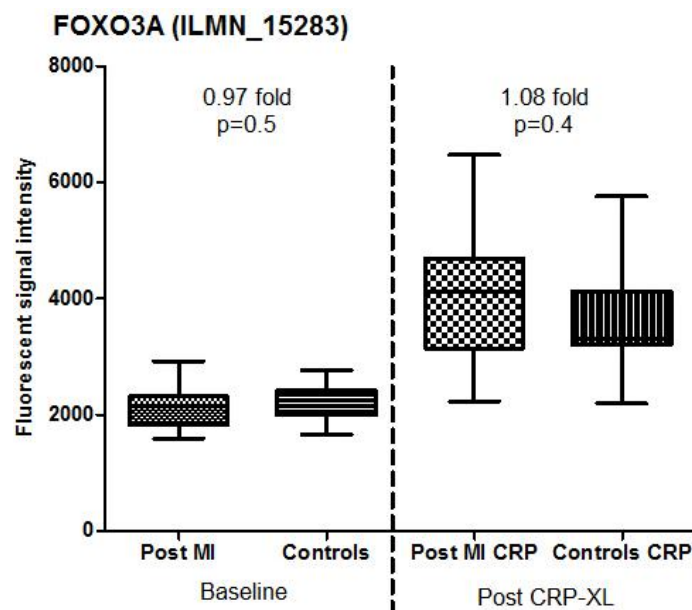


Figure 4.46: Microarray signal intensities of FOXO3A in Post MI patients and controls. Fluorescent signal intensities in Post MI patients and controls before and after platelet-mediated stimulation are shown. Error bars denote the range of expression. Fold changes and p values are provided.

Diversion of beta catenin to FOXO mediated transcription releases PPAR gamma (PPARG) from the inhibitory effect of beta catenin (Almeida et al., 2009). In both groups, there was only a modest rise in PPAR gamma following stimulation (Figure 4.47). In this Figure, the signal intensities in the Post MI group before and after stimulation are shown to the left of the dotted line and corresponding values for the controls are shown on the right. Very low levels of expression were noted which makes it difficult to draw conclusions about the trend of PPARG expression given that these intensities may fall below the resolution limit of the array scanner.

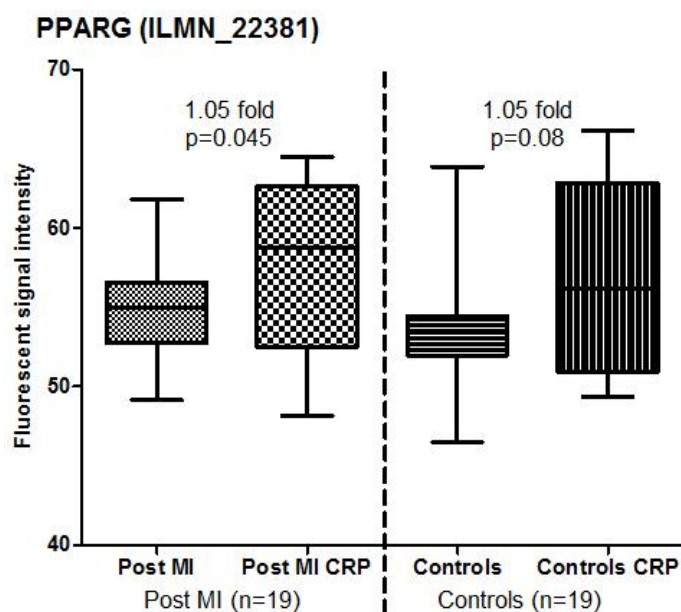


Figure 4.47: Microarray signal intensities of PPARG in Post MI patients and controls. Fluorescent signal intensities in Post MI patients and controls before and after platelet-mediated stimulation are shown. Error bars denote the range of expression. Fold changes and p values are provided.

4.9 DISCUSSION

This Chapter describes the differences in gene expression in monocytes from Post MI patients compared to healthy controls under two conditions: (i) in the resting state and (ii) after a platelet-mediated stimulation experiment using cross-linked collagen (CRP-XL).

It is apparent from the analysis of the differentially expressed genes that there are only modest differences in gene expression profiles in resting monocytes between the two groups. Such low numbers of differentially expressed genes with modest fold changes in expression levels between cases and controls have been previously noted in other transcriptome profiling studies in myocardial infarction (Healy et al., 2006). Shared phenotypic characteristics between the Post MI and control groups such as age may have contributed to the common trends in gene

expression. Alterations in monocyte gene expression as a result of ageing have been noted in human (Seidler et al., 2010) and animal (Futamura, 1994) studies. However, in this study, the transcriptome of the monocyte has been shown to be extremely responsive to platelet-mediated stimulation with over 200-fold changes in gene expression as noted in Chapter 3. This highlights the importance of a stimulus of pathophysiological relevance to reveal changes in global gene expression in circulating monocytes.

Following platelet-mediated stimulation, many more genes were differentially expressed in the Post MI group (169 transcripts vs. 27 transcripts in resting monocytes). All the candidate genes had significant p values after correction for multiple testing using the *fdr2D* algorithm. Many of these genes were not differentially expressed in resting monocytes but showed differential expression in monocytes stimulated by activated platelets. These included genes involved in haemostasis, cholesterol metabolism and transcriptional regulation, some of which have recognized roles in vascular inflammation and atherosclerosis.

Another interesting observation to emerge from this analysis is the modulation of the Wnt/beta catenin signalling pathway by some of the differentially expressed genes. This pathway plays an important role in cell motility, proliferation, tissue repair and apoptosis.

An important limitation of the analysis in this Chapter is the influence of pharmacotherapy on monocyte gene expression. HMGCoA reductase inhibitors (statins) and antiplatelet agents have been shown to influence monocyte gene expression (Sivapalaratnam et al., 2012). Cathepsin-L levels in atherosclerotic lesions are suppressed after statin therapy (Abisi et al., 2008) while expression of

Legumain is suppressed in monocytes from patients with coronary atherosclerosis (Wang et al., 2010b). Levels of both transcripts were significantly reduced in the Post MI group in this study. All subjects in this group were on statin therapy while none of the controls were on any medication. Another interesting observation in this analysis is the reduction in levels of CD86 after platelet-mediated stimulation which parallels the decrease in expression of this receptor following stimulation of monocytes with lipopolysaccharide (Yilmaz et al., 2006).

Although the effect of pharmacotherapy cannot be ruled out for the differences noted in gene expression, none of the other genes have previously reported interactions with these agents. Moreover, the replication of previously known influences of medication on monocyte gene expression in this study adds to the validity of the methods and especially proves that the microarray platform is able to detect these expected differences in gene expression.

In summary, this Chapter serves to substantiate the following hypotheses: that (i) variations in gene expression of the circulating peripheral blood monocyte determine individual susceptibility to atherosclerotic coronary artery disease, (ii) platelet driven stimulation of circulating monocytes plays an important role in the initiation, progression and manifestation of atherosclerotic coronary artery disease and (iii) gene expression analysis of peripheral blood monocytes under resting and stimulated conditions in individuals with and without premature coronary artery disease will identify differentially expressed genes, which underlie the pathogenesis, progression and outcome of coronary artery disease.

A particular limitation of studying subjects with established disease is that the differential gene expression cannot be reliably classified into primary i.e.,

contributing to the development of the disease or secondary i.e., a change in response to the disease. It is also difficult to separate the changes in gene expression primarily driven by pharmacotherapy such as statins or aspirin from the disease process itself. Although an attempt has been made in this chapter to identify probable effects of medication, the conclusions drawn from such analyses are speculative and based on available data from published literature.

Identification of differential gene expression that is driven by genetic susceptibility to disease can only be made by analysis of gene expression in subjects who are genetically predisposed to but not overtly affected by the disease. This question is addressed in the next Chapter which explores the differences in monocyte gene expression in the resting state and after platelet-mediated stimulation in young healthy male offspring of patients with premature MI compared to healthy Control offspring with no such family history of premature MI or CAD. None of the recruits in the offspring groups have clinical manifestations of coronary atherosclerosis and therefore the changes in gene expression are likely to be primary events which underlie the genetic predisposition to CAD and MI in these individuals.

CHAPTER 5: RESULTS

**Offspring of MI vs. Controls –
differences in monocyte gene
expression at baseline and after
platelet mediated stimulation**

5.1 INTRODUCTION

The experiments in this Chapter were performed to identify gene expression abnormalities in resting and stimulated monocytes that may be associated with the risk of premature MI. For this purpose we studied healthy young men with a two generational family history of premature coronary artery disease compared to healthy age and gender matched controls. The differences in resting monocyte gene expression ('baseline') are explored in the initial sections (Figure 5.1).

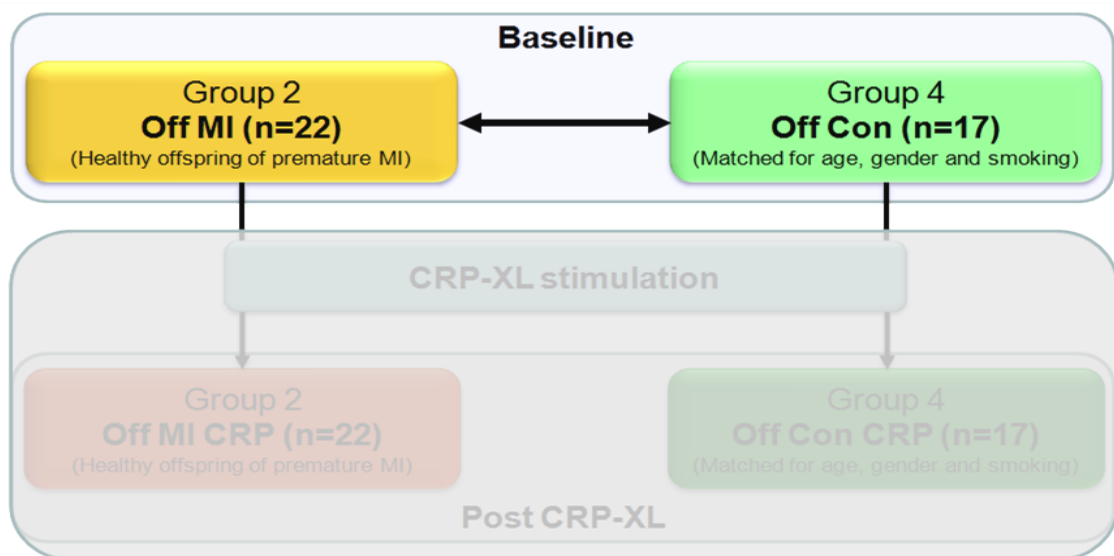


Figure 5.1: Scheme of analysis – Offspring of MI vs. Controls at baseline.

5.2 BASELINE GENE EXPRESSION: INITIAL ANALYSIS

Peripheral venous blood samples collected in EDTA were used to isolate CD14⁺ monocytes from which RNA was extracted in TRIzol within 50 minutes of venesection. Absence of platelet mediated monocyte activation was confirmed by flowcytometry. The microarray signal intensities were quantile normalised following which they were compared (Offspring of MI (Group 2) vs. Control offspring (Group 4) at baseline) and statistically analysed for significant differential expression.

Differential expression of transcripts in Offspring of MI in comparison to healthy Control offspring is shown in sigmoid plots (Figure 5.2). As explained in previous Chapters, the probe sets in the order of their ID numbers (x axis) corresponding to increasing signal intensities (y-axis) are shown.

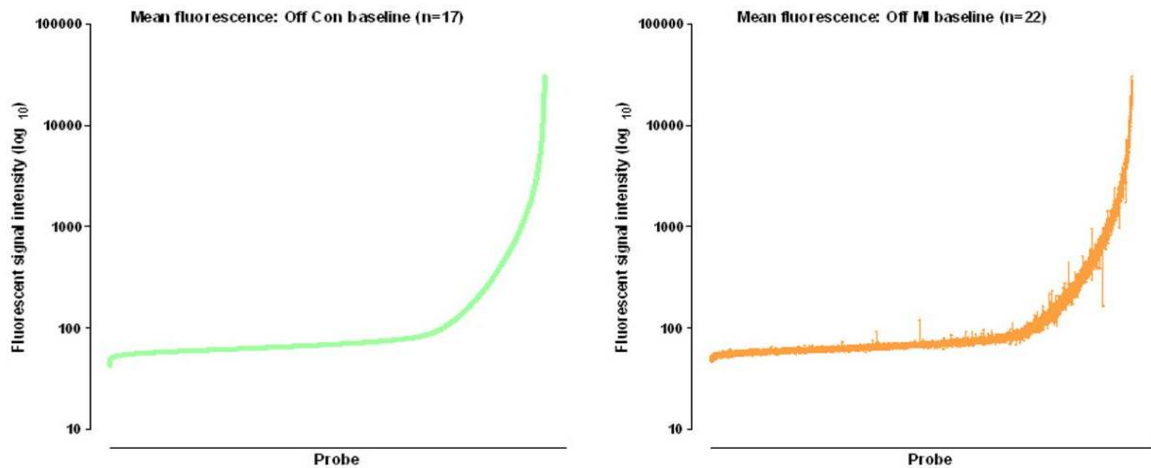


Figure 5.2: Sigmoid plots of fluorescent signal intensity in resting monocytes.

The graph shows baseline mean fluorescent signal intensities of all probe sets in healthy Control offspring (left) and corresponding changes in signal intensities in the Offspring of MI group (right).

Degree (fold change) and significance (p value) of each transcript probe set are graphically represented in Figure 5.3.

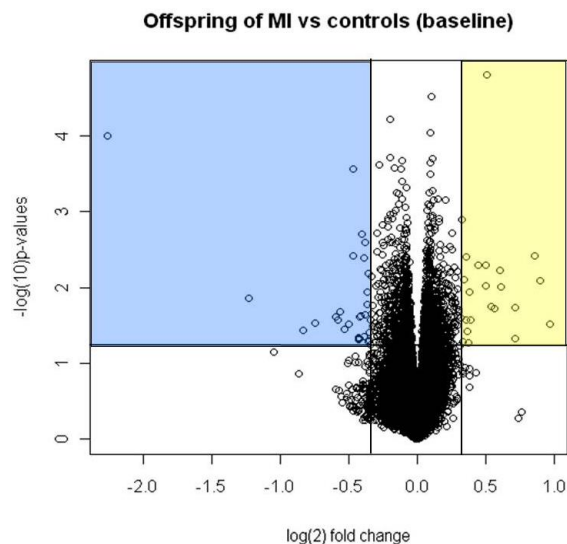


Figure 5.3: Volcano plot of Offspring of MI vs. controls at baseline.

Log₂ of fold change (Offspring of MI/controls) is plotted on the x-axis and log₁₀ of p-values (t test, uncorrected) is plotted on the y-axis. The yellow and blue shaded regions contain up and down regulated transcripts respectively which pass the filtering criteria for candidate gene analyses.

Differentially expressed genes were analysed according to the fold change in gene expression. The filtering protocol was as described before in Chapter 4 with a minor change in the strategy. As shown in Figure 5.4 below, when a stringent criterion was applied for the false discovery correction ($fdr_{2D} < 0.05$), only two genes were available for analysis (see Table 5.1 below), one of which (Probe ID: ILMN_30877, Gene ID: LOC650946) was no longer listed on the NCBI Gene database (withdrawn). However, there were transcripts with a higher magnitude of fold change which had fdr_{2D} values in the range 0.05-0.5. Therefore, for both the offspring group comparisons (baseline and after platelet-mediated stimulation) a less statistically stringent nonetheless biologically relevant filtering threshold was used ($p < 0.05$, $fdr_{2D} < 0.5$, fold change > 1.25 or < 0.8).

45 transcripts were considered for further analyses, of which 14 were up-regulated and 31 were down regulated in Offspring of MI compared to Control offspring.

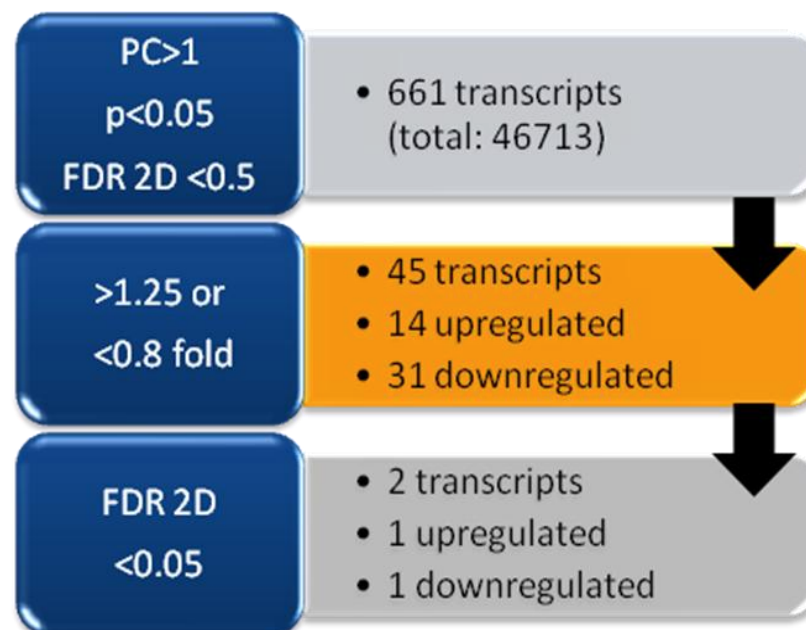


Figure 5.4: Gene transcript filtering strategy to identify differentially expressed genes. The orange panel highlights the filtering threshold used for subsequent candidate gene analyses. PC=present calls, fdr 2D=false detection rate in 2 dimensions.

Probe ID	Symbol	Fold change	p values	FDR2D
ILMN_13603	FOSB	1.86	0.01	0.22
ILMN_20932	EGR1	1.81	0.00	0.11
ILMN_13426	DCAL1 (CLECL1)	1.53	0.01	0.23
ILMN_22857	CCL3L3	1.52	0.01	0.20
ILMN_9681	BTG2	1.45	0.02	0.49
ILMN_2504	AOAH	1.42	0.00	3.08719E-08
ILMN_1999	CCL3	1.42	0.01	0.36
ILMN_35426	LOC652479	1.41	0.01	0.33
ILMN_2033	CYP27A1	1.36	0.01	0.45
ILMN_29203	TRIB1	1.30	0.01	0.44
ILMN_22082	FBN2	1.28	0.03	0.46
ILMN_6158	CCL3L1	1.28	0.00	0.42
ILMN_16430	DLG4 (LLGL1)	1.26	0.01	0.43
ILMN_18369	ARNT	1.25	0.00	0.40
ILMN_681	MAP7	0.80	0.02	0.39
ILMN_14906	C14orf166	0.80	0.03	0.36
ILMN_25742	LRRC57	0.79	0.01	0.41
ILMN_24114	CLEC12A	0.79	0.03	0.36
ILMN_6837	ZNF185	0.78	0.04	0.32
ILMN_28130	MYC	0.78	0.01	0.40
ILMN_10323	RSBN1L	0.78	0.01	0.38
ILMN_7870	EIF1B	0.77	0.02	0.34
ILMN_6185	ZNF274	0.77	0.00	0.39
ILMN_40471	LOC652616	0.77	0.04	0.28
ILMN_17602	ITGB1BP1	0.76	0.00	0.39
ILMN_16020	ZNF447	0.76	0.00	0.39
ILMN_6588	ACTA2	0.75	0.02	0.29
ILMN_27091	TMEM14B	0.74	0.05	0.23
ILMN_6353	SDHD	0.74	0.05	0.23
ILMN_39597	LOC645719	0.72	0.00	0.19
ILMN_4641	HLA-DPB1	0.72	0.00	0.36
ILMN_31638	LOC644191	0.71	0.03	0.22
ILMN_138738	NPM1	0.69	0.03	0.20
ILMN_43805	LOC649143	0.68	0.02	0.21
ILMN_43826	LOC644934	0.67	0.03	0.20
ILMN_46687	LOC644928	0.66	0.02	0.20
ILMN_38819	LOC643516	0.59	0.03	0.16
ILMN_41173	HLA-DQA1	0.43	0.01	0.14
ILMN_30877	LOC650946	0.21	0.00	3.08719E-08

Table 5.1: Offspring of MI vs. Controls – differentially expressed genes at baseline.

The up-regulated gene IDs are in yellow and the down regulated in blue. Fold changes (Offspring of MI/Controls) are tabulated. All transcripts fulfilled the filtering thresholds (present calls in >1, fold change >1.25 or < 0.8, uncorrected p value <0.05, false discovery rate [fdr2d] <0.5). Unmapped transcripts are not shown. The two probes with corrected p (fdr2d) <0.05 are highlighted in red. 6/31 down regulated probe IDs were unannotated in the genome and therefore excluded from this list.

5.3 BASELINE GENE EXPRESSION: LINKS WITH CAD

To identify known relationships of the candidate molecules with each other and with atherosclerosis, further text mining analysis was performed using ChiLiBot. The candidate genes were analysed for interactions within published literature with each other and with the following key words: atherogenesis, atherosclerosis, atherothrombosis, coronary artery disease, myocardial infarction, monocyte, macrophage and collagen.

16 of the differentially expressed genes had established links with the aforementioned key words in published literature. The genes with established links to atherosclerosis are shown in Figure 5.5. This analysis enabled the selection of genes with the strongest pathophysiological links to atherosclerosis from the genes which showed maximal differential expression in unstimulated monocytes.

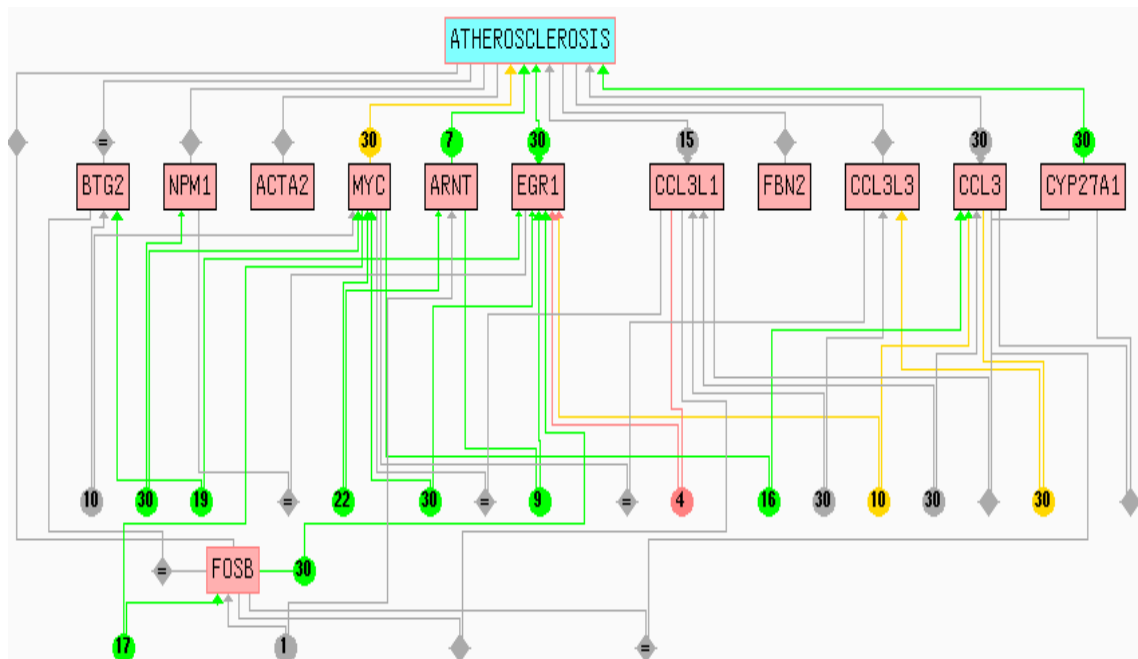


Figure 5.5: Interaction map (ChiLiBot) of candidate gene linked to atherosclerosis.

The arrows in green denote a positive association between terms (up-regulation, activation, enhancement etc), red arrows denote a negative association (inhibition, down regulation, suppression etc) while the grey arrows denote associations with no such directionality. The numbers within the circles denote the number of interactive sentences.

5.4 BASELINE GENE EXPRESSION: CANDIDATE GENES AND PATHWAYS

Resting peripheral blood monocytes showed differential gene expression in healthy subjects with a strong family history of premature myocardial infarction (Group 2) compared to healthy Control offspring (Group 4). The genes which were most differentially expressed with established or putative roles in atherosclerosis included transcription factors, chemokines and structural proteins. The most statistically significant differential expression was observed in the levels of Acyloxyacyl hydrolase which is described first followed by the other genes which were selected based on the relaxed filtering criterion discussed above.

5.4.1 Genes

5.4.1.1 Acyloxyacyl hydrolase (AOAH); Chr 7p14-p12

This gene encodes the enzyme that hydrolyses and detoxifies acyloxyacyl-linked fatty acyl chains from bacterial lipopolysaccharides (Hagen et al., 1991). An intronic SNP in this gene (rs2001600) has been linked to carotid intima media thickness which is a subclinical indicator of atherosclerotic arterial disease (Wang et al., 2012b). Other variants in this gene have been associated with asthma and related quantitative traits such as IgE and cytokine levels (Barnes et al., 2006). A potential mechanism is suggested by the observation that IgE levels are elevated in patients with MI and unstable angina (Wang et al., 2011b) and that IgE promotes cytokine expression and apoptosis in macrophages (Wang et al., 2011b). The latter study also showed that Fc ϵ R1, the specific receptor for IgE is highly expressed in monocyte derived macrophages in atherosclerotic lesions, but not in smooth muscle cells.

In this study, microarray signal intensities indicate that AOA_H is expressed in resting monocytes at moderate levels (1-3,000). Expression levels in Offspring of MI were 1.42 fold higher with a corrected p value of 3.05×10^{-8} (Figure 5.6). The microarray results were validated by PCR (Figure 5.7)

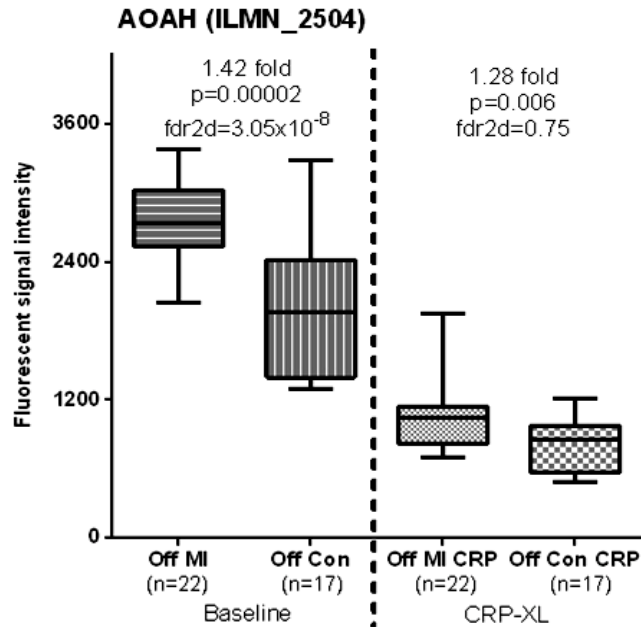


Figure 5.6: Microarray signal intensities of AOA_H in Offspring of MI and controls.

Fluorescent signal intensities in Offspring of MI (Off MI) and controls (Off Con) before and after platelet-mediated stimulation are shown. Error bars denote the range of expression. Fold changes, p values and false discovery rates are provided.

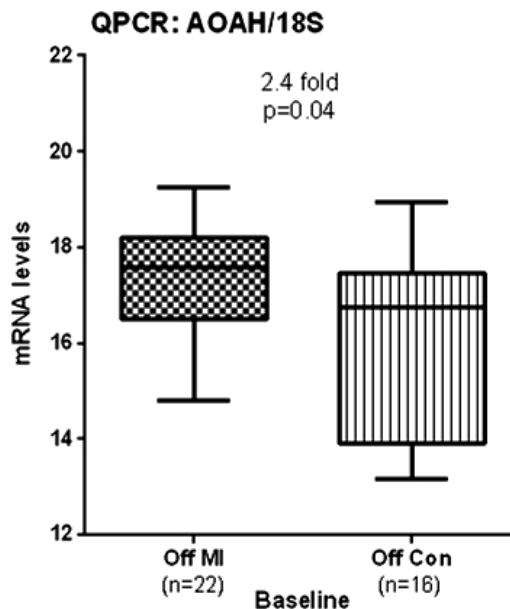


Figure 5.7: Quantitative PCR of AOA_H in Offspring of MI and controls.

Q-PCR of AOA_H with 18S as control gene is shown. Error bars denote the range of expression. Fold change and p value are provided.

5.4.1.2 Transcription factors

5.4.1.2.1 Early growth response protein 1 (EGR1); Chr 5q31.1

EGR1 is a C2H2 type zinc finger nuclear protein that functions as a transcriptional regulator. It is induced by hypoxia (Sperandio et al., 2009) and has been implicated in various cardiovascular pathological processes including atherosclerosis, vascular injury and angiogenesis (Khachigian, 2006). High levels of EGR1 were seen in human carotid atherosclerotic lesion caps in comparison to tunica media tissue (McCaffrey et al., 2000). EGR1 co-localises with macrophages in the shoulder of atherosclerotic lesions in ApoE deficient mice (Bea et al., 2003). EGR1 is induced in vascular smooth muscle cells (VSMCs) following exposure to atherogenic chylomicron particles (Takahashi et al., 2005). Exposure of VSMCs to oxidant stress induces EGR1 expression which then binds to promoter regions of tissue factor and plasminogen activator inhibitor-1 (Hasan and Schafer, 2008). Endothelial cells express higher levels of tissue factor following exposure to oxidized LDL in an EGR1 dependent manner (Bochkov et al., 2002). Bone marrow-derived EGR1 promotes macrophage accumulation, atherosclerotic lesion development, and lesion complexity (Albrecht et al., 2010). It is also involved in foam cell formation within atherosclerotic lesions (Kim et al., 2009). In human monocytes, oxidized LDL (Harja et al., 2004) and enzymatically modified LDL (Stoyanova et al., 2001) induces expression of EGR1. EGR1 expression in atherosclerotic lesions was decreased by the HMGCoA inhibitor, simvastatin (Bea et al., 2003).

Fluorescent signal intensities (Figure 5.8) indicate that EGR1 is expressed in resting monocytes at moderate levels (1-3,000). Expression levels in Offspring of MI were 1.8 fold higher with a p value of 0.004 which passed the fdr_{2d} threshold of

significance (<0.5). The differential expression of EGR-1 noted in the microarray experiment was validated by quantitative PCR (Figure 5.9).

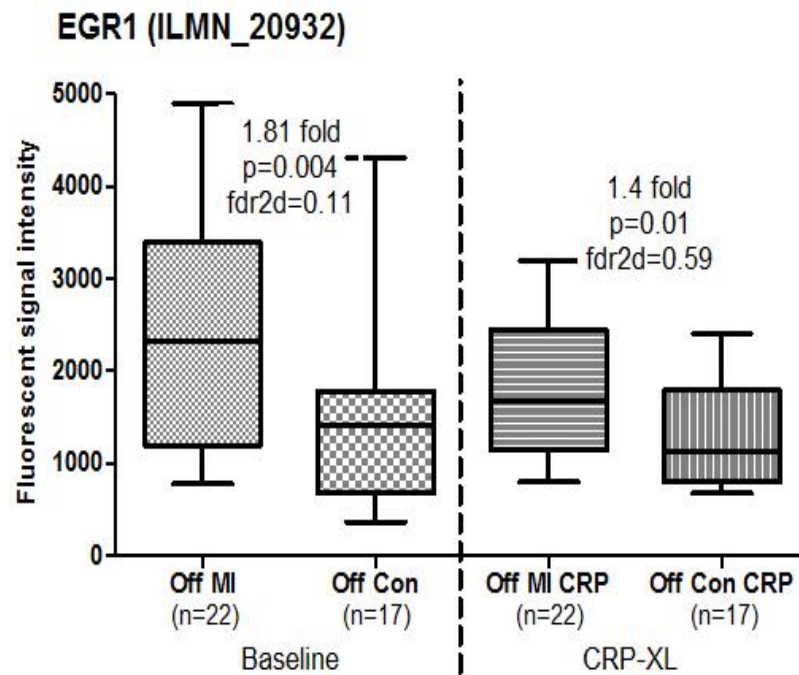


Figure 5.8: Microarray signal intensities of EGR1 in Offspring of MI and controls. Fluorescent signal intensities in Offspring of MI (Off MI) and controls (Off Con) before and after platelet-mediated stimulation are shown. Error bars denote the range of expression. Fold changes, p values and false discovery rates are provided.

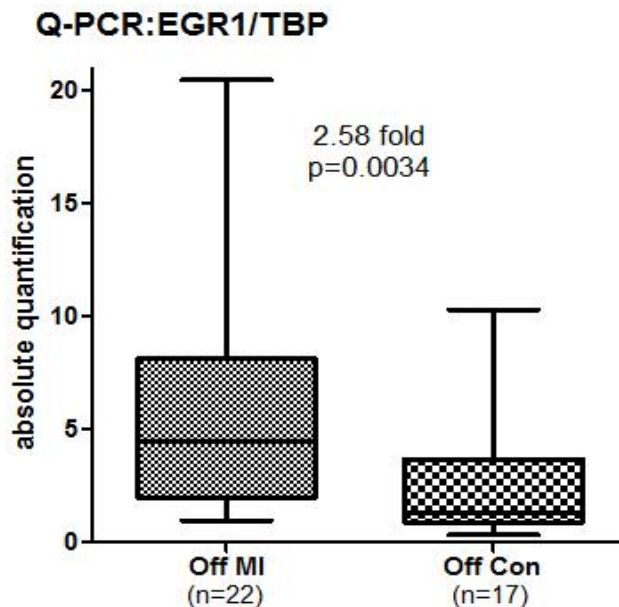


Figure 5.9: Quantitative PCR of EGR1 in Offspring of MI and controls. Q-PCR of EGR1 with TATA box protein as control gene is shown. Error bars denote the range of expression. Fold change and p value are provided.

5.4.1.2.2 Aryl hydrocarbon receptor nuclear translocator (ARNT/HIF1 β); Chr 1q21

ARNT is the constitutive beta subunit of the heterodimeric transcription factor hypoxia-inducible factor 1 (HIF1). Under hypoxic conditions it binds to the inducible alpha subunit and promotes atherosclerotic plaque angiogenesis (Moreno et al., 2006), macrophage infiltration and lesion progression. The HIF1 complex binds to hypoxia response elements (HREs) of target genes including vascular endothelial growth factor (VEGF), erythropoietin and inducible nitric oxide synthetase (iNOS) (Sharp et al., 2004). EGR1 and HIF1 share target genes (Sharp et al., 2004). In human macrophages, ARNT promotes ATP binding cassette transporter A1 (ABCA1) expression under hypoxic stress and facilitates ABCA1 mediated cholesterol efflux (Ugocsai et al., 2010).

Signal intensities in Figure 5.10 indicate that ARNT is expressed at low levels in monocytes. In resting monocytes, ARNT expression levels were 1.25 fold higher in the Offspring of MI group compared to healthy Control offspring.

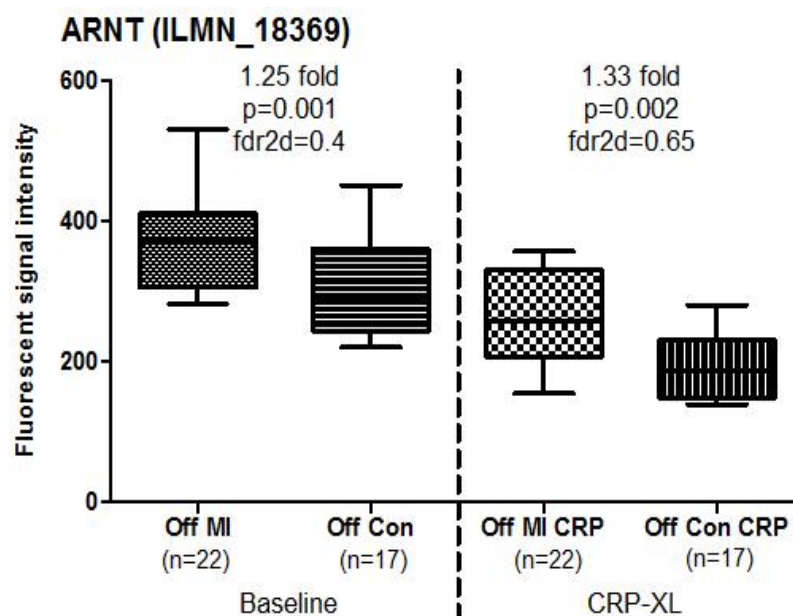


Figure 5.10: Microarray signal intensities of ARNT in Offspring of MI and controls.

Fluorescent signal intensities in Offspring of MI (Off MI) and controls (Off Con) before and after platelet-mediated stimulation are shown. Error bars denote the range of expression. Fold changes, p values and false discovery rates are provided.

5.4.1.2.3 Finkel-Biskis-Jinkins murine osteosarcoma viral oncogene homolog B (FOSB); Chr 19q13.32

FOSB is a leucine zipper protein that dimerises with members of the JUN family to form the transcription complex, activator protein-1 (AP-1) (Novotny et al., 1998). Experiments in mice suggest that FOSB along with HIF1 regulates the response of the carotid body to chronic hypoxia (Prabhakar and Jacono, 2005). Hypoxic stress induces matrix metalloproteinase 2 (MMP-2) in cardiac fibroblasts in a FOSB dependent manner (Bergman et al., 2003). Expression of FOSB and EGR1 was induced by angiotensin II and inhibited by the angiotensin II receptor type 1 (AT-1) blocker, losartan in rat brain tissue (Lebrun et al., 1995). Plasmin treated human monocytes demonstrated increased AP-1 binding and expressed interleukin-1alpha (IL-1alpha), IL-1beta, tumour necrosis factor-alpha (TNF-alpha) and tissue factor (TF) in a dose dependant manner (Syrovets et al., 2001).

FOSB is expressed at low levels in resting monocytes (Figure 5.11). FOSB expression levels were 1.86 fold higher in Offspring of MI ($p=0.008$, $fdr2d=0.22$).

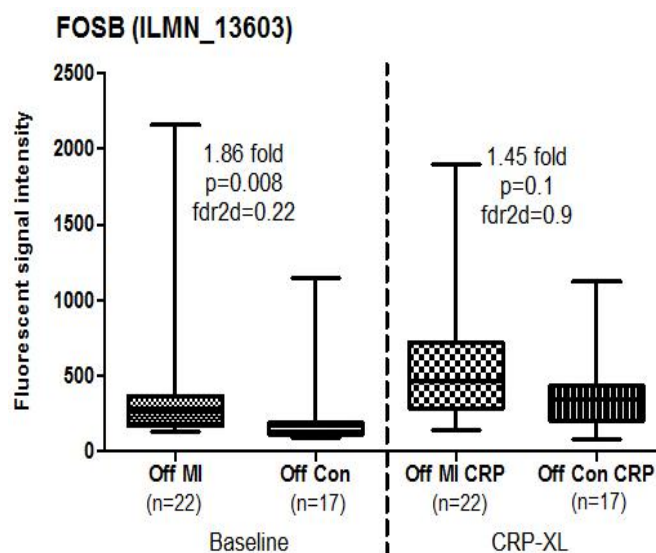


Figure 5.11: Microarray signal intensities of FOSB in Offspring of MI and controls.

Fluorescent signal intensities in Offspring of MI (Off MI) and controls (Off Con) before and after platelet-mediated stimulation are shown. Error bars denote the range of expression. Fold changes, p values and false discovery rates are provided.

5.4.1.2.4 V-myc myelocytomatosis viral oncogene homolog (MYC/c-MYC); 8q24.21

An atherogenic role has been proposed for MYC from the observation that expression levels were high in obese women at high cardiovascular risk and that the levels settled with weight loss in these subjects (Holvoet, 2008). Under conditions of chronic moderate hypoxia, human monocyte derived macrophages expressed matrix metalloproteinase-7 (MMP7), CD44 and MYC in addition to the alpha subunit of HIF1 (Deguchi et al., 2009). MYC co-localised with atherosclerotic lesions in cholesterol fed rabbits (Qin et al., 2005).

Figure 5.12 shows that MYC is expressed at low to moderate levels in resting monocytes. MYC levels were 0.78 fold lower in Offspring of MI at baseline ($p=0.006$, $fdr_{2d}=0.4$). Interestingly, in this study, MYC levels were significantly lower in the 'at risk' group (Offspring of MI) which may be a result of hypoxic stress. ARNT (up-regulated in Group 2, see above) has been shown to activate the MYC inhibitor MXI1 in response to hypoxia (Corn et al., 2005) and to competitively displace MYC from its DNA binding site (Swanson and Yang, 1999).

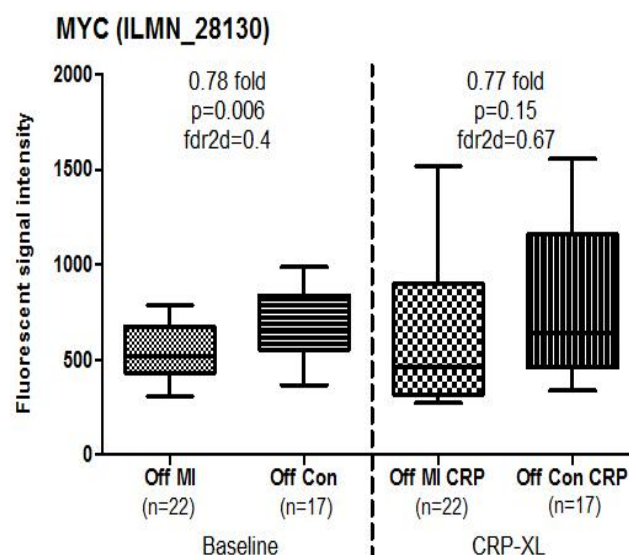


Figure 5.12: Microarray signal intensities of MYC in Offspring of MI and controls.

Fluorescent signal intensities in Offspring of MI (Off MI) and controls (Off Con) before and after platelet-mediated stimulation are shown. Error bars denote the range of expression. Fold changes, p values and false discovery rates are provided.

5.4.1.2.5 Zinc finger protein 274 (ZNF274); Chr 19qter

ZNF274 encodes a zinc finger protein containing five C2H2-type zinc finger domains, one or two Kruppel-associated box A (KRAB A) domains, and a leucine-rich domain which localises to the nucleolus (Yano et al., 2000). This promotes the binding of the histone methyl transferase SETDB1 to genomic locations resulting in the regulation (silencing) of transcription factors (Fietze et al., 2010). ZNF274 therefore plays a role in tissue specific gene silencing, especially of transcription factors to facilitate selective activation and expression of these factors.

As with all the other differentially expressed transcription factors described above, ZNF274 is expressed at low levels (500-1000) in resting monocytes (Figure 5.13). Levels in Offspring of MI were 0.77 fold lower compared to healthy controls ($p=0.003$, $fdr_{2d}=0.4$). Lower levels of this transcriptional repressor may suggest an early deregulation of transcription in the 'at risk' subjects.

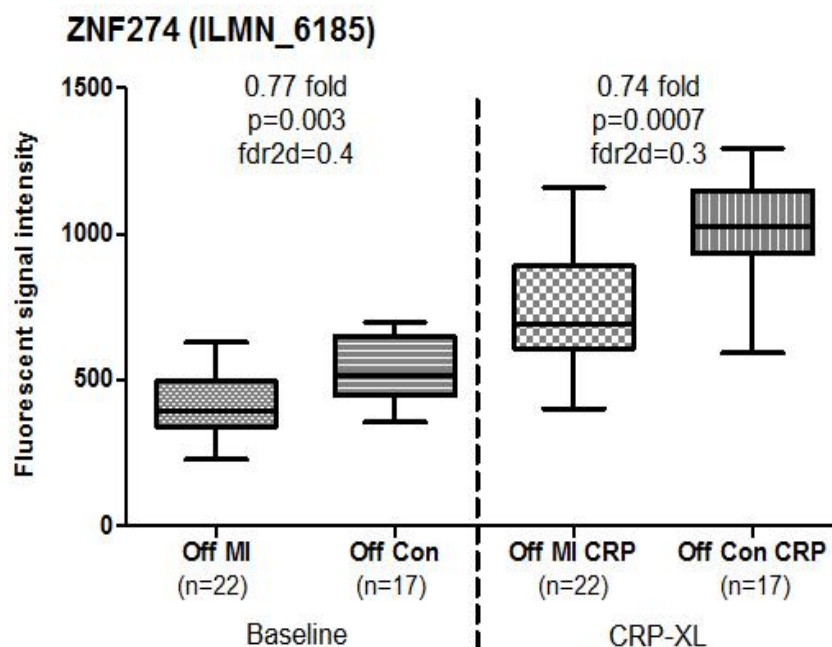


Figure 5.13 Microarray signal intensities of ZNF274 in Offspring of MI and controls.

Fluorescent signal intensities in Offspring of MI (Off MI) and controls (Off Con) before and after platelet-mediated stimulation are shown. Error bars denote the range of expression. Fold changes, p values and false discovery rates are provided.

5.4.1.2.6 Role of hypoxia in differential expression of transcription factors

A common theme that links the differentially expressed transcription factors in this comparison is hypoxic stress. This may explain the observed differences in gene expression in the Offspring of MI. In this group, there was a 25% increase in expression of ARNT which is the constitutive component of HIF1 with a direct role in plaque angiogenesis and monocyte infiltration. In addition, raised ARNT levels may also explain the down regulation of MYC seen in this analysis. EGR1, another transcription factor with significantly higher expression levels in the Offspring of MI group is induced in response to hypoxia and directly activates the inducible alpha component of HIF1 which then binds to ARNT. FOSB is also expressed in response to hypoxia (Knight et al., 2011) and regulates metalloproteinase activity in fibroblasts. Tissue factor, which plays a central role in thrombosis, is activated by both EGR1 and FOSB. The differential expression of transcription factors seen in this analysis is summarised in Figure 5.14.

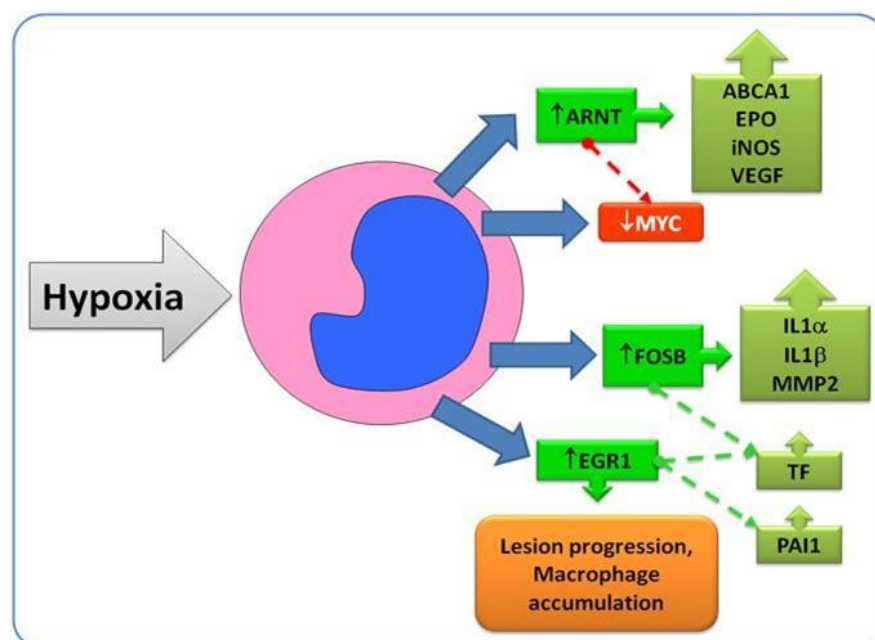


Figure 5.14: Monocyte mediated mechanisms of atherogenesis in Offspring of MI.

At baseline, the differences in expression of transcription factors in Offspring of MI appear to be mediated by hypoxic stress as depicted. The major transcription factors with recognized roles in atherosclerosis are shown.

5.4.1.3 Other genes

5.4.1.3.1 Cytochrome P450, family 27, subfamily A, polypeptide 1 (CYP27A1); Chr2q33-qter

This enzyme facilitates sterol elimination from macrophages. The atheroprotective effect of peroxisome proliferator activated receptor gamma (PPAR- γ) is partly mediated by up-regulation of CYP27A1 in human monocyte derived macrophages (Quinn et al., 2005). The raised levels seen in Offspring of MI may suggest a compensatory protective mechanism in response to a proinflammatory atherogenic state. This is suggested by the observation that CYP27A1 is a target for the JNK/c-JUN pathway (Norlin et al.), activated by apoptotic and proinflammatory stimuli such as TNF α and oxidised LDL (Go et al., 2001).

CYP27A1 is expressed at moderate levels in resting monocytes (Figure 5.15). Levels were 1.36 fold higher in Offspring of MI ($p=0.005$, $fdr_{2d}=0.45$). Levels were also significantly higher in the Post MI group after stimulation (Chapter 4).

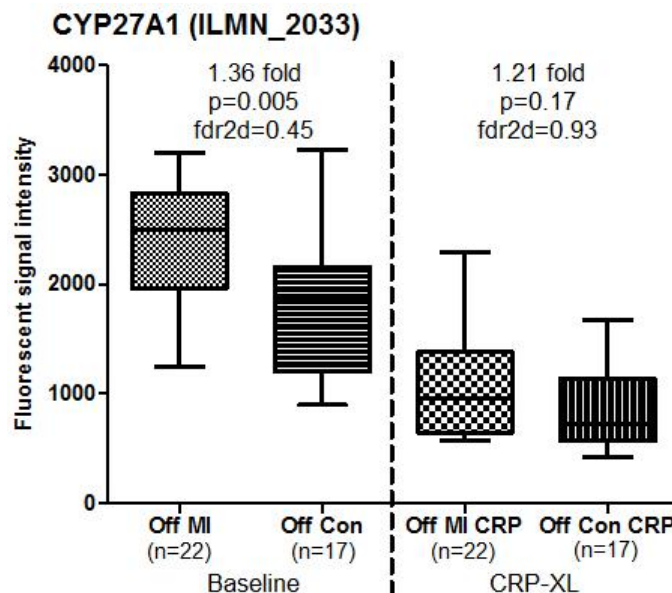


Figure 5.15: Microarray signal intensities of CYP27A1 in Offspring of MI and controls.

Fluorescent signal intensities in Offspring of MI (Off MI) and controls (Off Con) before and after platelet-mediated stimulation are shown. Error bars denote the range of expression. Fold changes, p values and false discovery rates are provided.

The findings on microarray were confirmed by Q-PCR (Figure 5.16).

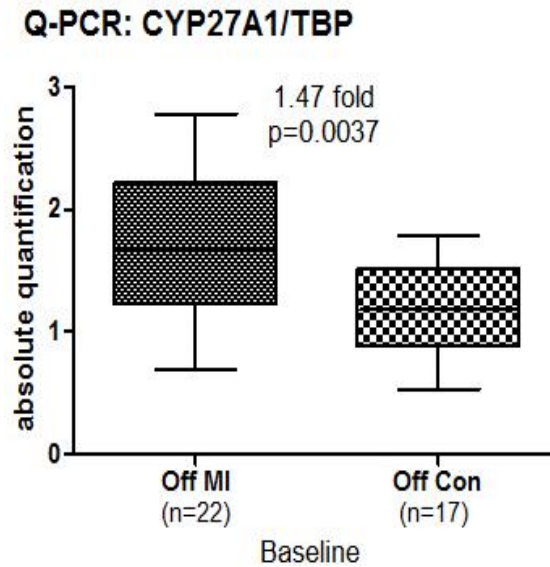


Figure 5.16: quantitative PCR of CYP27A1 in Offspring of MI and controls.

Q-PCR of CYP27A1 with TATA box protein as control gene is shown. Error bars denote the range of expression. Fold change and p value are provided.

5.4.1.3.2 Chemokine (C-C motif) ligand 3 (CCL3/macrophage inflammatory protein-1 α); Chr 17q11-q21

CCL3 is secreted by monocytes (Teupser et al., 2008) and is expressed in calcified plaques (Cagnin et al., 2009). Lipid peroxidation in endothelial cells induces CCL3 which then promotes atherogenesis by chemotaxis of circulating monocytes into the arterial intima (Yang et al., 2003). Serum levels of CCL3 are elevated in patients with significant CAD (Ardigo et al., 2007). The angiotensin II receptor (AT-1) antagonist, irbesartan reduces expression of CCL3 in atherosclerotic lesions in ApoE deficient mice (Dol et al., 2001). Monocyte-derived dendritic cells cultured with interleukin-3 (IL3), a potent atherogenic cytokine (Brizzi et al., 2001), over express both CCL3 and CYP27A1 (Hata et al., 2009) as seen in the Offspring of MI. CCL3 has also been implicated in lipid homeostasis in animal models of atherosclerosis (Kennedy et al., 2012).

Figure 5.17 shows that CCL3 is expressed at low levels in monocytes (100-400). Expression levels were 1.36 fold higher in Offspring of MI ($p=0.005$, $fdr_{2d}=0.45$) in resting monocytes. These findings were validated by Q-PCR (Figure 5.18).

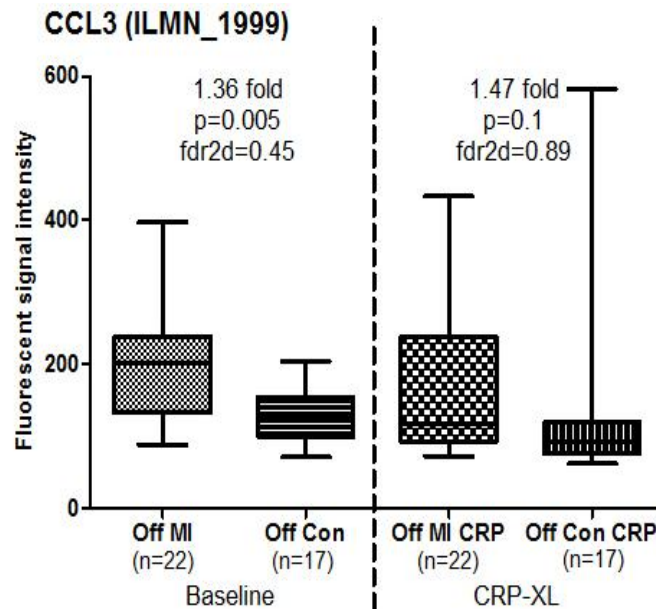


Figure 5.17: Microarray signal intensities of CCL3 in Offspring of MI and controls.

Fluorescent signal intensities in Offspring of MI (Off MI) and controls (Off Con) before and after platelet-mediated stimulation are shown. Error bars denote the range of expression. Fold changes, p values and false discovery rates are provided.

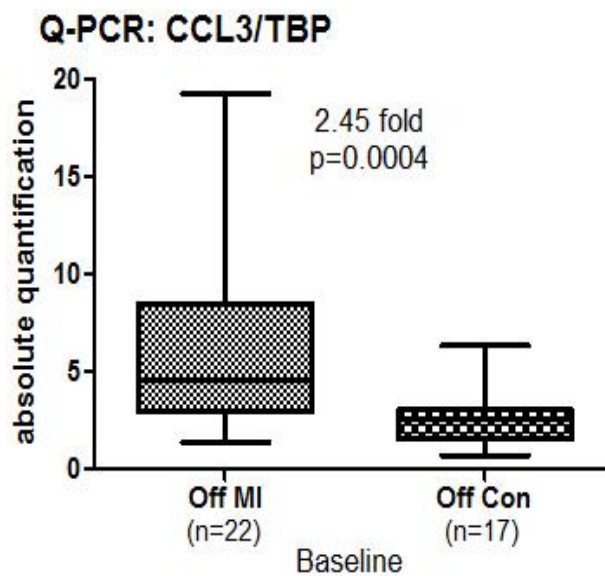


Figure 5.18: quantitative PCR of CCL3 in Offspring of MI and controls.

Q-PCR of CCL3 with TATA box protein as control gene is shown. Error bars denote the range of expression. Fold change and p value are provided.

Two copies of a related chemokine, CCL3L1 (telomeric copy) and CCL3L3 (centromeric copy) were also differentially expressed in Group 2 (Figure 5.19).

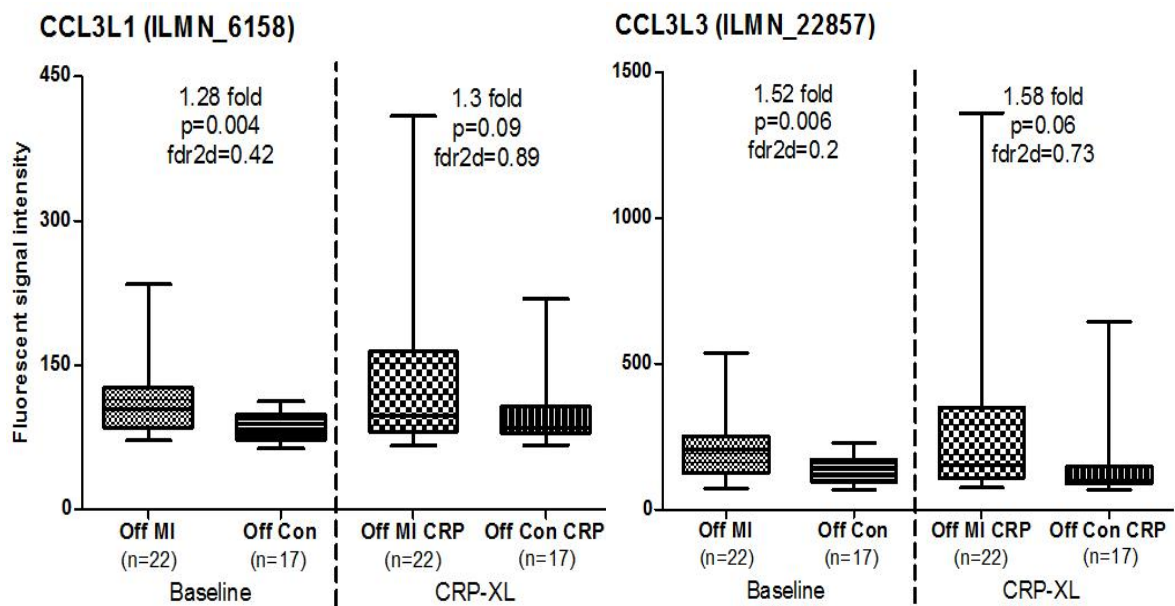


Figure 5.19: Signal intensities of CCL3L1 and CCL3L3 in Offspring of MI and controls.

Fluorescent signal intensities in Offspring of MI (Off MI) and controls (Off Con) before and after platelet-mediated stimulation are shown. Error bars denote the range of expression. Fold changes, p values and false discovery rates are provided.

Studies have focused on structural genetic variations in CCL3L1 and disease susceptibility. CCL3L1 copy number variations (CNV) have been associated with susceptibility to infections such as HIV (Nakajima et al., 2008) and hepatitis C (Grunhage et al., 2010). CNV in CCL3L1 correlates with the ratio of CCL3L1:CCL3 mRNA (Carpenter et al., 2012). Even more interesting from the perspective of CAD is the strong association of CCL3L1 copy number variation with Kawasaki's disease (KD) – a systemic inflammatory disorder affecting children which causes coronary aneurysms. A study of Japanese children with KD has shown that a variation from the population average copy number of CCL3L1 is associated with an increased risk of KD (Mamtani et al., 2010).

Further studies are needed to assess whether the significant increase in expression of CCL3, CCL3L1 and CCL3L3 in Offspring of MI may associate with CNVs in CCL3L1.

5.4.1.3.3 Actin, alpha 2, smooth muscle, aorta (ACTA2), Chr 10q23.3

This protein plays an important role in cell motility and integrity. Mutations in vascular smooth muscle cell ACTA2 results in premature coronary disease, stroke and thoracic aneurysms as suggested by a linkage analysis and association study of individuals in 20 families with ACTA2 mutations (Guo et al., 2009).

ACTA2 is expressed at low levels in monocytes (Figure 5.20) and levels were 0.75 fold lower in Offspring of MI ($p=0.024$, $fdr_{2d}=0.3$).

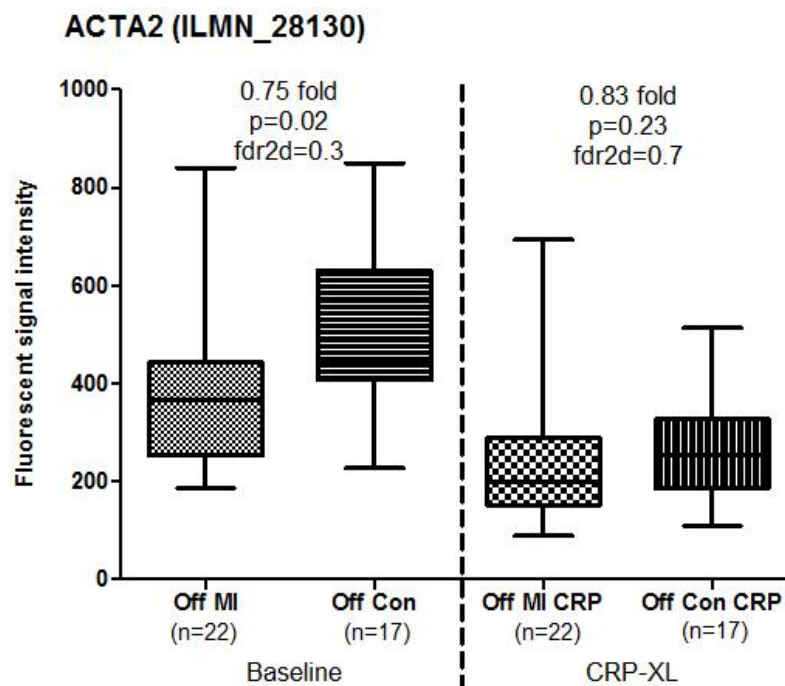


Figure 5.20: Microarray signal intensities of MYC in Offspring of MI and controls.

Fluorescent signal intensities in Offspring of MI (Off MI) and controls (Off Con) before and after platelet-mediated stimulation are shown. Error bars denote the range of expression. Fold changes, p values and false discovery rates are provided.

5.4.2 Pathways

5.4.2.1 VEGF signaling

Vascular endothelial growth factor promotes the growth and development of endothelial and lymphatic cells. In pathological states such as atherosclerosis, VEGF is induced by HIF1 in response to hypoxia or ischaemia (Forsythe et al., 1996) and is regulated by Wnt/beta catenin (Lee et al., 2009a). The binding of VEGF to its receptor (VEGF-R) results in cell proliferation, cell migration and pathological angiogenesis (Matsumoto and Mugishima, 2006). ARNT, the constitutional beta subunit of HIF1 is shown to regulate VEGF expression and promote angiogenesis under hypoxic conditions (Han et al., 2010). The significant over expression of ARNT in the Offspring of MI suggests an early activation of proinflammatory, atherogenic pathways in the absence of clinically apparent atherosclerosis. In addition, the inducible alpha subunit of HIF1 which activates VEGF is directly activated by EGR1, another of the candidate genes which was expressed at significantly higher levels in Offspring of MI. VEGF has also been shown to induce expression of FOSB in endothelial cells (Holmes and Zachary, 2004), another of the differentially expressed genes in this comparison. Given that there were no significant differences in environmental risk factor between the two groups, this is likely to suggest a genetically determined activation of a proatherogenic signalling pathway.

5.5 ANALYSIS OF DIFFERENTIALLY EXPRESSED MONOCYTES GENES AFTER PLATELET MEDIATED STIMULATION (CRP-XL)

Only a finite number of genes are differentially expressed in resting monocytes in healthy young men with contrasting familial history of premature MI. In this section, we focus on the gene expression profiles in monocytes from at risk individuals (Offspring of MI) when exposed to activated platelets (Figure 5.21).

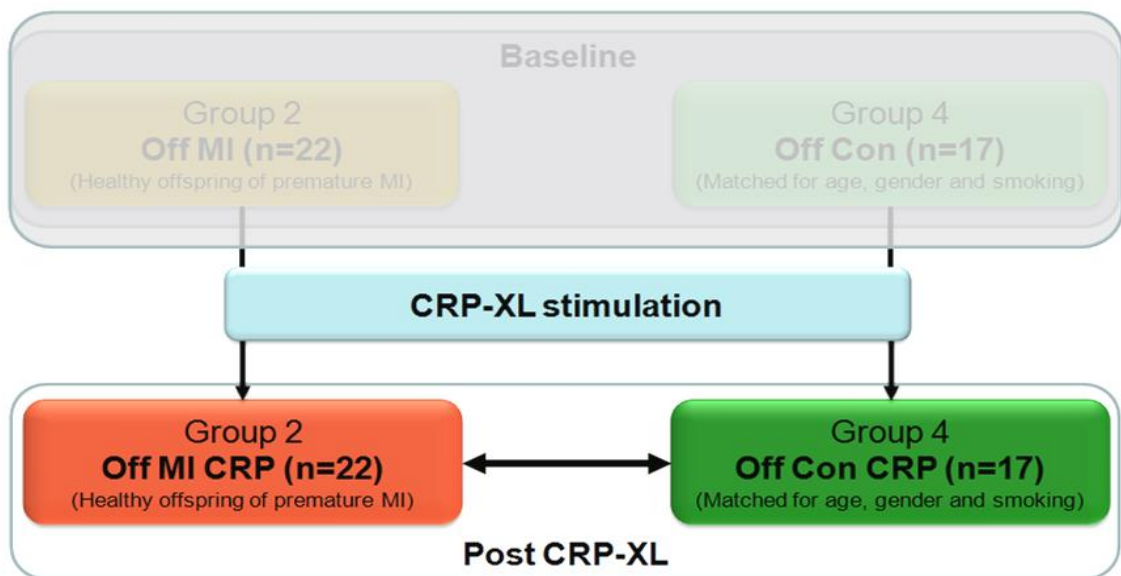


Figure 5.21: Offspring of MI vs. Controls after platelet-mediated stimulation.

5.6 DIFFERENTIAL GENE EXPRESSION IN ACTIVATED MONOCYTES: INITIAL ANALYSIS

Peripheral venous blood samples collected in citrate tubes were stimulated with activated platelets following which CD14⁺ monocytes were isolated and RNA was extracted in TRIzol. Platelet mediated monocyte activation was confirmed by MPA assay.

The normalized signal intensities were compared as previously described. Differential expression of transcripts in Offspring of MI in comparison to healthy Control offspring is shown in sigmoid plots (Figure 5.22).

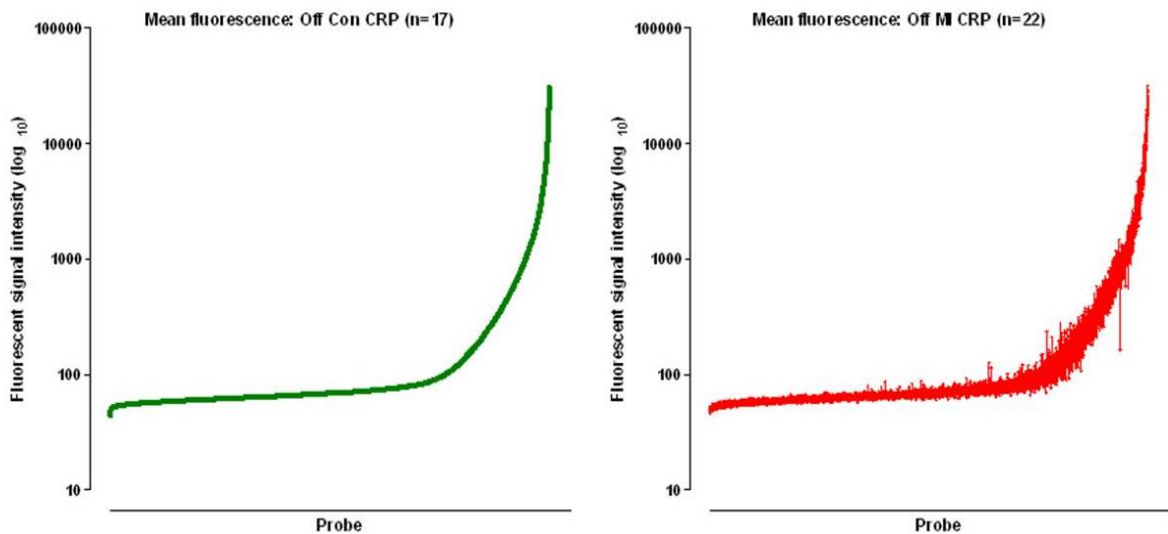


Figure 5.22: Sigmoid plots of fluorescent signal intensity in stimulated monocytes. Mean fluorescent signal intensities of all probe sets following stimulation in healthy Control offspring (left) and corresponding changes in signal intensities in the Offspring of MI group (right) are shown. The change in gene expression for each transcript is depicted in the right sided graph.

Degree (fold change) and significance (p value) of each transcript probe set are graphically represented in Figure 5.23.

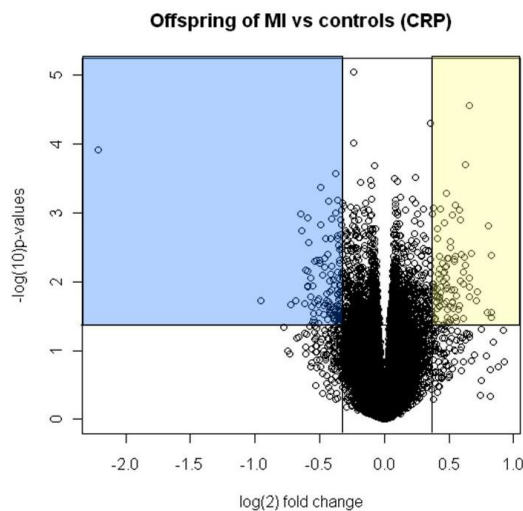


Figure 5.23: Volcano plot of Offspring of MI vs. controls after platelet-mediated stimulation. \log_2 transformed fold change (Offspring of MI/controls) is plotted on the x-axis and \log_{10} transformed p-values (t test; uncorrected for multiple comparisons) is plotted on the y-axis. The yellow and blue shaded regions contain up and down regulated transcripts respectively which fulfil the filtering criteria for subsequent candidate gene analyses.

As described in section 5.2, the filtering steps were modified for the analysis of the offspring groups. Similar to the trend in the baseline comparison, many genes with established roles in atherosclerosis which were differentially expressed between the groups would not have fulfilled the stringent criteria for statistical filtering. These were included in the analysis by relaxing the false discovery thresholds (Figure 5.24).

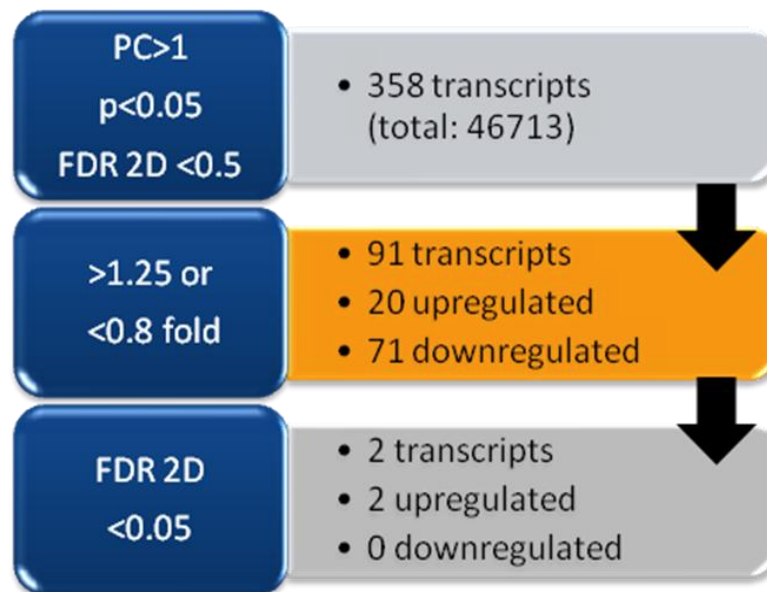


Figure 5.24: Gene transcript filtering strategy to identify differentially expressed genes. The orange panel highlights the filtering threshold used for subsequent candidate gene analyses. PC=present calls, FDR 2D=false detection rate in 2 dimensions.

Only two genes met the stringent *fdr2d* threshold. However 91 transcripts met these filtering criteria of intermediate stringency, of which 20 were up-regulated and 71 were down regulated in Offspring of MI compared to controls (Table 5.2).

Probe_ID	Symbol	Fold change	p values	FDR2D
ILMN_3272	WBP5	1.75	0.002	0.41
ILMN_9429	FKBP4	1.59	0.004	0.35
ILMN_11699	SLC5A3	1.58	0.009	0.49
ILMN_28761	STIP1	1.57	<0.001	0.0000084
ILMN_16430	DLG4	1.55	<0.001	0.19
ILMN_16000	HSP90AB1	1.54	0.006	0.35
ILMN_2942	HLA-DRB3	1.53	0.004	0.36
ILMN_6829	ID3	1.53	0.007	0.41
ILMN_9639	PAPSS2	1.50	0.001	0.39
ILMN_26999	TSPYL2	1.50	0.001	0.37
ILMN_10449	CXXC5	1.47	0.004	0.44
ILMN_3298	PVRL2	1.46	0.001	0.38
ILMN_547	BIN1	1.46	0.005	0.44
ILMN_20328	NT5DC2	1.45	0.005	0.45
ILMN_30967	LOC653158	1.43	0.003	0.49
ILMN_7651	DNAJB6	1.42	0.003	0.49
ILMN_2079	DGKD	1.28	<0.001	0.0000084
ILMN_9565	EEF1E1	0.80	0.017	0.42
ILMN_15728	ZNF329	0.80	0.004	0.31
ILMN_1275	ZMYM6	0.80	0.009	0.37
ILMN_24256	C20orf72	0.80	0.030	0.45
ILMN_11569	CIDEB	0.80	0.037	0.46
ILMN_138903	KENAE	0.80	0.001	0.24
ILMN_16611	MRPS28	0.80	0.032	0.45
ILMN_6467	TPK1	0.80	0.012	0.40
ILMN_138454	GRPEL2	0.80	0.014	0.42
ILMN_19845	STK39	0.79	0.007	0.36
ILMN_14063	DLEU7	0.79	0.003	0.30
ILMN_17415	MTFMT	0.79	0.003	0.30
ILMN_26395	ROPN1L	0.79	0.034	0.45
ILMN_27988	ACAD10	0.79	0.001	0.27
ILMN_4372	MGC2408	0.79	0.029	0.45
ILMN_29359	SURF6	0.79	0.002	0.28
ILMN_26271	TMEM5	0.79	0.001	0.26
ILMN_20316	PAG1	0.79	0.023	0.44
ILMN_25681	TM6SF1	0.79	0.028	0.45
ILMN_22373	GUSBL1	0.79	0.016	0.43
ILMN_4187	LRP10	0.79	0.014	0.42
ILMN_4112	ADARB1	0.79	0.027	0.45
ILMN_12202	TUFT1	0.79	0.009	0.39
ILMN_19229	FLJ38451	0.79	0.011	0.41
ILMN_19940	ATP8B2	0.79	0.003	0.30
ILMN_14646	CDCA7L	0.79	0.031	0.47
ILMN_4193	GNAT2	0.79	0.005	0.34
ILMN_12288	KIAA1505	0.79	0.015	0.43
ILMN_21747	TMC8	0.79	0.005	0.34
ILMN_16588	KIR2DL4	0.79	0.034	0.49

Probe_ID	Symbol	Fold change	p values	FDR2D
ILMN_1387	STAMBPL1	0.79	0.017	0.44
ILMN_8407	CACNG6	0.79	0.012	0.41
ILMN_21640	GPR77	0.78	0.018	0.44
ILMN_19169	MRPL3	0.78	0.034	0.50
ILMN_25107	CGI-115	0.78	0.023	0.45
ILMN_2369	PLA2G4A	0.78	0.018	0.44
ILMN_138056	MGC3207	0.78	0.009	0.40
ILMN_10998	RHOBTB3	0.78	0.002	0.29
ILMN_11121	WDR23	0.78	0.031	0.49
ILMN_22879	ARHGAP9	0.78	0.021	0.45
ILMN_12686	DHRS7	0.78	0.002	0.30
ILMN_25234	RAB3IL1	0.78	0.027	0.48
ILMN_438	ABCC5	0.78	0.007	0.39
ILMN_21245	OSGEP	0.78	0.015	0.44
ILMN_11666	CCBP2	0.78	0.001	0.24
ILMN_9525	NCOA7	0.78	0.015	0.44
ILMN_2603	PCK2	0.78	0.022	0.45
ILMN_1894	IL5RA	0.78	0.023	0.47
ILMN_17661	MGC29671	0.77	0.025	0.48
ILMN_14509	SLC16A6	0.77	0.026	0.50
ILMN_5909	ARV1	0.77	<0.001	0.23
ILMN_6226	PGM2	0.77	0.001	0.26
ILMN_14105	PARP4	0.76	0.010	0.43
ILMN_21992	SNX10	0.76	0.013	0.47
ILMN_29455	TAP2	0.75	0.006	0.42
ILMN_137811	FLJ45909	0.75	0.001	0.31
ILMN_20839	C1orf181	0.75	0.002	0.37
ILMN_3318	ACACB	0.75	0.008	0.44
ILMN_15545	DHRS1	0.75	0.010	0.46
ILMN_6185	ZNF274	0.74	0.001	0.30
ILMN_10044	LXN	0.74	0.004	0.42
ILMN_12195	PFKFB2	0.73	0.002	0.41
ILMN_2535	RAB33A	0.73	0.006	0.48
ILMN_2666	FLJ33641	0.73	0.005	0.45
ILMN_28720	FLJ10379	0.71	0.001	0.42
ILMN_19388	CPA3	0.71	<0.001	0.35
ILMN_6502	TFF3	0.66	0.001	0.45
ILMN_39819	TREML3	0.64	0.002	0.49
ILMN_16020	ZNF447	0.64	0.001	0.43

Table 5.2: Offspring of MI vs. Controls – differentially expressed genes in circulating monocytes after platelet-mediated stimulation.

All transcripts fulfilled the filtering thresholds (present calls in >1, fold change >1.25 [yellow] or < 0.8 [blue], uncorrected p value <0.05, false discovery rate [fdr2d] <0.5). Unmapped transcripts are not shown. The two genes with corrected p values (fdr2d) <0.05 are shown in red.

5.7 DIFFERENTIAL GENE EXPRESSION IN ACTIVATED MONOCYTES: LINKS WITH CAD

As previously described, text mining analysis was performed using ChiLiBot. The candidate genes were analysed for interactions within published literature with each other and with the following key words: atherogenesis, atherosclerosis, atherothrombosis, coronary artery disease, myocardial infarction, monocyte, macrophage and collagen.

Of the differentially expressed genes, 25 had established links with the aforementioned key words in published literature. This analysis enabled the selection of genes with the strongest pathophysiological links to atherosclerosis from the candidate genes which showed maximal differential expression following platelet-mediated stimulation (Figure 5.25).

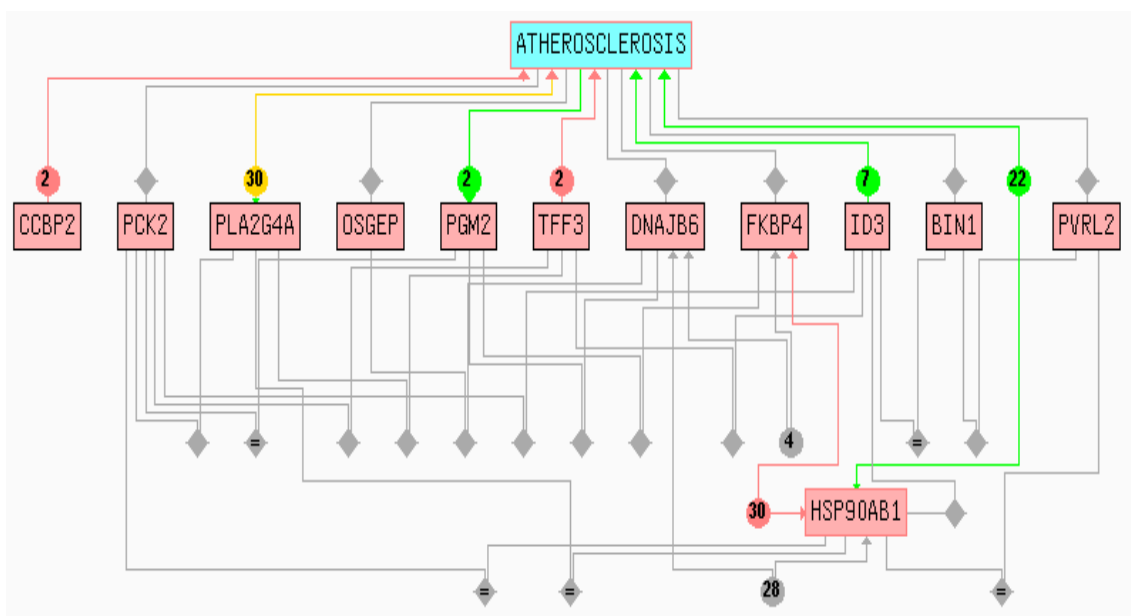


Figure 5.25: Interaction map (ChiLiBot) of candidate gene linked to atherosclerosis.

The arrows in green denote a positive association between terms (up-regulation, activation, enhancement etc), red arrows denote a negative association (inhibition, down regulation, suppression etc) while the grey arrows denote associations with no such directionality. The numbers within the circles denote the number of interactive sentences.

5.8 CANDIDATE GENES AND PATHWAYS

A significant number of the differentially expressed genes in Offspring of MI belonged to the heat shock protein family. These and other genes and pathways are discussed below.

5.8.1 Genes

5.8.1.1 Heat shock proteins

Following platelet-mediated stimulation, six members of the heat shock protein (HSP) family or their associated chaperone proteins were up-regulated in the Offspring of MI (Table 5.3). Four of these satisfied the false discovery threshold ($fdr_{2d} < 0.5$).

Gene	Array ID	Chr	Fold change	p value	fdr _{2D}
STIP1	ILMN_28761	11q13	1.57	0.00003	0.000008
DNAJB6	ILMN_7651	7q36.3	1.42	0.003	0.49
FKBP4	ILMN_9429	12p13.33	1.59	0.004	0.35
HSP90AB1	ILMN_16000	6p12	1.54	0.006	0.35
DNAJA4	ILMN_23222	15q25.1	1.49	0.02	0.64
HSPB1	ILMN_28967	7q11.23	1.77	0.03	0.62

Table 5.3: List of differentially expressed heat shock proteins.

Members of the heat shock protein family which were differentially expressed in Offspring of MI vs. controls following platelet-mediated stimulation are shown. The two genes in the shaded rows did not pass the false discovery correction threshold.

ChiLiBot analysis revealed that HSP90AB1 was the gene with the most number of interactions with the other differentially expressed genes and with established links with atherosclerosis (Figure 5.26). The other genes were FKBP4, DNAJB6 and STIP1, of which the latter had a highly significant p value after correcting for multiple testing. Although DNAJA4 and HSPB1 (HSP27) did not meet the criteria for false discovery correction, they were also included in this analysis.

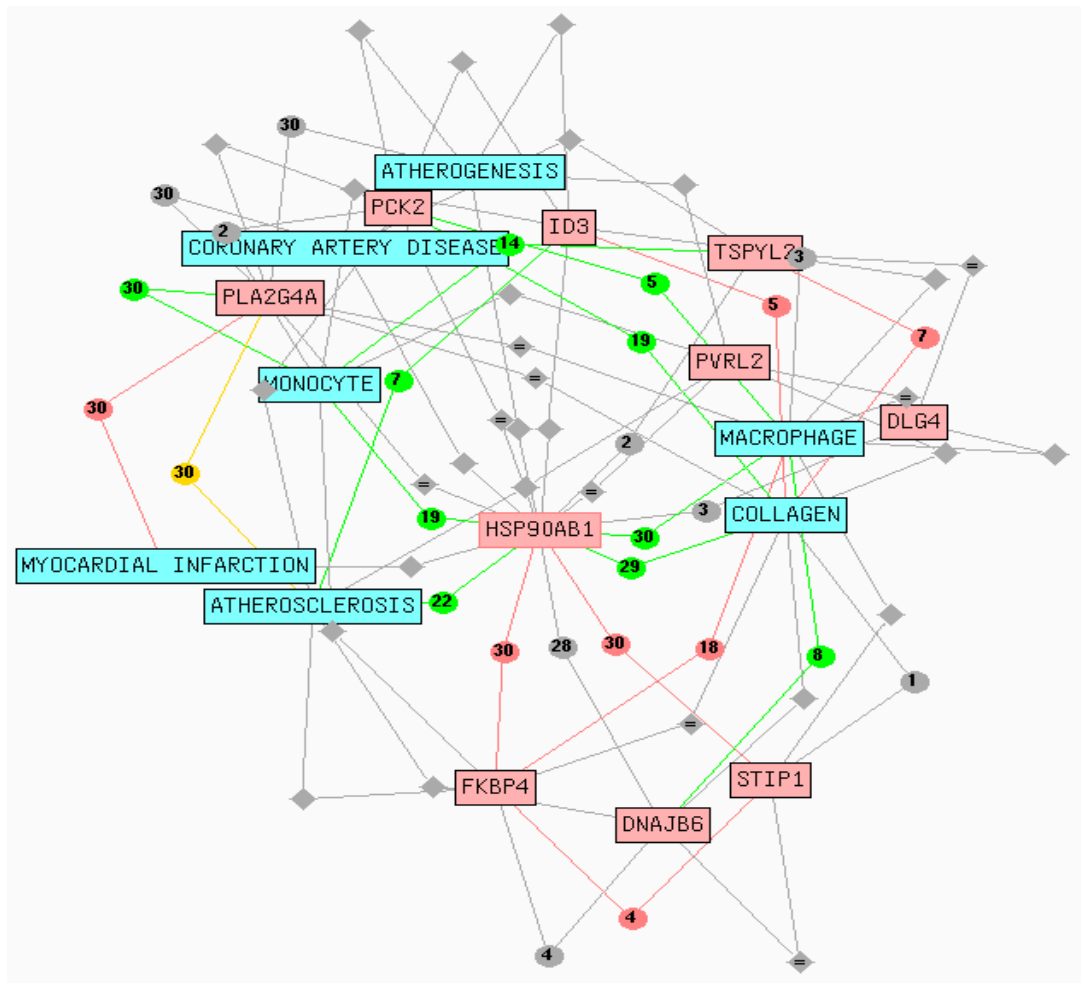


Figure 5.26: Interaction map (ChiLiBot) of key words and genes linked to HSP90AB1.

5.8.1.1.1 Heat shock protein 90kDa alpha (cytosolic), class B member 1 (HSP90AB1/HSP90β); Chr 6 p12

HSP90AB1 is a component of the constitutional cytosolic chaperone protein HSP90 with a role in protein folding and degradation (Freeman and Morimoto, 1996). It interacts with other heat shock proteins (HSP70 and DNAJB1 – the latter was differentially expressed in the Post MI group – see Chapter 4) to mediate protein folding, especially relevant to the synthesis of the glucocorticoid receptor (Morishima et al., 2001). HSP90, HSP70 and HSPB1 (see below) have anti-apoptotic roles and determine cell fate (Lanneau et al., 2007). Human endothelial cells exposed to ‘hyperlipidaemic stress’ express high levels of HSP90, HSP70

and HSPB1 (Ivan and Antohe, 2010). HSP90 associates with endothelial nitric oxide synthase (eNOS) and determines the balance between NO and superoxide (Stepp et al., 2002). In the presence of oxidized LDL, atorvastatin has been shown to increase the stimulatory interaction between HSP90 and endothelial nitric oxide synthetase (eNOS) (Feron et al., 2001). HSP90AB1 helps in regulation of the immune response by stabilizing microtubules in macrophages stimulated by interferon- γ and lipopolysaccharide (Patel et al., 2009). It also interacts with the transcription factor Nrf2 and has a role in mediating the oxidative stress response (Miller and Ramos, 2005).

HSP90AB1 expression levels in monocytes were comparable at baseline (Figure 5.27). Following platelet-mediated stimulation, expression was 1.54 fold higher in ($p=0.006$) in Offspring of MI ($p=0.005$, $fdr2d=0.35$).

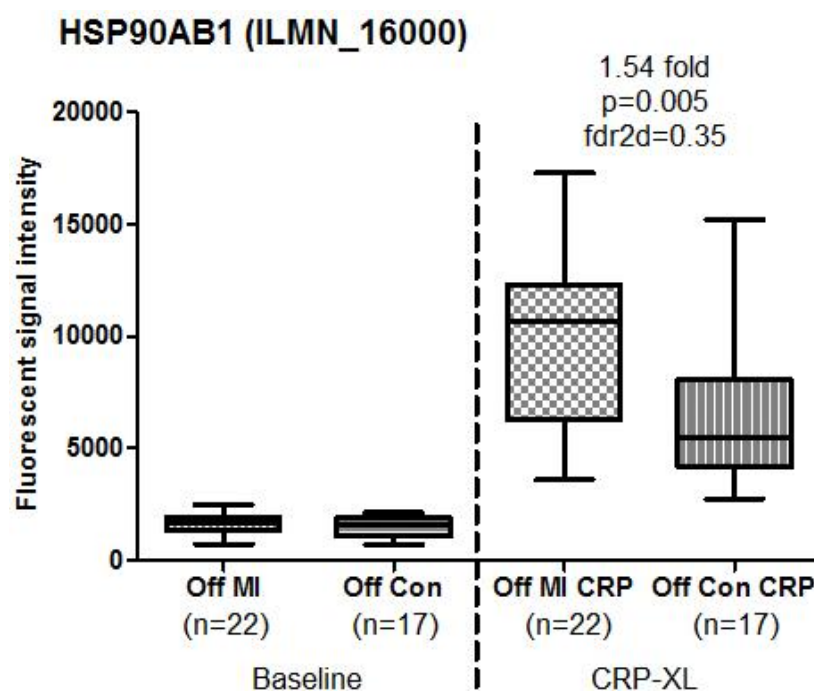


Figure 5.27: Microarray signal intensities of HSP90AB1 in Offspring of MI and controls. Fluorescent signal intensities in Offspring of MI (Off MI) and controls (Off Con) before and after platelet-mediated stimulation are shown. Error bars denote the range of expression. Fold changes, p values and false discovery rates are provided.

Although a numerically higher expression level (1.82 fold) was seen on Q-PCR, this was not statistically significant (Figure 5.28)

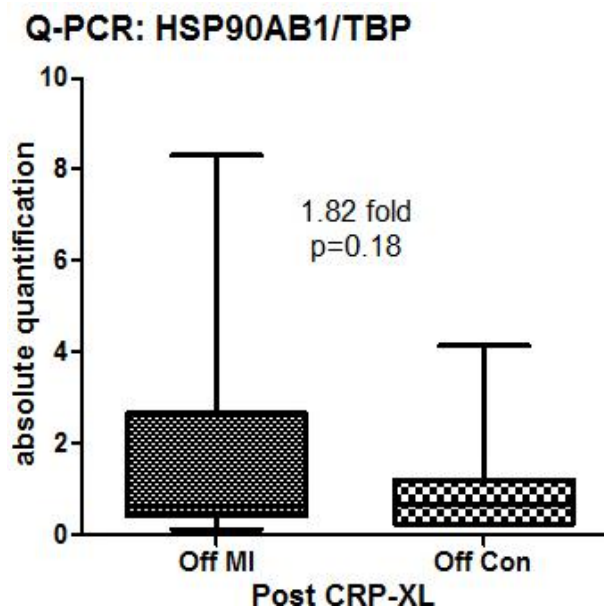


Figure 5.28: quantitative PCR of HSP90AB1 in Offspring of MI and controls. Q-PCR of HSP90AB1 with TATA box protein as control gene is shown. Error bars denote the range of expression. Fold change and p value are shown.

5.8.1.1.2 Stress induced phosphoprotein 1 (STIP1/P60/HOP/STI1); Chr 11q13

This co-chaperone protein co-ordinates the function of the protein folding complex HSP70/HSP90 and also independently regulates their function (Song and Masison, 2005). Following heat shock stress, STIP1 translocates from cytoplasm to nucleus (Daniel et al., 2008). It then binds to HSP90 via its tetratricopeptide repeat domain 2A (TPR2A) and with HSP70 via TPR1 (Odunuga et al., 2003). Macrophages express STIP1 in response to lipopolysaccharide (Heine et al., 1999) suggesting that this protein mediates other pathways in pro-inflammatory cellular stress of relevance to atherosclerosis. Recent studies also indicate that it has a role in angiogenesis (Li et al., 2012).

STIP1 expression levels were comparable between groups at baseline (Figure 5.29). Expression levels increased in both groups following CRP-XL stimulation with a 1.57 fold higher level in Offspring of MI compared to controls ($p=0.00003$, $fdr2d=0.000008$) in Offspring of MI (Figure 5.29). A higher expression level was noted on QPCR (Figure 5.30).

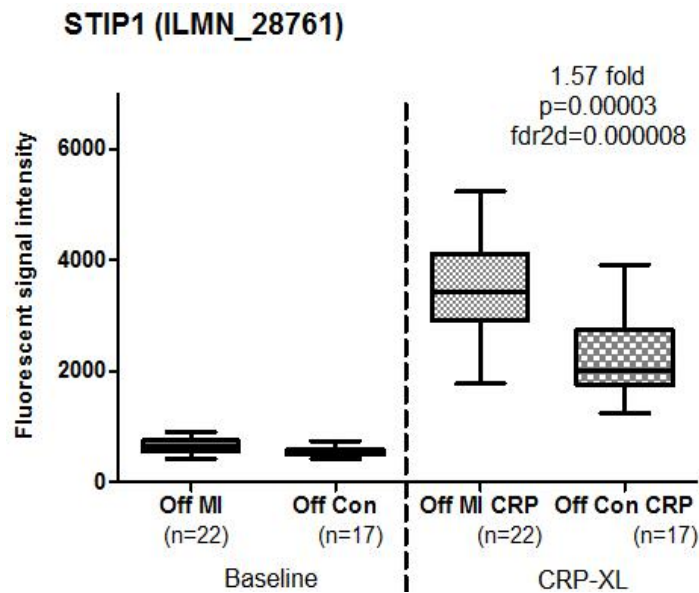


Figure 5.29: Microarray signal intensities of STIP1 in Offspring of MI and controls.

Fluorescent signal intensities in Offspring of MI (Off MI) and controls (Off Con) before and after platelet-mediated stimulation are shown. Error bars denote the range of expression. Fold changes, p values and false discovery rates are provided.

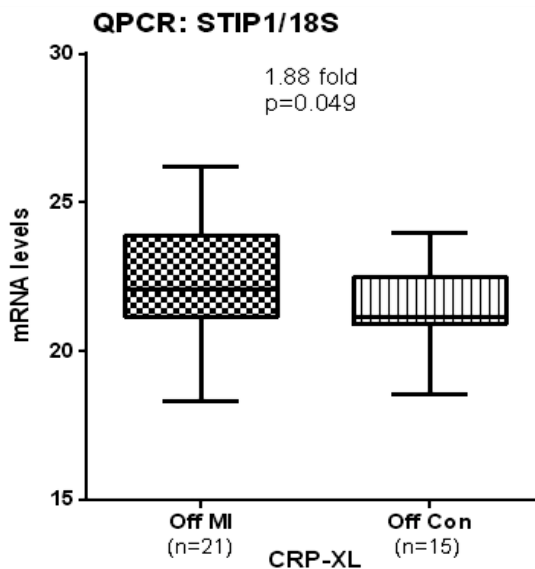


Figure 5.30: quantitative PCR of STIP1 in Offspring of MI and controls.

Q-PCR of STIP1 with 18S as control gene is shown. Error bars denote the range of expression. Fold change and p value are shown.

5.8.1.1.3 DnaJ (Hsp40) homolog, subfamily B, member 6 (DNAJB6; Ch4 7q36.3)

This is a co-chaperone that assists protein folding function of HSP70 (Farinha et al., 2002). It facilitates autophagy of damaged mitochondria by restoring function of the ligase, Parkin (Rose et al., 2011) and has been shown to be a negative regulator of T cell proliferation (Zhang et al., 2008). It exerts a regulatory role on the Wnt/beta catenin pathway by degrading beta catenin (Menezes et al., 2012) and reducing expression of its downstream target, osteopontin (Mitra et al., 2012).

DNAJB6 was expressed at similar levels in unstimulated monocytes (Figure 5.31). Following platelet-mediated stimulation, a 1.42 fold higher expression was noted in the Offspring of MI ($p=0.003$, $fdr_{2d}=0.49$).

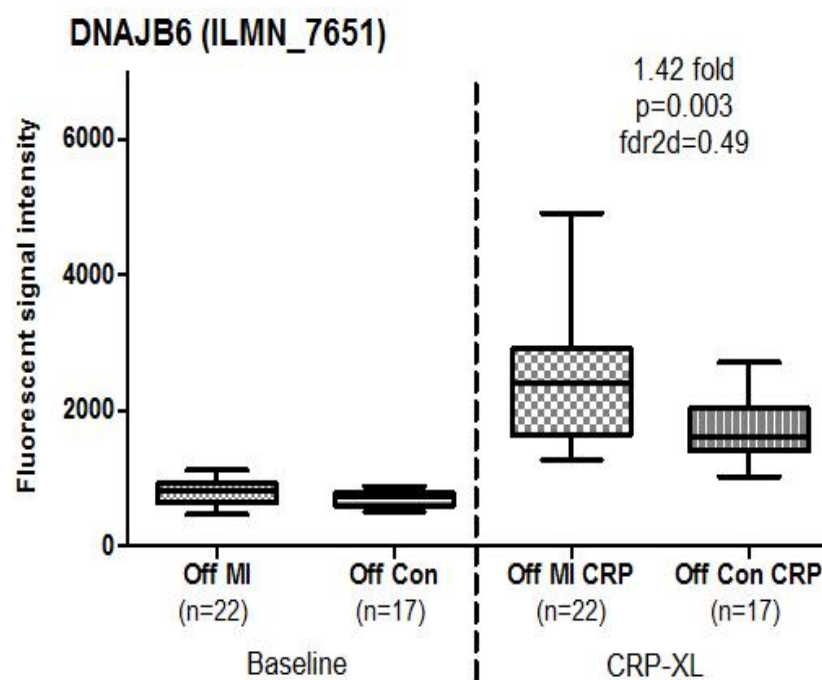


Figure 5.31: Microarray signal intensities of DNAJB6 in Offspring of MI and controls.

Fluorescent signal intensities in Offspring of MI (Off MI) and controls (Off Con) before and after platelet-mediated stimulation are shown. Error bars denote the range of expression. Fold changes, p values and false discovery rates are provided.

5.8.1.1.4 FKBP4 binding protein 4 (FKBP4/FKBP52/PPIase/HSP56; Chr 12p13.33)

This protein is a member of the immunophilin family and associates with two heat shock proteins, HSP70 and HSP90. It binds to HSP90 during ligand mediated activation of the glucocorticoid receptor (Park et al., 2007). Gene knockdown studies in mice have shown that this molecule regulates inflammation, angiogenesis and cell proliferation (Hirota et al., 2008).

Figure 5.32 shows that FKBP4 was expressed at low levels in unstimulated monocytes with no significant difference between cases and controls. A 1.59 fold up-regulation of FKBP4 gene expression was seen in Offspring of MI ($p=0.004$, $fdr_{2d}=0.35$) after platelet-mediated stimulation.

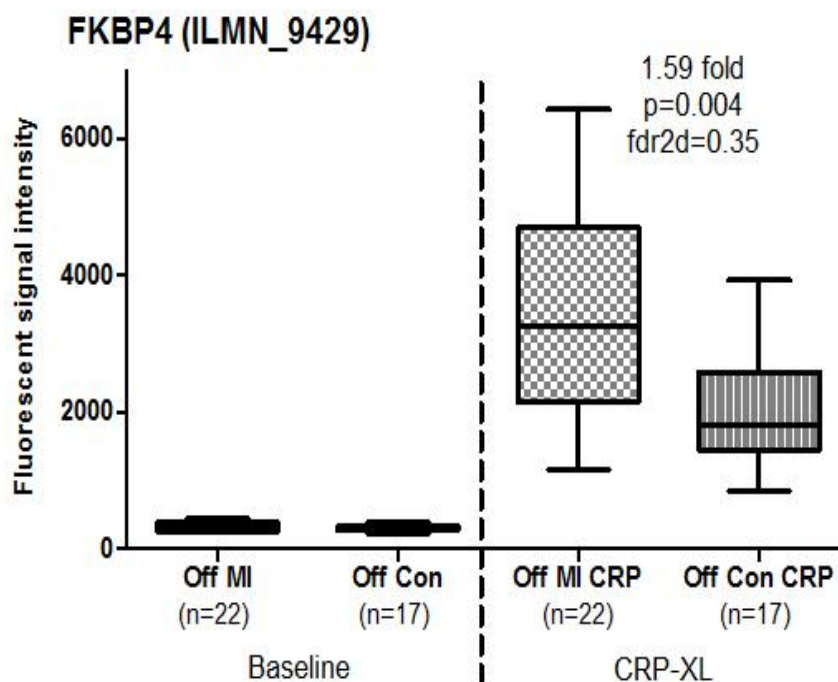


Figure 5.32: Microarray signal intensities of FKBP4 in Offspring of MI and controls.

Fluorescent signal intensities in Offspring of MI (Off MI) and controls (Off Con) before and after platelet-mediated stimulation are shown. Error bars denote the range of expression. Fold changes, p values and false discovery rates are provided.

5.8.1.1.5 DnaJ (Hsp40) homolog, subfamily A, member 4 (DNAJA4), Chr 15q25.1

This is a member of the HSP40 family and stabilizes the interaction of HSP70 with substrate proteins (Qiu et al., 2006). Of relevance to atherosclerosis is the observation that DNAJA4 is involved in cholesterol biosynthesis and increases activity of HMGCoA reductase, the rate limiting step in this pathway (Robichon et al., 2006).

DNAJA4 expression levels were comparable at baseline (Figure 5.33). Expression levels increased in both groups after CRP-XL stimulation. A 1.49 fold increased expression was seen in Offspring of MI ($p=0.02$, $fdr_{2d} >0.5$).

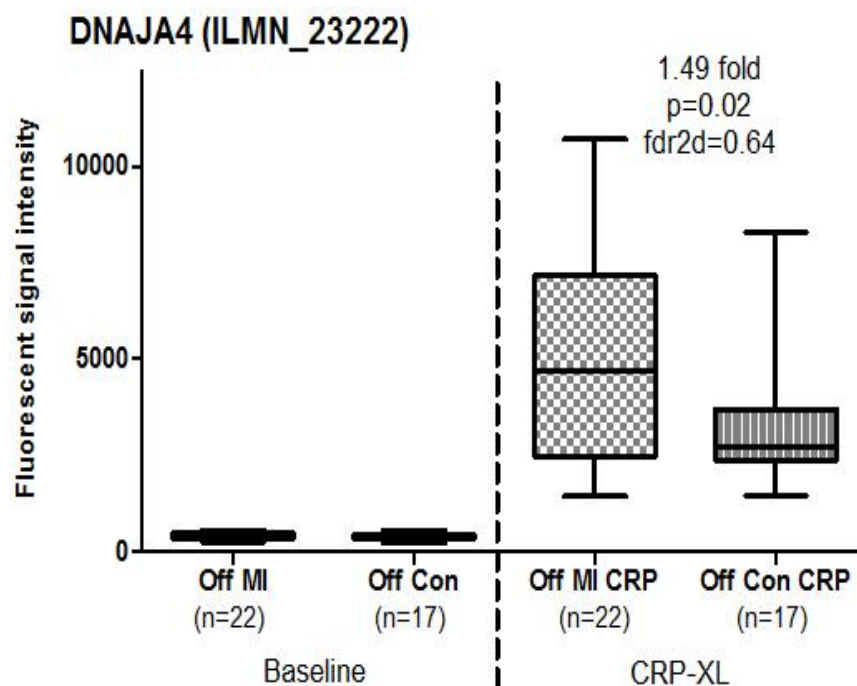


Figure 5.33: Microarray signal intensities of DNAJA4 in Offspring of MI and controls.

Fluorescent signal intensities in Offspring of MI (Off MI) and controls (Off Con) before and after platelet-mediated stimulation are shown. Error bars denote the range of expression. Fold changes, p values and false discovery rates are provided.

5.8.1.1.6 Heat shock protein B1 (HSPB1, HSP27); Chr 7q11.23

An atheroprotective role mediated by oestrogen is suggested for this protein (Rayner et al., 2009). HSPB1 is up-regulated in monocytes following hypoxic stress (Chakrabarti et al., 2009) and protects against hydrogen peroxide induced cytotoxicity by up regulating glutathione levels and preventing necrotic cell death (Salinthoné et al., 2007). Levels are increased following chronic oxidative stress and correlate with greater resistance to injury (Bailey et al., 2004). In vascular smooth muscle cells, LDL induces dephosphorylation of HSPB1 and translocation of the modified HSPB1 to the tips of actin stress fibres and focal adhesion structures on the cell surface (Garcia-Arguinzonis et al., 2010). HSPB1 gene silencing results in increased apoptotic death in vascular smooth muscle cells and its co localisation in the 'cap' region of atheromatous plaques has been proposed as a protective mechanism against plaque rupture (Martin-Ventura et al., 2006). HSPB1 surface expression in the arterial wall is inversely proportional to atherosclerotic burden (Park et al., 2006). HSPB1 surface expression is reduced in the shoulder regions of plaques which contain apoptotic cells and plasminogen, suggesting that HSPB1 is cleaved by plasmin (Figure 5.34) and released into circulation (Martin-Ventura et al., 2006). Interestingly, circulating HSPB1 levels are elevated in patients following plaque rupture events (Park et al., 2006).

As with other HSPs described above, HSPB1 was expressed at low levels in resting monocytes with no significant difference between groups. Following stimulation, levels were 1.77 fold higher in Offspring of MI (Figure 5.35) compared to controls ($p=0.03$, $fdr_{2d}>0.5$). This relative increase in the Offspring of MI may be a result of oxidative stress. As described in Chapter 3, CRP-XL stimulation results in up-regulation of genes attributable to an oxidative stress response. The higher

expression levels of HSPB1 seen in the Offspring of MI considered alongside the up-regulation of hypoxia driven transcriptions factors in resting monocytes may indicate a chronic oxidative stress in these individuals.

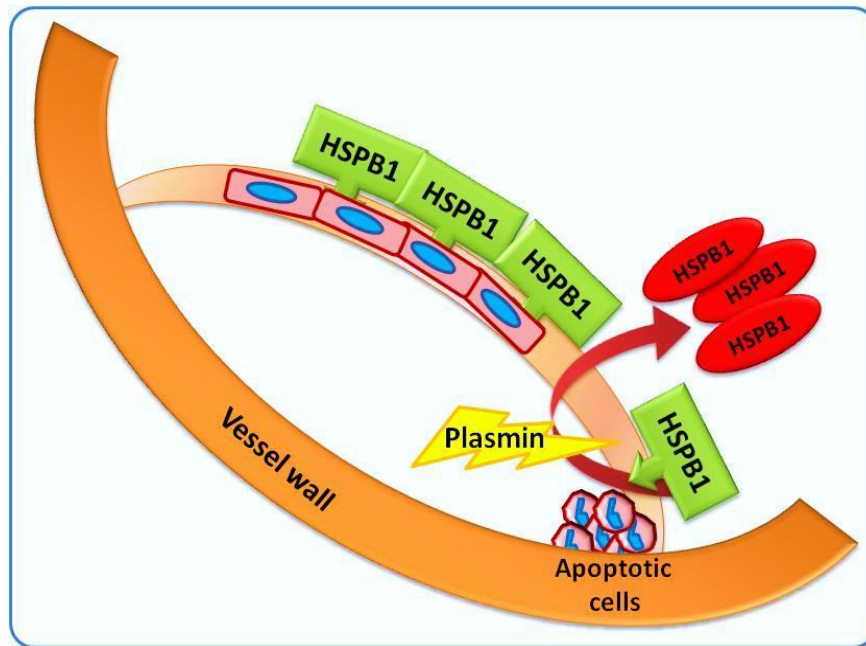


Figure 5.34: HSPB1 in the atherosclerotic plaque.

Active HSPB1 in the fibrous cap is shown in green and the inactive form in red. Plasmin which co localises with apoptotic cells in the shoulder regions of the plaque cleaves and inactivates cell surface HSPB1.

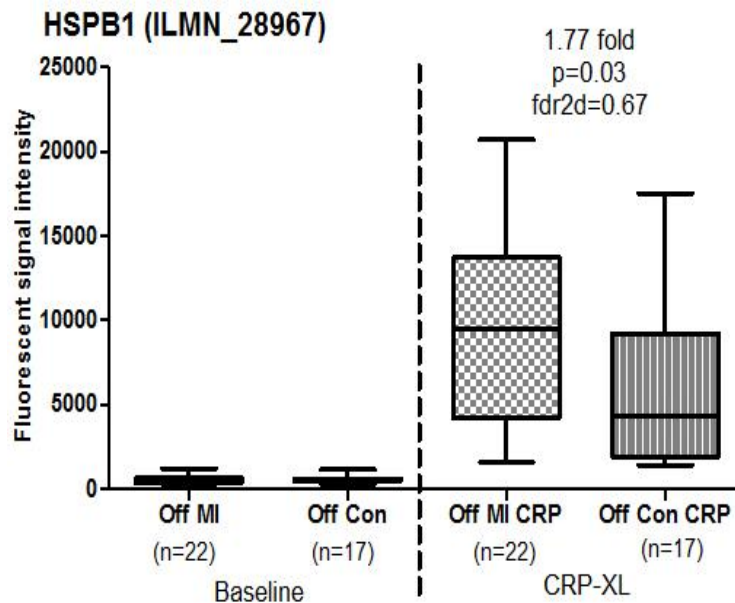


Figure 5.35: Microarray signal intensities of HSPB1 in Offspring of MI and controls.

Fluorescent signal intensities in Offspring of MI (Off MI) and controls (Off Con) before and after platelet-mediated stimulation are shown. Error bars denote the range of expression. Fold changes, p values and false discovery rates are provided.

5.8.1.2 Other candidate genes

5.8.1.2.1 Diacyl glycerol kinase delta (DGKD); Chr 2q37.1

DGKD is a member of a family of lipid kinases with the ability to regulate two lipid signalling cascades (Raben and Tu-Sekine, 2008). By transferring the gamma phosphate of ATP to diacyl glycerol (DG) to generate phosphatidic acid it acts as a switch between these second messengers. It also cycles between the cytoplasm and nucleus in response to agonists to bring about this second messenger regulation (Martelli et al., 2002). This has important implications for vascular function as DG is a second messenger for angiotensin-II, endothelin-1 and norepinephrine (Choi et al., 2009).

DGKD is expressed in low levels in resting monocytes (signal intensity <1000) but increase following platelet-mediated stimulation (Figure 5.36). A 1.28 fold increased expression was seen in Offspring of MI ($p=0.00005$, $fdr_{2D}=0.000008$). This was validated by PCR with 18S as control gene (Figure 5.37).

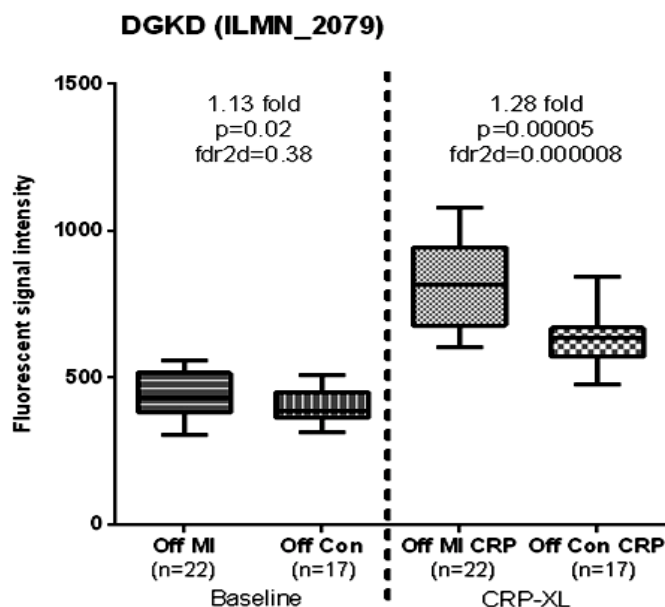


Figure 5.36: Microarray signal intensities of DGKD in Offspring of MI and controls.

Fluorescent signal intensities in Offspring of MI (Off MI) and controls (Off Con) before and after platelet-mediated stimulation are shown. Error bars denote the range of expression. Fold changes, p values and false discovery rates are provided.

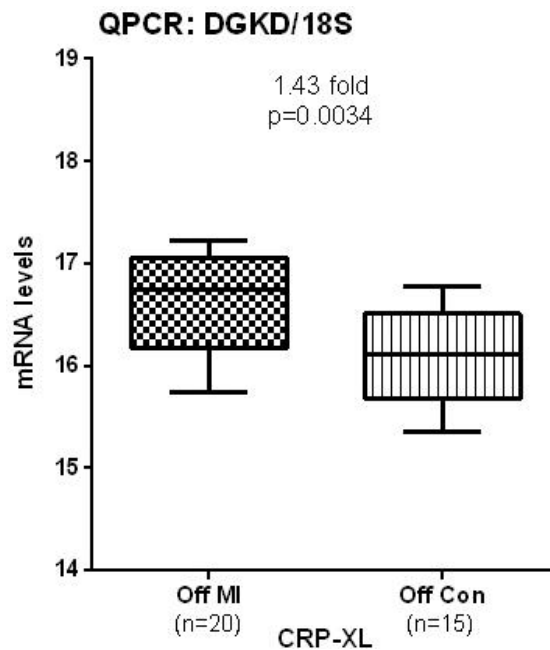


Figure 5.37: quantitative PCR of DGKD in Offspring of MI and controls.

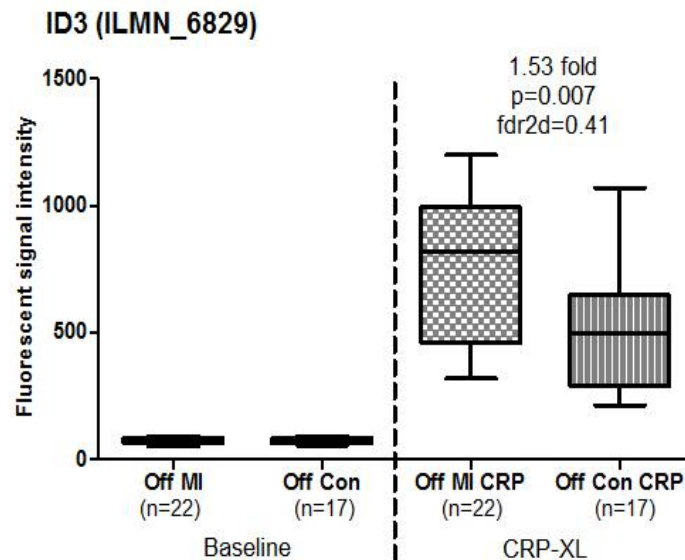
Q-PCR of DGKD with 18S as control gene is shown. Error bars denote the range of expression. Fold change and p value are shown.

5.8.1.2.2 Inhibitor of DNA binding 3 (ID3/HEIR-1); Chr 1p36.13-p36.12

ID3 is a helix-loop-helix protein which is expressed in atherosclerotic plaques (Matsumura et al., 2001). Angiotensin II mediates its proliferative effect on vascular smooth muscle cells through activation of ID3 (Mueller et al., 2002). This is a redox state sensitive transcription factor which is up-regulated in vascular smooth muscle cells following exposure to oxidized LDL (Taylor et al., 2006). It is also induced via superoxide by xanthine/xanthine oxidase in vascular smooth muscle cells and promotes cell proliferation (Nickenig et al., 2002). ID3 levels are increased in fibroblasts (Swiss 3T3 cell lines) in response to cigarette smoke exposure (Bosio et al., 2002).

ID3 was expressed at low levels in unstimulated monocytes (Figure 5.38). Following CRP-XL stimulation, levels increased significantly in both groups, with a 1.53 fold higher expression in Offspring of MI ($p=0.007$, $fdr_{2d}=0.41$). This is unlikely

to be an effect of cigarette smoke as the groups were matched for smoking status. It suggests that the Offspring of MI respond differently to oxidative stress, as also evidenced by the changes in other genes described above.



5.38: Microarray signal intensities of ID3 in Offspring of MI and controls.

Fluorescent signal intensities in Offspring of MI (Off MI) and controls (Off Con) before and after platelet-mediated stimulation are shown. Error bars denote the range of expression. Fold changes, p values and false discovery rates are provided.

5.8.1.2.3 Transporter 2, ATP-binding cassette, sub-family B (TAP2); Chr 6p21.3

TAP2 is a member of the MDR/TAP sub family of ATP-binding cassette transporter proteins. This molecule has a role in antigen presenting in monocyte derived dendritic cells (Tosello et al., 2009). Deficiency of TAP2 in patients with granulomatous diseases affecting the respiratory tract is associated with increased expression of CCR2 (monocyte chemoattractant protein-1 receptor) which mediates monocyte chemotaxis (Hanna et al., 2005). Increased CCR2 expression in TAP2 deficiency has been proposed as the mechanism for retention of natural killer cells in areas of chronic inflammation (Hanna et al., 2005).

At baseline, TAP2 expression levels were numerically lower in Offspring of MI although not statistically significant (Figure 5.39). Following CRP-XL stimulation,

no significant change was observed in control subjects. However, expression levels decreased in Offspring of MI to 0.75 fold when compared to controls ($p=0.006$, $fdr_{2d}=0.42$). This suggests that following oxidative stress injury, these individuals are more likely to have monocyte chemotaxis into sites of chronic inflammation (i.e., atherosclerotic lesions) and may explain how the increased familial risk of CAD is mediated through the circulating monocyte.

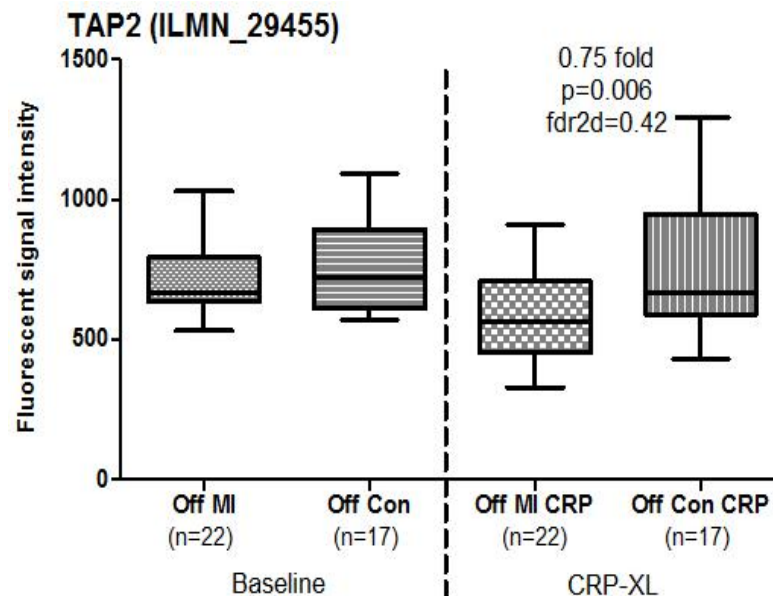


Figure 5.39: Microarray signal intensities of TAP2 in Offspring of MI and controls.

Fluorescent signal intensities in Offspring of MI (Off MI) and controls (Off Con) before and after platelet-mediated stimulation are shown. Error bars denote the range of expression. Fold changes, p values and false discovery rates are provided.

5.8.1.2.4 Latexin (LXN), Chr 3q25.32

LXN encodes the only known protein inhibitor of zinc-dependent metalloproteinase (MCP) A (Liang and Van Zant, 2008). MCPs are ubiquitous enzymes with proteolytic activity (Gomis-Ruth, 2003). LXN regulates haemopoietic stem cells (Liang et al., 2007) and has a tumour suppressor role in gastric cancer (Li et al.). It influences ageing of haemopoietic cells by reducing proliferation and increasing apoptosis (Liang and Van Zant, 2008). Latexin also prevents transformation to malignant stem cells (Liang and Van Zant, 2008).

Latexin is essential for tissue repair and healing and regulates the expression of types II and X collagen (Kadouchi et al., 2009). It is up-regulated alongside HSP27 (HSPB1) as a protective response to intracellular accumulation of abnormal toxic proteins (Yata et al.) and has a role in cell survival.

LXN expression at baseline was lower in Offspring of MI but not statistically significant (Figure 5.40). Following CRP-XL stimulation, there was no significant change in expression in control subjects. However, levels were 0.74 fold lower in Offspring of MI compared to controls ($p=0.004$, $fdr_{2d}=0.42$). The down regulation of latexin in the Offspring of MI following an oxidative stress stimulus suggests abnormalities in cell survival and homeostasis. Given its regulatory roles in cell proliferation and the protective response to accumulation of intracellular toxins, the significant reduction in LXN in the Offspring of MI suggests an impairment of tissue repair and apoptosis. Interestingly, a similar trend in LXN expression was seen in the premature MI group (0.75 fold, $p=0.02$) which will be discussed in Chapter 6.

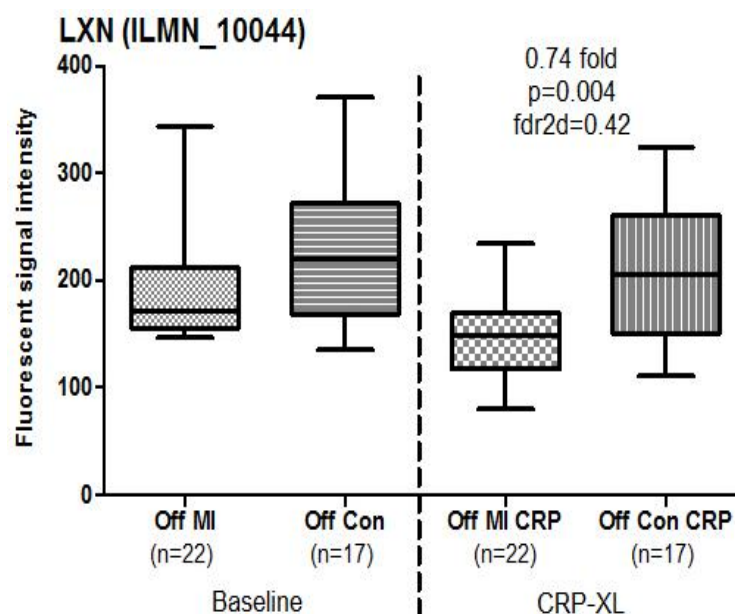


Figure 5.40: Microarray signal intensities of LXN in Offspring of MI and controls.

Fluorescent signal intensities in Offspring of MI (Off MI) and controls (Off Con) before and after platelet-mediated stimulation are shown. Error bars denote the range of expression. Fold changes, p values and false discovery rates are provided.

5.8.2 Pathways

5.8.2.1 Nrf2 mediated oxidative stress response

Nuclear factor-erythroid 2-related factor 2 (Nrf2) is a regulator of cellular response to oxidative stress. As part of this response, it activates heat shock proteins which aid protein folding and repair. Three members of the HSP family, STIP1, DNAJB6 and HSP90AB1 are involved in Nrf2 mediated oxidative stress response.

Oxidative stress plays an important role in atherogenesis and progression of atherosclerotic lesions. Nrf2 activation and translocation from cytoplasm to nucleus follows stimulation of murine macrophages with oxidised LDL (Ishii et al., 2004). In its dormant state, Nrf2 remains bound to its inhibitor I κ Nrf2 in the cytoplasm. HSP90 releases Nrf2 from its inhibitor and allows nuclear translocation of Nrf2 in response to cellular stress (Niture and Jaiswal, 2010). HSP90AB1 (up-regulated in Offspring of MI following platelet-mediated stimulation) has been noted to heterodimerise with Nrf2 and form part of the anti oxidant/electrophile response element (ARE/EpRE) (Miller and Ramos, 2005).

ARE/EpRE regulates c-Ha-ras which is a key target in oxidative stress response in vascular smooth muscle cells (Ramos, 1999). There is also evidence that Nrf2 mediates its oxidative stress response by modulating the expression of STIP1 (Yamada et al., 2011), which was significantly up-regulated in Offspring of MI following platelet-mediated stimulation. FKBP4 which is a co chaperone that binds HSP70, STIP1 and HSP90 to form tetramers was also up-regulated in the Offspring of MI following stimulation. In addition, another HSP molecule, DNAJB1 (HSP40), which was significantly up-regulated in patients with MI (Group 1) but not in Offspring of MI (Group 2), is also implicated in this pathway (Jacobs and

Marnett, 2007). The cholesterol hydroxylase enzyme CYP27A1 which is differentially expressed in both Offspring of MI and patients Post MI is dependent on HSP70 for mitochondrial translocation (Anandatheerthavarada et al., 2009). The up-regulation of HSP family members in this pathway maybe a response to increased oxidative stress in such individuals.

5.8.2.2 Wnt/beta catenin signalling

As previously noted in the transcriptome analysis of activated monocytes in the Post MI group (Chapter 4), transcripts with a role in this signalling pathway were differentially expressed in the Offspring of MI group after platelet-mediated stimulation. Oxidative stress has been shown to activate Wnt/beta catenin signalling along with Nrf2 signalling (Reuter et al., 2010). DNAJB6 regulates Wnt/beta catenin signalling in epithelial cells by activating DKK1 (dickkopf 1 homolog) which degrades beta catenin (Mitra et al., 2010). HSPB1 interacts directly with beta catenin and has a role in cell survival (Fanelli et al., 2008).

Figure 5.41 summarises the interactions of the various heat shock proteins, related co chaperones and signalling pathways discussed in this Chapter. Microarray data from resting and stimulated samples for all four groups (Post MI, Offspring of MI and the two control groups) were analysed to explore the trends in expression of HSPs and related molecules shown here. No significant differences were noted in the expression of HSP70 and HSPAA1. Four of the other molecules (HSP90AB1, STIP1, DNAJB6 and FKBP4) were up-regulated in Offspring of MI (Group 2) after platelet-mediated stimulation. DNAJB1 was up-regulated in the Post MI group (Group 1) after stimulation. The dotted lines in the Figure demarcate the molecules which have known physical interactions.

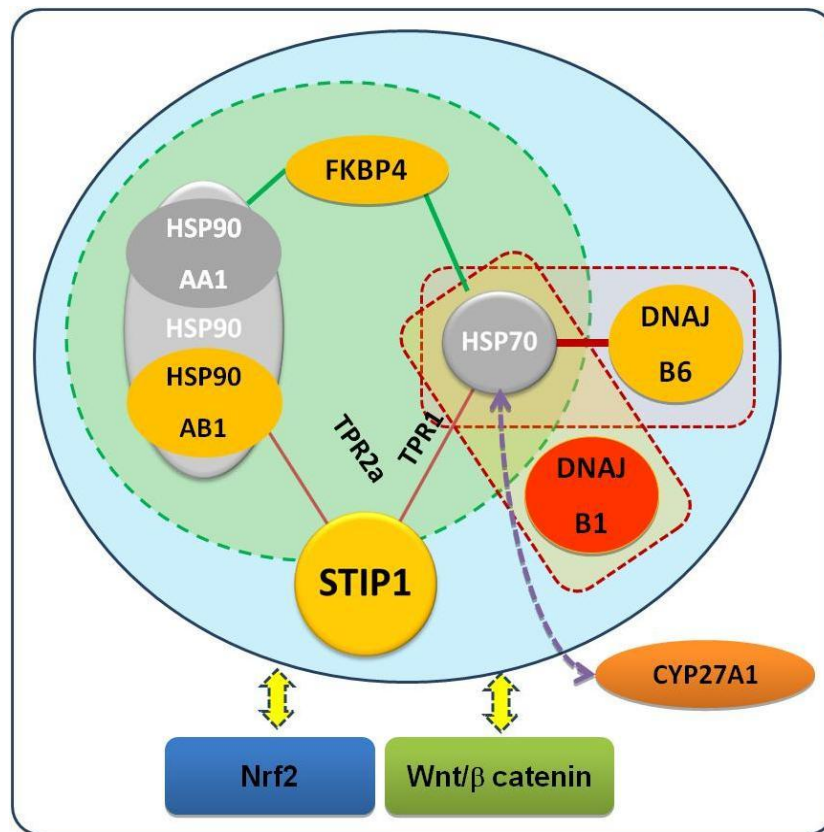


Figure 5.41: Heat shock proteins and their interactions.

The genes in yellow were differentially expressed in the Offspring of MI while the one in red was differentially expressed in patients with premature MI. There were no significant differences in HSP70 or HSP90A1 (in grey). The interaction between HSP70 and CYP27A1 is shown. Many of the HSPs are involved in Nrf2 and Wnt signalling.

5.9 DISCUSSION

This Chapter describes the differences in gene expression in monocytes in two groups of healthy young men, matched for age and smoking status with contrasting family history of premature CAD. All ‘cases’ (Group 2) had at least one parent with a premature MI (<55 years) and 50% had a grandparent with premature MI (<65 years). The controls (Group 4) were selected on the basis of not having a family history of premature coronary or cerebrovascular disease in their parents or grandparents.

Whole genome expression analysis of unstimulated (resting) monocytes from these two groups with a contrasting familial risk of CAD revealed differential expression of transcription factors which regulate the response to hypoxia, chemokines and cholesterol transport mediators. An important finding of relevance to atherosclerosis was the highly statistically significant up-regulation of the enzyme acyloxyacyl hydrolase (AOAH) in resting monocytes of subjects with an increased genetic risk of myocardial infarction (Offspring of MI, Group 2). Genetic variants in this gene have been recently linked with increased carotid intima media thickness and also regulate IgE levels which has been implicated in atherosclerosis and seen to co-localise with monocyte derived macrophages in vascular lesions. Further studies are needed to explore the role of this gene in atherogenesis.

Following platelet-mediated stimulation, more genes were differentially expressed in monocytes in the Offspring of MI (Group 2). The most significant observation is the increased levels of expression of various molecules belonging to the heat shock protein family of chaperone proteins. These are required for protein folding as part of synthesis or degradation. They also form part of an oxidative stress response. The highly statistically significant increase in levels of stress induced phosphoprotein-1 (STIP1) which is a co-chaperone molecule in the Nrf-2 regulated oxidative stress response suggests that these apparently healthy individuals have a higher genetic tendency to mount an oxidative stress response in response to an appropriate stimulus (platelet-mediated stimulation).

The other differentially expressed gene was the enzyme diacyl glycerol kinase delta (DGKD) which has a role in promoting vasoconstriction in response to

endothelin, angiotensin and other mediators. The increased levels seen in monocytes in Group 2 may be a surrogate reporter of vascular dysfunction (i.e., for gene expression in vascular smooth muscle cells) seen in such individuals with a genetic preponderance to MI.

In addition, the down regulation of TAP2 and latexin are indicative of abnormalities of tissue repair and apoptosis in these apparently healthy individuals. It is also interesting to note that these changes were not apparent at baseline, indicating that an appropriate stimulus of relevance to atherosclerosis helps to reveal such transcriptional alterations.

In summary, this Chapter therefore serves to substantiate the hypothesis that gene expression analysis of peripheral blood monocytes under basal and stimulated conditions in individuals with contrasting familial risk for coronary heart disease will identify differentially expressed genes, which underlie the genetic aetiology of coronary artery disease.

The next Chapter summarises the findings of the previous two Chapters (4, 5) and focuses on those genes with trends in expression shared between patient Post MI (Group 1) and Offspring of MI (Group 3).

CHAPTER 6: RESULTS

Genes shared between Post MI and Offspring of MI

6.1 INTRODUCTION

To understand heritable trends in monocyte gene expression of relevance to atherosclerosis, further analysis was performed with the most differentially expressed genes in each comparison experiment. These were investigated further to assess their expression profiles in the other experiments (Figure 6.1).

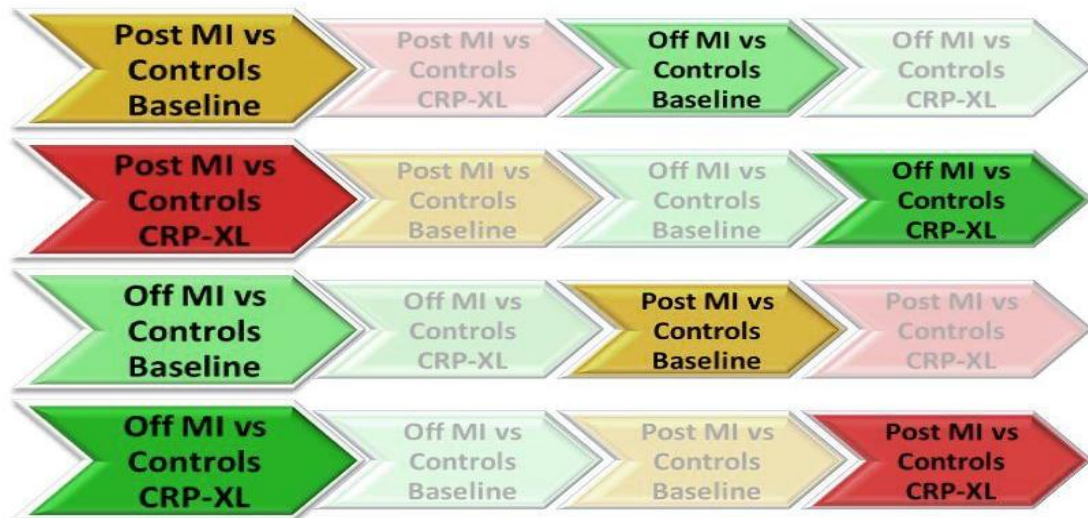


Figure 6.1: Trends in differential gene expression across experiments.

Differentially expressed genes in each comparison experiment were investigated in other comparisons to identify similar trends in expression and statistical significance. Each comparison is shown in a different colour panel.

To identify heritable trends in monocyte gene expression, further analysis was performed focused on the genes that had a similar direction and magnitude of differential gene expression across groups. The genes that emerged with similar trends in gene expression in Post MI (Group 1) and Offspring of MI (Group 2) compared to respective control groups (Group 3&4) both at baseline and after platelet-mediated stimulation are described in this Chapter. It is important to emphasise that apart from one individual, none of the twenty two subjects in the Offspring of MI group was related to a subject in the Post MI group. None of the Control offspring were related to the healthy controls recruited for the Post MI

group. Therefore the observed similarities are not explained by familial trends in gene expression.

Differentially expressed genes with similar trends in microarray fluorescent signal intensities in Post MI and Offspring of MI are listed in Tables 6.1 and 6.2 below.

Gene	Array ID	Post MI (Group 1)	Off MI (Group 2)	Function
		Fold change (p)	Fold change (p)	
IER2	12423	1.26 (0.01)	1.19 (0.11)	Transcription factor
Gene	Array ID	Off MI (Group 2)	Post MI (Group 1)	Function
		Fold change (p)	Fold change (p)	
EGR1	20932	1.81 (0.004)	1.37 (0.23)	Transcription factor
BTG2	9681	1.45 (0.02)	1.27 (0.14)	Cellular senescence
FOSB	13603	1.86 (0.008)	1.27 (0.28)	Transcription factor
CCL3L3	22857	1.52 (0.006)	1.26 (0.2)	Chemokine
CCL3	1999	1.42 (0.005)	1.18 (0.32)	Chemokine
CCL3L1	6158	1.28 (0.004)	1.12 (0.27)	Chemokine
ACTA2	6588	0.75 (0.02)	0.84 (0.2)	Cell motility

Table 6.1: Genes with shared trends in unstimulated monocytes (baseline).

Genes at baseline (higher levels when compared to controls – yellow, lower levels – blue) in patients Post MI which follow a similar trend in the Offspring of MI and vice versa are shown. Fold changes, p values and a brief description of the molecular function are also provided.

Gene	Array ID	Post MI CRP	Off MI CRP	Function
		Fold change (p)	Fold change (p)	
LEP	10827	3.36 (0.005)	1.68 (0.27)	Adipocyte metabolism
FAM13A1	10067	2.55 (0.002)	1.59 (0.14)	Response to hypoxia
DNAJB1	19740	1.85 (0.006)	1.5 (0.07)	Heat shock response
HIG2	8723	2.68 (0.007)	1.3 (0.5)	Response to hypoxia
HIP1	21141	1.55 (0.0005)	1.25 (0.11)	Ageing
CYP27A1	2033	1.66 (0.00008)	1.21 (0.17)	Cholesterol efflux
Wnt5A	14624	0.56 (0.001)	0.9 (0.46)	Wnt signalling
CCL7	24123	0.47 (0.0004)	0.73 (0.3)	Monocyte chemotaxis
Gene	Array ID	Off MI CRP	Post MI CRP	Function
		Fold change (p)	Fold change (p)	
FKBP4	9429	1.6 (0.004)	1.3 (0.15)	Heat shock response
SLC5A3	11699	1.58 (0.009)	1.31 (0.09)	Solute transport
WBP5	3262	1.75 (0.002)	1.2 (0.2)	Protein interaction
STIP1	28761	1.58 (0.003)	1.19 (0.2)	Heat shock response
DNAJB6	7651	1.42 (0.003)	1.15 (0.23)	Heat shock response
HSP90AB1	16000	1.54 (0.006)	1.14 (0.35)	Heat shock response
DLG4	16430	1.55 (0.0002)	1.13 (0.44)	Intracellular trafficking
CCBP2	11666	0.78 (0.0007)	0.88 (0.07)	Chemokine regulation
ACAD10	27988	0.79 (0.001)	0.86 (0.05)	Fatty acid oxidation
PCK2	2603	0.78 (0.02)	0.83 (0.14)	Mitochondrial kinase
ARV1	5909	0.77 (0.0003)	0.82 (0.08)	Sterol transport
LXN	10044	0.74 (0.004)	0.75 (0.024)	Tumour suppressor
KIR2DL4	16588	0.79 (0.03)	0.72 (0.03)	Cell surface receptor

Table 6.2: Genes with shared trends after platelet-mediated monocyte stimulation (CRP-XL).

Differentially expressed genes after platelet-mediated stimulation (higher levels when compared to controls – yellow, lower levels – blue) in patients Post MI which follow a similar trend in the Offspring of MI and vice versa are shown. The genes in the orange rows had the greatest statistical significance for the similar trends in expression in groups 1 and 2 (Post MI and Offspring of MI). Fold changes, p values and a brief description of the molecular function are also provided.

6.2 ANALYSIS OF SHARED GENES

Genes with a fold change >1.2 or <0.8 fold and $p < 0.05$ in either Post MI or Offspring of MI with similar trends in the other group were selected (Figure 6.2). These thresholds were chosen to include genes with a significant differential expression in one group and a similar trend in the other, which are most likely to have genetic trends in expression.

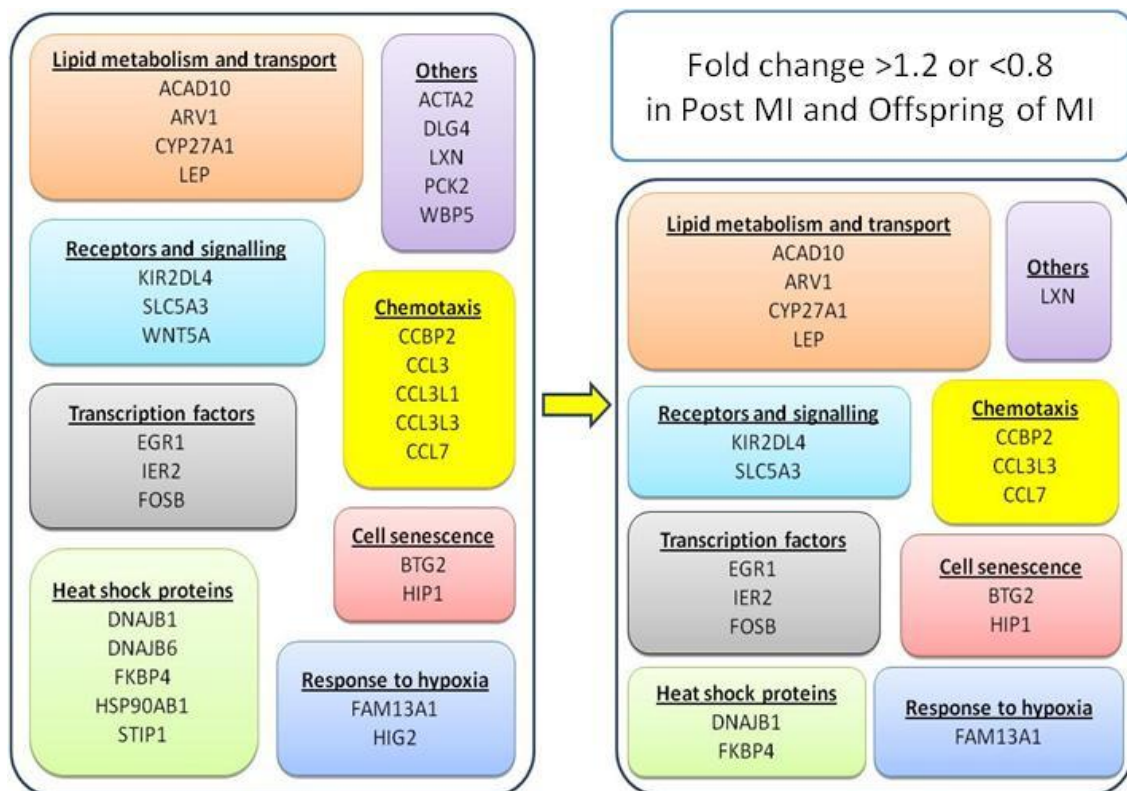


Figure 6.2: Classification of shared genes according to biological function.

29 genes with shared expression profiles were screened to identify those with the greatest fold change and statistical significance. 18 genes in the enriched gene list are shown on the right panel.

The 18 genes which passed the above screening threshold were analysed for established links with atherosclerosis using ChiLiBot. PubMed abstracts were analysed for associations with relevant key words as described in previous Chapters. The results of this analysis were filtered further to identify the strongest interactive relationships in published literature (Figure 6.3).

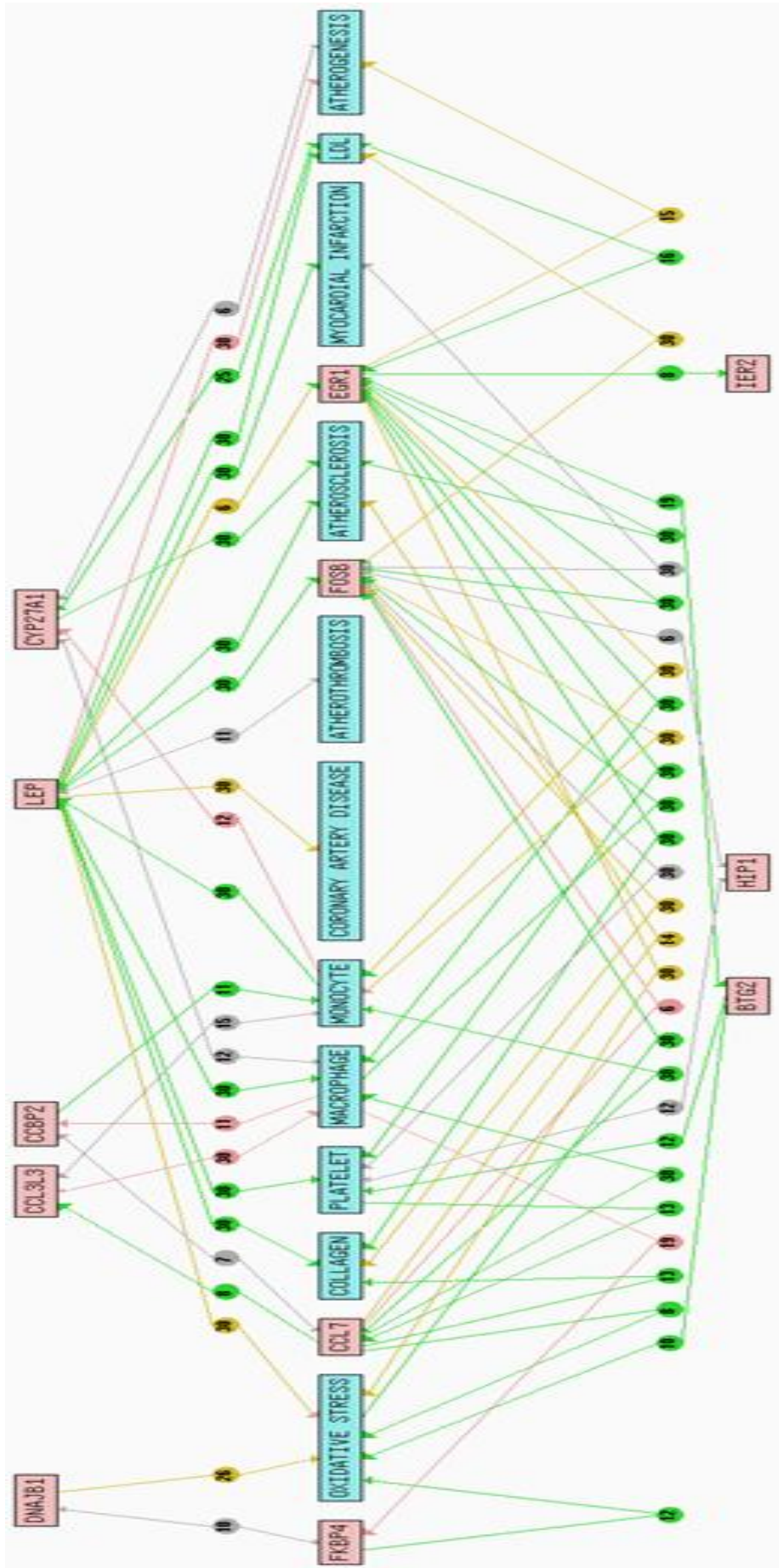


Figure 6.3: Interaction map (ChLiBot) of shared candidate gene to predefined search terms.

The arrows in green denote a positive association between terms (up-regulation, activation, enhancement etc), red arrows denote a negative association (inhibition, down regulation, suppression etc) while the grey arrows denote associations with no such directionality. The numbers within the circles denote the number of interactive sentences in published literature.

The genes are arranged in Table 6.3 in the order of established links to the keywords in published literature. This approach was used to select those genes with both statistical and biological significance from the analyses performed in previous Chapters. The number of links with the selected keywords in this analysis helped to provide an overview of the relative contribution of differentially expressed genes to atherosclerosis.

Gene	Chr locus	Post MI	Offspring of MI	Condition	Links
FOSB	19q13.12	1.27 (0.28)	1.86 (0.008)	Baseline	23
EGR1	5q31.1	1.37 (0.23)	1.81 (0.004)	Baseline	20
CCL7	17q11.2-q12	0.47 (0.0004)	0.73 (0.3)	CRP-XL	17
LEP	7q31.3	3.36 (0.005)	1.68 (0.27)	CRP-XL	16
BTG2	1q32	1.27 (0.14)	1.45 (0.02)	Baseline	12
DNAJB1	19p13.2	1.85 (0.006)	1.5 (0.07)	CRP-XL	11
CYP27A1	2q33-qter	1.66 (0.00008)	1.21 (0.17)	CRP-XL	10
FKBP4	12p13.33	1.3 (0.15)	1.6 (0.004)	CRP-XL	9
CCL3L3	17q21.1	1.26 (0.2)	1.52 (0.006)	Baseline	8
HIP1	7q11.23	1.55 (0.0005)	1.25 (0.11)	CRP-XL	6
CCBP2	3p21.3	0.88 (0.07)	0.78 (0.0007)	CRP-XL	6
KIR2DL4	19q13.4	0.72 (0.03)	0.79 (0.03)	CRP-XL	5
SLC5A3	21q22.12	1.31 (0.09)	1.58 (0.009)	CRP-XL	5
IER2	19p13.2	1.26 (0.01)	1.19 (0.11)	Baseline	3
LXN	3q25.32	0.74 (0.004)	0.75 (0.024)	CRP-XL	2

Table 6.3: Genes shared by Post MI and Offspring of MI groups linked to CAD.

Up-regulated genes are shown in yellow and down regulated genes in blue. Genes are arranged in descending order of known links in literature with the keywords relevant to CAD.

6.2.1 Transcription factors

6.2.1.1 FOSB (AP-1); Chr 19q13.32

FOSB forms a part of the activating protein-1 (AP-1) complex expressed in response to oscillatory shear stress in endothelial cells and facilitates monocyte binding by increasing expression of CCL2 (Zhou et al., 2011). It is induced in response to oxidised LDL and regulates the production of transforming growth factor beta (TGF β) (Zhou et al., 2002). The AP-1 complex is essential for hypoxia mediated gene expression in human monocyte derived macrophages (Bosco et al., 2008). Hydrogen peroxide induced oxidative injury increases expression of FOSB and EGR1 (Fratelli et al., 2005) suggesting that a primary increase in oxidative stress may explain the observed up-regulation of these transcription factors in both Offspring of MI and patients Post MI.

In resting monocytes, FOSB was expressed at low levels in the offspring groups and at moderate levels in the Post MI and control groups (Figure 6.4). Levels were significantly higher in Offspring of MI compared to controls ($p=0.008$) while a similar non significant trend was seen in the Post MI group ($p=0.28$). Platelet-mediated stimulation resulted in an increase in FOSB levels in all four groups. Although levels were numerically higher in the Offspring of MI and Post MI groups compared to controls, neither was statistically significant after stimulation. Given that oxidative stress increases FOSB expression, the increase in levels following stimulation in all groups suggests that collagen activated platelet stimulation of monocytes results in an oxidative stress response, as described previously in Chapter 3.

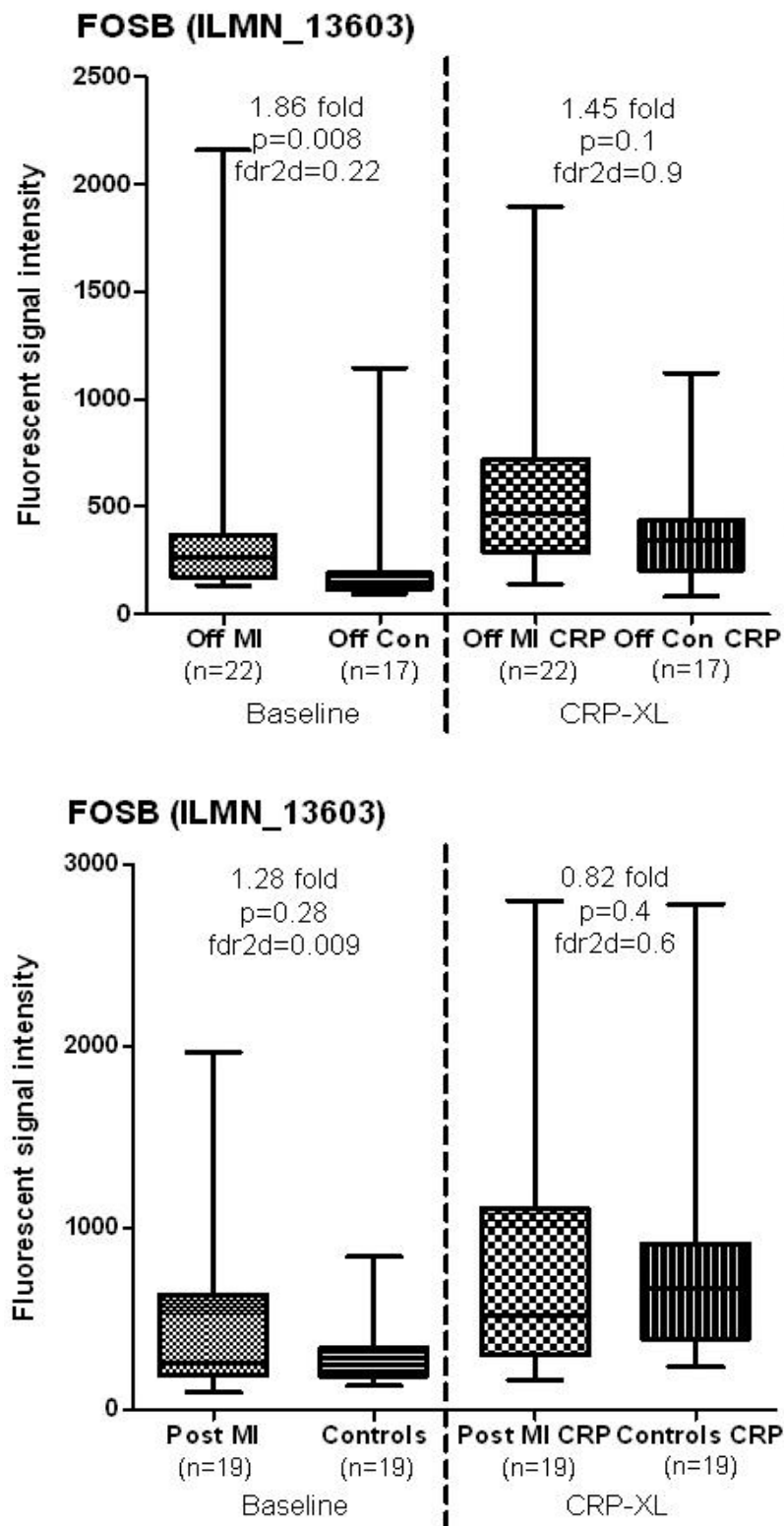


Figure 6.4: Differential expression of FOSB in Offspring of MI and patients Post MI.

Fluorescent signal intensities in Offspring of MI and controls following platelet-mediated stimulation are shown in the top panel. Corresponding signal intensities in the Post MI and controls are shown on the bottom panel. Error bars denote the range of expression. Fold changes, p values and false discovery rates are provided where applicable.

6.2.1.2 EGR1; Chr 5q31.1

EGR1 is a zinc finger transcription factor that plays a deterministic role in committing haemopoietic stem cells to the monocyte-macrophage lineage (Krishnaraju et al., 1995). EGR1 up-regulates LDL receptor expression by binding to its promoter region in response to the chemokine Oncostatin M (Zhang et al., 2002) and promotes atherosclerosis by inducing foam cell formation in bone marrow derived macrophages (Kim et al., 2009). In response to shear stress in aortic endothelial cells, EGR1 promotes platelet derived growth factor expression, suggesting a role in atherogenesis (Khachigian et al., 1997). EGR-1 regulates the expression of TGF β and plasminogen activator inhibitor-1 (PAI-1) suggesting a potential prothrombotic role (Liu et al., 1996). Both EGR1 and FOSB bind to the promoter region of tissue factor (Terasaka et al., 2005).

EGR1 is expressed at moderate levels in unstimulated monocytes in all four groups (Figure 6.5). In the Offspring of MI group, there was a significant 1.81 fold increased expression compared to levels in the Control offspring group ($p=0.004$). There was a numerically higher expression level in the Post MI group although this was not statistically significant ($p=0.23$), possibly due to an outlier value in the control group (see Figure 6.5 bottom panel – controls at baseline). Following platelet-mediated stimulation, although the levels were numerically higher in the Offspring of MI and Post MI groups, neither reached statistical significance.

EGR1 expression is stimulated by oxidative stress (Wang et al., 2006) and therefore the lack of difference in expression levels in the 'at risk' groups after platelet-mediated stimulation is surprising. Previous studies in mononuclear cells have shown that EGR1 levels increase as early as 20 minutes after stimulation

(Segel et al., 2003). The lack of difference may therefore be due to the single time point of sampling after stimulation at four hours. The lack of difference in levels between the Post MI and control groups may be a result of statin therapy which down regulates expression of EGR1 (Lamon et al., 2009, Zhang et al., 2007).

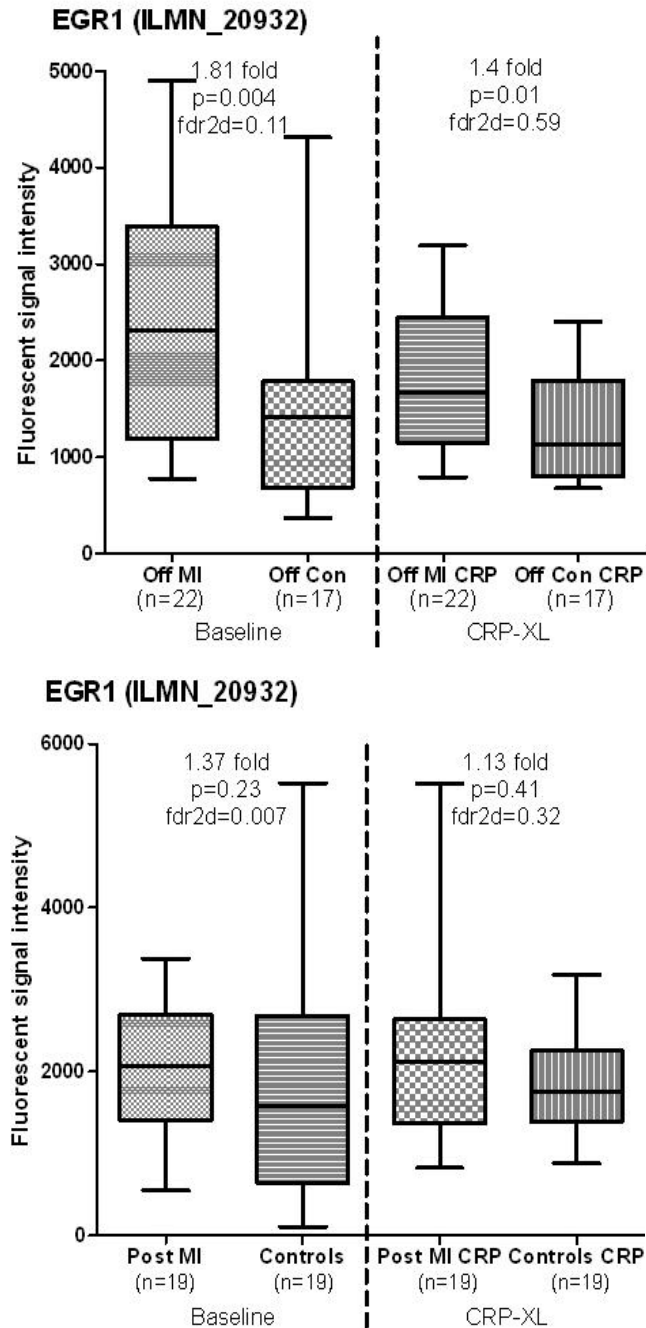


Figure 6.5: Differential expression of EGR1 in Offspring of MI and patients Post MI.

Fluorescent signal intensities in Offspring of MI and controls following platelet-mediated stimulation are shown on the left panel. Corresponding signal intensities in the Post MI and controls are shown on the right panel. Error bars denote the range of expression. Fold changes, p values and false discovery rates are provided where applicable.

6.2.1.3 Immediate early response 2 (IER2);Chr 19p13.2

IER2 is a transcription factor that is transiently up-regulated during macrophage differentiation (Shimizu et al., 1991). Although not directly linked to atherosclerosis, this gene regulates the expression of inositol-3-phosphate synthase 1 (ISYNA1), a cell signalling molecule (Takaya et al., 2009). Interestingly, ISYNA1 interacts closely with solute carrier family 5 member 3 (SLC5A3; differentially expressed in the Offspring of MI), which plays a role in the cellular response to hypertonic stress (Kwon et al., 1992). IER2 also promotes cell motility and tumour invasion (Neeb et al., 2011)

IER2 was expressed at low levels in resting monocytes in all four study groups (Figure 6.6). Levels at baseline were 26% higher in Offspring of MI compared to controls ($p=0.01$, $fdr_{2d}=0.01$). Although levels were numerically higher in the Post MI group, this was not statistically significant ($p=0.11$). Following stimulation with activated platelets, levels rose in all groups but there were no statistically significant differences between groups. Although not previously described, this may be an indicator of oxidative stress given that expression levels were consistently up-regulated in all groups following stimulation. As discussed regarding EGR1 above, the lack of difference after stimulation may be due to the timing of repeat sampling.

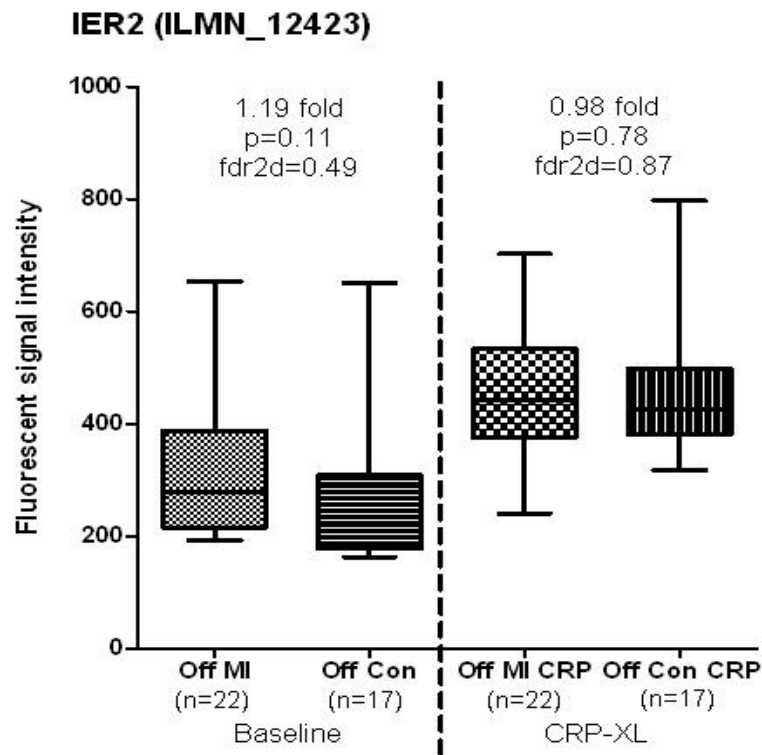
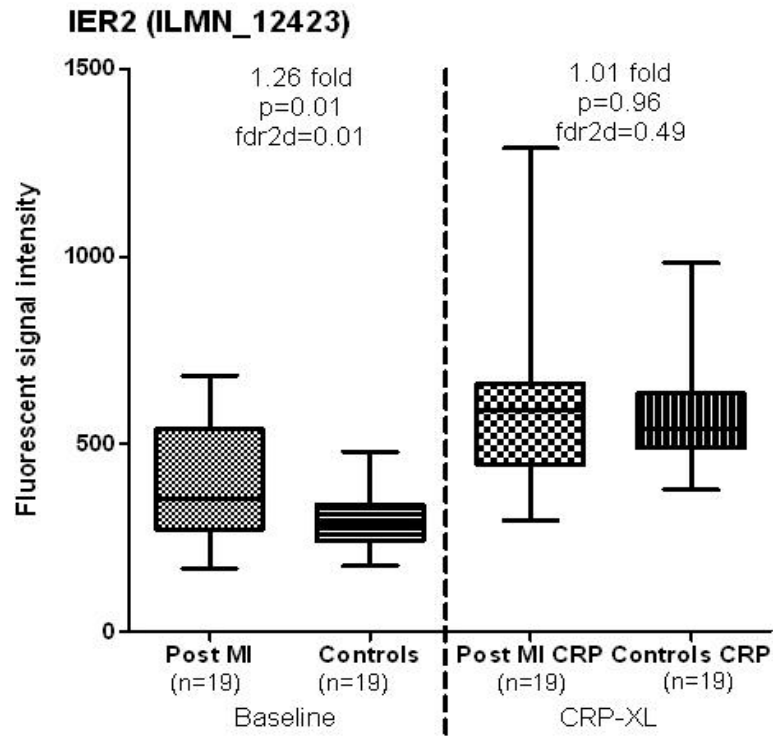


Figure 6.6: Differential expression of IER2 in patients Post MI and Offspring of MI.

Fluorescent signal intensities in patients Post MI and controls following platelet-mediated stimulation are shown on the left panel. Corresponding signal intensities in Offspring of MI and controls are shown on the right panel. Error bars denote the range of expression. Fold changes, p values and false discovery rates are provided where applicable.

6.2.2 Lipid metabolism and transport

6.2.2.1 Cytochrome P450, family 27, subfamily A, polypeptide 1 (CYP27A1); Chr2q33-qter

CYP27A1 is a mediator of cellular cholesterol efflux and is up-regulated following differentiation of monocytes to macrophages, suggesting an antiatherogenic role (Hansson et al., 2003). In addition, increased expression and function of CYP27A1 prevents foam cell formation (Bingham et al., 2012). An interesting recent development is the observation that 27 hydroxycholesterol, the product of cholesterol hydroxylation by CYP27A1 in peripheral tissues, is a selective oestrogen receptor modulator (SERM) and adversely affects oestrogen mediated cardiovascular protection and bone mineralization (Umetani and Shaul, 2011).

CYP27A1 is expressed at moderate levels in all groups at baseline (Figure 6.7). Levels were significantly higher in Offspring of MI compared to controls ($p=0.005$). However, at baseline, the levels were numerically lower in the Post MI group compared to healthy controls. Following platelet-mediated stimulation, levels were significantly lower in all groups suggesting that this is an atherogenic stimulus. However, the extent of the suppression was less in the Post MI and Offspring of MI groups resulting in a statistically significant relative increase in levels in the Post MI group and a numerically higher level in the Offspring of MI group. Hepatic CYP27A1 activity is induced by dietary cholesterol (Kushwaha and McGill, 1998). Offspring of MI had numerically higher but statistically non significant total cholesterol and LDL cholesterol levels which may explain the over expression seen at baseline and also account for the lower expression levels of this gene in patients Post MI compared to controls at baseline ($p=ns$) as the patients had lower

cholesterol levels due to pharmacotherapy and lifestyle modifications. Further studies are needed to establish the role of CYP27A1 in atherosclerosis.

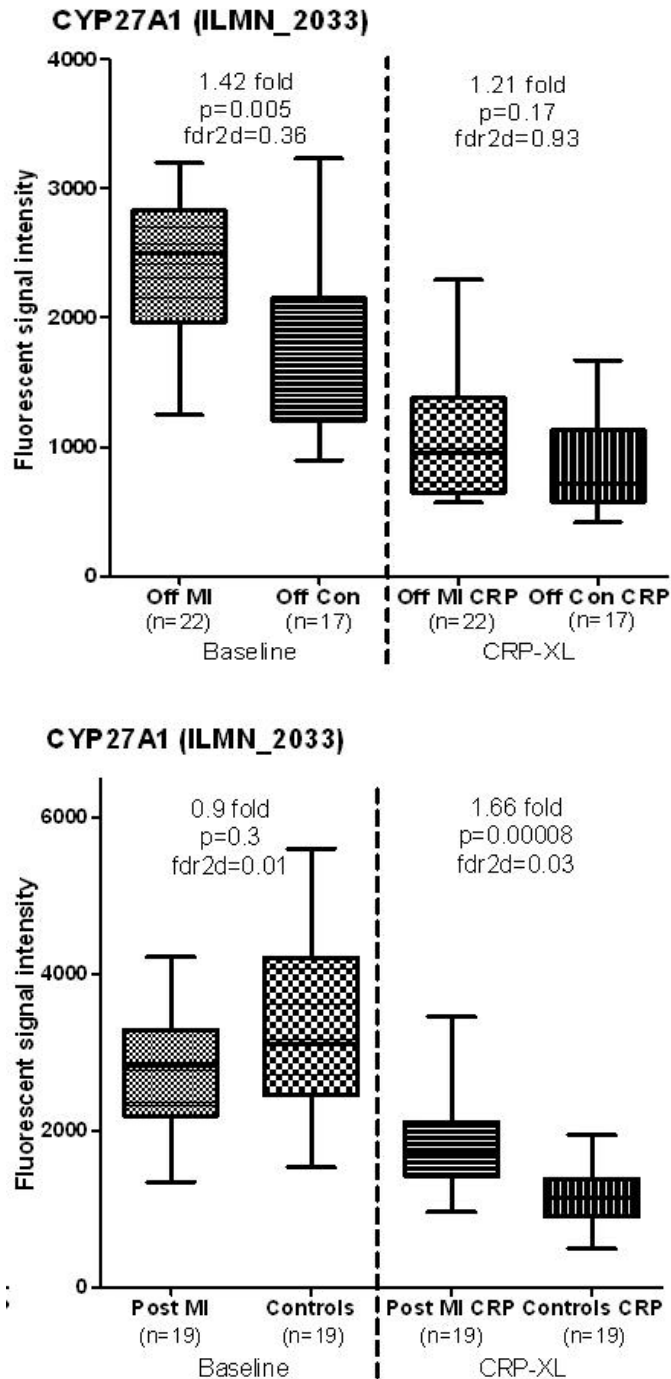


Figure 6.7: Differential expression of CYP27A1 in Offspring of MI and Post MI.

Fluorescent signal intensities in Offspring of MI and controls following platelet-mediated stimulation are shown on the left panel. Corresponding signal intensities in patients Post MI and controls are shown on the right panel. Error bars denote the range of expression. Fold changes, p values and false discovery rates are provided where applicable.

6.2.2.2 Leptin (LEP); Chr 7q31.3

Leptin is a regulator of energy homeostasis and has pro-inflammatory, pro-oxidative (Nseir et al., 2011) and prothrombotic effects (Katagiri et al., 2007). It up-regulates the transcription factors FOSB (Bendinelli et al., 2000) and EGR1 (de Lartigue et al., 2010) which have proatherogenic roles as previously described.

Leptin expression levels were low in all groups at baseline (Figure 6.8). Following stimulation, a significant >3 fold increase was seen in the Post MI group while a non significant increase was noted in the Offspring of MI group. This suggests that following a pro-atherogenic stimulus, leptin is preferentially increased in patients with established CAD and those with a high genetic predisposition to disease.

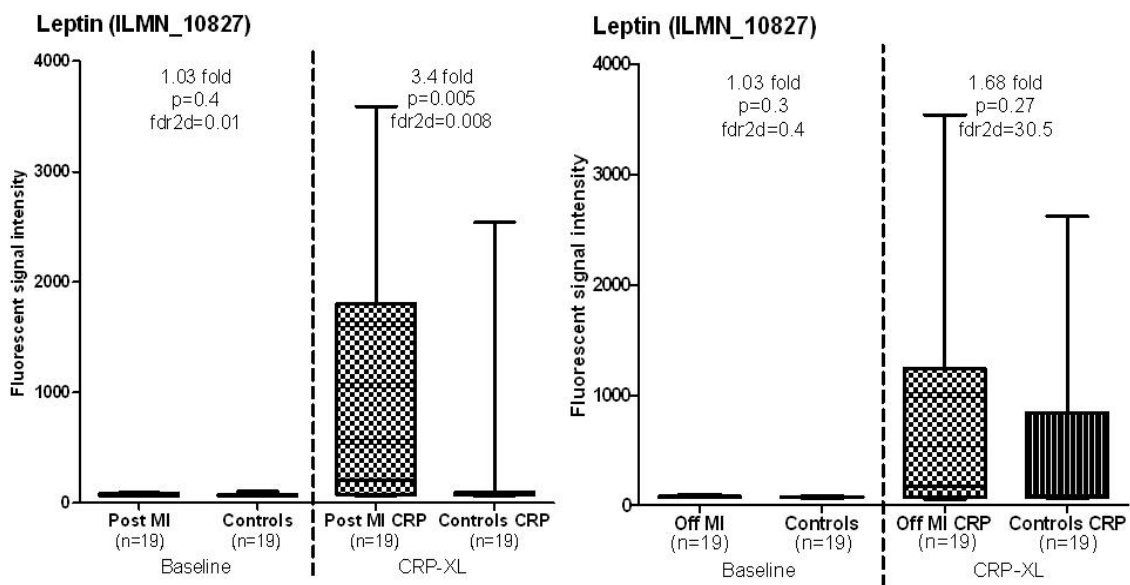


Figure 6.8: Differential expression of LEP in patients Post MI and Offspring of MI.

Fluorescent signal intensities in patients Post MI and controls following platelet-mediated stimulation are shown on the left panel. Corresponding signal intensities in Offspring of MI and controls are shown on the right panel. Error bars denote the range of expression. Fold changes, p values and false discovery rates are provided where applicable.

6.2.2.3 Acyl coenzyme A dehydrogenase family, member 10 (ACAD10); Chr 12q24.12

ACAD10 is an enzyme which participates in the beta oxidation of fatty acids in mitochondria. Genetic variations have been linked to abnormal lipid oxidation and predisposition to diabetes mellitus (Bian et al., 2010).

ACAD10 was expressed at low levels (fluorescent signal intensity <1000) in all four study groups with no significant differences at baseline (Figure 6.9). Following stimulation, levels were suppressed in all groups but more so in the Offspring of MI and Post MI groups compared to respective controls. A statistically significant relative reduction in gene expression was noted in both groups.

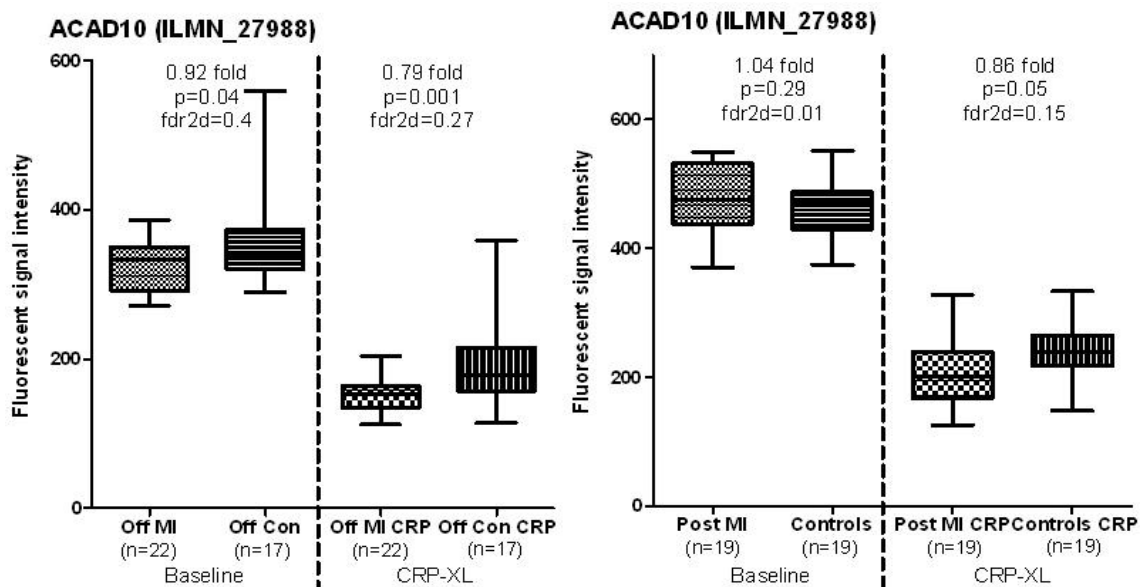


Figure 6.9: Differential expression of ACAD10 in Offspring of MI and Post MI.

Fluorescent signal intensities in Offspring of MI and controls following platelet-mediated stimulation are shown on the left panel. Corresponding signal intensities in patients Post MI and controls are shown on the right panel. Error bars denote the range of expression. Fold changes, p values and false discovery rates are provided where applicable.

6.2.2.4 ARV1 homolog (ARV1); Chr 1q42.2

ARV1 is a resident protein in the endoplasmic reticulum with a role in intracellular sterol transport (Tong et al., 2010). It mediates sterol transport from the endoplasmic reticulum to the plasma membrane (Shechtman et al., 2011). Defective ARV1 results in intracellular sterol accumulation and lipid droplet accumulation (Shechtman et al., 2011). ARV1 knockdown in murine macrophages results in apoptotic changes (Shechtman et al., 2011). Decreased ARV1 expression has been shown to induce hypercholesterolaemia and intracellular lipid accumulation with suppression of sterol regulatory element-binding proteins (SREBPs). SREBPs are key regulators of intracellular lipid transport and cholesterol homeostasis (Rawson, 2003).

ARV1 was expressed at low levels in all groups (Figure 6.10). In the Offspring of MI, expression levels were 10% lower than in controls at baseline ($p=0.003$, $fdr_{2d}=0.28$). No significant difference was noted in the Post MI group and their controls in resting monocytes. Following platelet-mediated stimulation, ARV1 gene expression was suppressed in all groups with lower transcript levels in the Offspring of MI and Post MI groups compared to their respective controls. The reduction was statistically significant in the Offspring group.

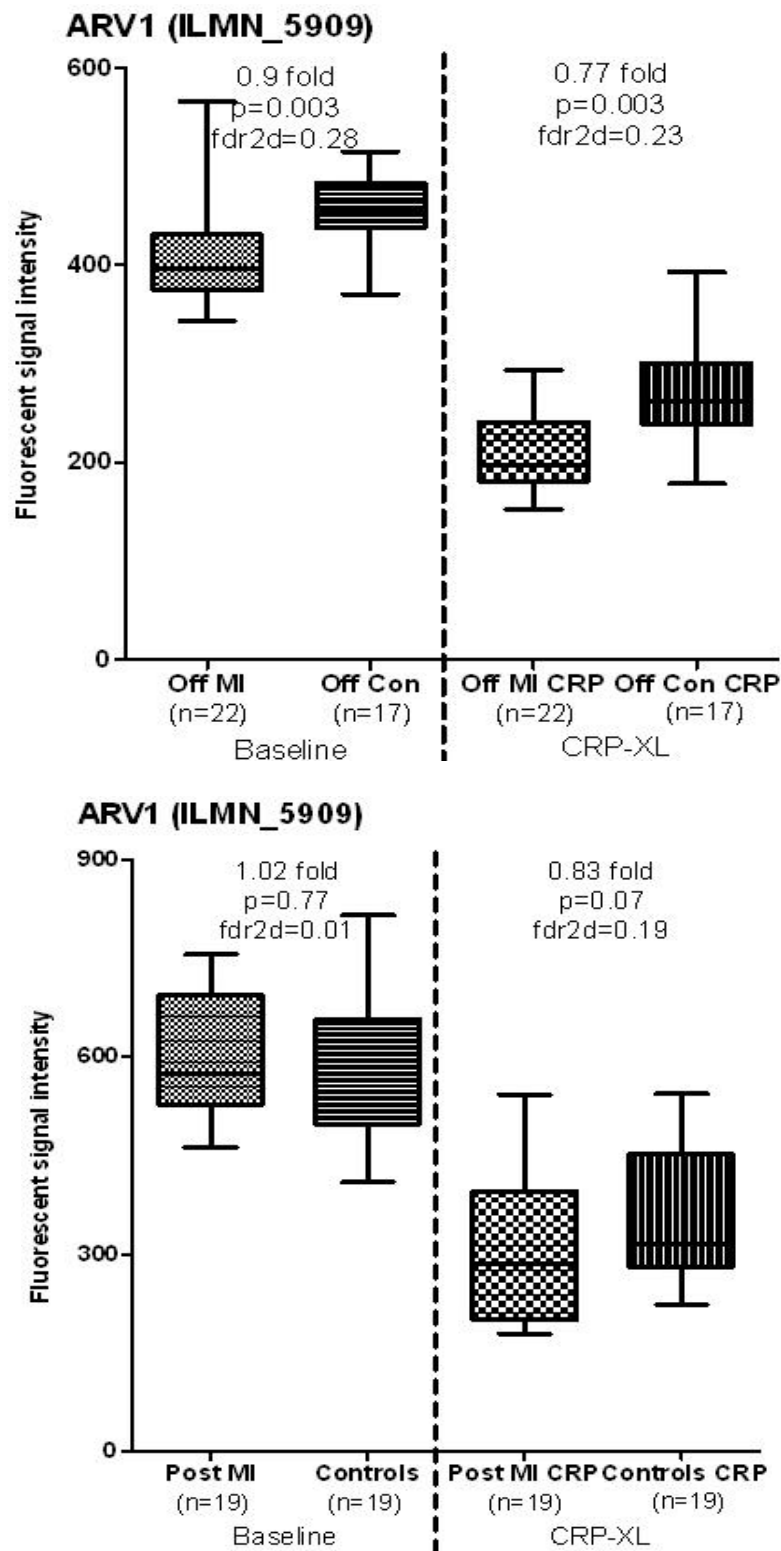


Figure 6.10: Differential expression of ARV1 in Offspring of MI and Post MI.

Fluorescent signal intensities in Offspring of MI and controls following platelet-mediated stimulation are shown on the left panel. Corresponding signal intensities in patients Post MI and controls are shown on the right panel. Error bars denote the range of expression. Fold changes, p values and false discovery rates are provided where applicable.

6.2.3 Chemokines

6.2.3.1 Chemokine (C-C motif) ligand 3-like 3 (CCL3L3); Chr 17q21.1

CCL3L3 is the centromeric full length copy of the gene CCL3L1 (Shrestha et al., 2010) and part of a chemokine gene cluster on Chr17q12 sharing homology with CCL3 and CCL3L2. Copy number variations in the telomeric copy of this gene, CCL3L1 has been linked to susceptibility to infections (Shrestha et al., 2010).

The three related genes, CCL3, CCL3L1 and CCL3L3 showed similar trends of expression in both Offspring of MI and patients Post MI in resting and stimulated monocytes, of which CCL3L3 passed the stringent filtering step (Figure 6.11).

Following platelet-mediated stimulation, expression levels were significantly higher in patients Post MI and to a lesser extent in Offspring of MI compared to respective controls.

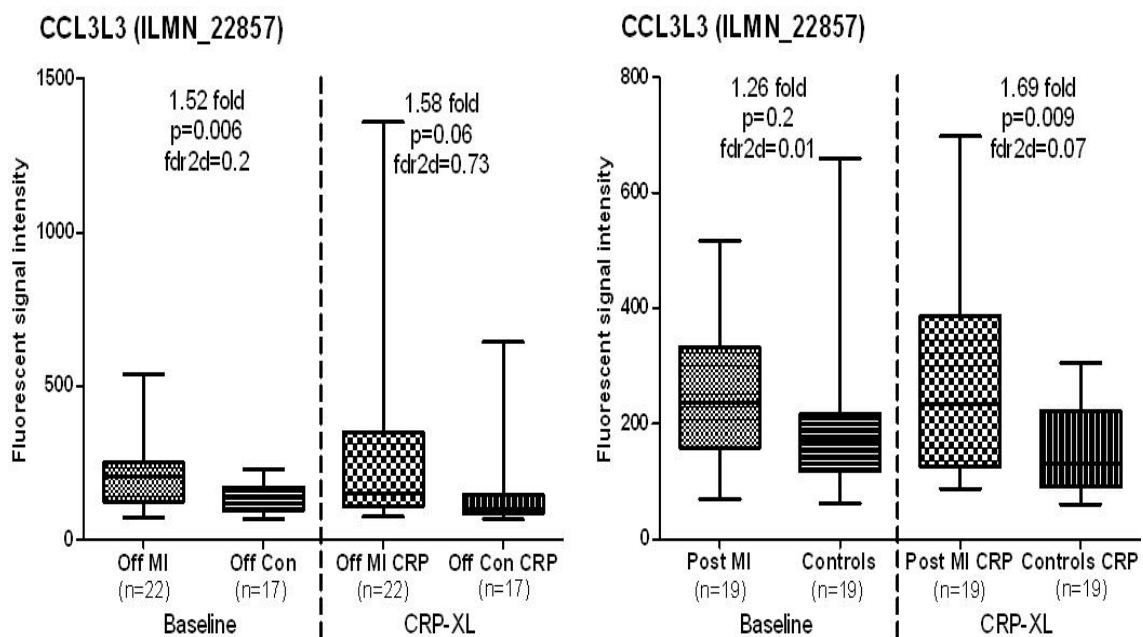


Figure 6.11: Differential expression of CCL3L3 in Offspring of MI and Post MI.

Fluorescent signal intensities in Offspring of MI and controls following platelet-mediated stimulation are shown on the left panel. Corresponding signal intensities in patients Post MI and controls are shown on the right panel. Error bars denote the range of expression. Fold changes, p values and false discovery rates are provided where applicable.

6.2.3.2 Chemokine (C-C ligand) 7 (CCL7/MCP3); Chr 17q11.2-q12

CCL7 (monocyte chemoattractant protein 3) is a pro-inflammatory cytokine that is chemotactic to monocytes. It has also been shown to induce smooth muscle proliferation in coronary arteries (Maddaluno et al., 2011). Atorvastatin reduces expression levels of CCL7 in circulating lymphocytes (Wang et al., 2011d).

CCL7 levels were low at baseline in all groups (Figure 6.12) but increased significantly following monocyte stimulation with collagen-activated platelets suggesting the pro-atherogenic potential of the stimulus. The relatively lower levels in the Post MI group are likely to be due to statin therapy. Although levels were numerically lower in Offspring of MI, the overlapping ranges of expression in both offspring groups suggest that the expression levels are not significantly different.

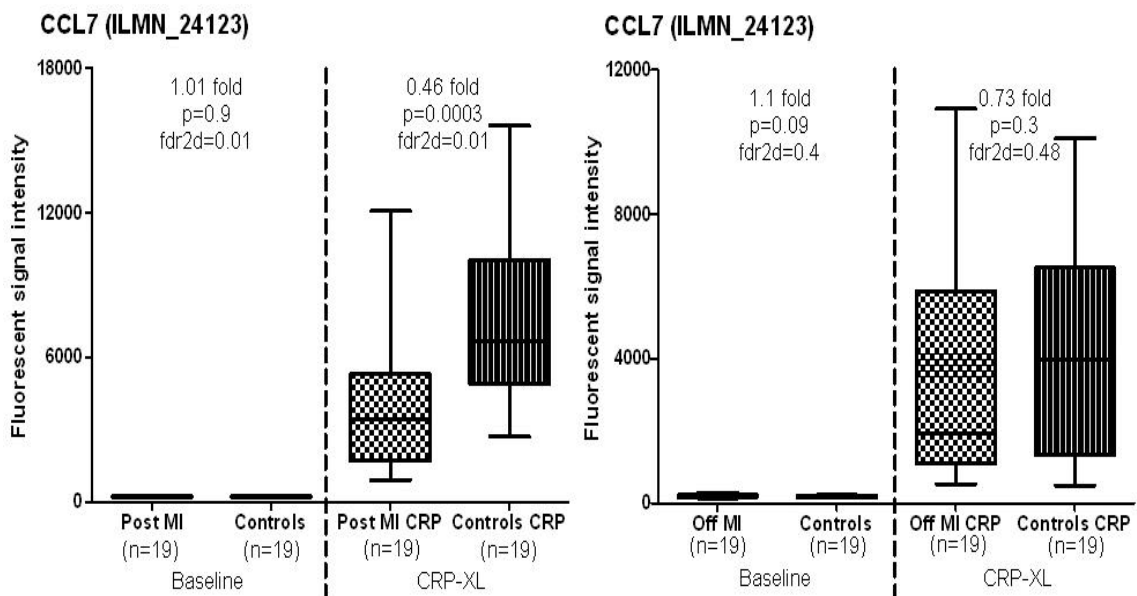


Figure 6.12: Differential expression of CCL7 in Post MI and Offspring of MI.

Fluorescent signal intensities in patients Post MI and controls following platelet-mediated stimulation are shown on the left panel. Corresponding signal intensities in Offspring of MI and controls are shown on the right panel. Error bars denote the range of expression. Fold changes, p values and false discovery rates are provided where applicable.

6.2.3.3 Chemokine binding protein 2 (CCBP2/D6/CCR9/CCR10); Chr 3p21.3

CCBP2 is a promiscuous decoy receptor that regulates inflammation and proliferation (Wu et al., 2008) which down regulates chemokines including CCL2 and CCL5. This 'silent' receptor does not promote chemotactic signalling, instead it binds the chemokines and transfers it from the cell surface to the endocytic compartment for degradation (Locati et al., 2005), This regulates the proinflammatory properties of these cytokines. Inflammatory chemokine activation has been noted in CCBP deficient animal models (Lee et al., 2011b).

CCBP is expressed at very low levels in resting monocytes in all groups (Figure 6.13). Following stimulation with activated platelets, levels increase in all groups but this response is subdued in both the Offspring of MI and Post MI groups. The relative reduction in levels was statistically significant in the Offspring of MI group compared to controls. This may promote up-regulation of CCL2, CCL3, CCL3L1 and CCL5 which are recognised ligands for this receptor (Hansell et al., 2011).

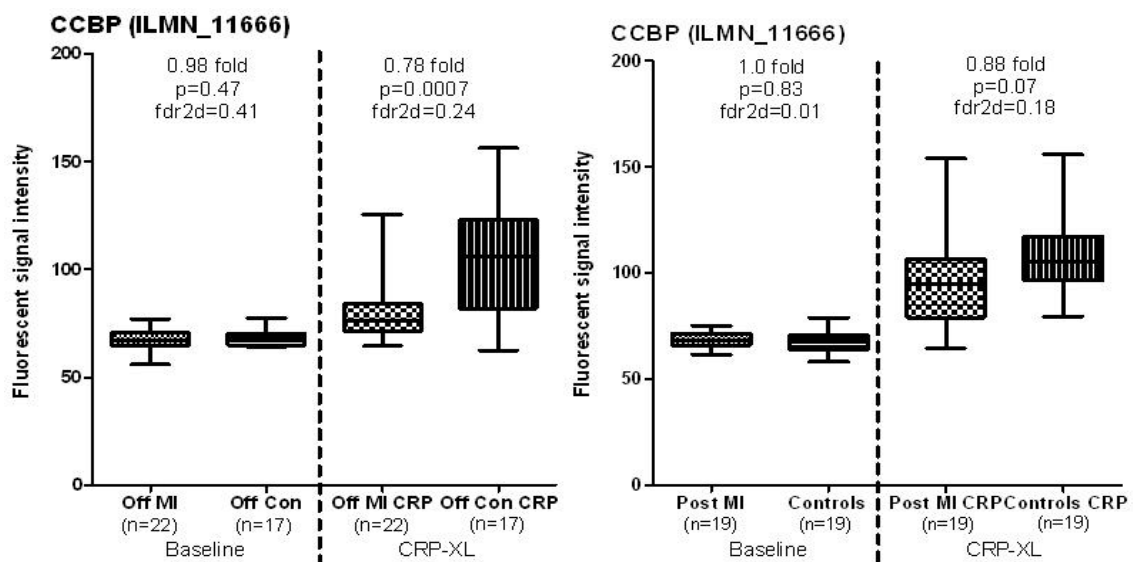


Figure 6.13: Differential expression of CCBP2 in Offspring of MI and Post MI.

Fluorescent signal intensities in Offspring of MI and controls following platelet-mediated stimulation are shown on the left panel. Corresponding signal intensities in patients Post MI and controls are shown on the right panel. Error bars denote the range of expression. Fold changes, p values and false discovery rates are provided where applicable.

6.2.4 Heat shock proteins

6.2.4.1 DnaJ (Hsp40) homolog, subfamily B, member 1 (DNAJB1/HSP40); Chr 19p13.2

DNAJB1 is a heat shock protein that is protective against oxidative stress (Kim et al., 2008b). This gene is up-regulated alongside the transcription factors FOSB and EGR1 following oxidative stress (Fratelli et al., 2005).

DNAJB1 levels were low in all groups at baseline (Figure 6.14). In patients Post MI, there was a statistically significant >2 fold up-regulation of this gene after platelet-mediated stimulation compared to controls. There was a similar trend in the Offspring of MI following stimulation of borderline statistical significance ($p=0.07$).

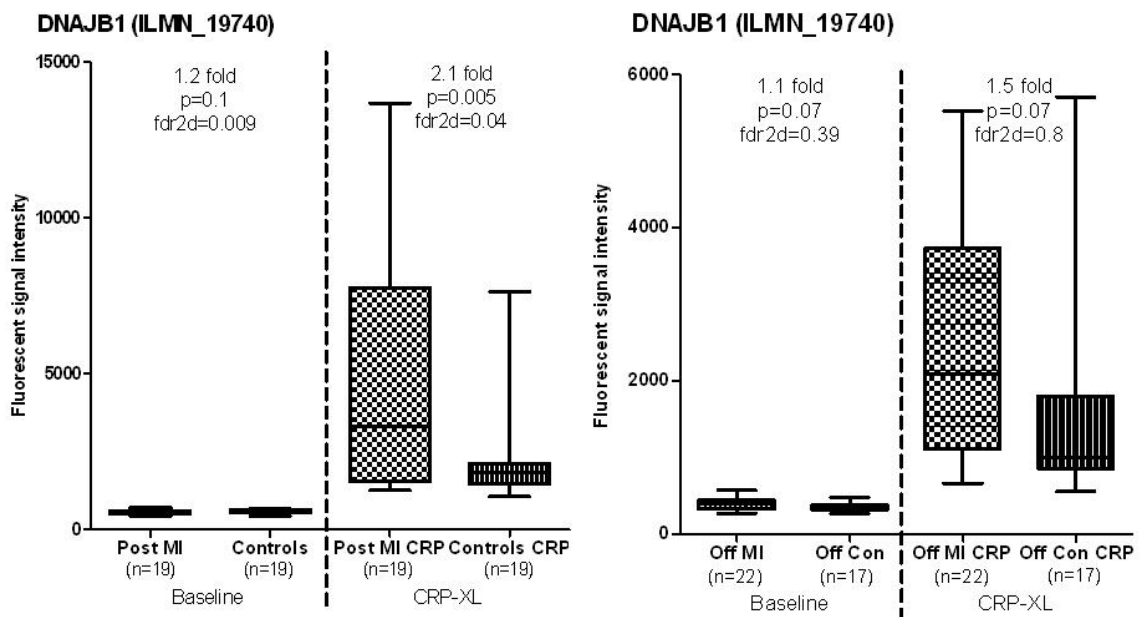


Figure 6.14: Differential expression of DNAJB1 in Post MI and Offspring of MI.

Fluorescent signal intensities in patients Post MI and controls following platelet-mediated stimulation are shown on the left panel. Corresponding signal intensities in Offspring of MI and controls are shown on the right panel. Error bars denote the range of expression. Fold changes, p values and false discovery rates are provided where applicable.

6.2.4.2 FKBP4 binding protein 4 (FKBP4/HSP56/PPIase); Chr 12p13.33

FKBP4 is a member of the immunophilin family that associates with HSPs 70 and 90. It translocates from mitochondria to nucleus and mediates an anti-apoptotic protective effect following oxidative stress (Gallo et al., 2011). In addition, along with other heat shock proteins, FKBP4 mediate stress induced steroid hormone signalling (Sivils et al., 2011).

FKBP4 was expressed at low levels in all four groups at baseline (Figure 6.15). Following platelet-mediated stimulation, FKBP4 levels increased in all groups suggesting that stimulation results in an oxidative stress response in monocytes. In the Offspring of MI, a statistically significant 1.6 fold relative increase in expression was noted compared to controls whilst in the Post MI group, the relative up-regulation approached statistical significance (p=0.15).

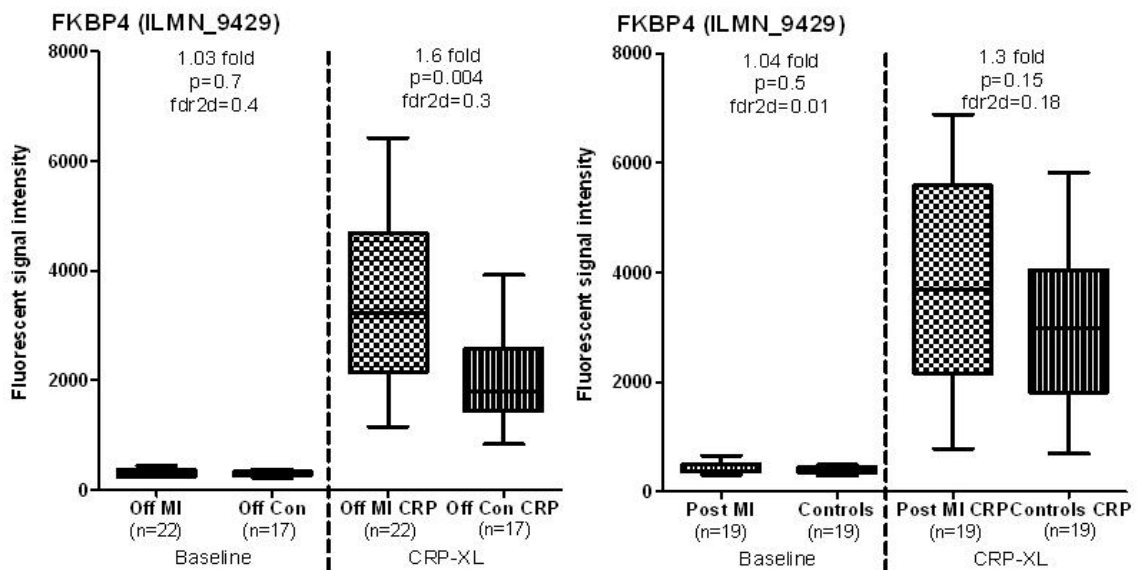


Figure 6.15: Differential expression of FKBP4 in Offspring of MI and Post MI.

Fluorescent signal intensities in Offspring of MI and controls following platelet-mediated stimulation are shown on the left panel. Corresponding signal intensities in patients Post MI and controls are shown on the right panel. Error bars denote the range of expression. Fold changes, p values and false discovery rates are provided where applicable.

6.2.5 Cell senescence

6.2.5.1 B cell translocation gene 2 (BTG2; Chr 1q32)

BTG2 is a regulator of the cell cycle with anti-proliferative properties. It is up-regulated in response to oxidative stress injury in animal models (Han et al., 2008). It regulates replicative senescence in a p-53 responsive manner (Wheaton et al., 2010) and has a tumour suppressor role (Zhang et al., 2010).

BTG2 was expressed at moderate levels in unstimulated monocytes (Figure 6.16) and no significant difference in levels was noted following platelet-mediated stimulation. In Offspring of MI, there was a statistically significant 1.45 fold up-regulation of BTG2 expression at baseline with a similar trend in patients with MI.

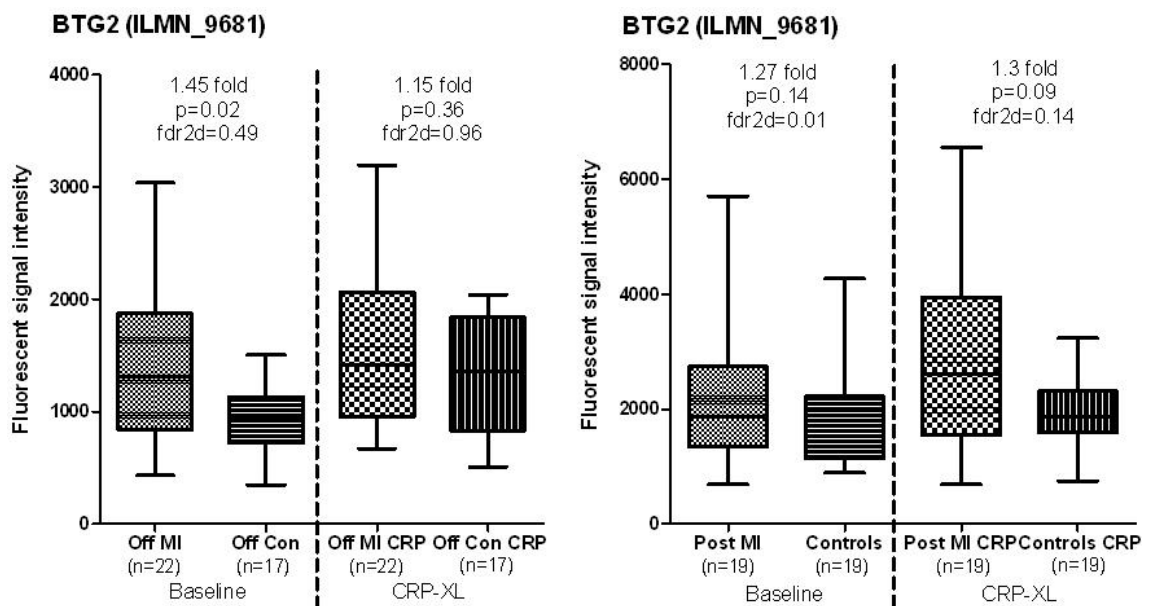


Figure 6.16: Differential expression of BTG2 in Offspring of MI and Post MI.

Fluorescent signal intensities in Offspring of MI and controls following platelet-mediated stimulation are shown on the left panel. Corresponding signal intensities in patients Post MI and controls are shown on the right panel. Error bars denote the range of expression. Fold changes, p values and false discovery rates are provided where applicable.

6.2.5.2 Huntington interacting protein 1 (HIP1); Chr 7q11.23

HIP1 is essential for cytoskeletal integrity (Wilbur et al., 2008) and has a role in cell senescence (Chigira et al., 2003) and growth factor receptor trafficking (Bradley et al., 2005). It also has a proapoptotic role by induction of caspase 8 (Wanker, 2002).

Low expression levels were noted in all groups at baseline (Figure 6.17). Levels increased in all groups following platelet-mediated stimulation with a 1.55 fold relative increase in the Offspring of MI compared to healthy controls ($p=0.0005$, $fdr_{2d}=0.05$). A similar non significant trend was noted in patients Post MI.

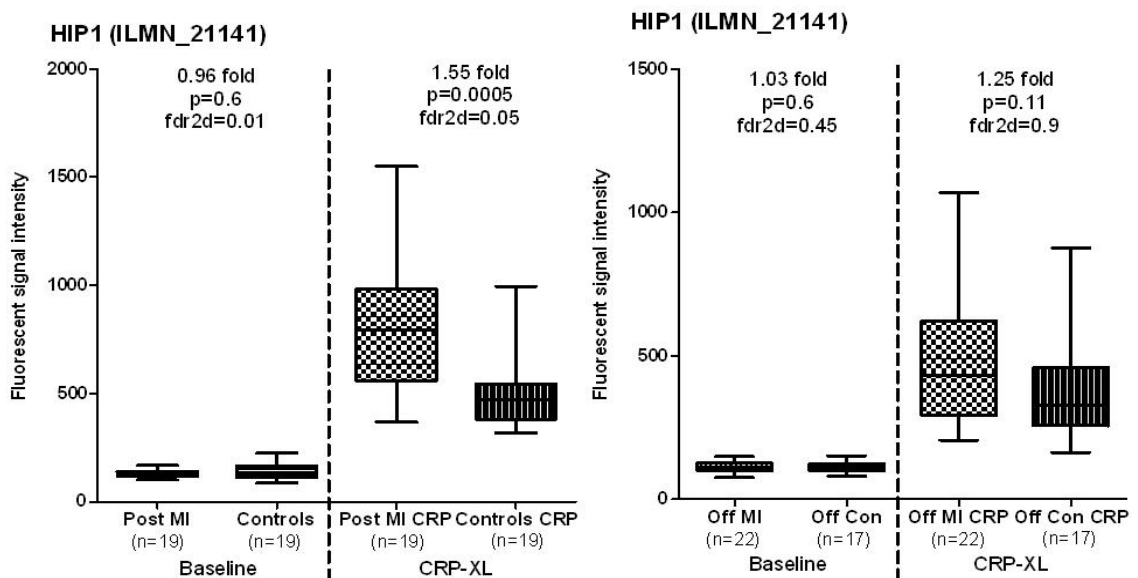


Figure 6.17: Differential expression of HIP1 in Post MI and Offspring of MI.

Fluorescent signal intensities in patients Post MI and controls following platelet-mediated stimulation are shown on the left panel. Corresponding signal intensities in Offspring of MI and controls are shown on the right panel. Error bars denote the range of expression. Fold changes, p values and false discovery rates are provided where applicable.

6.2.6 Response to hypoxia

6.2.6.1 Family with sequence similarity 13, member A (FAM13A1); Chr 4q22.1

FAM13A1 codes for a protein with a putative role in signalling and is expressed in response to hypoxia (Chi et al., 2006).

This gene was expressed at low levels (signal intensity <1000) in all groups at baseline (Figure 6.18). Following platelet-mediated stimulation, levels were lower in both control groups. However, there was an increase in expression levels in the Offspring of MI and Post MI groups. A significant 2.55 fold relative increase was noted in the Offspring of MI ($p=0.002$, $fdr_{2d}=0.02$). A similar but non-significant trend was noted in the Post MI group.

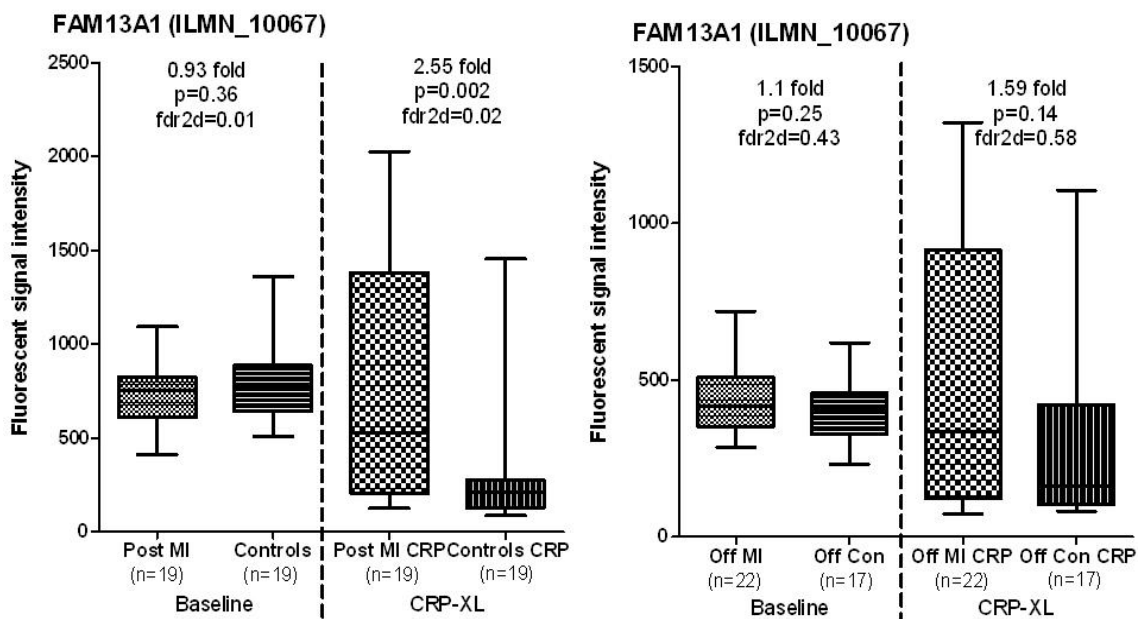


Figure 6.18: Differential expression of FAM13A1 in Post MI and Offspring of MI.

Fluorescent signal intensities in patients Post MI and controls following platelet-mediated stimulation are shown on the left panel. Corresponding signal intensities in Offspring of MI and controls are shown on the right panel. Error bars denote the range of expression. Fold changes, p values and false discovery rates are provided where applicable.

6.2.7 Tumour suppressor

6.2.7.1 Latexin (LXN); Chr 3q25.32

LXN is an inhibitor of zinc dependent metalloproteinase (MCP) which exhibits tumour suppressor properties (Li et al.). It regulates intracellular protein abundance in haemopoietic stem cells (HSC) and latexin suppression is seen in haematological malignancies (Mitsunaga et al., 2012). It is a natural brake on stem cell numbers and its expression is inversely correlated to the size of HSC populations.

LXN is expressed at low levels in monocytes both before and after stimulation (Figure 6.19). A 25% relative reduction in gene expression was seen in Offspring of MI following platelet-mediated stimulation ($p=0.004$, $fdr_{2d}=0.4$). A similar statistically significant trend ($p=0.02$) was noted in the Post MI patients.

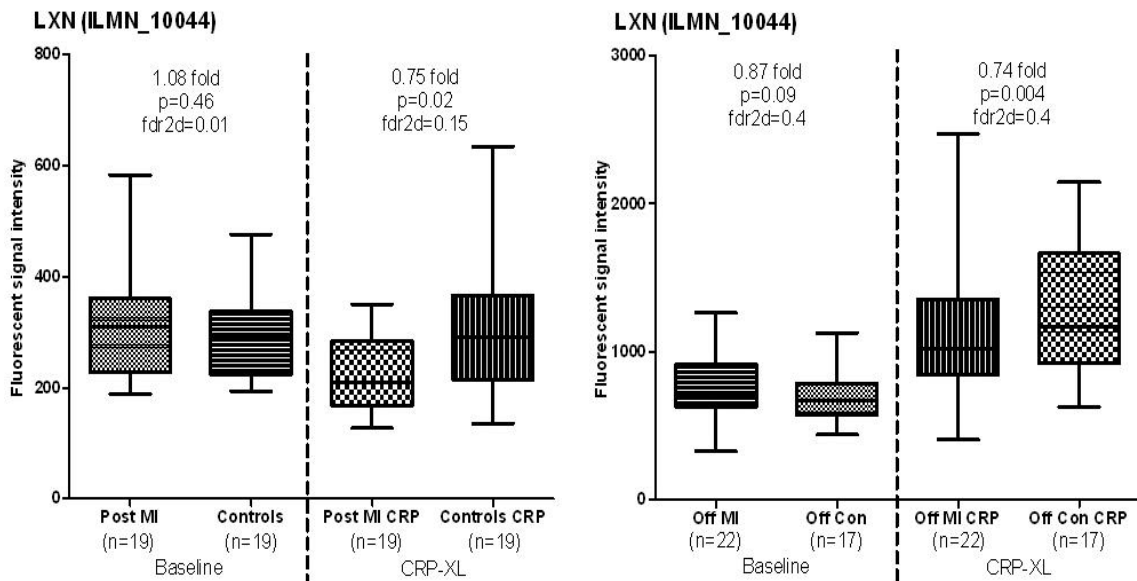


Figure 6.19: Differential expression of LXN in Post MI and Offspring of MI.

Fluorescent signal intensities in patients Post MI and controls following platelet-mediated stimulation are shown on the left panel. Corresponding signal intensities in Offspring of MI and controls are shown on the right panel. Error bars denote the range of expression. Fold changes, p values and false discovery rates are provided where applicable.

6.2.8 Receptors and signaling

6.2.8.1 Killer cell immunoglobulin-like receptor, two domains, long cytoplasmic tail, 4 (KIR2DL4/G9P/CD158D); 19q13.4

KIR2DL4 is a transmembrane glycoprotein receptor expressed in antigen presenting cells, natural killer cells and T cells which mediates immune tolerance and immune silencing through its ligand HLA-G (LeMaoult et al., 2005). It is unique in having both activating and inhibiting functions in response to ligand binding (Faure and Long, 2002).

Low levels of KIR2DL4 expression was seen in all groups at baseline (Figure 6.20). and levels increased in all groups after stimulation. However, a statistically significant relative lower in levels was noted in both Offspring of MI and Post MI groups when compared to their respective controls, suggesting an imbalance of immune response with preferential stimulation of pro-inflammatory cytokines (CCL2, CCL3, CCL3L1 and CCL3L3) and reduced expression of immunoregulatory receptors including CCBP2 (Figure 6.13) and KIR2DL4.

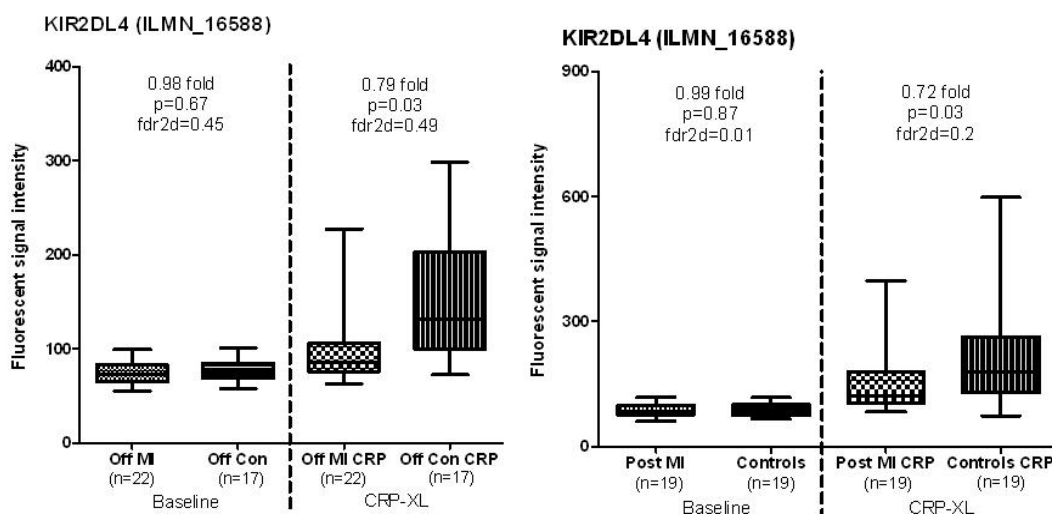


Figure 6.20: Differential expression of KIR2DL4 in Offspring of MI and Post MI.

Fluorescent signal intensities in Offspring of MI and controls following platelet-mediated stimulation are shown on the left panel. Corresponding signal intensities in patients Post MI and controls are shown on the right panel. Error bars denote the range of expression. Fold changes, p values and false discovery rates are provided where applicable.

6.2.8.2 Solute carrier family 5 (sodium/myo-inositol cotransporter), member 3 (SLC5A3/SMIT/SMIT2); Chr 21q22.12

SLC5A3 is a cellular osmoregulator (Mallee et al., 1997). A recent genome wide association study in coronary artery disease has identified a single nucleotide polymorphism with a strong association with coronary disease near the SLC5A3 locus (Kathiresan et al., 2009).

Low levels of SLC5A3 expression was seen in all four groups in resting monocytes (Figure 6.21). Levels increased in all four groups after platelet-mediated stimulation with a larger magnitude of increase in the Offspring of MI and Post MI groups. A 58% relative increase in expression was noted in the Offspring of MI group ($p=0.009$, $fdr_{2d}=0.49$). In the Post MI group, a similar relative up-regulation of borderline statistical significance was seen following stimulation ($p=0.09$).

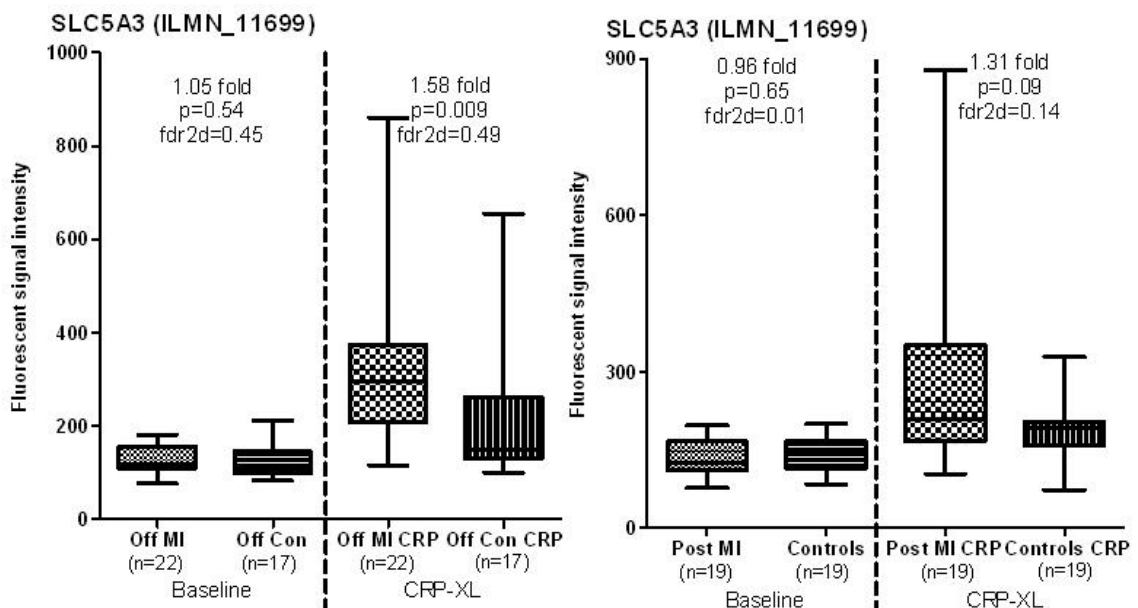


Figure 6.21: Differential expression of SLC5A3 in Offspring of MI and Post MI. Fluorescent signal intensities in Offspring of MI and controls following platelet-mediated stimulation are shown on the left panel. Corresponding signal intensities in patients Post MI and controls are shown on the right panel. Error bars denote the range of expression. Fold changes, p values and false discovery rates are provided where applicable.

6.2.9 Summary of shared trends in monocyte gene expression in high risk groups

In this section, trends in monocyte gene expression which were shared between two high risk groups were studied to identify novel mechanisms which may determine the genetic risk of CAD. Possible alterations in oxidative stress behaviour and heat shock response were two mechanisms that were identified (Figure 6.22). Transcription factors with recognized roles in oxidative stress response and atherogenesis were up-regulated (FOSB, EGR1). FOSB and EGR1 activate tissue factor by binding to its promoter region while EGR1 promotes LDL receptor gene expression in response to activation by Oncostatin M (Zhang et al., 2002). OSM is a chemokine that was significantly up-regulated following platelet-mediated stimulation in all groups (see Chapter 3; Figure 3.19). IER2, another transcription factor which was up-regulated in these groups regulates the expression of inositol-3-phosphate synthase 1 (ISYNA1), a cell signalling molecule which interacts closely with solute carrier family 5 member 3 (SLC5A3) which has a role in cellular response to hypertonic stress (Kwon et al., 1992). SLC5A3 was also preferentially increased in the two high risk groups and has been associated with CAD. In addition, proinflammatory cytokines such as Leptin and CCL3 are preferentially up-regulated in these subjects after platelet-mediated stimulation.

The down regulated genes CCBP2 and KIR2DL4 have immunomodulatory roles and counter the actions of the other pro-inflammatory cytokines which were up-regulated in these groups. This suggests an imbalance in regulation of the inflammatory response in these individuals. The three molecules which regulate intracellular lipid transport and metabolism (CYP27A1, ACAD10 and ARV1) which were differentially expressed in the Post MI and Offspring of MI groups compared to their respective control groups are shown in Figure 6.23.

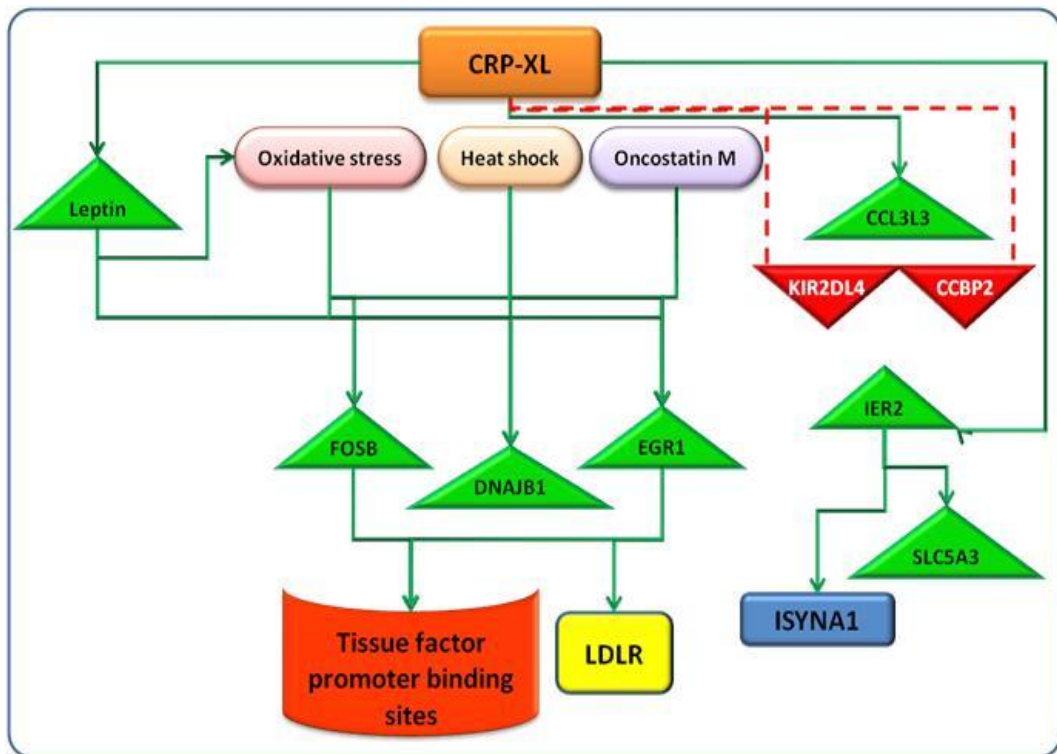


Figure 6.22: Summary of shared genes in Post MI and Offspring of MI.
 Up-regulated genes are shown in green triangles and down regulated genes in red triangles.

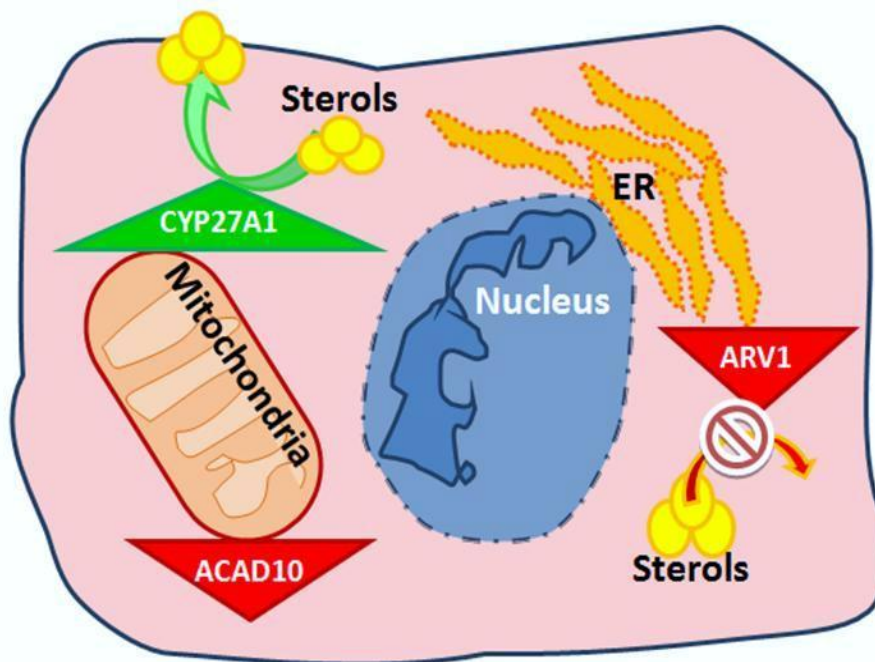


Figure 6.23: Perturbations in sterol metabolism in Post MI and Offspring of MI.
 Three genes involved in sterol metabolism were differentially expressed in the two ‘at risk’ groups. Down regulation of ARV1 and ACAD10 suggest alterations in intracellular sterol trafficking and fatty acid metabolism respectively. CYP27A1 up-regulation may represent a compensatory mechanism to improve cholesterol efflux from peripheral tissues.

6.3 VALIDATION OF KEY MICROARRAY RESULTS BY Q-PCR

Two genes were selected for validation by Q-PCR. This selection was based on their shared magnitude of fold change and statistical significance across the Post MI and Offspring of MI groups as well as their biological significance and recognised roles in atherosclerosis and coronary artery disease.

The transcription factor EGR1 and the mitochondrial enzyme CYP27A1 were selected for validation based on the above criteria.

6.3.1 EGR1 – validation by PCR

EGR1 was validated by Q-PCR in Offspring of MI (Figure 6.24) and patients Post MI (Figure 6.25) in resting monocytes (baseline). In the offspring group, a 1.81 fold up-regulation was seen on microarray. Q-PCR with TBP as the control gene validated this finding with a 2.58 fold up-regulation of EGR1 in Offspring of MI.

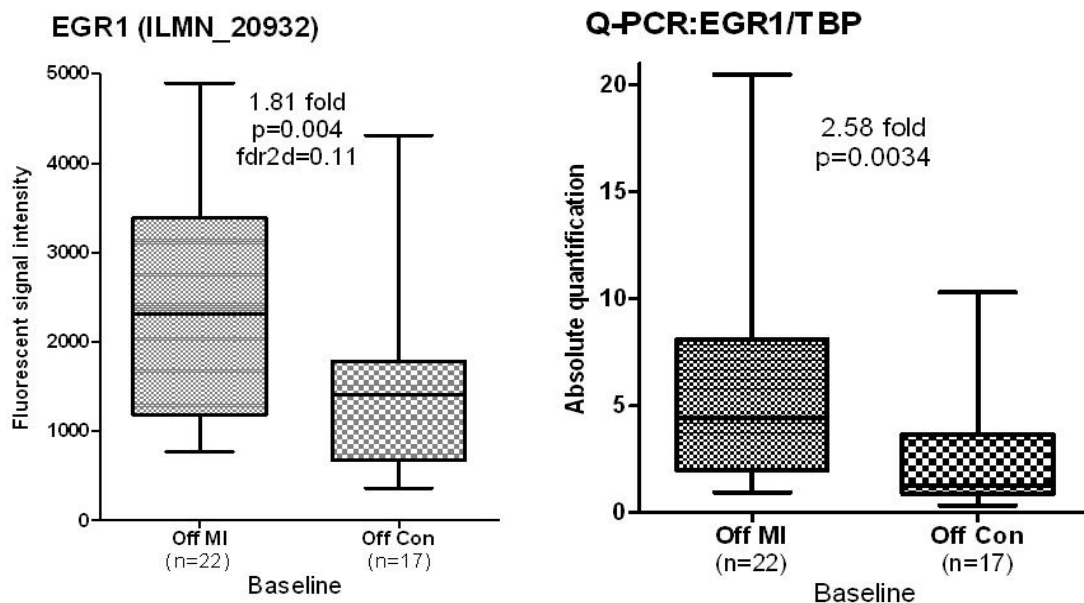


Figure 6.24: Microarray and Q-PCR results of EGR1 in Offspring of MI and controls.

Fluorescent signal intensities in Offspring of MI and controls at baseline are shown on the left panel. Q-PCR validation of the microarray results with TATA box protein as the control gene is shown on the right panel. Error bars denote the range of expression. Fold changes, p values and false discovery rates are provided where applicable.

In the Post MI group, a non significant 1.37 fold up-regulation was seen at baseline. Q-PCR confirmed a relative up-regulation (1.9 fold) of EGR1 in the Post MI groups of borderline statistical significance ($p=0.056$).

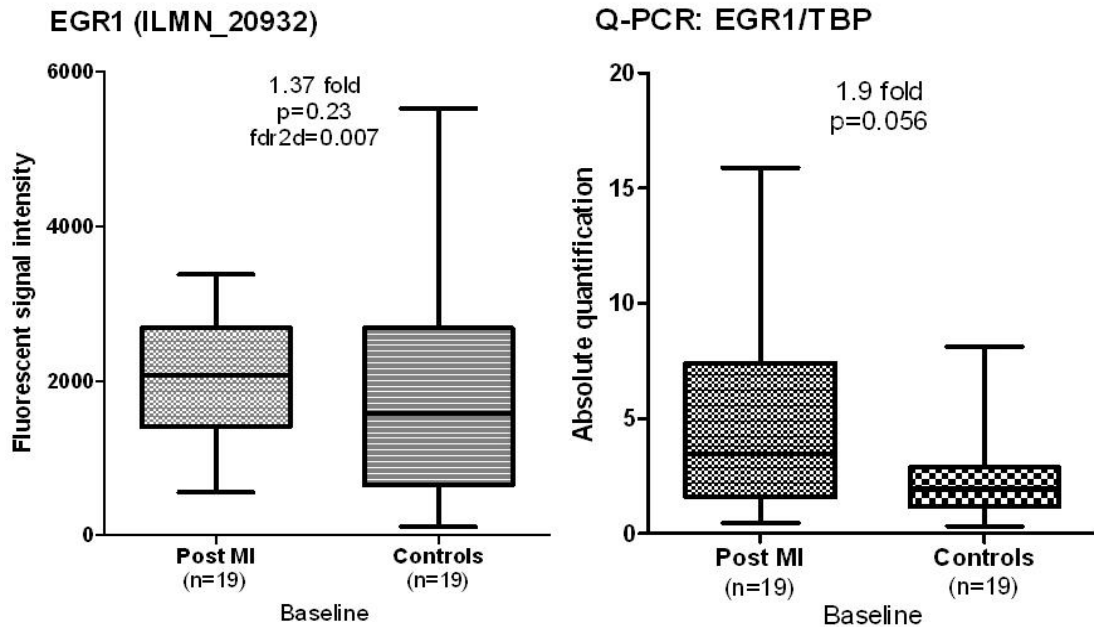


Figure 6.25: Microarray and Q-PCR results of EGR1 in patients Post MI and controls. Fluorescent signal intensities in patients Post MI and controls at baseline are shown on the left panel. Q-PCR validation of the microarray results with TATA box protein as the control gene is shown on the right panel. Error bars denote the range of expression. Fold changes, p values and false discovery rates are provided where applicable.

6.3.2 CYP27A1 – validation by PCR

CYP27A1 was validated by Q-PCR in Offspring of MI at baseline (Figure 8.26) and after CRP-XL stimulation (Figure 6.27). In the Post MI group, Q-PCR validation was performed to confirm differential expression after CRP-XL stimulation (Figure 6.26). Baseline Post MI and controls samples were not analysed by Q-PCR as there was no significant difference between groups before stimulation.

In Offspring of MI, a 42% relative increase in CYP27A1 levels was noted at baseline. A 47% up-regulation was confirmed on Q-PCR (Figure 6.26).

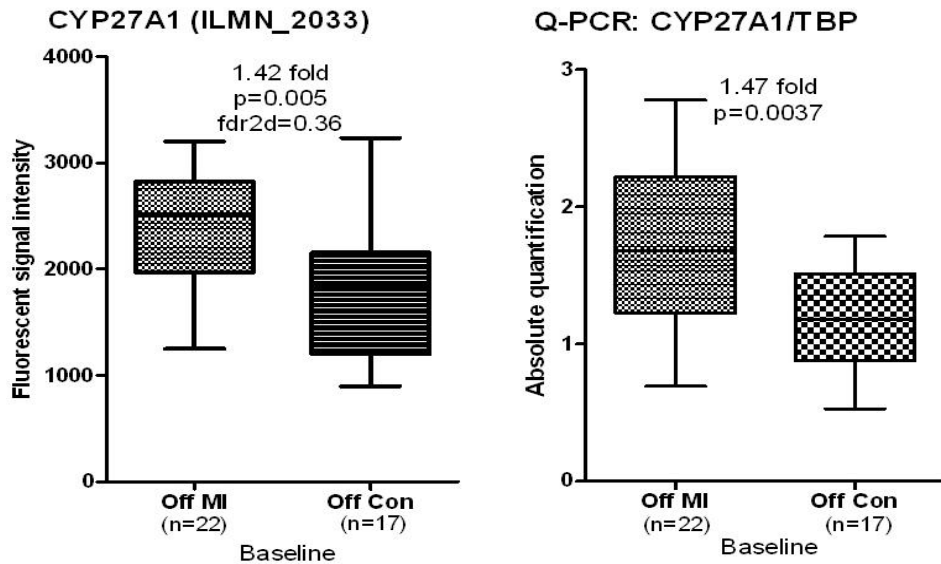


Figure 6.26: Microarray and Q-PCR for CYP27A1 in Offspring of MI and controls.

Fluorescent signal intensities in Offspring of MI and controls at baseline are shown on the left panel. Q-PCR validation of the microarray results with TATA box protein as the control gene is shown on the right panel. Error bars denote the range of expression. Error bars denote the range of expression. Fold changes, p values and false discovery rates are provided where applicable.

Following platelet-mediated stimulation a 21% relative up-regulation (p=ns) was noted in Offspring of MI. A corresponding 51% trend was confirmed on Q-PCR (Figure 6.27).

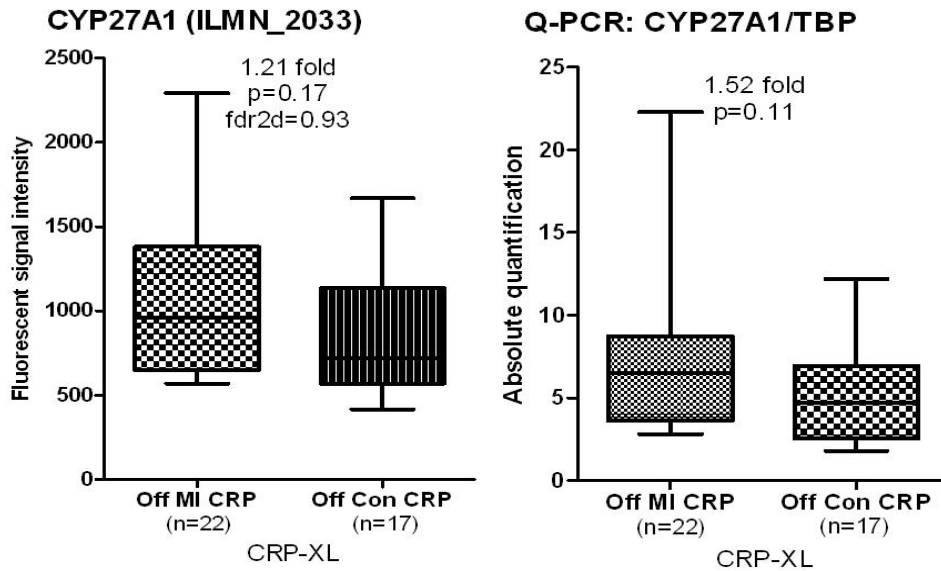


Figure 6.27: Microarray and Q-PCR for CYP27A1 in Offspring of MI and controls.

Fluorescent signal intensities in Offspring of MI and controls following platelet-mediated stimulation are shown on the left panel. Q-PCR validation of the microarray results with TATA box protein as the control gene is shown on the right panel. Error bars denote the range of expression. Error bars denote the range of expression. Fold changes, p values and false discovery rates are provided where applicable.

In the Post MI group, no significant difference in expression was noted at baseline compared to controls. Following platelet-mediated stimulation (Figure 6.28), a statistically significant 1.66 fold up-regulation in expression level was noted which was validated by Q-PCR. With TBP as control gene, a 3.24 fold up-regulation of CYP27A1 was noted in the Post MI group ($p < 0.0001$).

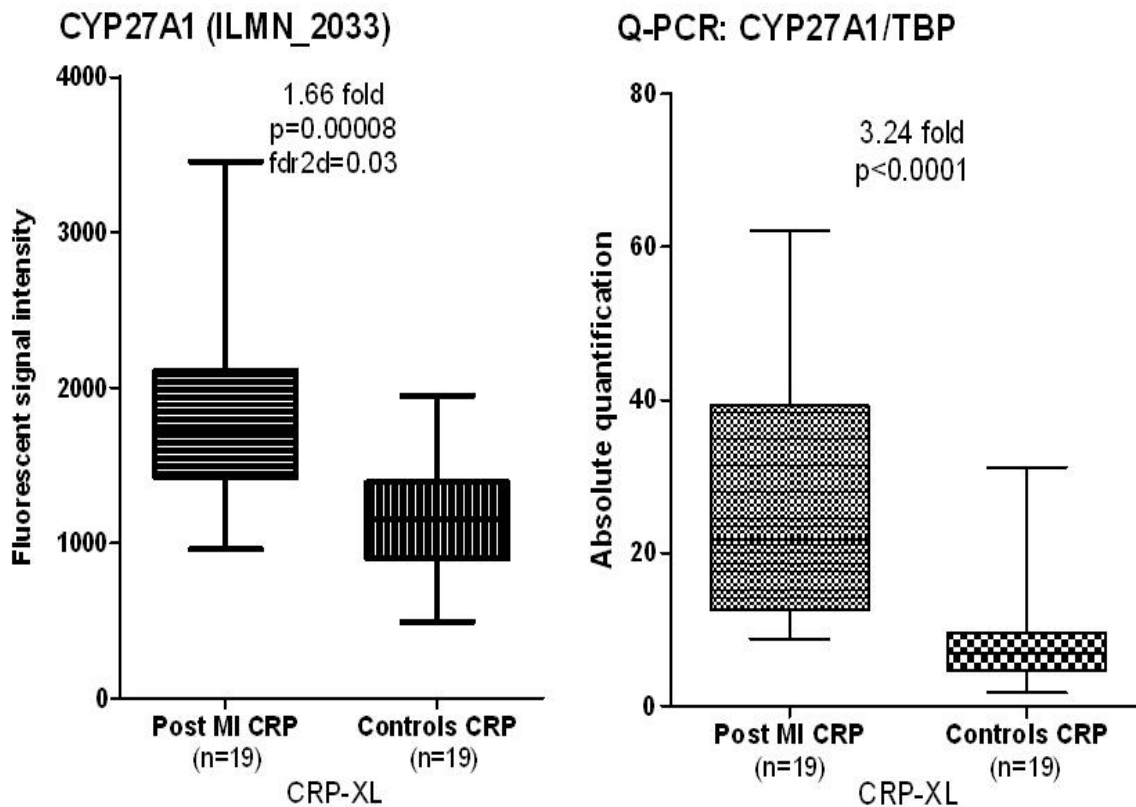


Figure 6.28: Microarray and Q-PCR results of CYP27A1 in Post MI and controls.

Fluorescent signal intensities in patients Post MI and controls following platelet-mediated stimulation are shown on the left panel. Q-PCR validation of the microarray results with TATA box protein as the control gene is shown on the right panel. Error bars denote the range of expression. Fold changes, p values and false discovery rates are provided where applicable.

6.4 CORRELATING GENETIC VARIANTS WITH MONOCYTE GENE EXPRESSION

The transcriptome is an integrator of genetic and environmental influences on complex diseases such as CAD and MI. Monocyte transcriptome analysis was performed in this study thesis to identify those genes which were differentially regulated in individuals with and at high genetic risk of premature MI. This allows further focused analysis of genetic variations which lie within or near the differentially expressed genes and assess (i) whether they are associated with risk of CAD or MI and/or (ii) whether they affect expression of the genes. A scheme of analysis is shown in Figure 6.29.

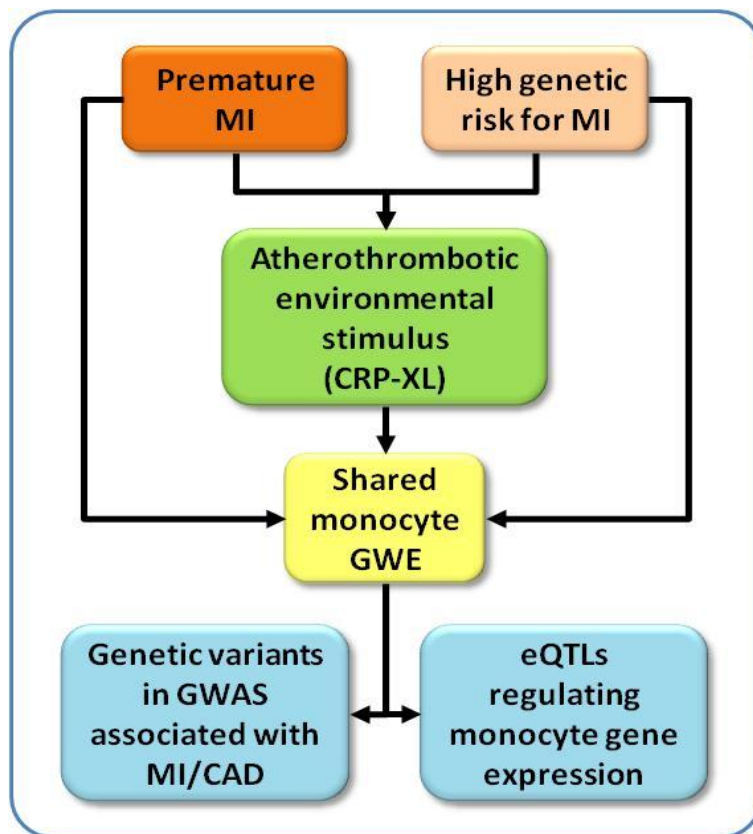


Figure 6.29: Correlating GWE with GWAS - scheme of analysis

Genes with shared expression profiles in monocytes before and after platelet-mediated stimulation in the Post MI and Offspring of MI groups were selected for this analysis. Existing databases were searched for genetic variants in these genes which strongly associate with CAD/MI and/or regulate monocyte gene expression.

6.4.1 Genetic variants in differentially expressed genes and their association with CAD and MI

6.4.1.1 CARDIoGRAM Study

GWAS have been published in recent years which have identified genetic variants with a strong association to both CAD and MI (Samani et al., 2007, Reilly et al., 2011, Consortium, 2011, Wang et al., 2011a, IBC_50K_CAD, 2011). The Coronary ARtery Disease Genome-wide Replication And Meta-analysis (CARDIoGRAM) consortium was formed to conduct a meta analysis of 14 genome wide association studies in CAD comprising 22,233 individuals with CAD (cases) and 64,762 controls of European descent. A proportion of the CAD cases had a history of MI and a meta-analysis was also done in MI patients only. Subjects in all studies were genotyped using one of the available GWA arrays and to allow data to be combined, all studied were imputed using HapMap CEU (HapMap3_r2) providing up to 2.5 million genotypes. A validation step was then performed by genotyping of top association signals in 56,682 additional individuals. (Preuss et al., 2010).

CARDIoGRAM identified 13 new loci associated with CAD at genome-wide significance level ($P < 5 \times 10^{-8}$) with the frequency of the risk allele ranging from 13% to 91% in the study, with each allele associated with a 6% to 17% increase in the risk of CAD. The study also confirmed 10 out of 12 previously reported genetic variants with strong association with CAD or MI (Schunkert et al., 2011). A further 6000 loci showed a nominal association with CAD or MI. In this study, 10 out of 13 new loci did not associate with classical CAD risk factors. The majority were in chromosomal regions with no recognized roles in the development or progression of CAD. These findings suggest that other approaches such as the one employed

in this thesis may help to prioritise and identify those loci amongst these that have a genuine genetic association with CAD but do not achieve the very stringent p values required in GWAS.

6.4.1.2 Selection of genes

47 differentially expressed genes were studied in this analysis (see Tables 6.4-6). This included 18 genes with shared trends in differential expression, 21 genes expressed in Post MI at baseline, 5 genes in Post MI after CRP-XL, 1 gene in Offspring of MI at baseline and 2 genes in Offspring of MI after CRP-XL stimulation. All genetic variants within or near (± 50 kb) the genes were tested for associations with CAD or MI within CARDIoGRAM.

Shared Genes: Post MI and Offspring of MI		
Gene	Chromosome	Gene Name
BTG2	1q32	BTG family, member 2
ARV1	1q42.2	ARV1 homolog (<i>S. cerevisiae</i>)
CYP27A1	2q33-qter	cytochrome P450, family 27, subfamily A, polypeptide 1
CCBP2	3p21.3	chemokine binding protein 2
LXN	3q25.32	Latexin
FAM13A1	4q22.1	family with sequence similarity 13, member A
EGR1	5q31.1	early growth response 1
HIP1	7q11.23	Huntington interacting protein 1
LEP	7q31.3	Leptin
FKBP4	12p13.33	FK506 binding protein 4, 59kDa
ACAD10	12q24.12	acyl-CoA dehydrogenase family, member 10
CCL7	17q11.2-q12	chemokine (C-C motif) ligand 7
CCL3L3	17q21.1	chemokine (C-C motif) ligand 3-like 3
DNAJB1	19p13.2	DnaJ (Hsp40) homolog, subfamily B, member 1
IER2	19p13.2	immediate early response 2
FOSB	19q13.32	FBJ murine osteosarcoma viral oncogene homolog B
KIR2DL4	19q13.4	killer cell immunoglobulin-like receptor, two domains, long cytoplasmic tail, 4
SLC5A3	21q22.12	solute carrier family 5 (sodium/myo-inositol co-transporter), member 3

Table 6.4: List of shared genes selected for CARDIoGRAM analysis

Post MI vs. Controls: Baseline (blue) and Stimulated (Orange)		
Gene	Chromosome	Gene Name
ANKRD35	1q21.1	ankyrin repeat domain 35
TRK1	1q21-q22	neurotrophic tyrosine kinase, receptor, type 1 (NTRK1)
OPN3	1q43	opsin3
DRD3	3q13.3	dopamine receptor D3
H1FX	3q21.3	H1 histone family, member X
CXXC5	5q31.2	CXXC finger protein 5
TNF	6p21.3	tumour necrosis factor
TES	7q31.2	testis derived transcript (3 LIM domains)
CLEC5A	7q33	C-type lectin domain family 5, member A
ORM1	9q31-q32	orosomuroid 1
OLFM1	9q34.3	olfactomedin 1
HBB	11p15.5	haemoglobin, beta
TIMM10	11q12.1-q12.3	translocase of inner mitochondrial membrane 10 homolog (yeast)
OAS1	12q24.2	2'-5'-oligoadenylate synthetase 1
HBA1	16p13.3	haemoglobin, alpha 1
SLC16A6	17q24.2	solute carrier family 16, member 6 (monocarboxylic acid transporter 7)
SS18	18q11.2	synovial sarcoma translocation, chromosome 18
PEX11G	19p13.2	peroxisomal biogenesis factor 11 gamma
PGLYRP1	19q13.2-q13.3	peptidoglycan recognition protein 1
SNX5	20p11	sortin nexin 5
PYGB	20p11.2-p11.1	phosphorylase, glycogen; brain
TFPI	2q32	tissue factor pathway inhibitor
CXCR7	2q37.3	chemokine (C-X-C motif) receptor 7 (CMKOR1)
LRRC33	3q29	leucine rich repeat containing 33
ITGB1	10p11.2	integrin, beta 1
CCDC47	17q23.3	coiled-coil domain containing 47

Table 6.5: List of genes in Post MI vs. Controls selected for CARDIoGRAM analysis

Offspring of MI vs. Controls: Baseline (blue) and Stimulated (Orange)		
Gene	Chromosome	Gene Name
AOAH	7p14-p12	acyloxyacyl hydrolase (neutrophil)
DGKD	2q37.1	diacylglycerol kinase, delta 130kDa
STIP1	11q13	stress-induced-phosphoprotein 1

Table 6.6: List of genes in Offspring of MI vs. Controls selected for CARDIoGRAM analysis

6.4.1.3 Findings

6.4.1.3.1 Association with CAD:

19 genes had SNPs which associated with CAD. 3 SNPs retained statistical significance after correction for multiple testing (Table 6.7). For each gene, the most statistically significant SNP was selected and then a Bonferroni correction was performed for the number of SNPs in the gene. For example, for the ACAD10 SNP rs2238151, the correction was performed as follows: corrected p value = uncorrected p value (0.000000136) x number of SNPs tested (43) = 0.00000585.

SNP	Gene	RA	RAF	p value	Corr. p value	OR	Group
rs2238151	ACAD10	T	0.63	1.36E-07	5.85E-06	1.08	Shared MI and Off MI
rs7649438	DRD3	C	0.74	1.84E-04	0.026	1.06	MI vs. Con baseline
rs11672503	PGLYRP1	T	0.84	2.34E-04	0.018	1.08	MI vs. Con baseline
rs1285933	CLEC5A	G	0.46	9.85E-04	0.064	1.05	MI vs. Con baseline
rs548829	OLFM1	T	0.02	0.001	0.254	1.14	MI vs. Con baseline
rs2238687	FOSB	T	0.87	0.001	0.057	1.09	Shared MI and Off MI
rs7636293	H1FX	C	0.33	0.002	0.073	1.05	MI vs. Con baseline
rs1046974	DGKD	A	0.43	0.003	0.356	1.04	Off MI vs. Con CRP
rs4846886	ARV1	G	0.33	0.003	0.229	1.05	Shared MI and Off MI
rs7801689	AOAH	C	0.89	0.003	1	1.07	Off MI vs. Con baseline
rs10488675	HBB	G	0.25	0.005	0.587	1.05	MI vs. Con baseline
rs3775378	FAM13A1	T	0.10	0.005	1	1.04	Shared MI and Off MI
rs2857706	TNF	T	0.17	0.006	0.813	1.05	MI vs. Con baseline
rs8044711	HBA1	T	0.12	0.007	0.184	1.07	MI vs. Con baseline
rs12534640	HIP1	C	0.97	0.007	1	1.25	Shared MI and Off MI
rs17738942	SLC5A3	C	0.93	0.008	0.437	1.08	Shared MI and Off MI
rs9832803	LXN	C	0.63	0.008	0.887	1.04	Shared MI and Off MI
rs9890694	SLC16A6	C	0.88	0.009	0.607	1.06	MI vs. Con baseline
rs17138532	TES	A	0.87	0.010	1	1.05	MI vs. Con baseline

Table 6.7: SNPs in differentially expressed genes with significant association with CAD

The 19 genes which were significantly associated with CAD in CARDIoGRAM are shown. The shaded rows are those genes which did not retain statistical significance after correction for multiple testing. RA= risk allele, RAF = risk allele frequency, OR = odds ratio.

The genetic variant with the strongest association with CAD (and MI; see below) was rs2238151 in ACAD10 (Figure 6.30). Expression of this gene was suppressed in both the Post MI and Offspring of MI groups after platelet mediated stimulation. This was significantly associated with both CAD and MI in CARDIoGRAM with an odds ratio of 1.08 for both ($p < 10^{-5}$ for both after correction for multiple testing). The risk allele frequency was 63% for CAD and 57% for MI.

ACAD 10 is a component of the mitochondrial enzyme complex which participates in beta oxidation of fatty acids. Other variants in this gene (rs601663 and rs659964) have been associated with insulin resistance and type II diabetes mellitus (Bian et al., 2010). Lower levels of lipid oxidation and larger adipocyte size were associated with these variants. The SNP rs2238151 itself has been associated with oxidative stress in the context of head and neck cancer in a previous study (Hakenewerth et al., 2011).

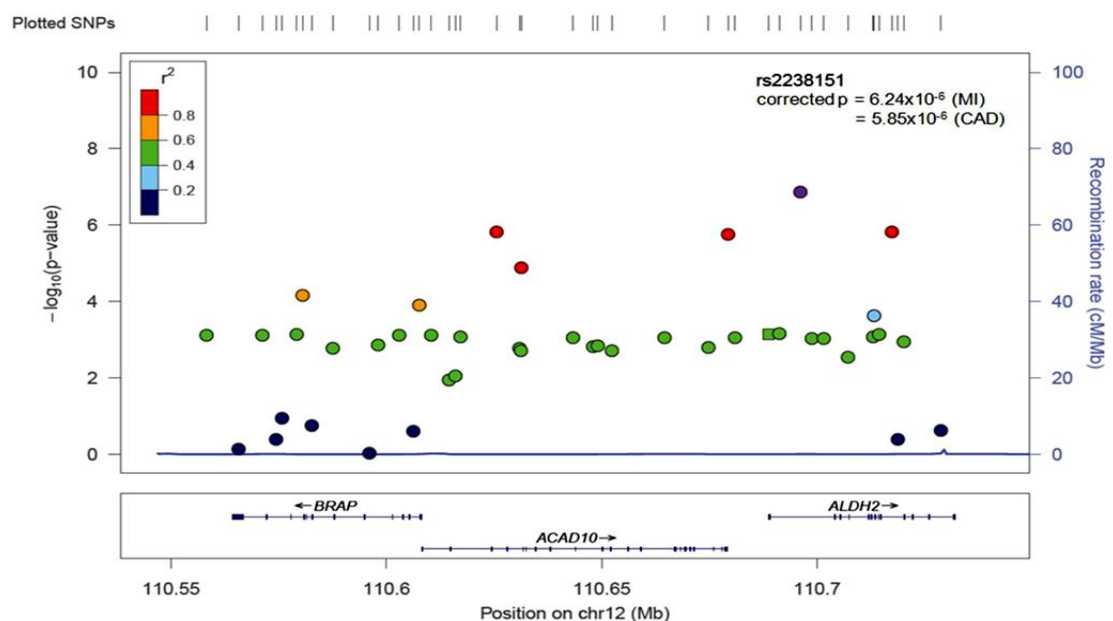


Figure 6.30: Genetic variant in ACAD10 (rs2238151) associated with CAD and MI.

The variant rs2238151 (purple dot) was strongly associated with CAD and MI. The left y-axis denotes the p value expressed as $-\log_{10}$. Recombination rate is depicted on the right y-axis and in this instance is the continuous blue line at the bottom of the image. The chromosome locus is shown on the x axis.

DRD3 and PGLYRP1 were the other two genes with variants which had a statistically significant association with CAD (Figures 6.31 and 6.32). Neither had a significant association with MI. In the Post MI group, DRD3 showed significantly lower levels before and after stimulation while PGLYRP1 levels were significantly higher under both conditions (Figure 6.33). These were not differentially expressed in the offspring groups.

PGLYRP1 is a receptor for peptidoglycan and expressed in human atherosclerotic lesions (Rohatgi et al., 2009). DRD3 is a dopamine receptor which is localized in the limbic areas and has no recognized role in CAD.

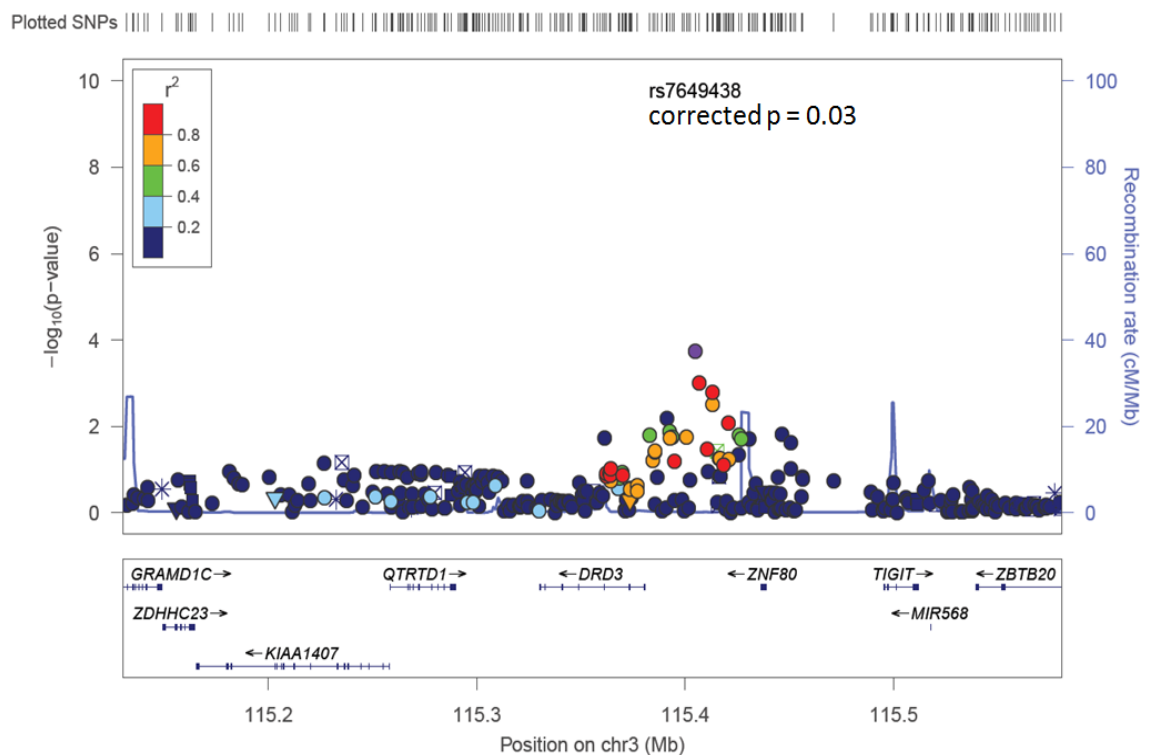


Figure 6.31: Genetic variant in DRD3 (rs7649438) associated with CAD.

The Figure shows the variant rs7649438 (purple dot) which is significantly associated with CAD. The risk allele frequency was 74% and the odds ratio was 1.06. The left y-axis denotes the p value expressed as $-\log_{10}$. Recombination rate is depicted on the right y-axis and in this instance is the blue line at the bottom of the image. The chromosome locus is shown on the x axis.

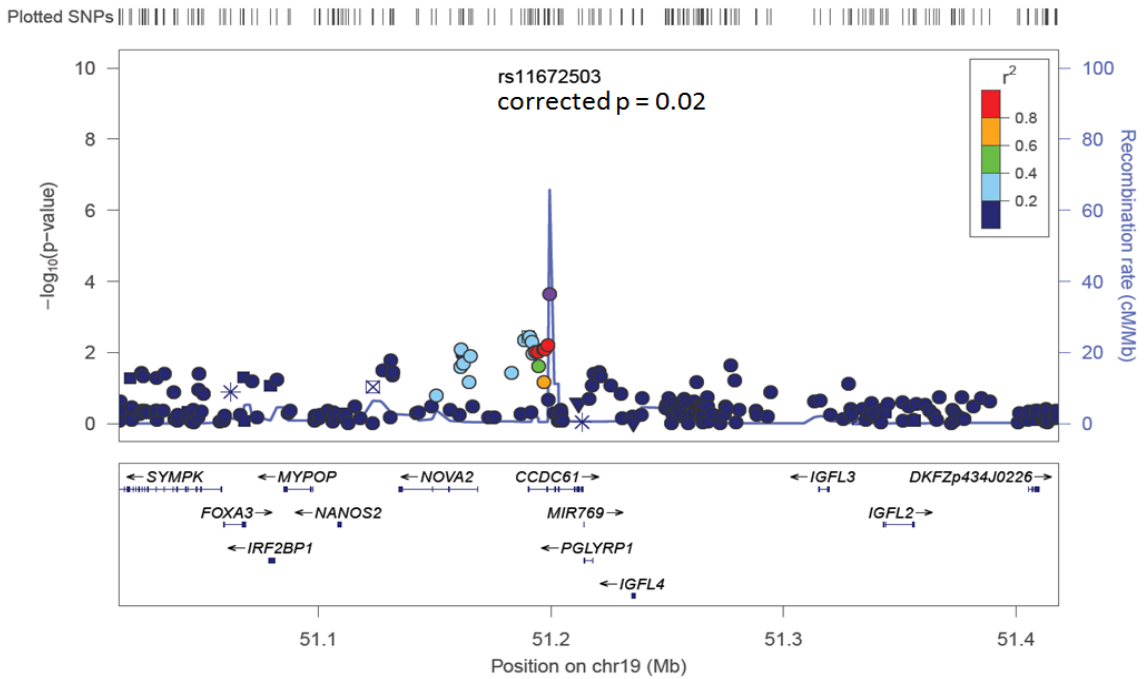


Figure 6.32: Genetic variant in PGLYRP1 (rs11672503) associated with CAD.

The variant rs11672503 (purple dot) is associated with CAD. The risk allele frequency was 84% and the odds ratio was 1.08. The left y-axis denotes the p value expressed as $-\log_{10}$. A recombination spot is seen in the region of the SNP. The chromosome locus is shown on the x axis.

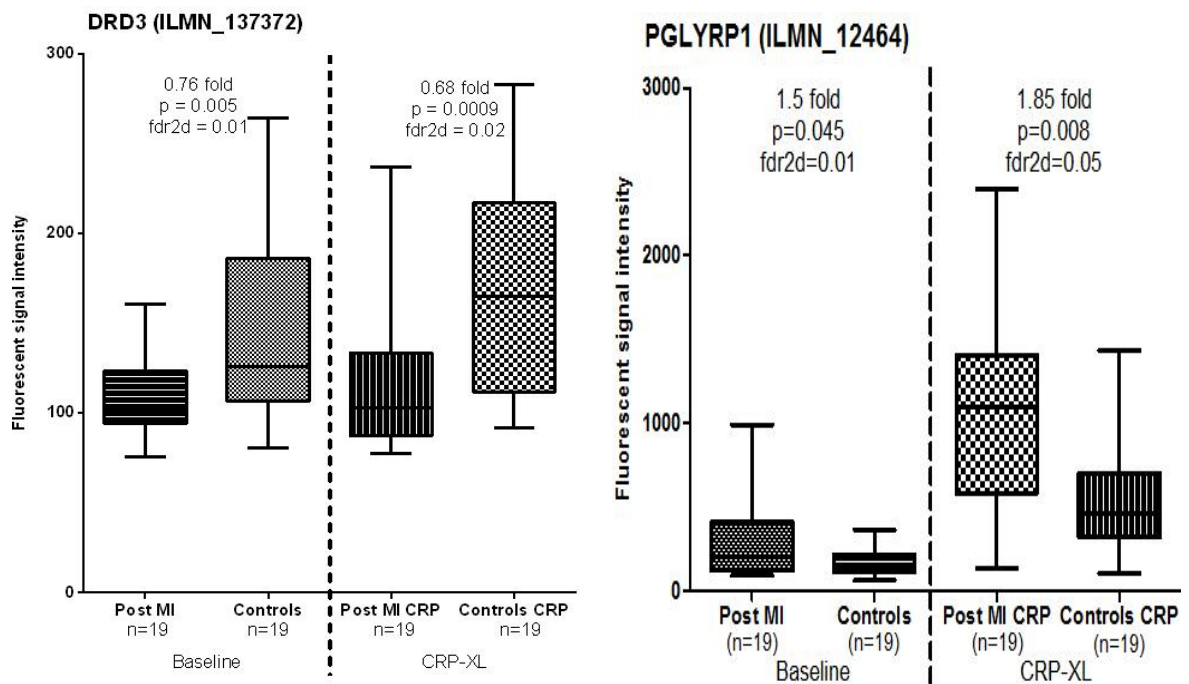


Figure 6.33: Differential expression of DRD3 and PGLYRP1 in Post MI.

Fluorescent signal intensities before and after platelet-mediated stimulation are shown. The left panel shows the expression levels of DRD3 in Post MI and controls and the right panel shows levels of PGLYRP1. Statistically significant differential expression is seen in both genes under both conditions. Error bars denote the range of expression. Fold changes, p values and false discovery rates are provided where applicable.

6.4.1.3.2 Association with MI:

The same set of 48 differentially expressed genes was tested of which 3 retained statistical significance after correction for multiple testing. These were rs2238151 in ACAD10, rs4506448 in ARV1 and rs991479 in CCL3L3 (Table 6.8).

SNP	Gene	RA	RAF	p value	Corr. p value	OR	Group
rs2238151	ACAD10	T	0.57	1.45E-07	6.24E-06	1.09	Shared MI and Off MI
rs4506448	ARV1	T	0.06	0.0003	0.027	1.12	Shared MI and Off MI
rs991479	CCL3L3	G	0.94	0.0004	0.002	1.28	Shared MI and Off MI
rs2034761	DGKD	G	0.45	0.0004	0.063	1.20	Off MI vs. Con CRP
rs6798102	DRD3	T	0.72	0.001	0.117	1.06	MI vs. Con baseline
rs2279562	LXN	A	0.78	0.001	0.127	1.07	Shared MI and Off MI
rs11770855	CLEC5A	C	0.33	0.001	0.087	1.07	MI vs. Con baseline
rs4766663	OAS1	G	0.63	0.002	0.248	1.08	MI vs. Con baseline
rs727508	TFPI	C	0.03	0.002	0.271	1.16	MI vs. Con CRP
rs12143768	TRK1	A	0.15	0.003	0.342	1.07	MI vs. Con baseline
rs3801300	AOAH	C	0.06	0.003	1	1.12	Off MI vs. Con baseline
rs17039656	OLFM1	C	0.86	0.005	1	1.07	MI vs. Con baseline
rs6979456	TES	G	0.13	0.005	0.893	1.08	MI vs. Con baseline
rs6439169	H1FX	A	0.31	0.006	0.226	1.05	MI vs. Con baseline
rs9909207	SLC16A6	C	0.91	0.006	0.422	1.09	MI vs. Con baseline
rs4835681	EGR1	C	0.58	0.007	0.277	1.05	Shared MI and Off MI
rs1980497	PYGB	G	0.91	0.007	0.652	1.11	MI vs. Con baseline
rs17738942	SLC5A3	C	0.93	0.007	0.370	1.10	Shared MI and Off MI
rs11672503	PGLYRP1	T	0.85	0.008	0.62	1.09	MI vs. Con baseline

Table 6.8: SNPs in differentially expressed genes with significant association with MI

The 19 genes which were significantly associated with MI in CARDIoGRAM are shown. The shaded rows are those genes which did not retain statistical significance after correction for multiple testing. RA= risk allele, RAF = risk allele frequency, OR = odds ratio.

As previously noted in section 6.2, expression levels of ACAD10 were significantly lower compared to controls after stimulation in both the Post MI and Offspring of MI groups. ARV1 levels were significantly lower in the Offspring of MI group at baseline and after stimulation whilst lower levels of borderline statistical significance were noted in the Post MI group. CCL3L3 levels were significantly higher in the Post MI group after stimulation with a similar trend of borderline statistical significance in the Offspring of MI group.

ARV1 (Figure 6.34) codes a resident protein in the endoplasmic reticulum that is essential for cholesterol homeostasis. Deficiency of this protein results in cellular organelle disruption and impaired hepatic cholesterol metabolism (Tong et al., 2010). The SNP rs4506448 was associated with MI in CARDIoGRAM with a risk allele frequency of 6% and an odds ratio of 1.12.

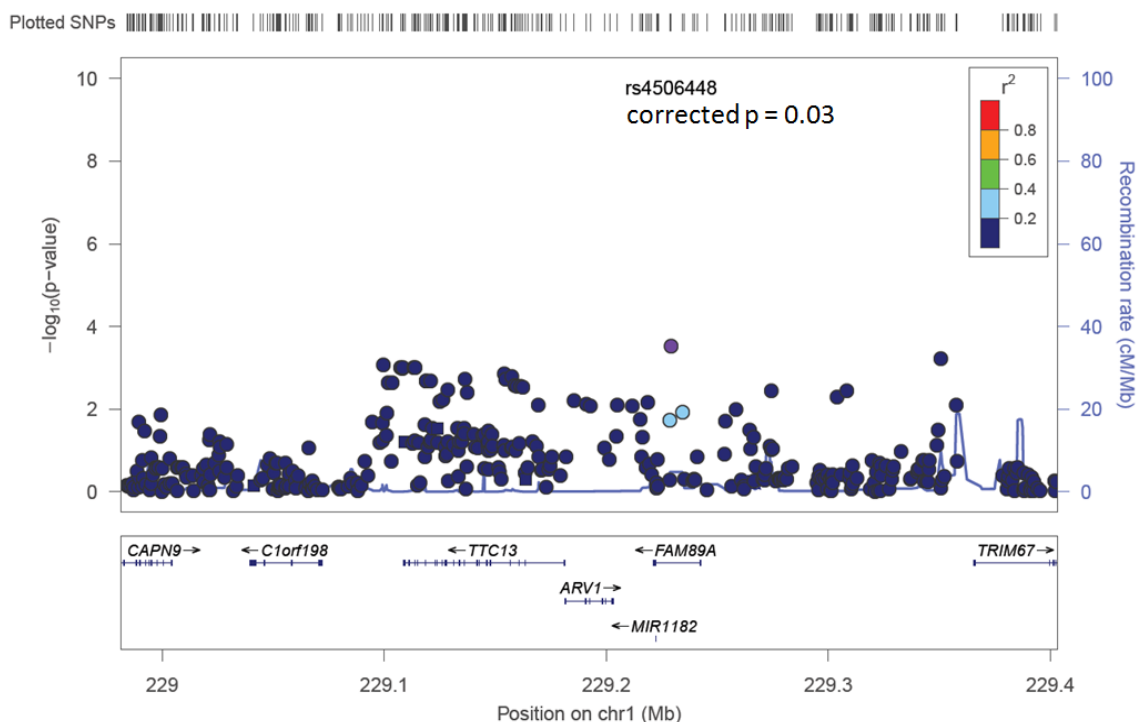


Figure 6.34: Genetic variant in ARV1 (rs4506448) associated with CAD.

The Figure shows the variant rs4506448 (purple dot) which is associated with CAD. The left y-axis denotes the p value expressed as $-\log_{10}$. The chromosome locus is shown on the x axis.

CCL3L3 (Figure 6.35) which is closely related to CCL3 and CCL3L1 is a chemokine that is part of a cluster of chemokine genes on chromosome 17q12. Copy number variations in this and associated genes have been associated with susceptibility to infections and perturbations in the immune response. The SNP rs991479 was associated with MI in CARDIoGRAM with a risk allele frequency of 94% and an odds ratio of 1.28.

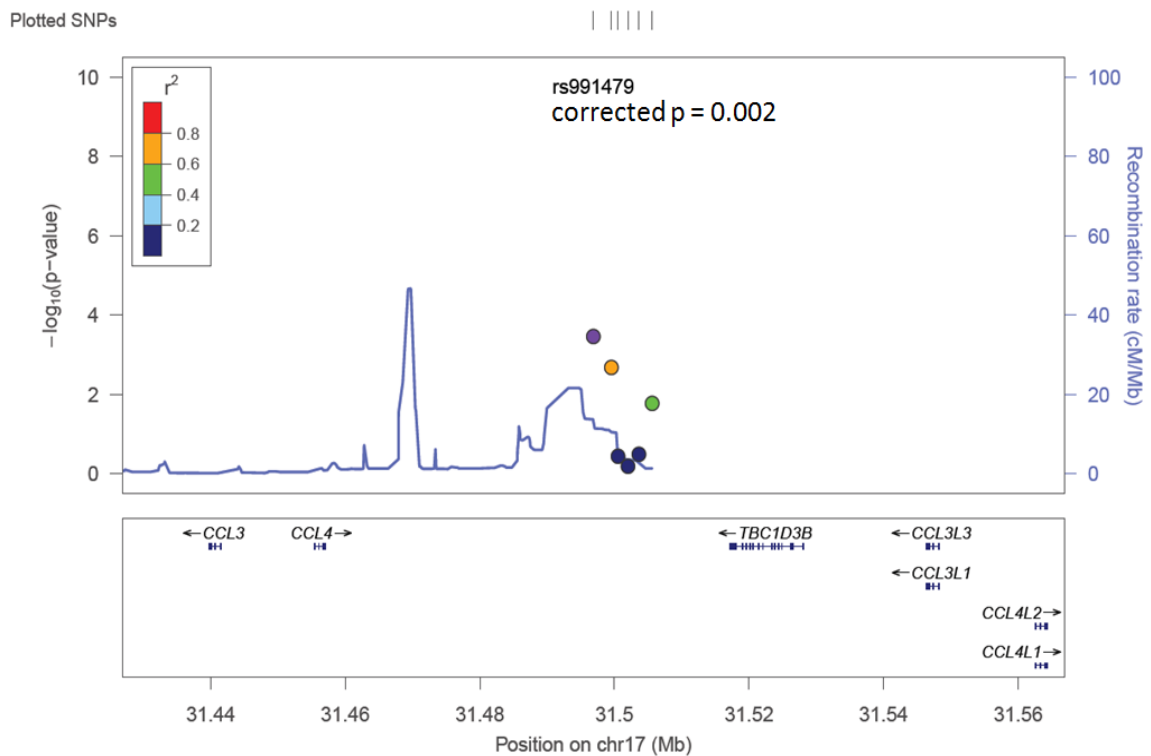


Figure 6.34: Genetic variant in CCL3L3 (rs991479) associated with CAD.

The Figure shows the variant rs991479 (purple dot) which is associated with CAD. The left y-axis denotes the p value expressed as $-\log_{10}$. A recombination spot is seen in the region of the SNP. The chromosome locus is shown on the x axis.

6.4.2 Genetic variants and monocyte gene expression

6.4.2.1 Background

The transcriptome has the potential to be the essential link between genetic variants and their associated disease by providing insights into the biological mechanisms that mediate the risk attributable to a genetic variant. One proposed mechanism by which genetic variants mediate risk would be by influencing the magnitude and direction of gene expression. Therefore the transcriptome can be considered as an intermediate phenotype of disease which can be quantified by microarray and PCR techniques. The genetic variants which determine these quantitative traits in gene expression are referred to as expression Quantitative Trait Loci or eQTL. By correlating GWE data with GWAS, those genetic variants that determine levels of gene expression (i.e., eQTL) can be identified.

6.4.2.2 Cardiogenics – a GWE/GWAS study of human monocytes

Cardiogenics is a multicentre study that investigated the monocyte/macrophage lineage in the context of atherosclerosis. Genome wide transcript abundance in the monocyte was studied to assess whether this correlates with genetic variants that associate with the risk of CAD. This study assessed the monocyte transcriptome in 363 CAD patients and 395 controls especially focusing on genetic variants which regulate monocyte gene expression, i.e., expression quantitative trait loci - eQTL (Rotival et al., 2011). This study therefore attempted to explore both genetic and environmental influences on monocyte gene expression.

Cardiogenics used the Illumina HT-12 v3 BeadChip array for transcriptome analysis which shares >75% of the probe sets with Illumina Human-6 expression BeadChip, the microarray platform used in the current study (Shi et al., 2010).

6.4.2.3 eQTLs in differentially expressed genes

The genes which showed the most significant differential expression in this study were investigated within the Cardiogenics dataset to identify genetic variants which determine levels of gene expression. 12 genes had cis-acting variants which associated with levels of gene expression (eQTLs) in monocytes according to genotype (Figure 6.35 and Table 6.9).

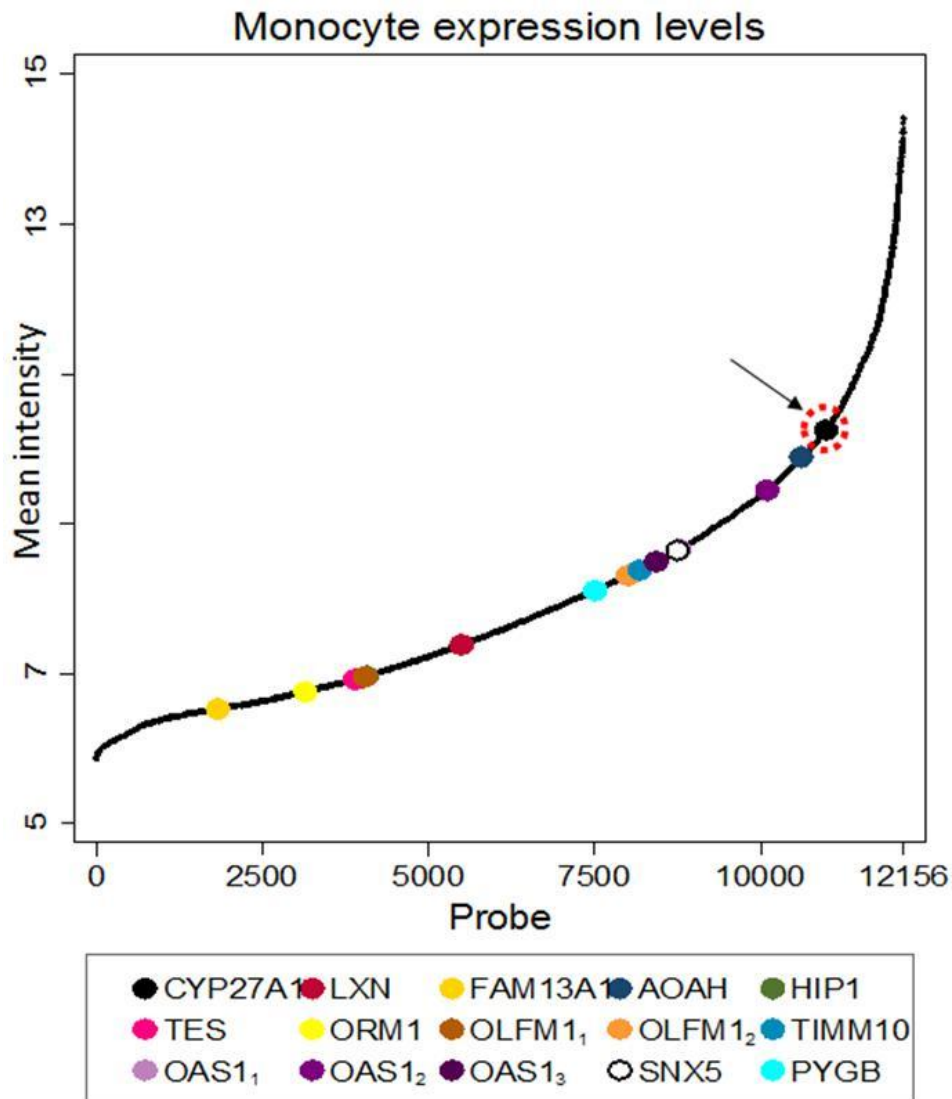


Figure 6.35: Candidate genes with eQTLs in Cardiogenics

The graph shows mean fluorescent signal intensities of 15 transcript probes representing 12 candidate genes (OLFM1 is represented by 2 probes and OAS1 with 3 probes on the array) with eQTLs in Cardiogenics. The Probe sets are arranged on the x-axis in ascending order of Probe ID. Mean fluorescent signal intensities (log₂ scale) are plotted on the y-axis. CYP27A1, with shared trends in expression profiles in the Post MI and Offspring of MI groups is highlighted in the red dotted circle (arrow).

Gene	Locus	Comparison	Condition	RNA levels	SNP (eQTL)	SNP p value
CYP27A1	2q33-qter	Post MI and Offspring of MI	Baseline & stimulated	↑	rs933994	2.9x10 ⁻⁷⁰
LXN	3q25.32	Post MI and Offspring of MI	Stimulated	↓	rs17699324	1.3x10 ⁻⁶⁰
FAM13A1	4q22.1	Post MI and Offspring of MI	Stimulated	↑	rs1965869	1.1x10 ⁻¹⁵
AOAH	7p14-p12	Offspring of MI	Baseline	↑	rs10275462	5.9x10 ⁻²¹
HIP1	7q11.23	Post MI	Stimulated	↑	rs1179620	2.4x10 ⁻⁵⁹
TES	7q31.2	Post MI	Baseline	↓	rs1048508	6.3x10 ⁻²⁵
ORM1	9q31-q32	Post MI	Both	↑	rs7851482	4.9x10 ⁻⁵²
OLFM1	9q34.3	Post MI	Baseline	↓	rs10120023	9.7x10 ⁻²⁶
OLFM1	9q34.3	Post MI	Baseline	↓	rs10858300	1.1x10 ⁻³⁴
TIMM10	11q12.1-q12.3	Post MI	Both	↓	rs2848630	1.2x10 ⁻²¹³
OAS1	12q24.2	Post MI	Baseline	↑	rs7965538	4.4x10 ⁻³⁰
OAS1	12q24.2	Post MI	Baseline	↑	rs3177979	1.1x10 ⁻¹⁷⁷
SNX5	20p11	Post MI	Baseline	↓	rs11696646	1.4x10 ⁻²²
PYGB	20p11.2-p11.1	Post MI	Both	↓	rs3746337	1.4x10 ⁻⁵⁷

Table 6.9: Candidate genes with eQTLs in Cardiogenics

The Table lists the genes which were differentially expressed in Post MI or Offspring of MI or both compared to respective controls. The column ‘RNA levels’ indicate whether the transcript levels were relatively higher or lower in these groups. The eQTL and corresponding p values in Cardiogenics are also shown. All genetic variants in this Table were cis-acting SNPs.

Of the 12 genes identified, detailed data for CYP27A1 as an example are presented below. CYP27A1 was selected for further eQTL analysis as it had shown similar trends in expression in both the Post MI and Offspring of MI groups which were also confirmed by Q-PCR. SNP rs933994 showed a significant association with gene expression according to genotype (Figures 6.36-37).

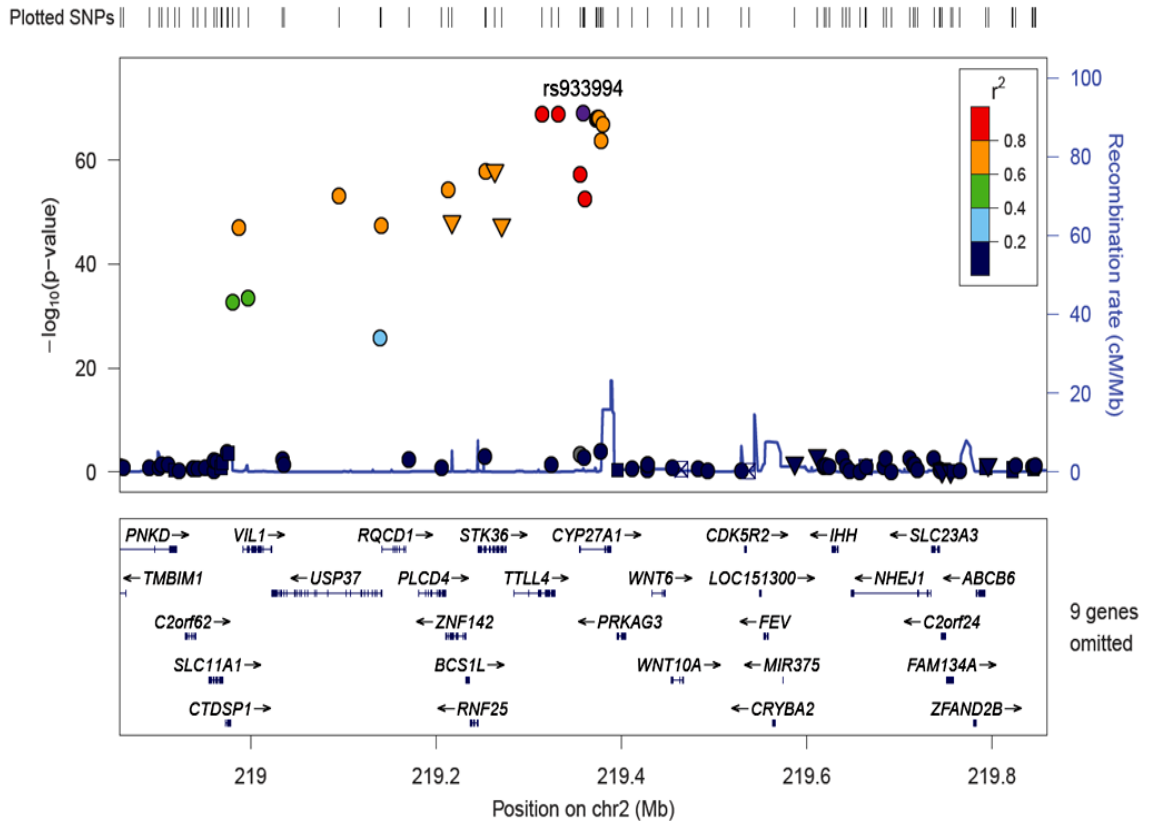


Figure 6.36: eQTL in gene CYP27A1

rs933994 shown in blue is an intronic SNP in the gene CYP27A1 which strongly associates with transcript levels according to genotype.

The fluorescent signal intensity for the CYP27A1 probe set in Cardiogenics is shown in Figure 6.37 according to genotype.

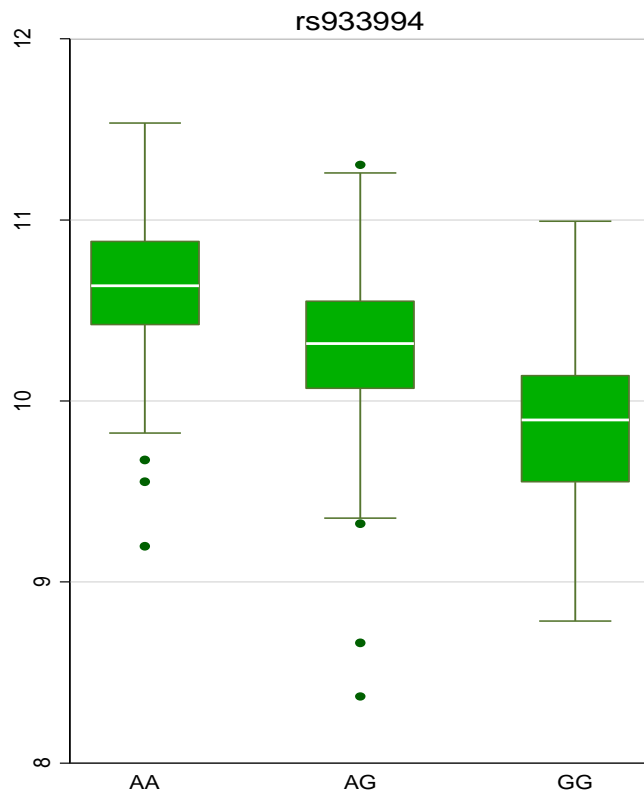


Figure 6.37: CYP27A1 gene expression according to genotype

The Figure shows relative levels of CYP27A1 gene expression (fluorescent signal intensity) according to genotype for the intronic SNP rs933994.

6.5 DISCUSSION

In the initial sections in this Chapter, shared trends were identified in the differential gene expression observed in two high risk groups: those with established premature coronary artery disease manifesting as acute myocardial infarction (Post MI; Group 1) and those with a strong genetic risk of premature myocardial infarction (Offspring of MI; Group 2).

The genes which showed higher expression levels in the two groups included transcription factors, enzymes regulating lipid metabolism, chemokines and heat shock proteins. The down regulated genes were modulators of inflammation. Selected genes were validated by Q-PCR to confirm the observed trends in expression. Similar trends in monocyte gene expression observed in these two groups with an increased genetic risk of myocardial infarction suggests that these may be genetically determined. Therefore differentially expressed genes were investigated to identify genetic variants which may either associate with CAD/MI or determine levels of gene expression in monocytes.

Arbitrary thresholds of fold changes and statistical significance were set to select genes with similar trends in gene expression in the Post MI and Offspring of MI groups. In doing so, it is possible that certain genes with less impressive shared trends in expression but nonetheless with genetic variants associated with CAD or MI were excluded from the analysis.

Interestingly five genes showing differential expression in monocytes also had genetic variants which associated with CAD/MI. Of these, ACAD10 was the most interesting gene as it fulfilled the following criteria:

- Differential expression in both Post MI and Offspring of MI groups after platelet-mediated monocyte stimulation.
- Presence of a genetic variant which had a statistically significant association with CAD and MI.

Two other genes, PGLYRP1 and DRD3 had variants with significant association with CAD while variants in CCL3L3 and ARV1 associated with MI in large scale GWAS. PGLYRP1 is expressed in atherosclerotic plaques while ARV1 has a role in intracellular sterol transport. In addition, CCL3, a pro-inflammatory chemokine which showed similar trends in gene expression is a closely related gene to CCL3L3 which had a genetic variant with a significant association with MI.

Analysis of the Cardiogenics data revealed 12 genes which were differentially expressed in either Post MI (Group 1), Offspring of MI (Group 2) or both that had genetic variants which determined levels of gene expression. CYP27A1 which showed similar trends in both Offspring of MI and Post MI groups had an eQTL (rs933994) which determined monocyte gene expression. This gene regulates non HDL-mediated cholesterol efflux from monocyte derived macrophages in atherosclerotic lesions and the shared trends in gene expression in individuals with premature MI and with high genetic risk of MI alongside the eQTL regulating monocyte gene expression strongly suggests a mechanism of genetic regulation of individual disease susceptibility to CAD. It is important to note that all the

genetic variants identified in this analysis were in non coding regions of their respective genes.

These findings provide evidence to substantiate the hypotheses that: (i) variations in gene expression of the circulating peripheral blood monocyte determine individual susceptibility to atherosclerotic coronary artery disease and that (ii) platelet driven stimulation of circulating monocytes plays an important role in the initiation, progression and manifestation of atherosclerotic coronary artery disease. This analysis helps to prioritise some of the genes identified by my work for further analysis which are discussed in the next Chapter.

CHAPTER 7

Discussion

7.1 THE CHALLENGE OF CAD IN THE 21ST CENTURY

Atherosclerotic coronary artery disease has gained prominence as a global phenomenon adversely affecting human health across the boundaries of age, gender, ethnicity and geographic location. This has prompted a consolidation of scientific knowledge on the epidemiology of CAD and the modifiable and non modifiable factors that contribute to this. In parallel to such population based studies, insights into pathophysiology of atherosclerosis have progressed significantly from the early works of Klotz and Baldauf on calcification in the aorta more than a century ago (Klotz, 1905, Baldauf, 1906) and the seminal observations of Bailey linking dietary excess of cholesterol to the development of aortic atheroma (Bailey, 1916). In the last three decades, the work of Russell Ross has led the way in delineating the complex cellular and molecular events which orchestrate this initially protective, but later deregulated, inflammatory, fibro-proliferative response to risk agents such as modified cholesterol (Ross and Glomset, 1973, Ross and Harker, 1976, Ross, 1993, Ross, 1999). In parallel to these developments investigating the mechanisms underlying atherosclerotic plaque progression, large scale epidemiological studies in the latter half of the 20th century have identified genetic and environmental risk factors that determine individual susceptibility to coronary atherosclerosis. CAD is now recognized as a disease phenotype with genetic and environmental contributors and interactions which mediate their influence at a cellular level through perturbations in monocyte and platelet biology and their effects on the vessel wall (Oemar et al., 1995).

The pace of basic science research in CAD has been aided by technological advances in molecular biology such as large scale genotyping, microarrays including exome arrays and platforms for proteomic analysis as well as the development of statistical and computational tools capable of handling the high throughput of data generated from such experiments. In addition, leading researchers in the field have actively collaborated through consortia such as Cardiogenics and CARDIoGRAM which has resulted in an exponential increase in the knowledge base in the genetics of CAD. This is evidenced by the fact that in the five years since the first report of a genetic risk variant for CAD in 2007 (McPherson et al., 2007, Helgadottir et al., 2007), a further 36 genetic variants have been identified and validated (Roberts and Stewart, 2012).

The challenge posed by CAD in the 21st century will be in the delineation of molecular pathways that determine the risk of development and progression of CAD in a particular individual. Generation of such highly accurate and person specific risk profiles is a prerequisite to the delivery of personalized healthcare to all patients (Desiere and Romano Spica, 2012).

7.2 RATIONALE, DESIGN AND OUTCOMES OF THE STUDY

7.2.1 Rationale for the use of transcriptome analysis

Transcriptomics is strategically placed at the crossroads of genetics and environment in CAD. The transcriptome is responsive both to genetic and environmental changes which may occur independently and in concert. Genome wide expression (GWE) analysis is a useful exploratory tool in understanding the mechanisms by which the various genetic risk variants in

CAD confer the increased risk, considering that the vast majority of these are in genomic regions with no obvious links to CAD (Schunkert et al., 2011).

7.2.2 Design of the current study

Gene expression profiling of circulating monocytes was performed using a whole genome microarray platform in phenotypically well characterised groups of individuals. The study design allowed an unbiased approach to the discovery of novel candidate genes which may influence the initiation, progression and clinical manifestations of atherosclerotic coronary artery disease.

This study was well suited to explore the genetic determinants underlying CAD which manifest as transcriptional changes in the monocyte in response to a physiologically relevant platelet mediated stimulus. The well defined subject groups studied under resting and stimulated conditions allowed maximal separation of monocyte phenotypes and attempted to minimise confounding variables. The microarray experiments, subsequent bioinformatic analyses and validation by TaqMan Q-PCR ensured that the results obtained were real, reproducible and of biological relevance.

Two types of variations in monocyte gene expression were studied:

1. Possible heritable variations by study of individuals with high familial risk of premature CAD.
2. Variations in response to external perturbations of pathophysiological relevance (stimulation of monocytes by collagen [CRP-XL] activated platelets).

In addition, the effects of two confounding factors were also explored.

1. Therapeutic interventions in established CAD including those intended to modify risk factors (primary prevention) and those aimed at limiting the pathophysiological alterations in established CAD (secondary prevention) are known to affect the monocyte transcriptome. Not surprisingly, the same medication has varying effects on gene expression of cells such as platelets, monocytes and endothelial cells depending on the clinical condition of the subject. For instance, hydroxyl methyl glutaryl coenzyme-A inhibitors (HMG Co-A inhibitors; 'statins') have effects on cellular stress and inflammation in those prone to CAD (without established disease) while they have antiproliferative effects in patients with a previous myocardial infarction.
2. Monocyte gene expression is also affected by tissue necrosis following myocardial infarction and tissue repair signalling in incipient or established congestive cardiac failure. Such changes also have an effect on the transcriptome which is distinct from the changes which underlie the development and progression of disease.

These issues were addressed by the stimulation experiment in the study. By using a physiologically relevant stimulus (addition of cross linked collagen related peptide – CRP-XL to activate platelets) we were able to drive monocyte gene expression in a direction which is of relevance to atherosclerosis and atherothrombosis. The decision to conduct the stimulation experiment in freshly isolated whole blood rather than in cultured monocyte derived macrophages adds to the pathophysiological relevance of the experiment by simulating the conditions which follow platelet-mediated stimulation in vivo.

This stimulation experiment has relevance to both arms of the study. In the established CAD arm (Post MI and their controls), the stimulation experiment prompted changes in the monocyte transcriptome which may occur *in vivo* when monocytes are stimulated by collagen-activated platelets, for instance after atherosclerotic plaque rupture. In the offspring cohort, this stimulation experiment revealed the changes in gene expression of relevance to the development of atherogenesis. Pertinent environmental stimuli are often required to reveal the genetically determined differences in gene expression. Monocyte transcriptome analysis after a stimulation experiment of relevance to the pathophysiology of CAD helped to explore the complex interactions between genetic and environmental influences.

7.2.2.1 Subject selection and definition of study groups

In complex phenotypes such as CAD with multiple strands of environmental and genetic influences ('classical' risk factors, haemostatic and thrombotic tendencies, inflammatory mediators and apoptosis amongst others), selection of study subjects will govern the 'signal to noise ratio' of experiments, especially those on a large scale such as transcriptomics.

In selecting the subjects with established CAD, stringent inclusion criteria were applied including ethnicity (Caucasians from a defined geographic region), age (<65 years), timing of recruitment (3-6 months after their first ever myocardial infarction) and clinical condition (stable, established on optimum and stable doses of relevant pharmacotherapy, no clinically evident heart failure at the time of recruitment).

Patients with diabetes mellitus, chronic inflammatory conditions and acute infections were excluded as these conditions are likely to affect monocyte transcriptome. All recruits had a confirmed diagnosis of ST segment elevation myocardial infarction (STEMI). The underlying pathology in STEMI is coronary atherosclerotic plaque rupture followed by total or near total thrombotic occlusion of the coronary artery resulting in acute myocardial ischaemia leading to infarction. Optical coherence tomography (OCT) of coronary arteries have shown that patients with STEMI have significantly longer regions of rupture with more missing areas (denudation) in the fibrous cap and have plaques with more lipid content than patients with NSTEMI (Toutouzas et al., 2011). Intravascular ultrasound (IVUS) studies have also shown that plaque burden, plaque rupture and intraluminal thrombus are significantly more prevalent in STEMI compared to NSTEMI (Hong et al., 2010, Lee et al., 2009b). Occlusive coronary thrombosis is also more prevalent in STEMI compared to other types of acute coronary syndromes (Koyama et al., 2002). Such lesions were associated with higher levels of C reactive protein (CRP) and were not present in patients with stable angina (Lee et al., 2009b). Selection of STEMI patients with internationally accepted diagnostic criteria based on the 12 lead ECG allowed unambiguous identification of appropriate study subjects.

The controls for the premature CAD group had no pre-existing diagnosis of chronic illnesses or classical risk factors for CAD and were not on pharmacotherapy. They were matched for age, gender and smoking status, as the latter is known to affect monocyte gene expression (Doyle et al., 2010, Chong et al., 2002).

The offspring groups were robustly selected based on the clear delineation of family history. The reported family history of premature myocardial infarction was confirmed by review of hospital records of parents. None of the Control offspring had a family history of sudden deaths, myocardial infarction or stroke. None of the study groups had subjects with chronic inflammatory conditions or platelet/haemostatic disorders.

7.2.2.2 Sample processing

All blood samples were collected in the fasting state to eliminate the effect of glycaemic changes on the monocyte transcriptome (Stan et al., 2011, Bao et al., 2010). The cell isolation method ensured that monocytes were isolated with minimal mechanical stress (no centrifugation steps or column based separation) as gene expression is also affected by mechanical stress (Kim et al., 2008a). RNA degradation was kept to a minimum by ensuring that RNA was extracted and stored at -80°C within one hour of venesection from all baseline samples.

7.2.3 Study objectives

The study explored the following aspects pertaining to monocyte gene expression in various stages of atherosclerotic coronary disease:

- Differences in monocyte gene expression before and after platelet-mediated stimulation in patients Post MI (Group 1) and controls (Group 3).
- Differences in monocyte gene expression before and after platelet-mediated stimulation in healthy men with contrasting familial risk of MI (groups 2, 4).
- Genetic link between differentially expressed genes and risk of CAD or gene expression.
- The effect of platelet-mediated stimulation on monocyte gene expression.

In the following sections, the main findings which answer each of the aforementioned questions are discussed.

7.2.3.1 Transcriptome of resting and stimulated monocytes in overt atherosclerotic coronary artery disease (Post MI vs Controls)

Pro-inflammatory molecules were up-regulated in patients with premature MI. Tumour necrosis factor alpha ($TNF\alpha$), Orosomucoid-1 (ORM1) and Peptidoglycan recognition protein-1 (PGLYRP1), all of which have been associated with inflammatory response, were up-regulated at baseline. In addition, the differentially expressed genes were noted to have regulatory roles in Wnt signalling which is known to play a role in inflammation and tissue repair.

Platelet driven stimulation of monocytes in the Post MI group resulted in differential expression of genes involved in coagulation, cholesterol metabolism and transcriptional regulation. In addition, there were differences in gene expression driven by pharmacotherapy, especially statins.

One of the most interesting observations, confirmed by Q-PCR is the relative reduction in expression of TFPI. This is a regulator of tissue factor in human monocytes which is expressed in high levels in resting monocytes and in proportion to an increase in tissue factor levels in LPS stimulated monocytes (Basavaraj et al., 2010). Tissue factor is expressed at very low levels in intact vasculature but at higher levels in atherosclerotic plaques. Its expression is enhanced many fold following plaque rupture (Jude et al., 2005). The significantly lower TFPI levels following platelet-mediated stimulation of resting monocytes from patients with premature MI suggests a defect in the regulation

of tissue factor activity following plaque rupture. This may be a reason for the occlusive thrombosis seen in STEMI patients following plaque rupture.

The changes in Wnt signalling pathway both in resting and stimulated monocytes from patients with MI suggests that oxidative stress response is significantly different in patients with MI compared to controls. There is a suggestion that Wnt signalling is diverted from repair and proliferation to stress signalling, cell senescence and apoptosis.

The effects of pharmacotherapy are apparent from the expression profiles of proinflammatory and prothrombotic genes which fail to be up-regulated following CRP-XL stimulation. Predominantly, these are seen to be a consequence of statin therapy.

7.2.3.2 Transcriptome of resting and stimulated monocytes in individuals with inherited risk of atherosclerosis

A number of transcription factors which mediate hypoxia induced signalling were up-regulated in resting monocytes in healthy Offspring of MI. Tissue hypoxia is recognised as an early event in atherogenesis and promotes intracellular lipid accumulation (Lattimore et al., 2005) and lipid oxidation (Rydberg et al., 2004). There is evidence suggesting that hypoxia promotes proinflammatory signalling in monocytes and endothelial cells (Chakrabarti et al., 2009). In addition, plaque development and progression have been shown to result in hypoxia and stimulate plaque angiogenesis as a result of specific signalling mediated by hypoxia-inducible factor (HIF). ARNT, one of the differentially expressed genes in this group is a constitutive component of HIF

which suggests that early atherosclerotic events may explain the observed up-regulation of this gene and transcription factors (Sluimer and Daemen, 2009).

The chemokine CCL3 and two related genes, CCL3L1 and CCL3L3 were up-regulated in Offspring of MI. A similar trend was seen in the Post MI group especially for CCL3L3. The role of CCL3 and its receptor CCR5 in atherogenesis is increasingly recognised, especially in recruitment of monocytes to atherosclerotic plaques (Jones et al., 2011). There is also evidence that CCL3 levels are increased in macrophages following exposure to very low density lipoproteins (VLDL) (Saraswathi and Hasty, 2006) and that simvastatin reduces surface expression of the CCL3 receptor, CCR5 (Veillard et al., 2006).

These changes suggest that in apparently healthy subjects with a high genetic risk profile for CAD, there are alterations in molecular pathways of relevance to the development and progression of atherosclerosis. The differentially expressed genes have established roles in atherogenesis and included chemokines and transcription factors.

There was significant differential expression of heat shock proteins (HSPs) in the Offspring of MI compared to controls. HSP90AB1, one of the components of the HSP90 complex was significantly up-regulated in Offspring of MI with no overt clinical evidence of CAD. HSP90 has been shown to co localise with areas of unstable atherosclerotic plaque and thin cap fibroatheroma (Madrigal-Matute et al.). STIP1 (CHOP), a co-chaperone for HSPs which is up-regulated by endoplasmic reticulum stress, was significantly up-regulated in Offspring of MI compared to controls.

7.2.3.3 Shared genes – Post MI and Offspring of MI

The pro-inflammatory transcription factor, EGR1 was up-regulated in both Offspring of MI and patients Post MI. This has atherogenic properties and is up-regulated following oxidised phospholipid exposure (Furnkranz et al., 2005, Kadl et al., 2002). EGR1 regulates the expression of pro-inflammatory and procoagulant genes (Harja et al., 2004). Interestingly, EGR1 also promotes tissue factor expression in endothelial cells.

The cholesterol efflux promoter CYP27A1 was up-regulated in both Offspring of MI and patients Post MI. There is evidence that this is up-regulated in individuals with ineffective HDL mediated cholesterol efflux (Weingartner et al.). Such compensatory increase in expression levels is also seen after administration of ritonavir which is known to precipitate premature coronary artery disease (Pou et al., 2008).

7.2.3.4 Genetic variations associate with gene expression

This study has provided evidence for the influence of the genome on the monocyte transcriptome in the context of atherosclerosis and CAD. The most significant findings are the variants rs2238151 and rs4506448 in the genes ACAD10 and ARV1 respectively. The former had a risk allele frequency of 57% (OR – 1.08) while the latter had an RAF of 6% (OR – 1.12). Both were down regulated with similar trends in Post MI and Offspring of MI groups. A deficiency of ACAD10 has been associated with oxidative stress while low levels of ARV1 results in disruption of cholesterol metabolism. In addition, A SNP in PGLYRP1, a peptidoglycan receptor expressed at relatively higher levels in the Post MI group was associated with CAD and a variant in CCL3L3 was associated with

MI. A total of 12 candidate genes which were differentially expressed in the study had eQTLs identified within Cardiogenics. Of these, three genes (CYP27A1, LXN and FAM13A1) shared similar expression trends in the Post MI and Offspring of MI groups. All of these loci were *cis*-eQTLs.

7.2.3.5 The effect of collagen activated platelets on monocyte gene expression

Collagen, a potential stimulus to resting platelets results in activation of platelets and initiation of pro-inflammatory and proatherosclerotic signalling (Lassila, 1993, Penz et al., 2005, Chesterman and Berndt, 1986). Such platelet activation and subsequent monocyte recruitment has been proposed as one of the initial events in atherogenesis (Seizer et al., 2008, Baltus et al., 2005) as well as the acute event in atherothrombosis (Freedman and Loscalzo, 2002).

In this study, the predominant effect of stimulation by collagen-activated platelets in monocytes was oxidative stress as evidenced by the up-regulation of OLR1, a receptor for oxidised LDL with an increasingly recognised role in atherogenesis and proliferation (Lu et al., 2011b). The consistent observation in all groups of nearly 200 fold up-regulation of this gene in monocytes following stimulation with activated platelets suggests the proinflammatory potential of the stimulation experiment 'priming' the monocyte to develop into lesion macrophages and foam cells. TGM2, CCL2, CCL7 and IL8 were other pro-inflammatory molecules which were up-regulated following CRP-XL stimulation. Taken together with the down regulation of the anti inflammatory molecules GPBAR1 and IL15, this suggests that CRP-XL-induced, platelet-driven stimulation of monocytes promotes a proatherosclerotic, proinflammatory phenotypic transformation of circulating monocytes.

7.4 MAIN CONCLUSIONS

This study has provided evidence to support the hypothesis that the circulating monocyte plays an important role in the various stages of atherosclerosis. The monocyte transcriptome has proven to be a relevant and responsive tool in exploring the mechanisms that mediate the genetic risk of CAD and MI. In both subject groups with a high genetic risk of MI (Post MI and Offspring of MI), monocyte transcriptome analysis has provided evidence of molecular perturbations which are of relevance to the initiation and progression of CAD and MI.

Stimulation of monocytes by collagen-activated platelets by administration of CRP-XL to freshly isolated venous blood samples has proven to be an effective and appropriate stimulus that drives the monocyte transcriptome in a direction of relevance to atherosclerosis (oxidative stress response driving the monocyte to a proatherogenic phenotype). The 200 fold up-regulation of Oxidised LDL Receptor 1 (OLR1) along with other differentially expressed genes indicates that platelet mediated stimulation does not simply induce a proinflammatory and apoptotic response in the monocyte such as the response to lipopolysaccharide (Sivapalaratnam et al., 2011b), but that it specifically facilitates changes of relevance to CAD.

In the group with established CAD (Post MI) the differentially expressed genes included inflammatory markers, regulators of haemostasis and metabolic modulators. Some of these differences are likely to be due to the effect of pharmacotherapeutic agents on the monocyte.

In the group of healthy young men with a high genetic risk of CAD (Offspring of MI), the most significant differentially expressed genes (i) mediated the response to hypoxic stress, (ii) regulated protein processing (heat shock response) and (iii) facilitated lipid transport. In addition, certain genes showed similar trends in expression profiles in both Post MI and Offspring of MI.

The most interesting observation in this study is the identification of interactions between genetic variation and gene expression, both of which independently correlate with CAD and MI. The most statistically significant differentially expressed genes in the study formed an enriched dataset to identify genetic variations which associate strongly with CAD and MI. This analysis revealed genes which had similar trends in expression in monocytes and also had variants within them with a strong association with CAD and/or MI. In addition, a genome wide interaction analysis was performed which identified eQTL which acted on monocyte gene expression.

The work in this thesis has highlighted the central role of the monocyte in coronary atherosclerosis. Gene expression in the monocyte is influenced by genetic factors, some of which contribute to the heritable risk of disease as well as environmental influences (as described in Figure 1.1), of which stimulation by activated platelets is highly relevant to atherosclerosis. The change in the immediate environment mediated by platelet driven stimulation revealed changes in expression of genes which also contribute to the genetic risk of CAD and MI. This study has therefore successfully integrated genetic and environmental risk factors which mediate their effect through the monocyte transcriptome in coronary artery disease (Figure 7.1). It is interesting to note

that differentially expressed genes such as TFPI and CYP27A1 have regulatory roles (anticoagulant, reverse cholesterol transport respectively) which suggest that CAD risk may be mediated not simply by activation of proinflammatory and prothrombotic pathways but also impairment of regulatory mechanisms.

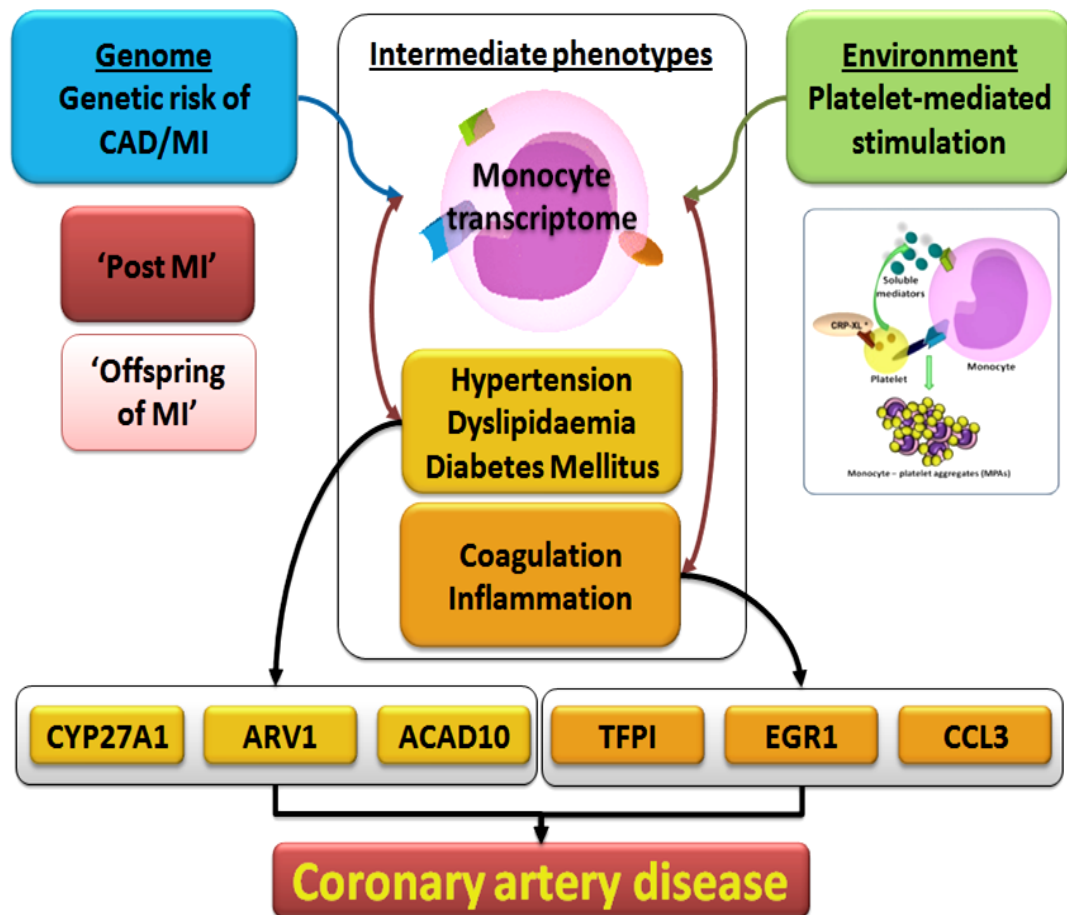


Figure 7.1: Role of monocyte transcriptome analysis in CAD

The monocyte transcriptome can be considered an intermediate phenotype at a molecular level under the influence of genetic and environmental variations. In this study, the most significant findings were seen in the expression of genes implicated in sterol and lipid metabolism, coagulation and inflammation. Similar trends in expression profiles were seen in some of these genes in the Post MI and Offspring of MI groups. Genetic variants associated with CAD/MI as well as eQTLs regulating monocyte gene expression were seen in some of these genes.

7.5 LIMITATIONS OF THE STUDY

The Post MI groups were all recruited at a stage where they were established on pharmacotherapy for secondary prevention. It was not ethical either to omit such medications at the time of recruitment or alternatively administer these drugs to the healthy controls. However, in the analysis of differential expression in these groups (see Chapter 4), published literature has been extensively reviewed to identify known influences of medication on gene expression. Furthermore, by identifying similar trends in expression of the same genes in the Offspring of MI group, in which no one was on regular medications, it has been possible to select those genes and pathways which are likely to a primary association with the disease rather than manifest the effect of medications or other secondary factors. It is also important to note that in a parallel study by our group investigating monocyte gene expression in matched groups of premature MI patients and healthy controls both treated with aspirin and statin, the differentially expressed genes were not the same as in the current study (Sivapalaratnam et al., 2012).

Another limitation is the single time point for analysis after stimulation by collagen-activated platelets. A four hour time point was selected based on previous work within the group where serial time point experiments have been used to study finite sets of candidate genes after platelet-mediated stimulation. These have shown that some genes demonstrate a rising trend in expression in the first few hours after stimulation and therefore, a four hour incubation period was selected to allow adequate stimulation of monocytes. It is possible that certain early response genes including transcription factors may have shown

differences in expression at earlier time points which may have been missed by choosing to study gene expression at four hours. However, by performing pathway analyses to delineate biological networks which integrate the differentially expressed genes, it has been possible to identify key regulatory elements such as the Wnt/beta catenin signalling system which may orchestrate some of the changes in gene expression.

Another limitation in this analysis is the possibility of contamination of the RNA samples by platelet transcripts. This is especially the case in the stimulated samples due to the formation of monocyte-platelet aggregates. However, monocytes contain >10,000 fold the amount of RNA compared to a platelet which makes substantial contamination unlikely. In addition, the differentially expressed genes were examined in the HaemAtlas database (<http://www.t1dbase.org/page/HaemAtlasHome>) to confirm that these genes are predominantly expressed in monocytes. In rare instances genes which were preferentially expressed in platelets were identified such as MEIS1 (relatively lower levels in Post MI compared to Controls) which were then excluded from further analysis.

The study used a version of the whole genome array which has since been superseded by newer and better annotated arrays with improved efficiency of hybridization and accuracy of post array analysis. Such 'next generation' platforms using sequencing of all the genes would allow a complete analysis of all genes expressed in any given cell or tissue.

The most significant differentially expressed genes were validated by Q-PCR. However, additional validation is desirable to prove that the transcribed genes are then translated to proteins, the final phenotype of functional relevance. However, in doing so, it is important to consider the cellular location of these molecules. A proportion of the differentially expressed genes code for intracellular organelle-related proteins, cell surface receptors or transcription factors without secreted components or surrogate markers which can be measured in plasma or serum by conventional methods such as ELISA. Other molecules such as CCL3 which was differentially expressed in Offspring of MI is a secreted chemokine which can be measured in plasma. This would be useful in confirming the difference in transcript levels seen in this study.

The bioinformatic analysis of differentially expressed genes in this thesis is focused on those that have either a recognised role or mechanistic relevance to atherosclerosis, coronary artery disease or other relevant pathological states such as hyperlipidaemia and oxidative stress. From the pathway analyses done in this study, genes selected for further integrative GWAS-GWE analysis were those with shared expression profiles in the two at risk groups (Post MI and Offspring of MI) and those which had plausible biological roles in the disease process. This strategy may exclude novel/unexplored transcripts/genes from a pool of differentially expressed ones taken forward for further pathway analysis. However in making this selection, the available literature on all differentially expressed genes were reviewed in detail to arrive at the shortlist of genes which were explored further for genetic variants.

The GWE-GWAS analysis described in Chapter 6 was performed using existing large databases of cases (MI and CAD) and controls. Genotyping of the study subjects would be a useful additional step to assess whether the observations from the large scale databases are also seen in the current study, however the small sample size may limit the use of this strategy. This is especially relevant to the offspring group experiments as the Offspring of MI group are different from the MI and CAD groups in GWAS analyses.

The GWAS-GWE analysis revealed that while some expressed RNAs are associated with eQTL variants (CARDIOGENICS) and some associated with CAD (CARDIOGRAM) – there are no examples where all three things are associated and so no clear evidence of causation. This may represent a type II error which may have arisen from a stringent selection of differentially expressed genes with shared trends in expression between Post MI and Offspring of MI groups.

Finally, genome wide expression analysis is a hypothesis-generating exercise. Differential expression of genes with already recognized roles in atherosclerosis helped to confirm the biological relevance of the stimulation experiment. However, a number of differentially expressed genes have no previously recognized roles in CAD or MI, but offer mechanistic insights into atherosclerosis by their contributions to the heat shock response, oxidative stress or the response to hypoxic environments, all of which have roles in the development and progression of atherosclerosis. It will require further functional studies to confirm the proposed roles of these differentially expressed genes.

7.6 FUTURE DIRECTIONS

This study has provided a useful foundation for further focused work in exploring the roles of differentially expressed genes in monocytes. The monocyte transcriptome in the resting state as well as after platelet-mediated stimulation was studied in subjects with contrasting genetic risk for CAD and MI. This study has confirmed that stimulation by activated platelets is an appropriate and useful experiment to study the monocyte in the context of atherosclerosis and that such a stimulus triggers an oxidative stress response in monocytes. Certain candidate genes from this study merit consideration of further studies to explore their pathophysiological roles.

The transcription factor EGR1, the chemokine CCL3 and the genes implicated in lipid and fatty acid metabolism such as the cholesterol export enzyme CYP27A1, the mitochondrial enzyme ACAD10 and the endoplasmic reticulum resident protein ARV1 are interesting candidates for such analyses.

CYP27A1 – a key regulator of cholesterol efflux

The cytochrome p450 enzyme, CYP27A1 located on the inner mitochondrial membrane shows the most promise as an indicator of plaque progression (Shanahan et al., 2001) and a potential therapeutic target in atherosclerosis. The co localisation of this enzyme with macrophages in shoulder regions of advanced atherosclerotic plaques and the proportional increase of this enzyme in macrophages according to the stage of plaque disease suggest that this may provide an inducible alternative pathway for non-HDL based cholesterol export from tissues. The enzyme has also been found in vascular smooth muscle cells

in the intimal layer but not in the media suggesting that this may have a role in cholesterol efflux in conditions of increased intracellular cholesterol accumulation. Animal knockout models studying non-alcoholic steatohepatitis (NASH) have shown that cholesterol accumulates in lysosomes within monocyte-derived phagocytic cells in the liver (Kupffer cells) in the absence of CYP27A1 and that such accumulation is reduced by the supplementation of 27 hydroxycholesterol synthesized by CYP27A1 from cholesterol (Bieghs et al., 2012). A brief outline of further experiments is provided in the following section.

Human monocyte derived macrophages in culture provide a useful experimental model for specific gene knockdown experiments using RNA interference (siRNA) targeted at CYP27A1. This would allow assessment of alterations in intracellular cholesterol storage and export of cholesterol from cells in the absence of this enzyme. Further stimulation experiments of cultured macrophages with oxidized LDL with and without CYP27A1 knockdown would help to delineate the role of this enzyme in response to a pro-inflammatory atherogenic stimulus.

Once the role of CYP27A1 in non HDL-dependent cholesterol efflux is established at a cellular level, the role of this enzyme in atherosclerotic plaque progression could be studied using animal knock out models. Currently available CYP27A1 (-/-) mouse would be an appropriate model for such studies. This along with double knock out models of CYP27A1 (-/-) and LDLR (-/-) or ApoE (-/-) can be used for further exploration of the role of CYP27A1 in progression of atherosclerosis. The observation that CYP27A1 co localises with macrophages in the vulnerable shoulder regions of atherosclerotic plaques

(Shanahan et al., 2001) also suggests that this enzyme may have a role in plaque stabilization.

Findings from the above experiments may open new opportunities for therapy. Currently available lipid modification strategies focus mainly on the absorption and synthesis of cholesterol. These agents have modest or no effect on reverse cholesterol transport which is primarily HDL driven. In this study raised levels of CYP27A1 have been observed as an early change in individuals at high genetic risk of coronary atherosclerosis. This indicates that this enzyme may be a compensatory protective response to aid cholesterol efflux in individuals. Therapeutic options may include supplementation of 27-hydroxycholesterol or ways of promoting the action of the enzyme by preventing its degradation. In addition, the eQTL in this gene can be investigated further to determine whether this regulates cholesterol efflux from monocyte derived macrophages.

CCL3 – a biomarker for early stage atherosclerosis

CCL3 which has been implicated in the progression of atherosclerosis is a chemokine that is released into plasma and therefore measurable by ELISA (Bandinelli et al., 2012). Increased levels of this chemokine seen in the Offspring of MI group in this study suggest that this is a potential biomarker for the early identification of individuals at risk of CAD. Large scale studies are required to validate this finding and to determine whether CCL3 levels would add to existing risk assessment tools which use classical risk factors for CAD and other inflammatory markers such as high sensitivity C reactive protein (HS-CRP). In addition, it would be important to establish that the CCL3 levels are not influenced by acute or chronic inflammatory conditions and to establish its

specificity for atherosclerotic disease. It is possible that CCL3 is a marker of atherosclerosis in general rather than coronary artery disease. Nonetheless it may be a marker with a high negative predictive value when used as a screening tool in a vulnerable population.

PGLYRP1 and ORM1 – plasma biomarkers for genetic risk of CAD

Both genes were expressed at significantly higher levels in the Post MI group at baseline and after platelet-mediated stimulation. The genetic variant rs11672503 in PGLYRP1 was noted to have a statistically significant association with CAD but not MI in the CARDIoGRAM analysis (Chapter 6). The locus rs7851482 within the ORM1 gene was seen to associate with levels of monocyte gene expression in the Cardiogenics analysis (Chapter 6). Previous studies have shown that both are potential plasma biomarkers for atherosclerosis (Chapelle et al., 1981, Rohatgi et al., 2009). Further studies in large well characterised clinical cohorts would allow validation of these biomarkers which may be specifically useful in the risk assessment of individuals with a high genetic risk of CAD.

7.7 CONCLUSION

In the wider context of genetic research in CAD, the next phase is genome wide interaction analysis which incorporates GWAS and GWE to understand the functional relationships between genetic variants and differential expressed genes in CAD. A detailed characterization of the monocyte transcriptome allows integration of genetic and environmental risk factors and further exploration and validation of key regulatory molecules and pathways with potential therapeutic applications. This would then promote translational research incorporating bedside diagnostic tools which would allow detailed and rapid characterization of such well validated molecular pathways in patients with CAD. Therapy can then be guided according to the patient-specific perturbations in these pathways, thereby achieving the Holy Grail of personalized medical care for all.

REFERENCES

- ABBOUD-JARROUS, G., ATZMON, R., PERETZ, T., PALERMO, C., GADEA, B. B., JOYCE, J. A. & VLODAVSKY, I. 2008. Cathepsin L is responsible for processing and activation of proheparanase through multiple cleavages of a linker segment. *J Biol Chem*, 283, 18167-76.
- ABISI, S., BURNAND, K. G., HUMPHRIES, J., WALTHAM, M., TAYLOR, P. & SMITH, A. 2008. Effect of statins on proteolytic activity in the wall of abdominal aortic aneurysms. *Br J Surg*, 95, 333-7.
- AIELLO, R. J., BOURASSA, P. A., LINDSEY, S., WENG, W., NATOLI, E., ROLLINS, B. J. & MILOS, P. M. 1999. Monocyte chemoattractant protein-1 accelerates atherosclerosis in apolipoprotein E-deficient mice. *Arterioscler Thromb Vasc Biol*, 19, 1518-25.
- AL-ALY, Z. 2008. Arterial calcification: a tumor necrosis factor-alpha mediated vascular Wnt-opathy. *Transl Res*, 151, 233-9.
- ALBASANZ-PUIG, A., MURRAY, J., PREUSCH, M., COAN, D., NAMEKATA, M., PATEL, Y., DONG, Z. M., ROSENFELD, M. E. & WIJELATH, E. S. 2011. Oncostatin M is expressed in atherosclerotic lesions: a role for Oncostatin M in the pathogenesis of atherosclerosis. *Atherosclerosis*, 216, 292-8.
- ALBRECHT, C., PREUSCH, M. R., HOFMANN, G., MORRIS-ROSENFELD, S., BLESSING, E., ROSENFELD, M. E., KATUS, H. A. & BEA, F. 2010. Egr-1 deficiency in bone marrow-derived cells reduces atherosclerotic lesion formation in a hyperlipidaemic mouse model. *Cardiovasc Res*, 86, 321-9.
- ALLENDER, S. 2007. Coronary Heart Disease Statistics.
- ALLENDER, S., SCARBOROUGH, P., PETO, V., RAYNER, M., LEAL, J., LUENGO-FERNANDEZ, R. & GRAY, A. 2008. European Cardiovascular Disease Statistics. In: NETWORK, E. H. (ed.). Brussels.
- ALMEIDA, M., AMBROGINI, E., HAN, L., MANOLAGAS, S. C. & JILKA, R. L. 2009. Increased lipid oxidation causes oxidative stress, increased peroxisome proliferator-activated receptor-gamma expression, and diminished pro-osteogenic Wnt signaling in the skeleton. *J Biol Chem*, 284, 27438-48.
- AMBROGINI, E., ALMEIDA, M., MARTIN-MILLAN, M., PAIK, J. H., DEPINHO, R. A., HAN, L., GOELLNER, J., WEINSTEIN, R. S., JILKA, R. L., O'BRIEN, C. A. & MANOLAGAS, S. C. 2010. FoxO-mediated defense against oxidative stress in osteoblasts is indispensable for skeletal homeostasis in mice. *Cell Metab*, 11, 136-46.
- ANANDATHEERTHAVARADA, H. K., SEPURI, N. B. & AVADHANI, N. G. 2009. Mitochondrial targeting of cytochrome P450 proteins containing NH2-terminal chimeric signals involves an unusual TOM20/TOM22 bypass mechanism. *J Biol Chem*, 284, 17352-63.
- ANDERSSON, T., SODERSTEN, E., DUCKWORTH, J. K., CASCANTE, A., FRITZ, N., SACCHETTI, P., CERVENKA, I., BRYJA, V. & HERMANSON, O. 2009. CXXC5 is a novel BMP4-regulated modulator of Wnt signaling in neural stem cells. *J Biol Chem*, 284, 3672-81.
- ANTONIADES, C., BAKOGIANNIS, C., TOUSOULIS, D., DEMOSTHENOUS, M., MARINO, K. & STEFANADIS, C. 2010. Platelet activation in atherogenesis associated with low-grade inflammation. *Inflamm Allergy Drug Targets*, 9, 334-45.
- AOYAMA, T., INOKUCHI, S., BRENNER, D. A. & SEKI, E. 2010. CX3CL1-CX3CR1 interaction prevents carbon tetrachloride-induced liver inflammation and fibrosis in mice. *Hepatology*, 52, 1390-400.
- ARCHACKI, S. R., ANGHELOIU, G., MORAVEC, C. S., LIU, H., TOPOL, E. J. & WANG, Q. K. 2012. Comparative gene expression analysis between coronary arteries

- and internal mammary arteries identifies a role for the TES gene in endothelial cell functions relevant to coronary artery disease. *Hum Mol Genet*, 21, 1364-73.
- ARDIGO, D., ASSIMES, T. L., FORTMANN, S. P., GO, A. S., HLATKY, M., HYTOPOULOS, E., IRIBARREN, C., TSAO, P. S., TABIBIAZAR, R. & QUERTERMOUS, T. 2007. Circulating chemokines accurately identify individuals with clinically significant atherosclerotic heart disease. *Physiol Genomics*, 31, 402-9.
- BABIKER, A., ANDERSSON, O., LUND, E., XIU, R. J., DEEB, S., RESHEF, A., LEITERSDORF, E., DICZFALUSY, U. & BJORKHEM, I. 1997. Elimination of cholesterol in macrophages and endothelial cells by the sterol 27-hydroxylase mechanism. Comparison with high density lipoprotein-mediated reverse cholesterol transport. *J Biol Chem*, 272, 26253-61.
- BAI, Z., CHENG, B., YU, Q., LI, C., HE, P. & MAO, X. 2004. Effects of leptin on expression of acyl-coenzyme A: cholesterol acyltransferase-1 in cultured human monocyte-macrophages. *J Huazhong Univ Sci Technolog Med Sci*, 24, 563-5, 590.
- BAILEY, C. H. 1916. Atheroma and Other Lesions Produced in Rabbits by Cholesterol Feeding. *J Exp Med*, 23, 69-84.
- BAILEY, T. A., KANUGA, N., ROMERO, I. A., GREENWOOD, J., LUTHERT, P. J. & CHEETHAM, M. E. 2004. Oxidative stress affects the junctional integrity of retinal pigment epithelial cells. *Invest Ophthalmol Vis Sci*, 45, 675-84.
- BALDAUF, L. K. 1906. The Chemistry of Atheroma and Calcification (Aorta). *J Med Res*, 15, 355-61.
- BALTUS, T., VON HUNDELSHAUSEN, P., MAUSE, S. F., BUHRE, W., ROSSAINT, R. & WEBER, C. 2005. Differential and additive effects of platelet-derived chemokines on monocyte arrest on inflamed endothelium under flow conditions. *J Leukoc Biol*, 78, 435-41.
- BANDINELLI, F., DEL ROSSO, A., GABRIELLI, A., GIACOMELLI, R., BARTOLI, F., GUIDUCCI, S. & MATUCCI CERINIC, M. 2012. CCL2, CCL3 and CCL5 chemokines in systemic sclerosis: the correlation with SSc clinical features and the effect of prostaglandin E1 treatment. *Clin Exp Rheumatol*, 30, S44-9.
- BAO, W., MIN, D., TWIGG, S. M., SHACKEL, N. A., WARNER, F. J., YUE, D. K. & MCLENNAN, S. V. 2010. Monocyte CD147 is induced by advanced glycation end products and high glucose concentration: possible role in diabetic complications. *Am J Physiol Cell Physiol*, 299, C1212-9.
- BAO, W., SRINIVASAN, S. R., WATTIGNEY, W. A. & BERENSON, G. S. 1995. The relation of parental cardiovascular disease to risk factors in children and young adults. The Bogalusa Heart Study. *Circulation*, 91, 365-71.
- BARLIC, J., SECHLER, J. M. & MURPHY, P. M. 2003. IL-15 and IL-2 oppositely regulate expression of the chemokine receptor CX3CR1. *Blood*, 102, 3494-503.
- BARNARD, M. R., LINDEN, M. D., FRELINGER, A. L., 3RD, LI, Y., FOX, M. L., FURMAN, M. I. & MICHELSON, A. D. 2005. Effects of platelet binding on whole blood flow cytometry assays of monocyte and neutrophil procoagulant activity. *J Thromb Haemost*, 3, 2563-70.
- BARNES, K. C., GRANT, A., GAO, P., BALTA DJIEVA, D., BERG, T., CHI, P., ZHANG, S., ZAMBELLI-WEINER, A., EHRLICH, E., ZARDKOOHI, O., BRUMMET, M. E., STOCKTON, M., WATKINS, T., GAO, L., GITTENS, M., WILLS-KARP, M., CHEADLE, C., BECK, L. A., BEATY, T. H., BECKER, K. G., GARCIA, J. G. & MATHIAS, R. A. 2006. Polymorphisms in the novel gene acyloxyacyl hydroxylase (AOAH) are associated with asthma and associated phenotypes. *J Allergy Clin Immunol*, 118, 70-7.

- BASAVARAJ, M. G., GRUBER, F. X., SOVERSHAEV, M., APPELBOM, H. I., OSTERUD, B., PETERSEN, L. C. & HANSEN, J. B. 2010. The role of TFPI in regulation of TF-induced thrombogenicity on the surface of human monocytes. *Thromb Res*, 126, 418-25.
- BATA, I. R., GREGOR, R. D., WOLF, H. K. & BROWNELL, B. 2006. Trends in five-year survival of patients discharged after acute myocardial infarction. *Can J Cardiol*, 22, 399-404.
- BEA, F., BLESSING, E., SHELLEY, M. I., SHULTZ, J. M. & ROSENFELD, M. E. 2003. Simvastatin inhibits expression of tissue factor in advanced atherosclerotic lesions of apolipoprotein E deficient mice independently of lipid lowering: potential role of simvastatin-mediated inhibition of Egr-1 expression and activation. *Atherosclerosis*, 167, 187-94.
- BEDÉL, A., NEGRE-SALVAYRE, A., HEENEMAN, S., GRAZIDE, M. H., THIERS, J. C., SALVAYRE, R. & MAUPAS-SCHWALM, F. 2008. E-cadherin/beta-catenin/T-cell factor pathway is involved in smooth muscle cell proliferation elicited by oxidized low-density lipoprotein. *Circ Res*, 103, 694-701.
- BELTOWSKI, J. 2008. Liver X receptors (LXR) as therapeutic targets in dyslipidemia. *Cardiovasc Ther*, 26, 297-316.
- BENDINELLI, P., MARONI, P., PECORI GIRALDI, F. & PICCOLETTI, R. 2000. Leptin activates Stat3, Stat1 and AP-1 in mouse adipose tissue. *Mol Cell Endocrinol*, 168, 11-20.
- BERG, K. 1990. Risk factor variability and coronary heart disease. *Acta Genet Med Gemellol (Roma)*, 39, 15-24.
- BERGMAN, M. R., CHENG, S., HONBO, N., PIACENTINI, L., KARLINER, J. S. & LOVETT, D. H. 2003. A functional activating protein 1 (AP-1) site regulates matrix metalloproteinase 2 (MMP-2) transcription by cardiac cells through interactions with JunB-Fra1 and JunB-FosB heterodimers. *Biochem J*, 369, 485-96.
- BIAN, L., HANSON, R. L., MULLER, Y. L., MA, L., KOBES, S., KNOWLER, W. C., BOGARDUS, C. & BAIER, L. J. 2010. Variants in ACAD10 are associated with type 2 diabetes, insulin resistance and lipid oxidation in Pima Indians. *Diabetologia*, 53, 1349-53.
- BIEGHS, V., HENDRIKX, T., VAN GORP, P. J., VERHEYEN, F., GUICHOT, Y. D., WALENBERGH, S. M., GIJBELS, M., RENSEN, S. S., BAST, A., PLAT, J., KALHAN, S. C., LEITERSDORF, E., HOFKER, M., LUTJOHANN, D. & SHIRISVERDLOV, R. 2012. The Cholesterol Derivative 27-Hydroxycholesterol Reduces Steatohepatitis in Mice. *Gastroenterology*.
- BINGHAM, T. C., PARATHATH, S., TIAN, H., REISS, A., CHAN, E., FISHER, E. A. & CRONSTEIN, B. N. 2012. Cholesterol 27-hydroxylase but not apolipoprotein apoE contributes to A2A adenosine receptor stimulated reverse cholesterol transport. *Inflammation*, 35, 49-57.
- BJORKHEM, I., ANDERSSON, O., DICZFALUSY, U., SEVASTIK, B., XIU, R. J., DUAN, C. & LUND, E. 1994. Atherosclerosis and sterol 27-hydroxylase: evidence for a role of this enzyme in elimination of cholesterol from human macrophages. *Proc Natl Acad Sci U S A*, 91, 8592-6.
- BLANKESTEIJN, W. M., VAN GIJN, M. E., ESSERS-JANSSEN, Y. P., DAEMEN, M. J. & SMITS, J. F. 2000. Beta-catenin, an inducer of uncontrolled cell proliferation and migration in malignancies, is localized in the cytoplasm of vascular endothelium during neovascularization after myocardial infarction. *Am J Pathol*, 157, 877-83.
- BLUMENTHAL, A., EHLERS, S., LAUBER, J., BUER, J., LANGE, C., GOLDMANN, T., HEINE, H., BRANDT, E. & REILING, N. 2006. The Wingless homolog WNT5A

- and its receptor Frizzled-5 regulate inflammatory responses of human mononuclear cells induced by microbial stimulation. *Blood*, 108, 965-73.
- BOCHKOV, V. N., MECHTCHERIAKOVA, D., LUCERNA, M., HUBER, J., MALLI, R., GRAIER, W. F., HOFER, E., BINDER, B. R. & LEITINGER, N. 2002. Oxidized phospholipids stimulate tissue factor expression in human endothelial cells via activation of ERK/EGR-1 and Ca(++)/NFAT. *Blood*, 99, 199-206.
- BOHR, D. C., KOCH, M., KRITZENBERGER, M., FUCHSHOFER, R. & TAMM, E. R. 2011. Increased expression of olfactomedin-1 and myocilin in podocytes during puromycin aminonucleoside nephrosis. *Nephrol Dial Transplant*, 26, 83-92.
- BOISVERT, W. A., ROSE, D. M., BOULLIER, A., QUEHENBERGER, O., SYDLASKE, A., JOHNSON, K. A., CURTISS, L. K. & TERKELTAUB, R. 2006. Leukocyte transglutaminase 2 expression limits atherosclerotic lesion size. *Arterioscler Thromb Vasc Biol*, 26, 563-9.
- BONOMINI, F., TENGATTINI, S., FABIANO, A., BIANCHI, R. & REZZANI, R. 2008. Atherosclerosis and oxidative stress. *Histol Histopathol*, 23, 381-90.
- BOSCO, M. C., PIEROBON, D., BLENGIO, F., RAGGI, F., VANNI, C., GATTORNO, M., EVA, A., NOVELLI, F., CAPPELLO, P., GIOVARELLI, M. & VAREGIO, L. 2011. Hypoxia modulates the gene expression profile of immunoregulatory receptors in human mature dendritic cells: identification of TREM-1 as a novel hypoxic marker in vitro and in vivo. *Blood*, 117, 2625-39.
- BOSCO, M. C., PUPPO, M., BLENGIO, F., FRAONE, T., CAPPELLO, P., GIOVARELLI, M. & VAREGIO, L. 2008. Monocytes and dendritic cells in a hypoxic environment: Spotlights on chemotaxis and migration. *Immunobiology*, 213, 733-49.
- BOSIO, A., KNORR, C., JANSSEN, U., GEBEL, S., HAUSSMANN, H. J. & MULLER, T. 2002. Kinetics of gene expression profiling in Swiss 3T3 cells exposed to aqueous extracts of cigarette smoke. *Carcinogenesis*, 23, 741-8.
- BRADLEY, S. V., ORAVECZ-WILSON, K. I., BOUGEARD, G., MIZUKAMI, I., LI, L., MUNACO, A. J., SREEKUMAR, A., CORRADETTI, M. N., CHINNAIYAN, A. M., SANDA, M. G. & ROSS, T. S. 2005. Serum antibodies to huntingtin interacting protein-1: a new blood test for prostate cancer. *Cancer Res*, 65, 4126-33.
- BRESLOW, J. L. 2000. Genetics of lipoprotein abnormalities associated with coronary artery disease susceptibility. *Annu Rev Genet*, 34, 233-254.
- BRIZZI, M. F., FORMATO, L., DENTELLI, P., ROSSO, A., PAVAN, M., GARBARINO, G., PEGORARO, M., CAMUSSI, G. & PEGORARO, L. 2001. Interleukin-3 stimulates migration and proliferation of vascular smooth muscle cells: a potential role in atherogenesis. *Circulation*, 103, 549-54.
- BURTON, D. G., GILES, P. J., SHEERIN, A. N., SMITH, S. K., LAWTON, J. J., OSTLER, E. L., RHYS-WILLIAMS, W., KIPLING, D. & FARAGHER, R. G. 2009. Microarray analysis of senescent vascular smooth muscle cells: A link to atherosclerosis and vascular calcification. *Exp Gerontol*, 44, 659-65.
- BUTTNER, P., MOSIG, S. & FUNKE, H. 2007a. Gene expression profiles of T lymphocytes are sensitive to the influence of heavy smoking: A pilot study. *Immunogenetics*, 59, 37-43.
- BUTTNER, P., MOSIG, S., LECHTERMANN, A., FUNKE, H. & MOOREN, F. C. 2007b. Exercise affects the gene expression profiles of human white blood cells. *J Appl Physiol*, 102, 26-36.
- CAGNIN, S., BISCUOLA, M., PATUZZO, C., TRABETTI, E., PASQUALI, A., LAVEDER, P., FAGGIAN, G., IAFRANCESCO, M., MAZZUCCO, A., PIGNATTI, P. F. & LANFRANCHI, G. 2009. Reconstruction and functional analysis of altered molecular pathways in human atherosclerotic arteries. *BMC Genomics*, 10, 13.

- CAPLICE, N. M., MUESKE, C. S., KLEPPE, L. S. & SIMARI, R. D. 1998. Presence of tissue factor pathway inhibitor in human atherosclerotic plaques is associated with reduced tissue factor activity. *Circulation*, 98, 1051-7.
- CARPENTER, D., MCINTOSH, R. S., PLEASS, R. J. & ARMOUR, J. A. 2012. Functional effects of CCL3L1 copy number. *Genes Immun*.
- CHAKRABARTI, S., RIZVI, M., PATHAK, D., KIRBER, M. T. & FREEDMAN, J. E. 2009. Hypoxia influences CD40-CD40L mediated inflammation in endothelial and monocytic cells. *Immunol Lett*, 122, 170-84.
- CHANG, T. Y., CHANG, C. C., LIN, S., YU, C., LI, B. L. & MIYAZAKI, A. 2001. Roles of acyl-coenzyme A:cholesterol acyltransferase-1 and -2. *Curr Opin Lipidol*, 12, 289-96.
- CHAPELLE, J. P., ALBERT, A., SMEETS, J. P., HEUSGHEM, C. & KULBERTUS, H. E. 1981. The prognostic significance of serum alpha 1-acid glycoprotein changes in acute myocardial infarction. *Clin Chim Acta*, 115, 199-209.
- CHAPMAN, J. M. & MASSEY, F. J., JR. 1964. The Interrelationship of Serum Cholesterol, Hypertension, Body Weight, and Risk of Coronary Disease. Results of the First Ten Years' Follow-up in the Los Angeles Heart Study. *J Chronic Dis*, 17, 933-49.
- CHEN, H. & SHARP, B. M. 2004. Content-rich biological network constructed by mining PubMed abstracts. *BMC Bioinformatics*, 5, 147.
- CHEN, J. & LOPEZ, J. A. 2005. Interactions of platelets with subendothelium and endothelium. *Microcirculation*, 12, 235-46.
- CHEN, Y. G., XU, F., ZHANG, Y., JI, Q. S., SUN, Y., LU, R. J. & LI, R. J. 2006. Effect of aspirin plus clopidogrel on inflammatory markers in patients with non-ST-segment elevation acute coronary syndrome. *Chin Med J (Engl)*, 119, 32-6.
- CHENG, C. W., YEH, J. C., FAN, T. P., SMITH, S. K. & CHARNOCK-JONES, D. S. 2008. Wnt5a-mediated non-canonical Wnt signalling regulates human endothelial cell proliferation and migration. *Biochem Biophys Res Commun*, 365, 285-90.
- CHESTERMAN, C. N. & BERNDT, M. C. 1986. Platelet and vessel wall interaction and the genesis of atherosclerosis. *Clin Haematol*, 15, 323-53.
- CHI, J. T., WANG, Z., NUYTEN, D. S., RODRIGUEZ, E. H., SCHANER, M. E., SALIM, A., WANG, Y., KRISTENSEN, G. B., HELLAND, A., BORRESEN-DALE, A. L., GIACCIA, A., LONGAKER, M. T., HASTIE, T., YANG, G. P., VAN DE VIJVER, M. J. & BROWN, P. O. 2006. Gene expression programs in response to hypoxia: cell type specificity and prognostic significance in human cancers. *PLoS Med*, 3, e47.
- CHIGIRA, S., SUGITA, K., KITA, K., SUGAYA, S., ARASE, Y., ICHINOSE, M., SHIRASAWA, H. & SUZUKI, N. 2003. Increased expression of the Huntingtin interacting protein-1 gene in cells from Hutchinson Gilford Syndrome (Progeria) patients and aged donors. *J Gerontol A Biol Sci Med Sci*, 58, B873-8.
- CHIODINI, B. D. & LEWIS, C. M. 2003. Meta-analysis of 4 coronary heart disease genome-wide linkage studies confirms a susceptibility locus on chromosome 3q. *Arterioscler Thromb Vasc Biol*, 23, 1863-8.
- CHO, B. R., KIM, M. K., SUH, D. H., HAHN, J. H., LEE, B. G., CHOI, Y. C., KWON, T. J., KIM, S. Y. & KIM, D. J. 2008. Increased tissue transglutaminase expression in human atherosclerotic coronary arteries. *Coron Artery Dis*, 19, 459-68.
- CHOI, H., ALLAHDADI, K. J., TOSTES, R. C. & WEBB, R. C. 2009. Diacylglycerol Kinase Inhibition and Vascular Function. *Curr Enzym Inhib*, 5, 148-152.
- CHONG, I. W., LIN, S. R., HWANG, J. J., HUANG, M. S., WANG, T. H., HUNG, J. Y. & PAULAUSKIS, J. D. 2002. Expression and regulation of the macrophage

- inflammatory protein-1 alpha gene by nicotine in rat alveolar macrophages. *Eur Cytokine Netw*, 13, 242-9.
- CHRISTMAN, M. A., 2ND, GOETZ, D. J., DICKERSON, E., MCCALL, K. D., LEWIS, C. J., BENENCIA, F., SILVER, M. J., KOHN, L. D. & MALGOR, R. 2008. Wnt5a is expressed in murine and human atherosclerotic lesions. *Am J Physiol Heart Circ Physiol*, 294, H2864-70.
- CLERIN, V., SHIH, H. H., DENG, N., HEBERT, G., RESMINI, C., SHIELDS, K. M., FELDMAN, J. L., WINKLER, A., ALBERT, L., MAGANTI, V., WONG, A., PAULSEN, J. E., KEITH, J. C., JR., VLASUK, G. P. & PITTMAN, D. D. 2008. Expression of the cysteine protease legumain in vascular lesions and functional implications in atherogenesis. *Atherosclerosis*, 201, 53-66.
- CONGRAINS, A., KAMIDE, K., KATSUYA, T., YASUDA, O., OGURO, R., YAMAMOTO, K., OHISHI, M. & RAKUGI, H. 2012a. CVD-associated non-coding RNA, ANRIL, modulates expression of atherogenic pathways in VSMC. *Biochem Biophys Res Commun*, 419, 612-6.
- CONGRAINS, A., KAMIDE, K., OGURO, R., YASUDA, O., MIYATA, K., YAMAMOTO, E., KAWAI, T., KUSUNOKI, H., YAMAMOTO, H., TAKEYA, Y., YAMAMOTO, K., ONISHI, M., SUGIMOTO, K., KATSUYA, T., AWATA, N., IKEBE, K., GONDO, Y., OIKE, Y., OHISHI, M. & RAKUGI, H. 2012b. Genetic variants at the 9p21 locus contribute to atherosclerosis through modulation of ANRIL and CDKN2A/B. *Atherosclerosis*, 220, 449-55.
- CONSORTIUM, C. A. D. C. D. G. 2011. A genome-wide association study in Europeans and South Asians identifies five new loci for coronary artery disease. *Nat Genet*, 43, 339-44.
- CORN, P. G., RICCI, M. S., SCATA, K. A., ARSHAM, A. M., SIMON, M. C., DICKER, D. T. & EL-DEIRY, W. S. 2005. Mxi1 is induced by hypoxia in a HIF-1-dependent manner and protects cells from c-Myc-induced apoptosis. *Cancer Biol Ther*, 4, 1285-94.
- CORREALE, M., BRUNETTI, N. D., DE GENNARO, L. & DI BIASE, M. 2008. Acute phase proteins in atherosclerosis (acute coronary syndrome). *Cardiovasc Hematol Agents Med Chem*, 6, 272-7.
- CRAWLEY, J., LUPU, F., WESTMUCKETT, A. D., SEVERS, N. J., KAKKAR, V. V. & LUPU, C. 2000. Expression, localization, and activity of tissue factor pathway inhibitor in normal and atherosclerotic human vessels. *Arterioscler Thromb Vasc Biol*, 20, 1362-73.
- CRUJEIRAS, A. B., PARRA, D., MILAGRO, F. I., GOYENECHEA, E., LARRARTE, E., MARGARETO, J. & MARTINEZ, J. A. 2008. Differential expression of oxidative stress and inflammation related genes in peripheral blood mononuclear cells in response to a low-calorie diet: a nutrigenomics study. *OMICS*, 12, 251-61.
- DA COSTA MARTINS, P. A., VAN GILS, J. M., MOL, A., HORDIJK, P. L. & ZWAGINGA, J. J. 2006. Platelet binding to monocytes increases the adhesive properties of monocytes by up-regulating the expression and functionality of beta1 and beta2 integrins. *J Leukoc Biol*, 79, 499-507.
- DANIEL, S., BRADLEY, G., LONGSHAW, V. M., SOTI, C., CSERMELY, P. & BLATCH, G. L. 2008. Nuclear translocation of the phosphoprotein Hop (Hsp70/Hsp90 organizing protein) occurs under heat shock, and its proposed nuclear localization signal is involved in Hsp90 binding. *Biochim Biophys Acta*, 1783, 1003-14.
- DAVI, G. & PATRONO, C. 2007. Platelet activation and atherothrombosis. *N Engl J Med*, 357, 2482-94.
- DE LARTIGUE, G., LUR, G., DIMALINE, R., VARRO, A., RAYBOULD, H. & DOCKRAY, G. J. 2010. EGR1 Is a target for cooperative interactions between

- cholecystokinin and leptin, and inhibition by ghrelin, in vagal afferent neurons. *Endocrinology*, 151, 3589-99.
- DE MAGALHAES, J. P., CURADO, J. & CHURCH, G. M. 2009. Meta-analysis of age-related gene expression profiles identifies common signatures of aging. *Bioinformatics*, 25, 875-81.
- DEGUCHI, J. O., YAMAZAKI, H., AIKAWA, E. & AIKAWA, M. 2009. Chronic hypoxia activates the Akt and beta-catenin pathways in human macrophages. *Arterioscler Thromb Vasc Biol*, 29, 1664-70.
- DELL'ACCIO, F., DE BARI, C., ELTAWIL, N. M., VANHUMMELEN, P. & PITZALIS, C. 2008. Identification of the molecular response of articular cartilage to injury, by microarray screening: Wnt-16 expression and signaling after injury and in osteoarthritis. *Arthritis Rheum*, 58, 1410-21.
- DEMETZ, G., SEITZ, I., STEIN, A., STEPPICH, B., GROHA, P., BRANDL, R., SCHOMIG, A. & OTT, I. Tissue Factor-Factor VIIa complex induces cytokine expression in coronary artery smooth muscle cells. *Atherosclerosis*.
- DESIERE, F. & ROMANO SPICA, V. 2012. Personalised Medicine in 2012: Editorial to the Special Issue of New Biotechnology on "MOLECULAR DIAGNOSTICS & PERSONALISED MEDICINE". *N Biotechnol*.
- DJE N'GUESSAN, P., RIEDIGER, F., VARDAROVA, K., SCHARF, S., EITEL, J., OPITZ, B., SLEVOGT, H., WEICHERT, W., HOCKE, A. C., SCHMECK, B., SUTTORP, N. & HIPPENSTIEL, S. 2009. Statins control oxidized LDL-mediated histone modifications and gene expression in cultured human endothelial cells. *Arterioscler Thromb Vasc Biol*, 29, 380-6.
- DOL, F., MARTIN, G., STAELS, B., MARES, A. M., CAZAUBON, C., NISATO, D., BIDOUCARD, J. P., JANIAC, P., SCHAEFFER, P. & HERBERT, J. M. 2001. Angiotensin AT1 receptor antagonist irbesartan decreases lesion size, chemokine expression, and macrophage accumulation in apolipoprotein E-deficient mice. *J Cardiovasc Pharmacol*, 38, 395-405.
- DOYLE, I., RATCLIFFE, M., WALDING, A., VANDEN BON, E., DYMOND, M., TOMLINSON, W., TILLEY, D., SHELTON, P. & DOUGALL, I. 2010. Differential gene expression analysis in human monocyte-derived macrophages: impact of cigarette smoke on host defence. *Mol Immunol*, 47, 1058-65.
- DRAUDE, G., VON HUNDELSHAUSEN, P., FRANKENBERGER, M., ZIEGLER-HEITBROCK, H. W. & WEBER, C. 1999. Distinct scavenger receptor expression and function in the human CD14(+)/CD16(+) monocyte subset. *Am J Physiol*, 276, H1144-9.
- DUAN, W., PAKA, L. & PILLARISSETTI, S. 2005. Distinct effects of glucose and glucosamine on vascular endothelial and smooth muscle cells: evidence for a protective role for glucosamine in atherosclerosis. *Cardiovasc Diabetol*, 4, 16.
- DUMONT, J., ZUREIK, M., COTTEL, D., MONTAYE, M., DUCIMETIERE, P., AMOUYEL, P. & BROUSSEAU, T. 2007. Association of arginase 1 gene polymorphisms with the risk of myocardial infarction and common carotid intima media thickness. *J Med Genet*, 44, 526-31.
- DZIARSKI, R. & GUPTA, D. 2010. Review: Mammalian peptidoglycan recognition proteins (PGRPs) in innate immunity. *Innate Immun*, 16, 168-74.
- EDWARDS, P. A., KENNEDY, M. A. & MAK, P. A. 2002. LXRs; oxysterol-activated nuclear receptors that regulate genes controlling lipid homeostasis. *Vascul Pharmacol*, 38, 249-56.
- EL-TANANI, M. K. 2008. Role of osteopontin in cellular signaling and metastatic phenotype. *Front Biosci*, 13, 4276-84.

- ELLIS, J. H., BURDEN, M. N., VINOGRADOV, D. V., LINGE, C. & CROWE, J. S. 1996. Interactions of CD80 and CD86 with CD28 and CTLA4. *J Immunol*, 156, 2700-9.
- ELLISEN, L. W. 2005. Growth control under stress: mTOR regulation through the REDD1-TSC pathway. *Cell Cycle*, 4, 1500-02.
- FANELLI, M. A., MONTT-GUEVARA, M., DIBLASI, A. M., GAGO, F. E., TELLO, O., CUELLO-CARRION, F. D., CALLEGARI, E., BAUSERO, M. A. & CIOCCA, D. R. 2008. P-cadherin and beta-catenin are useful prognostic markers in breast cancer patients; beta-catenin interacts with heat shock protein Hsp27. *Cell Stress Chaperones*, 13, 207-20.
- FARINHA, C. M., NOGUEIRA, P., MENDES, F., PENQUE, D. & AMARAL, M. D. 2002. The human DnaJ homologue (Hdj)-1/heat-shock protein (Hsp) 40 co-chaperone is required for the in vivo stabilization of the cystic fibrosis transmembrane conductance regulator by Hsp70. *Biochem J*, 366, 797-806.
- FARRALL, M., GREEN, F. R., PEDEN, J. F., OLSSON, P. G., CLARKE, R., HELLENIUS, M. L., RUST, S., LAGERCRANTZ, J., FRANZOSI, M. G., SCHULTE, H., CAREY, A., OLSSON, G., ASSMANN, G., TOGNONI, G., COLLINS, R., HAMSTEN, A. & WATKINS, H. 2006. Genome-wide mapping of susceptibility to coronary artery disease identifies a novel replicated locus on chromosome 17. *PLoS Genet*, 2, e72.
- FAURE, M. & LONG, E. O. 2002. KIR2DL4 (CD158d), an NK cell-activating receptor with inhibitory potential. *J Immunol*, 168, 6208-14.
- FERLAZZO, G., SPAGGIARI, G. M., SEMINO, C., MELIOLI, G. & MORETTA, L. 2000. Engagement of CD33 surface molecules prevents the generation of dendritic cells from both monocytes and CD34+ myeloid precursors. *Eur J Immunol*, 30, 827-33.
- FERON, O., DESSY, C., DESAGER, J. P. & BALLIGAND, J. L. 2001. Hydroxy-methylglutaryl-coenzyme A reductase inhibition promotes endothelial nitric oxide synthase activation through a decrease in caveolin abundance. *Circulation*, 103, 113-8.
- FINK, L., HOLSCHERMANN, H., KWAPISZEWSKA, G., MUYAL, J. P., LENGEMANN, B., BOHLE, R. M. & SANTOSO, S. 2003. Characterization of platelet-specific mRNA by real-time PCR after laser-assisted microdissection. *Thromb Haemost*, 90, 749-56.
- FISCHER, M., BROECKEL, U., HOLMER, S., BAESSLER, A., HENGSTENBERG, C., MAYER, B., ERDMANN, J., KLEIN, G., RIEGGER, G., JACOB, H. J. & SCHUNKERT, H. 2005. Distinct heritable patterns of angiographic coronary artery disease in families with myocardial infarction. *Circulation*, 111, 855-62.
- FORD, E. S., AJANI, U. A., CROFT, J. B., CRITCHLEY, J. A., LABARTHE, D. R., KOTTKE, T. E., GILES, W. H. & CAPEWELL, S. 2007. Explaining the decrease in U.S. deaths from coronary disease, 1980-2000. *N Engl J Med*, 356, 2388-98.
- FORSYTHE, J. A., JIANG, B. H., IYER, N. V., AGANI, F., LEUNG, S. W., KOOS, R. D. & SEMENZA, G. L. 1996. Activation of vascular endothelial growth factor gene transcription by hypoxia-inducible factor 1. *Mol Cell Biol*, 16, 4604-13.
- FOX, R., NHAN, T. Q., LAW, G. L., MORRIS, D. R., LILES, W. C. & SCHWARTZ, S. M. 2007. PSGL-1 and mTOR regulate translation of ROCK-1 and physiological functions of macrophages. *EMBO J*, 26, 505-15.
- FRATELLI, M., GOODWIN, L. O., OROM, U. A., LOMBARDI, S., TONELLI, R., MENGOZZI, M. & GHEZZI, P. 2005. Gene expression profiling reveals a signaling role of glutathione in redox regulation. *Proc Natl Acad Sci U S A*, 102, 13998-4003.
- FREEDMAN, J. E. & LOSCALZO, J. 2002. Platelet-monocyte aggregates: bridging thrombosis and inflammation. *Circulation*, 105, 2130-2.

- FREEMAN, B. C. & MORIMOTO, R. I. 1996. The human cytosolic molecular chaperones hsp90, hsp70 (hsc70) and hdj-1 have distinct roles in recognition of a non-native protein and protein refolding. *EMBO J*, 15, 2969-79.
- FRIETZE, S., O'GEEN, H., BLAHNIK, K. R., JIN, V. X. & FARNHAM, P. J. 2010. ZNF274 recruits the histone methyltransferase SETDB1 to the 3' ends of ZNF genes. *PLoS One*, 5, e15082.
- FURMAN, M. I., BARNARD, M. R., KRUEGER, L. A., FOX, M. L., SHILALE, E. A., LESSARD, D. M., MARCHESE, P., FRELINGER, A. L., 3RD, GOLDBERG, R. J. & MICHELSON, A. D. 2001. Circulating monocyte-platelet aggregates are an early marker of acute myocardial infarction. *J Am Coll Cardiol*, 38, 1002-6.
- FURNKRANZ, A., SCHOBER, A., BOCHKOV, V. N., BASHTRYKOV, P., KRONKE, G., KADL, A., BINDER, B. R., WEBER, C. & LEITINGER, N. 2005. Oxidized phospholipids trigger atherogenic inflammation in murine arteries. *Arterioscler Thromb Vasc Biol*, 25, 633-8.
- FUTAMURA, Y. 1994. [Strain- and age-associated changes in cytokine release from endotoxin-treated mouse monocytes]. *Jikken Dobutsu*, 43, 545-9.
- GALLO, L. I., LAGADARI, M., PIWIEN-PILIPUK, G. & GALIGNIANA, M. D. 2011. The Hsp90-binding immunophilin FKBP51 is a mitochondrial protein that translocates to the nucleus to protect cells against oxidative stress. *J Biol Chem*.
- GAO, C. & CHEN, Y. G. 2010. Dishevelled: The hub of Wnt signaling. *Cell Signal*, 22, 717-27.
- GARCIA-ARGUINZONIS, M., PADRO, T., LUGANO, R., LLORENTE-CORTES, V. & BADIMON, L. 2010. Low-density lipoproteins induce heat shock protein 27 dephosphorylation, oligomerization, and subcellular relocation in human vascular smooth muscle cells. *Arterioscler Thromb Vasc Biol*, 30, 1212-9.
- GAWAZ, M., STELLOS, K. & LANGER, H. F. 2008. Platelets modulate atherogenesis and progression of atherosclerotic plaques via interaction with progenitor and dendritic cells. *J Thromb Haemost*, 6, 235-42.
- GILAD, Y., RIFKIN, S. A. & PRITCHARD, J. K. 2008. Revealing the architecture of gene regulation: the promise of eQTL studies. *Trends Genet*, 24, 408-15.
- GO, Y. M., LEVONEN, A. L., MOELLERING, D., RAMACHANDRAN, A., PATEL, R. P., JO, H. & DARLEY-USMAR, V. M. 2001. Endothelial NOS-dependent activation of c-Jun NH(2)- terminal kinase by oxidized low-density lipoprotein. *Am J Physiol Heart Circ Physiol*, 281, H2705-13.
- GOLDBERG, R. J., GLATFELTER, K., BURBANK-SCHMIDT, E., LESSARD, D. & GORE, J. M. 2006. Trends in community mortality due to coronary heart disease. *Am Heart J*, 151, 501-7.
- GOMIS-RUTH, F. X. 2003. Structural aspects of the metzincin clan of metalloendopeptidases. *Mol Biotechnol*, 24, 157-202.
- GORDON, T. & KANNEL, W. B. 1971. Premature mortality from coronary heart disease. The Framingham study. *JAMA*, 215, 1617-25.
- GORDON, T. & KANNEL, W. B. 1976. Obesity and cardiovascular diseases: the Framingham study. *Clin Endocrinol Metab*, 5, 367-75.
- GRUNHAGE, F., NATTERMANN, J., GRESSNER, O. A., WASMUTH, H. E., HELLERBRAND, C., SAUERBRUCH, T., SPENGLER, U. & LAMMERT, F. 2010. Lower copy numbers of the chemokine CCL3L1 gene in patients with chronic hepatitis C. *J Hepatol*, 52, 153-9.
- GUO, D. C., PAPKE, C. L., TRAN-FADULU, V., REGALADO, E. S., AVIDAN, N., JOHNSON, R. J., KIM, D. H., PANNU, H., WILLING, M. C., SPARKS, E., PYERITZ, R. E., SINGH, M. N., DALMAN, R. L., GROTTA, J. C., MARIAN, A. J.,

- BOERWINKLE, E. A., FRAZIER, L. Q., LEMAIRE, S. A., COSELLI, J. S., ESTRERA, A. L., SAFI, H. J., VEERARAGHAVAN, S., MUZNY, D. M., WHEELER, D. A., WILLERSON, J. T., YU, R. K., SHETE, S. S., SCHERER, S. E., RAMAN, C. S., BUJA, L. M. & MILEWICZ, D. M. 2009. Mutations in smooth muscle alpha-actin (ACTA2) cause coronary artery disease, stroke, and Moyamoya disease, along with thoracic aortic disease. *Am J Hum Genet*, 84, 617-27.
- GUSTAFSON, B. & SMITH, U. 2006. Cytokines promote Wnt signaling and inflammation and impair the normal differentiation and lipid accumulation in 3T3-L1 preadipocytes. *J Biol Chem*, 281, 9507-16.
- HAGEN, F. S., GRANT, F. J., KUIJPER, J. L., SLAUGHTER, C. A., MOOMAW, C. R., ORTH, K., O'HARA, P. J. & MUNFORD, R. S. 1991. Expression and characterization of recombinant human acyloxyacyl hydrolase, a leukocyte enzyme that deacylates bacterial lipopolysaccharides. *Biochemistry*, 30, 8415-23.
- HAJJAR, K. A., GAVISH, D., BRESLOW, J. L. & NACHMAN, R. L. 1989. Lipoprotein(a) modulation of endothelial cell surface fibrinolysis and its potential role in atherosclerosis. *Nature*, 339, 303-5.
- HAKENEWERTH, A. M., MILLIKAN, R. C., RUSYN, I., HERRING, A. H., NORTH, K. E., BARNHOLTZ-SLOAN, J. S., FUNKHOUSER, W. F., WEISSLER, M. C. & OLSHAN, A. F. 2011. Joint effects of alcohol consumption and polymorphisms in alcohol and oxidative stress metabolism genes on risk of head and neck cancer. *Cancer Epidemiol Biomarkers Prev*, 20, 2438-49.
- HAN, E. S., MULLER, F. L., PEREZ, V. I., QI, W., LIANG, H., XI, L., FU, C., DOYLE, E., HICKEY, M., CORNELL, J., EPSTEIN, C. J., ROBERTS, L. J., VAN REMMEN, H. & RICHARDSON, A. 2008. The in vivo gene expression signature of oxidative stress. *Physiol Genomics*, 34, 112-26.
- HAN, Y., KUANG, S. Z., GOMER, A. & RAMIREZ-BERGERON, D. L. 2010. Hypoxia influences the vascular expansion and differentiation of embryonic stem cell cultures through the temporal expression of vascular endothelial growth factor receptors in an ARNT-dependent manner. *Stem Cells*, 28, 799-809.
- HANNA, J., MUSSAFFI, H., STEUER, G., HANNA, S., DEEB, M., BLAU, H., ARNON, T. I., WEIZMAN, N. & MANDELBOIM, O. 2005. Functional aberrant expression of CCR2 receptor on chronically activated NK cells in patients with TAP-2 deficiency. *Blood*, 106, 3465-73.
- HANSELL, C. A., HURSON, C. E. & NIBBS, R. J. 2011. DARC and D6: silent partners in chemokine regulation? *Immunol Cell Biol*, 89, 197-206.
- HANSSON, M., ELLIS, E., HUNT, M. C., SCHMITZ, G. & BABIKER, A. 2003. Marked induction of sterol 27-hydroxylase activity and mRNA levels during differentiation of human cultured monocytes into macrophages. *Biochim Biophys Acta*, 1593, 283-9.
- HARISMENDY, O., NOTANI, D., SONG, X., RAHIM, N. G., TANASA, B., HEINTZMAN, N., REN, B., FU, X. D., TOPOL, E. J., ROSENFELD, M. G. & FRAZER, K. A. 2011. 9p21 DNA variants associated with coronary artery disease impair interferon-gamma signalling response. *Nature*, 470, 264-8.
- HARJA, E., BUCCIARELLI, L. G., LU, Y., STERN, D. M., ZOU, Y. S., SCHMIDT, A. M. & YAN, S. F. 2004. Early growth response-1 promotes atherogenesis: mice deficient in early growth response-1 and apolipoprotein E display decreased atherosclerosis and vascular inflammation. *Circ Res*, 94, 333-9.
- HAROON, Z. A., WANNENBURG, T., GUPTA, M., GREENBERG, C. S., WALLIN, R. & SANE, D. C. 2001. Localization of tissue transglutaminase in human carotid and coronary artery atherosclerosis: implications for plaque stability and progression. *Lab Invest*, 81, 83-93.

- HARVALD, B. 1967. Genetic perspectives in diabetes mellitus. *Acta Med Scand Suppl*, 476, 17-27.
- HASAN, R. N. & SCHAFER, A. I. 2008. Hemin upregulates Egr-1 expression in vascular smooth muscle cells via reactive oxygen species ERK-1/2-Elk-1 and NF-kappaB. *Circ Res*, 102, 42-50.
- HATA, M., TAKAHARA, S., TSUZAKI, H., ISHII, Y., NAKATA, K., AKAGAWA, K. S. & SATOH, K. 2009. Expression of Th2-skewed pathology mediators in monocyte-derived type 2 of dendritic cells (DC2). *Immunol Lett*, 126, 29-36.
- HAUSER, E. R., CROSSMAN, D. C., GRANGER, C. B., HAINES, J. L., JONES, C. J., MOOSER, V., MCADAM, B., WINKELMANN, B. R., WISEMAN, A. H., MUHLESTEIN, J. B., BARTEL, A. G., DENNIS, C. A., DOWDY, E., ESTABROOKS, S., EGGLESTON, K., FRANCIS, S., ROCHE, K., CLEVINGER, P. W., HUANG, L., PEDERSEN, B., SHAH, S., SCHMIDT, S., HAYNES, C., WEST, S., ASPER, D., BOOZE, M., SHARMA, S., SUNDSETH, S., MIDDLETON, L., ROSES, A. D., HAUSER, M. A., VANCE, J. M., PERICAK-VANCE, M. A. & KRAUS, W. E. 2004. A genomewide scan for early-onset coronary artery disease in 438 families: the GENECARD Study. *Am J Hum Genet*, 75, 436-47.
- HAYASHIDA, K., KUME, N., MURASE, T., MINAMI, M., NAKAGAWA, D., INADA, T., TANAKA, M., UEDA, A., KOMINAMI, G., KAMBARA, H., KIMURA, T. & KITA, T. 2005. Serum soluble lectin-like oxidized low-density lipoprotein receptor-1 levels are elevated in acute coronary syndrome: a novel marker for early diagnosis. *Circulation*, 112, 812-8.
- HEALY, A. M., PICKARD, M. D., PRADHAN, A. D., WANG, Y., CHEN, Z., CROCE, K., SAKUMA, M., SHI, C., ZAGO, A. C., GARASIC, J., DAMOKOSH, A. I., DOWIE, T. L., POISSON, L., LILLIE, J., LIBBY, P., RIDKER, P. M. & SIMON, D. I. 2006. Platelet expression profiling and clinical validation of myeloid-related protein-14 as a novel determinant of cardiovascular events. *Circulation*, 113, 2278-84.
- HEINE, H., DELUDE, R. L., MONKS, B. G., ESPEVIK, T. & GOLENBOCK, D. T. 1999. Bacterial lipopolysaccharide induces expression of the stress response genes hop and H411. *J Biol Chem*, 274, 21049-55.
- HELGADOTTIR, A., THORLEIFSSON, G., MANOLESCU, A., GRETARSDOTTIR, S., BLONDAL, T., JONASDOTTIR, A., SIGURDSSON, A., BAKER, A., PALSSON, A., MASSON, G., GUDBJARTSSON, D. F., MAGNUSSON, K. P., ANDERSEN, K., LEVEY, A. I., BACKMAN, V. M., MATTHIASDOTTIR, S., JONSDOTTIR, T., PALSSON, S., EINARSDOTTIR, H., GUNNARSDOTTIR, S., GYLFASSON, A., VACCARINO, V., HOOPER, W. C., REILLY, M. P., GRANGER, C. B., AUSTIN, H., RADER, D. J., SHAH, S. H., QUYYUMI, A. A., GULCHER, J. R., THORGEIRSSON, G., THORSTEINSDOTTIR, U., KONG, A. & STEFANSSON, K. 2007. A common variant on chromosome 9p21 affects the risk of myocardial infarction. *Science*, 316, 1491-3.
- HIROTA, Y., TRANGUCH, S., DAIKOKU, T., HASEGAWA, A., OSUGA, Y., TAKETANI, Y. & DEY, S. K. 2008. Deficiency of immunophilin FKBP52 promotes endometriosis. *Am J Pathol*, 173, 1747-57.
- HOLDT, L. M., SASS, K., GABEL, G., BERGERT, H., THIERY, J. & TEUPSER, D. 2011. Expression of Chr9p21 genes CDKN2B (p15(INK4b)), CDKN2A (p16(INK4a)), p14(ARF) and MTAP in human atherosclerotic plaque. *Atherosclerosis*, 214, 264-70.
- HOLDT, L. M. & TEUPSER, D. 2012. Recent studies of the human chromosome 9p21 locus, which is associated with atherosclerosis in human populations. *Arterioscler Thromb Vasc Biol*, 32, 196-206.

- HOLM, T., DAMAS, J. K., HOLVEN, K., NORDOY, I., BROSSTAD, F. R., UELAND, T., WAHRE, T., KJEKSHUS, J., FROLAND, S. S., EIKEN, H. G., SOLUM, N. O., GULLESTAD, L., NENSETER, M. & AUKRUST, P. 2003. CXC-chemokines in coronary artery disease: possible pathogenic role of interactions between oxidized low-density lipoprotein, platelets and peripheral blood mononuclear cells. *J Thromb Haemost*, 1, 257-62.
- HOLMES, D. I. & ZACHARY, I. 2004. Placental growth factor induces FosB and c-Fos gene expression via Flt-1 receptors. *FEBS Lett*, 557, 93-8.
- HOLVOET, P. 2008. Relations between metabolic syndrome, oxidative stress and inflammation and cardiovascular disease. *Verh K Acad Geneesk Belg*, 70, 193-219.
- HONG, Y. J., JEONG, M. H., CHOI, Y. H., MA, E. H., KO, J. S., LEE, M. G., PARK, K. H., SIM, D. S., YOON, N. S., YOUN, H. J., KIM, K. H., PARK, H. W., KIM, J. H., AHN, Y., CHO, J. G., PARK, J. C. & KANG, J. C. 2010. Differences in intravascular ultrasound findings in culprit lesions in infarct-related arteries between ST segment elevation myocardial infarction and non-ST segment elevation myocardial infarction. *J Cardiol*, 56, 15-22.
- HOPKINS, P. N., WILLIAMS, R. R., KUIDA, H., STULTS, B. M., HUNT, S. C., BARLOW, G. K. & ASH, K. O. 1988. Family history as an independent risk factor for incident coronary artery disease in a high-risk cohort in Utah. *Am J Cardiol*, 62, 703-7.
- HORREVOETS, A. J., FONTIJN, R. D., VAN ZONNEVELD, A. J., DE VRIES, C. J., TEN CATE, J. W. & PANNEKOEK, H. 1999. Vascular endothelial genes that are responsive to tumor necrosis factor-alpha in vitro are expressed in atherosclerotic lesions, including inhibitor of apoptosis protein-1, stannin, and two novel genes. *Blood*, 93, 3418-31.
- HU, C., DANDAPAT, A., CHEN, J., LIU, Y., HERMONAT, P. L., CAREY, R. M. & MEHTA, J. L. 2008. Over-expression of angiotensin II type 2 receptor (agtr2) reduces atherogenesis and modulates LOX-1, endothelial nitric oxide synthase and heme-oxygenase-1 expression. *Atherosclerosis*, 199, 288-94.
- HUNG, C. F., HUANG, T. F., CHEN, B. H., SHIEH, J. M., WU, P. H. & WU, W. B. 2008. Lycopene inhibits TNF-alpha-induced endothelial ICAM-1 expression and monocyte-endothelial adhesion. *Eur J Pharmacol*, 586, 275-82.
- IBC_50K_CAD 2011. Large-scale gene-centric analysis identifies novel variants for coronary artery disease. *PLoS Genet*, 7, e1002260.
- IENTILE, R., CACCAMO, D. & GRIFFIN, M. 2007. Tissue transglutaminase and the stress response. *Amino Acids*, 33, 385-94.
- IMAIZUMI, T., YOSHIDA, H. & SATOH, K. 2004. Regulation of CX3CL1/fractalkine expression in endothelial cells. *J Atheroscler Thromb*, 11, 15-21.
- INOUE, O., SUZUKI-INOUE, K. & OZAKI, Y. 2008. Redundant mechanism of platelet adhesion to laminin and collagen under flow: involvement of von Willebrand factor and glycoprotein Ib-IX-V. *J Biol Chem*, 283, 16279-82.
- IOANNIDIS, J. P. & LAU, J. 1997. The impact of high-risk patients on the results of clinical trials. *J Clin Epidemiol*, 50, 1089-98.
- IRITA, J., OKURA, T., JOTOKU, M., NAGAO, T., ENOMOTO, D., KURATA, M., DESILVA, V. R., MIYOSHI, K., MATSUI, Y., UEDE, T., DENHARDT, D. T., RITTLING, S. R. & HIGAKI, J. 2011. Osteopontin deficiency protects against aldosterone-induced inflammation, oxidative stress, and interstitial fibrosis in the kidney. *Am J Physiol Renal Physiol*, 301, F833-44.
- ISHIDA, Y., GAO, J. L. & MURPHY, P. M. 2008. Chemokine receptor CX3CR1 mediates skin wound healing by promoting macrophage and fibroblast accumulation and function. *J Immunol*, 180, 569-79.

- ISHII, T., ITOH, K., RUIZ, E., LEAKE, D. S., UNOKI, H., YAMAMOTO, M. & MANN, G. E. 2004. Role of Nrf2 in the regulation of CD36 and stress protein expression in murine macrophages: activation by oxidatively modified LDL and 4-hydroxynonenal. *Circ Res*, 94, 609-16.
- ISHITANI, T., KISHIDA, S., HYODO-MIURA, J., UENO, N., YASUDA, J., WATERMAN, M., SHIBUYA, H., MOON, R. T., NINOMIYA-TSUJI, J. & MATSUMOTO, K. 2003. The TAK1-NLK mitogen-activated protein kinase cascade functions in the Wnt-5a/Ca(2+) pathway to antagonize Wnt/beta-catenin signaling. *Mol Cell Biol*, 23, 131-9.
- IVAN, L. & ANTOHE, F. 2010. Hyperlipidemia induces endothelial-derived foam cells in culture. *J Recept Signal Transduct Res*, 30, 106-14.
- JACOBS, A. T. & MARNETT, L. J. 2007. Heat shock factor 1 attenuates 4-Hydroxynonenal-mediated apoptosis: critical role for heat shock protein 70 induction and stabilization of Bcl-XL. *J Biol Chem*, 282, 33412-20.
- JAWIEN, J. 2008. New insights into immunological aspects of atherosclerosis. *Pol Arch Med Wewn*, 118, 127-31.
- JIN, T., GEORGE FANTUS, I. & SUN, J. 2008. Wnt and beyond Wnt: multiple mechanisms control the transcriptional property of beta-catenin. *Cell Signal*, 20, 1697-704.
- JOHANSEN, C. T., LANKTREE, M. B. & HEGELE, R. A. 2010. Translating genomic analyses into improved management of coronary artery disease. *Future Cardiol*, 6, 507-21.
- JOHNSON, K. A., POLEWSKI, M. & TERKELTAUB, R. A. 2008. Transglutaminase 2 is central to induction of the arterial calcification program by smooth muscle cells. *Circ Res*, 102, 529-37.
- JONES, K. L., MAGUIRE, J. J. & DAVENPORT, A. P. 2011. Chemokine receptor CCR5: from AIDS to atherosclerosis. *Br J Pharmacol*, 162, 1453-69.
- JUDE, B., ZAWADZKI, C., SUSEN, S. & CORSEAU, D. 2005. Relevance of tissue factor in cardiovascular disease. *Arch Mal Coeur Vaiss*, 98, 667-71.
- JUNG, S. M. & MOROI, M. 2008. Platelet glycoprotein VI. *Adv Exp Med Biol*, 640, 53-63.
- JUNG, S. M., TSUJI, K. & MOROI, M. 2009. Glycoprotein (GP) VI dimer as a major collagen-binding site of native platelets: direct evidence obtained with dimeric GPVI-specific Fabs. *J Thromb Haemost*, 7, 1347-55.
- KAARTINEN, M. T., MURSHED, M., KARSENTY, G. & MCKEE, M. D. 2007. Osteopontin upregulation and polymerization by transglutaminase 2 in calcified arteries of Matrix Gla protein-deficient mice. *J Histochem Cytochem*, 55, 375-86.
- KADL, A., HUBER, J., GRUBER, F., BOCHKOV, V. N., BINDER, B. R. & LEITINGER, N. 2002. Analysis of inflammatory gene induction by oxidized phospholipids in vivo by quantitative real-time RT-PCR in comparison with effects of LPS. *Vascul Pharmacol*, 38, 219-27.
- KADOUCHI, I., SAKAMOTO, K., TANGJIAO, L., MURAKAMI, T., KOBAYASHI, E., HOSHINO, Y. & YAMAGUCHI, A. 2009. Latexin is involved in bone morphogenetic protein-2-induced chondrocyte differentiation. *Biochem Biophys Res Commun*, 378, 600-4.
- KAKUTANI, M., MASAKI, T. & SAWAMURA, T. 2000. A platelet-endothelium interaction mediated by lectin-like oxidized low-density lipoprotein receptor-1. *Proc Natl Acad Sci U S A*, 97, 360-4.
- KAMANNA, V. S. & KASHYAP, M. L. 2007. Nicotinic acid (niacin) receptor agonists: will they be useful therapeutic agents? *Am J Cardiol*, 100, S53-61.

- KAMEZAKI, F., YAMASHITA, K., TASAKI, H., KUME, N., MITSUOKA, H., KITA, T., ADACHI, T. & OTSUJI, Y. 2009. Serum soluble lectin-like oxidized low-density lipoprotein receptor-1 correlates with oxidative stress markers in stable coronary artery disease. *Int J Cardiol*, 134, 285-7.
- KANNEL, W. B. 2000. Fifty years of Framingham Study contributions to understanding hypertension. *J Hum Hypertens*, 14, 83-90.
- KANNEL, W. B., CASTELLI, W. P., GORDON, T. & MCNAMARA, P. M. 1971. Serum cholesterol, lipoproteins, and the risk of coronary heart disease. The Framingham study. *Ann Intern Med*, 74, 1-12.
- KANNEL, W. B., CASTELLI, W. P. & MCNAMARA, P. M. 1968. Cigarette smoking and risk of coronary heart disease. Epidemiologic clues to pathogenesis. The Framingham Study. *Natl Cancer Inst Monogr*, 28, 9-20.
- KANNEL, W. B., DAWBER, T. R., KAGAN, A., REVOTSKIE, N. & STOKES, J., 3RD 1961. Factors of risk in the development of coronary heart disease--six year follow-up experience. The Framingham Study. *Ann Intern Med*, 55, 33-50.
- KANNEL, W. B., DAWBER, T. R. & MCGEE, D. L. 1980. Perspectives on systolic hypertension. The Framingham study. *Circulation*, 61, 1179-82.
- KANNEL, W. B., DAWBER, T. R., THOMAS, H. E., JR. & MCNAMARA, P. M. 1965. Comparison of Serum Lipids in the Prediction of Coronary Heart Disease. Framingham Study Indicates That Cholesterol Level and Blood Pressure Are Major Factors in Coronary Heart Disease; Effect of Obesity and Cigarette Smoking Also Noted. *R I Med J*, 48, 243-50.
- KANNEL, W. B. & MCGEE, D. L. 1979. Diabetes and cardiovascular risk factors: the Framingham study. *Circulation*, 59, 8-13.
- KASTL, S. P., SPEIDL, W. S., KATSAROS, K. M., KAUN, C., REGA, G., ASSADIAN, A., HAGMUELLER, G. W., HOETH, M., DE MARTIN, R., MA, Y., MAURER, G., HUBER, K. & WOJTA, J. 2009. Thrombin induces the expression of oncostatin M via AP-1 activation in human macrophages: a link between coagulation and inflammation. *Blood*, 114, 2812-8.
- KATAGIRI, H., YAMADA, T. & OKA, Y. 2007. Adiposity and cardiovascular disorders: disturbance of the regulatory system consisting of humoral and neuronal signals. *Circ Res*, 101, 27-39.
- KATHIRESAN, S., VOIGHT, B. F., PURCELL, S., MUSUNURU, K., ARDISSINO, D., MANNUCCI, P. M., ANAND, S., ENGERT, J. C., SAMANI, N. J., SCHUNKERT, H., ERDMANN, J., REILLY, M. P., RADER, D. J., MORGAN, T., SPERTUS, J. A., STOLL, M., GIRELLI, D., MCKEOWN, P. P., PATTERSON, C. C., SISCOVICK, D. S., O'DONNELL, C. J., ELOSUA, R., PELTONEN, L., SALOMAA, V., SCHWARTZ, S. M., MELANDER, O., ALTSHULER, D., MERLINI, P. A., BERZUINI, C., BERNARDINELLI, L., PEYVANDI, F., TUBARO, M., CELLI, P., FERRARIO, M., FETIVEAU, R., MARZILIANO, N., CASARI, G., GALLI, M., RIBICHINI, F., ROSSI, M., BERNARDI, F., ZONZIN, P., PIAZZA, A., YEE, J., FRIEDLANDER, Y., MARRUGAT, J., LUCAS, G., SUBIRANA, I., SALA, J., RAMOS, R., MEIGS, J. B., WILLIAMS, G., NATHAN, D. M., MACRAE, C. A., HAVULINNA, A. S., BERGLUND, G., HIRSCHHORN, J. N., ASSELTA, R., DUGA, S., SPREAFICO, M., DALY, M. J., NEMESH, J., KORN, J. M., MCCARROLL, S. A., SURTI, A., GUIDUCCI, C., GIANNINY, L., MIREL, D., PARKIN, M., BURTT, N., GABRIEL, S. B., THOMPSON, J. R., BRAUND, P. S., WRIGHT, B. J., BALMFORTH, A. J., BALL, S. G., HALL, A. S., LINSEL-NITSCHKE, P., LIEB, W., ZIEGLER, A., KONIG, I., HENGSTENBERG, C., FISCHER, M., STARK, K., GROSSHENNIG, A., PREUSS, M., WICHMANN, H. E., SCHREIBER, S., OUWEHAND, W.,

- DELOUKAS, P., SCHOLZ, M., CAMBIEN, F., LI, M., CHEN, Z., WILENSKY, R., MATTHAI, W., QASIM, A., HAKONARSON, H. H., DEVANEY, J., BURNETT, M. S., et al. 2009. Genome-wide association of early-onset myocardial infarction with single nucleotide polymorphisms and copy number variants. *Nat Genet*, 41, 334-41.
- KATIYAR, S., LIU, E., KNUTZEN, C. A., LANG, E. S., LOMBARDO, C. R., SANKAR, S., TOTH, J. I., PETROSKI, M. D., RONAI, Z. & CHIANG, G. G. 2009. REDD1, an inhibitor of mTOR signalling, is regulated by the CUL4A-DDB1 ubiquitin ligase. *EMBO Rep*, 10, 866-72.
- KATO, A., OGASAWARA, T., HOMMA, T., SAITO, H. & MATSUMOTO, K. 2004. Lipopolysaccharide-binding protein critically regulates lipopolysaccharide-induced IFN-beta signaling pathway in human monocytes. *J Immunol*, 172, 6185-94.
- KATOH, M. 2008. WNT signaling in stem cell biology and regenerative medicine. *Curr Drug Targets*, 9, 565-70.
- KAWAMATA, Y., FUJII, R., HOSOYA, M., HARADA, M., YOSHIDA, H., MIWA, M., FUKUSUMI, S., HABATA, Y., ITOH, T., SHINTANI, Y., HINUMA, S., FUJISAWA, Y. & FUJINO, M. 2003. A G protein-coupled receptor responsive to bile acids. *J Biol Chem*, 278, 9435-40.
- KEHREL, B., WIERWILLE, S., CLEMETSON, K. J., ANDERS, O., STEINER, M., KNIGHT, C. G., FARNDAL, R. W., OKUMA, M. & BARNES, M. J. 1998. Glycoprotein VI is a major collagen receptor for platelet activation: it recognizes the platelet-activating quaternary structure of collagen, whereas CD36, glycoprotein IIb/IIIa, and von Willebrand factor do not. *Blood*, 91, 491-9.
- KENNEDY, A., GRUEN, M. L., GUTIERREZ, D. A., SURMI, B. K., ORR, J. S., WEBB, C. D. & HASTY, A. H. 2012. Impact of macrophage inflammatory protein-1alpha deficiency on atherosclerotic lesion formation, hepatic steatosis, and adipose tissue expansion. *PLoS One*, 7, e31508.
- KENT, D. M., ALSHEIKH-ALI, A. & HAYWARD, R. A. 2008. Competing risk and heterogeneity of treatment effect in clinical trials. *Trials*, 9, 30.
- KHACHIGIAN, L. M. 2006. Early growth response-1 in cardiovascular pathobiology. *Circ Res*, 98, 186-91.
- KHACHIGIAN, L. M., ANDERSON, K. R., HALNON, N. J., GIMBRONE, M. A., JR., RESNICK, N. & COLLINS, T. 1997. Egr-1 is activated in endothelial cells exposed to fluid shear stress and interacts with a novel shear-stress-response element in the PDGF A-chain promoter. *Arterioscler Thromb Vasc Biol*, 17, 2280-6.
- KHOT, U. N., KHOT, M. B., BAJZER, C. T., SAPP, S. K., OHMAN, E. M., BRENER, S. J., ELLIS, S. G., LINCOFF, A. M. & TOPOL, E. J. 2003. Prevalence of conventional risk factors in patients with coronary heart disease. *JAMA*, 290, 898-904.
- KIM, H. G., KIM, J. Y., GIM, M. G., LEE, J. M. & CHUNG, D. K. 2008a. Mechanical stress induces tumor necrosis factor- α production through Ca²⁺ release-dependent TLR2 signaling. *Am J Physiol Cell Physiol*, 295, C432-9.
- KIM, J. S., PARK, D. W., LEE, H. K., KIM, J. R. & BAEK, S. H. 2009. Early growth response-1 is involved in foam cell formation and is upregulated by the TLR9-MyD88-ERK1/2 pathway. *Biochem Biophys Res Commun*, 390, 196-200.
- KIM, M. S., YOON, S. K., BOLLIG, F., KITAGAKI, J., HUR, W., WHYE, N. J., WU, Y. P., RIVERA, M. N., PARK, J. Y., KIM, H. S., MALIK, K., BELL, D. W., ENGLERT, C., PERANTONI, A. O. & LEE, S. B. 2010. A novel Wilms tumor 1 (WT1) target gene negatively regulates the WNT signaling pathway. *J Biol Chem*, 285, 14585-93.
- KIM, S. A., CHANG, S., YOON, J. H. & AHN, S. G. 2008b. TAT-Hsp40 inhibits oxidative stress-mediated cytotoxicity via the inhibition of Hsp70 ubiquitination. *FEBS Lett*, 582, 734-40.

- KLOS, K. L., KARDIA, S. L., FERRELL, R. E., TURNER, S. T., BOERWINKLE, E. & SING, C. F. 2001. Genome-wide linkage analysis reveals evidence of multiple regions that influence variation in plasma lipid and apolipoprotein levels associated with risk of coronary heart disease. *Arterioscler Thromb Vasc Biol*, 21, 971-8.
- KLOTZ, O. 1905. Studies Upon Calcareous Degeneration : I. The Process of Pathological Calcification. *J Exp Med*, 7, 633-74.
- KNIGHT, W. D., LITTLE, J. T., CARRENO, F. R., TONEY, G. M., MIFFLIN, S. W. & CUNNINGHAM, J. T. 2011. Chronic intermittent hypoxia increases blood pressure and expression of FosB/DeltaFosB in central autonomic regions. *Am J Physiol Regul Integr Comp Physiol*, 301, R131-9.
- KOJIMA, S., NARA, K. & RIFKIN, D. B. 1993. Requirement for transglutaminase in the activation of latent transforming growth factor-beta in bovine endothelial cells. *J Cell Biol*, 121, 439-48.
- KOOPERBERG, C., SIIPIONE, S., LEBLANC, M., STRAND, A. D., CATTANEO, E. & OLSON, J. M. 2002. Evaluating test statistics to select interesting genes in microarray experiments. *Hum Mol Genet*, 11, 2223-32.
- KOYAMA, Y., HANSEN, P. S., HANRATTY, C. G., NELSON, G. I. & RASMUSSEN, H. H. 2002. Prevalence of coronary occlusion and outcome of an immediate invasive strategy in suspected acute myocardial infarction with and without ST-segment elevation. *Am J Cardiol*, 90, 579-84.
- KRISHNARAJU, K., NGUYEN, H. Q., LIEBERMANN, D. A. & HOFFMAN, B. 1995. The zinc finger transcription factor Egr-1 potentiates macrophage differentiation of hematopoietic cells. *Mol Cell Biol*, 15, 5499-507.
- KUGE, Y., KUME, N., ISHINO, S., TAKAI, N., OGAWA, Y., MUKAI, T., MINAMI, M., SHIOMI, M. & SAJI, H. 2008. Prominent lectin-like oxidized low density lipoprotein (LDL) receptor-1 (LOX-1) expression in atherosclerotic lesions is associated with tissue factor expression and apoptosis in hypercholesterolemic rabbits. *Biol Pharm Bull*, 31, 1475-82.
- KULLER, L. H., TRACY, R. P., SHATEN, J. & MEILAHN, E. N. 1996. Relation of C-reactive protein and coronary heart disease in the MRFIT nested case-control study. Multiple Risk Factor Intervention Trial. *Am J Epidemiol*, 144, 537-47.
- KUME, N., MITSUOKA, H., HAYASHIDA, K., TANAKA, M., KOMINAMI, G. & KITA, T. 2010. Soluble lectin-like oxidized LDL receptor-1 (sLOX-1) as a sensitive and specific biomarker for acute coronary syndrome--comparison with other biomarkers. *J Cardiol*, 56, 159-65.
- KUSHWAHA, R. S. & MCGILL, H. C., JR. 1998. Diet, plasma lipoproteins and experimental atherosclerosis in baboons (*Papio* sp.). *Hum Reprod Update*, 4, 420-9.
- KVASNICKA, T., KVASNICKA, J., CESKA, R. & VRABLIK, M. 2003. Increase of inflammatory state in overweight adults with combined hyperlipidemia. *Nutr Metab Cardiovasc Dis*, 13, 227-31.
- KWON, H. M., YAMAUCHI, A., UCHIDA, S., PRESTON, A. S., GARCIA-PEREZ, A., BURG, M. B. & HANDLER, J. S. 1992. Cloning of the cDNA for a Na⁺/myo-inositol cotransporter, a hypertonicity stress protein. *J Biol Chem*, 267, 6297-301.
- LAI, C. F., SHAO, J. S., BEHRMANN, A., KRCHMA, K., CHENG, S. L. & TOWLER, D. A. 2012. TNFR1-Activated Reactive Oxidative Species Signals Up-Regulate Osteogenic Msx2 Programs in Aortic Myofibroblasts. *Endocrinology*, 153, 3897-910.
- LAMON, B. D., SUMMERS, B. D., GOTTO, A. M., JR. & HAJJAR, D. P. 2009. Pitavastatin suppresses mitogen activated protein kinase-mediated Erg-1 induction in human vascular smooth muscle cells. *Eur J Pharmacol*, 606, 72-6.

- LANE, P. 1997. Regulation of T and B cell responses by modulating interactions between CD28/CTLA4 and their ligands, CD80 and CD86. *Ann N Y Acad Sci*, 815, 392-400.
- LANNEAU, D., DE THONEL, A., MAUREL, S., DIDELOT, C. & GARRIDO, C. 2007. Apoptosis versus cell differentiation: role of heat shock proteins HSP90, HSP70 and HSP27. *Prion*, 1, 53-60.
- LASSILA, R. 1993. Inflammation in atheroma: implications for plaque rupture and platelet-collagen interaction. *Eur Heart J*, 14 Suppl K, 94-7.
- LATTIMORE, J. D., WILCOX, I., NAKHLA, S., LANGENFELD, M., JESSUP, W. & CELERMAJER, D. S. 2005. Repetitive hypoxia increases lipid loading in human macrophages—a potentially atherogenic effect. *Atherosclerosis*, 179, 255-9.
- LAWRENCE, S., TANG, Y., FRANK, M. B., DOZMOROV, I., JIANG, K., CHEN, Y., CADWELL, C., TURNER, S., CENTOLA, M. & JARVIS, J. N. 2007. A dynamic model of gene expression in monocytes reveals differences in immediate/early response genes between adult and neonatal cells. *J Inflamm (Lond)*, 4, 4.
- LEBRUN, C. J., BLUME, A., HERDEGEN, T., SEIFERT, K., BRAVO, R. & UNGER, T. 1995. Angiotensin II induces a complex activation of transcription factors in the rat brain: expression of Fos, Jun and Krox proteins. *Neuroscience*, 65, 93-9.
- LEE, A. K., AHN, S. G., YOON, J. H. & KIM, S. A. 2011a. Sox4 stimulates ss-catenin activity through induction of CK2. *Oncol Rep*, 25, 559-65.
- LEE, D. K., NATHAN GRANTHAM, R., TRACHTE, A. L., MANNION, J. D. & WILSON, C. L. 2006. Activation of the canonical Wnt/beta-catenin pathway enhances monocyte adhesion to endothelial cells. *Biochem Biophys Res Commun*, 347, 109-16.
- LEE, H. L., WOO, K. M., RYOO, H. M. & BAEK, J. H. 2010. Tumor necrosis factor- α increases alkaline phosphatase expression in vascular smooth muscle cells via MSX2 induction. *Biochem Biophys Res Commun*, 391, 1087-92.
- LEE, K. M., MCKIMMIE, C. S., GILCHRIST, D. S., PALLAS, K. J., NIBBS, R. J., GARSIDE, P., MCDONALD, V., JENKINS, C., RANSOHOFF, R., LIU, L., MILLING, S., CEROVIC, V. & GRAHAM, G. J. 2011b. D6 facilitates cellular migration and fluid flow to lymph nodes by suppressing lymphatic congestion. *Blood*, 118, 6220-9.
- LEE, S. H., KIM, M. H. & HAN, H. J. 2009a. Arachidonic acid potentiates hypoxia-induced VEGF expression in mouse embryonic stem cells: involvement of Notch, Wnt, and HIF-1 α . *Am J Physiol Cell Physiol*, 297, C207-16.
- LEE, S. Y., MINTZ, G. S., KIM, S. Y., HONG, Y. J., KIM, S. W., OKABE, T., PICHARD, A. D., SATLER, L. F., KENT, K. M., SUDDATH, W. O., WAKSMAN, R. & WEISSMAN, N. J. 2009b. Attenuated plaque detected by intravascular ultrasound: clinical, angiographic, and morphologic features and post-percutaneous coronary intervention complications in patients with acute coronary syndromes. *JACC Cardiovasc Interv*, 2, 65-72.
- LEMAOULT, J., ZAFARANLOO, K., LE DANFF, C. & CAROSELLA, E. D. 2005. HLA-G up-regulates ILT2, ILT3, ILT4, and KIR2DL4 in antigen presenting cells, NK cells, and T cells. *FASEB J*, 19, 662-4.
- LI, J., SUN, X., WANG, Z., CHEN, L., LI, D., ZHOU, J. & LIU, M. 2012. Regulation of vascular endothelial cell polarization and migration by Hsp70/Hsp90-organizing protein. *PLoS One*, 7, e36389.
- LI, W., KORNMARK, L., JONASSON, L., FORSSELL, C. & YUAN, X. M. 2009a. Cathepsin L is significantly associated with apoptosis and plaque destabilization in human atherosclerosis. *Atherosclerosis*, 202, 92-102.

- LI, Y., BASANG, Z., DING, H., LU, Z., NING, T., WEI, H., CAI, H. & KE, Y. Latexin expression is downregulated in human gastric carcinomas and exhibits tumor suppressor potential. *BMC Cancer*, 11, 121.
- LI, Y., BASANG, Z., DING, H., LU, Z., NING, T., WEI, H., CAI, H. & KE, Y. 2011. Latexin expression is downregulated in human gastric carcinomas and exhibits tumor suppressor potential. *BMC Cancer*, 11, 121.
- LI, Y. H., LIU, S. L., SHI, G. Y., TSENG, G. H., LIU, P. Y. & WU, H. L. 2006. Thrombomodulin plays an important role in arterial remodeling and neointima formation in mouse carotid ligation model. *Thromb Haemost*, 95, 128-33.
- LI, Y. H., SHI, G. Y. & WU, H. L. 2009b. Thrombomodulin in the treatment of atherothrombotic diseases. *Front Biosci (Schol Ed)*, 1, 33-8.
- LIANG, Y., JANSEN, M., ARONOW, B., GEIGER, H. & VAN ZANT, G. 2007. The quantitative trait gene latexin influences the size of the hematopoietic stem cell population in mice. *Nat Genet*, 39, 178-88.
- LIANG, Y. & VAN ZANT, G. 2008. Aging stem cells, latexin, and longevity. *Exp Cell Res*, 314, 1962-72.
- LIBBY, P. 2002. Inflammation in atherosclerosis. *Nature*, 420, 868-74.
- LIN, C. I., CHEN, C. N., LIN, P. W., CHANG, K. J., HSIEH, F. J. & LEE, H. 2007. Lysophosphatidic acid regulates inflammation-related genes in human endothelial cells through LPA1 and LPA3. *Biochem Biophys Res Commun*, 363, 1001-8.
- LIN, C. L., CHENG, H., TUNG, C. W., HUANG, W. J., CHANG, P. J., YANG, J. T. & WANG, J. Y. 2008. Simvastatin reverses high glucose-induced apoptosis of mesangial cells via modulation of Wnt signaling pathway. *Am J Nephrol*, 28, 290-7.
- LINDEN, M. D. & JACKSON, D. E. 2010. Platelets: pleiotropic roles in atherogenesis and atherothrombosis. *Int J Biochem Cell Biol*, 42, 1762-6.
- LIPPI, G., MONTAGNANA, M., SALVAGNO, G. L., CICORELLA, N., DEGAN, M., MINUZ, P., LECHI, C. & GUIDI, G. C. 2007. Risk stratification of patients with acute myocardial infarction by quantification of circulating monocyte-platelet aggregates. *Int J Cardiol*, 115, 101-2.
- LIU, C., ADAMSON, E. & MERCOLA, D. 1996. Transcription factor EGR-1 suppresses the growth and transformation of human HT-1080 fibrosarcoma cells by induction of transforming growth factor beta 1. *Proc Natl Acad Sci U S A*, 93, 11831-6.
- LIU, J., SUKHOVA, G. K., YANG, J. T., SUN, J., MA, L., REN, A., XU, W. H., FU, H., DOLGANOV, G. M., HU, C., LIBBY, P. & SHI, G. P. 2006. Cathepsin L expression and regulation in human abdominal aortic aneurysm, atherosclerosis, and vascular cells. *Atherosclerosis*, 184, 302-11.
- LLOYD-JONES, D. M., NAM, B. H., D'AGOSTINO, R. B., SR., LEVY, D., MURABITO, J. M., WANG, T. J., WILSON, P. W. & O'DONNELL, C. J. 2004. Parental cardiovascular disease as a risk factor for cardiovascular disease in middle-aged adults: a prospective study of parents and offspring. *Jama*, 291, 2204-11.
- LLUIS-GANELLA, C., LUCAS, G., SUBIRANA, I., ESCURRIOL, V., TOMAS, M., SENTI, M., SALA, J., MARRUGAT, J. & ELOSUA, R. 2009. Qualitative assessment of previous evidence and an updated meta-analysis confirms lack of association between the ESR1 rs2234693 (PvuII) variant and coronary heart disease in men and women. *Atherosclerosis*, 207, 480-6.
- LOCATI, M., TORRE, Y. M., GALLIERA, E., BONECCHI, R., BODDULURI, H., VAGO, G., VECCHI, A. & MANTOVANI, A. 2005. Silent chemoattractant receptors: D6 as a decoy and scavenger receptor for inflammatory CC chemokines. *Cytokine Growth Factor Rev*, 16, 679-86.

- LU, J., MITRA, S., WANG, X., KHAIDAKOV, M. & MEHTA, J. L. 2011a. Oxidative stress and lectin-like ox-LDL-receptor LOX-1 in atherogenesis and tumorigenesis. *Antioxid Redox Signal*, 15, 2301-33.
- LU, J., MITRA, S., WANG, X., KHAIDAKOV, M. & MEHTA, J. L. 2011b. Oxidative Stress and Lectin-Like Ox-LDL-Receptor LOX-1 in Atherogenesis and Tumorigenesis. *Antioxid Redox Signal*.
- MADAMANCHI, N. R., VENDROV, A. & RUNGE, M. S. 2005. Oxidative stress and vascular disease. *Arterioscler Thromb Vasc Biol*, 25, 29-38.
- MADDALUNO, M., DI LAURO, M., DI PASCALE, A., SANTAMARIA, R., GUGLIELMOTTI, A., GRASSIA, G. & IALENTI, A. 2011. Monocyte chemotactic protein-3 induces human coronary smooth muscle cell proliferation. *Atherosclerosis*, 217, 113-9.
- MADRIGAL-MATUTE, J., LOPEZ-FRANCO, O., BLANCO-COLIO, L. M., MUNOZ-GARCIA, B., RAMOS-MOZO, P., ORTEGA, L., EGIDO, J. & MARTIN-VENTURA, J. L. Heat shock protein 90 inhibitors attenuate inflammatory responses in atherosclerosis. *Cardiovasc Res*, 86, 330-7.
- MALLEE, J. J., ATTA, M. G., LORICA, V., RIM, J. S., KWON, H. M., LUCENTE, A. D., WANG, Y. & BERRY, G. T. 1997. The structural organization of the human Na⁺/myo-inositol cotransporter (SLC5A3) gene and characterization of the promoter. *Genomics*, 46, 459-65.
- MAMTANI, M., MATSUBARA, T., SHIMIZU, C., FURUKAWA, S., AKAGI, T., ONOUCHI, Y., HATA, A., FUJINO, A., HE, W., AHUJA, S. K. & BURNS, J. C. 2010. Association of CCR2-CCR5 haplotypes and CCL3L1 copy number with Kawasaki Disease, coronary artery lesions, and IVIG responses in Japanese children. *PLoS One*, 5, e11458.
- MARENBERG, M. E., RISCH, N., BERKMAN, L. F., FLODERUS, B. & DE FAIRE, U. 1994. Genetic susceptibility to death from coronary heart disease in a study of twins. *N Engl J Med*, 330, 1041-6.
- MARTELLI, A. M., BORTUL, R., TABELLINI, G., BAREGGI, R., MANZOLI, L., NARDUCCI, P. & COCCO, L. 2002. Diacylglycerol kinases in nuclear lipid-dependent signal transduction pathways. *Cell Mol Life Sci*, 59, 1129-37.
- MARTIN-VENTURA, J. L., NICOLAS, V., HOUARD, X., BLANCO-COLIO, L. M., LECLERCQ, A., EGIDO, J., VRANCKX, R., MICHEL, J. B. & MEILHAC, O. 2006. Biological significance of decreased HSP27 in human atherosclerosis. *Arterioscler Thromb Vasc Biol*, 26, 1337-43.
- MARUYAMA, T., TANAKA, K., SUZUKI, J., MIYOSHI, H., HARADA, N., NAKAMURA, T., MIYAMOTO, Y., KANATANI, A. & TAMAI, Y. 2006. Targeted disruption of G protein-coupled bile acid receptor 1 (Gpbar1/M-Bar) in mice. *J Endocrinol*, 191, 197-205.
- MASAI, N., TATEBE, J., YOSHINO, G. & MORITA, T. 2010. Indoxyl sulfate stimulates monocyte chemoattractant protein-1 expression in human umbilical vein endothelial cells by inducing oxidative stress through activation of the NADPH oxidase-nuclear factor-kappaB pathway. *Circ J*, 74, 2216-24.
- MASSBERG, S., BRAND, K., GRUNER, S., PAGE, S., MULLER, E., MULLER, I., BERGMEIER, W., RICHTER, T., LORENZ, M., KONRAD, I., NIESWANDT, B. & GAWAZ, M. 2002. A critical role of platelet adhesion in the initiation of atherosclerotic lesion formation. *J Exp Med*, 196, 887-96.
- MATHERS, C. D. & LONCAR, D. 2006. Projections of global mortality and burden of disease from 2002 to 2030. *PLoS Med*, 3, e442.

- MATSUMOTO, T. & MUGISHIMA, H. 2006. Signal transduction via vascular endothelial growth factor (VEGF) receptors and their roles in atherogenesis. *J Atheroscler Thromb*, 13, 130-5.
- MATSUMURA, M. E., LI, F., BERTHOUX, L., WEI, B., LOBE, D. R., JEON, C., HAMMARSKJOLD, M. L. & MCNAMARA, C. A. 2001. Vascular injury induces posttranscriptional regulation of the Id3 gene: cloning of a novel Id3 isoform expressed during vascular lesion formation in rat and human atherosclerosis. *Arterioscler Thromb Vasc Biol*, 21, 752-8.
- MATTOCK, K. L., GOUGH, P. J., HUMPHRIES, J., BURNAND, K., PATEL, L., SUCKLING, K. E., CUELLO, F., WATTS, C., GAUTEL, M., AVKIRAN, M. & SMITH, A. 2010. Legumain and cathepsin-L expression in human unstable carotid plaque. *Atherosclerosis*, 208, 83-9.
- MAYER, B., ERDMANN, J. & SCHUNKERT, H. 2007. Genetics and heritability of coronary artery disease and myocardial infarction. *Clin Res Cardiol*, 96, 1-7.
- MCCAFFREY, T. A., FU, C., DU, B., EKSINAR, S., KENT, K. C., BUSH, H., JR., KREIGER, K., ROSENGART, T., CYBULSKY, M. I., SILVERMAN, E. S. & COLLINS, T. 2000. High-level expression of Egr-1 and Egr-1-inducible genes in mouse and human atherosclerosis. *J Clin Invest*, 105, 653-62.
- MCCLAIN, K. L., CAI, Y. H., HICKS, J., PETERSON, L. E., YAN, X. T., CHE, S. & GINSBERG, S. D. 2005. Expression profiling using human tissues in combination with RNA amplification and microarray analysis: assessment of Langerhans cell histiocytosis. *Amino Acids*, 28, 279-90.
- MCGREGOR, L., MARTIN, J. & MCGREGOR, J. L. 2006. Platelet-leukocyte aggregates and derived microparticles in inflammation, vascular remodelling and thrombosis. *Front Biosci*, 11, 830-7.
- MCPHERSON, R., PERTSEMLIDIS, A., KAVASLAR, N., STEWART, A., ROBERTS, R., COX, D. R., HINDS, D. A., PENNACCHIO, L. A., TYBJAERG-HANSEN, A., FOLSOM, A. R., BOERWINKLE, E., HOBBS, H. H. & COHEN, J. C. 2007. A common allele on chromosome 9 associated with coronary heart disease. *Science*, 316, 1488-91.
- MEDINA, P., NAVARRO, S., CORRAL, J., ZORIO, E., ROLDAN, V., ESTELLES, A., SANTAMARIA, A., MARIN, F., RUEDA, J., BERTINA, R. M. & ESPANA, F. 2008. Endothelial protein C receptor polymorphisms and risk of myocardial infarction. *Haematologica*, 93, 1358-63.
- MENEZES, M. E., MITRA, A., SHEVDE, L. A. & SAMANT, R. S. 2012. DNAB6 governs a novel regulatory loop determining Wnt/beta-catenin signalling activity. *Biochem J*, 444, 573-80.
- MICHALEC, L., CHOUDHURY, B. K., POSTLETHWAIT, E., WILD, J. S., ALAM, R., LETT-BROWN, M. & SUR, S. 2002. CCL7 and CXCL10 orchestrate oxidative stress-induced neutrophilic lung inflammation. *J Immunol*, 168, 846-52.
- MICHELSON, A. D., BARNARD, M. R., KRUEGER, L. A., VALERI, C. R. & FURMAN, M. I. 2001. Circulating monocyte-platelet aggregates are a more sensitive marker of in vivo platelet activation than platelet surface P-selectin: studies in baboons, human coronary intervention, and human acute myocardial infarction. *Circulation*, 104, 1533-7.
- MIKELS, A. J. & NUSSE, R. 2006. Purified Wnt5a protein activates or inhibits beta-catenin-TCF signaling depending on receptor context. *PLoS Biol*, 4, e115.
- MILLER, K. P. & RAMOS, K. S. 2005. DNA sequence determinants of nuclear protein binding to the c-Ha-ras antioxidant/electrophile response element in vascular smooth

- muscle cells: identification of Nrf2 and heat shock protein 90 beta as heterocomplex components. *Cell Stress Chaperones*, 10, 114-25.
- MITRA, A., MENEZES, M. E., PANNELL, L. K., MULEKAR, M. S., HONKANEN, R. E., SHEVDE, L. A. & SAMANT, R. S. 2012. DNAJB6 chaperones PP2A mediated dephosphorylation of GSK3beta to downregulate beta-catenin transcription target, osteopontin. *Oncogene*.
- MITRA, A., MENEZES, M. E., SHEVDE, L. A. & SAMANT, R. S. 2010. DNAJB6 induces degradation of beta-catenin and causes partial reversal of mesenchymal phenotype. *J Biol Chem*, 285, 24686-94.
- MITSUNAGA, K., KIKUCHI, J., WADA, T. & FURUKAWA, Y. 2012. Latexin regulates the abundance of multiple cellular proteins in hematopoietic stem cells. *J Cell Physiol*, 227, 1138-47.
- MORAWIETZ, H. 2010. [LOX-1 receptor as a novel target in endothelial dysfunction and atherosclerosis]. *Dtsch Med Wochenschr*, 135, 308-12.
- MORENO, P. R., PURUSHOTHAMAN, K. R., SIROL, M., LEVY, A. P. & FUSTER, V. 2006. Neovascularization in human atherosclerosis. *Circulation*, 113, 2245-52.
- MORISHIMA, Y., KANELAKIS, K. C., MURPHY, P. J., SHEWACH, D. S. & PRATT, W. B. 2001. Evidence for iterative ratcheting of receptor-bound hsp70 between its ATP and ADP conformations during assembly of glucocorticoid receptor.hsp90 heterocomplexes. *Biochemistry*, 40, 1109-16.
- MORO, C., JOUAN, M. G., RAKOTOVAO, A., TOUFEKTSIAN, M. C., ORMEZZANO, O., NAGY, N., TOSAKI, A., DE LEIRIS, J. & BOUCHER, F. 2007. Delayed expression of cytokines after reperfused myocardial infarction: possible trigger for cardiac dysfunction and ventricular remodeling. *Am J Physiol Heart Circ Physiol*, 293, H3014-9.
- MUELLER, C., BAUDLER, S., WELZEL, H., BOHM, M. & NICKENIG, G. 2002. Identification of a novel redox-sensitive gene, Id3, which mediates angiotensin II-induced cell growth. *Circulation*, 105, 2423-8.
- MURRY, B. P., GREITER-WILKE, A., PAULSEN, D. P., HIATT, K. M., BELTRAMI, C. A. & MARCHETTI, D. 2005. Selective heparanase localization in malignant melanoma. *Int J Oncol*, 26, 345-52.
- MUSIL, V., MAJER, M. & JURESA, V. 2012. Elevated blood pressure in school children and adolescents--prevalence and associated risk factors. *Coll Antropol*, 36 Suppl 1, 147-55.
- MUSUNURU, K., POST, W. S., HERZOG, W., SHEN, H., O'CONNELL, J. R., MCARDLE, P. F., RYAN, K. A., GIBSON, Q., CHENG, Y. C., CLEARFIELD, E., JOHNSON, A. D., TOFLER, G., YANG, Q., O'DONNELL, C. J., BECKER, D. M., YANEK, L. R., BECKER, L. C., FARADAY, N., BIELAK, L. F., PEYSER, P. A., SHULDINER, A. R. & MITCHELL, B. D. 2010. Association of single nucleotide polymorphisms on chromosome 9p21.3 with platelet reactivity: a potential mechanism for increased vascular disease. *Circ Cardiovasc Genet*, 3, 445-53.
- MYLER, H. A., LIPKE, E. A., RICE, E. E. & WEST, J. L. 2006. Novel heparanase-inhibiting antibody reduces neointima formation. *J Biochem*, 139, 339-45.
- NADIR, Y., BRENNER, B., GINGIS-VELITSKI, S., LEVY-ADAM, F., ILAN, N., ZCHARIA, E., NADIR, E. & VLODAVSKY, I. 2008. Heparanase induces tissue factor pathway inhibitor expression and extracellular accumulation in endothelial and tumor cells. *Thromb Haemost*, 99, 133-41.
- NAKAJIMA, T., KAUR, G., MEHRA, N. & KIMURA, A. 2008. HIV-1/AIDS susceptibility and copy number variation in CCL3L1, a gene encoding a natural ligand for HIV-1 co-receptor CCR5. *Cytogenet Genome Res*, 123, 156-60.

- NAKAYA, N., LEE, H. S., TAKADA, Y., TZCHORI, I. & TOMAREV, S. I. 2008. Zebrafish olfactomedin 1 regulates retinal axon elongation in vivo and is a modulator of Wnt signaling pathway. *J Neurosci*, 28, 7900-10.
- NAN, B., YANG, H., YAN, S., LIN, P. H., LUMSDEN, A. B., YAO, Q. & CHEN, C. 2005. C-reactive protein decreases expression of thrombomodulin and endothelial protein C receptor in human endothelial cells. *Surgery*, 138, 212-22.
- NAPOLI, C., D'ARMIENTO, F. P., MANCINI, F. P., POSTIGLIONE, A., WITZTUM, J. L., PALUMBO, G. & PALINSKI, W. 1997. Fatty streak formation occurs in human fetal aortas and is greatly enhanced by maternal hypercholesterolemia. Intimal accumulation of low density lipoprotein and its oxidation precede monocyte recruitment into early atherosclerotic lesions. *J Clin Invest*, 100, 2680-90.
- NAVAB, M., ANANTHRAMAIAH, G. M., REDDY, S. T., VAN LENTEN, B. J., ANSELL, B. J., FONAROW, G. C., VAHABZADEH, K., HAMA, S., HOUGH, G., KAMRANPOUR, N., BERLINER, J. A., LUSIS, A. J. & FOGELMAN, A. M. 2004. The oxidation hypothesis of atherogenesis: the role of oxidized phospholipids and HDL. *J Lipid Res*, 45, 993-1007.
- NEEB, A., WALLBAUM, S., NOVAC, N., DUKOVIC-SCHULZE, S., SCHOLL, I., SCHREIBER, C., SCHLAG, P., MOLL, J., STEIN, U. & SLEEMAN, J. P. 2011. The immediate early gene *Ier2* promotes tumor cell motility and metastasis, and predicts poor survival of colorectal cancer patients. *Oncogene*.
- NERI, M., CERRETANI, D., FIASCHI, A. I., LAGHI, P. F., LAZZERINI, P. E., MAFFIONE, A. B., MICHELI, L., BRUNI, G., NENCINI, C., GIORGI, G., D'ERRICO, S., FIORE, C., POMARA, C., RIEZZO, I., TURILLAZZI, E. & FINESCHI, V. 2007. Correlation between cardiac oxidative stress and myocardial pathology due to acute and chronic norepinephrine administration in rats. *J Cell Mol Med*, 11, 156-70.
- NGUYEN, T. Q., JARAMILLO, A., THOMPSON, R. W., DINTZIS, S., OPPAT, W. F., ALLEN, B. T., SICARD, G. A. & MOHANAKUMAR, T. 2001. Increased expression of HDJ-2 (hsp40) in carotid artery atherosclerosis: a novel heat shock protein associated with luminal stenosis and plaque ulceration. *J Vasc Surg*, 33, 1065-71.
- NICA, A. C. & DERMITZAKIS, E. T. 2008. Using gene expression to investigate the genetic basis of complex disorders. *Hum Mol Genet*, 17, R129-34.
- NICKENIG, G., BAUDLER, S., MULLER, C., WERNER, C., WERNER, N., WELZEL, H., STREHLOW, K. & BOHM, M. 2002. Redox-sensitive vascular smooth muscle cell proliferation is mediated by GKLf and Id3 in vitro and in vivo. *FASEB J*, 16, 1077-86.
- NITURE, S. K. & JAISWAL, A. K. 2010. Hsp90 interaction with INrf2(Keap1) mediates stress-induced Nrf2 activation. *J Biol Chem*, 285, 36865-75.
- NOMURA, S., SHOUZU, A., OMOTO, S., INAMI, N., SHIMAZU, T., SATOH, D., KAJIURA, T., YAMADA, K., URASE, F., MAEDA, Y. & IWASAKA, T. 2009. Effects of pitavastatin on monocyte chemoattractant protein-1 in hyperlipidemic patients. *Blood Coagul Fibrinolysis*, 20, 440-7.
- NOMURA, S., TANDON, N. N., NAKAMURA, T., CONE, J., FUKUHARA, S. & KAMBAYASHI, J. 2001. High-shear-stress-induced activation of platelets and microparticles enhances expression of cell adhesion molecules in THP-1 and endothelial cells. *Atherosclerosis*, 158, 277-87.
- NOOKAEW, I., GABRIELSSON, B. G., HOLMANG, A., SANDBERG, A. S. & NIELSEN, J. 2010. Identifying molecular effects of diet through systems biology: influence of herring diet on sterol metabolism and protein turnover in mice. *PLoS One*, 5, e12361.

- NORLIN, M., PETTERSSON, H., TANG, W. & WIKVALL, K. Androgen receptor-mediated regulation of the anti-atherogenic enzyme CYP27A1 involves the JNK/c-jun pathway. *Arch Biochem Biophys*, 506, 236-41.
- NOVOTNY, V., PRIESCHL, E. E., CSONGA, R., FABJANI, G. & BAUMRUKER, T. 1998. Nrf1 in a complex with fosB, c-jun, junD and ATF2 forms the AP1 component at the TNF alpha promoter in stimulated mast cells. *Nucleic Acids Res*, 26, 5480-5.
- NSEIR, W., SHALATA, A., MARMOR, A. & ASSY, N. 2011. Mechanisms Linking Nonalcoholic Fatty Liver Disease with Coronary Artery Disease. *Dig Dis Sci*.
- NYSTROM, T., DUNER, P. & HULTGARDH-NILSSON, A. 2007. A constitutive endogenous osteopontin production is important for macrophage function and differentiation. *Exp Cell Res*, 313, 1149-60.
- ODUNUGA, O. O., HORNBY, J. A., BIES, C., ZIMMERMANN, R., PUGH, D. J. & BLATCH, G. L. 2003. Tetratricopeptide repeat motif-mediated Hsc70-mSTII interaction. Molecular characterization of the critical contacts for successful binding and specificity. *J Biol Chem*, 278, 6896-904.
- OEMAR, B. S., YANG, Z. & LUSCHER, T. F. 1995. Molecular and cellular mechanisms of atherosclerosis. *Curr Opin Nephrol Hypertens*, 4, 82-91.
- OERLEMANS, M. I., GOUMANS, M. J., VAN MIDDELAAR, B., CLEVERS, H., DOEVENDANS, P. A. & SLUIJTER, J. P. 2010. Active Wnt signaling in response to cardiac injury. *Basic Res Cardiol*, 105, 631-41.
- OGAWA, M. 1993. Differentiation and proliferation of hematopoietic stem cells. *Blood*, 81, 2844-53.
- OHSHIRO, T., MATSUDA, D., SAKAI, K., DEGIROLAMO, C., YAGYU, H., RUDEL, L. L., OMURA, S., ISHIBASHI, S. & TOMODA, H. 2011. Pyripyropene A, an acyl-coenzyme A:cholesterol acyltransferase 2-selective inhibitor, attenuates hypercholesterolemia and atherosclerosis in murine models of hyperlipidemia. *Arterioscler Thromb Vasc Biol*, 31, 1108-15.
- ORN, S., BRELAND, U. M., MOLLNES, T. E., MANHENKE, C., DICKSTEIN, K., AUKRUST, P. & UELAND, T. 2009. The chemokine network in relation to infarct size and left ventricular remodeling following acute myocardial infarction. *Am J Cardiol*, 104, 1179-83.
- OVECHKIN, A. V., LOMINADZE, D., SEDORIS, K. C., ROBINSON, T. W., TYAGI, S. C. & ROBERTS, A. M. 2007. Lung ischemia-reperfusion injury: implications of oxidative stress and platelet-arteriolar wall interactions. *Arch Physiol Biochem*, 113, 1-12.
- OVSTEBE, R., OLSTAD, O. K., BRUSLETTO, B., MOLLER, A. S., AASE, A., HAUG, K. B., BRANDTZAEG, P. & KIERULF, P. 2008. Identification of genes particularly sensitive to lipopolysaccharide (LPS) in human monocytes induced by wild-type versus LPS-deficient *Neisseria meningitidis* strains. *Infect Immun*, 76, 2685-95.
- PARINI, P., JIANG, Z. Y., EINARSSON, C., EGGERTSEN, G., ZHANG, S. D., RUDEL, L. L., HAN, T. Q. & ERIKSSON, M. 2009. ACAT2 and human hepatic cholesterol metabolism: identification of important gender-related differences in normolipidemic, non-obese Chinese patients. *Atherosclerosis*, 207, 266-71.
- PARK, H. K., PARK, E. C., BAE, S. W., PARK, M. Y., KIM, S. W., YOO, H. S., TUDEV, M., KO, Y. H., CHOI, Y. H., KIM, S., KIM, D. I., KIM, Y. W., LEE, B. B., YOON, J. B. & PARK, J. E. 2006. Expression of heat shock protein 27 in human atherosclerotic plaques and increased plasma level of heat shock protein 27 in patients with acute coronary syndrome. *Circulation*, 114, 886-93.
- PARK, J., KIM, M., NA, G., JEON, I., KWON, Y. K., KIM, J. H., YOUN, H. & KOO, Y. 2007. Glucocorticoids modulate NF-kappaB-dependent gene expression by up-

- regulating FKBP51 expression in Newcastle disease virus-infected chickens. *Mol Cell Endocrinol*, 278, 7-17.
- PARK, Y. M., FEBBRAIO, M. & SILVERSTEIN, R. L. 2009. CD36 modulates migration of mouse and human macrophages in response to oxidized LDL and may contribute to macrophage trapping in the arterial intima. *J Clin Invest*, 119, 136-45.
- PATEL, P. C., FISHER, K. H., YANG, E. C., DEANE, C. M. & HARRISON, R. E. 2009. Proteomic analysis of microtubule-associated proteins during macrophage activation. *Mol Cell Proteomics*, 8, 2500-14.
- PATINO, W. D., MIAN, O. Y., KANG, J. G., MATOBA, S., BARTLETT, L. D., HOLBROOK, B., TROUT, H. H., 3RD, KOZLOFF, L. & HWANG, P. M. 2005. Circulating transcriptome reveals markers of atherosclerosis. *Proc Natl Acad Sci U S A*, 102, 3423-8.
- PENDINO, F., NGUYEN, E., JONASSEN, I., DYSVIK, B., AZOUZ, A., LANOTTE, M., SEGAL-BENDIRDJIAN, E. & LILLEHAUG, J. R. 2009. Functional involvement of RINF, retinoid-inducible nuclear factor (CXXC5), in normal and tumoral human myelopoiesis. *Blood*, 113, 3172-81.
- PENZ, S., REININGER, A. J., BRANDL, R., GOYAL, P., RABIE, T., BERNLOCHNER, I., ROTHER, E., GOETZ, C., ENGELMANN, B., SMETHURST, P. A., OUWEHAND, W. H., FARNDAL, R., NIESWANDT, B. & SIESS, W. 2005. Human atheromatous plaques stimulate thrombus formation by activating platelet glycoprotein VI. *FASEB J*, 19, 898-909.
- PERSAD, S., RUPP, H., JINDAL, R., ARNEJA, J. & DHALLA, N. S. 1998. Modification of cardiac beta-adrenoceptor mechanisms by H₂O₂. *Am J Physiol*, 274, H416-23.
- PHILIPS, B., DE LEMOS, J. A., PATEL, M. J., MCGUIRE, D. K. & KHERA, A. 2007. Relation of family history of myocardial infarction and the presence of coronary arterial calcium in various age and risk factor groups. *Am J Cardiol*, 99, 825-9.
- PIKULEVA, I. A., BABIKER, A., WATERMAN, M. R. & BJORKHEM, I. 1998. Activities of recombinant human cytochrome P450c27 (CYP27) which produce intermediates of alternative bile acid biosynthetic pathways. *J Biol Chem*, 273, 18153-60.
- PILLARISSETTI, S. 2000. Lipoprotein modulation of subendothelial heparan sulfate proteoglycans (perlecan) and atherogenicity. *Trends Cardiovasc Med*, 10, 60-5.
- PILLARISSETTI, S., PAKA, L., OBUNIKE, J. C., BERGLUND, L. & GOLDBERG, I. J. 1997. Subendothelial retention of lipoprotein (a). Evidence that reduced heparan sulfate promotes lipoprotein binding to subendothelial matrix. *J Clin Invest*, 100, 867-74.
- PLONER, A., CALZA, S., GUSNANTO, A. & PAWITAN, Y. 2006. Multidimensional local false discovery rate for microarray studies. *Bioinformatics*, 22, 556-65.
- POLANOWSKA-GRABOWSKA, R., GIBBINS, J. M. & GEAR, A. R. 2003. Platelet adhesion to collagen and collagen-related peptide under flow: roles of the [alpha]2[beta]1 integrin, GPVI, and Src tyrosine kinases. *Arterioscler Thromb Vasc Biol*, 23, 1934-40.
- POU, J., REBOLLO, A., ROGLANS, N., SANCHEZ, R. M., VAZQUEZ-CARRERA, M., LAGUNA, J. C., PEDRO-BOTET, J. & ALEGRET, M. 2008. Ritonavir increases CD36, ABCA1 and CYP27 expression in THP-1 macrophages. *Exp Biol Med (Maywood)*, 233, 1572-82.
- PRABHAKAR, N. R. & JACONO, F. J. 2005. Cellular and molecular mechanisms associated with carotid body adaptations to chronic hypoxia. *High Alt Med Biol*, 6, 112-20.

- PRAMFALK, C., ANGELIN, B., ERIKSSON, M. & PARINI, P. 2007. Cholesterol regulates ACAT2 gene expression and enzyme activity in human hepatoma cells. *Biochem Biophys Res Commun*, 364, 402-9.
- PREUSS, M., KONIG, I. R., THOMPSON, J. R., ERDMANN, J., ABSHER, D., ASSIMES, T. L., BLANKENBERG, S., BOERWINKLE, E., CHEN, L., CUPPLES, L. A., HALL, A. S., HALPERIN, E., HENGSTENBERG, C., HOLM, H., LAAKSONEN, R., LI, M., MARZ, W., MCPHERSON, R., MUSUNURU, K., NELSON, C. P., BURNETT, M. S., EPSTEIN, S. E., O'DONNELL, C. J., QUERTERMOUS, T., RADER, D. J., ROBERTS, R., SCHILLERT, A., STEFANSSON, K., STEWART, A. F., THORLEIFSSON, G., VOIGHT, B. F., WELLS, G. A., ZIEGLER, A., KATHIRESAN, S., REILLY, M. P., SAMANI, N. J. & SCHUNKERT, H. 2010. Design of the Coronary ARtery Disease Genome-Wide Replication And Meta-Analysis (CARDIoGRAM) Study: A Genome-wide association meta-analysis involving more than 22 000 cases and 60 000 controls. *Circ Cardiovasc Genet*, 3, 475-83.
- PUC CETTI, L., SAWAMURA, T., PASQUI, A. L., PASTORELLI, M., AUTERI, A. & BRUNI, F. 2005. Atorvastatin reduces platelet-oxidized-LDL receptor expression in hypercholesterolaemic patients. *Eur J Clin Invest*, 35, 47-51.
- PUGH, N., SIMPSON, A. M., SMETHURST, P. A., DE GROOT, P. G., RAYNAL, N. & FARNDAL E, R. W. 2010. Synergism between platelet collagen receptors defined using receptor-specific collagen-mimetic peptide substrata in flowing blood. *Blood*, 115, 5069-79.
- QIN, G., ZHANG, Y., CAO, W., AN, R., GAO, Z., LI, G., XU, W., ZHANG, K. & LI, S. 2005. Molecular imaging of atherosclerotic plaques with technetium-99m-labelled antisense oligonucleotides. *Eur J Nucl Med Mol Imaging*, 32, 6-14.
- QIN, L. X. & KERR, K. F. 2004. Empirical evaluation of data transformations and ranking statistics for microarray analysis. *Nucleic Acids Res*, 32, 5471-9.
- QIU, X. B., SHAO, Y. M., MIAO, S. & WANG, L. 2006. The diversity of the DnaJ/Hsp40 family, the crucial partners for Hsp70 chaperones. *Cell Mol Life Sci*, 63, 2560-70.
- QUASNICHKA, H., SLATER, S. C., BEECHING, C. A., BOEHM, M., SALA-NEWBY, G. B. & GEORGE, S. J. 2006. Regulation of smooth muscle cell proliferation by beta-catenin/T-cell factor signaling involves modulation of cyclin D1 and p21 expression. *Circ Res*, 99, 1329-37.
- QUINN, C. M., JESSUP, W., WONG, J., KRITHARIDES, L. & BROWN, A. J. 2005. Expression and regulation of sterol 27-hydroxylase (CYP27A1) in human macrophages: a role for RXR and PPARgamma ligands. *Biochem J*, 385, 823-30.
- RABEN, D. M. & TU-SEKINE, B. 2008. Nuclear diacylglycerol kinases: regulation and roles. *Front Biosci*, 13, 590-7.
- RAJAVASHISTH, T. B., ANDALIBI, A., TERRITO, M. C., BERLINER, J. A., NAVAB, M., FOGELMAN, A. M. & LUSIS, A. J. 1990. Induction of endothelial cell expression of granulocyte and macrophage colony-stimulating factors by modified low-density lipoproteins. *Nature*, 344, 254-7.
- RAMOS, K. S. 1999. Redox regulation of c-Ha-ras and osteopontin signaling in vascular smooth muscle cells: implications in chemical atherogenesis. *Annu Rev Pharmacol Toxicol*, 39, 243-65.
- RAO, R. M., YANG, L., GARCIA-CARDENA, G. & LUSCINSKAS, F. W. 2007. Endothelial-dependent mechanisms of leukocyte recruitment to the vascular wall. *Circ Res*, 101, 234-47.
- RAWSON, R. B. 2003. Control of lipid metabolism by regulated intramembrane proteolysis of sterol regulatory element binding proteins (SREBPs). *Biochem Soc Symp*, 221-31.

- RAYNER, K., SUN, J., CHEN, Y. X., MCNULTY, M., SIMARD, T., ZHAO, X., WELLS, D. J., DE BELLEROCHE, J. & O'BRIEN, E. R. 2009. Heat shock protein 27 protects against atherogenesis via an estrogen-dependent mechanism: role of selective estrogen receptor beta modulation. *Arterioscler Thromb Vasc Biol*, 29, 1751-6.
- REILLY, M. P., LI, M., HE, J., FERGUSON, J. F., STYLIANOU, I. M., MEHTA, N. N., BURNETT, M. S., DEVANEY, J. M., KNOUFF, C. W., THOMPSON, J. R., HORNE, B. D., STEWART, A. F., ASSIMES, T. L., WILD, P. S., ALLAYEE, H., NITSCHKE, P. L., PATEL, R. S., MARTINELLI, N., GIRELLI, D., QUYYUMI, A. A., ANDERSON, J. L., ERDMANN, J., HALL, A. S., SCHUNKERT, H., QUERTERMOUS, T., BLANKENBERG, S., HAZEN, S. L., ROBERTS, R., KATHIRESAN, S., SAMANI, N. J., EPSTEIN, S. E. & RADER, D. J. 2011. Identification of ADAMTS7 as a novel locus for coronary atherosclerosis and association of ABO with myocardial infarction in the presence of coronary atherosclerosis: two genome-wide association studies. *Lancet*, 377, 383-92.
- REUTER, S., GUPTA, S. C., CHATURVEDI, M. M. & AGGARWAL, B. B. 2010. Oxidative stress, inflammation, and cancer: how are they linked? *Free Radic Biol Med*, 49, 1603-16.
- RICHMAN, J. G., KANEMITSU-PARKS, M., GAIDAROV, I., CAMERON, J. S., GRIFFIN, P., ZHENG, H., GUERRA, N. C., CHAM, L., MACIEJEWSKI-LENOIR, D., BEHAN, D. P., BOATMAN, D., CHEN, R., SKINNER, P., ORNELAS, P., WATERS, M. G., WRIGHT, S. D., SEMPLE, G. & CONNOLLY, D. T. 2007. Nicotinic acid receptor agonists differentially activate downstream effectors. *J Biol Chem*, 282, 18028-36.
- RISSANEN, A. M. 1979a. Familial aggregation of coronary heart disease in a high incidence area (North Karelia, Finland). *Br Heart J*, 42, 294-303.
- RISSANEN, A. M. 1979b. Familial occurrence of coronary heart disease: effect of age at diagnosis. *Am J Cardiol*, 44, 60-6.
- RISSANEN, A. M. & NIKKILA, E. A. 1979. Aggregation of coronary risk factors in families of men with fatal and non-fatal coronary heart disease. *Br Heart J*, 42, 373-80.
- ROBERTS, R. & STEWART, A. F. 2012. Genetics of Coronary Artery Disease in the 21st Century. *Clin Cardiol*.
- ROBICHON, C., VARRET, M., LE LIEPVRE, X., LASNIER, F., HAJDUCH, E., FERRE, P. & DUGAIL, I. 2006. DnaJA4 is a SREBP-regulated chaperone involved in the cholesterol biosynthesis pathway. *Biochim Biophys Acta*, 1761, 1107-13.
- ROHATGI, A., AYERS, C. R., KHERA, A., MCGUIRE, D. K., DAS, S. R., MATULEVICIUS, S., TIMARAN, C. H., ROSERO, E. B. & DE LEMOS, J. A. 2009. The association between peptidoglycan recognition protein-1 and coronary and peripheral atherosclerosis: Observations from the Dallas Heart Study. *Atherosclerosis*, 203, 569-75.
- ROSE, J. M., NOVOSELOV, S. S., ROBINSON, P. A. & CHEETHAM, M. E. 2011. Molecular chaperone-mediated rescue of mitophagy by a Parkin RING1 domain mutant. *Hum Mol Genet*, 20, 16-27.
- ROSENSON, R. S. 2001. Pluripotential mechanisms of cardioprotection with HMG-CoA reductase inhibitor therapy. *Am J Cardiovasc Drugs*, 1, 411-20.
- ROSS, R. 1993. The pathogenesis of atherosclerosis: a perspective for the 1990s. *Nature*, 362, 801-9.
- ROSS, R. 1995. Cell biology of atherosclerosis. *Annu Rev Physiol*, 57, 791-804.
- ROSS, R. 1999. Atherosclerosis--an inflammatory disease. *N Engl J Med*, 340, 115-26.

- ROSS, R. & GLOMSET, J. A. 1973. Atherosclerosis and the arterial smooth muscle cell: Proliferation of smooth muscle is a key event in the genesis of the lesions of atherosclerosis. *Science*, 180, 1332-9.
- ROSS, R. & HARKER, L. 1976. Hyperlipidemia and atherosclerosis. *Science*, 193, 1094-100.
- ROTIVAL, M., ZELLER, T., WILD, P. S., MAOUCHE, S., SZYMCZAK, S., SCHILLERT, A., CASTAGNE, R., DEISEROTH, A., PROUST, C., BROCHETON, J., GODEFROY, T., PERRET, C., GERMAIN, M., ELEFThERIADIS, M., SINNING, C. R., SCHNABEL, R. B., LUBOS, E., LACKNER, K. J., ROSSMANN, H., MUNZEL, T., RENDON, A., ERDMANN, J., DELOUKAS, P., HENGSTENBERG, C., DIEMERT, P., MONTALESCOT, G., OUWEHAND, W. H., SAMANI, N. J., SCHUNKERT, H., TREGOUET, D. A., ZIEGLER, A., GOODALL, A. H., CAMBIEN, F., TIRET, L. & BLANKENBERG, S. 2011. Integrating genome-wide genetic variations and monocyte expression data reveals trans-regulated gene modules in humans. *PLoS Genet*, 7, e1002367.
- RYDBERG, E. K., KRETTEK, A., ULLSTROM, C., EKSTROM, K., SVENSSON, P. A., CARLSSON, L. M., JONSSON-RYLANDER, A. C., HANSSON, G. I., MCPHEAT, W., WIKLUND, O., OHLSSON, B. G. & HULTEN, L. M. 2004. Hypoxia increases LDL oxidation and expression of 15-lipoxygenase-2 in human macrophages. *Arterioscler Thromb Vasc Biol*, 24, 2040-5.
- RYZHOVA, L. M., SUKHANOVA, G. A., KOVALEV, I. A. & FILIPPOV, G. P. 2001. [Lipids of lymphocyte plasma membranes in patients with atherosclerosis and their children]. *Klin Lab Diagn*, 10-2.
- SADLIER, D. M., OUYANG, X., MCMAHON, B., MU, W., OHASHI, R., RODGERS, K., MURRAY, D., NAKAGAWA, T., GODSON, C., DORAN, P., BRADY, H. R. & JOHNSON, R. J. 2005. Microarray and bioinformatic detection of novel and established genes expressed in experimental anti-Thy1 nephritis. *Kidney Int*, 68, 2542-61.
- SAGOO, G. S., TATT, I., SALANTI, G., BUTTERWORTH, A. S., SARWAR, N., VAN MAARLE, M., JUKEMA, J. W., WIMAN, B., KASTELEIN, J. J., BENNET, A. M., DE FAIRE, U., DANESH, J. & HIGGINS, J. P. 2008. Seven lipoprotein lipase gene polymorphisms, lipid fractions, and coronary disease: a HuGE association review and meta-analysis. *Am J Epidemiol*, 168, 1233-46.
- SAITO, H., MARUYAMA, I., SHIMAZAKI, S., YAMAMOTO, Y., AIKAWA, N., OHNO, R., HIRAYAMA, A., MATSUDA, T., ASAKURA, H., NAKASHIMA, M. & AOKI, N. 2007a. Efficacy and safety of recombinant human soluble thrombomodulin (ART-123) in disseminated intravascular coagulation: results of a phase III, randomized, double-blind clinical trial. *J Thromb Haemost*, 5, 31-41.
- SAITO, Y., FUJIOKA, D., KAWABATA, K., KOBAYASHI, T., YANO, T., NAKAMURA, T., KODAMA, Y., TAKANO, H., KITTA, Y., OBATA, J. E. & KUGIYAMA, K. 2007b. Statin reverses reduction of adiponectin receptor expression in infarcted heart and in TNF-alpha-treated cardiomyocytes in association with improved glucose uptake. *Am J Physiol Heart Circ Physiol*, 293, H3490-7.
- SAKURAI, K. & SAWAMURA, T. 2003. Stress and vascular responses: endothelial dysfunction via lectin-like oxidized low-density lipoprotein receptor-1: close relationships with oxidative stress. *J Pharmacol Sci*, 91, 182-6.
- SALINTHONE, S., BA, M., HANSON, L., MARTIN, J. L., HALAYKO, A. J. & GERTHOFFER, W. T. 2007. Overexpression of human Hsp27 inhibits serum-induced proliferation in airway smooth muscle myocytes and confers resistance to hydrogen peroxide cytotoxicity. *Am J Physiol Lung Cell Mol Physiol*, 293, L1194-207.

- SAMANI, N. J., BURTON, P., MANGINO, M., BALL, S. G., BALMFORTH, A. J., BARRETT, J., BISHOP, T. & HALL, A. 2005. A genomewide linkage study of 1,933 families affected by premature coronary artery disease: The British Heart Foundation (BHF) Family Heart Study. *Am J Hum Genet*, 77, 1011-20.
- SAMANI, N. J., ERDMANN, J., HALL, A. S., HENGSTENBERG, C., MANGINO, M., MAYER, B., DIXON, R. J., MEITINGER, T., BRAUND, P., WICHMANN, H. E., BARRETT, J. H., KONIG, I. R., STEVENS, S. E., SZYMCZAK, S., TREGOUET, D. A., ILES, M. M., PAHLKE, F., POLLARD, H., LIEB, W., CAMBIEN, F., FISCHER, M., OUWEHAND, W., BLANKENBERG, S., BALMFORTH, A. J., BAESSLER, A., BALL, S. G., STROM, T. M., BRAENNE, I., GIEGER, C., DELOUKAS, P., TOBIN, M. D., ZIEGLER, A., THOMPSON, J. R. & SCHUNKERT, H. 2007. Genomewide association analysis of coronary artery disease. *N Engl J Med*, 357, 443-53.
- SANGUIGNI, V., FERRO, D., PIGNATELLI, P., DEL BEN, M., NADIA, T., SALIOLA, M., SORGE, R. & VIOLI, F. 2005. CD40 ligand enhances monocyte tissue factor expression and thrombin generation via oxidative stress in patients with hypercholesterolemia. *J Am Coll Cardiol*, 45, 35-42.
- SARASWATHI, V. & HASTY, A. H. 2006. The role of lipolysis in mediating the proinflammatory effects of very low density lipoproteins in mouse peritoneal macrophages. *J Lipid Res*, 47, 1406-15.
- SAWADA, N., SAKAKI, T., OHTA, M. & INOUE, K. 2000. Metabolism of vitamin D(3) by human CYP27A1. *Biochem Biophys Res Commun*, 273, 977-84.
- SCHELLEMAN, H., KLUNGEL, O. H., WITTEMAN, J. C., HOFMAN, A., VAN DUIJN, C. M., DE BOER, A. & STRICKER, B. H. 2007. Pharmacogenetic interactions of three candidate gene polymorphisms with ACE-inhibitors or beta-blockers and the risk of atherosclerosis. *Br J Clin Pharmacol*, 64, 57-66.
- SCHENA, M., SHALON, D., DAVIS, R. W. & BROWN, P. O. 1995. Quantitative monitoring of gene expression patterns with a complementary DNA microarray. *Science*, 270, 467-70.
- SCHENK, M., BOUCHON, A., SEIBOLD, F. & MUELLER, C. 2007. TREM-1--expressing intestinal macrophages crucially amplify chronic inflammation in experimental colitis and inflammatory bowel diseases. *J Clin Invest*, 117, 3097-106.
- SCHILDKRAUT, J. M., MYERS, R. H., CUPPLES, L. A., KIELY, D. K. & KANNEL, W. B. 1989. Coronary risk associated with age and sex of parental heart disease in the Framingham Study. *Am J Cardiol*, 64, 555-9.
- SCHMIDT, M. I., DUNCAN, B. B., SHARRETT, A. R., LINDBERG, G., SAVAGE, P. J., OFFENBACHER, S., AZAMBUJA, M. I., TRACY, R. P. & HEISS, G. 1999. Markers of inflammation and prediction of diabetes mellitus in adults (Atherosclerosis Risk in Communities study): a cohort study. *Lancet*, 353, 1649-52.
- SCHUNKERT, H., KONIG, I. R., KATHIRESAN, S., REILLY, M. P., ASSIMES, T. L., HOLM, H., PREUSS, M., STEWART, A. F., BARBALIC, M., GIEGER, C., ABSHER, D., AHERRAHROU, Z., ALLAYEE, H., ALTSHULER, D., ANAND, S. S., ANDERSEN, K., ANDERSON, J. L., ARDISSINO, D., BALL, S. G., BALMFORTH, A. J., BARNES, T. A., BECKER, D. M., BECKER, L. C., BERGER, K., BIS, J. C., BOEKHOLDT, S. M., BOERWINKLE, E., BRAUND, P. S., BROWN, M. J., BURNETT, M. S., BUYSSCHAERT, I., CARLQUIST, J. F., CHEN, L., CICHON, S., CODD, V., DAVIES, R. W., DEDOISSIS, G., DEGHAN, A., DEMISSIE, S., DEVANEY, J. M., DIEMERT, P., DO, R., DOERING, A., EIFERT, S., MOKHTARI, N. E., ELLIS, S. G., ELOSUA, R., ENGERT, J. C., EPSTEIN, S. E., DE FAIRE, U., FISCHER, M., FOLSOM, A. R., FREYER, J., GIGANTE, B., GIRELLI, D., GRETARSDOTTIR, S., GUDNASON, V., GULCHER, J. R., HALPERIN, E.,

- HAMMOND, N., HAZEN, S. L., HOFMAN, A., HORNE, B. D., ILLIG, T., IRIBARREN, C., JONES, G. T., JUKEMA, J. W., KAISER, M. A., KAPLAN, L. M., KASTELEIN, J. J., KHAW, K. T., KNOWLES, J. W., KOLOVOU, G., KONG, A., LAAKSONEN, R., LAMBRECHTS, D., LEANDER, K., LETTRE, G., LI, M., LIEB, W., LOLEY, C., LOTERY, A. J., MANNUCCI, P. M., MAOUCHE, S., MARTINELLI, N., MCKEOWN, P. P., MEISINGER, C., MEITINGER, T., MELANDER, O., MERLINI, P. A., MOOSER, V., MORGAN, T., MUHLEISEN, T. W., MUHLESTEIN, J. B., MUNZEL, T., MUSUNURU, K., NAHRSTAEDT, J., NELSON, C. P., NOTHEN, M. M., OLIVIERI, O., et al. 2011. Large-scale association analysis identifies 13 new susceptibility loci for coronary artery disease. *Nat Genet*, 43, 333-8.
- SEGEL, G. B., WOODLOCK, T. J., XU, J., LI, L., FELGAR, R. E., RYAN, D. H., LICHTMAN, M. A. & WANG, N. 2003. Early gene activation in chronic leukemic B lymphocytes induced toward a plasma cell phenotype. *Blood Cells Mol Dis*, 30, 277-87.
- SEIDLER, S., ZIMMERMANN, H. W., BARTNECK, M., TRAUTWEIN, C. & TACKE, F. 2010. Age-dependent alterations of monocyte subsets and monocyte-related chemokine pathways in healthy adults. *BMC Immunol*, 11, 30.
- SEIZER, P., GAWAZ, M. & MAY, A. E. 2008. Platelet-monocyte interactions--a dangerous liaison linking thrombosis, inflammation and atherosclerosis. *Curr Med Chem*, 15, 1976-80.
- SENER, A., OZSAVCI, D., OBA, R., DEMIREL, G. Y., URAS, F. & YARDIMCI, K. T. 2005. Do platelet apoptosis, activation, aggregation, lipid peroxidation and platelet-leukocyte aggregate formation occur simultaneously in hyperlipidemia? *Clin Biochem*, 38, 1081-7.
- SHANAHAN, C. M., CARPENTER, K. L. & CARY, N. R. 2001. A potential role for sterol 27-hydroxylase in atherogenesis. *Atherosclerosis*, 154, 269-76.
- SHAO, J. S., ALY, Z. A., LAI, C. F., CHENG, S. L., CAI, J., HUANG, E., BEHRMANN, A. & TOWLER, D. A. 2007. Vascular Bmp Msx2 Wnt signaling and oxidative stress in arterial calcification. *Ann N Y Acad Sci*, 1117, 40-50.
- SHAO, J. S., CHENG, S. L., PINGSTERHAUS, J. M., CHARLTON-KACHIGIAN, N., LOEWY, A. P. & TOWLER, D. A. 2005. Msx2 promotes cardiovascular calcification by activating paracrine Wnt signals. *J Clin Invest*, 115, 1210-20.
- SHARP, F. R., RAN, R., LU, A., TANG, Y., STRAUSS, K. I., GLASS, T., ARDIZZONE, T. & BERNAUDIN, M. 2004. Hypoxic preconditioning protects against ischemic brain injury. *NeuroRx*, 1, 26-35.
- SHARRETT, A. R., BALLANTYNE, C. M., COADY, S. A., HEISS, G., SORLIE, P. D., CATELLIER, D. & PATSCH, W. 2001. Coronary heart disease prediction from lipoprotein cholesterol levels, triglycerides, lipoprotein(a), apolipoproteins A-I and B, and HDL density subfractions: The Atherosclerosis Risk in Communities (ARIC) Study. *Circulation*, 104, 1108-13.
- SHECHTMAN, C. F., HENNEBERRY, A. L., SEIMON, T. A., TINKELBERG, A. H., WILCOX, L. J., LEE, E., FAZLOLLAHI, M., MUNKACSI, A. B., BUSSEMAKER, H. J., TABAS, I. & STURLEY, S. L. 2011. Loss of subcellular lipid transport due to ARV1 deficiency disrupts organelle homeostasis and activates the unfolded protein response. *J Biol Chem*, 286, 11951-9.
- SHI, W., DE GRAAF, C. A., KINKEL, S. A., ACHTMAN, A. H., BALDWIN, T., SCHOFIELD, L., SCOTT, H. S., HILTON, D. J. & SMYTH, G. K. 2010. Estimating the proportion of microarray probes expressed in an RNA sample. *Nucleic Acids Res*, 38, 2168-76.

- SHIMIZU, N., OHTA, M., FUJIWARA, C., SAGARA, J., MOCHIZUKI, N., ODA, T. & UTIYAMA, H. 1991. Expression of a novel immediate early gene during 12-O-tetradecanoylphorbol-13-acetate-induced macrophagic differentiation of HL-60 cells. *J Biol Chem*, 266, 12157-61.
- SHIN, D. M., JEON, J. H., KIM, C. W., CHO, S. Y., LEE, H. J., JANG, G. Y., JEONG, E. M., LEE, D. S., KANG, J. H., MELINO, G., PARK, S. C. & KIM, I. G. 2008. TGFbeta mediates activation of transglutaminase 2 in response to oxidative stress that leads to protein aggregation. *FASEB J*, 22, 2498-507.
- SHRESTHA, S., NYAKU, M. & EDBERG, J. C. 2010. Variations in CCL3L gene cluster sequence and non-specific gene copy numbers. *BMC Res Notes*, 3, 74.
- SINNER, D., KORDICH, J. J., SPENCE, J. R., OPOKA, R., RANKIN, S., LIN, S. C., JONATAN, D., ZORN, A. M. & WELLS, J. M. 2007. Sox17 and Sox4 differentially regulate beta-catenin/T-cell factor activity and proliferation of colon carcinoma cells. *Mol Cell Biol*, 27, 7802-15.
- SIVAPALARATNAM, S., BASART, H., WATKINS, N. A., MAIWALD, S., RENDON, A., KRISHNAN, U., SONDERMEIJER, B. M., CREEMERS, E. E., PINTO-SIETSMA, S. J., HOVINGH, K., OUWEHAND, W. H., KASTELEIN, J. J., GOODALL, A. H. & TRIP, M. D. 2012. Monocyte gene expression signature of patients with early onset coronary artery disease. *PLoS One*, 7, e32166.
- SIVAPALARATNAM, S., FARRUGIA, R., NIEUWDORP, M., LANGFORD, C. F., VAN BEEM, R. T., MAIWALD, S., ZWAGINGA, J. J., GUSNANTO, A., WATKINS, N. A., TRIP, M. D. & OUWEHAND, W. H. 2011a. Identification of candidate genes linking systemic inflammation to atherosclerosis; results of a human in vivo LPS infusion study. *BMC Med Genomics*, 4, 64.
- SIVAPALARATNAM, S., FARRUGIA, R., NIEUWDORP, M., LANGFORD, C. F., VAN BEEM, R. T., MAIWALD, S., ZWAGINGA, J. J., GUSNANTO, A., WATKINS, N. A., TRIP, M. D. & OUWEHAND, W. H. 2011b. Identification of candidate genes linking systemic inflammation to atherosclerosis; results of a human in vivo LPS infusion study. *BMC Med Genomics*, 4, 64.
- SIVILS, J. C., STORER, C. L., GALIGNIANA, M. D. & COX, M. B. 2011. Regulation of steroid hormone receptor function by the 52-kDa FK506-binding protein (FKBP52). *Curr Opin Pharmacol*, 11, 314-9.
- SLUIMER, J. C. & DAEMEN, M. J. 2009. Novel concepts in atherogenesis: angiogenesis and hypoxia in atherosclerosis. *J Pathol*, 218, 7-29.
- SMETANINA, I. N., VAULIN, N. A., MASENKO, V. P. & GRATSIANSKII, N. A. 2006. [Short term simvastatin use in patients with heart failure of ischemic origin. Changes of blood lipids, markers of inflammation and left ventricular function]. *Kardiologiia*, 46, 44-9.
- SMITH, J. D., PENG, D. Q., DANSKY, H. M., SETTLE, M., BAGLIONE, J., LE GOFF, W., CHAKRABARTI, E., XU, Y. & PENG, X. 2006. Transcriptome profile of macrophages from atherosclerosis-sensitive and atherosclerosis-resistant mice. *Mamm Genome*, 17, 220-9.
- SNAPP, K. R., HEITZIG, C. E. & KANSAS, G. S. 2002. Attachment of the PSGL-1 cytoplasmic domain to the actin cytoskeleton is essential for leukocyte rolling on P-selectin. *Blood*, 99, 4494-502.
- SOMMER, G., KRALISCH, S., STANGL, V., VIETZKE, A., KOHLER, U., STEPAN, H., FABER, R., SCHUBERT, A., LOSSNER, U., BLUHER, M., STUMVOLL, M. & FASSHAUER, M. 2009. Secretory products from human adipocytes stimulate proinflammatory cytokine secretion from human endothelial cells. *J Cell Biochem*, 106, 729-37.

- SONG, H., KIM, B. K., CHANG, W., LIM, S., SONG, B. W., CHA, M. J., JANG, Y. & HWANG, K. C. 2011. Tissue transglutaminase 2 promotes apoptosis of rat neonatal cardiomyocytes under oxidative stress. *J Recept Signal Transduct Res*, 31, 66-74.
- SONG, Y. & MASISON, D. C. 2005. Independent regulation of Hsp70 and Hsp90 chaperones by Hsp70/Hsp90-organizing protein Sti1 (Hop1). *J Biol Chem*, 280, 34178-85.
- SOVERSHAEV, M. A., EGORINA, E. M., GRUBER, F. X., OLSEN, J. O. & OSTERUD, B. 2007. High tissue factor-expressing human monocytes carry low surface CD36: application to intersubject variability. *J Thromb Haemost*, 5, 2453-60.
- SPERANDIO, S., FORTIN, J., SASIK, R., ROBITAILLE, L., CORBEIL, J. & DE BELLE, I. 2009. The transcription factor Egr1 regulates the HIF-1alpha gene during hypoxia. *Mol Carcinog*, 48, 38-44.
- ST HILAIRE, C., ZIEGLER, S. G., MARKELLO, T. C., BRUSCO, A., GRODEN, C., GILL, F., CARLSON-DONOHUE, H., LEDERMAN, R. J., CHEN, M. Y., YANG, D., SIEGENTHALER, M. P., ARDUINO, C., MANCINI, C., FREUDENTHAL, B., STANESCU, H. C., ZDEBIK, A. A., CHAGANTI, R. K., NUSSBAUM, R. L., KLETA, R., GAHL, W. A. & BOEHM, M. 2011. NT5E mutations and arterial calcifications. *N Engl J Med*, 364, 432-42.
- STAN, D., CALIN, M., MANDUTEANU, I., PIRVULESCU, M., GAN, A. M., BUTOI, E. D., SIMION, V. & SIMIONESCU, M. 2011. High glucose induces enhanced expression of resistin in human U937 monocyte-like cell line by MAPK- and NF-kB-dependent mechanisms; the modulating effect of insulin. *Cell Tissue Res*, 343, 379-87.
- STEPP, D. W., OU, J., ACKERMAN, A. W., WELAK, S., KLICK, D. & PRITCHARD, K. A., JR. 2002. Native LDL and minimally oxidized LDL differentially regulate superoxide anion in vascular endothelium in situ. *Am J Physiol Heart Circ Physiol*, 283, H750-9.
- STOYANOVA, E., TESCH, A., ARMSTRONG, V. W. & WIELAND, E. 2001. Enzymatically degraded low density lipoproteins are more potent inducers of egr-1 mRNA than oxidized or native low density lipoproteins. *Clin Biochem*, 34, 483-90.
- STUMPF, C., SEYBOLD, K., PETZI, S., WASMEIER, G., RAAZ, D., YILMAZ, A., ANGER, T., DANIEL, W. G. & GARLICH, C. D. 2008. Interleukin-10 improves left ventricular function in rats with heart failure subsequent to myocardial infarction. *Eur J Heart Fail*, 10, 733-9.
- SWANSON, H. I. & YANG, J. H. 1999. Specificity of DNA binding of the c-Myc/Max and ARNT/ARNT dimers at the CACGTG recognition site. *Nucleic Acids Res*, 27, 3205-12.
- SWIRSKI, F. K., PITTET, M. J., KIRCHER, M. F., AIKAWA, E., JAFFER, F. A., LIBBY, P. & WEISSLEDER, R. 2006. Monocyte accumulation in mouse atherogenesis is progressive and proportional to extent of disease. *Proc Natl Acad Sci U S A*, 103, 10340-5.
- SYROVETS, T., JENDRACH, M., ROHWEDDER, A., SCHULE, A. & SIMMET, T. 2001. Plasmin-induced expression of cytokines and tissue factor in human monocytes involves AP-1 and IKKbeta-mediated NF-kappaB activation. *Blood*, 97, 3941-50.
- SZONDY, Z., SARANG, Z., MOLNAR, P., NEMETH, T., PIACENTINI, M., MASTROBERARDINO, P. G., FALASCA, L., AESCHLIMANN, D., KOVACS, J., KISS, I., SZEGEZDI, E., LAKOS, G., RAJNAVOLGYI, E., BIRCKBICHLER, P. J., MELINO, G. & FESUS, L. 2003. Transglutaminase 2^{-/-} mice reveal a phagocytosis-associated crosstalk between macrophages and apoptotic cells. *Proc Natl Acad Sci U S A*, 100, 7812-7.

- TACKE, F. & RANDOLPH, G. J. 2006. Migratory fate and differentiation of blood monocyte subsets. *Immunobiology*, 211, 609-18.
- TADDEI, S., VIRDIS, A., GHIADONI, L., SALVETTI, G. & SALVETTI, A. 2000. Endothelial dysfunction in hypertension. *J Nephrol*, 13, 205-10.
- TAKAHASHI, M., MASUYAMA, J., IKEDA, U., KASAHARA, T., KITAGAWA, S., TAKAHASHI, Y., SHIMADA, K. & KANO, S. 1995a. Induction of monocyte chemoattractant protein-1 synthesis in human monocytes during transendothelial migration in vitro. *Circ Res*, 76, 750-7.
- TAKAHASHI, M., MASUYAMA, J., IKEDA, U., KITAGAWA, S., KASAHARA, T., SAITO, M., KANO, S. & SHIMADA, K. 1995b. Suppressive role of endogenous endothelial monocyte chemoattractant protein-1 on monocyte transendothelial migration in vitro. *Arterioscler Thromb Vasc Biol*, 15, 629-36.
- TAKAHASHI, Y., FUJIOKA, Y., TAKAHASHI, T., DOMOTO, K., TAKAHASHI, A., TANIGUCHI, T., ISHIKAWA, Y. & YOKOYAMA, M. 2005. Chylomicron remnants regulate early growth response factor-1 in vascular smooth muscle cells. *Life Sci*, 77, 670-82.
- TAKAYA, T., KASATANI, K., NOGUCHI, S. & NIKAWA, J. 2009. Functional analyses of immediate early gene ETR101 expressed in yeast. *Biosci Biotechnol Biochem*, 73, 1653-60.
- TAKEMOTO, M., YOKOTE, K., NISHIMURA, M., SHIGEMATSU, T., HASEGAWA, T., KON, S., UEDE, T., MATSUMOTO, T., SAITO, Y. & MORI, S. 2000. Enhanced expression of osteopontin in human diabetic artery and analysis of its functional role in accelerated atherogenesis. *Arterioscler Thromb Vasc Biol*, 20, 624-8.
- TAURINO, C., MILLER, W. H., MCBRIDE, M. W., MCCLURE, J. D., KHANIN, R., MORENO, M. U., DYMOTT, J. A., DELLES, C. & DOMINICZAK, A. F. 2010. Gene expression profiling in whole blood of patients with coronary artery disease. *Clin Sci (Lond)*, 119, 335-43.
- TAYLOR, A. M., LI, F., THIMMALAPURA, P., GERRITY, R. G., SAREMBOCK, I. J., FORREST, S., RUTHERFORD, S. & MCNAMARA, C. A. 2006. Hyperlipemia and oxidation of LDL induce vascular smooth muscle cell growth: an effect mediated by the HLH factor Id3. *J Vasc Res*, 43, 123-30.
- TEMEL, R. E., HOU, L., RUDEL, L. L. & SHELNESS, G. S. 2007. ACAT2 stimulates cholesteryl ester secretion in apoB-containing lipoproteins. *J Lipid Res*, 48, 1618-27.
- TERASAKA, N., HIROSHIMA, A., ARIGA, A., HONZUMI, S., KOIEYAMA, T., INABA, T. & FUJIWARA, T. 2005. Liver X receptor agonists inhibit tissue factor expression in macrophages. *FEBS J*, 272, 1546-56.
- TESSARZ, A. S., WEILER, S., ZANZINGER, K., ANGELISOVA, P., HOREJSI, V. & CERWENKA, A. 2007. Non-T cell activation linker (NTAL) negatively regulates TREM-1/DAP12-induced inflammatory cytokine production in myeloid cells. *J Immunol*, 178, 1991-9.
- TETIK, S., AK, K., SAHIN, Y., GULSOY, O., ISBIR, S., ARSAN, S. & YARDIMCI, T. 2010. Postoperative Statin Therapy Attenuates the Intensity of Systemic Inflammation and Increases Fibrinolysis After Coronary Artery Bypass Grafting. *Clin Appl Thromb Hemost*.
- TEUPSER, D., BURKHARDT, R., WILFERT, W., HAFFNER, I., NEBENDAHL, K. & THIERY, J. 2006. Identification of macrophage arginase I as a new candidate gene of atherosclerosis resistance. *Arterioscler Thromb Vasc Biol*, 26, 365-71.
- TEUPSER, D., MUELLER, M. A., KOGLIN, J., WILFERT, W., ERNST, J., VON SCHEIDT, W., STEINBECK, G., SEIDEL, D. & THIERY, J. 2008. CD36 mRNA

- expression is increased in CD14+ monocytes of patients with coronary heart disease. *Clin Exp Pharmacol Physiol*, 35, 552-6.
- THEVENOD, F. & CHAKRABORTY, P. K. 2010. The role of Wnt/beta-catenin signaling in renal carcinogenesis: lessons from cadmium toxicity studies. *Curr Mol Med*, 10, 387-404.
- THUM, T. & BORLAK, J. 2008. LOX-1 receptor blockade abrogates oxLDL-induced oxidative DNA damage and prevents activation of the transcriptional repressor Oct-1 in human coronary arterial endothelium. *J Biol Chem*, 283, 19456-64.
- TONG, F., BILLHEIMER, J., SHECHTMAN, C. F., LIU, Y., CROOKE, R., GRAHAM, M., COHEN, D. E., STURLEY, S. L. & RADER, D. J. 2010. Decreased expression of ARV1 results in cholesterol retention in the endoplasmic reticulum and abnormal bile acid metabolism. *J Biol Chem*, 285, 33632-41.
- TOSELLO, V., ZAMARCHI, R., MERLO, A., GORZA, M., PIOVAN, E., MANDRUZZATO, S., BRONTE, V., WANG, X., FERRONE, S., AMADORI, A. & ZANOVELLO, P. 2009. Differential expression of constitutive and inducible proteasome subunits in human monocyte-derived DC differentiated in the presence of IFN-alpha or IL-4. *Eur J Immunol*, 39, 56-66.
- TOUTOUZAS, K., KARANASOS, A., TSIAMIS, E., RIGA, M., DRAKOPOULOU, M., SYNETOS, A., PAPANIKOLAOU, A., TSIOUFIS, C., ANDROULAKIS, A., STEFANADI, E., TOUSOULIS, D. & STEFANADIS, C. 2011. New insights by optical coherence tomography into the differences and similarities of culprit ruptured plaque morphology in non-ST-elevation myocardial infarction and ST-elevation myocardial infarction. *Am Heart J*, 161, 1192-9.
- TRAUNER, M., CLAUDEL, T., FICKERT, P., MOUSTAFA, T. & WAGNER, M. 2010. Bile acids as regulators of hepatic lipid and glucose metabolism. *Dig Dis*, 28, 220-4.
- TSOUKNOS, A., NASH, G. B. & RAINGER, G. E. 2003. Monocytes initiate a cycle of leukocyte recruitment when cocultured with endothelial cells. *Atherosclerosis*, 170, 49-58.
- UGOCSAI, P., HOHENSTATT, A., PARAGH, G., LIEBISCH, G., LANGMANN, T., WOLF, Z., WEISS, T., GROITL, P., DOBNER, T., KASPRZAK, P., GOBOLOS, L., FALKERT, A., SEELBACH-GOEBEL, B., GELLHAUS, A., WINTERHAGER, E., SCHMIDT, M., SEMENZA, G. L. & SCHMITZ, G. 2010. HIF-1beta determines ABCA1 expression under hypoxia in human macrophages. *Int J Biochem Cell Biol*, 42, 241-52.
- UMETANI, M. & SHAUL, P. W. 2011. 27-Hydroxycholesterol: the first identified endogenous SERM. *Trends Endocrinol Metab*, 22, 130-5.
- UREN, A., WOLF, V., SUN, Y. F., AZARI, A., RUBIN, J. S. & TORETSKY, J. A. 2004. Wnt/Frizzled signaling in Ewing sarcoma. *Pediatr Blood Cancer*, 43, 243-9.
- VADYSIRISACK, D. D. & ELLISEN, L. W. 2012. mTOR activity under hypoxia. *Methods Mol Biol*, 821, 45-58.
- VAN ASSCHE, T., HENDRICKX, J., CRAUWELS, H. M., GUNS, P. J., MARTINET, W., FRANSEN, P., RAES, M. & BULT, H. 2011. Transcription profiles of aortic smooth muscle cells from atherosclerosis-prone and -resistant regions in young apolipoprotein E-deficient mice before plaque development. *J Vasc Res*, 48, 31-42.
- VAN DE WOUWER, M., COLLEN, D. & CONWAY, E. M. 2004. Thrombomodulin-protein C-EPCR system: integrated to regulate coagulation and inflammation. *Arterioscler Thromb Vasc Biol*, 24, 1374-83.
- VAN DER MEER, J. J., DE BOER, O. J., TEELING, P., VAN DER LOOS, C. M., DESSING, M. C. & VAN DER WAL, A. C. 2011. Smooth muscle homeostasis in

- human atherosclerotic plaques through interleukin 15 signalling. *Int J Clin Exp Pathol*, 4, 287-94.
- VAN GILS, J. M., ZWAGINGA, J. J. & HORDIJK, P. L. 2009. Molecular and functional interactions among monocytes, platelets, and endothelial cells and their relevance for cardiovascular diseases. *J Leukoc Biol*, 85, 195-204.
- VAN HERCK, J. L., SCHRIJVERS, D. M., DE MEYER, G. R., MARTINET, W., VAN HOVE, C. E., BULT, H., VRINTS, C. J. & HERMAN, A. G. 2010. Transglutaminase 2 deficiency decreases plaque fibrosis and increases plaque inflammation in apolipoprotein-E-deficient mice. *J Vasc Res*, 47, 231-40.
- VANPATTEN, S., RANGINANI, N., SHEFER, S., NGUYEN, L. B., ROSSETTI, L. & COHEN, D. E. 2001. Impaired biliary lipid secretion in obese Zucker rats: leptin promotes hepatic cholesterol clearance. *Am J Physiol Gastrointest Liver Physiol*, 281, G393-404.
- VASSE, M., POURTAU, J., TROCHON, V., MURAINÉ, M., VANNIER, J. P., LU, H., SORIA, J. & SORIA, C. 1999. Oncostatin M induces angiogenesis in vitro and in vivo. *Arterioscler Thromb Vasc Biol*, 19, 1835-42.
- VEILLARD, N. R., BRAUNERSREUTHER, V., ARNAUD, C., BURGER, F., PELLI, G., STEFFENS, S. & MACH, F. 2006. Simvastatin modulates chemokine and chemokine receptor expression by geranylgeranyl isoprenoid pathway in human endothelial cells and macrophages. *Atherosclerosis*, 188, 51-8.
- VIEIRA, J. M., JR., RODRIGUES, L. T., MANTOVANI, E., DELLE, H., MATTAR, A. L., MALHEIROS, D. M., NORONHA, I. L., FUJIHARA, C. K. & ZATZ, R. 2005. Statin monotherapy attenuates renal injury in a salt-sensitive hypertension model of renal disease. *Nephron Physiol*, 101, p82-91.
- VLODAVSKY, I., ELKIN, M., ABOUD-JARROUS, G., LEVI-ADAM, F., FUKS, L., SHAFAT, I. & ILAN, N. 2008. Heparanase: one molecule with multiple functions in cancer progression. *Connect Tissue Res*, 49, 207-10.
- VOELLMY, R. & BOELLMANN, F. 2007. Chaperone regulation of the heat shock protein response. *Adv Exp Med Biol*, 594, 89-99.
- VON HUNDELSHAUSEN, P., KOENEN, R. R., SACK, M., MAUSE, S. F., ADRIAENS, W., PROUDFOOT, A. E., HACKENG, T. M. & WEBER, C. 2005. Heterophilic interactions of platelet factor 4 and RANTES promote monocyte arrest on endothelium. *Blood*, 105, 924-30.
- VON HUNDELSHAUSEN, P., WEBER, K. S., HUO, Y., PROUDFOOT, A. E., NELSON, P. J., LEY, K. & WEBER, C. 2001. RANTES deposition by platelets triggers monocyte arrest on inflamed and atherosclerotic endothelium. *Circulation*, 103, 1772-7.
- VORA, D. K., FANG, Z. T., LIVA, S. M., TYNER, T. R., PARHAMI, F., WATSON, A. D., DRAKE, T. A., TERRITO, M. C. & BERLINER, J. A. 1997. Induction of P-selectin by oxidized lipoproteins. Separate effects on synthesis and surface expression. *Circ Res*, 80, 810-8.
- WANG, C. C., SHARMA, G. & DRAZNIN, B. 2006. Early growth response gene-1 expression in vascular smooth muscle cells effects of insulin and oxidant stress. *Am J Hypertens*, 19, 366-72.
- WANG, F., LIU, S., WU, S., ZHU, Q., OU, G., LIU, C., WANG, Y., LIAO, Y. & SUN, Z. 2012a. Blocking TREM-1 signaling prolongs survival of mice with *Pseudomonas aeruginosa* induced sepsis. *Cell Immunol*, 272, 251-8.
- WANG, F., XU, C. Q., HE, Q., CAI, J. P., LI, X. C., WANG, D., XIONG, X., LIAO, Y. H., ZENG, Q. T., YANG, Y. Z., CHENG, X., LI, C., YANG, R., WANG, C. C., WU, G., LU, Q. L., BAI, Y., HUANG, Y. F., YIN, D., YANG, Q., WANG, X. J., DAI, D. P.,

- ZHANG, R. F., WAN, J., REN, J. H., LI, S. S., ZHAO, Y. Y., FU, F. F., HUANG, Y., LI, Q. X., SHI, S. W., LIN, N., PAN, Z. W., LI, Y., YU, B., WU, Y. X., KE, Y. H., LEI, J., WANG, N., LUO, C. Y., JI, L. Y., GAO, L. J., LI, L., LIU, H., HUANG, E. W., CUI, J., JIA, N., REN, X., LI, H., KE, T., ZHANG, X. Q., LIU, J. Y., LIU, M. G., XIA, H., YANG, B., SHI, L. S., XIA, Y. L., TU, X. & WANG, Q. K. 2011a. Genome-wide association identifies a susceptibility locus for coronary artery disease in the Chinese Han population. *Nat Genet*, 43, 345-9.
- WANG, J., CHENG, X., XIANG, M. X., ALANNE-KINNUNEN, M., WANG, J. A., CHEN, H., HE, A., SUN, X., LIN, Y., TANG, T. T., TU, X., SJOBERG, S., SUKHOVA, G. K., LIAO, Y. H., CONRAD, D. H., YU, L., KAWAKAMI, T., KOVANEN, P. T., LIBBY, P. & SHI, G. P. 2011b. IgE stimulates human and mouse arterial cell apoptosis and cytokine expression and promotes atherogenesis in Apoe^{-/-} mice. *J Clin Invest*, 121, 3564-77.
- WANG, L., BEECHAM, A., ZHUO, D., DONG, C., BLANTON, S. H., RUNDEK, T. & SACCO, R. L. 2012b. Fine mapping study reveals novel candidate genes for carotid intima-media thickness in Dominican Republican families. *Circ Cardiovasc Genet*, 5, 234-41.
- WANG, L., FAN, C., TOPOL, S. E., TOPOL, E. J. & WANG, Q. 2003. Mutation of MEF2A in an inherited disorder with features of coronary artery disease. *Science*, 302, 1578-81.
- WANG, M., LANG, X., ZOU, L., HUANG, S. & XU, Z. 2011c. Four genetic polymorphisms of paraoxonase gene and risk of coronary heart disease: a meta-analysis based on 88 case-control studies. *Atherosclerosis*, 214, 377-85.
- WANG, X., LI, X., YUE, T. L. & OHLSTEIN, E. H. 2000. Expression of monocyte chemotactic protein-3 mRNA in rat vascular smooth muscle cells and in carotid artery after balloon angioplasty. *Biochim Biophys Acta*, 1500, 41-8.
- WANG, X., XIAO, Y., MOU, Y., ZHAO, Y., BLANKESTEIJN, W. M. & HALL, J. L. 2002. A role for the beta-catenin/T-cell factor signaling cascade in vascular remodeling. *Circ Res*, 90, 340-7.
- WANG, Y., CHANG, H., ZOU, J., JIN, X. & QI, Z. 2011d. The effect of atorvastatin on mRNA levels of inflammatory genes expression in human peripheral blood lymphocytes by DNA microarray. *Biomed Pharmacother*, 65, 118-22.
- WANG, Y., FU, W., XIE, F., CHU, X., WANG, H., SHEN, M., SUN, W., LEI, R., YANG, L., WU, H., FOO, J., LIU, J., JIN, L. & HUANG, W. 2010a. Common polymorphisms in ITGA2, PON1 and THBS2 are associated with coronary atherosclerosis in a candidate gene association study of the Chinese Han population. *J Hum Genet*, 55, 490-4.
- WANG, Y. D., CHEN, W. D., YU, D., FORMAN, B. M. & HUANG, W. 2011e. The G-protein coupled bile acid receptor Gpbar1 (TGR5) negatively regulates hepatic inflammatory response through antagonizing Nuclear Factor kappaB. *Hepatology*.
- WANG, Z. H., LIU, X. L., ZHONG, M., ZHANG, L. P., SHANG, Y. Y., HU, X. Y., LI, L., ZHANG, Y., DENG, J. T. & ZHANG, W. 2010b. Pleiotropic effects of atorvastatin on monocytes in atherosclerotic patients. *J Clin Pharmacol*, 50, 311-9.
- WANKER, E. E. 2002. Hip1 and Hippi participate in a novel cell death-signaling pathway. *Dev Cell*, 2, 126-8.
- WATKINS, N. A., GUSNANTO, A., DE BONO, B., DE, S., MIRANDA-SAAVEDRA, D., HARDIE, D. L., ANGENENT, W. G., ATTWOOD, A. P., ELLIS, P. D., ERBER, W., FOAD, N. S., GARNER, S. F., ISACKE, C. M., JOLLEY, J., KOCH, K., MACAULAY, I. C., MORLEY, S. L., RENDON, A., RICE, K. M., TAYLOR, N., THIJSSEN-TIMMER, D. C., THIJSSEN, M. R., VAN DER SCHOOT, C. E.,

- WERNISCH, L., WINZER, T., DUDBRIDGE, F., BUCKLEY, C. D., LANGFORD, C. F., TEICHMANN, S., GOTTGENS, B. & OUWEHAND, W. H. 2009. A HaemAtlas: characterizing gene expression in differentiated human blood cells. *Blood*, 113, e1-9.
- WE, G. C., SIROI, M. G., QU, R., LIU, P. & ROULEA, J. L. 2002. Effects of quinapril on myocardial function, ventricular remodeling and cardiac cytokine expression in congestive heart failure in the rat. *Cardiovasc Drugs Ther*, 16, 29-36.
- WEINGARTNER, O., LAUFS, U., BOHM, M. & LUTJOHANN, D. An alternative pathway of reverse cholesterol transport: the oxysterol 27-hydroxycholesterol. *Atherosclerosis*, 209, 39-41.
- WEYRICH, A. S., ELSTAD, M. R., MCEVER, R. P., MCINTYRE, T. M., MOORE, K. L., MORRISSEY, J. H., PRESCOTT, S. M. & ZIMMERMAN, G. A. 1996. Activated platelets signal chemokine synthesis by human monocytes. *J Clin Invest*, 97, 1525-34.
- WHEATON, K., MUIR, J., MA, W. & BENCHIMOL, S. 2010. BTG2 antagonizes Pin1 in response to mitogens and telomere disruption during replicative senescence. *Aging Cell*, 9, 747-60.
- WILBUR, J. D., CHEN, C. Y., MANALO, V., HWANG, P. K., FLETTERICK, R. J. & BRODSKY, F. M. 2008. Actin binding by Hip1 (huntingtin-interacting protein 1) and Hip1R (Hip1-related protein) is regulated by clathrin light chain. *J Biol Chem*, 283, 32870-9.
- WILLIAMS, R. R., HUNT, S. C., HASSTEDT, S. J., BERRY, T. D., WU, L. L., BARLOW, G. K., STULTS, B. M. & KUIDA, H. 1988. Definition of genetic factors in hypertension: a search for major genes, polygenes, and homogeneous subtypes. *J Cardiovasc Pharmacol*, 12 Suppl 3, S7-20.
- WILLIAMS, R. R., HUNT, S. C., HEISS, G., PROVINCE, M. A., BENSEN, J. T., HIGGINS, M., CHAMBERLAIN, R. M., WARE, J. & HOPKINS, P. N. 2001. Usefulness of cardiovascular family history data for population-based preventive medicine and medical research (the Health Family Tree Study and the NHLBI Family Heart Study). *Am J Cardiol*, 87, 129-35.
- WINKELMANN, B. R. & HAGER, J. 2000. Genetic variation in coronary heart disease and myocardial infarction: methodological overview and clinical evidence. *Pharmacogenomics*, 1, 73-94.
- WU, F. Y., OU, Z. L., FENG, L. Y., LUO, J. M., WANG, L. P., SHEN, Z. Z. & SHAO, Z. M. 2008. Chemokine decoy receptor d6 plays a negative role in human breast cancer. *Mol Cancer Res*, 6, 1276-88.
- WU, Y., ZHANG, Y., ZHANG, H., YANG, X., WANG, Y., REN, F., LIU, H., ZHAI, Y., JIA, B., YU, J. & CHANG, Z. 2010. p15RS attenuates Wnt/ β -catenin signaling by disrupting β -catenin.TCF4 Interaction. *J Biol Chem*, 285, 34621-31.
- XIE, J., ZHU, H., GUO, L., RUAN, Y., WANG, L., SUN, L., ZHOU, L., WU, W., YUN, X., SHEN, A. & GU, J. 2010. Lectin-like oxidized low-density lipoprotein receptor-1 delivers heat shock protein 60-fused antigen into the MHC class I presentation pathway. *J Immunol*, 185, 2306-13.
- XUE, M., MARCH, L., SAMBROOK, P. N., FUKUDOME, K. & JACKSON, C. J. 2007. Endothelial protein C receptor is overexpressed in rheumatoid arthritic (RA) synovium and mediates the anti-inflammatory effects of activated protein C in RA monocytes. *Ann Rheum Dis*, 66, 1574-80.
- YAMADA, R., CAO, X., BUTKEVICH, A. N., MILLARD, M., ODDE, S., MORDWINKIN, N., GUNDLA, R., ZANDI, E., LOUIE, S. G., PETASIS, N. A. & NEAMATI, N. 2011. Discovery and preclinical evaluation of a novel class of cytotoxic propynoic acid carbamoyl methyl amides (PACMAs). *J Med Chem*, 54, 2902-14.

- YAMASHITA, S., HIRANO, K., KUWASAKO, T., JANABI, M., TOYAMA, Y., ISHIGAMI, M. & SAKAI, N. 2007. Physiological and pathological roles of a multi-ligand receptor CD36 in atherogenesis; insights from CD36-deficient patients. *Mol Cell Biochem*, 299, 19-22.
- YANG, L., ZHU, X., ZHAO, X. & DENG, Z. 2003. Expression of macrophage inflammatory protein 1 alpha in the endothelial cells exposed to diamide. *J Huazhong Univ Sci Technolog Med Sci*, 23, 219-22, 233.
- YANO, K., UEKI, N., ODA, T., SEKI, N., MASUHO, Y. & MURAMATSU, M. 2000. Identification and characterization of human ZNF274 cDNA, which encodes a novel kruppel-type zinc-finger protein having nucleolar targeting ability. *Genomics*, 65, 75-80.
- YATA, K., OIKAWA, S., SASAKI, R., SHINDO, A., YANG, R., MURATA, M., KANAMARU, K. & TOMIMOTO, H. 2011. Astrocytic neuroprotection through induction of cytoprotective molecules; a proteomic analysis of mutant P301S tau-transgenic mouse. *Brain Res*.
- YILMAZ, A., REISS, C., WENG, A., CICHA, I., STUMPF, C., STEINKASSERER, A., DANIEL, W. G. & GARLICH, C. D. 2006. Differential effects of statins on relevant functions of human monocyte-derived dendritic cells. *J Leukoc Biol*, 79, 529-38.
- YOSHIDA, T., METT, I., BHUNIA, A. K., BOWMAN, J., PEREZ, M., ZHANG, L., GANDJEVA, A., ZHEN, L., CHUKWUEKE, U., MAO, T., RICHTER, A., BROWN, E., ASHUSH, H., NOTKIN, N., GELFAND, A., THIMMULAPPA, R. K., RANGASAMY, T., SUSSAN, T., COSGROVE, G., MOUDED, M., SHAPIRO, S. D., PETRACHE, I., BISWAL, S., FEINSTEIN, E. & TUDER, R. M. 2010. Rtp801, a suppressor of mTOR signaling, is an essential mediator of cigarette smoke-induced pulmonary injury and emphysema. *Nat Med*, 16, 767-73.
- YUAN, Y., NIU, C. C., DENG, G., LI, Z. Q., PAN, J., ZHAO, C., YANG, Z. L. & SI, W. K. 2011. The Wnt5a/Ror2 noncanonical signaling pathway inhibits canonical Wnt signaling in K562 cells. *Int J Mol Med*, 27, 63-9.
- YUSUF, S., HAWKEN, S., OUNPUU, S., DANS, T., AVEZUM, A., LANAS, F., MCQUEEN, M., BUDAJ, A., PAIS, P., VARIGOS, J. & LISHENG, L. 2004. Effect of potentially modifiable risk factors associated with myocardial infarction in 52 countries (the INTERHEART study): case-control study. *Lancet*, 364, 937-52.
- ZAWADZKI, C., SUSEN, S., RICHARD, F., HAULON, S., CORSEAU, D., JEANPIERRE, E., VINCENTELLI, A., LUCAS, C., TORPIER, G., MARTIN, A., VAN BELLE, E., STAELS, B. & JUDE, B. 2007. Dyslipidemia shifts the tissue factor/tissue factor pathway inhibitor balance toward increased thrombogenicity in atherosclerotic plaques: evidence for a corrective effect of statins. *Atherosclerosis*, 195, e117-25.
- ZELLER, T., WILD, P., SZYMCZAK, S., ROTIVAL, M., SCHILLERT, A., CASTAGNE, R., MAUCHE, S., GERMAIN, M., LACKNER, K., ROSSMANN, H., ELEFThERiADIS, M., SINNING, C. R., SCHNABEL, R. B., LUBOS, E., MENNERICH, D., RUST, W., PERRET, C., PROUST, C., NICAUD, V., LOSCALZO, J., HUBNER, N., TREGOUET, D., MUNZEL, T., ZIEGLER, A., TIRET, L., BLANKENBERG, S. & CAMBIEN, F. 2010. Genetics and beyond--the transcriptome of human monocytes and disease susceptibility. *PLoS One*, 5, e10693.
- ZHANG, C., HEIN, T. W., WANG, W., REN, Y., SHIPLEY, R. D. & KUO, L. 2006. Activation of JNK and xanthine oxidase by TNF-alpha impairs nitric oxide-mediated dilation of coronary arterioles. *J Mol Cell Cardiol*, 40, 247-57.
- ZHANG, F., AHLBORN, T. E., LI, C., KRAEMER, F. B. & LIU, J. 2002. Identification of Egr1 as the oncostatin M-induced transcription activator that binds to sterol-

- independent regulatory element of human LDL receptor promoter. *J Lipid Res*, 43, 1477-85.
- ZHANG, L., HUANG, H., WU, K., WANG, M. & WU, B. 2010. Impact of BTG2 expression on proliferation and invasion of gastric cancer cells in vitro. *Mol Biol Rep*, 37, 2579-86.
- ZHANG, L., TIAN, F., HAN, D., NIU, J. & LIU, X. 2009a. [Effect of simvastatin on mRNA expressions of some components of Wnt signaling pathway in differentiation process of osteoblasts derived from BMSCs of rats]. *Zhongguo Xiu Fu Chong Jian Wai Ke Za Zhi*, 23, 1371-5.
- ZHANG, L., ZHANG, Z. G., LIU, X. S., HOZESKA-SOLGOT, A. & CHOPP, M. 2007. The PI3K/Akt pathway mediates the neuroprotective effect of atorvastatin in extending thrombolytic therapy after embolic stroke in the rat. *Arterioscler Thromb Vasc Biol*, 27, 2470-5.
- ZHANG, Y., YANG, Z., CAO, Y., ZHANG, S., LI, H., HUANG, Y., DING, Y. Q. & LIU, X. 2008. The Hsp40 family chaperone protein DnaJB6 enhances Schlafen1 nuclear localization which is critical for promotion of cell-cycle arrest in T-cells. *Biochem J*, 413, 239-50.
- ZHANG, Z., DEB, A., PACHORI, A., HE, W., GUO, J., PRATT, R. & DZAU, V. J. 2009b. Secreted frizzled related protein 2 protects cells from apoptosis by blocking the effect of canonical Wnt3a. *J Mol Cell Cardiol*, 46, 370-7.
- ZHAO, X. Q., ZHANG, M. W., WANG, F., ZHAO, Y. X., LI, J. J., WANG, X. P., BU, P. L., YANG, J. M., LIU, X. L., ZHANG, M. X., GAO, F., ZHANG, C. & ZHANG, Y. 2011. CRP enhances soluble LOX-1 release from macrophages by activating TNF-alpha converting enzyme. *J Lipid Res*, 52, 923-33.
- ZHOU, J., WANG, K. C., WU, W., SUBRAMANIAM, S., SHYY, J. Y., CHIU, J. J., LI, J. Y. & CHIEN, S. 2011. MicroRNA-21 targets peroxisome proliferators-activated receptor-alpha in an autoregulatory loop to modulate flow-induced endothelial inflammation. *Proc Natl Acad Sci U S A*, 108, 10355-60.
- ZHOU, Q., LAN, Y., WANG, Y., ZHAO, Y. & WU, Z. 2002. [Activating protein-1 complex regulates oxidized low density lipoprotein-induced overproduction of rat TGF-beta1 at transcriptional level]. *Zhonghua Yi Xue Za Zhi*, 82, 1346-50.
- ZHU, L., BISGAIER, C. L., AVIRAM, M. & NEWTON, R. S. 1999. 9-cis retinoic acid induces monocyte chemoattractant protein-1 secretion in human monocytic THP-1 cells. *Arterioscler Thromb Vasc Biol*, 19, 2105-11.
- ZINEH, I., BEITELSHEES, A. L., WELDER, G. J., HOU, W., CHEGINI, N., WU, J., CRESCI, S., PROVINCE, M. A. & SPERTUS, J. A. 2008. Epithelial neutrophil-activating peptide (ENA-78), acute coronary syndrome prognosis, and modulatory effect of statins. *PLoS One*, 3, e3117.

APPENDIX

Optimisation of methods and protocols

PLATELET-MEDIATED STIMULATION EXPERIMENT (CRP-XL)

Two forms of commercially available collagen related peptide (CRP) were compared for consistency and effectiveness of platelet activation, CRP-18 and CRP-XL. Optimisation experiments were carried out in three doses of each reagent: 10, 1.0 and 0.1 micrograms per ml sample. The extent of platelet activation (measured by fibrinogen binding and expressed in percentage) ranged from 74 to 94% with increasing doses of CRP-18, whilst the response with CRP-XL was less variable, ranging from 89% to 95%. Based on these experiments, it was decided that 0.5micrograms of CRP-XL per ml of whole blood would provide optimum stimulation.

Following CRP-XL stimulation, appropriate platelet activation and platelet-monocyte interaction were confirmed by fibrinogen binding, surface expression of P-selectin and by formation of monocyte-platelet aggregates (MPAs).

PLATELET FLOW CYTOMETRY

Fibrinogen binding and P-selectin expression

Reagents

Hepes buffered saline (HBS) (10mM HEPES; 150mM NaCl; 1mM MgSO₄; 5mM KCl; pH 7.4, filter sterilised through a 0.22µm filter) (HBS)

0.2% formyl saline (0.2% formaldehyde in 0.9% NaCl)

Agonists:

Agonist	Source	Stock concentrations	Storage	Volume to use
ADP	Sigma A6646	10-6M	-80°C (do not refreeze)	5µl (final conc: 10-7M)
CRP-XL	Richard Farndale	Stock conc: 9.3mg/ml (~10,000µg/ml) Prepare a working solution of 5µg/ml	Stock solution at 4°C dilute daily (see methods)	5µl of 5µg/ml (final conc: 0.5µg/ml)
TRAP	Bachem (H-2936)	2x10-5M	-80°C (do not refreeze)	5µl (final conc 2x10-6M)

Antibodies:

Antigen	CD No	Antibody	Source	Comments	Vol
Fibrinogen		Rabbit anti-fibrinogen .FITC	Dako F011	Activation marker Measures fibrinogen binding to activated GpIIb/IIIa	2µl
P-selectin	CD62P	Mouse-anti human P-selectin. FITC	R&D #BBA34	Activation marker Measures degranulation (α-granules) dilute 1 in 100 before use	2µl
-ve isotype for P-Selectin		IgG1 (CFS)	R&D #IC002F		2µl

Other reagents:

Reagent	Function	Source	Comments	Volume to add
Hirudin	Inhibition of all actions of thrombin	Fluka biochemika #94581	5µl of a 1000U/ml stock (100X conc.) to give final conc. of 10U/ml Stored at -80°C	5µl of 100X conc to 500µl whole blood
Aspirin	Blocks arachidonic metabolism via COX-1 in platelets	Sigma (A5376)	5µl of 1x10-2M stock (100X conc) to 500µl blood to give final conc. of 1x10-4M Stored at 4°C	5µl of 100X conc to 500µl whole blood
Apyrase	Cleaves ADP thereby inhibiting its action	Sigma (A6535)	Stock conc 40U/ml =10X conc. Final conc. of 4U/ml	5µl
EDTA	Chelates calcium	Sigma (E7889)	Stock 140mM. Add 2µl/LP3 tube. Final conc. of 6mM Stored at 4°C.	2µl

Fibrinogen binding and P-selectin expression

METHOD (Refer to Experiment Plan)

USE ASPIRIN & HIRUDIN TREATED WHOLE BLOOD THROUGHOUT

Diluted CRP-XL to working solution of 5µg/ml as follows:

- Dilute the conc. stock of 9.3mg/ml 1/100 to give 100µg/ml
- Take 50µl of this + 50µl HBS = 50µg/ml
- Dilute this by 1/10 by taking 10µl of this + 90µl HBS = 5µg/ml

Obtain all antibodies and agonists from freezer, keep on ice. Label LP3 tubes (duplicates for each test point) and place in a rack. Set up and label corresponding LP4 tubes each containing 0.5ml 0.2% formyl saline. Assay tubes should be prepared no more than 30 minutes before blood sample is taken. Ensure all tubes and reagents are at room temperature. Add HBS to each LP3 tube, taking care that the solution is placed in the bottom of each tube. HBS should be at room temperature. Using a Barmy pipette add specific antibodies to the appropriate tubes. Using a Barmy pipette add agonists (or no agonist see expt plan) to each tube. Add apyrase to each tube where appropriate. At this point the tubes can be left for up to 30 minutes before the blood is added. If there is a delay in blood collection place the tubes in the fridge for up to 1 hour but ensure tubes reach room temperature before adding blood. Once a sample is booked in carefully remove 500µl of blood from the first citrate tube using a pastette and transfer to a clean screw cap tube. Add 5µl 10mM aspirin, and 5µl 1000U/ml hirudin to the 500µl blood. Leave for 5 minutes to allow aspirin to permeate platelets. Samples must be analysed within 10-15 minutes of blood. Using a Barmy pipette add 5µl

aliquots of aspirinated and hirudinised blood to the assay tubes. Change the tip between each tube. Wipe tip on tissue before adding to tubes. Incubate assay tubes for 20 minutes at RT. Add 0.5ml of 0.2% formyl saline to each assay tube and incubate for 10 minutes at RT. Transfer 50µl of the fixed sample into the corresponding LP4 tubes containing 0.5ml 0.2% formyl saline. Analyse in the Coulter XL-MCL using protocol BLOODOMICS/P-SELECTIN, within 2 hours, using the two –ve controls to set the background fluorescence to 2%.

Whole blood MPA flow cytometric assay – Optilyse®C method

Method for analysing MPAs without prior isolation of monocytes

Reagents	Sample	SOP
Optilyse®C (Beckman Coulter#A11895) PBS pH 7.4 Hepes buffered saline	Citrated blood	Coulter XL-MCL flowcytometer Preparation of HBS

Antibody	Supplier	Stored in Bloodomics box in fridge
MOPC31C IgG1k	Sigma M9035	5µL
P-Selectin blocking Mab 9E1	R&D BBA30	2µL
CD14-RPE-Cy5 MouseαHuman	Serotec MCA1568C	5µL
RPE-Cy5 IgG2a isotype –ve control (for CD14.RPEcy5)	Serotec MCA 929C	2µL
CD42b-RPE MouseαHuman	DAKO R7014	2µL
RPE IgG2a –ve isotype (for CD42b)	DAKO X0950	2µL

Label 4 LP4 tubes and place in rack. Ensure all tubes and reagents are at room temperature. Add 50µL HBS to each tube and add the following antibodies (volumes should be checked with current titrations):

Whole blood Annexin binding assay (see Tube Plan below).

Label LP3 tubes (duplicates for each test point) and place in a rack. Add HBS to the control and HBS+Ca to all other tubes. Add MOPC21-PE isotype control and CD42b-RPE to tubes as appropriate. Using a Barmy pipette add agonist (or no agonist see below) to each tube.

Once a sample is booked in carefully remove 500µl of blood from the first citrate tube using a pastette and transfer to a clean screw cap tube. Samples must be analysed within 10-15 minutes of blood collection. Add 5µl of whole citrated blood to each tube. Incubate for 10 minutes at room temperature. Then Add 5µl Annexin V-FITC to each tube. Incubate for further 10 minutes at room temperature. Add 450µl HBS to Isotype tubes and HBS + Ca to other tubes. Label 1 set of LP4 tubes corresponding to each LP3; add 450µl appropriate HBS or HBS + Ca to LP4 tubes. Remove 50µl of diluted sample and add to appropriate LP4. Run these diluted tubes on the flowcytometer on Bloodomics CD42b/Annexin V protocol.

R SCRIPTS FOR STATISTICAL ANALYSIS

Analysis script for Post MI vs. controls

```
# Date of analysis 28-04-08
a <- read.Table("original_Leicester_MI_gene_profile.csv", skip=6, header=T, sep=",")
clin <- read.Table("original_MI_sample_list.txt", header=T, sep="\t")
# The ordering of samples should match the arrays
ncol.a <- ncol(a)
nrow.a <- nrow(a)
nrep.col <- 8 # number of columns repeated per array
starting.column <- 3 # starting column to be picked up
avg.signal <- a[, seq(starting.column,ncol.a,nrep.col)] # Average signal, our main interest
starting.column <- 7 # starting column to be picked up
sd.signal <- a[, seq(starting.column,ncol.a,nrep.col)]
starting.column <- 8 # starting column to be picked up
n.bead <- a[, seq(starting.column,ncol.a,nrep.col)]
starting.column <- 9 # starting column to be picked up
det.signal <- a[, seq(starting.column,ncol.a,nrep.col)]
order.clin.samples<- order(clin$Serial_No)
clin2 <- clin[order.clin.samples,]
group <- clin2$Group # AMI, PMIt0, PMIt4, CONt0, CONt4, PMIt0ex
group.id <- c(group) # Levels: AMI=1 CONt0=2 CONt4=3 PMIt0=4 PMIt0ex=5 PMIt4=6
avg.signal <- avg.signal[,order.clin.samples]
det.signal <- det.signal[,order.clin.samples]
### This section for getting normalized data from unnormalized data.
require(affy)
log.avg.signal <- as.matrix(log(avg.signal,2))
exp.normalized <- normalize.quantiles(log.avg.signal)
colnames(exp.normalized) <- names(avg.signal)
rownames(exp.normalized) <- as.character(a[,1])
exp.normalized.lin<-2^exp.normalized
# Output normalized linear signal intensities
write.csv(exp.normalized.lin, file="Leic_MIarrays_norm_intensity.csv")
#.... End of normalization step for non-normalized data.
# Obtain mean intensities per group
mean.AMI<-apply(exp.normalized[,group=="AMI"],1,mean)
mean.PMIt0<-apply(exp.normalized[,group=="PMIt0"],1,mean)
mean.PMIt4<-apply(exp.normalized[,group=="PMIt4"],1,mean)
mean.CONt0<-apply(exp.normalized[,group=="CONt0"],1,mean)
mean.CONt4<-apply(exp.normalized[,group=="CONt4"],1,mean)
# Determine genes that are present in each group
detection.threshold <- 0.99
temp <- function(a) sum(a>=detection.threshold)
present.AMI <- apply(det.signal[,group=="AMI"],1,temp)
present.PMIt0 <- apply(det.signal[,group=="PMIt0"],1,temp)
present.PMIt4 <- apply(det.signal[,group=="PMIt4"],1,temp)
present.CONt0 <- apply(det.signal[,group=="CONt0"],1,temp)
present.CONt4 <- apply(det.signal[,group=="CONt4"],1,temp)
#####
```

Analysis 1: PMIt4 vs CONt4

```
p.values1 <- apply(exp.normalized,1,function(a) t.test(a[group=="PMIt4"],
a[group=="CONt4"], paired=FALSE, var.equal=T)$p.val)
t.stat1 <- apply(exp.normalized,1,function(a) t.test(a[group=="PMIt4"], a[group=="CONt4"],
paired=FALSE, var.equal=T)$stat)
# Define and apply the function to get the average log fold change (PMIt4/CONt4)
avg.logfold1<-function(a){return(mean(a[group=="PMIt4"]-a[group=="CONt4"]))}
avg.log.fold1 <-apply(exp.normalized,1,avg.logfold1)
## Generate objects for PMIt4 vs. CONt4 from exp.normalized
clin.1 <- clin2[c(26:44,64:82),]
exp.normalized1 <- exp.normalized[,c(group=="PMIt4" | group=="CONt4")]
order.clin.samples<- order(clin.1$Serial_No)
clin.1 <- clin.1[order.clin.samples,]
group1 <- clin.1$Group # PMIt4, CONt4
group.id1 <- c(group1) # PMIt4=3 CONt4=5
exp.normalized1 <- exp.normalized1[,order.clin.samples]
#OCplus - FDR2d correction
require (OCplus)
result.2d1<-fdr2d(exp.normalized1, group.id1, nperm=500, smooth=0.01, paired=FALSE)
fdr.values1<-result.2d1$fdr
# Create summary Table
summary.Table1<-data.frame(gene.ID=as.character(rownames(exp.normalized)),
log.fold=avg.log.fold1, fold.change=2^avg.log.fold1, present.PMIt4, present.CONt4,
t.statistics=t.stat1, p.values=p.values1, fdr2d=fdr.values1)
write.csv(summary.Table1, file="original_Mlarrays_CRP_PMIvsCON.csv")
#volcano plot
plot(avg.log.fold1, -log(p.values1,10),xlab="log(2) fold change",ylab="-log(10)p-
values",main="PMI vs. CON CRP")
```

```
#####
```

Analysis 2: PMIt0 vs CONt0

```
p.values2 <- apply(exp.normalized,1,function(a) t.test(a[group=="PMIt0"],
a[group=="CONt0"], paired=FALSE, var.equal=T)$p.val)
t.stat2 <- apply(exp.normalized,1,function(a) t.test(a[group=="PMIt0"], a[group=="CONt0"],
paired=FALSE, var.equal=T)$stat)
# Define and apply the function to get the average log fold change (PMIt0/CONt0)
avg.logfold2<-function(a){return(mean(a[group=="PMIt0"]-a[group=="CONt0"]))}
avg.log.fold2 <-apply(exp.normalized,1,avg.logfold2)
## Generate objects for PMIt0 vs. CONt0 from exp.normalized
clin.2 <- clin2[c(6:14,16:25,45:63),]
exp.normalized2 <- exp.normalized[,c(group=="PMIt0" | group=="CONt0")]
order.clin.samples<- order(clin.2$Serial_No)
clin.2 <- clin.2[order.clin.samples,]
group2 <- clin.2$Group # PMIt0, CONt0
group.id2 <- c(group2) # PMIt0=5 CONt0=2
exp.normalized2 <- exp.normalized2[,order.clin.samples]
#OCplus - FDR2d correction
require (OCplus)
result.2d2<-fdr2d(exp.normalized2, group.id2, nperm=500, smooth=0.01, paired=FALSE)
fdr.values2<-result.2d2$fdr
# Create summary Table
summary.Table2<-data.frame(gene.ID=as.character(rownames(exp.normalized)),
log.fold=avg.log.fold2, fold.change=2^avg.log.fold2, present.PMIt0, present.CONt0,
t.statistics=t.stat2, p.values=p.values2, fdr2d=fdr.values2)
write.csv(summary.Table2, file="original_Mlarrays_baseline_PMIvsCON.csv")
#volcano plot
plot(avg.log.fold2, -log(p.values2,10),xlab="log(2) fold change",ylab="-log(10)p-
values",main="PMI vs. CON baseline")
```

```
#####
```

Analysis 3: PMIt4 vs PMIt0

```
p.values3 <- apply(exp.normalized,1,function(a) t.test(a[group=="PMIt4"],
a[group=="PMIt0"], paired=TRUE, var.equal=T)$p.val)
t.stat3 <- apply(exp.normalized,1,function(a) t.test(a[group=="PMIt4"], a[group=="PMIt0"],
paired=TRUE, var.equal=T)$stat)
# Define and apply the function to get the average log fold change (PMIt4/PMIt0)
avg.logfold3<-function(a){return(mean(a[group=="PMIt4"]-a[group=="PMIt0"]))}
avg.log.fold3 <-apply(exp.normalized,1,avg.logfold3)
## Generate objects for PMIt4 vs. PMIt0 from exp.normalized
clin.3 <- clin2[c(6:14,16:44),]
exp.normalized3 <- exp.normalized[,c(group=="PMIt4" | group=="PMIt0")]
order.clin.samples<- order(clin.3$Sample_ID)
clin.3 <- clin.3[order.clin.samples,]
group3 <- clin.3$Group # PMIt4=5 PMIt0=4
group.id3 <- c(group3) # PMIt4=5 PMIt0=4
exp.normalized3 <- exp.normalized3[,order.clin.samples]
#OCplus - FDR2d correction
require (OCplus)
result.2d3<-fdr2d(exp.normalized3, group.id3, nperm=500, smooth=0.04, paired=TRUE)
fdr.values3<-result.2d3$fdr
# Create summary Table
summary.Table3<-data.frame(gene.ID=as.character(rownames(exp.normalized)),
log.fold=avg.log.fold3, fold.change=2^avg.log.fold3, present.PMIt4, present.PMIt0,
t.statistics=t.stat3, p.values=p.values3, fdr2d=fdr.values3)
write.csv(summary.Table3, file="Post_MI_arrays_baseline vs. CRP.csv")
#volcano plot
plot(avg.log.fold3, -log(p.values3,10),xlab="log(2) fold change",ylab="-log(10) p-
values",main="Post MI baseline vs. CRP")
```

```
#####
```

Analysis 4: CONt4 vs CONt0

```
p.values4 <- apply(exp.normalized,1,function(a) t.test(a[group=="CONt4"],
a[group=="CONt0"], paired=TRUE, var.equal=T)$p.val)
t.stat4 <- apply(exp.normalized,1,function(a) t.test(a[group=="CONt4"],
a[group=="CONt0"], paired=TRUE, var.equal=T)$stat)
# Define and apply the function to get the average log fold change (CONt4/CONt0)
avg.logfold4<-function(a){return(mean(a[group=="CONt4"]-a[group=="CONt0"]))}
avg.log.fold4 <-apply(exp.normalized,1,avg.logfold4)
## Generate objects for CONt4 vs. CONt0 from exp.normalized
clin.4 <- clin2[c(45:82),]
exp.normalized4 <- exp.normalized[,c(group=="CONt4" | group=="CONt0")]
order.clin.samples<- order(clin.4$Sample_ID)
clin.4 <- clin.4[order.clin.samples,]
group4 <- clin.4$Group # CONt4=3 CONt0=4
group.id4 <- c(group4) # CONt4=1 CONt0=2
exp.normalized4 <- exp.normalized4[,order.clin.samples]
#OCplus - FDR2d correction
require (OCplus)
result.2d4<-fdr2d(exp.normalized4, group.id4, nperm=500, smooth=0.04, paired=TRUE)
fdr.values4<-result.2d4$fdr
# Create summary Table
summary.Table4<-data.frame(gene.ID=as.character(rownames(exp.normalized)),
log.fold=avg.log.fold4, fold.change=2^avg.log.fold4, present.CONt4, present.CONt0,
t.statistics=t.stat4, p.values=p.values4, fdr2d=fdr.values4)
write.csv(summary.Table4, file="MI Controls_baseline vs. CRP.csv")
#volcano plot
plot(avg.log.fold4, -log(p.values4,10),xlab="log(2) fold change",ylab="-log(10)p-
values",main="MI Controls baseline vs. CRP")
```

```
#####
```

Analysis script for Offspring of MI vs. controls

```
# Date of analysis 29-04-08
a <- read.Table("offspring_gene_profile_final.csv", skip=6, header=T, sep=",")
clin <- read.Table("offspring_sample_sheet_final.txt", header=T, sep="\t")
# The ordering of samples should match the arrays
ncol.a <- ncol(a)
nrow.a <- nrow(a)
nrep.col <- 8 # number of columns repeated per array
starting.column <- 3 # starting column to be picked up
avg.signal <- a[, seq(starting.column,ncol.a,nrep.col)] # Average signal, our main interest
starting.column <- 7 # starting column to be picked up
sd.signal <- a[, seq(starting.column,ncol.a,nrep.col)]
starting.column <- 8 # starting column to be picked up
n.bead <- a[, seq(starting.column,ncol.a,nrep.col)]
starting.column <- 9 # starting column to be picked up
det.signal <- a[, seq(starting.column,ncol.a,nrep.col)]
order.clin.samples<- order(clin$SerialNo)
clin2 <- clin[order.clin.samples,]
group <- clin2$Group # CB, CC, MB, MC, MDB, MDC, XMB, XMC
group.id <- c(group) # CB=1 CC=2 MB=3 MC=4 MDB=5 MDC=6, XMB=7, XMC=8
avg.signal <- avg.signal[,order.clin.samples]
det.signal <- det.signal[,order.clin.samples]
### This section for getting normalized data from unnormalized data.
require(affy)
log.avg.signal <- as.matrix(log(avg.signal,2))
exp.normalized <- normalize.quantiles(log.avg.signal)
colnames(exp.normalized) <- names(avg.signal)
rownames(exp.normalized) <- as.character(a[,1])
exp.normalized.lin<-2^exp.normalized
# Output normalized linear signal intensities
write.csv(exp.normalized.lin, file="Offspring_normalised_signal_final.csv")
#... End of normalization step for non-normalized data.
# Obtain mean intensities per group
mean.cb<-apply(exp.normalized[,group=="CB"],1,mean)
mean.cc<-apply(exp.normalized[,group=="CC"],1,mean)
mean.mb<-apply(exp.normalized[,group=="MB"],1,mean)
mean.mc<-apply(exp.normalized[,group=="MC"],1,mean)
# Determine genes that are present in each group
detection.threshold <- 0.99
temp <- function(a) sum(a>=detection.threshold)
present.CB <- apply(det.signal[,group=="CB"],1,temp)
present.CC <- apply(det.signal[,group=="CC"],1,temp)
present.MB <- apply(det.signal[,group=="MB"],1,temp)
present.MC <- apply(det.signal[,group=="MC"],1,temp)

#####
```

Analysis 1: CB vs CC

```
p.values1 <- apply(exp.normalized,1,function(a) t.test(a[group=="CB"], a[group=="CC"],
paired=TRUE, var.equal=T)$p.val)
t.stat1 <- apply(exp.normalized,1,function(a) t.test(a[group=="CB"], a[group=="CC"],
paired=TRUE, var.equal=T)$stat)
# Define and apply the function to get the average log fold change (CC/CB)
avg.logfold1<-function(a){return(mean(a[group=="CC"]-a[group=="CB"]))}
avg.log.fold1 <-apply(exp.normalized,1,avg.logfold1)
## Generate objects for CB vs. CC from exp.normalized
clin.1 <- clin2[c(1:34),]
exp.normalized1 <- exp.normalized[,c(group=="CB" | group=="CC")]
order.clin.samples<- order(clin.1$SampleID)
clin.1 <- clin.1[order.clin.samples,] group1 <- clin.1$Group # CB, CC
group.id1 <- c(group1) # CB=1 CC=2
exp.normalized1 <- exp.normalized1[,order.clin.samples]
#OCplus - FDR2d correction
require (OCplus)
result.2d1<-fdr2d(exp.normalized1, group.id1, nperm=500, smooth=0.01, paired=TRUE)
fdr.values1<-result.2d1$fdr
# Create summary Table
summary.Table1<-data.frame(gene.ID=as.character(rownames(exp.normalized)),
log.fold=avg.log.fold1, fold.change=2^avg.log.fold1, present.CB, present.CC,
t.statistics=t.stat1, p.values=p.values1, fdr2d=fdr.values1)
write.csv(summary.Table1, file="Control offspring baseline vs. CRP.csv")
#volcano plot
plot(avg.log.fold1, -log(p.values1,10),xlab="log(2) fold change",ylab="-log(10)p-
values",main="Control offspring baseline vs. CRP")

#####
```

Analysis 2: MB vs MC

```
p.values2 <- apply(exp.normalized,1,function(a) t.test(a[group=="MB"], a[group=="MC"],
paired=TRUE, var.equal=T)$p.val)
t.stat2 <- apply(exp.normalized,1,function(a) t.test(a[group=="MB"], a[group=="MC"],
paired=TRUE, var.equal=T)$stat)
# Define and apply the function to get the average log fold change (MC/MB)
avg.logfold2<-function(a){return(mean(a[group=="MC"]-a[group=="MB"]))}
avg.log.fold2 <-apply(exp.normalized,1,avg.logfold2)
## Generate objects for MB vs. MC from exp.normalized
clin.2 <- clin2[c(37:58,61:82),]
exp.normalized2 <- exp.normalized[,c(group=="MB" | group=="MC")]
order.clin.samples<- order(clin.2$SampleID)
clin.2 <- clin.2[order.clin.samples,]
group2 <- clin.2$Group # MB, MC
group.id2 <- c(group2) # MB=3 MC=4
exp.normalized2 <- exp.normalized2[,order.clin.samples]
#OCplus - FDR2d correction
require (OCplus)
result.2d2<-fdr2d(exp.normalized2, group.id2, nperm=500, smooth=0.01, paired=TRUE)
fdr.values2<-result.2d2$fdr
# fdr correction
fdr.p.values2=fdr.pval(p.values2)
# Create summary Table
summary.Table2<-data.frame(gene.ID=as.character(rownames(exp.normalized)),
log.fold=avg.log.fold2, fold.change=2^avg.log.fold2, present.MB, present.MC,
t.statistics=t.stat2, p.values=p.values2, fdr2d=fdr.values2)
write.csv(summary.Table2, file="Offspring of MI baseline vs. CRP.csv")
#volcano plot
plot(avg.log.fold2, -log(p.values2,10),xlab="log(2) fold change",ylab="-log(10)p-
values",main="Offspring of MI baseline vs. CRP")

#####
```

Analysis 3: MB vs CB

```
p.values3 <- apply(exp.normalized,1,function(a) t.test(a[group=="MB"], a[group=="CB"],
paired=FALSE, var.equal=T)$p.val)
t.stat3 <- apply(exp.normalized,1,function(a) t.test(a[group=="MB"], a[group=="CB"],
paired=FALSE, var.equal=T)$stat)
# Define and apply the function to get the average log fold change (MB/CB)
avg.log.fold3 <- mean.mb-mean.cb
## Generate objects for MB vs. CB from exp.normalized
clin.3 <- clin2[c(1:17,37:58),]
exp.normalized3 <- exp.normalized[,c(group=="MB" | group=="CB")]
order.clin.samples<- order(clin.3$Group)
clin.3 <- clin.3[order.clin.samples,]
group3 <- clin.3$Group # MB, CB
group.id3 <- c(group3) # MB=3 CB=1
exp.normalized3 <- exp.normalized3[,order.clin.samples]
#OCplus - FDR2d correction
require (OCplus)
result.2d3<-fdr2d(exp.normalized3, group.id3, nperm=500, smooth=0.01, paired=FALSE)
fdr.values3<-result.2d3$fdr
# fdr correction
fdr.p.values3=fdr.pval(p.values3)
# Create summary Table
summary.Table3<-data.frame(gene.ID=as.character(rownames(exp.normalized)),
log.fold=avg.log.fold3,
fold.change=2^avg.log.fold3, present.MB, present.CB, t.statistics=t.stat3,
p.values=p.values3,
fdr2d=fdr.values3)
write.csv(summary.Table3, file="Offspring_MI_vs_CON_baseline.csv")
#volcano plot
plot(avg.log.fold3, -log(p.values3,10),xlab="log fold change",ylab="-log(10)p-
values",main="Offspring of MI vs. controls (baseline)")

#####
```

Analysis 4: MC vs CC

```
p.values4 <- apply(exp.normalized,1,function(a) t.test(a[group=="MC"], a[group=="CC"],
paired=FALSE, var.equal=T)$p.val)
t.stat4 <- apply(exp.normalized,1,function(a) t.test(a[group=="MC"], a[group=="CC"],
paired=FALSE, var.equal=T)$stat)
# Define and apply the function to get the average log fold change (MC/CC)
avg.log.fold4 <- mean.mc-mean.cc
# Define and apply the function to get the average log fold change (MC/CC)
#the following will not work if the number of samples are not the same!
avg.logfold4<-function(a){return(mean(a[group=="MC"]-a[group=="CC"]))}
avg.log.fold4 <-apply(exp.normalized,1,avg.logfold4)
## Generate objects for MC vs. CC from exp.normalized
clin.4 <- clin2[c(18:34,61:82),]
exp.normalized4 <- exp.normalized[,c(group=="MC" | group=="CC")]
order.clin.samples<- order(clin.4$Group)
clin.4 <- clin.4[order.clin.samples,]
group4 <- clin.4$Group # MC, CC
group.id4 <- c(group4) # MC=4 CC=2
exp.normalized4 <- exp.normalized4[,order.clin.samples]
#OCplus - FDR2d correction
require (OCplus)
result.2d4<-fdr2d(exp.normalized4, group.id4, nperm=500, smooth=0.01, paired=FALSE)
fdr.values4<-result.2d4$fdr
# fdr correction
fdr.p.values4=fdr.pval(p.values4)
# Create summary Table
summary.Table4<-data.frame(gene.ID=as.character(rownames(exp.normalized)),
log.fold=avg.log.fold4, fold.change=2^avg.log.fold4, present.MC, present.CC,
t.statistics=t.stat4, p.values=p.values4, fdr2d=fdr.values4)
write.csv(summary.Table4, file="Offspring_MI_vs_CON_CRP.csv")
#volcano plot
plot(avg.log.fold4, -log(p.values4,10),xlab="log(2) fold change",ylab="-log(10)p-
values",main="Offspring of MI vs. controls (CRP)")

#####
```

SELECTION OF A CONTROL GENE

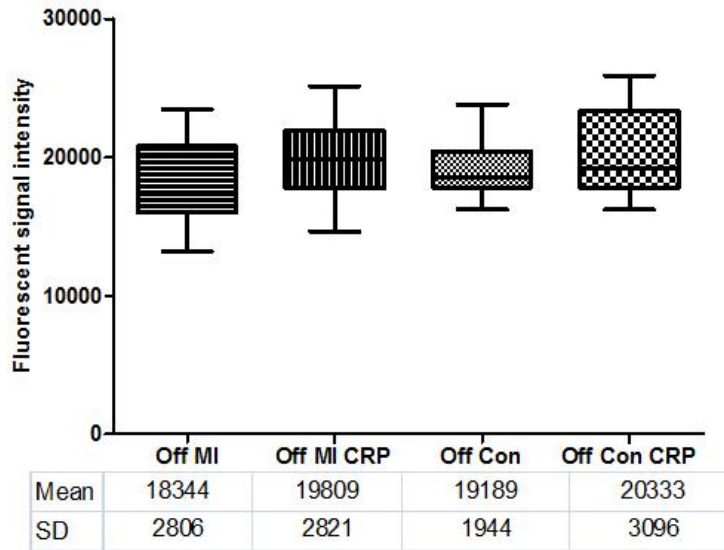
The first step was the identification of a suitable control gene. Although genes such as 18S and GAPDH are regularly used ubiquitous control genes in Q-PCR, there were important issues to consider in these analyses.

The cycle lengths of the control gene and the gene of interest should be comparable. As one cycle of Q-PCR equates to a two fold increase in sample, high abundance genes such as 18S which may frequently amplify 10-12 cycles prior to low abundance candidate gene would mask the small fold change in gene expression between the groups of samples.

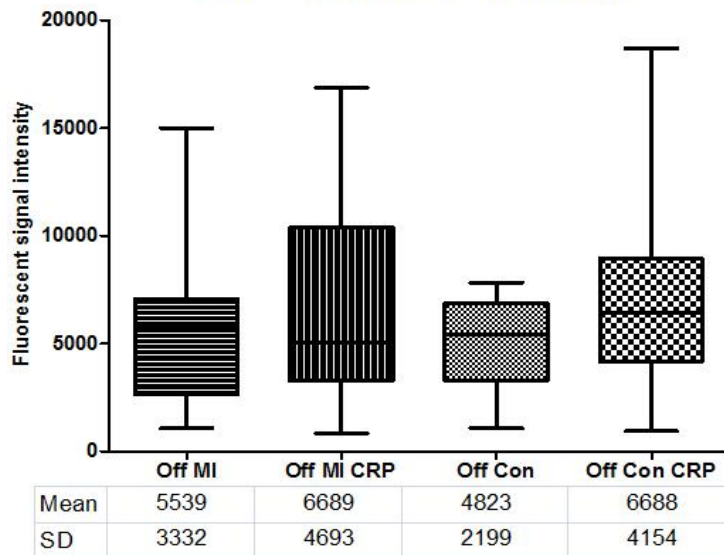
The use of a stimulus – cross linked collagen related peptide affects the expression of many genes, including commonly used control genes. To assess this further, GeneSpring GX was used to visualise signal intensities of commonly used control genes. Then, the absolute signal intensities were plotted graphically to identify the gene which had least variation following stimulation experiments. The genes studied were β 2 microglobulin, β actin, cyclophilin A, GAPDH, HMBS, HPRT1, PLA2 G4B, RPL13A, RPLP, SDH and TBP.

The gene that satisfied the two criteria mentioned above was TATA box protein (TBP). This was used in all Q-PCR experiments as control gene.

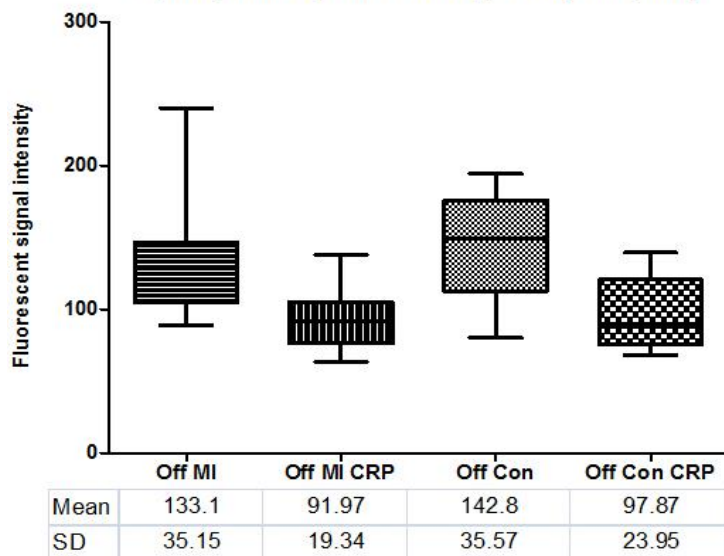
Beta 2 microglobulin (ILMN_19648) offspring



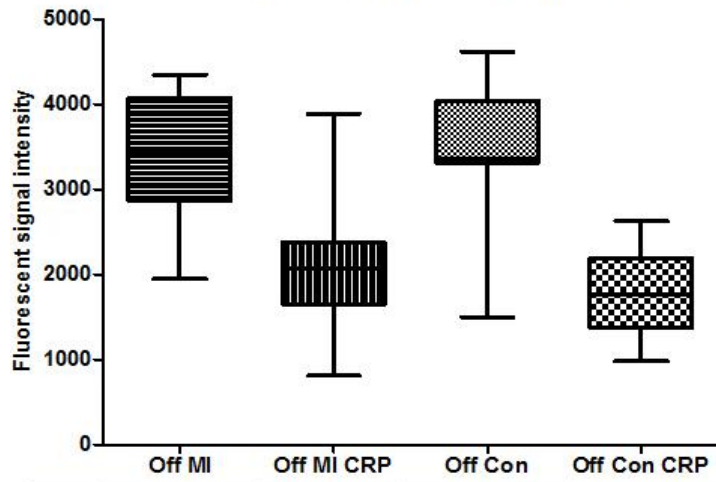
Beta actin (ILMN_2565) offspring



Cyclophilin A (PPIA - ILMN_22626) offspring

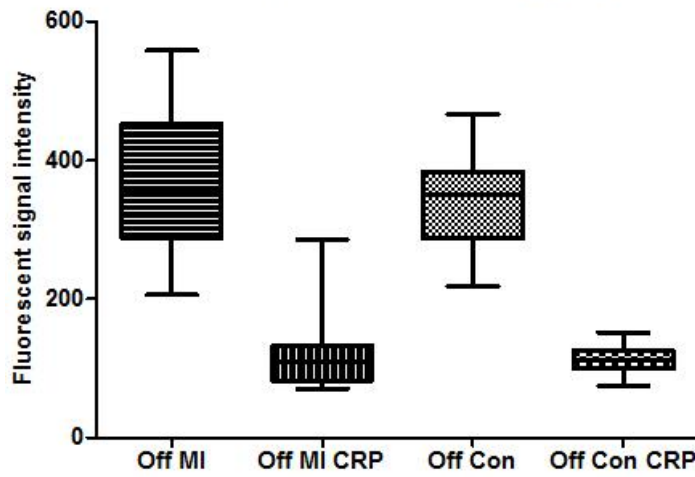


EIF3S5 (ILMN_138136) offspring



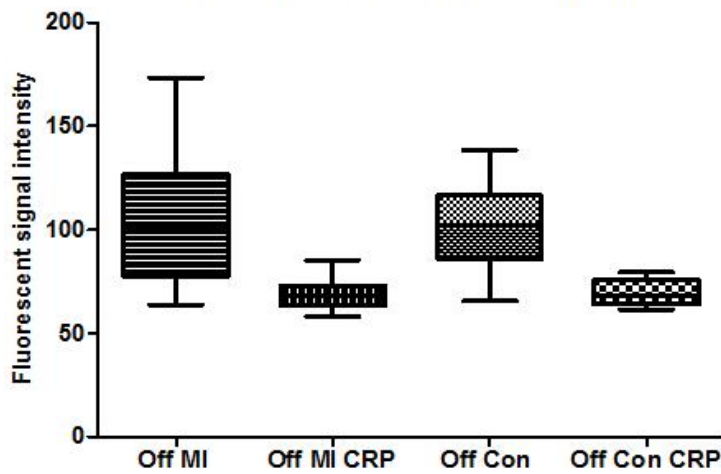
Mean	3414	2048	3511	1832
SD	759.2	680.3	833.1	510.3

HMBS (ILMN_15879) offspring



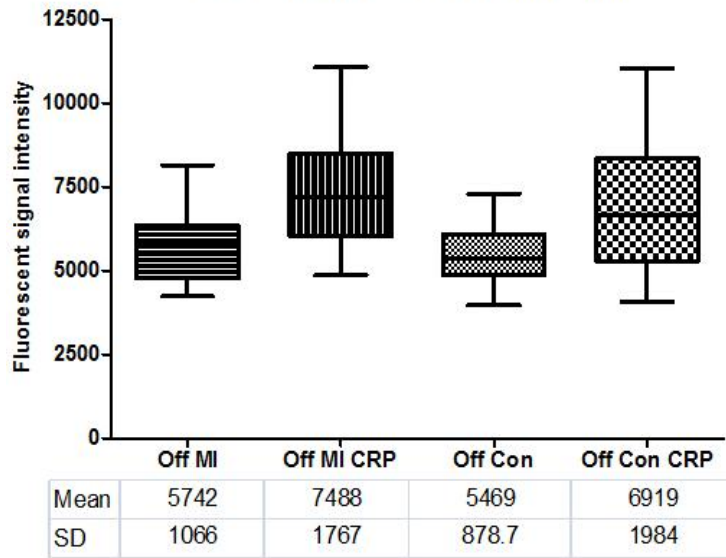
Mean	362.5	116.3	344	111.7
SD	100.9	45.44	59.72	21.05

HMBS (ILMN_16358) offspring

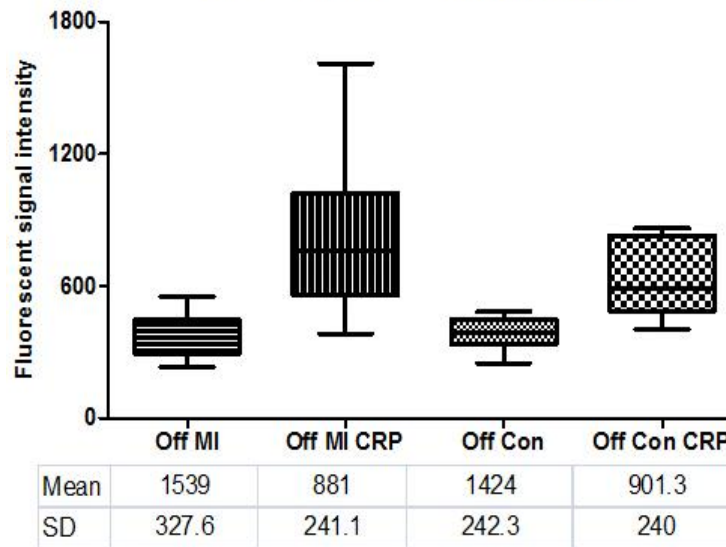


Mean	104.5	68.57	101.1	69.15
SD	30.7	7.196	19.13	6.048

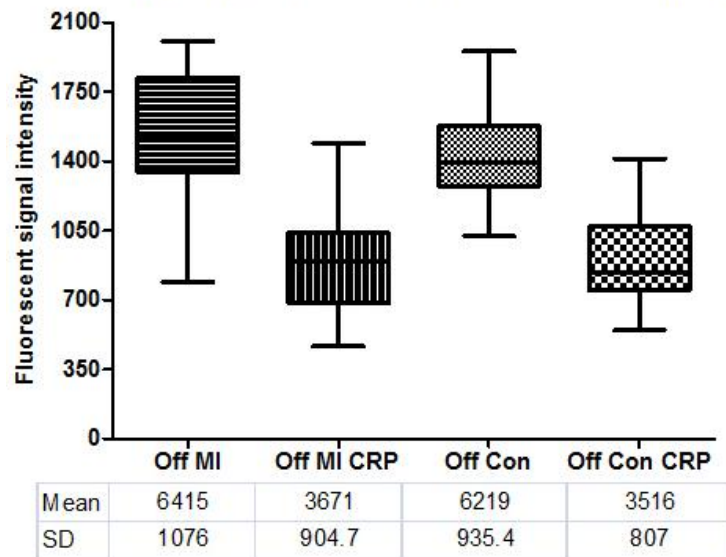
GAPDH (ILMN_137405) offspring



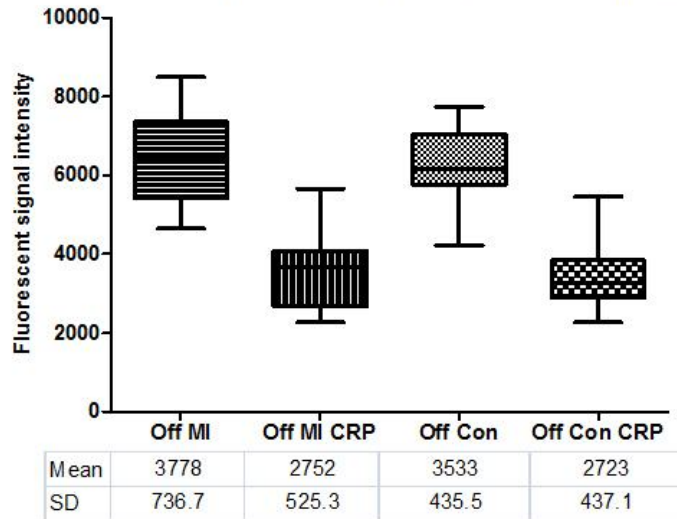
HPRT1 (ILMN_23394) offspring



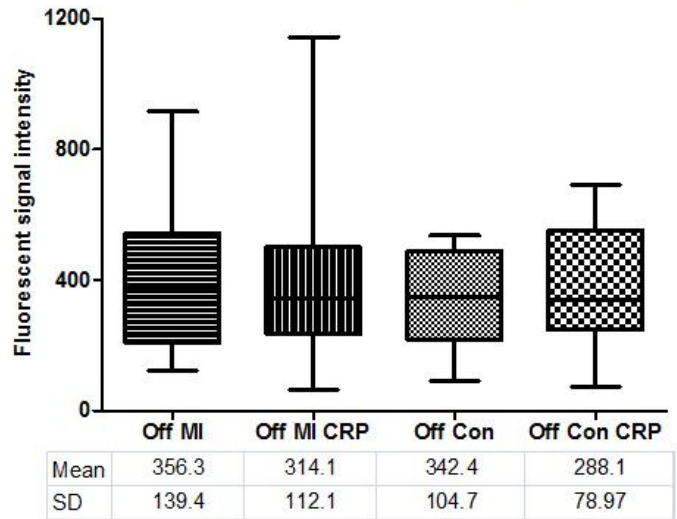
Phospholipase A2 G4B (ILMN_6705) offspring



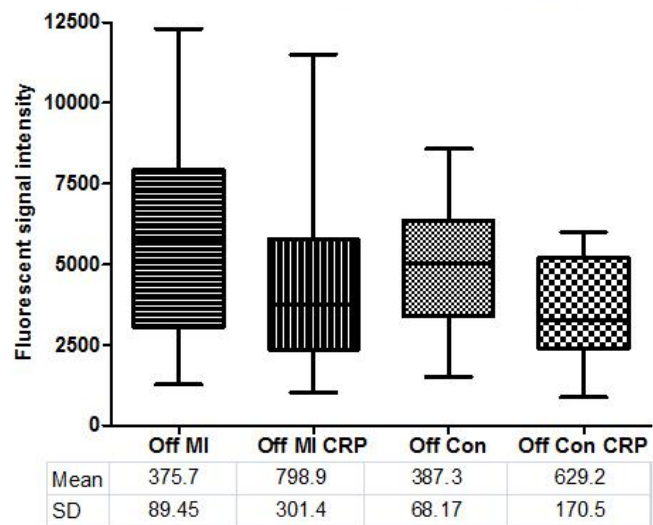
Ribosomal protein L13A (ILMN_2500) offspring



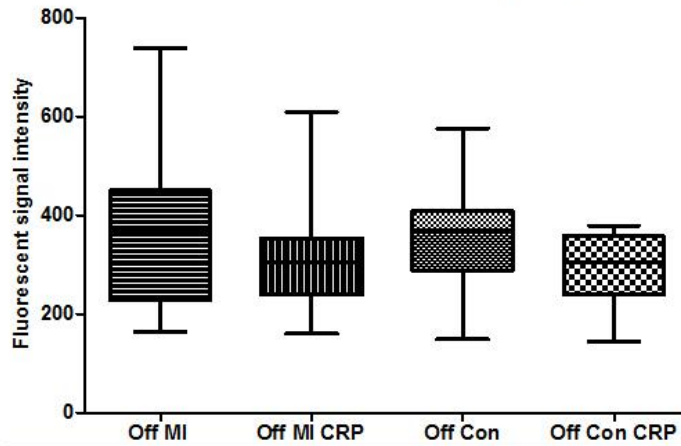
RPLP0 ILMN_22851 offspring



RPLP0 ILMN_22954 offspring

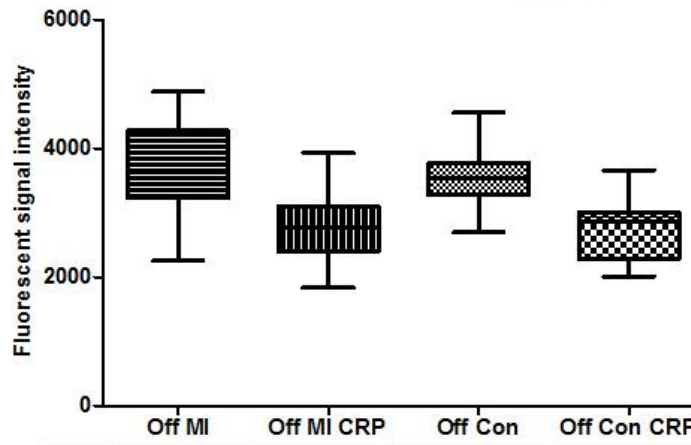


SDH A (ILMN_22058) offspring



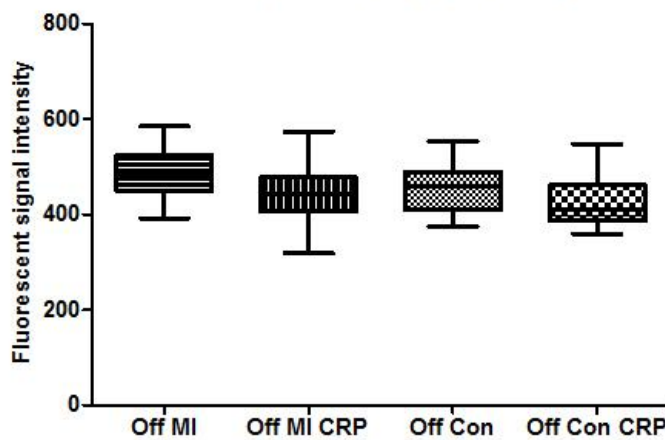
	Off MI	Off MI CRP	Off Con	Off Con CRP
Mean	407.9	414.4	348.3	377.3
SD	224.1	276.3	142.6	181.1

SDH B (ILMN_12116) offspring



	Off MI	Off MI CRP	Off Con	Off Con CRP
Mean	5704	4382	4917	3643
SD	2755	2811	1818	1626

TBP (ILMN_3293) offspring



	Off MI	Off MI CRP	Off Con	Off Con CRP
Mean	487.4	441.3	454.8	427.1
SD	52.87	52.46	53.41	51.56

